CONF-9409304--

SAND95-0116
UC-712
Unlimited Release

Workshop on Transport for a Common Ion Driver

September 20-21, 1994
Sandia National Laboratories
Albuquerque, New Mexico

Chairmen: C. Olson (SNL), E. Lee (LBL), B. Langdon (LLNL)

This work was supported by the United States Department of Energy under Contract DE-AC04-94AL85000.

SAND95-0116
UC-712
Unlimited Release

Workshop on Transport for a Common Ion Driver

September 20-21, 1994
Sandia National Laboratories
Albuquerque, New Mexico

Chairmen: C. Olson (SNL), E. Lee (LBL), B. Langdon (LLNL)

This work was supported by the United States Department
of Energy under Contract DE-AC04-94AL85000.

Table of Contents

Appendix: Presentations

Self-Pinched Transport

HIF and LIF transport, and Relevance to Common Ion Driver

LIF and HIF Reactor Concepts and Relevance to Common Ion Driver

Atomic Physics for Common Ion Driver

Code Capabilities and Needed Improvement

Workshop Working Discussion

Motivation for Workshop

A Tri-Laboratory meeting was held on February 8, 1994, in Livermore, California, for the purpose of considering the possibility of a "Common Ion Driver." This was an informal discussion with the following persons in attendance:

LLNL (Grant Logan, Mike Campbell, John Lindl, Alex Friedman)

LBL (Roger Bangerter, Ed Lee, Andy Faltens)

SNL (Don Cook, Jeff Quintenz, Craig Olson, Keith Matzen)

The intent of the meeting was to consider the possibility of a middle-weight ion driver that could be used for a combined Laboratory Microfusion Facility (LMF)/Engineering Test Facility (ETF), and to ultimately advise both DOE Defense Programs (DP) and DOE Energy Research (ER) of this possibility. A result of this meeting was the recommendation that working groups be formed in the areas of ion beam transport, accelerator concepts, and targets. The transport group, consisting of

SNL (Craig Olson)

LBL (Ed Lee)

LLNL (Bruce Langdon)

was commissioned to begin, since it was felt that the greatest commonality between Light Ion Fusion (LIF) and Heavy Ion Fusion (HIF) appeared to be in the area of ion beam transport. Results of the February 8, 1994 Tri-Lab meeting were reported in a Tri-Lab letter to

DOE DP (Marshall Sluyter)

DOE ER (David Crandall)

on February 11, 1994 (copy included in this Report).

The Transport Working Group met at LBL on June 5, 1994 and decided that a useful method for assessing ion beam transport would be to hold an informal workshop. This Workshop on Ion Beam Transport for a Common Ion Driver resulted.

Purpose of Workshop

Ion Beam drivers for Inertial Confinement Fusion (ICF) have been under development since the mid-1970's in two primary areas -- LIF drivers and HIF drivers. The LIF drivers are based on pulsed power driven 1- or 2-stage diodes, and typically use low atomic number ions ($A \lesssim 10$). The HIF drivers are based on conventional multi-gap accelerator technology (induction linacs in the US; RF accelerators/storage rings in Europe), and typically use high atomic number ions ($A \gtrsim 50$). Interest in middle-weight ions, and the concept of a multi-gap accelerator with neutralization between gaps, has arisen occasionally, but there has been no strong development of this area to date. Ion beam transport methods for both LIF and HIF have been examined during the same time period.

Following demonstration of ICF ignition using a glass laser in the National Ignition Facility (NIF), there are presently two future development options - LMF and ETF. The LMF is a high-yield, single-shot facility, for which an LIF driver is a prime candidate. The ETF is a lower-yield, rep-rated facility, for which an HIF driver is the prime candidate. Following LMF and ETF, the long-range goal is energy production, for which a single Demonstration Facility is envisioned. It is possible that a middle-weight ion, multi-gap accelerator might be conceived that could combine the LMF and ETF goals into a single facility. It appears prudent to at least consider the possibility of such a facility at this time.

The purpose of this workshop was to assess the physics of ion beam transport for this Common Ion Driver. Transport for LIF and HIF were to be discussed, but the emphasis was to be on encouraging comments and discussion on the possible advantages of a middle weight ion. Therefore, the scope of the workshop was to include:

1. all forms of final transport and focusing for LIF, HIF, and a middle-weight ion
2. neutralization between gaps in a multi-gap accelerator
3. all supporting areas for the above; including experiments, code development, and atomic physics

Neutralization between gaps was considered to be a transport issue, since the physics of this neutralization can be similar to some of the neutralization schemes for final transport.

The Workshop

The Workshop on Ion Beam Transport for a Common Ion Driver was held at Sandia National Laboratories in Albuquerque, New Mexico on September 20-21, 1994. A total of 32 people attended, with representatives from SNL, LBL, LLNL, NRL, MRC, U. Wisconsin, UNM, and DOE (see attendance list). The Workshop was organized into the following sessions:

1. motivation for common ion driver
2. multi-gap ion acceleration
3. neutralization with electrons
4. neutralization with gas
5. self-pinched transport
6. HIF and LIF transport and relevance to Common Ion Driver
7. LIF and HIF reactor concepts and relevance to Common Ion Driver
8. atomics physics for common ion driver
9. code capabilities and needed development
10. working discussion

There were no pre-determined conclusions for this Workshop. It was expected that several transport modes, and especially self-pinched transport, would be of interest for all ions. Advantages and disadvantages of each concept were to be discussed, and discussion of relevance toward a common ion was encouraged.

Summary of Workshop Sessions

In the following we briefly summarize the main results of each session.

(1) Motivation for a common ion driver

• Although LIF typically has ions with A $\lesssim$ 10, and HIF typically uses A $\gtrsim$ 50, there was virtually no consensus to assume 10 $\lesssim$ A $\lesssim$ 50 represents a middle-weight ion. The basic tendency of some HIF supporters was to assume that low A's could be used with the present HIF approach. However, during talk number 17 it was noted that the HIF approach for A $\lesssim$ 50 becomes impractical due to the cost of the low energy end. So it stands that a reasonable exploratory space for a middle-weight ion is 10 $\lesssim$ A $\lesssim$ 50, at least for the purposes of this study.

• It was emphasized that this Workshop is on transport, but that transport parameters will depend on the accelerator concept and target concept (which will be the subjects of two other working groups).

• An argument was made that a common ion driver will require multi-gap acceleration with neutralization between the gaps. This is a consequence of the small value of the Maschke current limit for space-charge dominated beams using vacuum quadrupole transport.

(2) Multi-gap ion acceleration

• The PULSELAC concept of multi-gap acceleration with neutralization between gaps was tested in initial experiments over a decade ago with ion beams from various sources (C^+; N^+ from gas puff source; proton/C from flashover source) with ion energies in the range of 100-300 keV. The best results for PULSELAC C-U for a 50 cm transport length to gap 2 show 25% transport with or without plasma wall sources, and 90% transport with a gas-puff. Since a common ion driver would have many such transport sections, the transport efficiency would have to be very close to 100% in each section for a practical accelerator. Although the present results are not very encouraging, more work could clearly be done in this area to complete a definitive assessment of this concept. This issue should also be addressed in the accelerator working group.

• In addition to efficiency of transport, a fundamental issue raised for the PULSELAC was beam emittance growth associated with field aberrations around the magnet supports. Since solenoids are interior to an annular beam in PULSELAC, this appears to be an unavoidable phenomena.

(3) Neutralization with electrons

• 1-D and 2-D numerical simulations of electron neutralization of ion beams have been performed at SNL over the past 15 years. Results for transverse electron neutralization for no external magnetic field ($B_0 = 0$) show poor neutralization (~ 60%) unless dissipative processes can occur. A tilted $B_0 \neq 0$ improves neutralization considerably. Results for axial neutralization show that the net potentials are not reduced to zero, but to $e\phi \approx \alpha(1/2\, m_e V_i^2)$ where V_i is the initial ion beam velocity and $1 \lesssim \alpha \lesssim 4$. These results occur for a wide variety of phenomena (including the Pierce instability saturation, and the micro charge non-neutrality problem). Sizeable microdivergence values can result.

• Modeling at LLNL concentrates on the low-density, near-ballistic regime (chamber vapor density ~ 10^{13} molecules/cc), and seeks to extend the boundaries of that mode of operation. The BICrz code has been used to model processes by which an unneutralized ion beam from the accelerator becomes partially neutralized, by entraining electrons from a pre-formed plasma cloud and from collisionally-ionized chamber vapor. We strive to establish that charge neutralization can reduce space charge sufficiently that intensity-dependent beamlet aiming/focusing, and stripping, are not an important complication at chamber conditions desired by reactor designers. We calculate that neutralization fractions > 80% are readily achievable if a means is found to form the plasma cloud. The remaining electric field, however is quite nonlinear, as we predicted. Thus far this has prevented us from focusing lighter ions onto the same focal spot as A = 200 ions. As predicted by Olson, the entraining electrons have energy $\gtrsim$ 25 keV; as predicted by Lemons and Jones, the neutralization by these electrons decreases as the beam approaches the target and the entrained electrons are compressed to higher temperatures. With a plasma column extending all the way to the target, simulations show spot sizes smaller than predicted by the vacuum envelope equation.

Ionization of chamber vapor (by collisions with beam ions, photoionization...) is helpful to neutralization. Ionization of beam ions, by collisions with vapor ('stripping') and photoionization by thermal x-rays emitted by the heated target, leads to emittance growth in residual electric fields. The ratio of beam ionization to vapor ionization, by collisions, is an ingredient in modeling of low density chambers. Initial neutralization by a pre-formed plasma reduces the damage done to the focal spot by stripping.

• For transverse electron neutralization, QUICKSILVER simulations show electrons remain tied to magnetic field lines despite development of fluctuations. ALIAS ion beam experiments will be used to assess these predictions.

(4) Gas neutralization

• Gas neutralization is used in many transport schemes for LIF and HIF, including ballistic transport and self-pinched transport. For LIF ballistic transport excellent current neutralization is needed ($\gtrsim$ 99.9%). For LIF and HIF self-pinched transport, lesser current neutralization is needed (~ 90-98%). The key to obtaining the desired current neutralization is to fully understand the physics of gas breakdown.

• Fast electrons must be included to model gas breakdown correctly. In the "-1 Torr regime," fast electrons have λ_{mfp} of the order of the beam radius and cause non-local breakdown effects. Fast electrons result from ion impact ionization, knock-on collisions, and runaway electrons during avalanching.

• The IPROP 3-D EM hybrid code is the first ion beam/gas breakdown code to correctly include fast electrons. IPROP has ion PIC, electron PIC for electron energies above some E_0 (typically 100 eV), and an electron fluid for energies below E_0.

• Gas breakdown experiments on GAMBLE II at NRL for helium and argon show good agreement with net currents as predicted by IPROP. The results indicate that fast electrons create a conducting channel outside the beam. This is very important since a significant portion of the return current can flow in the halo region.

• The effects of a transverse B on the gas breakdown and net current have been studied theoretically for beam injection into a preformed plasma.

(5) Self-pinched transport

• Self-pinched transport for HIF starts with a quadrupole or plasma lens focussing system located either just outside the fusion chamber or at the end of the accelerator system located several hundred meters from the chamber. In both cases the beam is rapidly stripped to a very high charge state at small radius and subsequently propagates in low pressure gas to the fusion target in an electrically neutralized, magnetically pinched condition. The available stripped beam electrical current is typically 40 kA or more; this implies current neutralization fractions of ~ 98% or lower are needed to confine the transverse pressure of the emittance. Although the physics of this transport mode is more complicated and uncertain than the standard final focus in vacuum, there are very substantial beneficial features for the fusion chamber and final focus configurations, and possibly a relaxation of requirements on accelerator wave form control. The main issues, now under study at LBL, are (1) the effectiveness of formation of the pinch, (2) stability of the beam against hose, sausage and two-stream modes, and (3) possible beam loss processes involving scattering and channel expansion. The PIC/Fluid Code IPROP, developed at MRC to study self-pinched transport for light ion beams, may be suitable for the heavy ion parameters. LBL computations now employ a PIC (r, z, t) model for beam and plasma under the assumption that electrons will be hot ($\gtrsim$ 1.0 keV) in the low pressure ranges considered.

• Self-pinched transport for LIF includes (1) ballistic focusing to a channel entrance; (2) self-pinched propagation in a guide tube for $\gtrsim$ 1 meter to establish equilibrium, a propagation axis for aiming, and some phase mixing; and (3) self-pinched propagation in the reactor chamber for many meters to a target. Present IPROP simulations suggest pressures of ~1 Torr for region (1) and $\lesssim$ 0.1 Torr for regions (2) and (3). This transport scheme should be ideal for all ions (LIF, common ion, HIF), and for all power plant schemes. IPROP simulations have been performed for a number of self-pinched schemes (including annular plasma transport), and they demonstrate that substantial net currents are possible.

• Early simulations of self-pinched transport at NRL using a collisionless preionized plasma channel showed strong pinching. Further simulation studies and analytical results predict weak pinching for beam injection into a dense plasma channel. Note that time-dependent gas breakdown with non-local breakdown effects was not addressed in this work.

• Experiments to demonstrate self-pinched transport have been proposed for SABRE or GAMBLE II. All of the basic features should be demonstrable including ballistic focusing to a channel entrance, self-pinched transport in a guide tube, and self-pinched transport in a large radius chamber. The results would be of considerable importance to LIF, HIF, and a common ion driver.

(6) HIF and LIF transport and relevance to a Common Ion Driver

• HIF mainline transport consists of a moderate number (N = 4-24) of vacuum beam lines comprised of magnetic quadrupole and bends and culminating in 4-6 large aperture final focus quadrupoles on each line. Focal spot size is limited by the momentum spread, transverse phase space area, various aberrations, and space charge. Each of these limitations is fairly well understood, provided the transport in the chamber can be assumed to be equivalent to vacuum. However this is not the case for most power reactor configurations since a residual pressure of 10^{-4}-10^{-2} Torr FLIBE or other vapor is present. Stripping and ionization will significantly effect beam dynamics in the chamber by altering the electrodynamics in ways that are only partially understood at present. A program of simulation study has begun at LBL and LLNL to scope such phenomena and address issues. This has proven to be a difficult task due to the complexity of the system, lack of good cross sections for some important atomic processes, and the short time scales dictated by the high plasma frequency in some scenarios. An additional related area of high value research is the interface between the chamber and final focus beam lines. Design must treat significant fluxes of neutron, gas and x-rays into the vacuum system.

• LIF mainline transport (for LMF and LIBRA-LiTE) is an achromatic lens system that consists of the high current extraction diode (which acts as a self-field lens) and a solenoidal lens. The beam is transported ballistically in gas from the lens to the target over a distance L, is focused by the lens, and then transported ballistically in gas from the lens to the target over a distance F. For LMF, L = 300 cm, and F = 100 cm. The gas is assumed to provide charge and current neutralization. The diode lens and solenoidal lens act together to form a system that is achromatic to lowest order in the diode voltage ramp variations. The basic elements of this system (diode lens effect, gas neutralization, and solenoidal lens effect) are all routinely observed on PBFA II, although a complete extracted beam, achromatic system has not been demonstrated. Key issues (which are all being addressed) include gas breakdown and current neutralization in the presence of transverse B fields, total system transport efficiencies, and the possibility of the filamentation instability.

• Channel transport and wire-guided transport are back-up transport methods for LIF (and they could also be used for HIF). For either "channel-like" scheme, the beam from the diode is first focused down to a small radius (< 1 cm) and then transported at small radius over several meters to the target. For LIF LMF parameters, all channel-like schemes require a channel current of ~ 50 kA. The current can be from a preformed discharge (well-confined transport) or a wire (wire-guided transport). Both channel transport and wire-guided transport have been thoroughly demonstrated at low energy (1 MeV p) and are expected to work at LMF energies (35 MeV Li), but require some transport apparatus (low mass tubes or wires) inside the containment chamber.

These schemes could be used for LMF (but not ETF or IFE).

• Channel issues affect all ion schemes (LIF, HIF, common ion) and should be addressed. Free-standing (laser-created) channels have high voltage breakdown as an unresolved issue. Channel expansion problems indicate small radius ($\lesssim$ 0.5 cm) channels will not work; larger radius channels ($\gtrsim$ 0.5 cm) will work. This issue is important because it implies, e.g., that HIF can use channels only for large spot radii targets.

(7) LIF and HIF reactor concepts and relevance to a Common Ion Driver

• LIF reactor concepts include three versions of the LIBRA concept. The original LIBRA used free-standing laser created channels. LIBRA-LiTE used ballistic transport with solenoidal lens focusing. LIBRA-SP, currently under study, uses self-pinched propagation. A common ion would easily apply to the chamber concept used in LIBRA-SP, and work on this scheme should be encouraged.

• HIF reactor concepts may be essentially classified according to the way x-rays are stopped (the "first wall") and the type and temperature of the coolant or breeding blanket. Three features have a profound effect on the final transport physics since they determine the gas environment of the beam and the gas load into the final transport beamlines. Most recently, the HYLIFE II design employs jets of FLIBE (Li-Be-F) to simultaneously perform all the first wall/ coolant/blanket functions. Compared with pure Li, this has reduced the standoff distance to the final magnet by several meters and increased the cross sections for stripping and ionization. Other recent design concepts are several forms of "wetted" walls using porous tubes for the breeding coolant. Examples are HIBALL II using Li-Pb, and Osiris using FLIBE. Much lower gas pressures are realized in this way, but at the cost of introducing fabricated components into the direct neutron flux from the microexplosions. Alternatives are Prometheus-H using Li-Pb in SiC channels and Cascade, using solid granules for the first wall/breader/coolant; pressures are similar to HYLIFE II but the gas type includes carbon and other species. From the point of view of final transport, any proposed reactor generates a beam environment which must be carefully considered for issues such as stripping effects, etc. In addition, the interface to the Final Focus system must be designed to take account of the gas load.

(8) Atomic physics needs for a common ion driver

• There is clearly a need for accurate cross sections for ion impact ionization, stripping, charge exchange, etc. In the presentations, the need was clear for both HIF and LIF, and certainly accurate cross sections will be needed for a common ion.

• A number of atomic physics modeling capabilities exists at the University of Wisconsin. These could be used to the benefit of LIF, HIF, and a common ion.

(9) Code capabilities and needed development

• IPROP is a quasi-3D code with full electromagnetic fields; it uses arbitrary orthogonal coordinates with the third dimension Fourier analyzed into an arbitrary number of modes. IPROP has micro-particle and thermal-fluid components for the electrons. Typically electrons with energies < 100 eV constitute a tensor conductivity; electrons at higher energies are followed as particles, and ions are followed as particles. Simple atomic physics models are included in IPROP. IPROP is ideal for many problems such as gas breakdown and current neutralization with non-local effects.

• BIC (beam-in-chamber) code models propagation of a particle beam from the wall of the target chamber to the target. BIC has two parts; both are particle-in-cell (PIC) models with a tapered field mesh that concentrates resolution near the target. BICxy follows a cross-sectional slice of the beam or a bundle of beamlets. In the moving frame of the slice, the fields are dominantly electrostatic. It has been used to assess the importance of photoionization of beam ions by thermal x-rays from the heated target, interaction of beamlets as they merge and overlap at the target, and other topics. BICrz is an r-z axisymmetric model with full electromagnetic fields; the mesh is stationary in the laboratory frame. Given cross-sections for beam stripping by the chamber vapor, and for collisional ionization of the vapor by the beam, BICrz models the effect of these processes on the beam propagation and deposition pattern. Normally the electrons are PIC modeled, although there is a fluid electron model under development that has promise for modeling electrons dense enough to charge-neutralize very well. BICrz needs cross-sections with higher credibility than those we have now. A number of refinements are in progress regarding boundary conditions. Photoionization of beam ions and of chamber vapor will be modeled. In the future, a description of the ion beam should be linked from WARP, and the beam deposition linked to the target modeling code.

• WARP is a multidimensional discrete-particle beam simulation program being developed and used at LLNL in collaboration with NRL and LBL. It is being designed and optimized for heavy ion fusion accelerator physics studies. At present it incorporates a 3-D description, an axisymmetric (r,z) description, and a simple envelope model used primarily to obtain a well-matched initial state. The code is built atop the BASIS development and run-time system, which affords a flexible and powerful interpretive user interface, and a means for splitting a code into "physics packages," which can be developed (almost) independently. The WARP code combines the particle-in-cell (PIC) technique commonly used for plasma modeling with a description of the accelerator "lattice" of elements. A fully general set of finite-length accelerator elements can be specified, including quadrupole focusing, dipole bending, accelerator, and more general elements specified via their axially dependent multipolar composition. Another set of elements in the 3-D model specifies the locations and curvatures of bends. These are not physical elements, but are the appropriate coordinate transformations needed to follow the beam around the bends. The calculation of the self-consistent fields is also altered to include the curvature of this "warped" space.

WARP has been used for a wide variety of applications. Both the 3-D and axisymmetric models have been used to study long time behavior of beams, beam confinement, and compression. The longitudinal microwave instability has been studied using the axisymmetric model. The 3-D model was used in the analysis of results of the LBL MBE-4 experiment, and in the analysis and design of the electrostatic quadrupole injector for the ILSE program. It has also been used to understand emittance growth processes associated with changing curvature. Most recently, the 3-D model has been used in the study of LLNL's small recirculator experiments. Eventually we expect to use WARP to follow HIF beams from the source through all manipulations up to and including the final focusing lens.

• QUICKSILVER is a 3D, time domain, finite-difference PIC code used for the simulation of complex structures. QUICKSILVER simulates electromagnetics and also, with the inclusion of charged particles, high-current, high-voltage plasma physics. The code can model geometrically complex systems of conductors and dielectrics, and a wide range of boundary conditions are available. The QUICKSILVER suite of codes has successfully been used on many problems, including: LIF diode diocotron and ion mode instabilities, PBFA vacuum voltage adder, post hole convolutes, extraction diodes, etc.

• BUCKSHOT is a 3-D "gridless" particle code for end-to-end, high-current particle accelerator research. In BUCKSHOT, particles are spheres or cylindrical filaments that interact magnetostatically. Particles feel their neighbors charge and currents, and particles move self-consistently with self and applied forces. Multi-species particles with realistic charge/mass ratios are used, which allows study of background plasmas, channels, and charge neutralization. Gaps, bends, boundaries, and laser or beam-driven ionization can be included. BUCKSHOT is easy to use, and is 10-1000 times faster than 3-D EM PIC. BUCKSHOT has been used for many problems, including: IFR relativistic electron beam transport; recirculating and spiral line accelerator end-to-end design; SSC H-injector, LEBT, and RFQ; and electron and ion beam lithography.

(10) Working discussion

An open discussion session was held to discuss (1) a common set of ion parameters, (2) transport issues, and (3) recommendations for future work. General results are as follows:

• No consensus was reached as to a common set of ICF ion beam parameters, such as atomic number, spot-size radius, etc. It appears that it is premature at this time to force a fixed range of parameters on the ion fusion community. Both LIF and HIF are evolving, and the new awareness of a middle-weight ion regime should help guide current research.

• Several transport issues and areas were itemized for future research, including:

self-pinched transport:	small radius equilibrium
	adequate net current
	efficiency of trapping
	stability
	target charge-up?
	beam overlap at target
	aiming and tracking
charge-neutralized transport:	ballistic focus
	neutralization between gaps
channel issues:	small radius limit
	free-standing channel HV breakdown
HIF lens:	aberrations
	realistic lenses

LIF lens:	current neutralization in B
	demonstration

ICF system sensitivity study

systematic evaluation of a common ion for transport

interface region - accelerator/final transport

diagnostics - I_{net}, electrical conductivity, etc.

- Several recommendations for future work were made, including:

experiments:	self-pinched transport on SABRE
	ILSE neutralization experiment
	LIF machine neutralization experiment
	pre-formed channels
	stripping, etc. for A > 1
code development:	IPROP: self-pinch for LIF, HIF, common ion
	WARP 3D: multi-gap with neutralization?
	BICrz: ballistic with plasma (HIF, LIF)
	QUICKSILVER: beam overlap problem (HIF, LIF)
	BUCKSHOT: delta ray for HIF stripping
	Z-Discharge codes

equilibrium and stability theory: first look for trouble

atomic physics:	ion impact cross sections
	stripping cross sections
	diagnostic signatures
	relevant gas chemistry

Conclusions

• There is an excellent commonality in the physics of transport for LIF and HIF. Workers in both HIF and LIF have already worked together, and they share a vision of increased cooperation. A synergy between HIF and LIF exists and it should continue to be nurtured.

• Certain LIF and HIF transport schemes will be useful for all ions. In particular, self-pinched transport looks very attractive for LIF, HIF, and a common ion. It should be noted that no resonance was detected for any particular middle-weight ion or any particular middle-weight ion transport scheme.

• Experiments to demonstrate self-pinched transport should be performed on SABRE or GAMBLE II. The results should be of great importance for LIF, HIF, and a common ion driver.

• Charge-neutralized transport is important for HIF, common ion driver schemes, and possibly LIF. Research should continue in all of these areas, and neutralized transport experiments should be performed on ILSE and LIF machines.

• Code development (IPROP, WARP 3D, BICrz, QUICKSILVER, BUCKSHOT, etc.) and cross utilization of codes (LIF codes for HIF problems, and vice-versa) should be encouraged.

• Channel issues should be resolved so that an allowed range of channel radii for HIF and LIF can be justified.

• Accurate atomic physics cross sections (impact ionization, stripping, recombination, etc.) are needed for all ions.

• A common ion target might involve concepts somewhere between the traditional HIF two spot irradiator targets and LIF spherical targets. No consensus could be reached for a target spot-size parameter range because of the variety of possibilities. This issue should be of prime concern for the target working group.

• A common ion accelerator might presumably involve a new technology somewhere between present accelerator concepts for LIF and HIF. However, no consensus was reached as to what middle-weight ion parameters might be ($20 < A < 50$?), or if a multi-gap accelerator with charge neutralization is required. This issue should be of prime concern for the accelerator concepts working group.

Workshop on Transport for a Common Ion Driver

September 20-21, 1994
Sandia National Laboratories
Albuquerque, New Mexico
Area IV, Building 962, Room 1402

Chairmen: C. Olson (SNL), E. Lee (LBL), B. Langdon (LLNL)

Tuesday, September 20, 1994

8:30 a.m.	Welcome	C. Olson	5 min.
8:35	Purpose of Workshop	C. Olson, E. Lee, B. Langdon	15 min.
8:50	National Ion Program	J. Quintenz	10 min.
9:00	Tri-Lab Interest in Common Ion Driver for LMF/ETF	G. Logan	10 min.
9:10	Common Ion Driver needs for multi-gap acceleration, neutralization, and transport	C. Olson	20 min.

Multi-Gap Ion Acceleration (Experiments)

9:30	Pulselac	S. Humphries, T. Lockner	45 min.
10:15	BREAK		

Neutralization with Electrons (Theory)

10:30	Simulations in 1D, 2D	J. Poukey	30 min.
11:00	Plasma neutralization	B. Langdon, D. Callahan	45 min.
11:45	Neutralization simulations	S. Slutz	30 min.
12:15 p.m.	LUNCH		

Gas Neutralization

1:00 p.m.	NRL experiments	J. Neri	30 min.
1:30	IPROP simulations	D. Welch	30 min.
2:00	Transverse B effects	B. Oliver	30 min.
2:30	BREAK		

Self-Pinched Transport

2:45	HIF Concept	E. Lee, K. Hahn	45 min.
3:30	LIF Concept	C. Olson, D. Welch	45 min.
4:15	NRL Concept	R. Hubbard	30 min.
4:45	SABRE/Gamble II possible experiment	C. Olson	15 min.
5:00	Tour: SABRE/Hermes III	M. Cuneo, D. Hanson	60 min.
6:00	ADJOURN		
7:30	DINNER		

Wednesday, September 21, 1994

HIF and LIF Transport, and Relevance to Common Ion Driver

8:30 a.m.	HIF mainline transport (ballistic/near vacuum + quadrupole triplet focus)	E. Lee	30 min.
9:00	LIF mainline transport (ballistic/gas + solenoid focus)	C. Olson, P. Ottinger	30 min.
9:30	Channel transport and wire-guided transport	P. Ottinger	30 min.
10:00	Channel issues	C. Olson	15 min.
10:15	BREAK		

LIF and HIF Reactor Concepts, and Relevance to Common Ion Driver

10:30 a.m.	LIF Reactors	R. Peterson	30 min.
11:00	HIF Reactors	R. Moir	30 min.

Atomic Physics for Common Ion Driver

11:30	U. Wisc. atomic modeling capabilities	J. MacFarlane	30 min.
12:00 p.m.	LUNCH		

Code Capabilities and Needed Development

1:00	IPROP, IVORY	D. Welch	15 min.
1:15	WARP (Recirc)	A. Friedman	15 min.
1:30	BIC RZ	B. Langdon	15 min.
1:45	QUICKSILVER, TWOQUICK	D. Seidel	15 min.
2:00	BUCKSHOT (RLA)	J. Wagner	15 min.
2:15	BREAK		

Workshop Working Discussion

2:30	Common set of parameters (LIF, HIF, Common Ion for LMF, ETF, Power) Transport Issues Pro's, Con's of Common Ion Recommendations for: Experiments, Code development, Cross sections, Stability theory, ...	E. Lee, B. Langdon, C. Olson	90 min.
4:00	Concluding Comments	B. Langdon, C. Olson, E. Lee	25 min.
4:25	Workshp Close	C. Olson	5 min.
4:30	ADJOURN		

Workshop on Transport for a Common Ion Driver

September 20-21, 1994
Sandia National Laboratories
Albuquerque, New Mexico
Area IV, Building 962, Room 1402

Chairmen: C. Olson (SNL), E. Lee (LBL), B. Langdon (LLNL)

ATTENDEES denoted by *:

* James E. Bailey, MS-1196
Sandia National Laboratories
P. O. Box 5800
Albuquerque, NM 87185-1196
505/845-7203
505/845-7820 FAX

Roger O. Bangerter, MS-47-112
Lawrence Berkeley Laboratory
1 Cyclotron Road
Berkeley, CA 94720
510/486-6376
510/486-5392 FAX

* Doug D. Bloomquist, MS-1193
Sandia National Laboratories
P. O. Box 5800
Albuquerque, NM 87185-1193
505/845-7455
505/845-7864 FAX

* Debra A. Callahan-Miller, L-440
Lawrence Livermore National Laboratory
P. O. Box 808
Livermore, CA 94550
510/423-5926
510/423-2664 FAX

E. Michael Campbell, L-481
Lawrence Livermore National Laboratory
P. O. Box 808
Livermore, CA 94550
510/422-0400
510/423-6212 FAX

Gary M. Chenevert
U.S. Department of Energy
DP-11/GTN
Washington, DC 20585
301/903-3397
301/903-4096 FAX

David H. Crandall
U.S. Department of Energy
ER-54/GTN
Washington, DC 20585
301/903-4596
301/903-1225 FAX

* Michael E. Cuneo, MS-1193
Sandia National Laboratories
P. O. Box 5800
Albuquerque, NM 87185-1193
505/845-8767
505/845-7864 FAX

William F. Dove
U.S. Department of Energy
ER-543/GTN
Washington, DC 20585
301/903-4598
301/903-1225 FAX

William M. Fawley, MS-47-112
Lawrence Berkeley Laboratory
1 Cyclotron Road
Berkeley, CA 94720
510/486-6229
510/486-5392 FAX

* Alex Friedman, L-440
Lawrence Livermore National Laboratory
P. O. Box 808
Livermore, CA 94550
510/422-0827
510/423-2664 FAX

* Kyoung D. Hahn, MS-47-112
Lawrence Berkeley Laboratory
1 Cyclotron Road
Berkeley, CA 94720
510/486-5286
510/486-5392 FAX

David A. Hammer
Cornell University
Laboratory of Plasma Studies
369 Upson Hall
Ithica, NY 14853
607/255-3916
607/255-3004 FAX

* David L. Hanson, MS-1193
Sandia National Laboratories
P. O. Box 5800
Albuquerque, NM 87185-1193
505/845-7547
505/845-7864 FAX

* William B. Herrmannsfeldt, MS-26
Stanford Linear Accelerator Center
P. O. Box 4349
Stanford, CA 94309
415/926-3342
415/926-4999 FAX

Carl B. Hilland
U.S. Department of Energy
DP-11/GTN
Washington, DC 20585
301/903-3687
301/903-4096 FAX

Richard F. Hubbard, Code 6791
Naval Research Laboratory
4555 Overlook Ave. SW
Washington, DC 20375-5320
202/767-2927
202/767-0631 FAX

* Stanley Humphries, Jr.
Electrical Engineering Dept.
University of New Mexico
Albuquerque, NM 87131
505/275-6509
505/294-0222 FAX

Martin Lampe, Code 6792
Naval Research Laboratory
4555 Overlook Ave. SW
Washington, DC 20375-5320
202/767-3200
202/767-0631 FAX

* A. Bruce Langdon, L-472
Lawrence Livermore National Laboratory
P. O. Box 808
Livermore, CA 94550
510/422-5444
510/423-9969 FAX

Janice Lawson
U.S. Department of Energy
DP-11/GTN
Washington, DC 20585
301/903-4919
301/903-4096 FAX

* Edward Lee, MS-47-112
Lawrence Berkeley Laboratory
1 Cyclotron Road
Berkeley, CA 94720
510/486-7345
510/486-5392 FAX

* Raymond W. Lemke, MS-1186
Sandia National Laboratories
P. O. Box 5800
Albuquerque, NM 87185-1186
505/845-7423
505/845-7890 FAX

John D. Lindl, L-472
Lawrence Livermore National Laboratory
P. O. Box 808
Livermore, CA 94550
510/422-5430
510/423-6212 FAX

* Thomas R. Lockner, MS-1196
Sandia National Laboratories
P. O. Box 5800
Albuquerque, NM 87185-1196
505/845-7272
505/845-7820 FAX

* B. Grant Logan, L-481
Lawrence Livermore National Laboratory
P. O. Box 808
Livermore, CA 94550
510/422-9816
510/423-6212 FAX

* Joseph J. MacFarlane
Fusion Technology Institute
University of Wisconsin
1500 Johnson Drive
Madison, WI 53706-1687
608/263-4789
608/263-4499 FAX

* Michael G. Mazarakis, MS-1193
Sandia National Laboratories
P. O. Box 5800
Albuquerque, NM 87185-1193
505/845-7138
505/845-7864 FAX

* Eugene J. McGuire, MS-1187
Sandia National Laboratories
P. O. Box 5800
Albuquerque, NM 87185-1187
505/845-7524
505/845-7890 FAX

* Wayne R. Meier
W. J. Schafer Associates, Inc.
303 Lindbergh Ave.
Livermore, CA 94550-9511
510/447-0555
510/447-0544 FAX

* Ralph W. Moir, L-637
Lawrence Livermore National Laboratory
P. O. Box 808
Livermore, CA 94550
510/422-9808
510/424-6401 FAX

* Jesse M. Neri, Code 6771
Naval Research Laboratory
4555 Overlook Ave. SW
Washington, DC 20375-5000
202/404-7567
202/767-0436 FAX

Brian Oliver, Code 6771
Naval Research Laboratory
4555 Overlook Ave. SW
Washington, DC 20375-5000
202/404-7567
202/767-0436 FAX

* Craig L. Olson, MS-1186
Sandia National Laboratories
P. O. Box 5800
Albuquerque, NM 87185-1186
505/845-7303
505/845-7890 FAX

* Richard E. Olson, MS-1187
Sandia National Laboratories
P. O. Box 5800
Albuquerque, NM 87185-1187
505/845-7527
505/845-7890 FAX

* Paul F. Ottinger, Code 6771
Naval Research Laboratory
4550 Overlook Ave. SW
Washington, DC 20375-5000
202/404-7567
202/767-0436 FAX

* Robert R. Peterson
Fusion Technology Institute
University of Wisconsin
1500 Johnson Drive
Madison, WI 53706-1687
608/263-5646
608/263-4499 FAX

* James W. Poukey, MS-1186
Sandia National Laboratories
P. O. Box 5800
Albuquerque, NM 87185-1186
505/845-7302
505/845-7890 FAX

Tony Russo
U.S. Department of Energy
DP-11/GTN
Washington, DC 20585
301/903-6288
301/903-4096 FAX

*Jeffrey P. Quintenz, MS-1195
Sandia National Laboratories
P. O. Box 5800
Albuquerque, NM 87185-1195
505/845-7245
505/845-7864 FAX

* Thomas W. L. Sanford, MS-1193
Sandia National Laboratories
P. O. Box 5800
Albuquerque, NM 87185-1193
505/845-7816
505/845-7864 FAX

* David B. Seidel, MS-1186
Sandia National Laboratories
P. O. Box 5800
Albuquerque, NM 87185-1186
505/845-8355
505/845-7890 FAX

* Stephen A. Slutz, MS-1186
Sandia National Laboratories
P. O. Box 5800
Albuquerque, NM 87185-1186
505/845-7310
505/845-7890 FAX

Marshal M. Sluyter
U.S. Department of Energy
DP-11/GTN
Washington, DC 20585
301/903-5491
301/903-9743 FAX

Ravi N. Sudan
Cornell University
Laboratory of Plasma Studies
369 Upson Hall
Ithica, NY 14853
607/255-4127
607/255-3004 FAX

*William S. Varnum, DP-11 GTN
U.S. Department of Energy
Washington, DC 20585
301/903-4919
301/903-4096 FAX

* John S. Wagner, MS-1186
Sandia National Laboratories
P. O. Box 5800
Albuquerque, NM 87185-1186
505/845-7295
505/845-7890 FAX

* Dale R. Welch
Mission Research Corporation
1720 Randolph Road SE
Albuquerque, NM 87106
505/768-7723
505/768-7601 FAX

Mark A. Wilson
U.S. Department of Energy
ER-543/GTN
Washington, DC 20585
301/903-5048
301/903-4716 FAX

Simon S. Yu, MS-47-112
Lawrence Berkeley Laboratory
1 Cyclotron Road
Berkeley, CA 94720
510/486-6372
510/486-5392 FAX

Lawrence Livermore National Laboratory

February 11, 1994

Marshall Sluyter, Acting Director
Office of Research and Inertial Confinement Fusion
U.S. Department of Energy, DP-28
19901 Germantown Road
Germantown, MD 20874

David Crandall, Director
Division of Advanced
Physics and Technology
Office of Fusion Energy
Office of Energy Research
U.S. Department of Energy
Washington, DC 20585

Dear Marshall and Dave,

Recognizing the resource limitations that the DOE and U.S. Government will be facing for the foreseeable future, we believe that it is necessary to evaluate the possibility of structuring long range strategic research activities for the widest possible benefit to multiple DOE missions. Following suggestions made at the joint DP/ER workshop in Washington last summer, we have begun informal discussions to assess the technical feasibility of a combined LMF/ETF facility with multiple target chambers sharing a common ion driver. We believe that ion drivers currently have great potential for providing the durability, efficiency, and rep rate required for energy. Most system studies for energy indicate that the optimum target yield is a few hundred megajoules. This matches the desired LMF yield for defense programs applications.

The goal of these discussions is to identify a research program that would provide the more demanding driver requirements for energy production, at a reasonably small incremental cost compared to the cost for the LMF's single shot needs. If such a driver could be identified, DOE would then be able to satisfy the needs of two of its major missions, advanced energy technology for fusion and nuclear defense, with a single facility. With the significant declassification of ICF, it should even be possible for this facility to play a major role in an international program.

Recycled

An Equal Opportunity Employer • University of California • P.O. Box 808 Livermore, CA 94551-9900 • Telephone (510) 422-1100 • Twx 910-386-8339 UCLLL LVMR

So far, we have identified chamber transport as a critical issue for both the defense program and energy application of ions, and we have established a technical working group to assess ways in which we could coordinate our research activities. We anticipate that other working groups addressing the issues of ion driven targets and novel acceleration concepts would also be of benefit to the national ion program. When we have a more definite proposal for coordinated activities, we will contact your offices to schedule formal discussions.

Sincerely,

John Lindl Acting ICF Program Leader, LLNL	Jeff Quintenz Light Ion Program Manager SNL	Roger Bangerter Program Head, Fusion Energy Research Program, LBL

cc:
E. M. Campbell, LLNL
D. L. Cook, SNL, ALBQ
G. Logan, LLNL
A. Friedman, LLNL

APPENDIX:

Presentations

Workshop on Transport for a Common Ion Driver

September 20-21, 1994
Sandia National Laboratories
Albuquerque, New Mexico
Area IV, Building 962, Room 1402

Chairmen: C. Olson (SNL), E. Lee (LBL), B. Langdon (LLNL)

Purpose of Workshop

The purpose of this workshop is to assess the physics of ion beam transport for a common ion driver for inertial confinement fusion. Transport for heavy ion fusion (HIF) and light ion fusion (LIF) will be discussed, but the emphasis will be on exploring the possible advantages of a middle-weight ion. If a middle-weight ion appears favorable, then a common ion driver could be conceived that would support both high yield (LMF) and energy (ETF), and offer a unified ion beam approach toward the future of energy production.

Periodic Table of the Elements

L/F

1 **H** 1.008																	2 **He** 4.003
3 **Li** 6.941	4 **Be** 9.012											5 **B** 10.81	6 **C** 12.01	7 **N** 14.01	8 **O** 16.00	9 **F** 19.00	10 **Ne** 20.18
11 **Na** 22.99	12 **Mg** 24.31											13 **Al** 26.98	14 **Si** 28.09	15 **P** 30.97	16 **S** 32.07	17 **Cl** 35.45	18 **Ar** 39.95
19 **K** 39.10	20 **Ca** 40.08	21 **Sc** 44.96	22 **Ti** 47.88	23 **V** 50.94	24 **Cr** 52.00	25 **Mn** 54.94	26 **Fe** 55.85	27 **Co** 58.93	28 **Ni** 58.69	29 **Cu** 63.55	30 **Zn** 65.39	31 **Ga** 69.72	32 **Ge** 72.61	33 **As** 74.92	34 **Se** 78.96	35 **Br** 79.90	36 **Kr** 83.80
37 **Rb** 85.47	38 **Sr** 87.62	39 **Y** 88.91	40 **Zr** 91.22	41 **Nb** 92.91	42 **Mo** 95.94	43 **Tc** (98)	44 **Ru** 101.07	45 **Rh** 102.91	46 **Pd** 106.42	47 **Ag** 107.87	48 **Cd** 112.41	49 **In** 114.82	50 **Sn** 118.71	51 **Sb** 121.75	52 **Te** 127.60	53 **I** 126.90	54 **Xe** 131.29
55 **Cs** 132.91	56 **Ba** 137.33	57–71 Lanthanide series*	72 **Hf** 178.49	73 **Ta** 180.95	74 **W** 183.85	75 **Re** 186.21	76 **Os** 190.2	77 **Ir** 192.22	78 **Pt** 195.08	79 **Au** 196.97	80 **Hg** 200.59	81 **Tl** 204.38	82 **Pb** 207.2	83 **Bi** 208.98	84 **Po** (209)	85 **At** (210)	86 **Rn** (222)
87 **Fr** (223)	88 **Ra** (226)	89–103 Actinide series†	104 **Unq** (261)	105 **Unp** (262)	106 **Unh** (263)	107 **Uns** (262)	108 **Uno** (265)	109 **Une** (266)									

H/F

*Lanthanide Series	57 **La** 138.91	58 **Ce** 140.12	59 **Pr** 140.91	60 **Nd** 144.24	61 **Pm** (145)	62 **Sm** 150.36	63 **Eu** 151.97	64 **Gd** 157.25	65 **Tb** 158.93	66 **Dy** 162.50	67 **Ho** 164.93	68 **Er** 167.26	69 **Tm** 168.93	70 **Yb** 173.04	71 **Lu** 174.97
†Actinide Series	89 **Ac** (227)	90 **Th** 232.04	91 **Pa** (231.04)	92 **U** 238.03	93 **Np** (237)	94 **Pu** (244)	95 **Am** (243)	96 **Cm** (247)	97 **Bk** (247)	98 **Cf** (251)	99 **Es** (252)	100 **Fm** (257)	101 **Md** (258)	102 **No** (259)	103 **Lr** (260)

***Atomic mass is average over abundances of stable isotopes. For radioactive elements, mass is in parentheses and is that of the most stable important (in availability, etc.) isotope.**

A wide parameter space is available for development of a Common Ion Driver

Table I. Energy and Current for Ion Beams with Optimum Ion Range at Fixed Power of 250 TW*

Ion	Lithium	Carbon	Sodium	Aluminum	Sulfur	Potassium	Titanium	Iron	Copper	Krypton	Bismuth
Mass	7	12	23	27	32	39	48	56	59	84	209
At. No.	3	6	11	13	16	19	22	26	29	36	83
E (MeV)	32	83	211	270	362	475	609	778	891	1320	4800
P (TW)	250	250	250	250	250	250	250	250	250	250	250
I (kA)	7,813	3,012	1,185	926	691	526	411	321	281	189	52

LIF — **middle-weight ion** — **HIF**

*D. L. Cook, J. Fusion Energy 11, 69 (1992).

A common ion driver would offer a unified ion approach toward energy

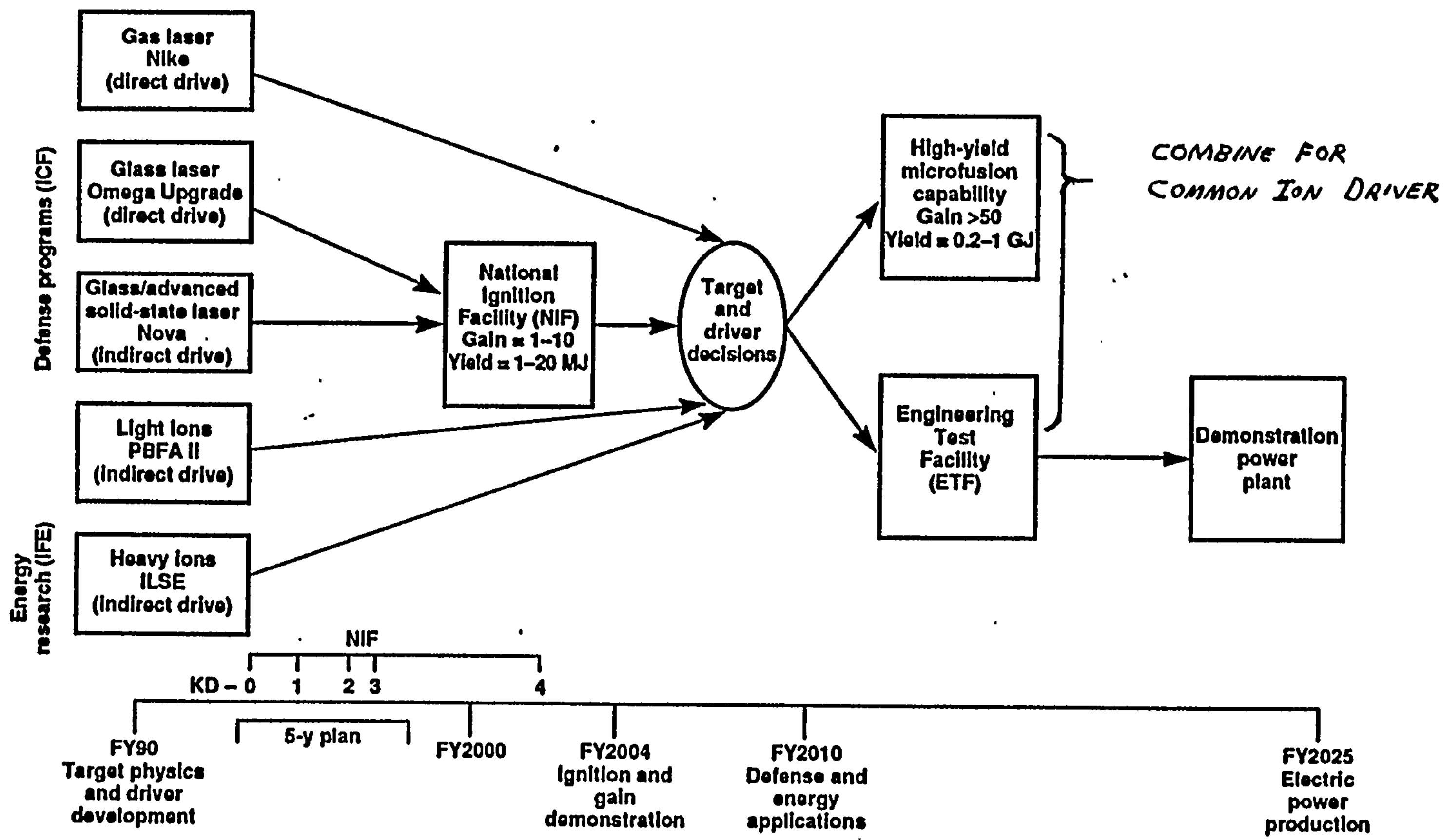

The existing DOE ICF strategy [from the 5-year ICF Program Plan (revised)].

There is Growing Interest in a Common Ion Driver for Defense and Energy Missions

LMF + ETF
LIF • • • HIF

February 8, 1994 Tri-Lab Meeting:

- LLNL (Grant Logan, Mike Campbell, John Lindl, Alex Fieldman)
- LBL (Roger Bangerter, Ed Lee, Andy Faltens)
- SNL (Don Cook, Jeff Quintenz, Craig Olson)

February 11, 1994 Tri-Lab Letter to: Marshal Sluyter (DP) and David Crandall (ER)

Tri-Lab-White Paper in progess

Transport Working Group established:

- SNL (Craig Olson)
- LBL (Ed Lee)
- LLNL (Bruce Langdon)

Other working groups proposed (Targets, Accelerator Concepts)

Common ion driver options for ETF/LMF involve transport

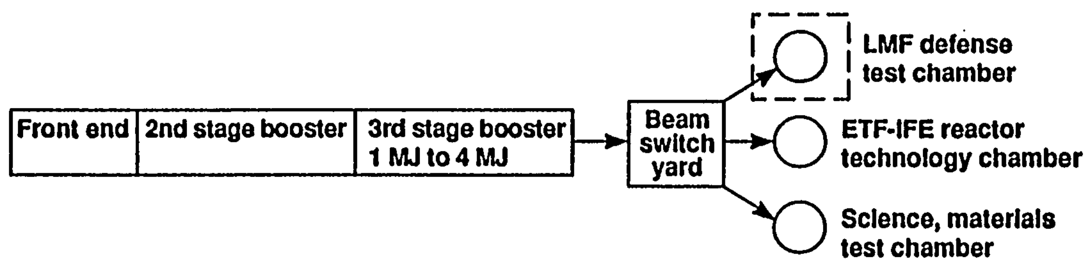

HIF-like

Common ion system?

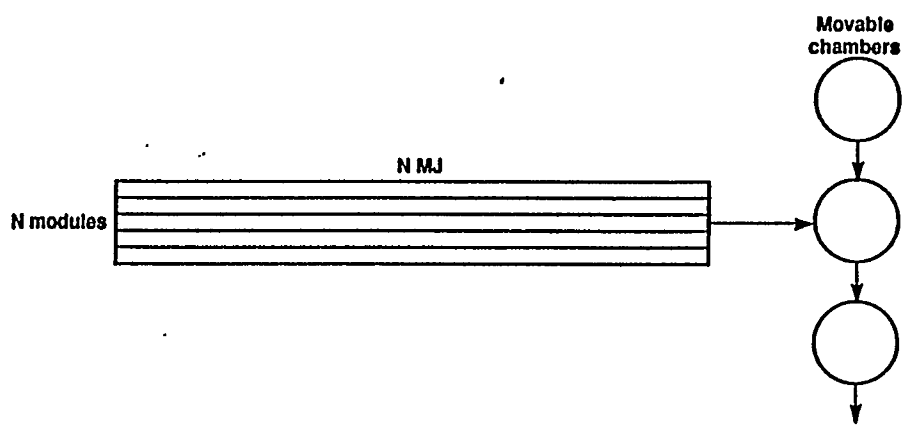

LIF-like

This workshop is on <u>transport</u> for a common ion driver

(proposed working group)	THIS WORKSHOP	(proposed working group)
Accelerator	**Transport**	**Target**
energy	neutralization with electrons	range
current	neutralization with gas	spot size r_t
A, Z, q	self-pinched transport	power
beam radius R	mainline HIF, LIF transport	uniformity
emittance E	mainline LIF, HIF power plants	•
uniformity	atomic physics	•
•	codes	•
•	•	•
•	•	•

Workshop Guidelines

Working workshop

Present existing work (HIF, LIF) with comments and conjectures toward common ion

Results: will help guide HIF, LIF research
will feed into White Paper
will be summarized in Tri-Lab paper at IAEA, Paris, November 14-18, 1994

"National Ion Program"

J. Quintenz

On February 8, 1994, representatives from LBL, LLNL, and SNL met to discuss issues of common interest to the light and heavy ion ICF programs. The discussion was prompted as a result of the new interest in looking at the possibility of a combined LMF/ETF using an ion driver. An ion driver is the leading candidate for such a combined facility because of the potential for lower cost, higher efficiency and repetitive pulse operation. It is the opinion of the participants that there would be great advantage to a common facility if it could be built at small incremental cost to either facility being built separately. At this meeting the term "National Ion Program" was coined to describe the collaborative research activities that could be performed that would benefit both the light and heavy ion ICF programs. Several areas were suggested as possibilities for this collaborative research, including: ion beam transport, ion driven targets and alternative acceleration concepts. At this meeting we also asked that the ion beam transport group be formed and begin to look at ways that the light and heavy ion programs could collaborate in investigating various transport scenarios. This workshop is the result of that initiative.

In summary, the purpose of the effort to look at the light ion and heavy ion ICF programs in a common setting is several fold:

- Identify those areas of research common to both concepts that would benefit from a coordinated research plan
- Describe computer codes that might be of use to both communities
- Begin to explore the possibility of defining an optimum ion driver or ion charge/mass for a combined LMF/ETF

My expectations for this workshop are that there be a very interactive flow of information and that proposals for collaboration in theory, calculations, and experiments be developed. I do not expect solutions or answers from this workshop but rather a better feel for the questions.

Finally, the Program Managers have agreed not to force an early down selection of drivers so emphasis at this workshop should be on science, not politics.

FUTURE PLANS FOR TRI-LAB COOPERATION

Grant Logan, Sandia National Laboratory Albuquerque, Sept. 21, 1994

- We need to plan another Tri-Lab meeting before the end of CY 95. This third meeting should be held at LBL, in the rotation order.
- We will need to review the results of this beam transport workshop at the LBL meeting. Can we have a draft of the beam transport white paper by then, assuming the LBL meeting was in December, after the Paris IAEA meeting in November? (Answer was, possibly, or a good start on one)
- To find an optimum middle weight candidate for a common ion driver, we will need to initiate other working groups on generic ion target scaling, and on generic induction accelerator scaling, and integrate the results. This will take some time before we know if an optimum middle-weight ion driver/target combination exists, probably 2 to 3 years.
- Even if we find no preferred middle weight ion driver/target for an LMF/ETF facility, both light and heavy-ion programs will benefit from shared data and ideas in ion beam transport and targets, and high ave. power induction core technology.
- In particular, it appears that SABRE offers a very useful facility for joint beam transport physics relevant to both light and heavy ions. The beam transport group needs to identify in the white paper possible experiments on SABRE that can test the physics models of the various particle simulation codes.
- Personally, I'd sure like to understand from this workshop why self-pinched beam transport should be a natural, robust mode of intense beam transport.

3

Common Ion Driver needs for:

multi-gap acceleration

neutralization

transport

What is a middle-weight ion for the Common Ion Driver?

LIF	Middle-Weight Ion (example)	HIF
30 MeV Li	300 MeV - 500 MeV	5 GeV Pb
20 MA (for 600TW)	2 MA - 1.2 MA	120 kA(for 600TW)
5 MeV/nucleon	5 MeV/nucleon < ε/A < 25 MeV/nucleon	25 MeV/nucleon
$\beta = 0.1$	$0.1 \leq \beta \lesssim 0.25$	$\beta \leq 0.25$
$A = 7$	$A = 20 - 60$	$A = 209$
$Z = 3$	$Z = 10 - 30$	$Z = 82$
$q = 1$	$q = ?$	$q = 1 - 3$

REQUIRES

multi-gaps
neutralization between gaps
neutralized transport

Multi-gap acceleration is needed for a common ion driver

LIF	Common Ion	HIF
1-2 stage diode	multi-gap, high current Pulselac experiments new technology needed?	multi-gap induction linac

2-Stage Diodes Offer Divergence Reduction and Independent Control of Voltage and Current

<u>ALIAS 2-Stage</u>	demonstrated divergence reduction first stage: $\theta \sim 19$ mrad (< 0.6 MeV) second stage: $\theta \sim 10$ mrad (> 1 MeV)
<u>PBFA II 2-Stage</u>	barrel 2-stage diode demonstrated generation and post acceleration of p and Li beams
<u>Multistage diode</u>	theory developed, including ion emission in final stage

Neutralization is needed for a Common Ion Driver:

Neutralization is needed between accelerating gaps (stripping NOT allowed):

Maschke current limit I_M for space charge dominated beam with vacuum transport

$$I_m = \pi\varepsilon_0 \left(\frac{mv^3}{2qe}\right)\left(\frac{a}{L}\right)^2 \sigma_0^2 \qquad \sigma_0 \sim \frac{B_p \eta L^2}{mva_p}$$

Neutralization is needed for final focus (stripping is allowed)

Radial space charge spreading current I_{RS} for unneutralized beam in vacuum

$$I_p^{RS} = (1/4)\beta_i^3\gamma_i\left(A/Z^2\right)\left(M_p c^3/e\right) \times \left(R^2/L^2\right)\left[\ln\left(R/r_p\right)\right]^{-1}$$

Neutralized transport is needed for a Common Ion Driver:

<u>Neutralization with electrons is needed between gaps</u>

<u>Neutralized final transport is needed</u>

- self-pinched transport is attractive
- other LIF/HIF modes may also work

All tranport modes for LIF and HIF may be grouped into eight categories

Ballistic transport

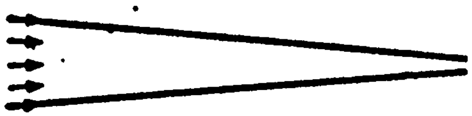

Ballistic transport with bare beam.

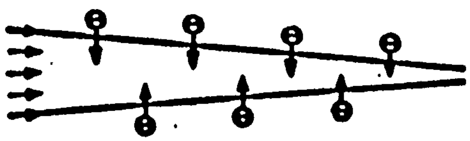

Ballistic transport with transversely-available electrons.

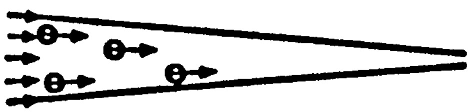

Ballistic transport with axially-available electrons.

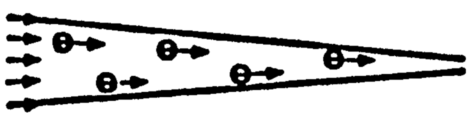

Ballistic transport with co-moving electrons.

Ballistic transport in gas or plasma.

Channel-like transport

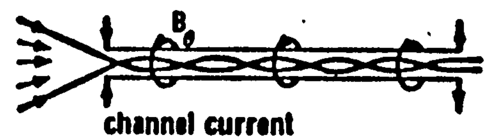

Beam in pre-formed channel

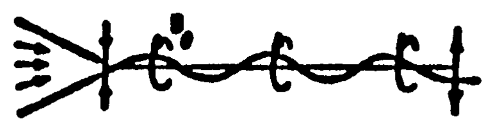

Wire-guided.

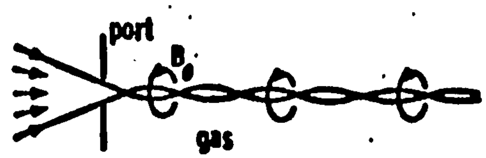

Self-pinched transport in gas.

LIF Transport

Gas-neutralized ballistic transport and self-pinched transport are highest priority for LIF

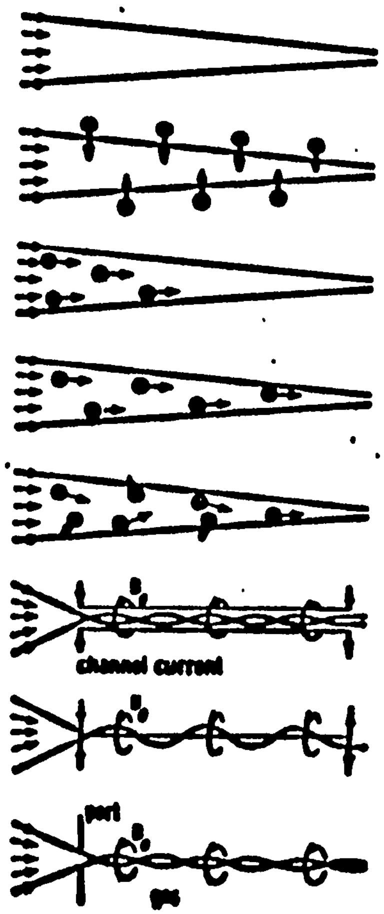

	LIF	PBFA II	LMF	LIBRA
1. Ballistic transport with bare beam.				
2. Ballistic transport with transversely-available electrons.	●	●		
3. Ballistic transport with axially-available electrons.	●			
4. Ballistic transport with co-moving electrons.	●			
→ 5. Ballistic transport in gas or plasma.	●	●	●	●
6. Beam in pre-formed channel	●		●	●
7. Wire-guided.	●		●	
→ 8. Self-pinched transport in gas.	●		●	●

Charge-neutralized ballistic transport and self-pinched transport are highest priority for HIF

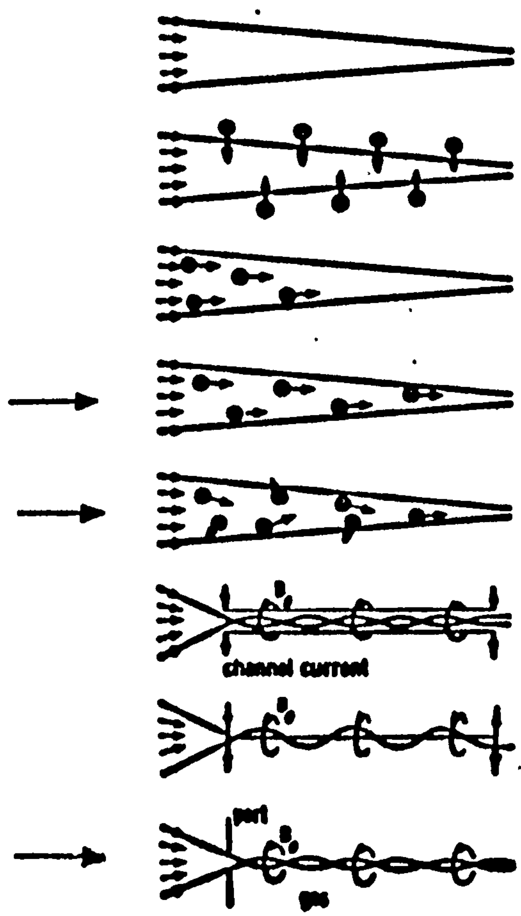

	Transport method	HIF	LMF	Reactor Studies
1.	Ballistic transport with bare beam.	●		●
2.	Ballistic transport with transversely-available electrons.	●		
3.	Ballistic transport with axially-available electrons.	●		
4.	Ballistic transport with co-moving electrons.	●	●	●
5.	Ballistic transport in gas or plasma.	●		●
6.	Beam in pre-formed channel	●		●
7.	Wire-guided.	●		
8.	Self-pinched transport in gas.	●		●

Transport Status

LIF	LMF	Reactor	Comments
acromatic lens	•	•	mainline approach
low-mass, wall-confined channel	•		demonstrated & "guaranteed to work"
wire-guided transport	•		demonstrated & "guaranteed to work"
self-pinched transport	•	•	continuing study (IPROP)
free-standing channel		•	high voltage breakdown issue

HIF	LMF	Reactor	COMMENTS
bare beam ($p \lesssim 10^{-3}$ Torr)		•	"guaranteed to work"
charge neutralization ($p > 10^{-3}$ Torr, plasma, etc.)	•	•	mainline approach
self-pinched transport		•	continuing study
free-standing channel		•	high voltage breakdown issue small radius channel issue

Workshop Sections

Multi-gap ion acceleration (experiments)
Neutralization with electrons (theory)
Gas neutralization
Self-pinched transport
HIF and LIF transport, and relevance to Common Ion Driver
LIF and HIF reactor concepts, and relevance to Common Ion Driver
Atomic physics for Common Ion Driver
Code capabilities and needed development
Workshop working discussion

Pulselac

Multi-stage acceleration of intense ion beams with space-charge neutralized transport

Tom Lockner

Department 1277

Sandia National Laboratory
Albuquerque, New Mexico

Presented to:

Workshop on Transport for a Common Ion Driver

Albuquerque, New Mexico
September 20, 1994

5

The Pulselac concept uses space-charge neutralization for higher current at a given radius

Magnetically insulated gaps
- virtual electrodes
- diamagnetic effects
- electrostatic focusing

Space-charge neutralization fraction

Emittance growth

Longitudinal stability

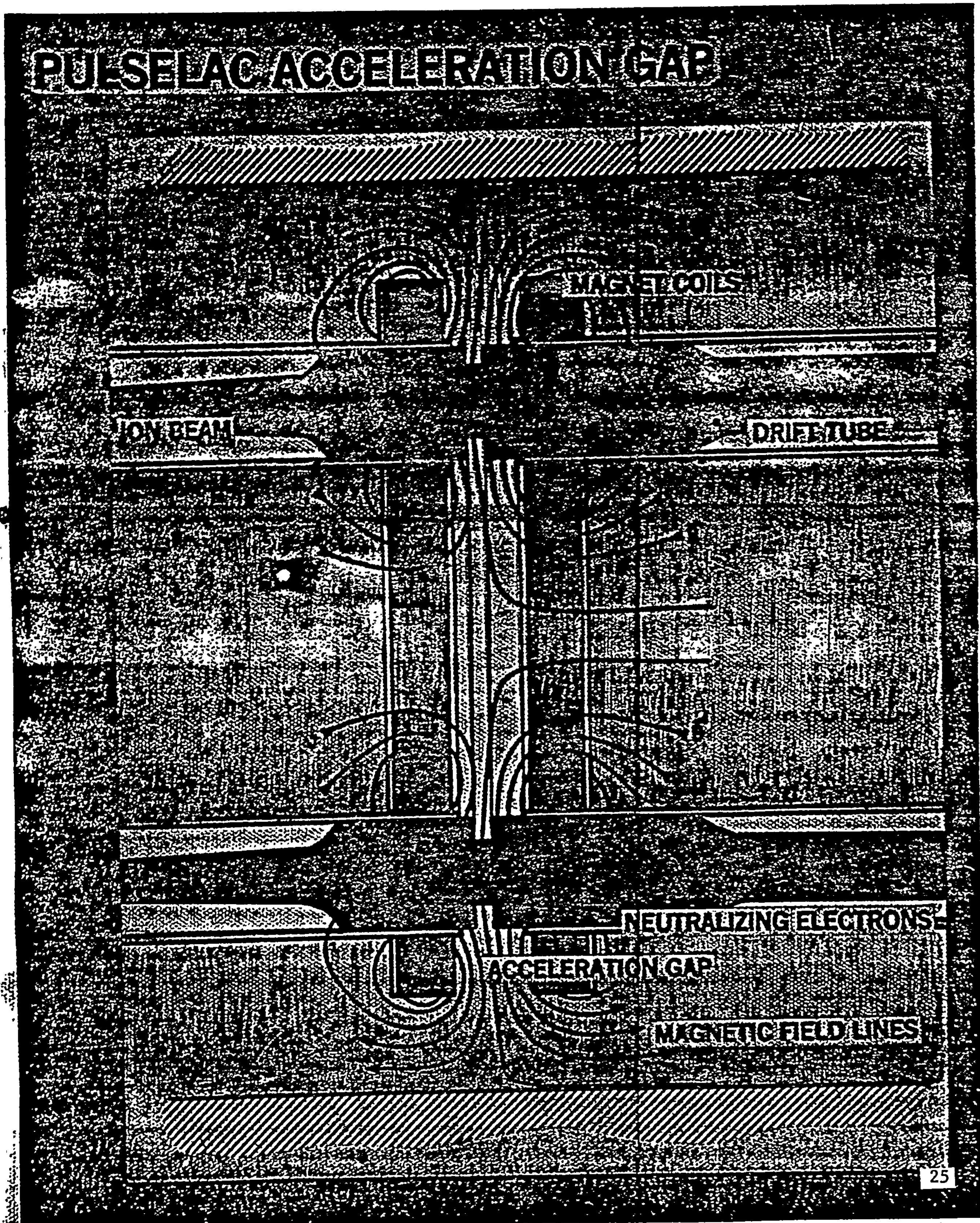
PULSELAC ACCELERATION GAP
MAGNET COILS
ION BEAM
DRIFT TUBE
NEUTRALIZING ELECTRONS
ACCELERATION GAP
MAGNETIC FIELD LINES
25

Pulselac B demonstrated neutralization for long pulse carbon beam

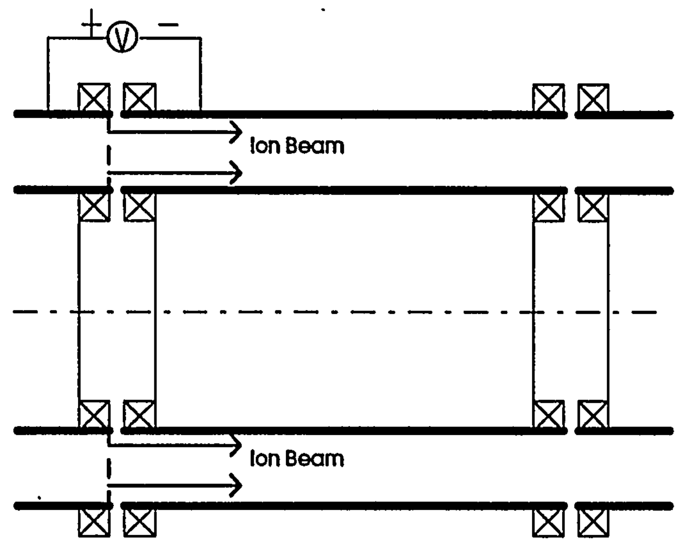

No
Active
Neutralization

120 keV C+

20 A/cm^2

30 cm propagation with 70% transport

0.5 - 1.0 μs pulse

Long pulse similar to Anaconda at LLNL

Post Acceleration (electrostatic)

The Pulselac C accelerator demonstrated high current ion beam inductive post acceleration

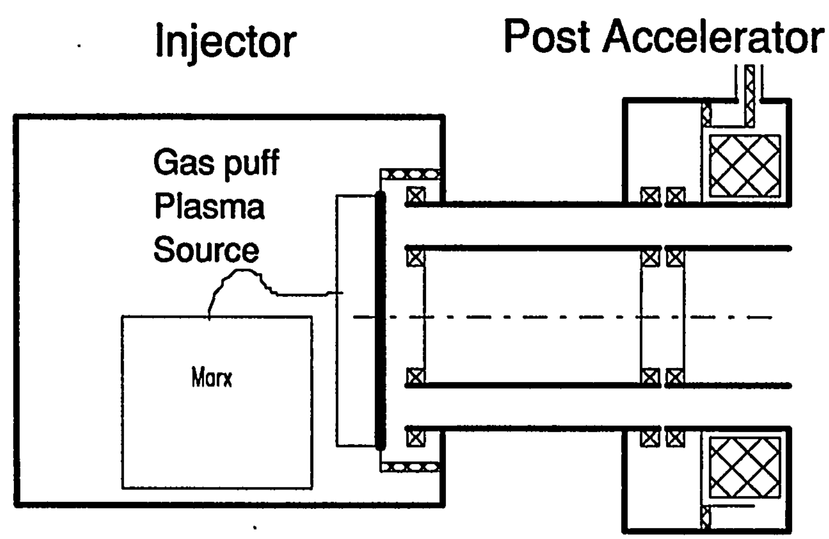

50 A/cm^2 source of N+, Ar+, etc.

10 kA of 100 kV N+ in 500 ns

Post Acceleration

- **4 kA of N+ accelerated to 350 keV**
- **high current efficiency in second gap**

PULSELAC C-U
with
PROPAGATION EXP

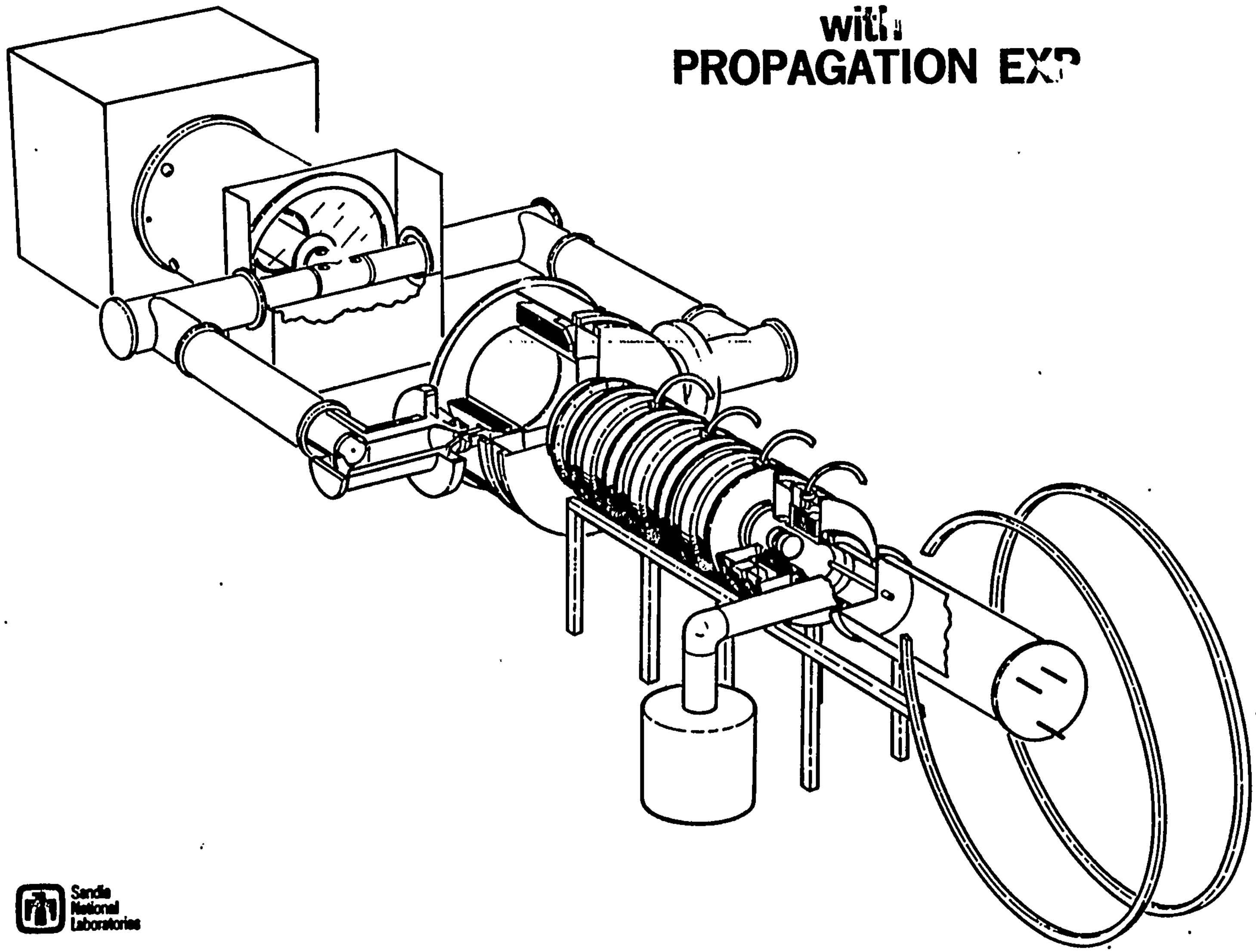

Sandia National Laboratories

Pulselac C-U demonstrated limit of wall neutralization for short pulse beams

Proton/carbon flashover source

50 ns pulse width

20 kA   100-200 A/cm^2, 300 keV injected ion beam

50 cm transport to gap 2

- 25% transport with or without plasma sources on wall
- 90% transport with gas puff

Effects observed

- Poor neutralization in applied field without neutral gas
- Electrostatic defocusing from gap in beam space-charge
- Electrostatic focusing of post-acceleration gap
- Inductive drop from Idot into second stage
- solenoidal focusing from applied field coils

Conclusion: 3 general areas of concern were identified with some experimental results

Space-charge neutralization

- Long pulse (~1 μs) neutralization from walls can be significant
- Short pulse (~50 ns) neutralization from walls is limited

Longitudinal stability

- Gap inductive effects critical for bunched beam (efficiency)

Emittance growth

- Beam azimuthal uniformity is critical in post-acceleration gap

We do not know if:

- Gap focusing will allow small enough emittance growth
- Inner coil rib can be made small enough for space-charge gap
- Limited wall neutralization can be balanced with lower current
- Inductive effects can be adequately controlled

PIC Simulations of Ion-Beam Charge Neutralization **6**

J. W. Poukey, et al., 9/20/94

<1964 I. 1-D theory (transverse neut.)

<1964 II. 1-D theory (longitudinal neut.)

1979 III. 1-D simulations (transverse, longitudinal, add applied B, beam risetime, SCL bc vs injected-e beam bc, beam pulse length, elec. temp.)

80 IV. 2-D simulations, no applied B

1979-1984 V. Pulselac gap simulations in 2-D

1991 VI. Charge fluctuations and microdivergence

1993 VII. Ion Beam Focusing – Space Charge Limit

1-D Theory of Transverse Neutralization

E. Stuhlinger <u>Ion Propulsion for Space Flight</u> 1964

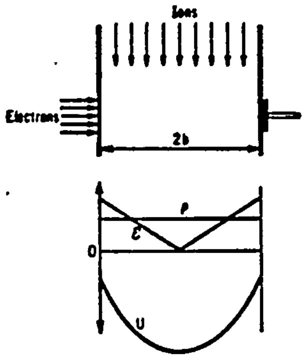

FIG. 5-36. Ion beam with lateral electron injection. Charge density, field strength, and potential before injection.

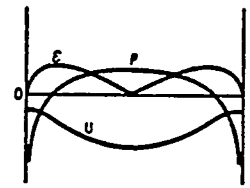

FIG. 5-37. Charge density, field strength, and potential with electron injection. $v_{e0} = 0$, incomplete neutralization. ($\rho \neq 0$.)

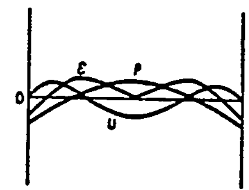

FIG. 5-38. Charge density, field strength, and potential with electron injection. $v_{e0} \neq 0$, complete neutralization. ($\rho = 0$.)

No electrons: $\Phi_{max}^{no\,e} = \dfrac{\rho_i b^2}{2\epsilon_0}$

Potential reduction with SCL electrons

$$\frac{\Phi_{max}^{w/e}}{\Phi_{max}^{no\,e}} = \frac{4}{(2m+1)^2\pi^2} \qquad (m = \#\text{ pot. max across beam} - 1)$$

For $m=0$ get "60% neut" and beam expands to wall in distance of order b.

Note: always <u>under</u>neutral in middle of beam, <u>over</u>neutral at edges.

1-D Theory and Simulation of Longitudinal Neutralization

(See Stuhlinger and Humphries, 1981)

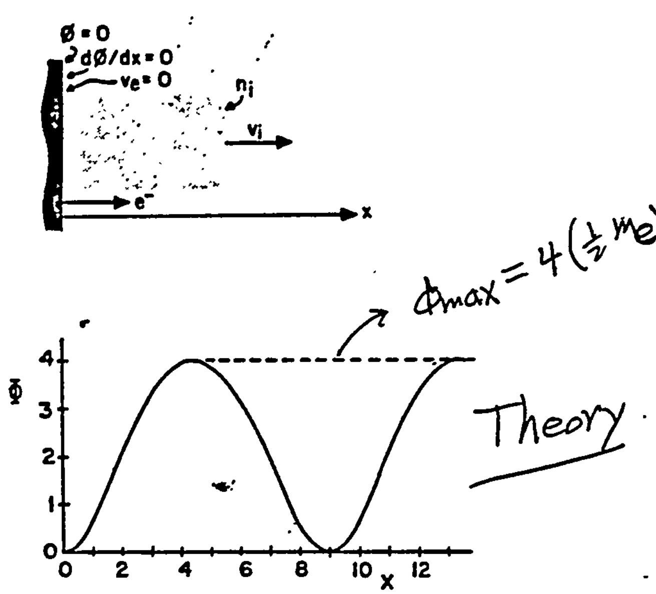

FIG. 1. Longitudinal autoneutralization. Top, geometry and entrance boundary conditions for propagation of an ion beam through a cold electron source into free space; bottom, analytic solutions—solid line is the solution to Eq. (1) for a uniform ion density and dotted line is the solution with the motion of the ion front included (from Ref. 13).

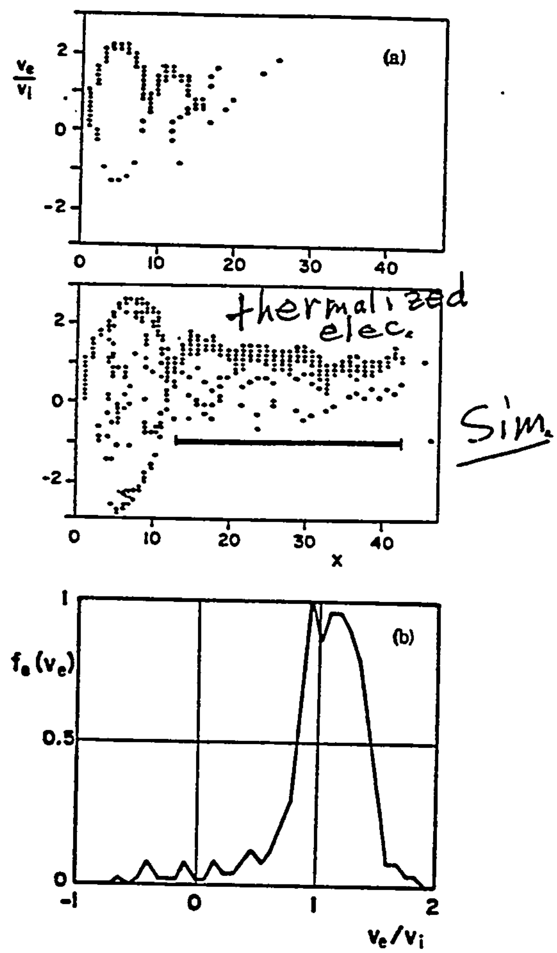

FIG. 2. Results of computer simulations. (a) Phase-space plots of the electron distribution at two times. (b) Relative velocity distribution of the downstream electrons taken over the region indicated by a bar in the second phase-space plot.

[Note: if add 2^{nd} wall at $x = L$, have possibility of Pierce instability

if $\frac{L}{V_0} > \frac{\pi}{\omega_p}$ $\left(\omega_p^2 \equiv \frac{n_i e^2}{m_e \epsilon_0}\right)$

Growth rate $\doteq \frac{V_0}{L} = \frac{1}{\text{transit time}}$]

Experimental verification: Kraft + Kusse, JAP, 1987

1-D Simulations of Transverse Neutralization with applied B (Poukey + Humphries, 1979)

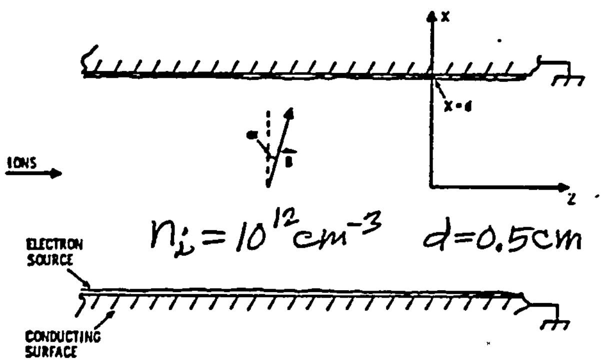

FIG. 1. Schematic of ion beam transverse neutralization problem.

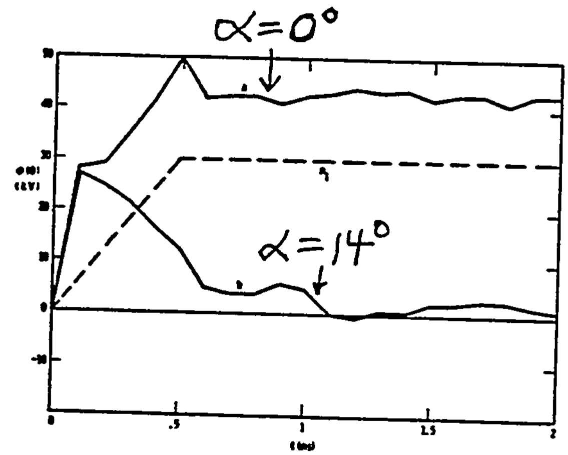

FIG. 2. Potential $\phi(x=0)$ at center of drift section versus time for cases (a) $B=0$ (or $\alpha=0$), (b) $B=2.06$ kG at $\alpha=14°$. Only average curves are shown; the actual curves would have small oscillations superimposed (amplitude of a few kV, period $2\pi/\omega_p \approx 0.1$ nsec). The ion density is indicated by the dashed line.

For $\alpha = 0°$ or no applied B, get poor neutralization, but if B lines are tilted, get good (not perfect) neutralization.

Why? A tilted B (or any elastic deflection) allows electrons to acquire energy parallel to walls, so ions in middle better neutralized, and electrons cannot return to walls, allowing emission of more electrons.

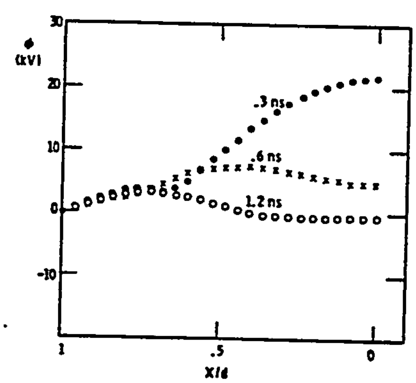

FIG. 3. Spatial dependence of potential ϕ for case of Fig. 2, curve (b). $\phi(x)$ is shown for three times t (nsec).

Neutralization is fast! And, larger α makes it even faster. (But, larger risetime slows neutraliz.)

2-D Simulations, no applied B

(Poukey, Quintenz, + Olson, 1980)

Case: 57 MeV H^+ beam, annular, cylindrical geometry. The Pierce limit is (non-rel.)

$$I_{lim} = 3\left[1 + (1.31R/L)^2\right] I_{ea}$$

where SCL for electrons alone is (mks)

$$I_{ea} = 66 \times 10^{-6} \left(\frac{mV_0^2}{2e}\right)^{3/2}$$

For constant ion density we find →

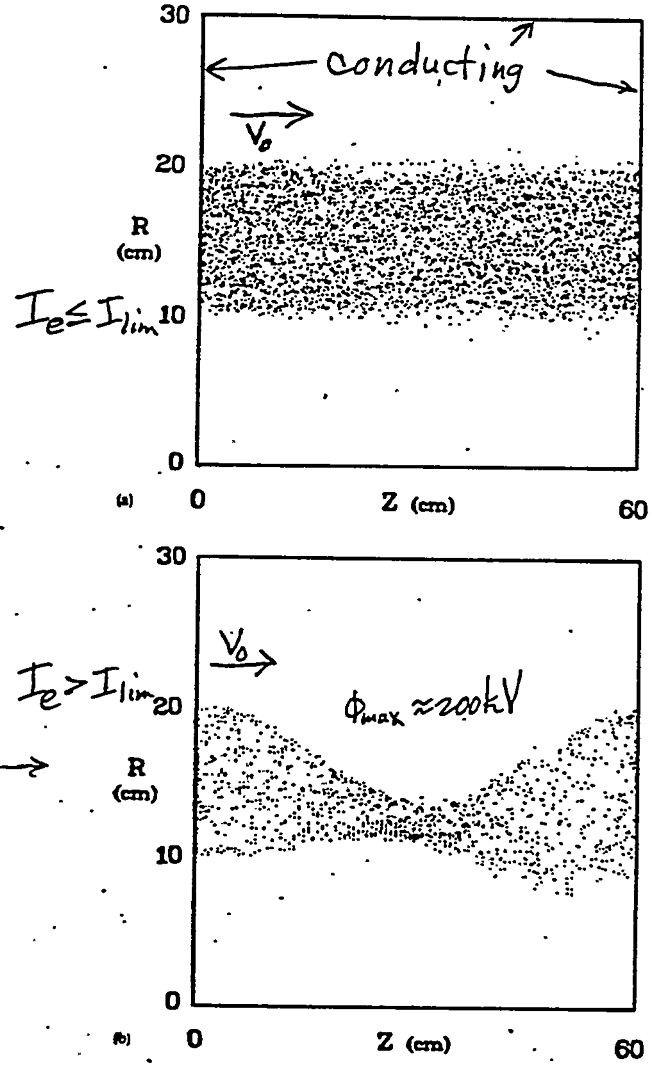

FIG. 2. Electrons in 2-*D* particle simulation of ion beam neutralization. Electrons move from left to right, and electron-absorbing conducting walls are located at $z = 0$ and 60 cm. (a) Injected current 250 A, less than the threshold current for instability ($I_e/I_t = 1$). (b) Injected current 5 kA, well above the threshold for instability ($I_e/I_t = 20$). These parameters correspond to the attempted neutralization of a 57-MeV proton beam with co-moving electrons ($r_0 = 10$ cm, $r_b = 20$ cm, $R = 30$ cm).

Max. potentials in unstable cases are of order $2m_eV_0^2/e$ as in 1-D theory

Cases shown used injected (co-moving) electrons, but similar result is obtained for SCL emission (slightly smaller ϕ values).

Estimated effect on ions:

$$\text{Div} \approx \left(\frac{m_e}{m_i}\right)^{1/2}$$

What is it? A standing Langmuir wave in "saturated" state, or an "electron pinch".

Pulselac Gap Simulations in 2-D (1979)
(Poukey + Humphries)

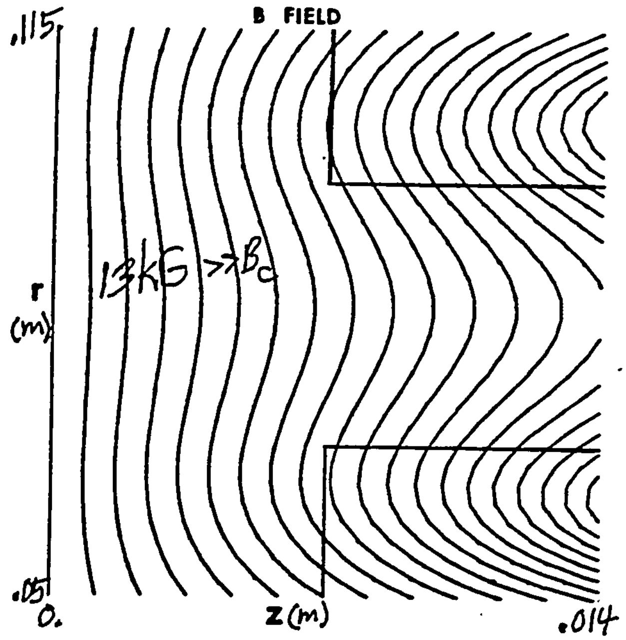

Figure 61. Geometry of Simulated Pulselac Gap and Applied $\vec{B}$. Total z-length of system is 1.4 cm; radial coordinate r runs from 5 to 11.5 cm.

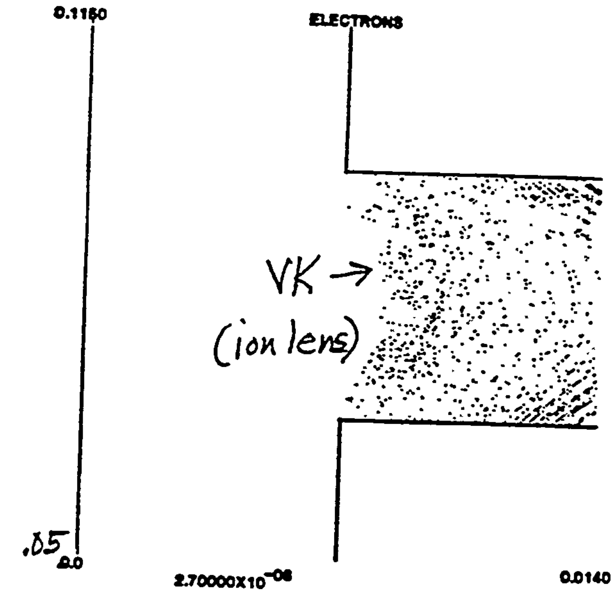

Figure 63. Electron Map Corresponding to Figure 62 at t = 27 ns.

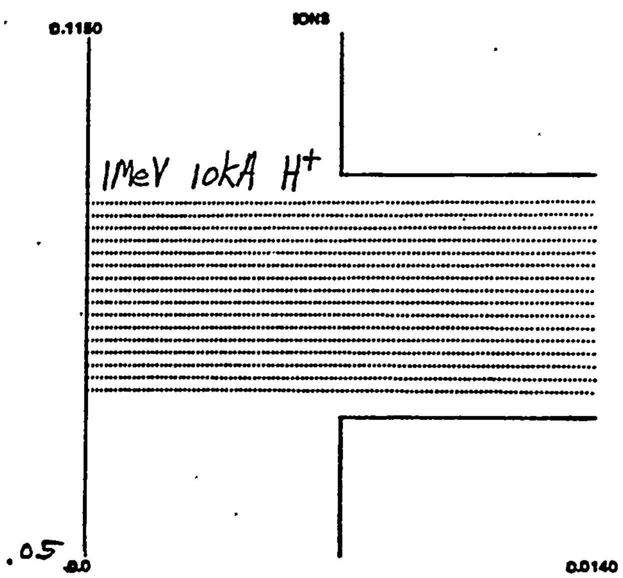

Figure 62. Ion Map for Strong-Applied $\vec{B}$ Case. The 10-kA, 1-MeV ion beam is accelerated from left to right through 200 kV.

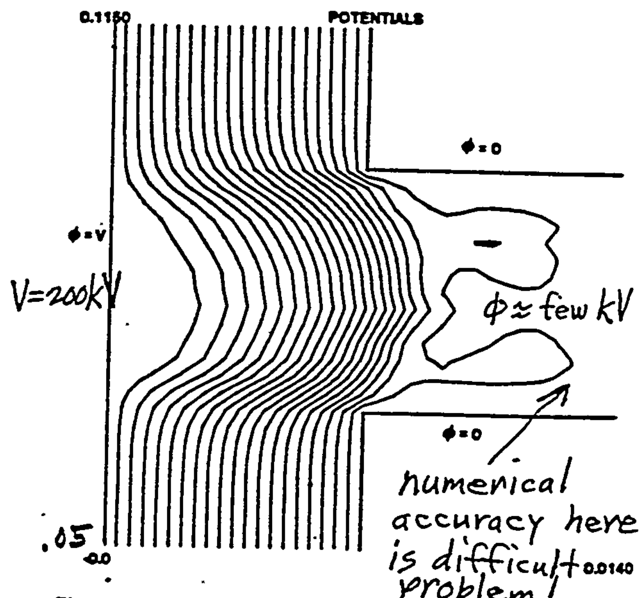

Figure 64. Equipotentials Corresponding to Figures 62 and 63.

Result: For this case, good neutralization in drift tube. (Actually, slightly underneutralized because gap between wall and ion beam edge contains electrons, and we use $\vec{E}=0$ boundary condition on emitting surfaces) Case with weaker B(applied) (still slightly $> B_c$) yielded poorer neutralization (+ larger div.)

Pulselac Gap Simulations (1984)
(Pulselac C parameters) (Lockner, Quintenz, + Poukey)

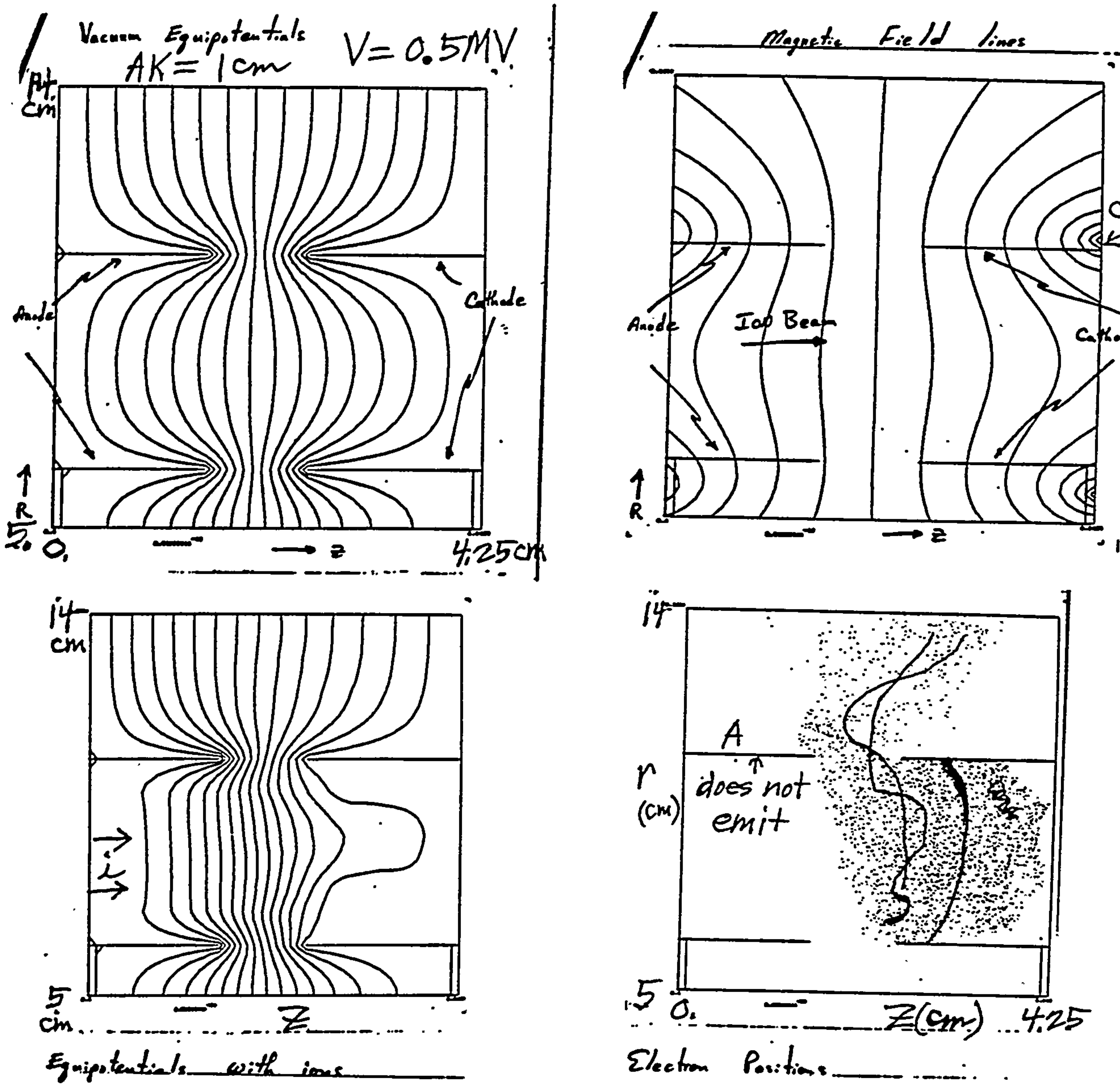

For this case, $n_i = 10^{11}\,cm^{-3}$, negligible emission from anode side of gap, get somewhat better neutralization with finite ion beam risetime, neutralization not great ($\Phi_{max}^{w/e} / \Phi_{max}^{no\,e} \approx .2$). Moving A-K gap with respect to B lines had only small effect. For good electrostatic focus, anode shaping?

Charge Fluctuations + Microdivergence (Olson + Poukey, 1991)

CHARGE FLUCTUATIONS TRAVELING WITH ION BEAM HAVE ϕ_{MIN} SET BY ELECTRON TRAPPING

In perturbation frame:

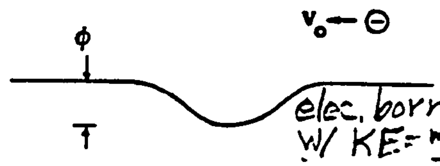

elec. born W/ KE = $\frac{m_e V_0^2}{2}$, if well deeper than this, elec trapped + well depth decreases until $e\phi_{min}$, at which elec. escape

$$e\phi_{MIN} \approx 1/2\, m_e V_0^2$$

Typically $\phi = a\phi_{MIN}$ $\quad 1 < a < 4$;

J. Poukey, SNL Report SAND80-2545 (1980).
J. Poukey, J. Quintenz, C. Olson, J. Appl. Phys. 52, 3016 (1981).
S. Humphries, Jr., Nucl. Fusion 20, 1549 (1980).
R. Sudan, Cornell U. Report LPS 280 (1980).
C. Olson, J. Fusion Energy 1, (1982).

MINIMUM VALUES OF FLUCTUATION POTENTIALS PREDICT A FUNDAMENTAL MICRODIVERGENCE LIMIT

for each species

$$e\phi_{MIN} = a\tfrac{1}{2} m_e \beta_i^2 c^2 \quad (a \geq 1)$$

If one species
ions see potential in ⊥ direction

$$\theta_\mu = \sqrt{a}\sqrt{\frac{m_e Z_t}{M_p A}}$$ Z_t is ion charge state during transport

If multi-species
consider one non-protonic species + protons
each species has its own ϕ_{MIN}
if non-protonic species feels ϕ_{MIN} of protons,

$$\theta_\mu = \sqrt{a}\sqrt{\frac{m_e}{M_p}\frac{Z_t}{Z_d}}$$ Z_d = charge state in diode

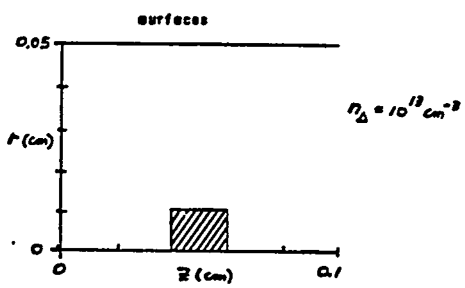

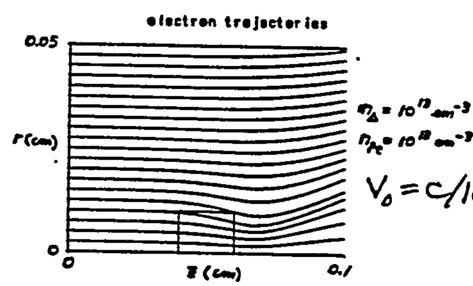

$V_0 = c/10$

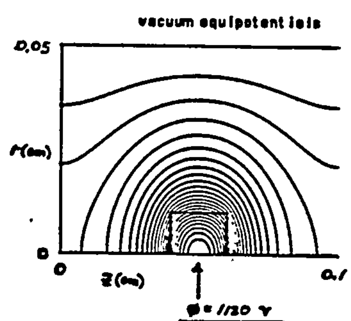

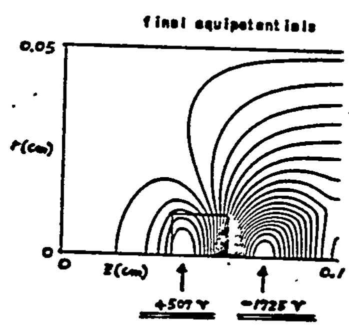

$$\frac{\frac{1}{2} m_e V_0^2}{e} = 2.5\,kV$$

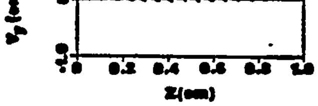

Fig. 4 MAGIC simulation showing growth of transverse ion momentum spread with distance. θ_μ grows to ~9 mrad in 1 cm.

Ion density fluctuations are produced by noise or source non-uniformities. They lead to divergence which scales like $\sqrt{\frac{m_e}{m_i}}$. Relevant to Pulselac?

Ion Beam Focusing – Space Charge Limit
(Poukey + Mendel, 1993)

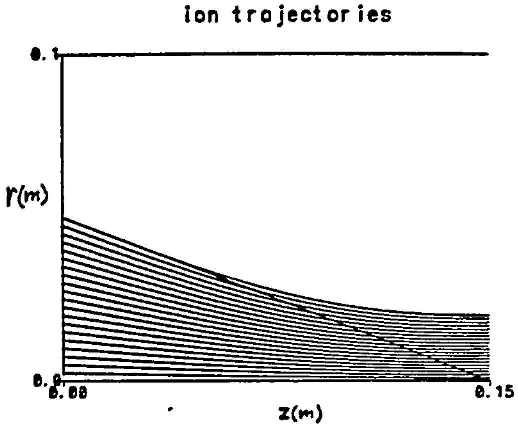

2a

Fig. 1. TRAJ equilibrium for 20 MeV, 79 kA Li+ beam injected into 15 cm-long metal can filled with background electrons such that $f = n_e/n_i = 0.95$ at all points. (a) Ion trajectories, which are initially aimed at a geometric focus (straight line). (b) equipotentials (max ϕ = 5 MV). See run 6, Table I.

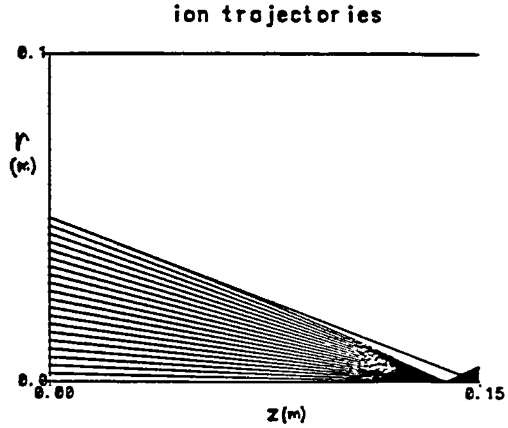

Fig. 2. As in Fig. 1 but $f = 1.0$, so the only force is self-magnetic, causing beam to focus slightly faster than geometrically. See run 8, Table I.

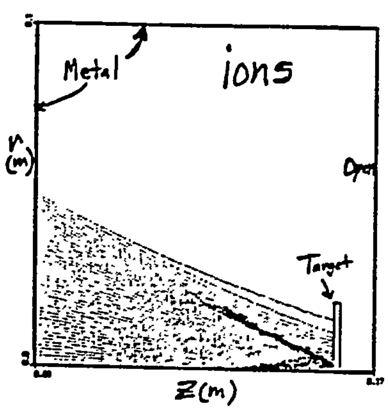

4a

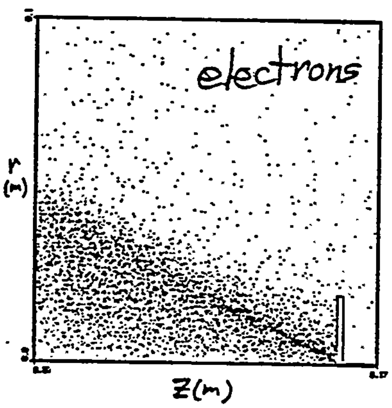

4b

Fig. 4. Same as Fig. 3 but "floating" target at L_z = 15 cm, z = 17 cm = the beam geometric focal point, a_0 = 0, SCL emission lhs only. (Ion beam: Li+, 80 kA, 20 MeV, edge radius 5 cm.) Result: Div = 42 mrad. See run 14, Table II. (a) ions, (b) electrons.

Two models of the final focus of a high-current Li^+ beam: top–fixed neutralization at all points inside beam; bottom–electrons emitted from left wall.

Result for latter case: $\theta_\mu = 42$ mrad ($\sqrt{\frac{m_e}{m_i}} = 9$ mrad $\quad \frac{1}{2} m_e V_0^2 = 1.55$ keV)

Hypothesis:

$\text{Div} > \sqrt{\frac{m_e\, q_i}{m_i\, e}}$ because ions will always ~~[illegible]~~ acquire transverse energy from fluctuating $\vec{E}$ of electrons

Propagation of partially-neutralized ion beams in the reactor

A. Bruce Langdon and Debra A. Callahan
Lawrence Livermore National Laboratory
University of California

for

Chamber Propagation Workshop

Autumnal Equinox, 1994

7

Motivation

We need *at least* one final-focus/chamber/target scenario documented that is not vulnerable to engineering or to physical or to political scrutiny.

If we can't do better, I *think* such a case can use singly-ionized 200 amu ions at 10 GeV, parameters that make it easiest for unneutralized 'vacuum' propagation.

Any flexibility that is uncovered in chamber propagation and target design is to be exploited in end-to-end modeling to optimize the HIF system.

Roger Bangerter said, in part:

In my opinion, it is critically important to understand what can and cannot be done. We need to understand the relationships among the following variables:

focal spot size
pulse length
power
beam energy
ion kinetic energy
ion mass
emittance
$\delta p/p$
pulse shape
density and composition of chamber gas
standoff distance
lens strength
vacuum
repetition rate
numbers of beams
beam geometry

Beam propagation may be possible in two density regions: low density or channel transport

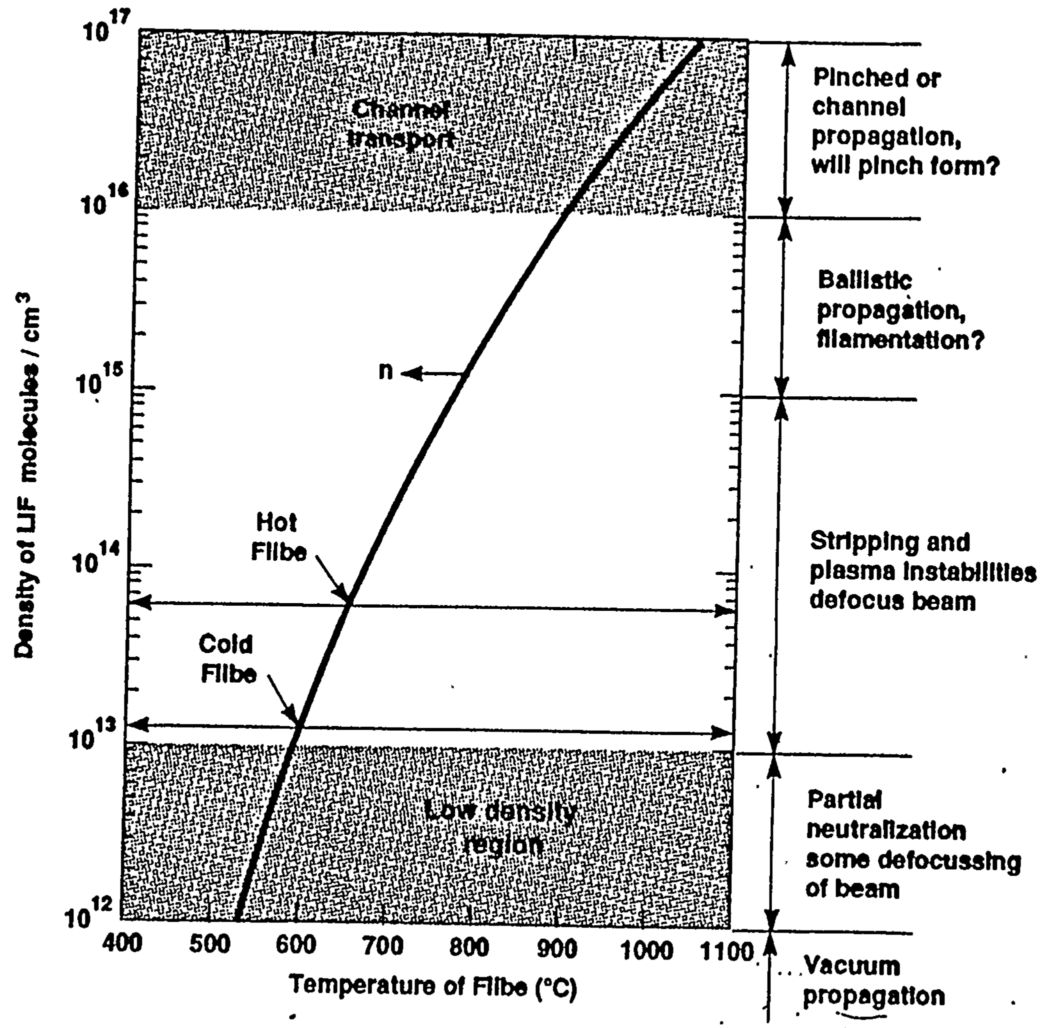

$(LiF)_2(BeF_2)$

Ralph Moir

TB-S36-U-12097-25

Direction of current work

We concentrate on the low-density, near-ballistic regime (chamber vapor density $\sim 10^{13}$ molecules/cc), and seek to extend the boundaries of that mode of operation.

We strive to establish that charge neutralization can reduce space charge sufficiently that intensity-dependent beamlet aiming/focusing, and stripping, are not an important complication at chamber conditions desired by reactor designers.

We are using the electromagnetic PIC code `BICrz`, developed for this purpose, which has a converging mesh capability to match the beam.

Any flexibility that is uncovered in chamber propagation and target design is to be exploited in end-to-end modeling to optimize the HIF system.

Outline

Propagation through near-vacuum has been considered a conservative option.

Problems with unneutralized vacuum transport.

Options for charge neutralization.

Axisymmetric PIC simulations of neutralization by preformed plasma

Subsequent additional neutralization.

Stripping, photoionization

Next steps

Complications of unneutralized vacuum transport

Perveance limitations (f-number, distance to target)

Keeping chamber pressure low enough to avoid collisional ionization and stripping is an undesirable constraint on reactor design.

Intensity-dependent focus
  Ho, Crandall and Haber (*Particle Accelerators*)

Aiming of beamlets in a cluster: intensity-dependence and finite-length effects
  Hofmann, Hasse, Reiser (Frascati)
Cluster acts somewhat like a short, fat nonuniform beam
Time dependent aiming?

Partial charge neutralization helps these problems but may increase emittance relative to idealized vacuum propagation.

Neutralization of an ion beam is more complicated than neutralization of an electron beam

For electron beam propagation, electrons produced by ionization of the gas are readily expelled, leaving an ion background to provide neutralization

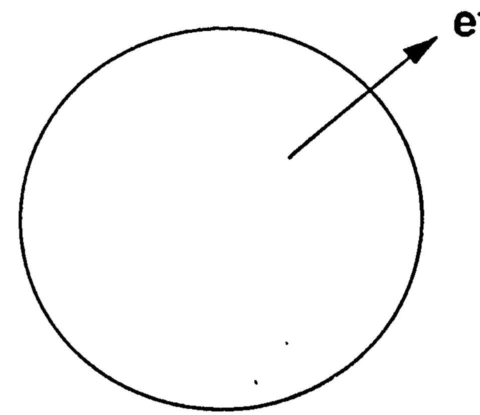

electron beam
cross section

For ion beam propagation, neutralization requires expulsion of plasma ions, or that electrons be somehow entrained axially or radially

Electrons produced by ionization within the beam do not reduce the net positive charge of the beam

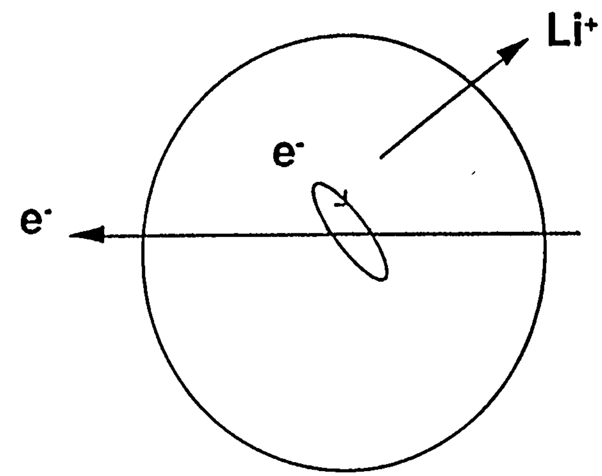

ion beam
cross section

axial entrainment

BICrz

Code features chosen for propagation model

- Electromagnetic fields, particle-in-cell ions
  - Need at least a time-dependent r, z model with self-consistent electrostatic, inductive electric, and magnetic fields (Darwin model also provides this).

- Orthogonal curvilinear quadrilateral mesh
  - concentrates expensive resolution where it is needed: near the target.

- Particle-in-cell electrons created by photoionization and collisions
  - Unless neutralization is quite complete, electrons will be energetic enough to warrant kinetic modeling.

Space and time scales

Some numbers...

At the target:

200 TW into a spot of 3 mm radius, of 10 GeV ions moving at 0.3c, means ion beam density $n_b = 5 \times 10^{13}\text{cm}^{-3}$.

Suppose $n_e = 3n_b$. Then $\omega_{pe} = 7 \times 10^{11}\text{sec}^{-1}$, skin depth $c/\omega_{pe} = 0.44$ mm, $v_{\text{beam}}/\omega_{pe} = 0.13$ mm.

This suggests $\Delta t \sim 0.3$ ps (30 ns = 100,000 time steps –maybe possible) cell size $\Delta x_{1,2} \sim 0.2$ mm near target (impractical over whole beam path).

Therefore, concentrate resolution near target.

Count on not modeling details of physics that are too close to the target to affect deposition.

Perhaps subcycle the time integration near the target.

Limitations on time step, due to electromagnetic Courant and to electron plasma frequency, are similar.

Compare $c\Delta t/\Delta r$ and $\omega_{pe}\Delta t$:

Suppose the ion beam has density uniform in a cross section of radius r_b, carries electrical current I_b at speed $v_b = \beta_b c$, and is charge neutralized.

Then

$$\frac{(\omega_{pe}\Delta t)^2}{(c\Delta t/\Delta r)^2} = \frac{4}{\beta_b}\frac{I_b}{17\text{ kA}}\left(\frac{\Delta r}{r_b}\right)^2$$

For example, with $(\omega_{pe}\Delta t)^2 = 0.1$, $(c\Delta t/\Delta r)^2 = 0.5$, $\beta_b = 0.3$, and $I_b = 12.5$ kA, we find that the electromagnetic Courant condition is more restrictive if $\Delta r < r_b/7$.

Either full electromagnetic or Darwin fields can be considered.

Beamlet parameters:

beamlets

- total charge 2.5×10^{-5} coulombs each
- total energy 2.5×10^{5} joules each, $\beta_b = 0.3$
- parabolic $I(t)$, duration $\tau_b = 8$ ns
- maximum current 4688 A (perveance $\sim 4 \times 10^{-5}$)
- ellipsoidal shape, uniform density $\Rightarrow$ linear self fields
- initial radius 10 cm

plasma cylinder and annulus

- $\omega_{\rm pe} \sim 10$ ns^{-1}
- outer radius 30 cm, length 60 cm
- inner radius 0 or 12 cm

Beam neutralization by electron pickup from preformed plasma

Purpose is to reduce net charge promptly and thoroughly, before beam emittance is degraded, without waiting for other neutralization mechanisms.

Plasma cylinder

models preionization of chamber vapor in beam path near beamlet ports (perhaps by microwave discharge?)

Plasma annulus

models preionization of chamber vapor outside beam path near ports (perhaps by electrical discharge?)

Space-charge-limited radial current from plasma annulus

Need to draw an electron current $= \lambda_b v_b = 2\pi r L J$ from the inner surface of the annulus across a gap d with an electric field at the beam surface given by $2\pi r \epsilon_0 E = (1-f)\lambda_b$, or $E \equiv (1-f)E_0$.

The space-charge-limited C-L result can be written $(\epsilon_0 E)^3 = 6J^2 \epsilon_0 \frac{m}{e} d$.

Combining,

$$\frac{e}{m} E_0 \left(\frac{L}{v_b}\right)^2 (1-f)^3 = 6d$$

For our parameters, this indicates $f \sim 90\%$.

BICrz results on pickup of neutralizing electrons

Achieve about 85% neutralization with the plasma cylinder,
and about 80% neutralization with the plasma annulus.

(with total electron charge = 30× total beam ion charge, and $\omega_{\mathrm{pe}} L / v_b \sim 60$.)

Because of symmetry of the r, z code, the electrons have little angular momentum, which enhances their density near the axis.

This effect, and the high temperature of the entrained electrons, leads to anharmonic radial fields and emittance growth visible in plots of $\delta\dot{r}/r$.

Collisional ionization of the chamber vapor provides additional neutralizing electrons.

We find $\sim 80 - 90\%$ neutralization by electron pickup from ionized chamber vapor, but again some degradation of emittance occurs.

RMS envelope equation

With variables normalized to correspond to the KV envelope equation

$$\frac{d^2a}{dz^2} = \frac{2U}{a} + \frac{\epsilon}{a^3}$$

where $a = \sqrt{2\langle r^2 \rangle}$ is the edge radius for a uniform beam,

$$\epsilon^2 = 16\left(\langle x^2\rangle\langle x'^2\rangle - \langle xx'\rangle^2\right)$$
$$= 4\left(\langle r^2\rangle\langle r'^2\rangle - \langle \mathbf{r}\cdot\mathbf{r}'\rangle^2\right)$$

is the edge emittance for a KV beam, and

$$2U = \frac{2Z_b e}{\gamma_b m_b v_b^2}\langle r\,(E_r - v_b B_\theta)\rangle \quad \text{(MKS)}$$
$$= \frac{2Z_b e}{\gamma_b^3 m_b v_b^2}\,\frac{\int dr\; r\rho_b\, rE_r}{\int dr\; r\rho_b}$$

Evaluation of the space charge term

If the only charge is that of the beam ions,

$$
\begin{aligned}
2U &= \frac{2Z_b e}{\gamma_b^3 m_b v_b^2} \left(\tfrac{1}{2} r E_r\right)_{r>a} \\
&= \frac{1}{4\pi\epsilon_0} \frac{2Z_b e I_b}{\gamma_b^3 m_b v_b^3} \quad \text{independent of the radial distribution of current} \\
&= K, \quad \text{the perveance}
\end{aligned}
$$

This envelope equation is accurate in the paraxial limit, however the variation of ϵ limits its usefulness.

For a partially neutralized beam,

$$2U = \frac{2Z_b e}{\gamma_b m_b v_b^2} \langle r \left(E_r - v_b B_\theta\right) \rangle$$

may be compared to K as a measure of degree of neutralization.

Neutralization by preformed plasma

Shielding by co-flowing electrons decreases on approach to the target

The entrained electrons are hot, $\beta_{te} \sim .3$.

As the beam approaches the target, it compresses radially, heating the electrons.

As the Debye length increases toward the beam radius, neutralization is impaired.†*

Collisional ionization and photoionization of chamber vapor are supplemental sources of neutralizing electrons.

† "...Emittance, Space Charge and Electron Pressure Effects on Focusing of Neutralized Ion Beams", D. S. Lemons and M. E. Jones, in proceedings of the 1986 HIF Symposium, AIP, 1986

* Section 11.4, "Charged Particle Beams", S. Humphries, Wiley, 1990

Collisional ionization of chamber vapor *versus* beam stripping

Ionization of chamber vapor helps supply electrons to be entrained in the beam, helping neutralization.

Stripping of beam ions increases their response to radial fields, leading to emittance growth.

Both effects increase with density.

HIPPO code results ($\sim$ 1981) assuming Li vapor showed benefits of collisional ionization *versus* beam stripping.

In recent reactor concepts using FLiBe, the vapor consists mainly of BeF_2.

Will BeF_2 degrade the ratio (vapor ionization)/(beam stripping)?

We need atomic physics information on BeF_2, or at least plausible recipes with which to compare results of various models.

Model for collisional ionization of the chamber vapor

This is not implemented as a Poisson process but by a near-deterministic algorithm:

Each ion has an accumulator, N_b, initialized to a random number in $(0, 1)$.

At each beam advance, N_b is incremented by $\frac{v\Delta t}{\lambda_{gi}}\frac{q_b}{q_{ei}}$ where q_b are the (variable) weighted beam ion charges, and q_{ei} is the charge of each electron created.

For each ion with $N_b > 1$, a cold electron is created at the position of the ion, the fixed background ion charge density is incremented, and N_b is decremented by 1.

Thus the total electron charge created by collisional ionization is

$$N_{ei}q_{ei} \simeq \frac{\sum z_b q_b}{\lambda_{gi}}$$

λ_{gi} is the path length over which a beam ion collisionally produces additional electron charge equal to its own charge.

Thermal X-rays from the heated target photoionize the chamber vapor

(photoionization of beam ions was discussed at Monterey 1990 HIF meeting)

When the focal spot on the outside of the target reaches ~ 100 eV, it emits $\sim 10^{13}$W/cm^2 through an area of ~ 0.3cm^2.

This corresponds to ~ 300 eV photons produced at a rate $\sim 10^{28}$ sec^{-1}.

Taking an ionization cross section $\sim 10^{-18}$cm^2 and density $\sim 10^{13}$, suggests that photoionization could produce photoelectron charge $\gg$ beam charge – most of it not in the beam path.

This process might benefit the (high energy, expensive) final section of the drive pulse.

Atomic physics data is needed in several areas:

Whatever data is needed to help find a cheap, chamber-survivable means to preionize chamber vapor.

Photoionization cross sections for FLiBe due to thermal radiation from heated target, $h\nu < 1$ keV.

Collisional ionization at speeds $\sim 0.3c$
- stripping of beam ions
- collisional ionization of chamber vapor
  - (e.g. ratio of vapor ionization to stripping in FLiBe versus Li)
- ionization by electron swarm

We need at least plausible recipes with which to compare results of various models.

The HYLIFE-II reactor design parameters were used

Beams enter the chamber with a beam radius of 5.2 cm and converge with a 1 degree angle in the 3 meter chamber.

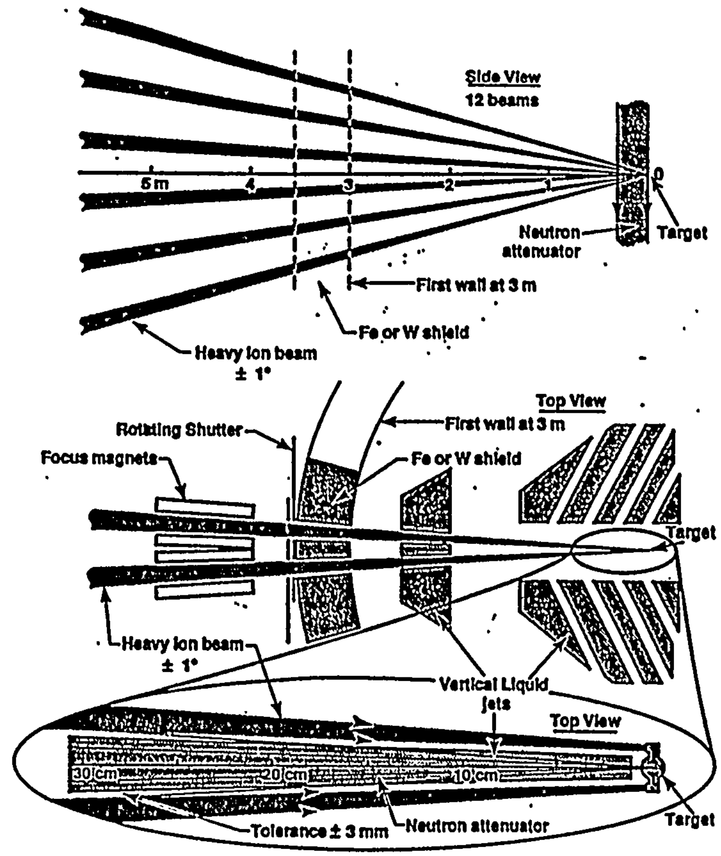

See R. Moir, et. al., "Hylife-II: A molten salt inertial fusion energy power plant design-final report," Fusion Technology, 25, 1994.

The converging grid maintains radial resolution as the beam radius decreases from 5.2 cm to a few millimeters.

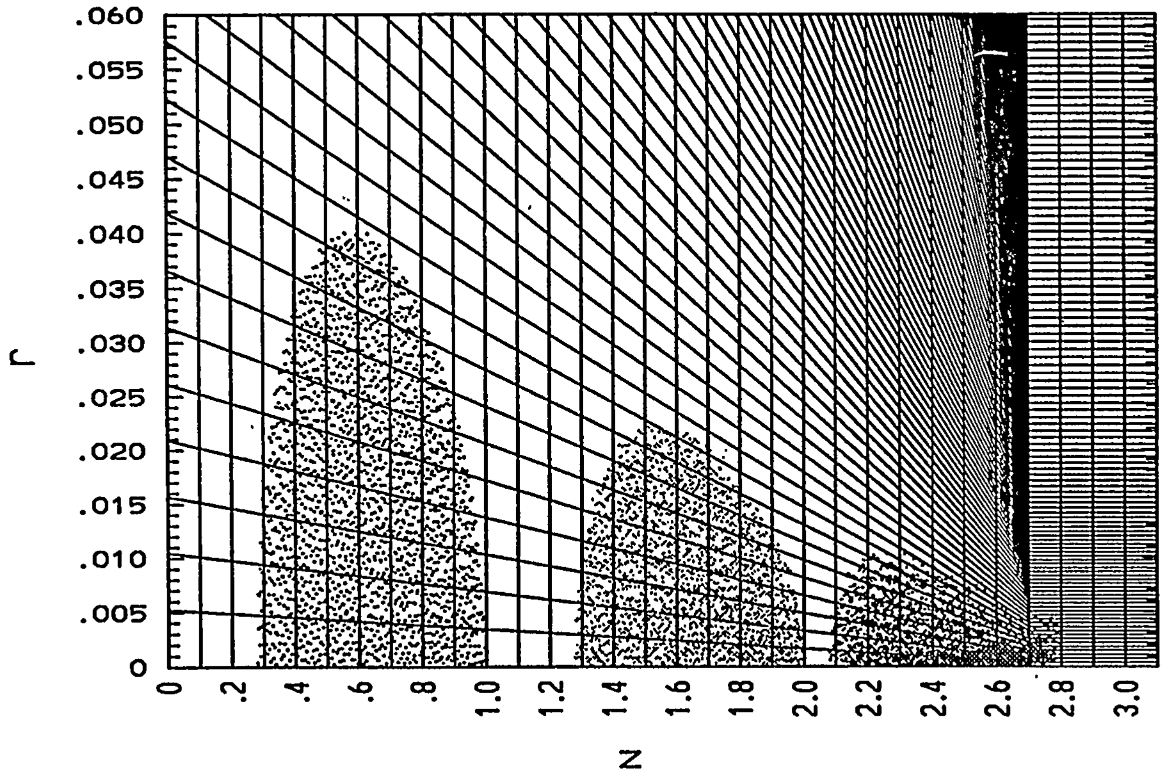

Every 10th z-cell is shown. The grid extends well beyond this plot in the radial direction.

Simulations without stripping or collisional ionization agree well with the beam envelope solution.

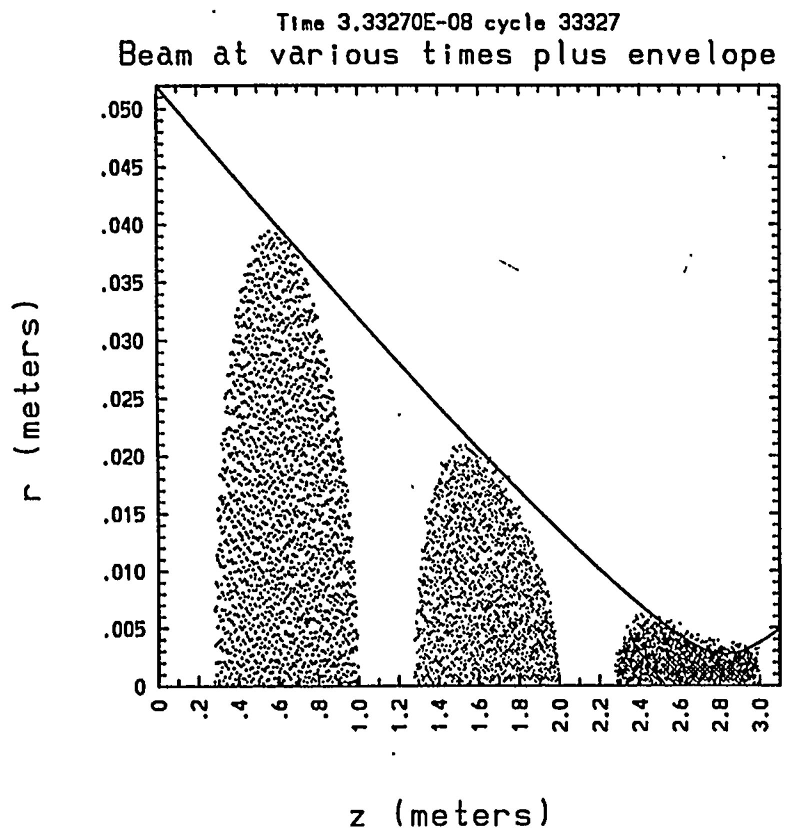

A parabolic beam as the beam head reaches 1 meter, 2 meters and 3 meters. Ballistically transporting the particles to the best focus gives 95% of the charge falling within a 2.6 mm radius at 2.82 meters. The envelope solution gives the best focus at 2.83 meters with beam radius 2.7 mm.

Necessary cross section data has been difficult to obtain.

In the HYLIFE-II reactor design, the chamber wall is protected by jets of liquid Flibe, $(LiF)_2(BeF_2)$. This molecule dissociates into BeF_2 and LiF. BeF_2 is much more volatile than LiF and at the temperatures of interest the gas should be rich in BeF_2 by about a factor of 10.

The cross sections for stripping 10 GeV lead ions by BeF_2 and collisional ionization of BeF_2 by the lead ions have been difficult to obtain. Some work by Gillespie and Janda was done for uranium ions in a Li gas chamber.

Currently, our best estimates are:
Stripping of lead ion: 5×10^{-17} - 1.6×10^{-16} cm^2
Collisional ionization of BeF_2: 8×10^{-18} - 1×10^{-16} cm^2

If we know the ratio of these cross sections, we have some flexibility in the chamber temperature (and hence, the chamber density) which effects the mean-free-paths. We will be working with atomic physicists to get better cross section data.

Beam stripping and collisional ionization sensitivity studies

Given that our knowledge of the cross sections is incomplete, we ran a number of simulations to test the sensitivity of the beam spot size at the target to the cross sections.

The procedure was as follows:

- Run the simulation until the beam is close to the target.
- Ballistically transport the ions ahead and find the distance at which the best focus occurs, z_{foc}.
- Run the simulation until the beam head reaches z_{foc}
- Ballistically transport the ions to z_{foc} and calculate the spot size.

In each simulation, the beam ions had a thermal speed of $\beta_{ti} = 1.0 \times 10^{-4}$. The RMS envelope solution with this temperature and no space-charge (*ie* fully neutralized beam) gives a minimum spot size of 2 mm.

Beam parameters used in the simulations

The main pulse should deliver 4 MJ of energy to the target. The beam has a parabolic shape which gives linear self fields. Each of the 16 beams have the following:

Current: 3.125 kA average, 4.688 kA maximum
Beam velocity: .3 c
Charge: 2.5×10^{-5} C
Beam duration: 8×10^{-9} sec
Radius at chamber entrance: 5.2 cm
Charge density (at entrance): 6.1×10^{-3} C/m^{-3}
Ion thermal speed: 1.0×10^{-4} c

Varying the stripping and collisional ionization mean-free-paths can result in spot sizes as large as 8 mm or as small as 2.9 mm

l_{strip} (m)	l_{CI} (m)	Angle	z_{foc} (m)	90% (mm)	95% (mm)
∞	∞	1.17	2.82	2.3	2.6
1.20	∞	1.10	3.00	6.6	8.0
1.20	3.0	1.05	3.03	4.5	5.4
1.20	0.4	1.05	2.92	3.0	3.7
5.25	∞	1.11	3.05	3.5	4.3
5.25	3.0	1.11	2.83	2.8	3.4
3.20	1.0	1.05	2.93	2.6	3.1
12.80	4.0	1.10	2.90	2.4	2.9

Nonlinear electric fields make it more difficult to focus the beam. In addition, the stripped ions respond more strongly to the electric fields.

Adding electrons to the system results in nonlinear radial electric fields

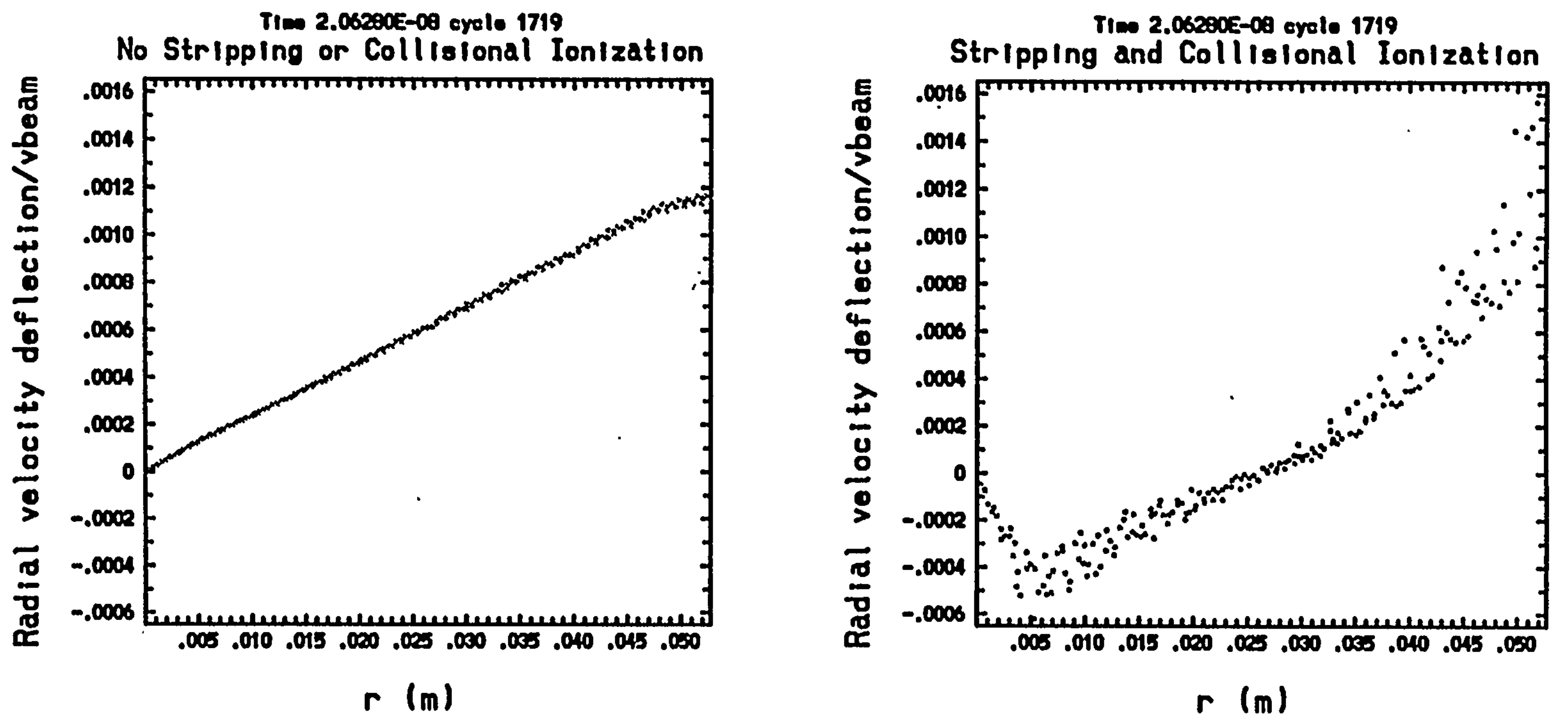

Particle color shows charge state, green = +1, red = +2, blue = +3 for ions near the beam center after 1.5 meters.

We can compensate for the linear electric field by increasing the focusing angle. We cannot compensate for the nonlinear fields in this way.

Additional electrons in the chamber can partially neutralize the beam.

- Neutralizing an ion beam is more difficult than neutralizing an electron beam.
  - When an electron beam passes through a plasma, the plasma electrons are moved out of the beam path by the beam self field. The beam is then neutralized by the immobile ions.
  - An ion beam must pull electrons in from outside the beam path.

- An electron produced by collisional ionization only reduces the net charge after the beam has left the gas ion behind.

- A preformed plasma annulus outside the beam path can partially neutralize if electrons are entrained by the beam. This leaves a positively charged plasma behind.
  - Electrons entrained by the beam are hot ($\beta_{te} \geq .3$). As the beam compresses near the target, these electrons will be less effective at neutralizing the beam.

A preformed plasma annulus was put just inside the chamber entrance.

A .3 meter long (40% of the beam length) annulus was placed near the entrance to the chamber. The annulus had radial extent to fit between the beams in the HYLIFE-II reactor design. The annulus (a neutral plasma) had an electron charge of 4 times the beam charge.

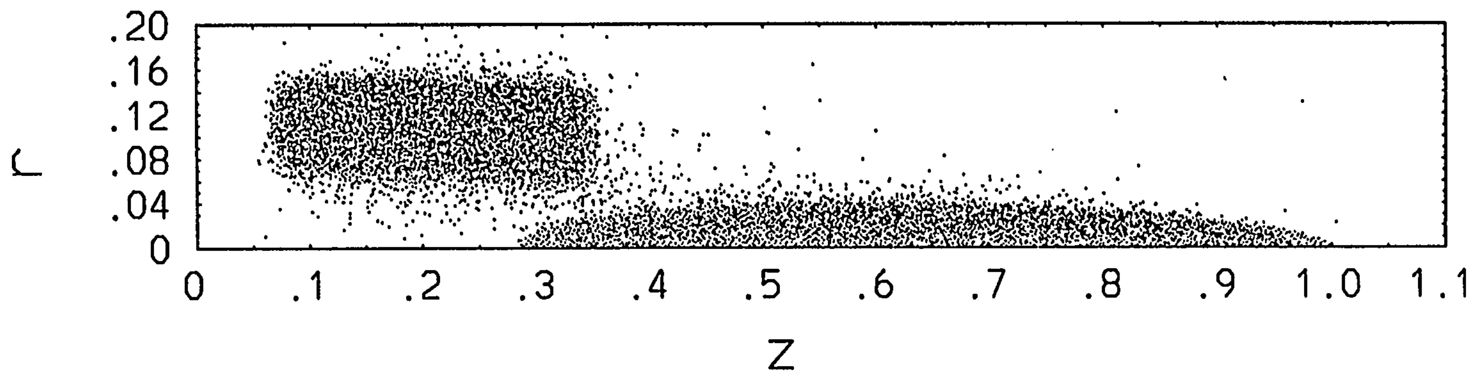

Beam ions shown in red, electrons (from stripping and plasma annulus) shown in black.

A preformed plasma annulus reduces the spot size.

Annulus	l_{strip}	l_{CI}	90% (mm)	95% (mm)
No annulus	1.2	∞	6.6	8.0
Cool annulus	1.2	∞	2.7	3.1
Warm annulus	1.2	∞	2.9	3.5
Warm annulus	1.2	3.0	2.5	3.0
Cool annulus	3.2	1.0	2.0	2.4

The cool annulus had an electron temperature of 100 eV. This small temperature give the electrons little angular momentum and enhances their effect near the origin. To give the electrons more angular momentum, an annulus with temperature 7.4 keV ("warm annulus") was also run. With the multiple beams, the HYLIFE-II chamber is not axisymmetric and the electrons will have angular momentum.

Effective perveance shows partial neutralization by ionization of the chamber gas and a plasma annulus.

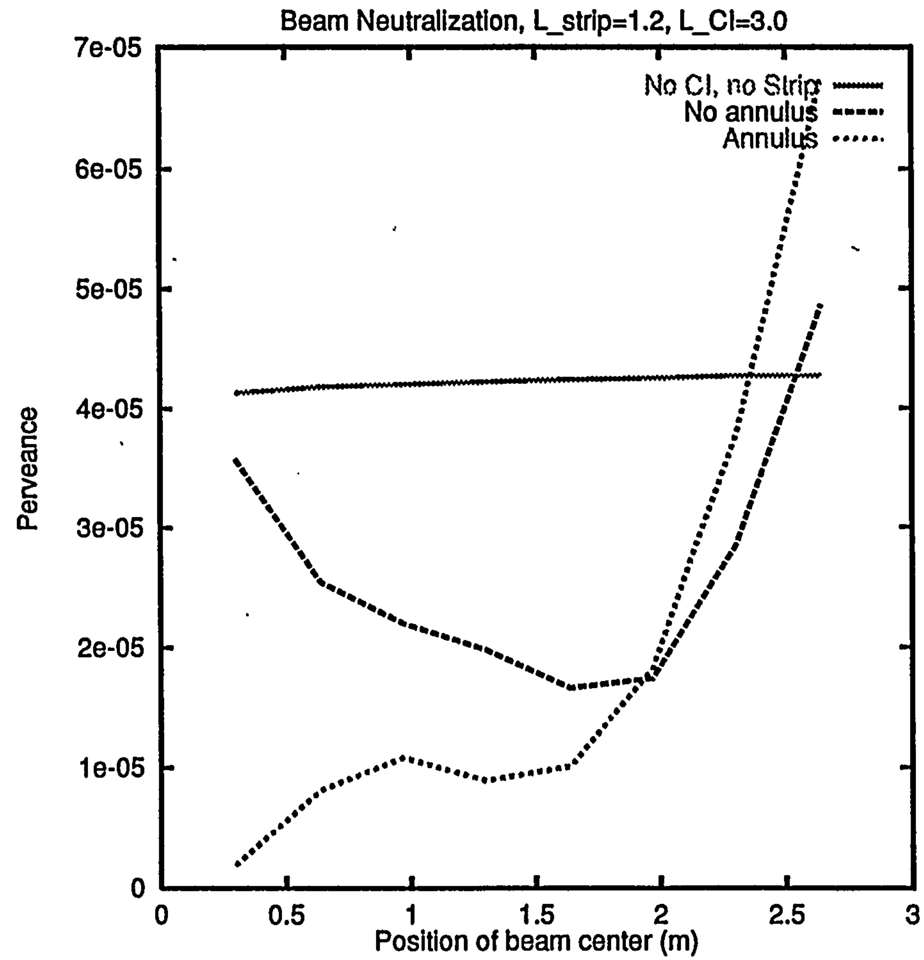

Three dimensional numerical simulations of vacuum charge-neutralization

Steve Slutz*, Tom Lockner*, and Stan Humphries+

*Sandia National Laboratories
Albuquerque, New Mexico 87185

+University of New Mexico
Albuquerque, New Mexico

Workshop on Transport for a Common Ion Driver
Sept 20-21, 1994 Albuquerque, N.M.

8

Beam space-charge drives the cost of high current induction linacs

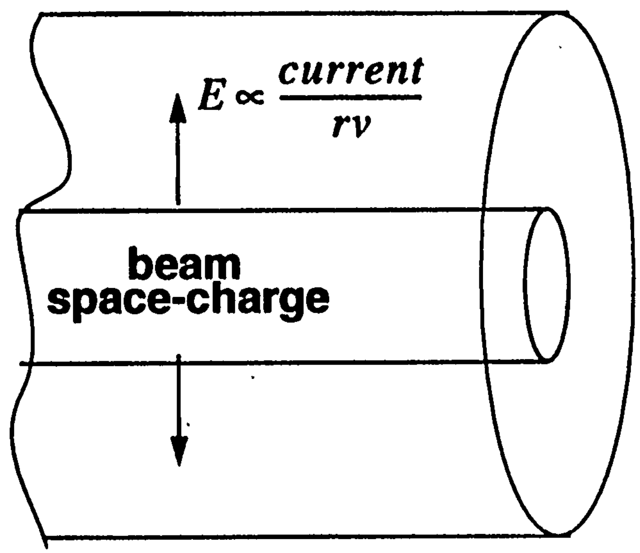

- High energy requires a long accelerator
- Large beams: induction core cost is proportional to r-V-s
- Many beam lines

Heavy ion accelerator designs for fusion use many beamlets to overcome the space-charge limitation

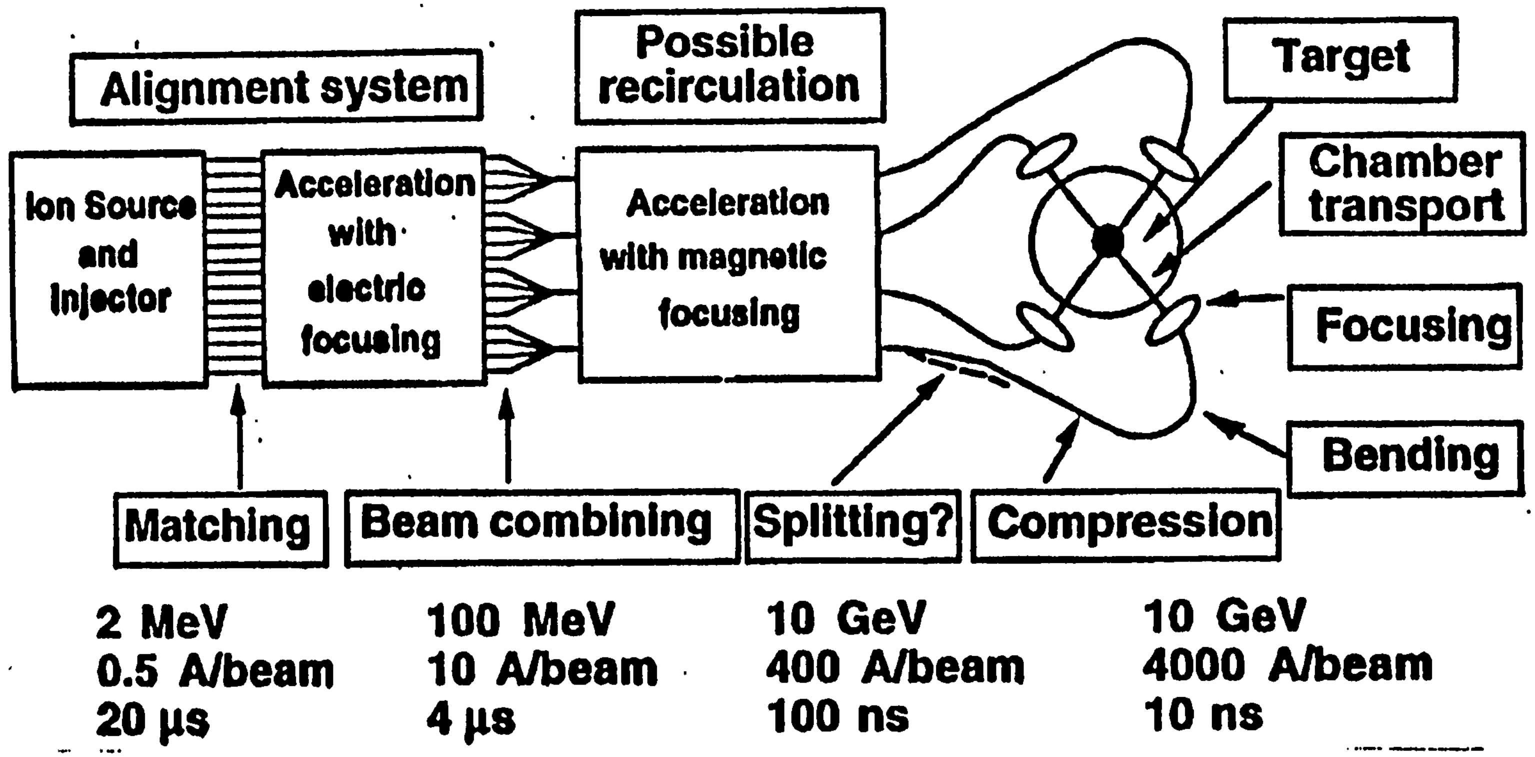

- "The optimal design for Heavy Ion accelerators may well be ones that have higher current, lower energy beams"

Pulselac results indicate ~90% charge-neutralization may be possible in vacuum

- This would allow roughly a facter of ten increase in beam current per line.
- The final voltage could be reduced proportionally, while still maintaining the same output power.
- Lower final voltage implies a shorter accelerator with fewer inductive cores.
- Reducing the amount of magnetic core material has a significant impact on the cost of the accelerator.

Pulselac required >99% space-charge neutralization and thus a plasma background

- Charge stripping during acceleration leads to a spread in the ion charge states
- Ions of different charge states are accelerated to different energies. This results in a spread of ion ranges in the target.
- Focussing forces depend of the charge state. Thus ions will be lost during transport and focussing.
- Near the output of the accelerator ions will be nearly fully stripped, which negates the advantage of using heavy ions.

Vacuum space-charge neutralization depends on the dynamics of electrons entering the beam

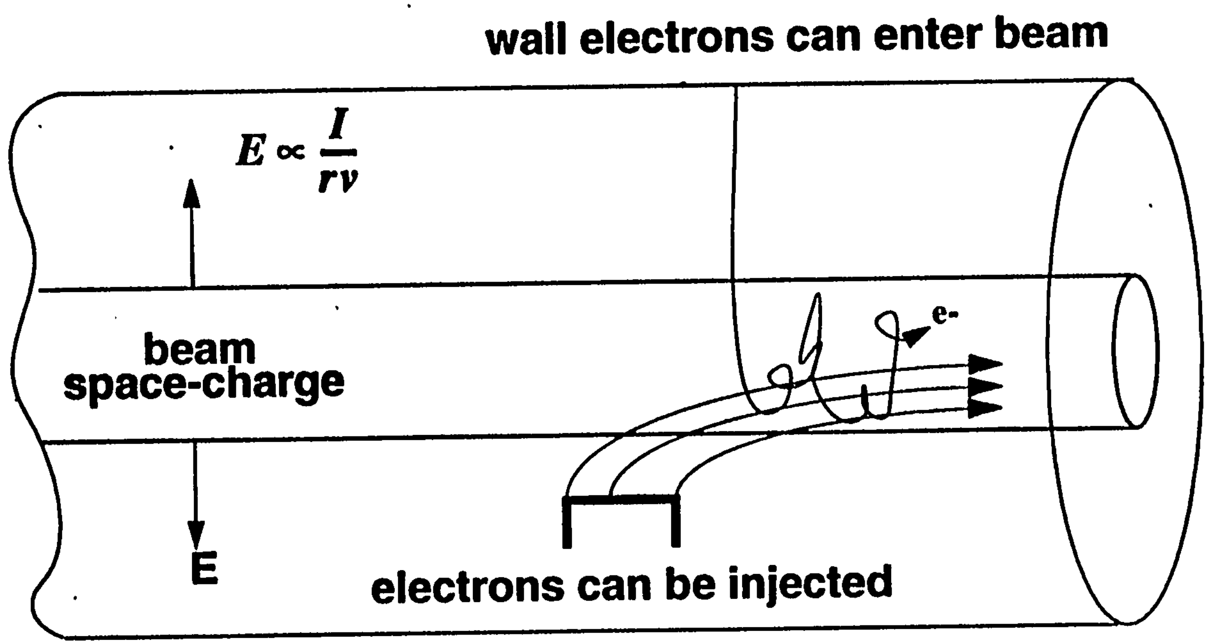

Three dimensional particle-in-cell simulations will be used to study charge neutralization

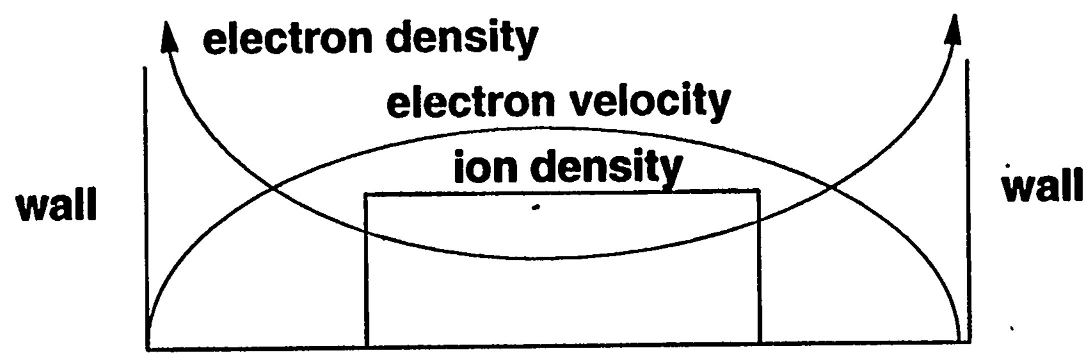

- Two-stream and diocotron instabilities may randomize the electron motion
- Instabilities could also lead to beam emittance growth

We simulated a proton beam injected between two electron emitting electrodes

- Set $J = J_{max}$, where $J_{max} = 2\varepsilon_0 \sqrt{\frac{2q}{M}} \frac{W^{3/2}}{x^2}$, W=1 MV

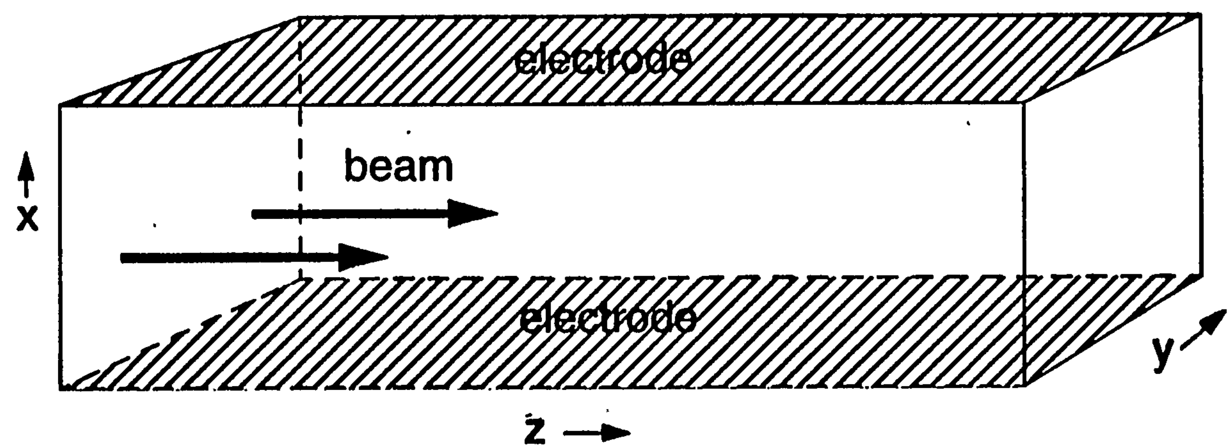

Wall electrons can provide up to 95% charge neutralization

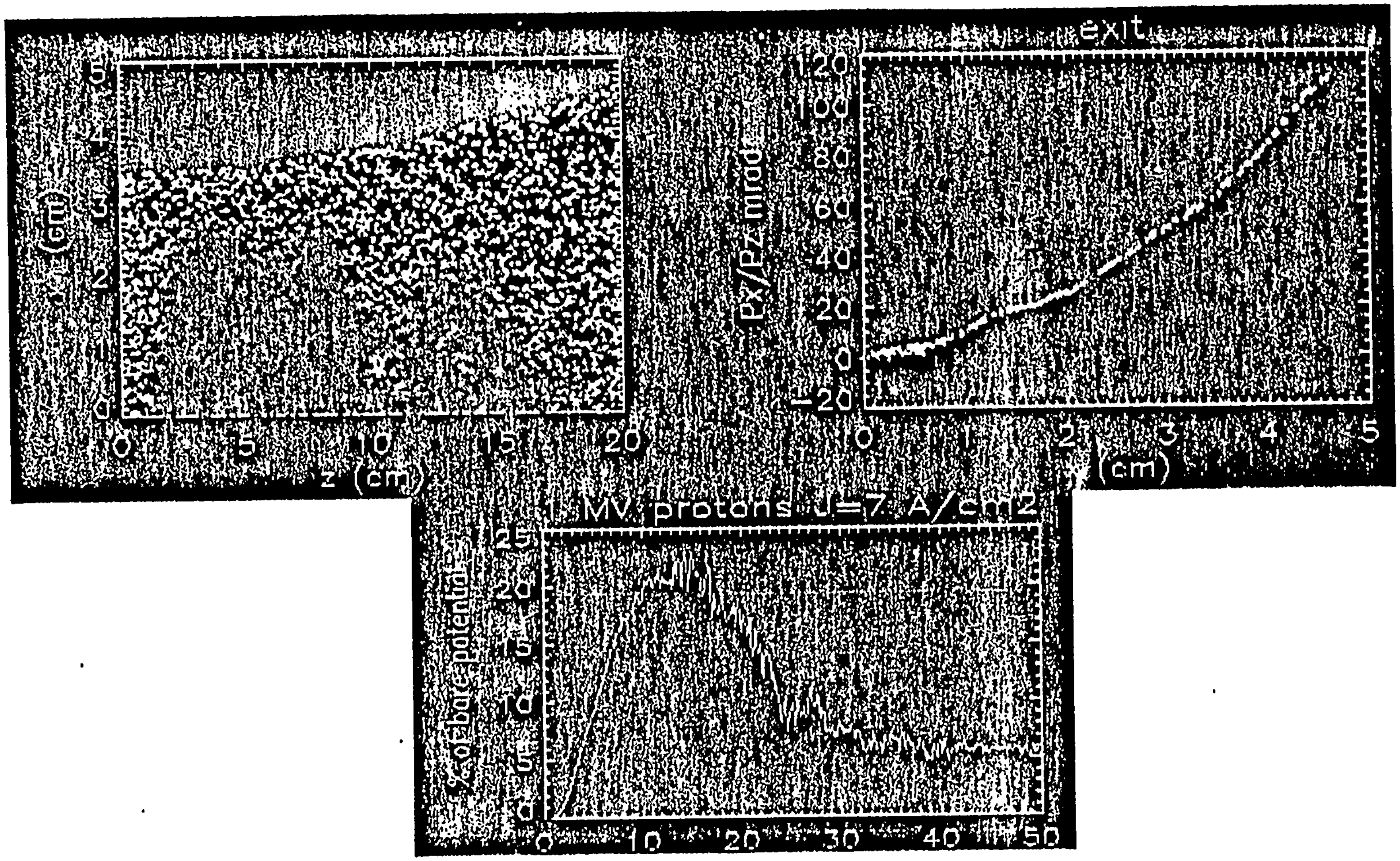

S.A.S. Workshop Sept. 1994

The acceleration gaps must be magnetically insulated

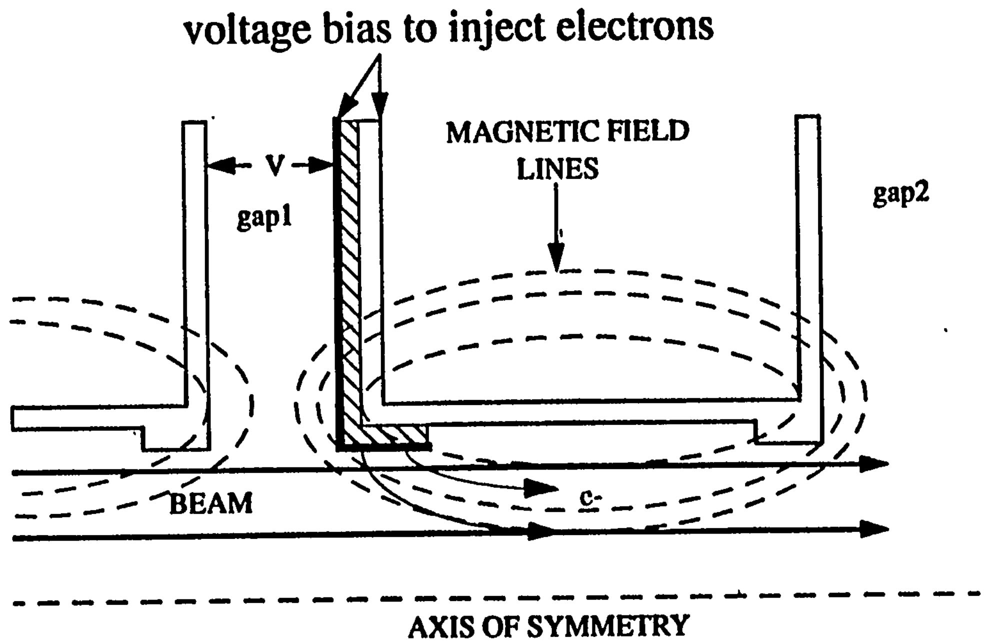

- A cusp magnetic field requires no inner conductor, provides solenoidal focussing, and allows electron injection into the beam.

The electrons remain tied to magnetic field lines despite the development of fluctuations

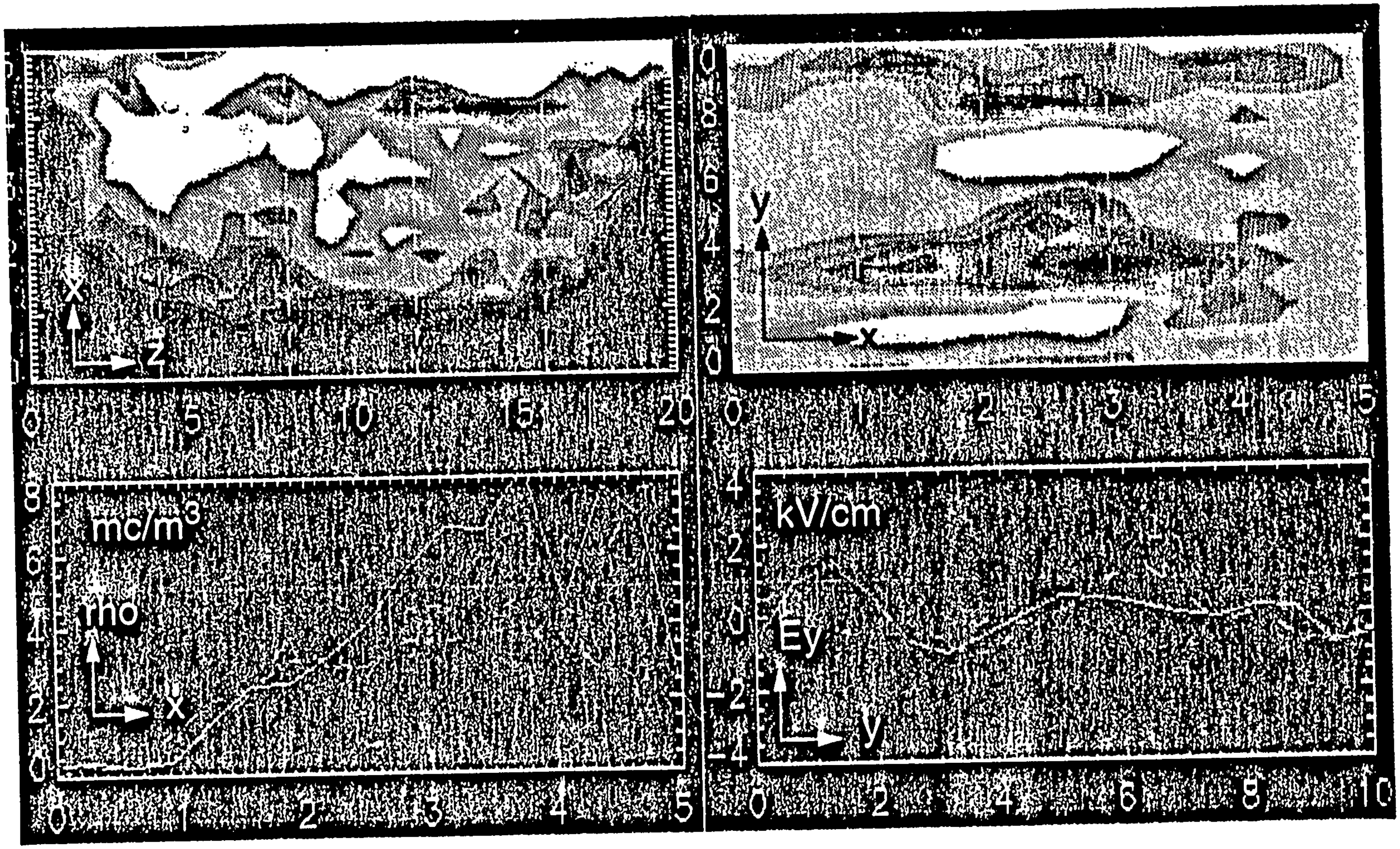

Simple additions to the existing ALIAS facility will be used to confirm the 3-D PIC simulations

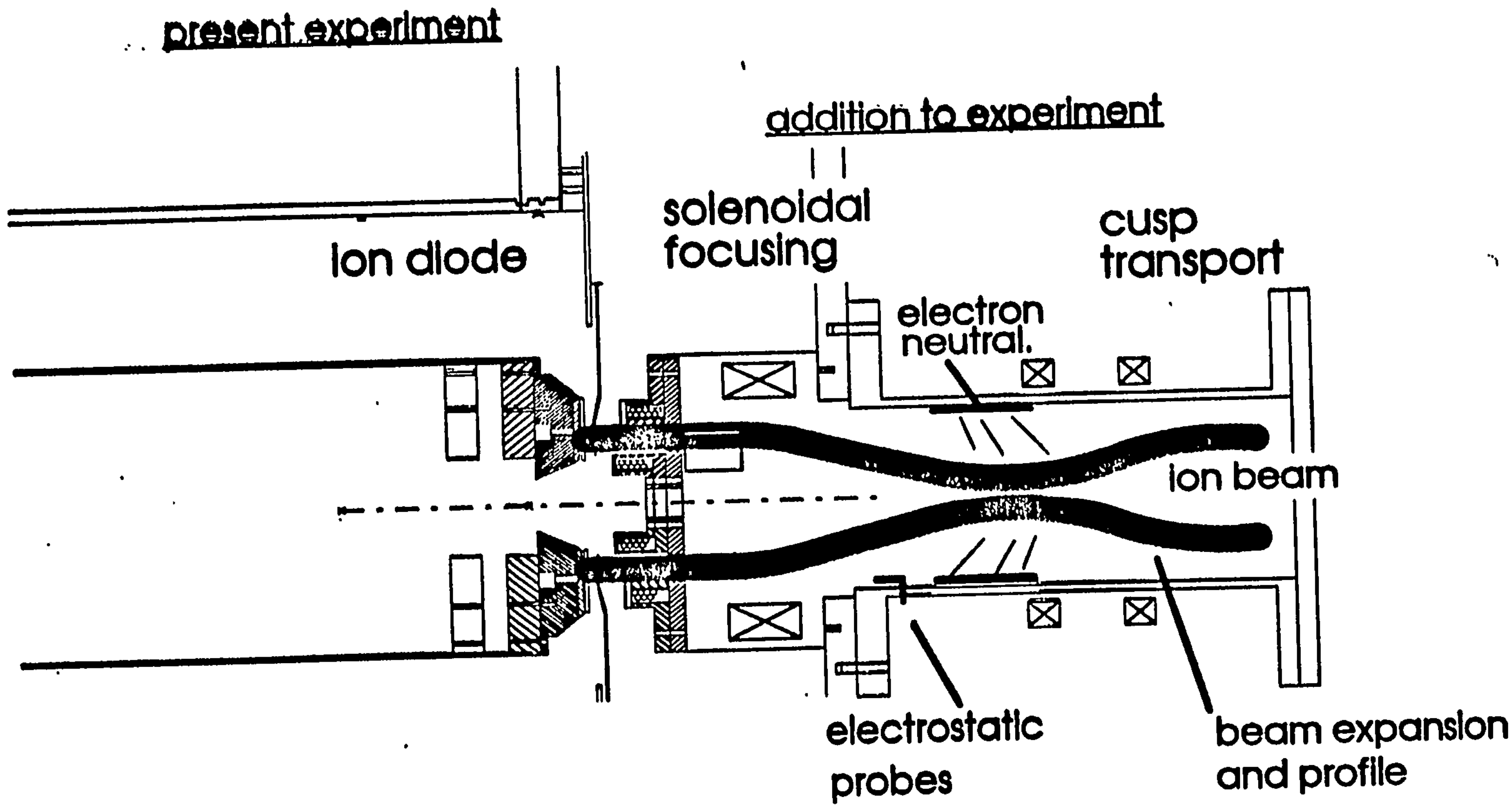

Future Work

- Simulate post acceleration. We expect larger fluctuations and greater electron transport
- Study the emittance growth of the beam during post acceleration and minimize the nonlinearity.
- Bias the cathodes to inject electrons into the beam
- Test simulations experimentally with the ALIAS facility

Current Neutralization of Intense MeV Proton Beams Transported in Low-Pressure Gases*

presented at the
APS Plasma Physics Division Meeting
St. Louis, Missouri
November 1, 1993

by

Frank C. Young
Plasma Physics Division
Naval Research Laboratory
Washington, DC

Workshop on Transport for a Common Ion Driver

Jess Neri at Sandia Nat. Labs 9/20/94

*Work supported by U.S. DOE through Sandia National Laboratories

9

Current Neutralization of Intense MeV Proton Beams Transported in Low-Pressure Gases*

presented at the
APS Plasma Physics Division Meeting
St. Louis, Missouri
November 1, 1993

by

Frank C. Young
Plasma Physics Division
Naval Research Laboratory
Washington, DC

* Work supported by U.S. DOE through Sandia National Laboratories

COLLABORATION

NRL		SNL
Experiment	Theory	Theory
F.C. Young	P.F. Ottinger	C.L. Olson
D.D. Hinshelwood*	D.V. Rose*	D.R. Welch+
S.J. Stephanakis	M. Lampe	
J.M. Neri	R.F. Hubbard	
	S.P. Slinker	

*JAYCOR, Inc., Vienna, VA.

+Mission Research Corp., Albuquerque, NM.

INTRODUCTION

- Ion-beam transport for light-ion beam ICF requires charge and current neutralization in low-pressure gas.
  - Transport is required for standoff and bunching.
  - Ballistic transport is baseline approach. Z-discharge and self-pinched transport are alternatives.

- Understanding gas ionization and plasma conductivity growth is necessary to determine transport feasibility.
  - Charge and current neutralization are necessary for focusing.
  - Large conductivity is required to avoid filamentation.

- Beam-plasma interaction is complicated in 1-Torr gas regime.
  - Conditions are intermediate between collisionless and collisional (resistive) models.
  - knock-on and fast electrons may lead to non-local secondary ionization.
  - Fast-electron population may alter plasma conductivity.

PROTON TRANSPORT EXPERIMENT

- Ion beam: 1-MeV protons, 5 to 7 kA, 0.7 to 1 kA/cm^2.

- Low-pressure gas: He, Ne, Ar, or air at 0.25 to 4 Torr.

- Measure net currents and electron densities in these gases.
  - Net currents are small: 2 to 8%.
  - Gases are only weakly ionized: 0.6 to 5%.

- Compare results with two different simulations.
  - Fast electrons play important role in generating net current.
  - Larger net currents may exist within the beam.

EXPERIMENTAL ARRANGEMENT

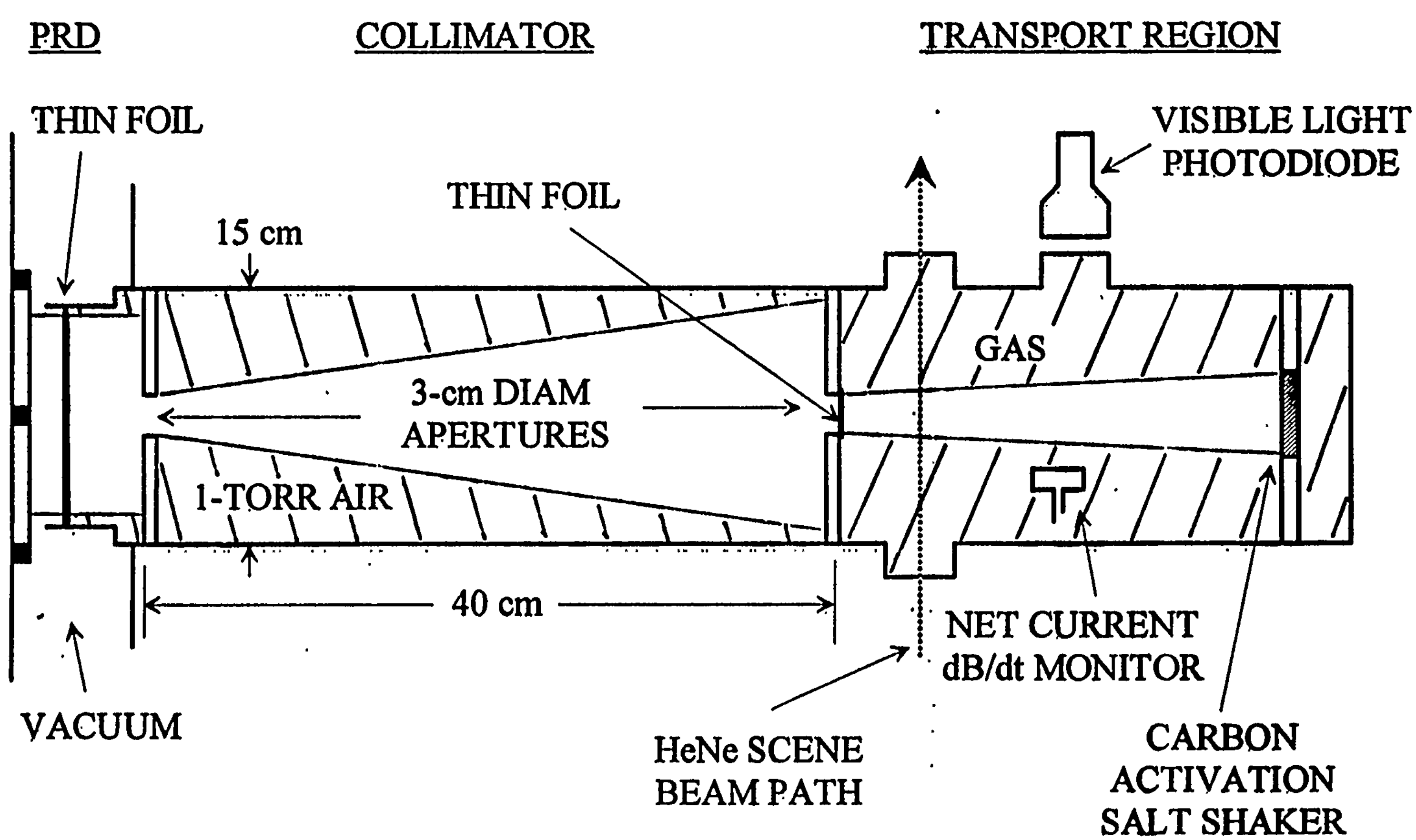

BEAM DIAMETER AND UNIFORMITY

Diagnostics at different distances from the collimator exit:

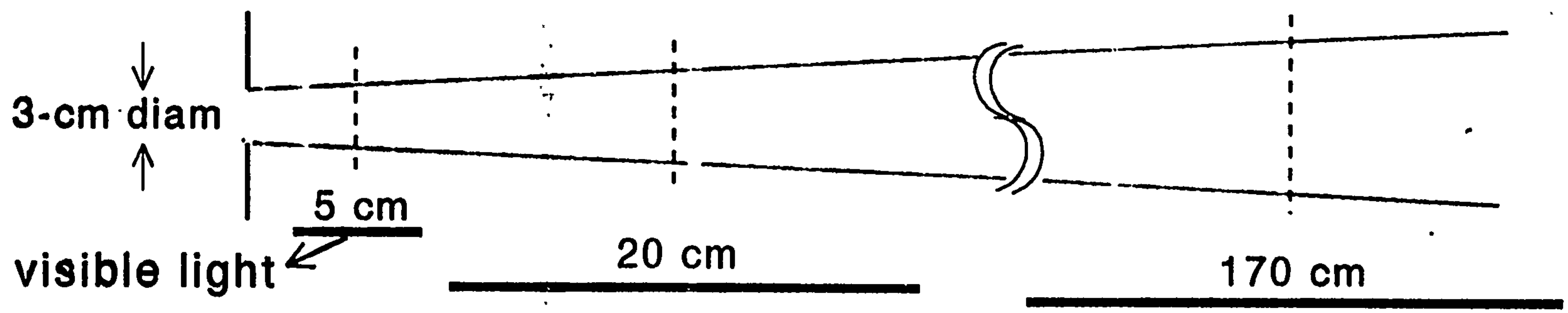

visible light image

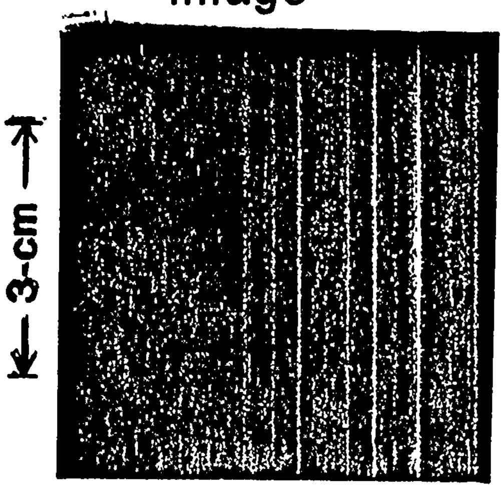

20 cm

- witness plate:
  beam diam = 5 cm
- Al K-α image:
  beam diam = 4.8 cm
  no filaments or
  structure

Beam divergence = 50 mrad

170 cm

radiachromic film
exposed
behind 0.25-mil Al

beam diam:
uniform image - 19 cm
with penumbra - 28 cm

= 50 mrad
= 75 mrad
(with penumbra)

BEAM TRANSPORT EXPERIMENT

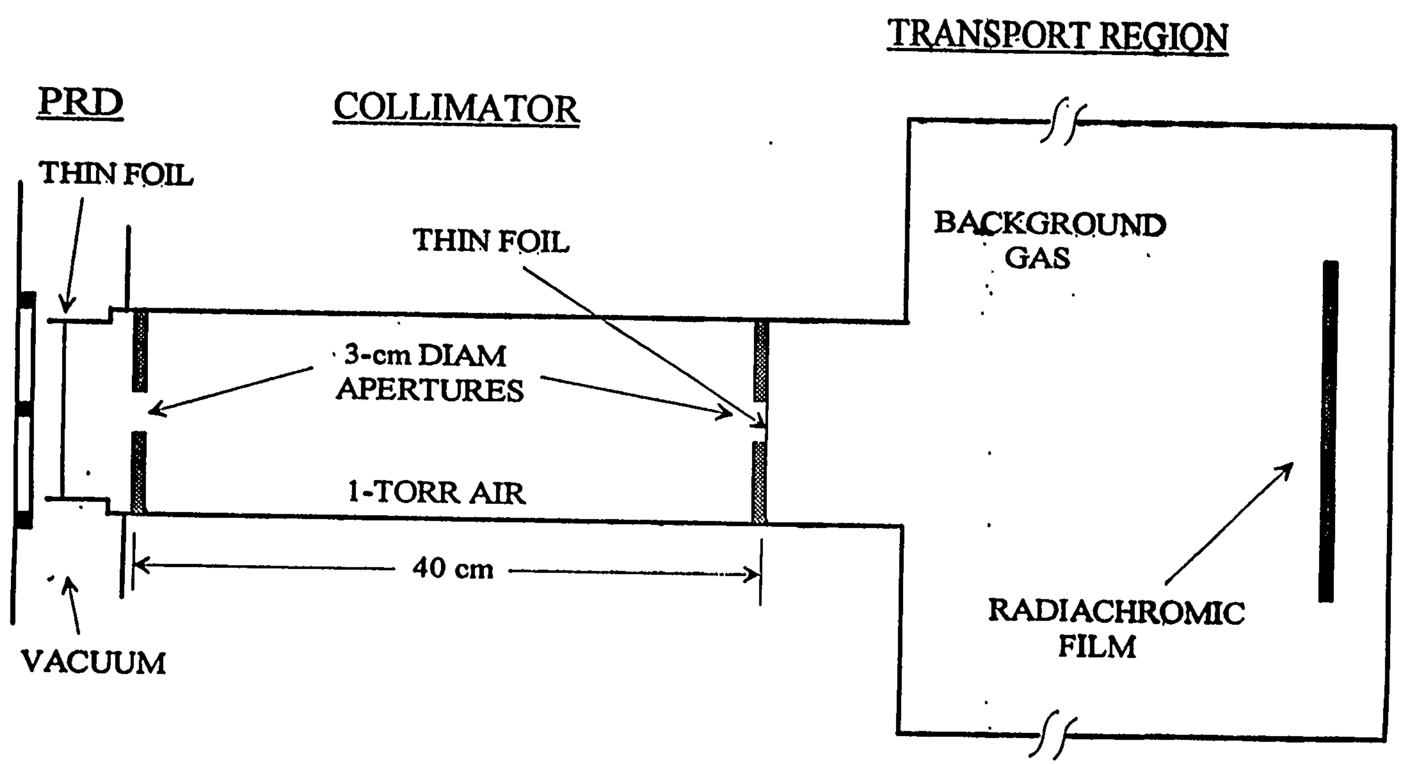

PROFILE 1.7 M BEYOND COLLIMATOR

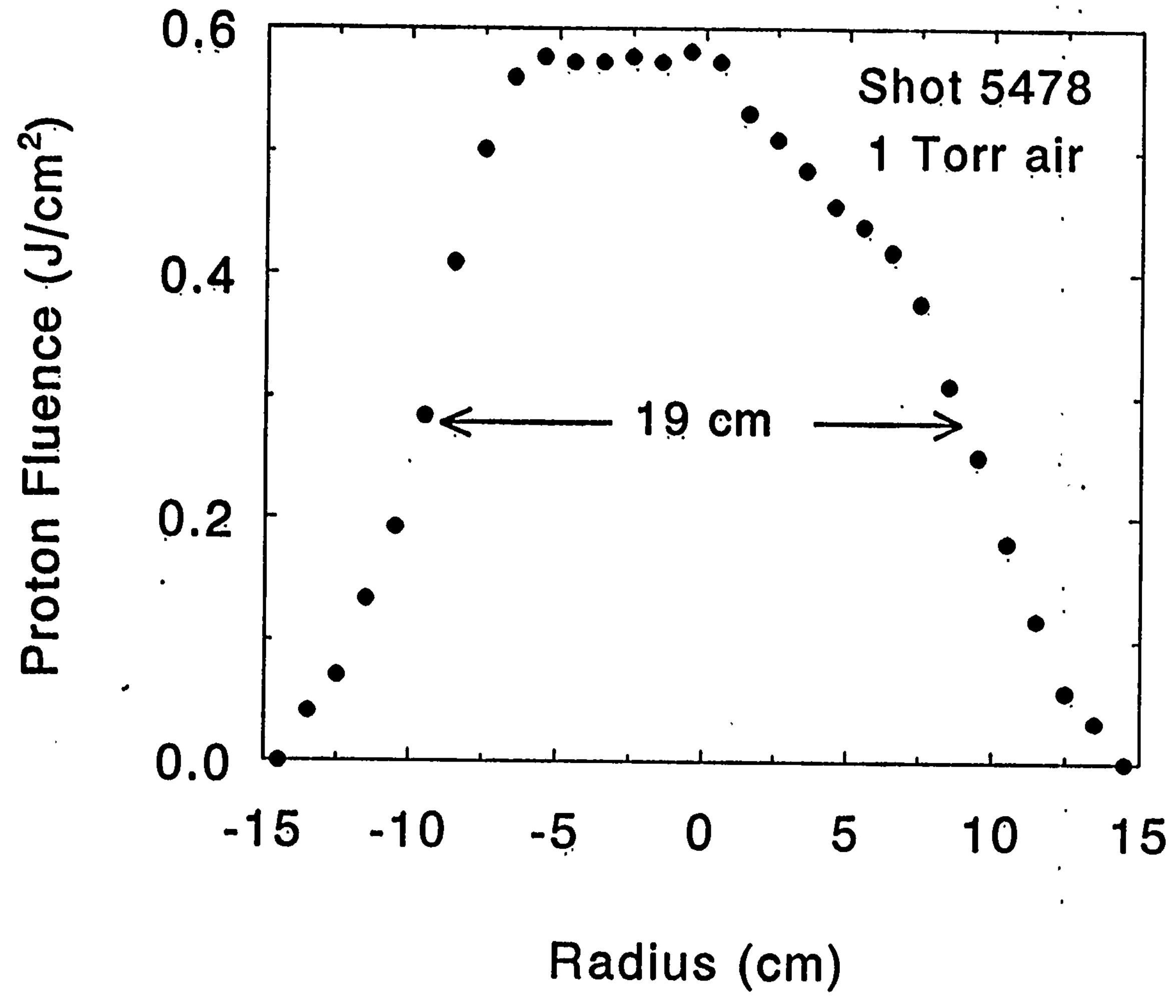

SPATIAL DISTRIBUTION OF TRANSPORTED BEAM

Array of Detectors

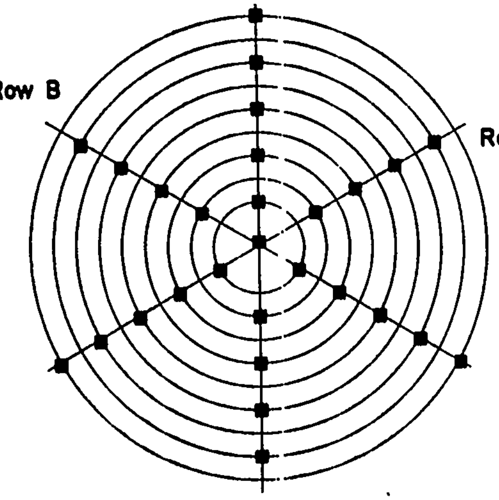

Radial Profiles

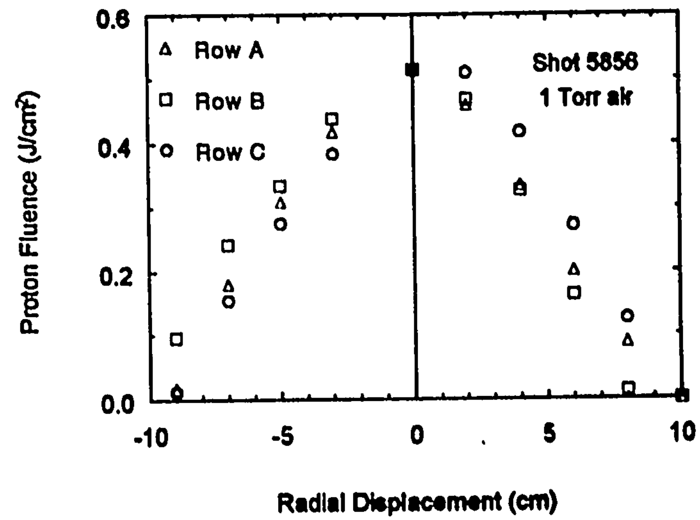

Contours of Fluence (Joules/cm²)

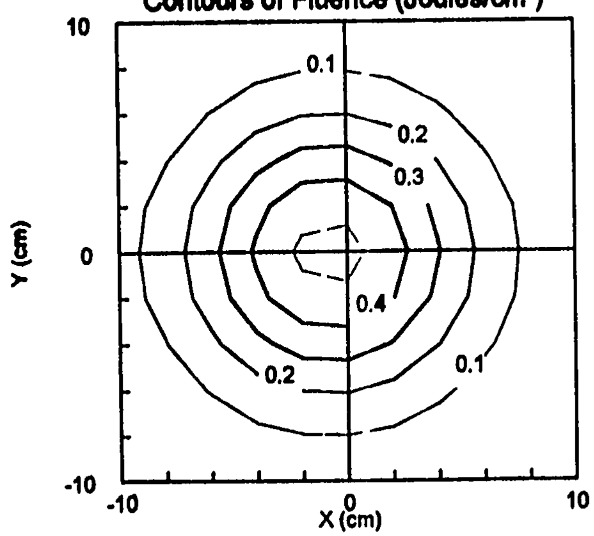

3D Fluence Map

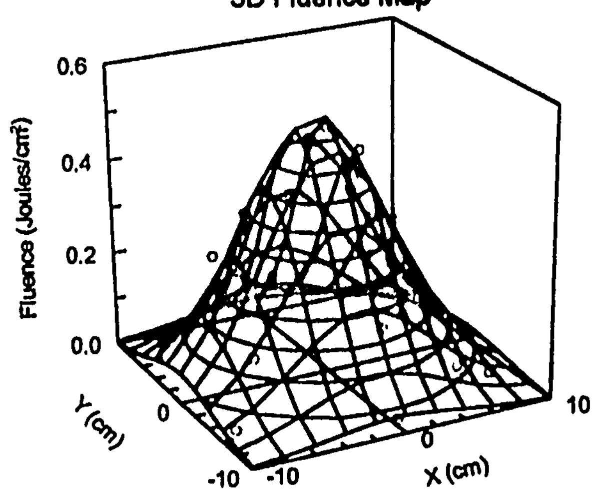

WAVEFORMS IN DIODE AND TRANSPORT REGIONS

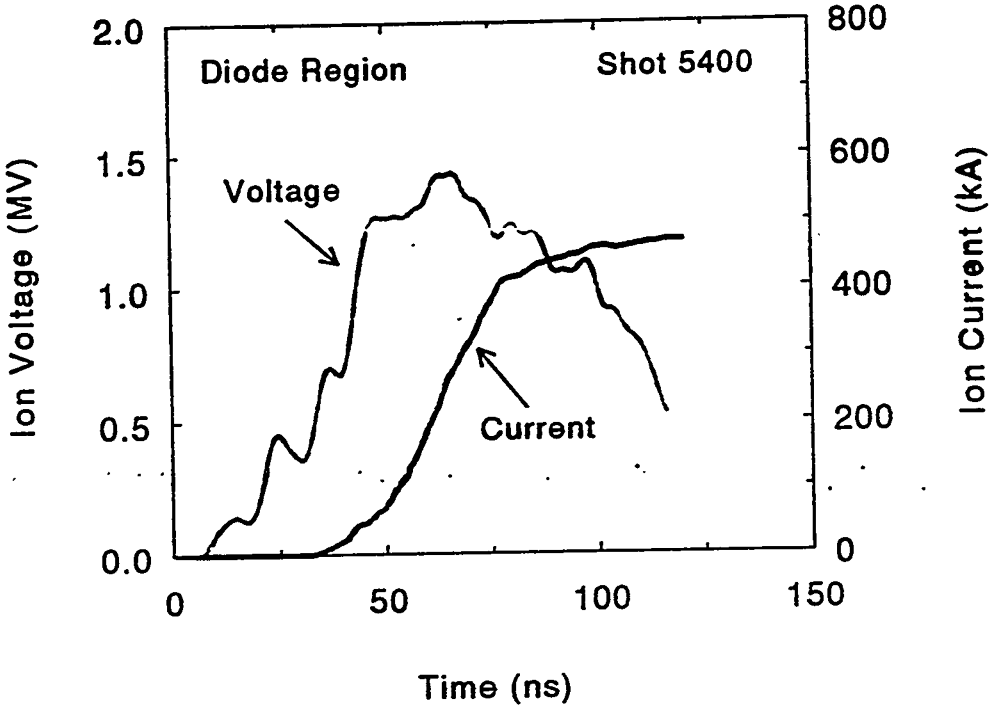

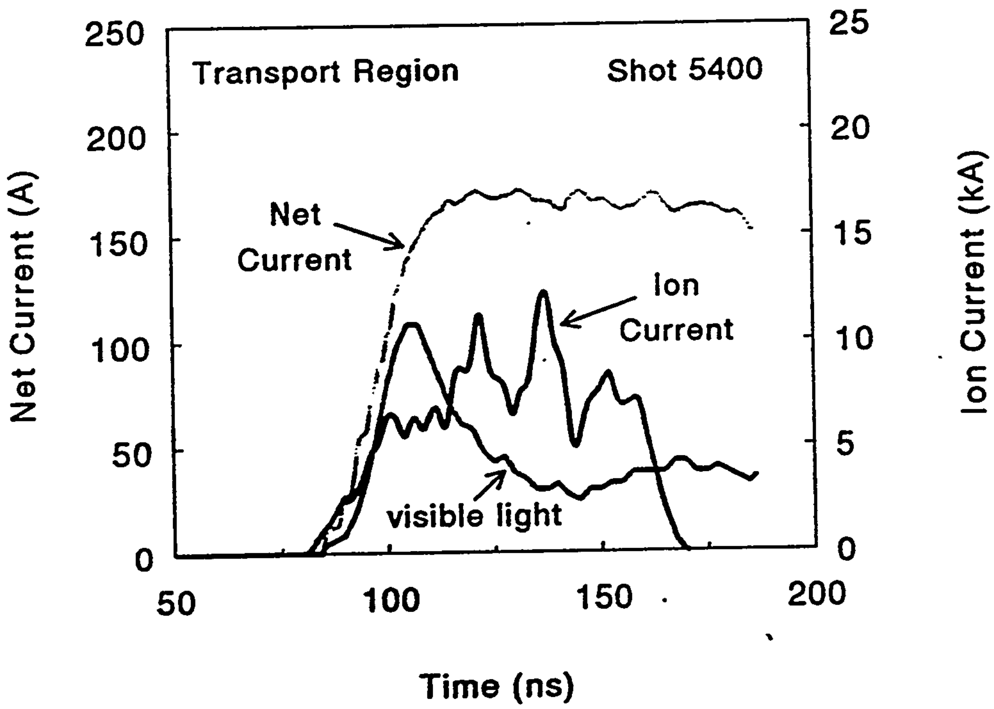

Ion energy measurements indicate energy loss at the head of the beam

Two Independent Ion Energy Measurements

- Proton Spectrum
  - stacked-foil carbon activation.
- Deuteron Energy
  - d(d,n) neutron time-of-flight.

Proton Number Spectra

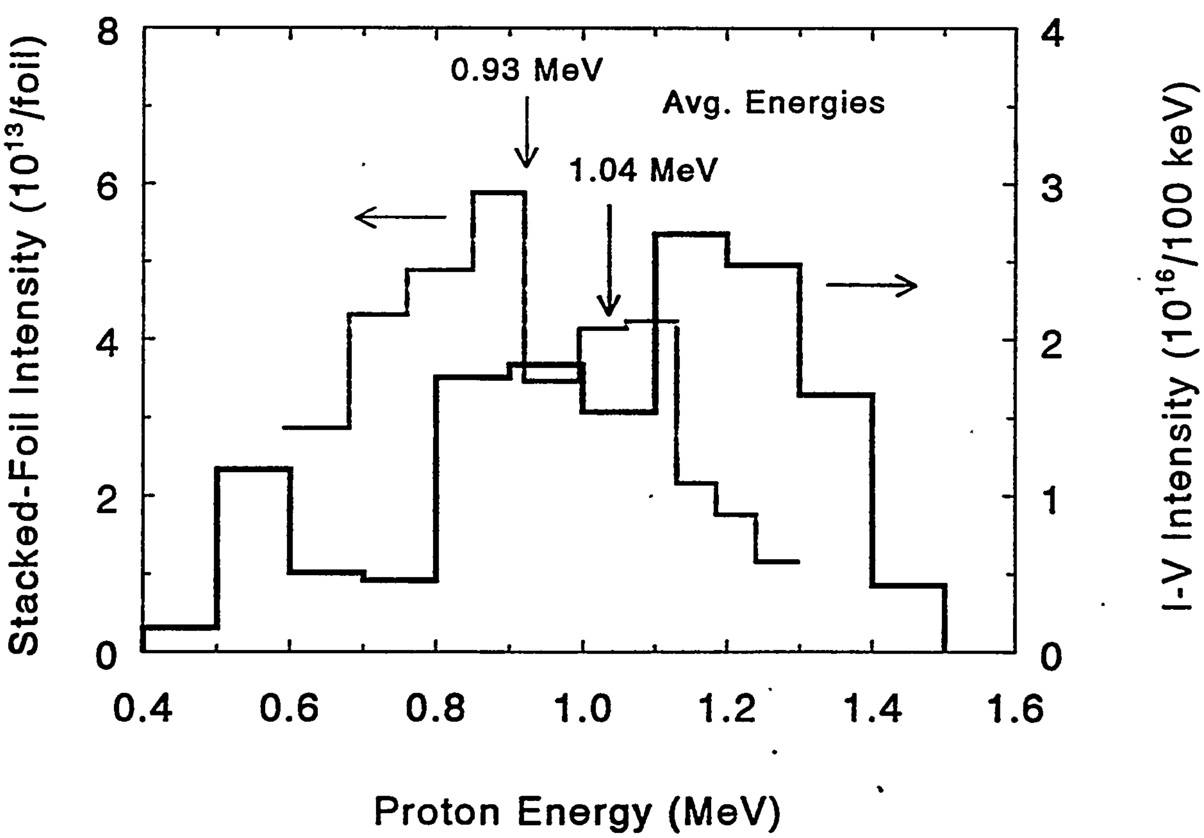

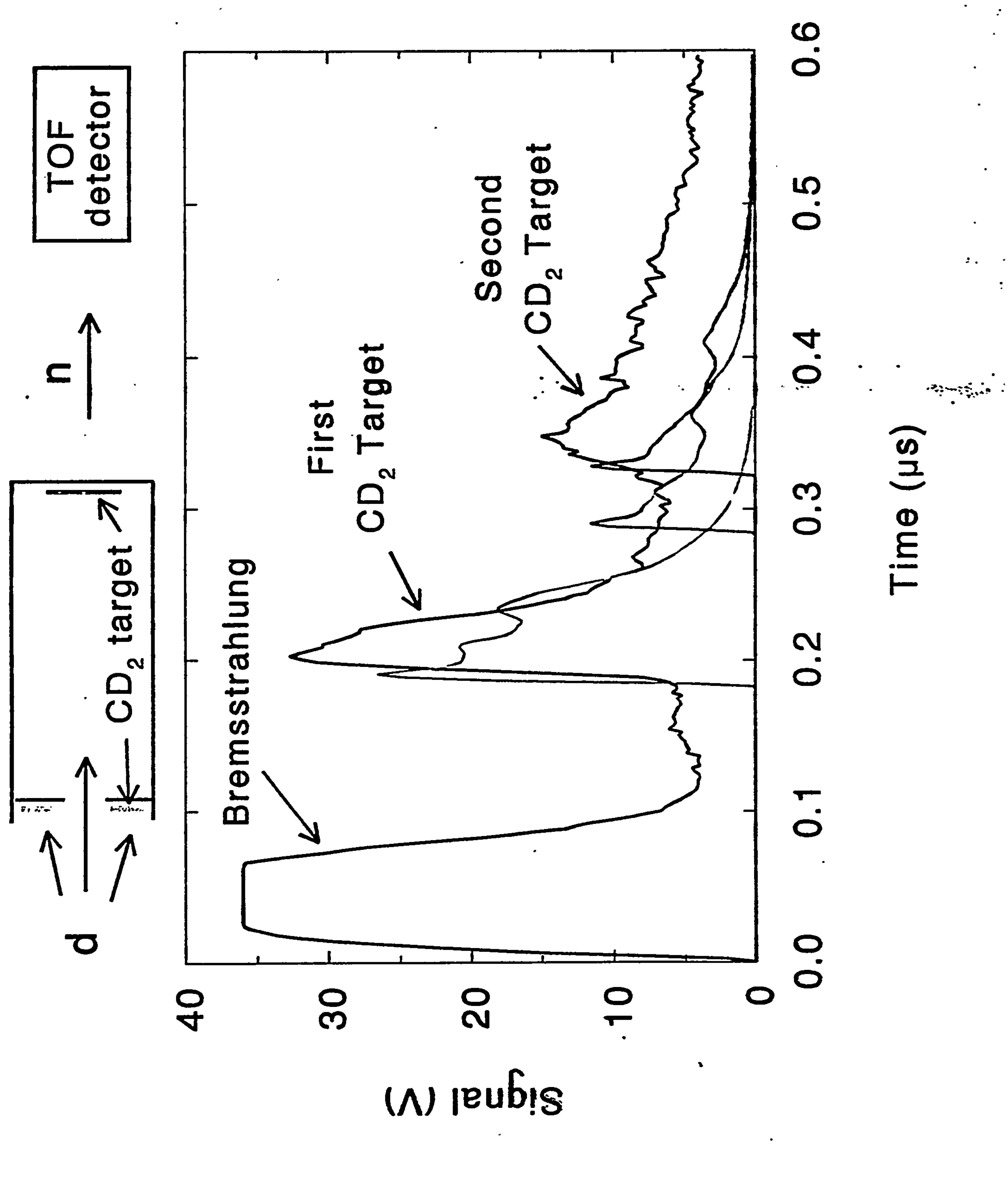

TOF detector
n
d
CD2 target
Bremsstrahlung
First CD2 Target
Second CD2 Target
Signal (V)
0
10
20
30
40
Time (μs)
0.0
0.1
0.2
0.3
0.4
0.5
0.6

Net-Current Waveforms Are Similar For Different Gases

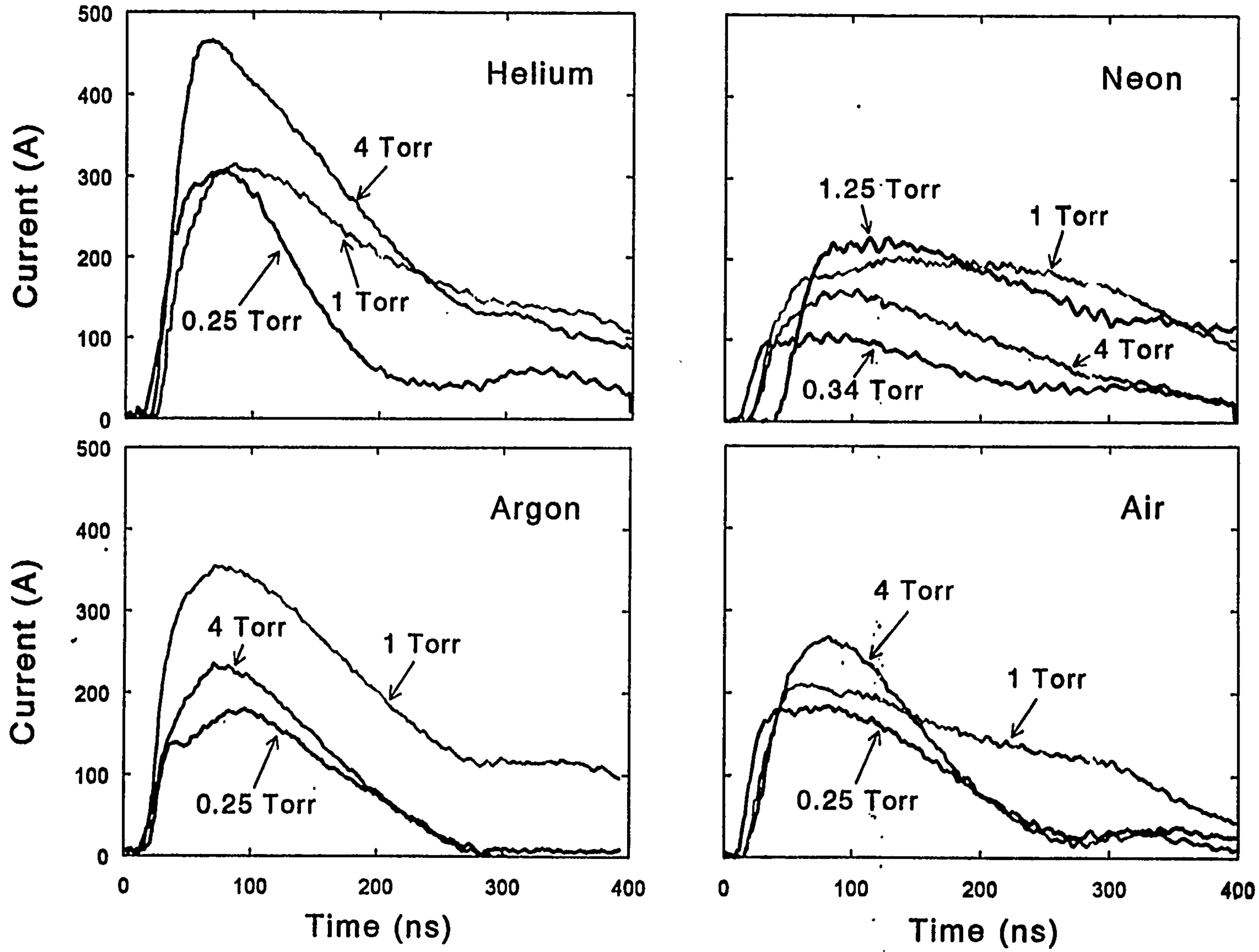

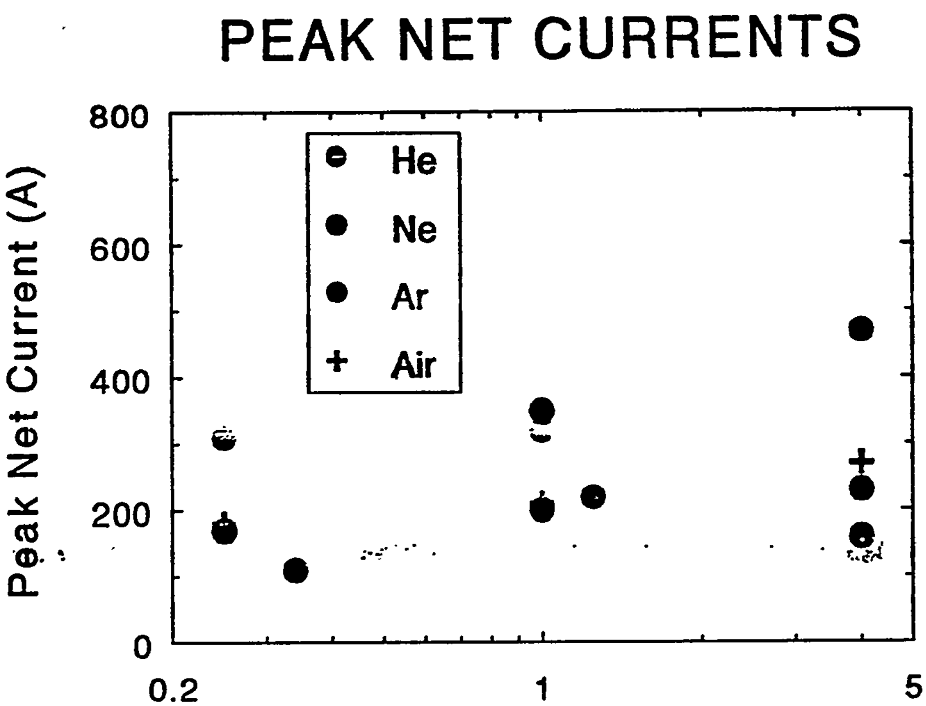
PEAK NET CURRENTS
Peak Net Current (A)
800
600
400
200
0
0.2
1
5
He
Ne
Ar
Air

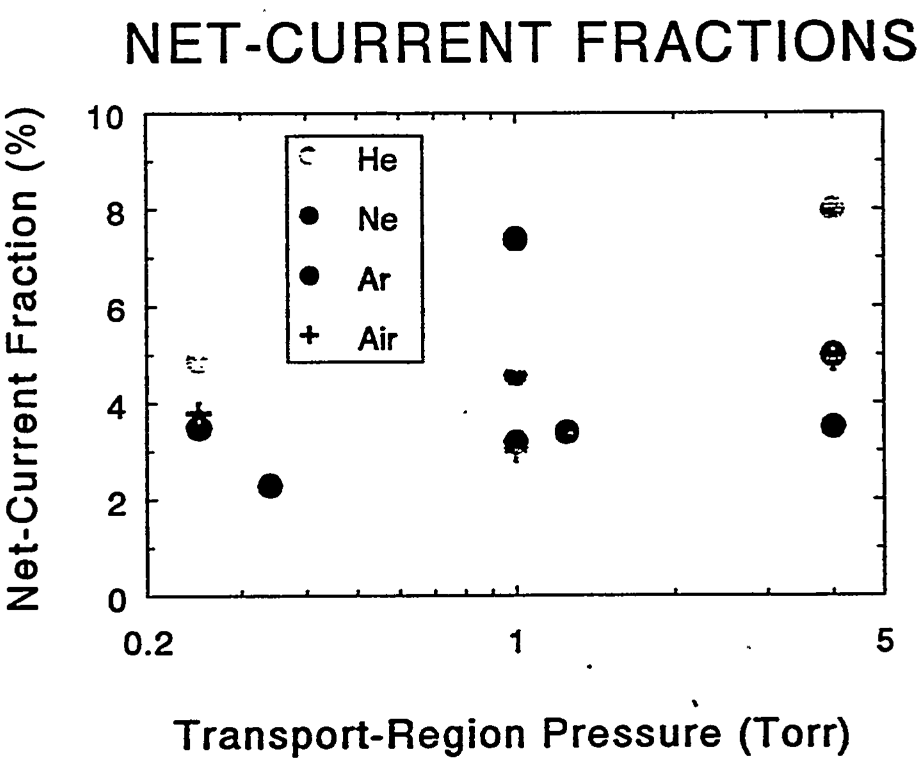
NET-CURRENT FRACTIONS
Net-Current Fraction (%)
10
8
6
4
2
0
0.2
1
5
He
Ne
Ar
Air
Transport-Region Pressure (Torr)

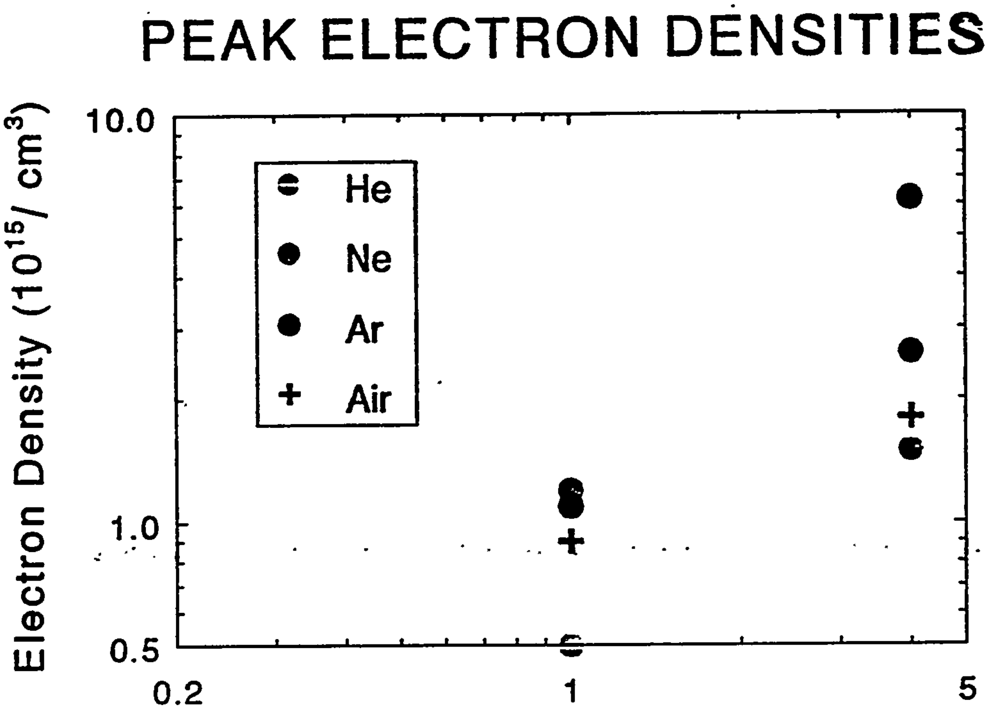
PEAK ELECTRON DENSITIES
Electron Density (10^{15}/ cm^3)
10.0
1.0
0.5
0.2
1
5
He
Ne
Ar
Air

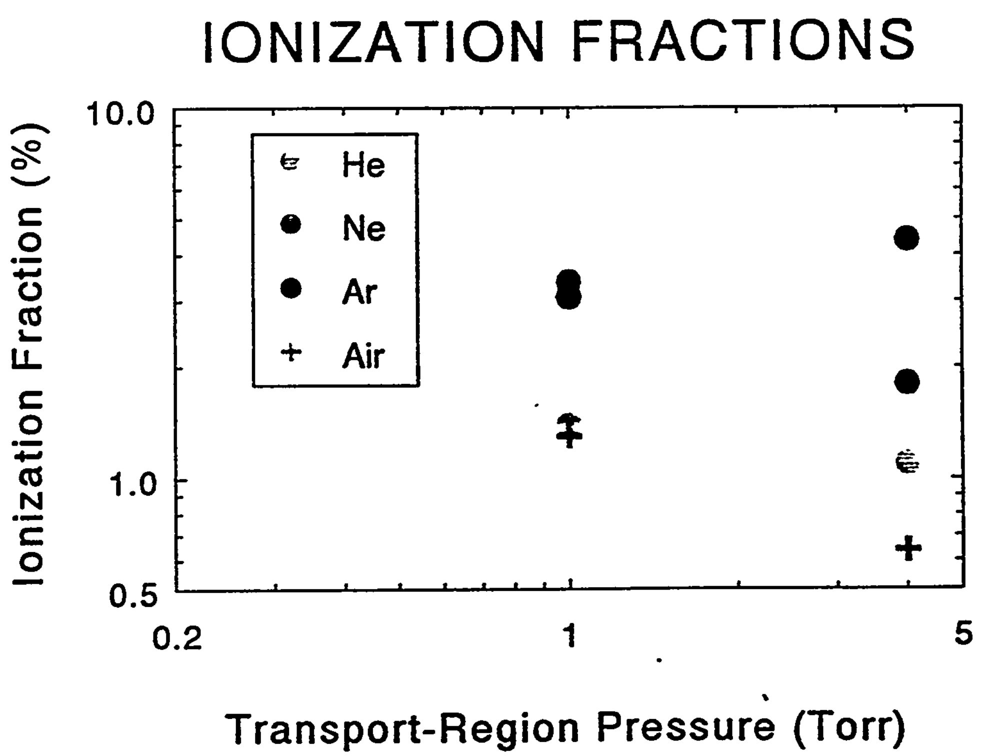
IONIZATION FRACTIONS
Ionization Fraction (%)
10.0
1.0
0.5
0.2
1
5
He
Ne
Ar
Air
Transport-Region Pressure (Torr)

Measured electron densities are consistent with ion impact ionization as the dominant mechanism

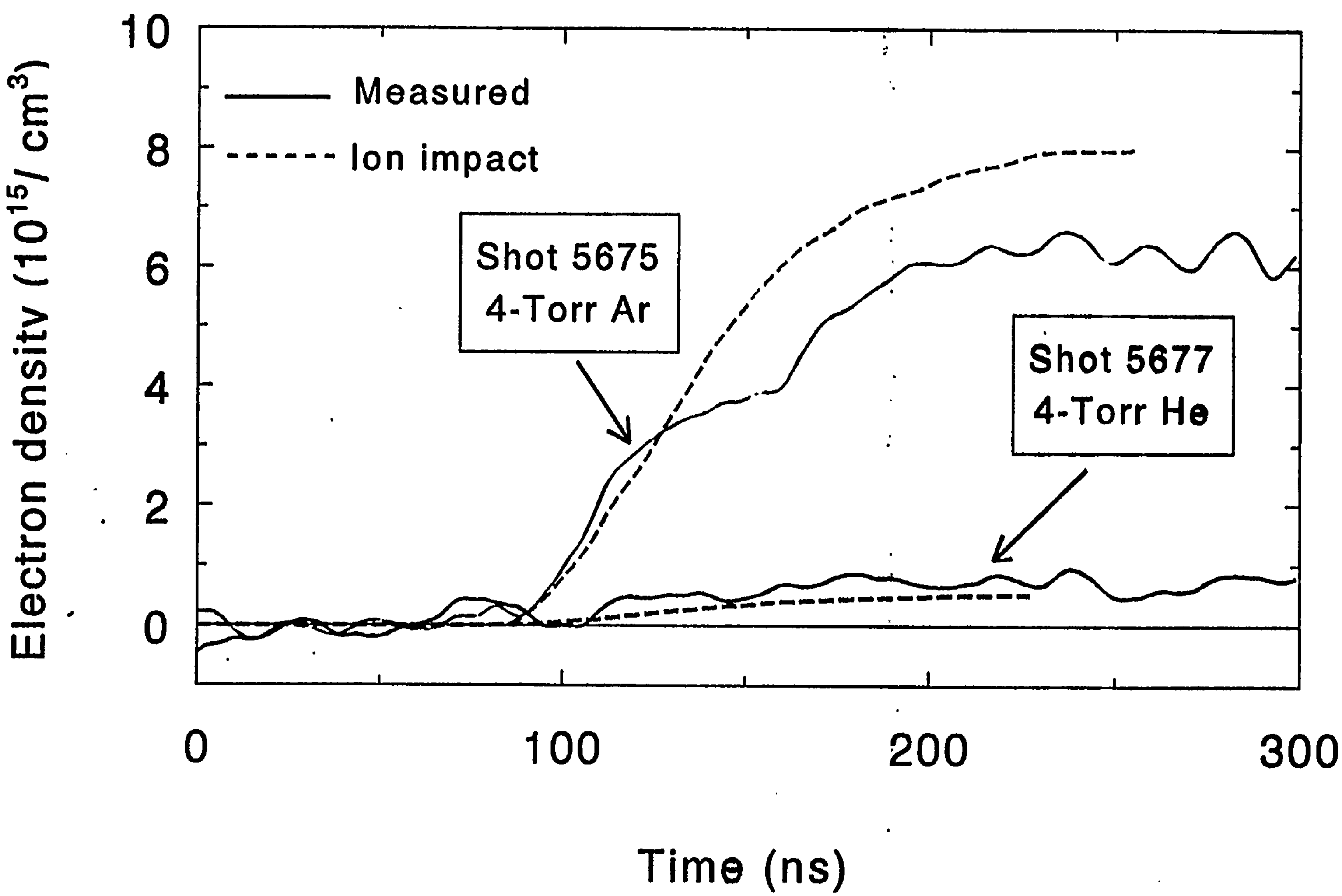

CODES TO SIMULATE ION-BEAM/GAS INTERACTION

DYNAPROP	IPROP
1-D Resistive Model (axially resolved)	3-D Hybrid Model
Thermal electrons - fluid Beam ions - envelope and emittance equations	Thermal electrons - resistive medium Beam ions and fast electrons - particles
Rate equations for n_e, T_e and σ	Rate equations for n_e and n_i
Net current from circuit equation	Maxwell's equations for fields
Effective net current - radially averaged, weighted by ion current	Radially resolved net current

NET-CURRENT COMPARISONS WITH THEORY

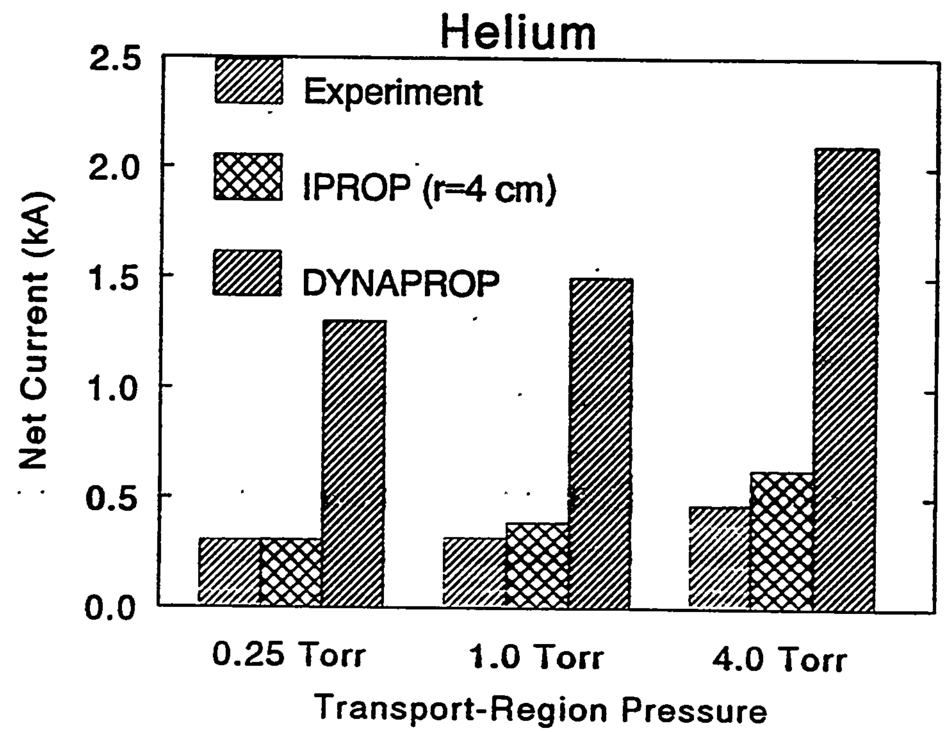

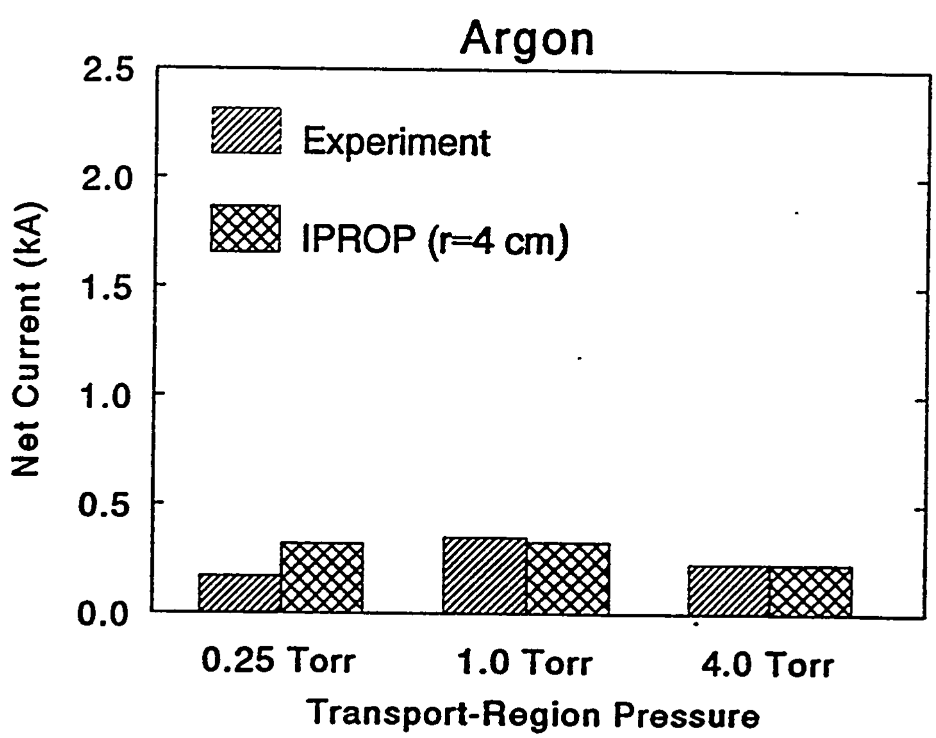

Radial profile has large net current within the beam envelope

IPROP Profiles for helium at monitor location 70 ns after beam starts

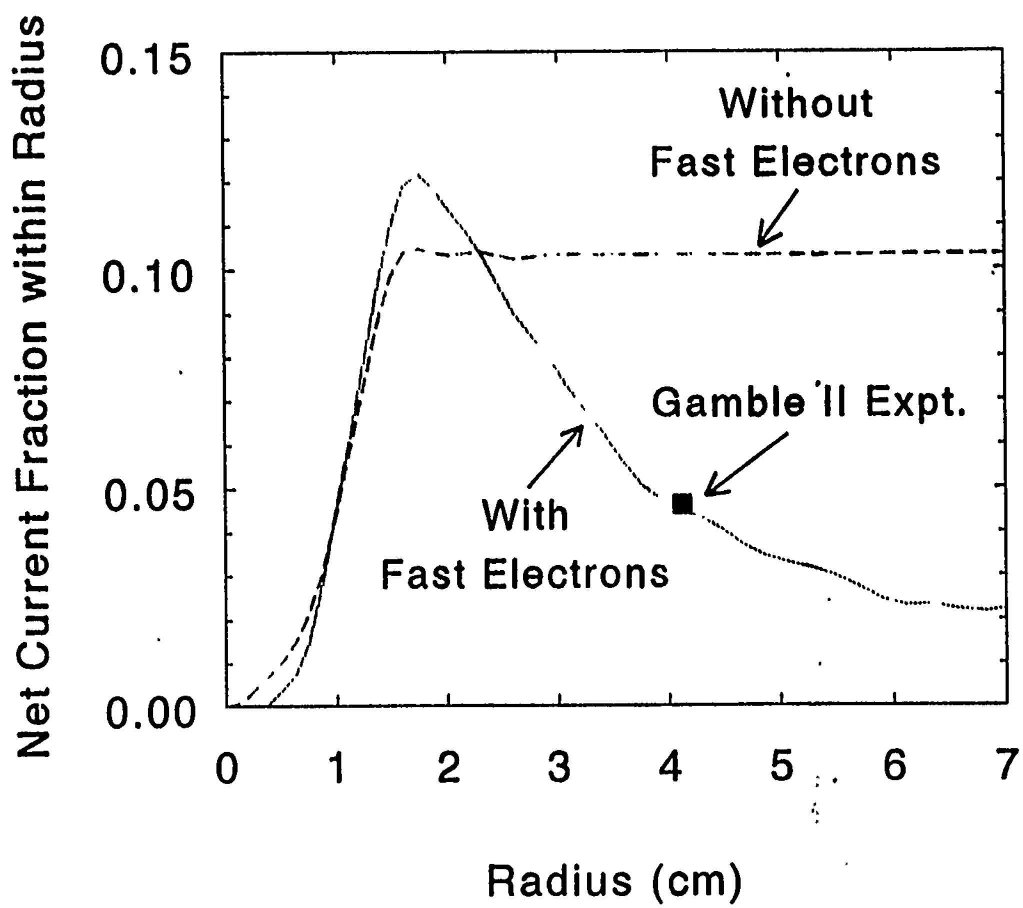

DENSITY COMPARISONS WITH THEORY

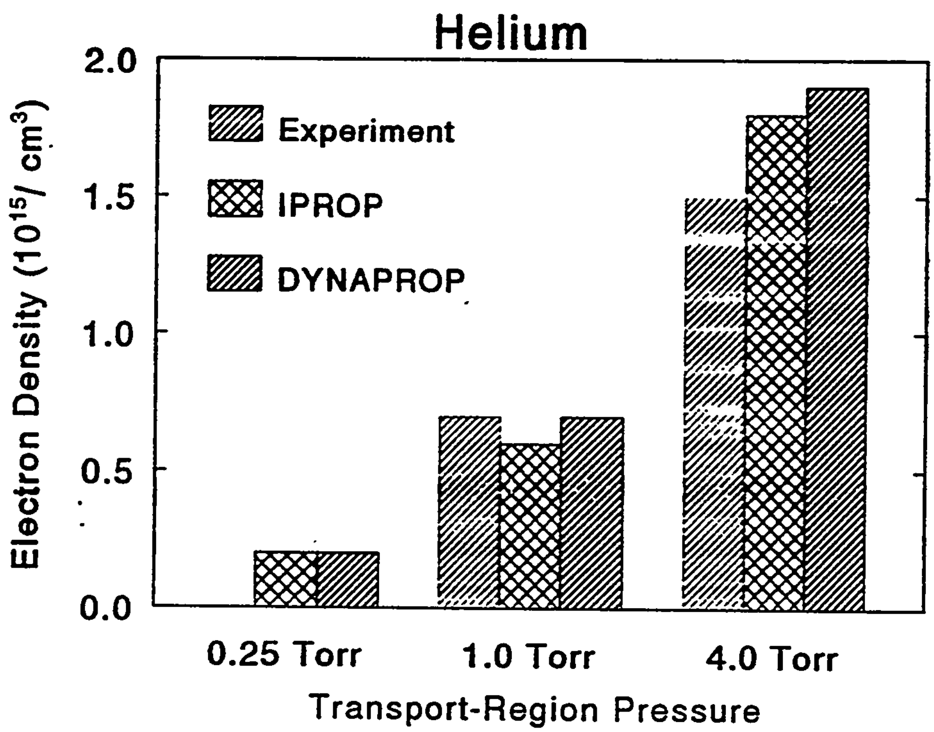

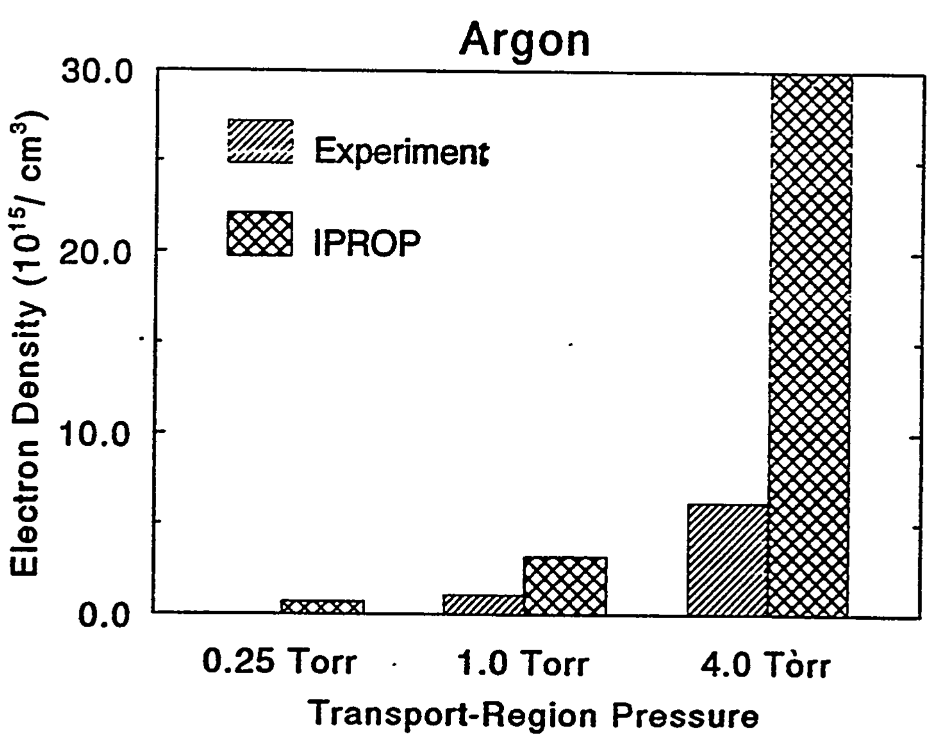

CONCLUSIONS

NET CURRENTS:

- The net currents are only weakly dependent on the background gas pressure in the range from 0.25 to 4 Torr.

- Net currents are largest for helium: 300-400 A
  smaller for argon and air: 200-300 A
  smallest for neon: 100-200 A

- Gas-breakdown transport calculations with ionization by local processes (DYNAPROP) predict larger currents at the edge of the beam (R = 1.5 cm).

- Calculations including non-local plasma deposition and fast electrons (IPROP) are consistent with these net currents measured at R = 4 cm.

CONCLUSIONS CONTINUED

ELECTRON DENSITIES:

- The gases are only weakly ionized by the kA/cm^2 proton beam.
  Ionization fractions are $\leq$ 1 % for air,
  = 1-2 % for helium,
  = 2-4 % for neon, and
  = 3-4 % for argon.

- Measured densities are consistent with ion impact ionization as the dominant ionization process at this current density. For larger currents, avalanche is expected to be dominant.

- For helium, gas-breakdown transport calculations with IPROP and DYNAPROP are consistent with the measured electron densities.

- For argon, densities predicted by IPROP calculations are 3 to 5 $\times$ larger than the measured densities.

ISSUES FOR FUTURE EXPERIMENTS

- Measure magnetic fields (net currents) within the beam envelope to look for larger currents as predicted by IPROP.

- Understand the mechanism for energy losses observed at the front of the beam.

- Scale experiments to larger ion-beam current for ICF.
  - Ideal is zero net-current: ballistic transport.
  - For net-current fraction ~0.1%: ballistic transport with adjustment for ion-beam focusing.
  - For net-current fraction ~1%: self-pinched transport may be developed.

- Benchmark the code (IPROP) to give predictive capability to scale to MA ion currents required for ICF.

IPROP Gas Breakdown Simulations

D. R. Welch
Mission Research Corporation
1720 Randolph Rd, Albuquerque NM 87106

September 20, 1994

Presented at the Workshop on Transport for a Common Ion Driver

10

TALK OUTLINE

- Quick description of IPROP code
- Gas breakdown modeling
- Simulations of GAMBLE II

IPROP IS A FLUID-PARTICLE HYBRID CODE

- Electromagnetic fields with tensor conductivity associated with (< 100 eV) fluid electrons
- PIC description of energetic ions and electrons from collisions, runaway and injection sources
- 3D, Fourier analyzed in third dimension
- Self-consistent N_2, Ar and He chemistries
- Simple MHD model for plasma motion

IPROP NOW EMPLOYS A TWO-COMPONENT MODEL FOR PLASMA ELECTRONS

Electron with energies $E < 100$ eV are treated as a fluid with a temperature T_e, momentum transfer frequency ν_m, and avalanche rate α -- all functions of $|E|/p$ and p

Electron number density at each grid point is determined by

$$\frac{dn_e}{dt} = (Wv)^{-1} \sum_i f_i \frac{dE}{dt_i} N_i + \alpha n_e - R(E/p,p) + S$$

where

- dE/dt is the slowing down rate due to collisions
- W is the energy required per ionization pair
- f is the fraction of electrons born with $E < 100$ eV
- R is the sink due to runaway electrons in the presence of E
- S is the source due to PIC electrons slowing down below 100 eV

PIC electrons are created with $E > 100$ eV in a forward scattered ionization event and from the runaway source R, they are absorbed into the low temperature fluid as they slow down below 100 eV

Fluid modeling of plasma electrons

$$\frac{dv}{dt}=E+vxB-\nu v_m \quad with \quad v_{max}=\sqrt{\frac{\xi_{cut}}{2m}}$$

$$\frac{d\xi}{dt}=\frac{E^2}{\nu_m(1+\frac{\omega_c^2}{\nu_m^2})}-\xi\nu_e \quad with \quad \xi_{max}=\xi_{cut}$$

- electrons are assumed to either drift or free stream, i.e.
- Fluid quantities T_e, avalanche, runaway and V_m are calculated with swarm version of IPROP with neutral gas and uniform E/p. An effective E/p with magnetic fields is taken as

$$\frac{E}{p}=\sqrt{\frac{E_{\parallel}^2}{p^2}+\frac{E_{\perp}^2}{p^2}(1+\frac{\omega_c^2}{\nu_m^2})^{-1}}$$

HELIUM CHEMISTRY DERIVED FROM EXPERIMENT AND SWARM CALCULATIONS

Input cross sections used in IPROP Monte Carlo model to determine swarm parameters and rate of electron runaway, electrons were absorbed as they reached 100 eV

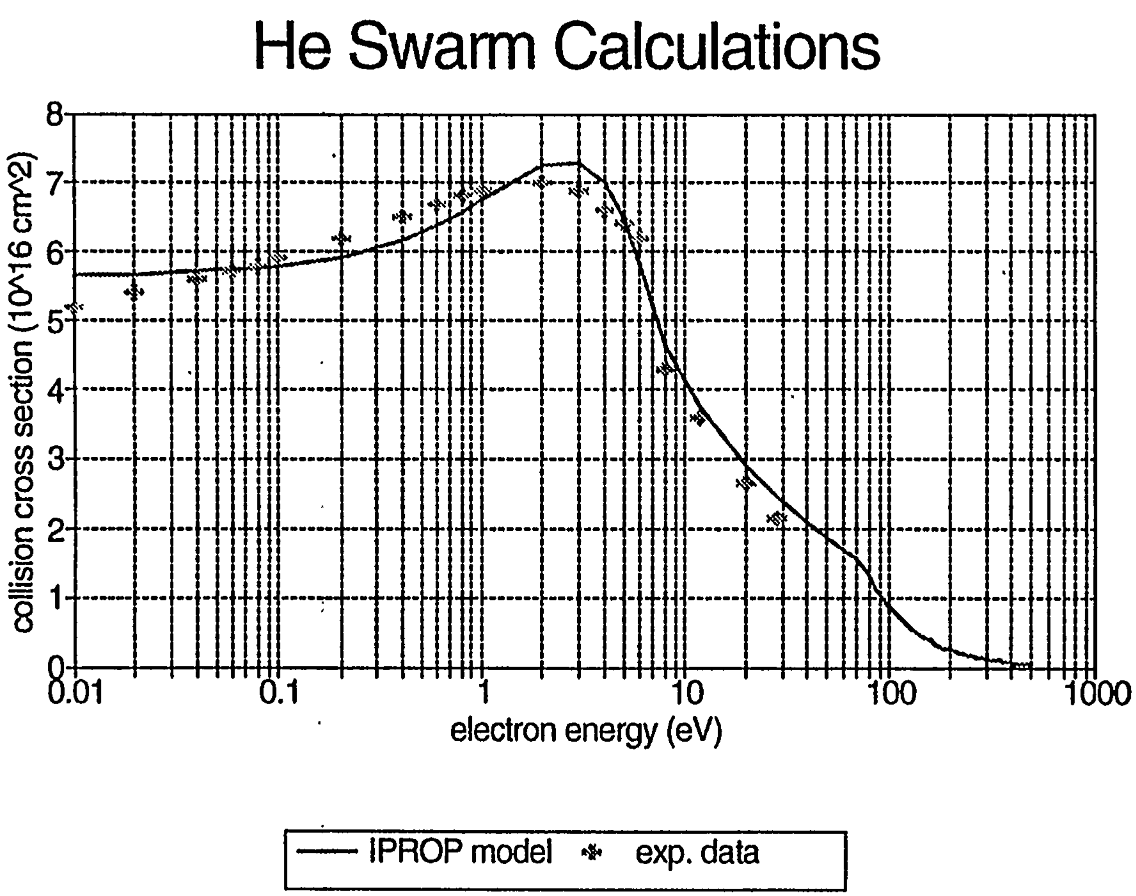

MOMENTUM TRANSFER FREQUENCIES IN ROUGH AGREEMENT WITH EXPERIMENT

strong electron runaway occurs for E/p > 150 kV/cm-atm

He Swarm Calculations

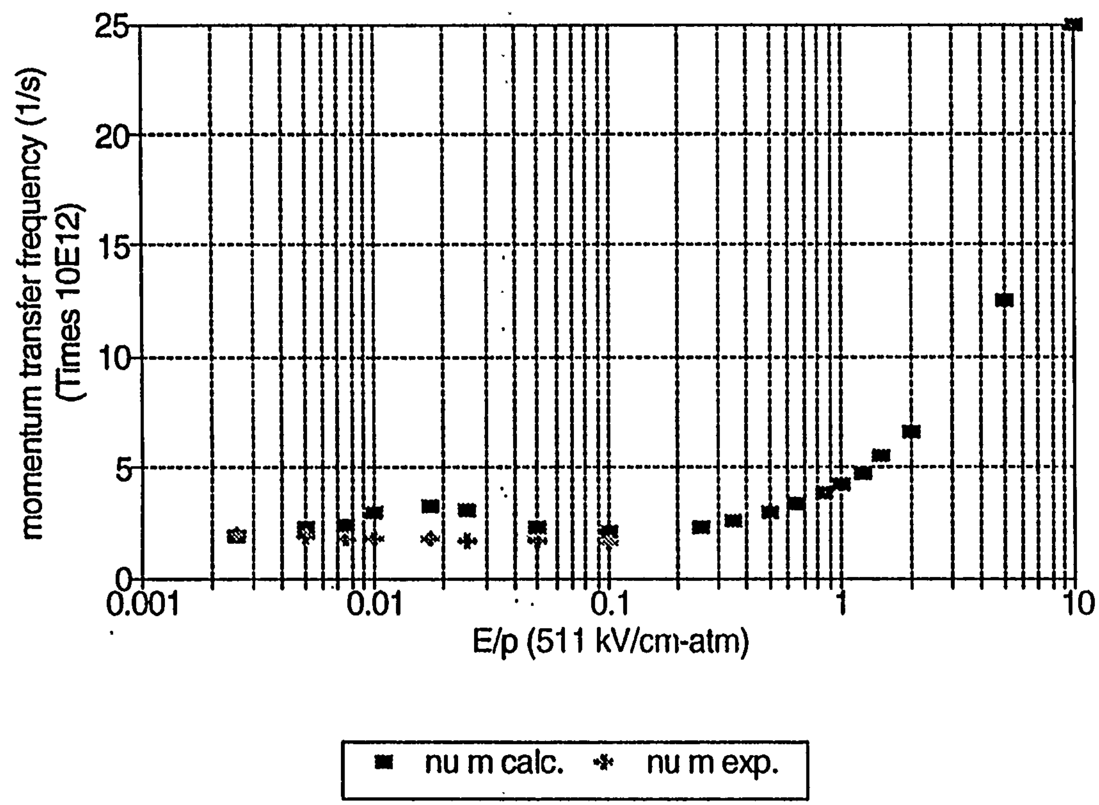

RUNAWAY SOURCE IS QUADRATIC IN E/p

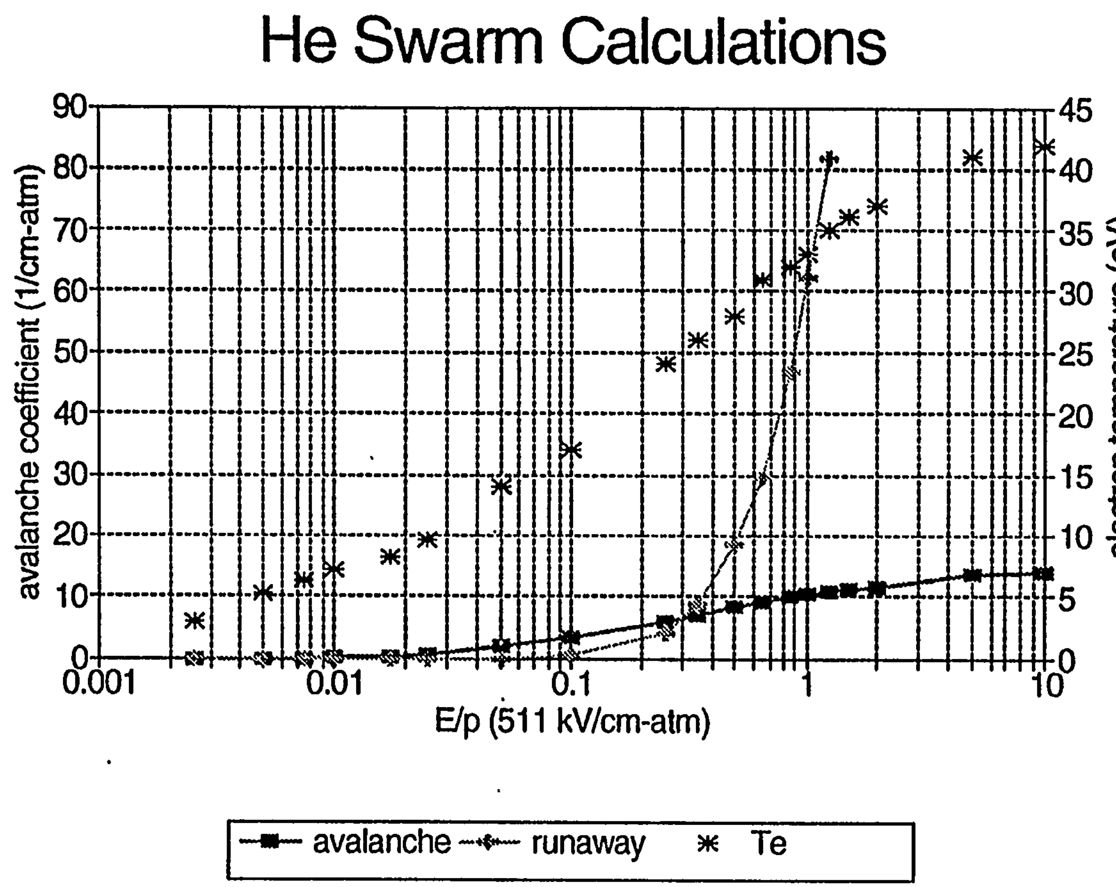

MAGNETIC FIELD EFFECTS ON CONDUCTIVITY IMPORTANT AS ω_c/ν_m NEARS UNITY

Conductivity parallel to **B**,

$$\sigma_{\parallel}=\frac{e^2 n_e}{m_e \nu_m}$$

where ν_m is from electron-neutral ($\nu^{e\text{-}n}$) and electron-ion ($\nu^{e\text{-}i}$) collisions

Conductivity perpendicular to **B**,

$$\sigma_{\perp}=\frac{\sigma_{\parallel}}{1+\left(\frac{\omega_c}{\nu_m}\right)^2}$$

ExB drift assuming uniform E and B

$$v_{ExB}=\frac{ExB}{B^2\left(1+\left(\frac{\nu_m}{\omega_c}\right)^2\right.}$$

Drifts obtained by modeling fluid with

$$J_p=\sigma(E+vxB),\ \frac{dv}{dt}=-v\nu_m+\frac{e}{m}(E+vxB)=0$$

IPROP SIMULATIONS OF 1-MV 6-kA GAMBLE II PROTON EXPERIMENT

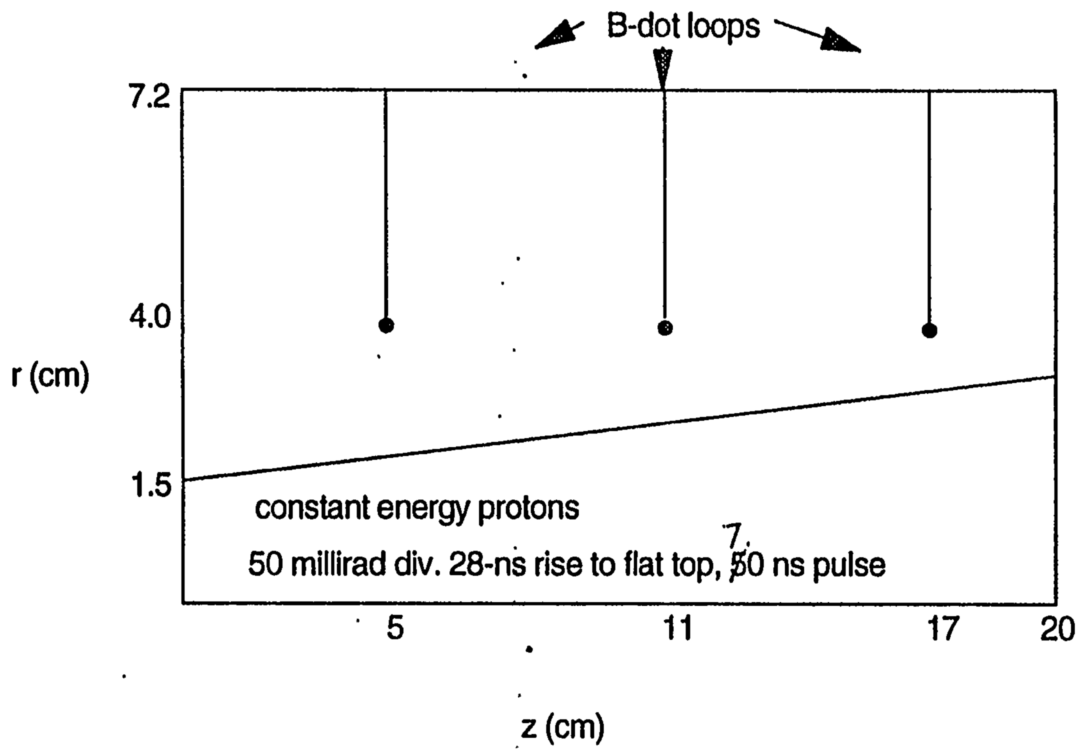

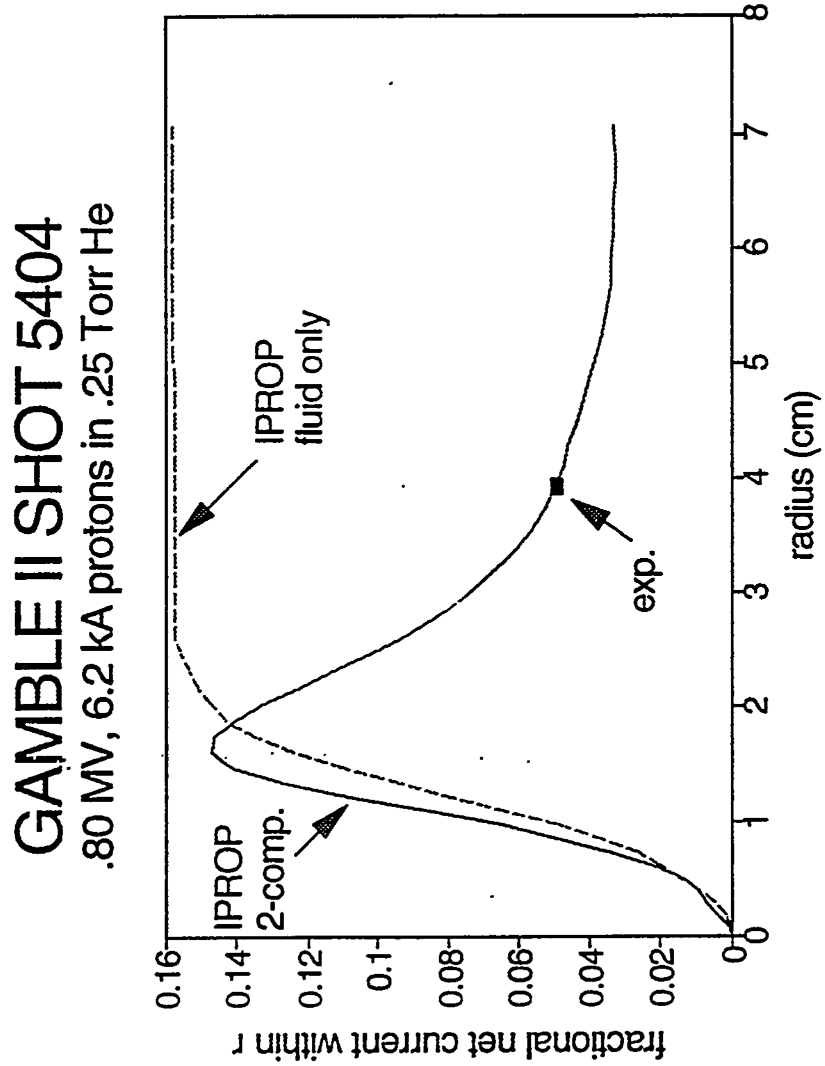

GAMBLE II SHOT 5404
.80 MV, 6.2 kA protons in .25 Torr He
IPROP
fluid only
IPROP
2-comp.
exp.
fractional net current within r
radius (cm)
0.16
0.14
0.12
0.1
0.08
0.06
0.04
0.02
0
0
1
2
3
4
5
6
7
8

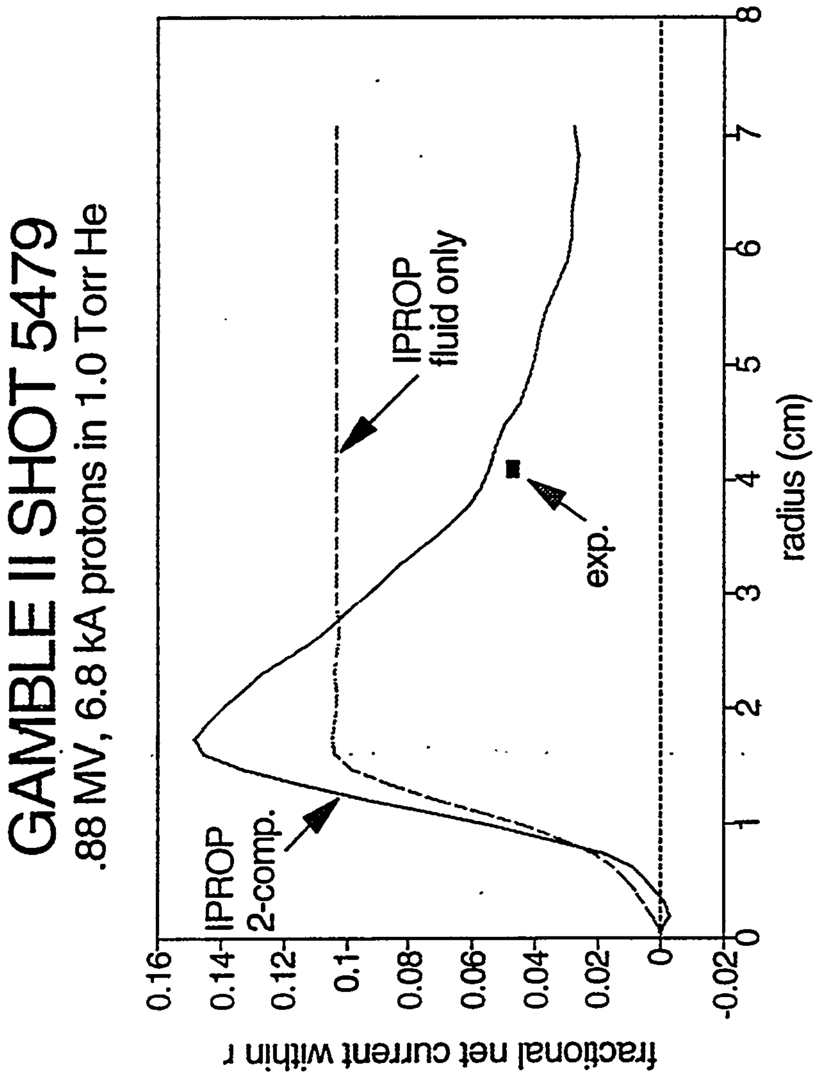
GAMBLE II SHOT 5479
.88 MV, 6.8 kA protons in 1.0 Torr He
IPROP 2-comp.
IPROP fluid only
exp.
fractional net current within r
radius (cm)
0.16
0.14
0.12
0.1
0.08
0.06
0.04
0.02
0
-0.02
0
1
2
3
4
5
6
7
8

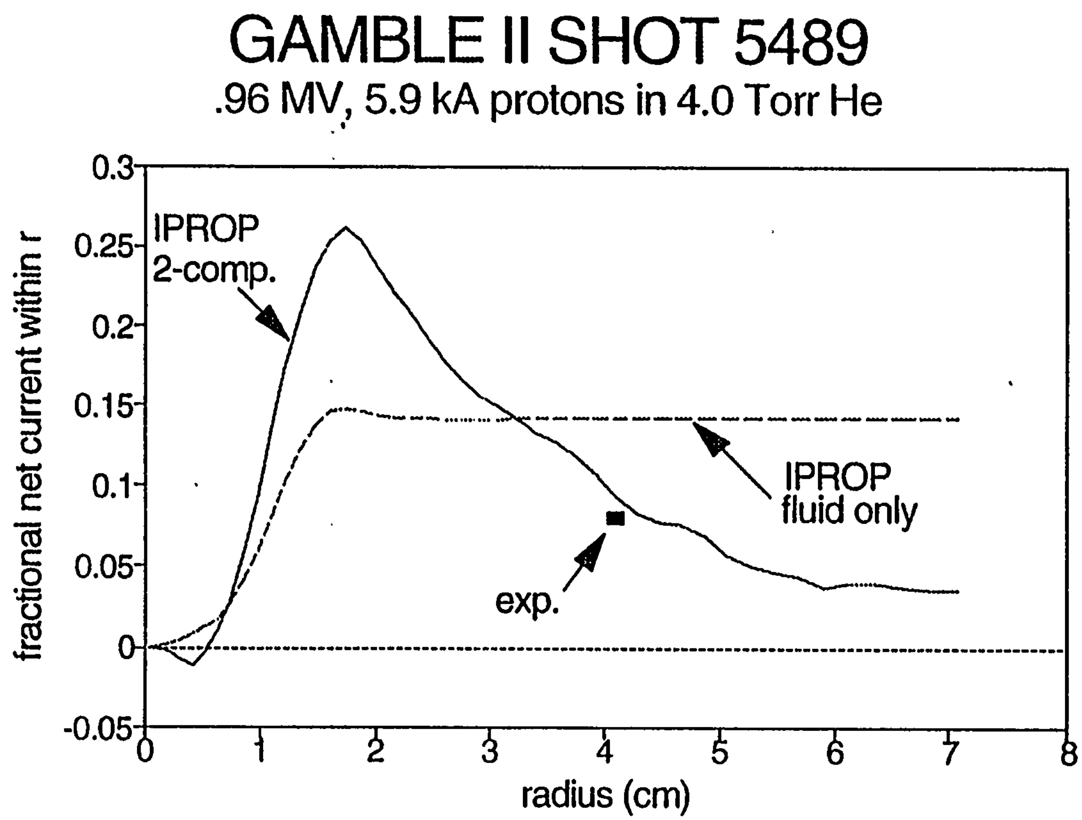
GAMBLE II SHOT 5489
.96 MV, 5.9 kA protons in 4.0 Torr He
fractional net current within r
radius (cm)
IPROP
2-comp.
IPROP
fluid only
exp.
0.3
0.25
0.2
0.15
0.1
0.05
0
-0.05
0
1
2
3
4
5
6
7
8

Net current at 4 cm radius shows initial jump with slow subsequent rise

- closely resembles experiment

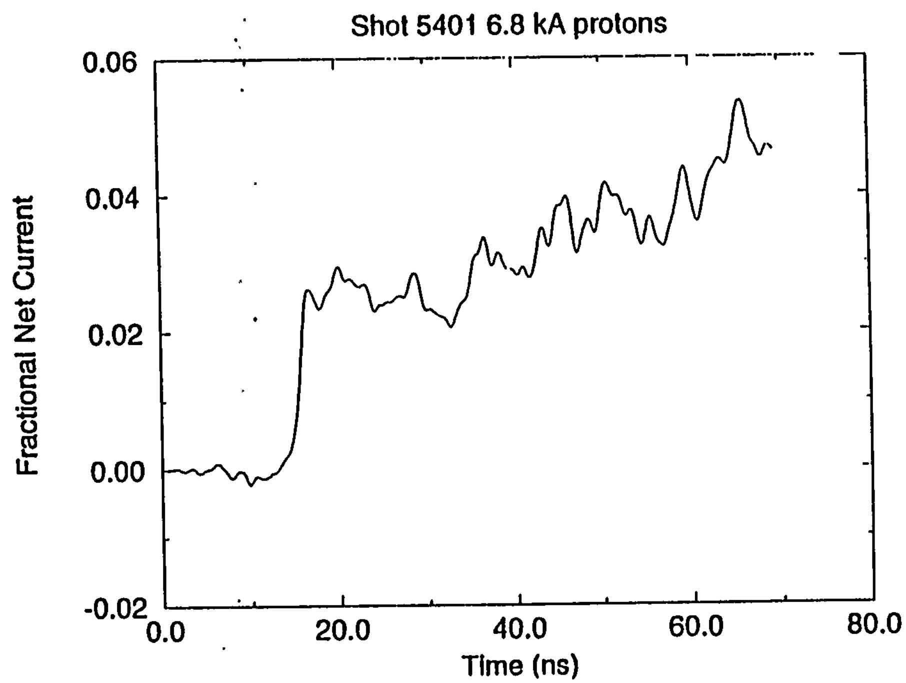

RUNAWAYS FORM HIGHLY CONDUCTIVE HALO ABOUT PROTON BEAM (Shot 5479)

t = 13 ns

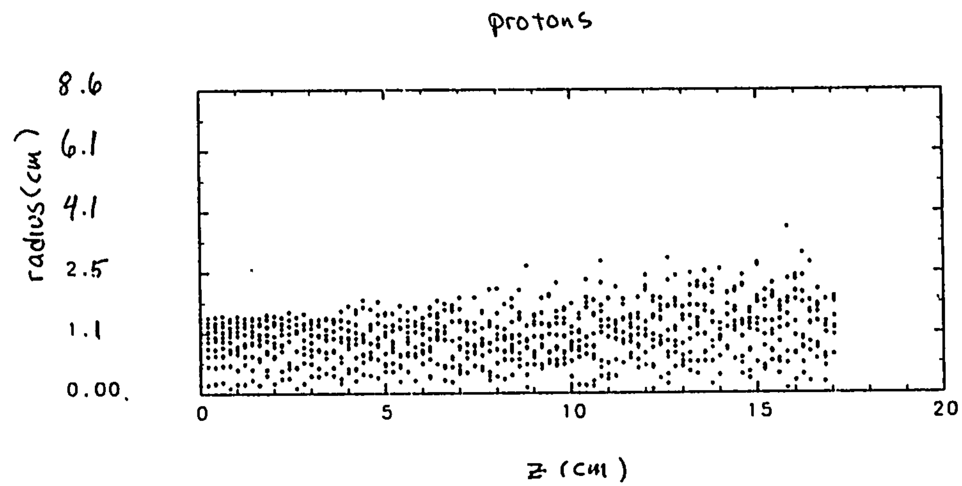

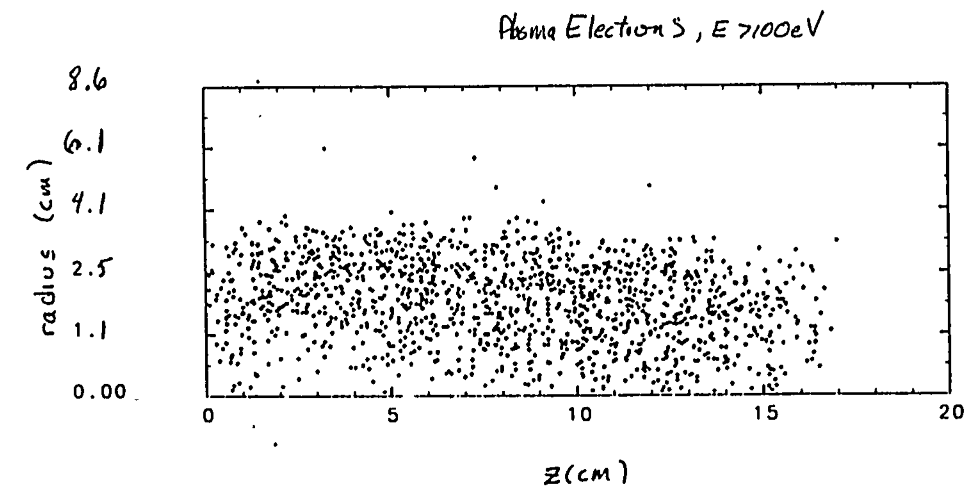

CONT.

t = 53 ns

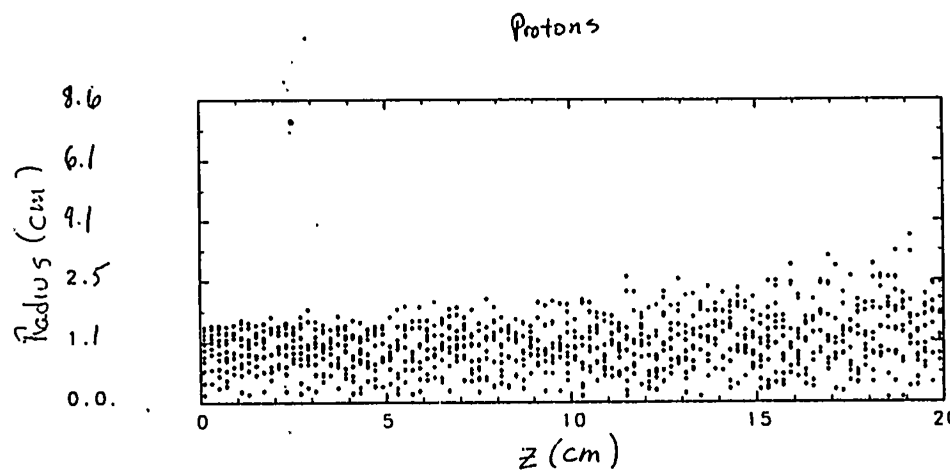

Protons
8.6
6.1
4.1
2.5
1.1
0.0.
Radius (cm)
0
5
10
15
20
Z (cm)

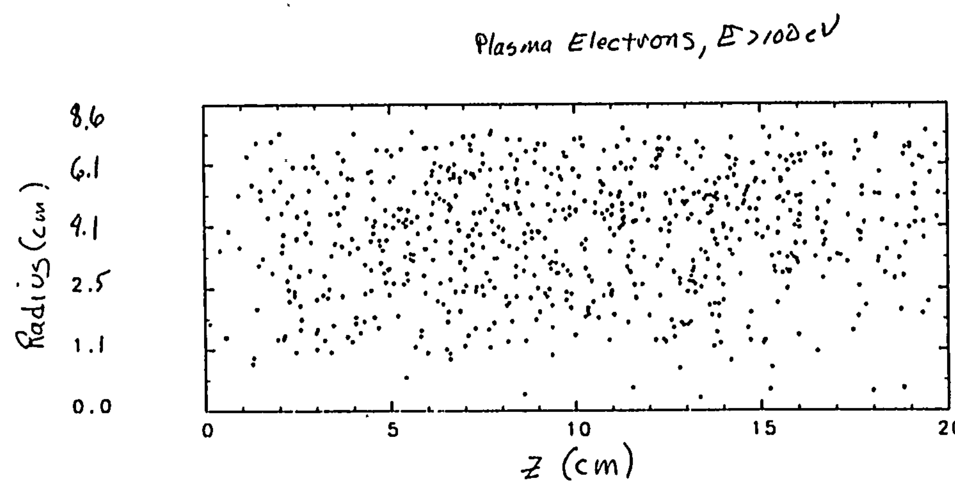

Plasma Electrons, E>100eV
8.6
6.1
4.1
2.5
1.1
0.0
Radius (cm)
0
5
10
15
20
Z (cm)

INCLUDING ENERGETIC ELECTRONS REDUCES NET CURRENTS AT LARGE RADIUS

Energetic weakly-collisional electrons are ejected radially from beam

At larger radius with smaller magnetic fields, energetic electrons are highly conductive

Energetic electrons deposition their energy at larger radius creating more secondaries

Conductive electron halo causes magnetic fields to diffuse much slower at the larger radii

"TRANSVERSE B EFFECTS" B. OLIVER

(PRESENTED BY P. OTTINGER)

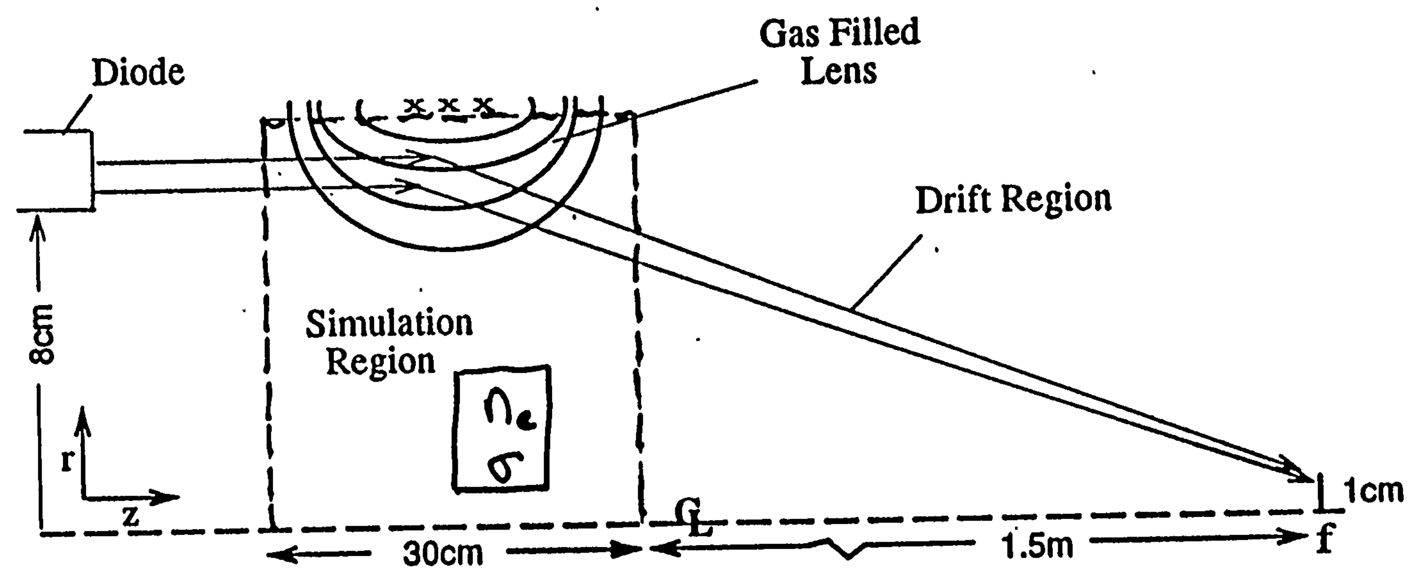

11

Analysis assumes:

- immobile background ions ($v_A \tau_b \ll r_b$)
- inertialess e^- fluid (collisional)
- particle beam ions
- quasineutrality ($n_e = Z_b n_b + Z_i n_i$)
- axisymmetry

Equations:

Ohm's Law $\quad \underset{\sim}{j_e} = \sigma \left(\underset{\sim}{E} + \frac{1}{c} \underset{\sim}{v_e} \times \underset{\sim}{B} \right)$

Faraday's Law $\quad \underset{\sim}{\nabla} \times \underset{\sim}{E} = - \frac{1}{c} \frac{\partial B}{\partial t}$

Ampere's Law $\quad j_e = \frac{c}{4\pi} (\underset{\sim}{\nabla} \times \underset{\sim}{B}) - j_b \qquad \left(\frac{\partial E}{\partial t} \to 0 \right)$

- Solving for magnetic field yields

$$\frac{\partial B}{\partial t} = \underbrace{\nabla \times V_e \times \underset{\sim}{B}}_{\text{advection}} - \underbrace{\nabla \times \eta \left(\nabla \times B - \frac{4\pi}{c} j_b \right)}_{\text{diffusion}}$$

where $\eta = \frac{c^2}{4\pi\sigma}$ is the magnetic diffusivity

- Advection dominates if η is small

⇒ "beam will act as a diamagnetic body and drag the trapped magnetic field with it"

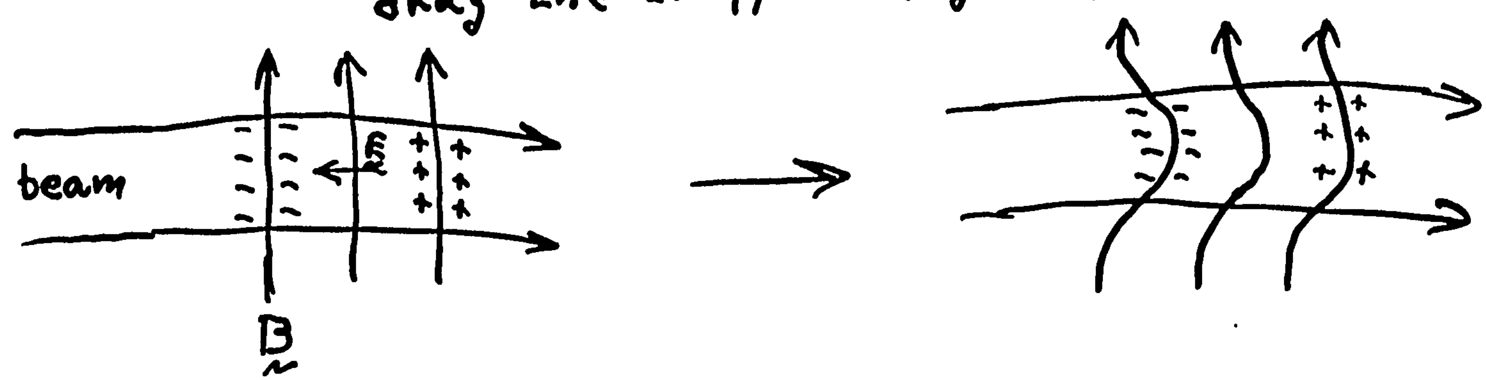

— Requiring the diffusive velocity $\left[\frac{d}{dt}\left(c^2 t/4\pi\sigma\right)^{1/2} \sim \frac{1}{2}\eta\tau_b^{-1/2}\right]$ to be greater than the e^- drag velocity $\left[v_e \sim \frac{n_b}{n_e} v_b \right]$

$$\Longrightarrow \quad \sigma < \sigma^* = \frac{1}{8\pi}\left(\frac{n_e}{n_b}\right)^2\left(\frac{c}{v_b}\right)^2\frac{1}{\tau_b}$$

(not to be confused with σ^* for filamentation)

— Thus,

for $\sigma > \sigma^*$ advection limits focusing

for $\sigma << \sigma^*$ resistive diffusion of the return current exposes the beam current and distorts focusing

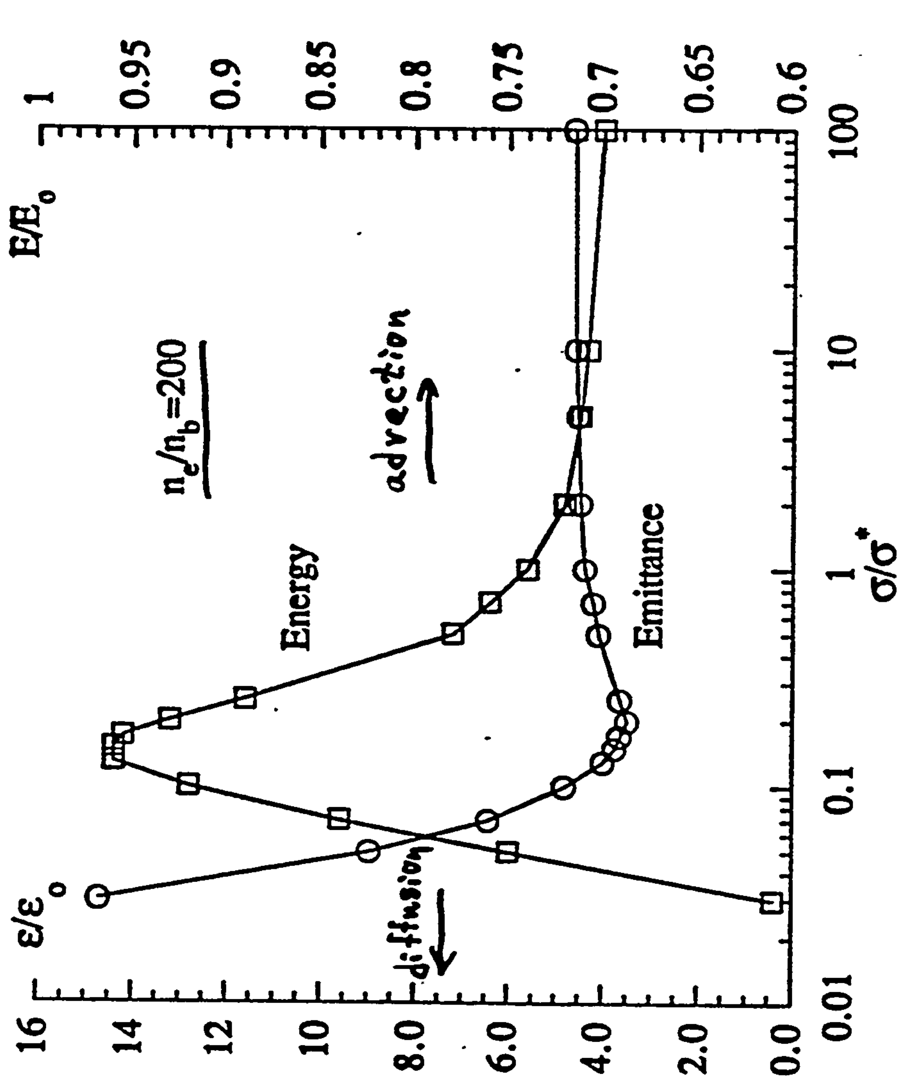
ε/ε$_o$
E/E$_o$
n_e/n_b=200
advection
diffusion
Energy
Emittance
σ/σ*
16
14
12
10
8.0
6.0
4.0
2.0
0.0
1
0.95
0.9
0.85
0.8
0.75
0.7
0.65
0.6
0.01
0.1
1
10
100

size of distortion is a function of distance the e^- are displaced during beam transport

⇒ **distortion (defocusing) decreases as $\frac{n_e}{n_b}$ increases**

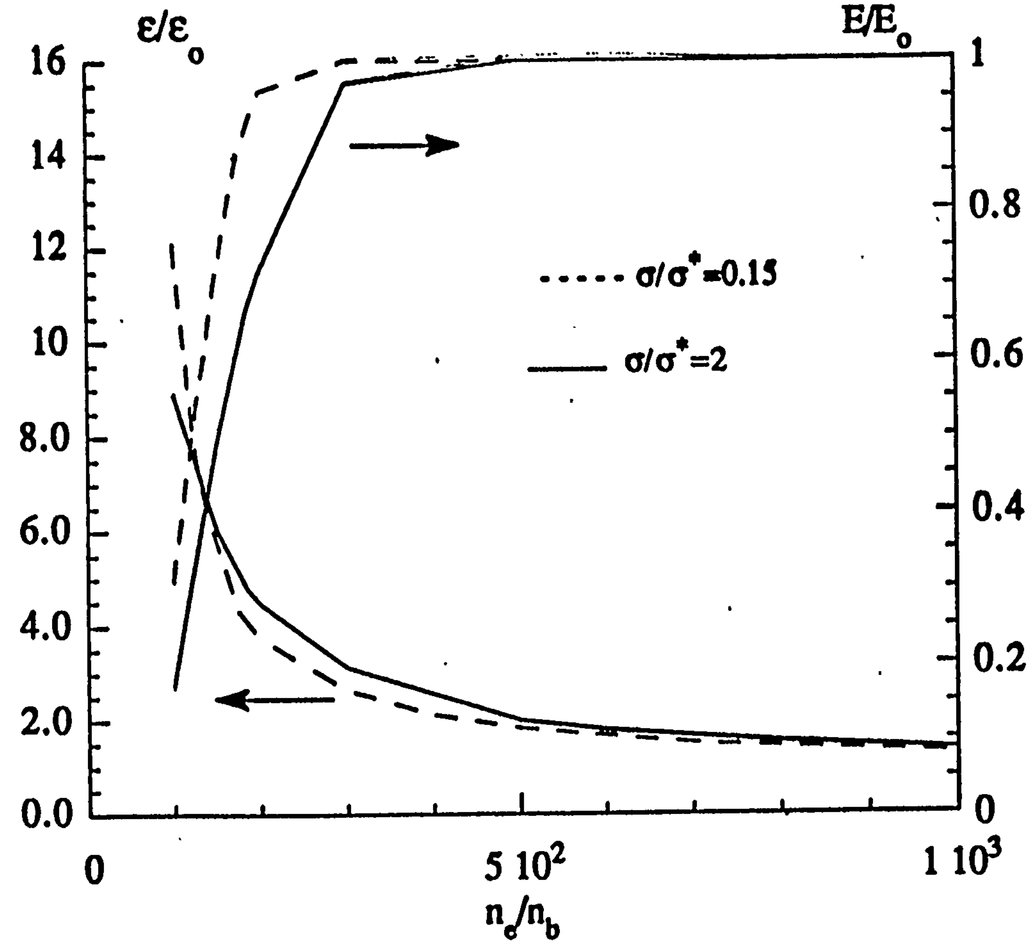

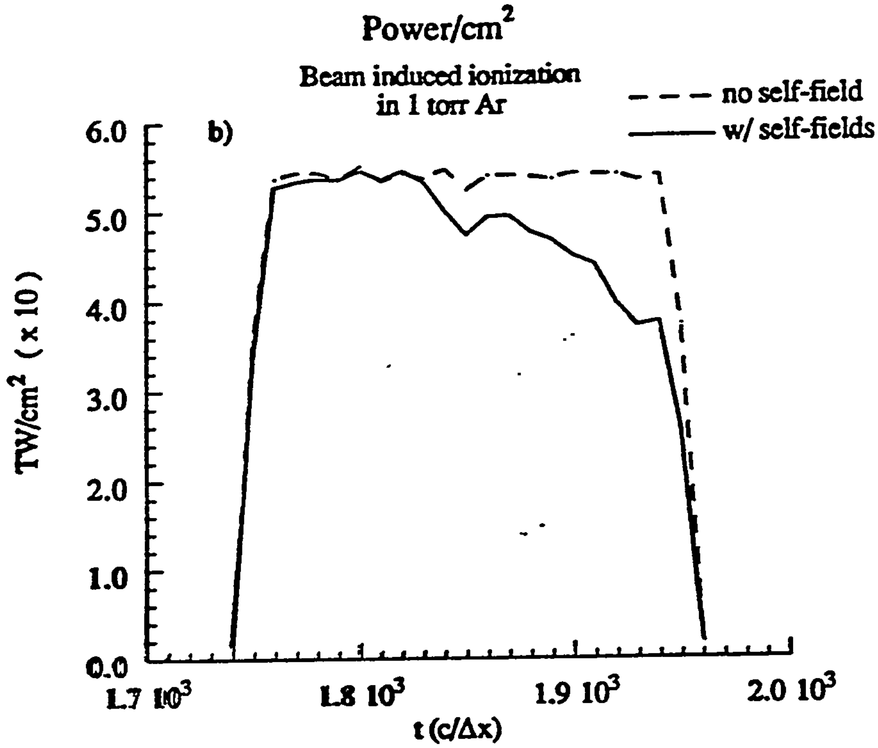
Power/cm²
Beam induced ionization
in 1 torr Ar
no self-field
w/ self-fields
b)
TW/cm² (x 10)
6.0
5.0
4.0
3.0
2.0
1.0
0.0
1.7 10³
1.8 10³
1.9 10³
2.0 10³
t (c/Δx)

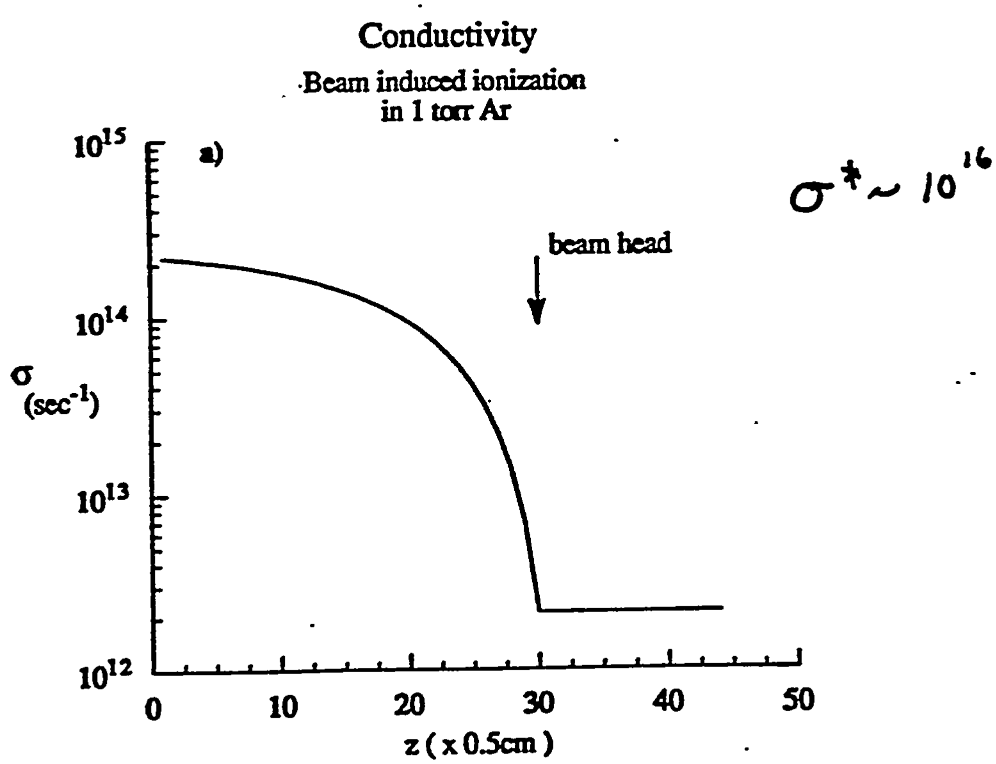
Conductivity
Beam induced ionization
in 1 torr Ar
a)
beam head
σ
(sec⁻¹)
10¹⁵
10¹⁴
10¹³
10¹²
0
10
20
30
40
50
z (x 0.5cm)
σ* ~ 10¹⁶

CONCLUSIONS

- High density ($n_e/n_b \gtrsim 500$), high conductivity plasma ($\sigma > 10^{13}\,s^{-1}$) greatly reduced self-field defocusing

- Tail of beam affected by frozen in field from early time ionization of gas (maybe preionize)

- Sharp beam fronts in high conductivity plasma ($\nu_e < \Omega_e$) may drive whistlers + distort field

12

Self-Pinched Transport of Heavy Ions

E. Lee, K. Hahn
Lawrence Berkeley Laboratory

Workshop on Transport for a Common Ion Driver

Sandia National Laboratory

September 20-21, 1994

Ballistic Final Focus

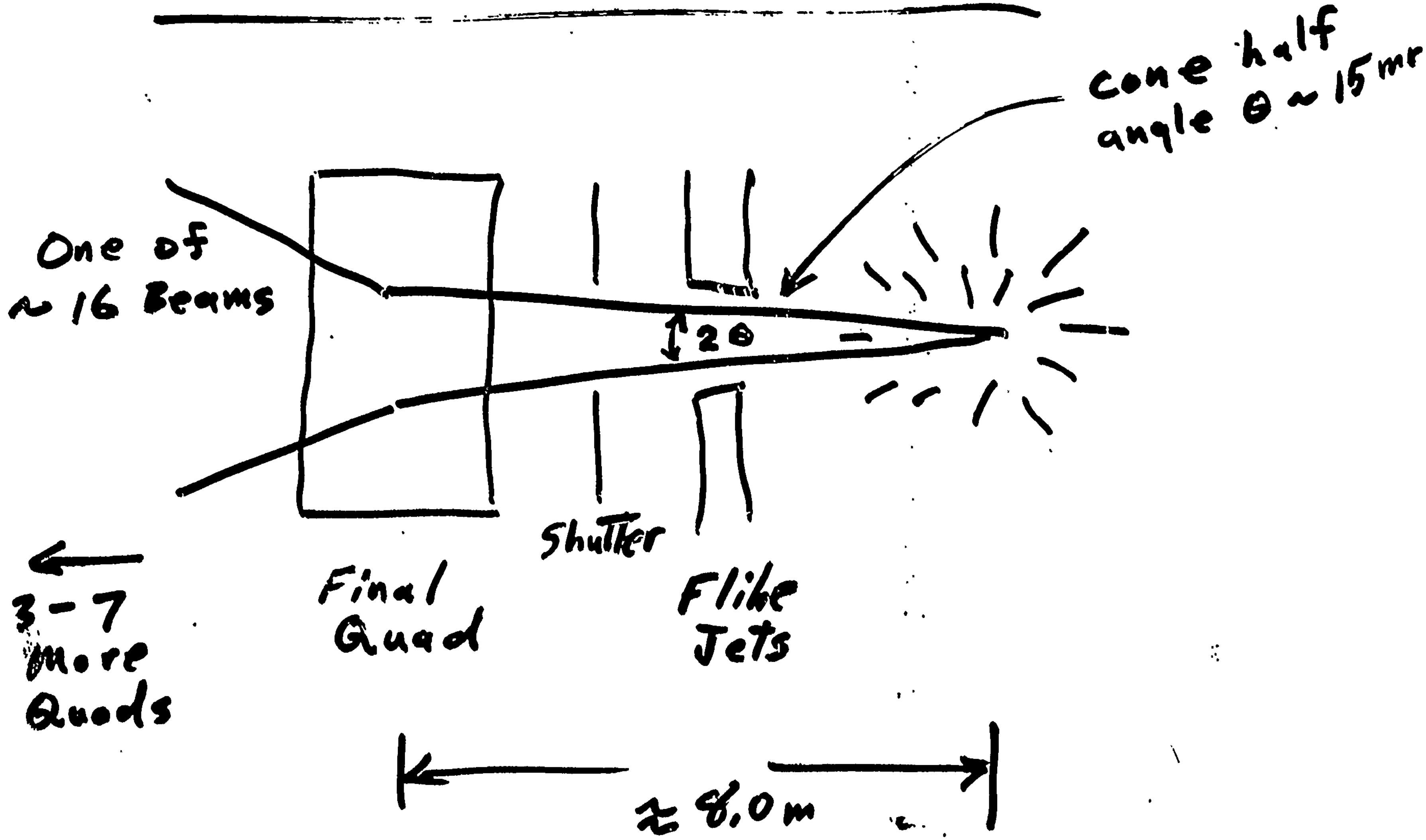

Typical Final Beam Parameters:

Total Energy	W =	5.0 MJ
Ion Type	Cs^{+}	A = 132.9 amu
Ion Range	R =	.1 gm/cm^2
Ion Energy	E =	5.33 GeV
Spot Radius	r_s =	2.0 mm
Gain	G =	90
Yield	Y = WG =	450 MJ
Peak Power	P =	480 TW

{Two Sided Indirect Drive}

See R. Bangerter + D. Ho
Proc. 1990 Linac Conf.
also HIFAN-470

Beam Parameters – Cont.

Assume There are $N = 16$ beams & We Use 12 For Peak Power

$$\text{Current Per Beam} = \frac{P}{12\,E} = \frac{480\,TW}{12 \times 5.33\,GV} = \underline{7.5\,kA}$$

This has been compressed by an order of magnitude in final ~400 m

Current/beam in Linac $= \underline{750 \text{ Amperes}}$

Ballistic Final Focus Has Some Unpleasant Features

Large Magnets → $$ + Space

Gas Load From Chamber → Shutters

Neutrons + Xrays up Beam Line

Momentum Spread $\lesssim$ Few $\times 10^{-4}$ in Accelerator

Neutralization May be Needed

Effects of Stripping Poorly Known

A Typical Beam Cone $\frac{1}{2}$ Angle

$\Theta = .015$ Radians

Larger Θ: Good For Emittance

Good For Space Charge

Bad For Chromatic Aberation

Bad For Geometric Aberation

Bad For Flux of { Neutrons, Gas, X rays }

Bad For Magnet Size

Maximum Beam Radius in Final Focus $\approx 3F\Theta = 3 \times 8 \times .015$

$= .32\ m$

Drift- Compression Lines ~400m Long

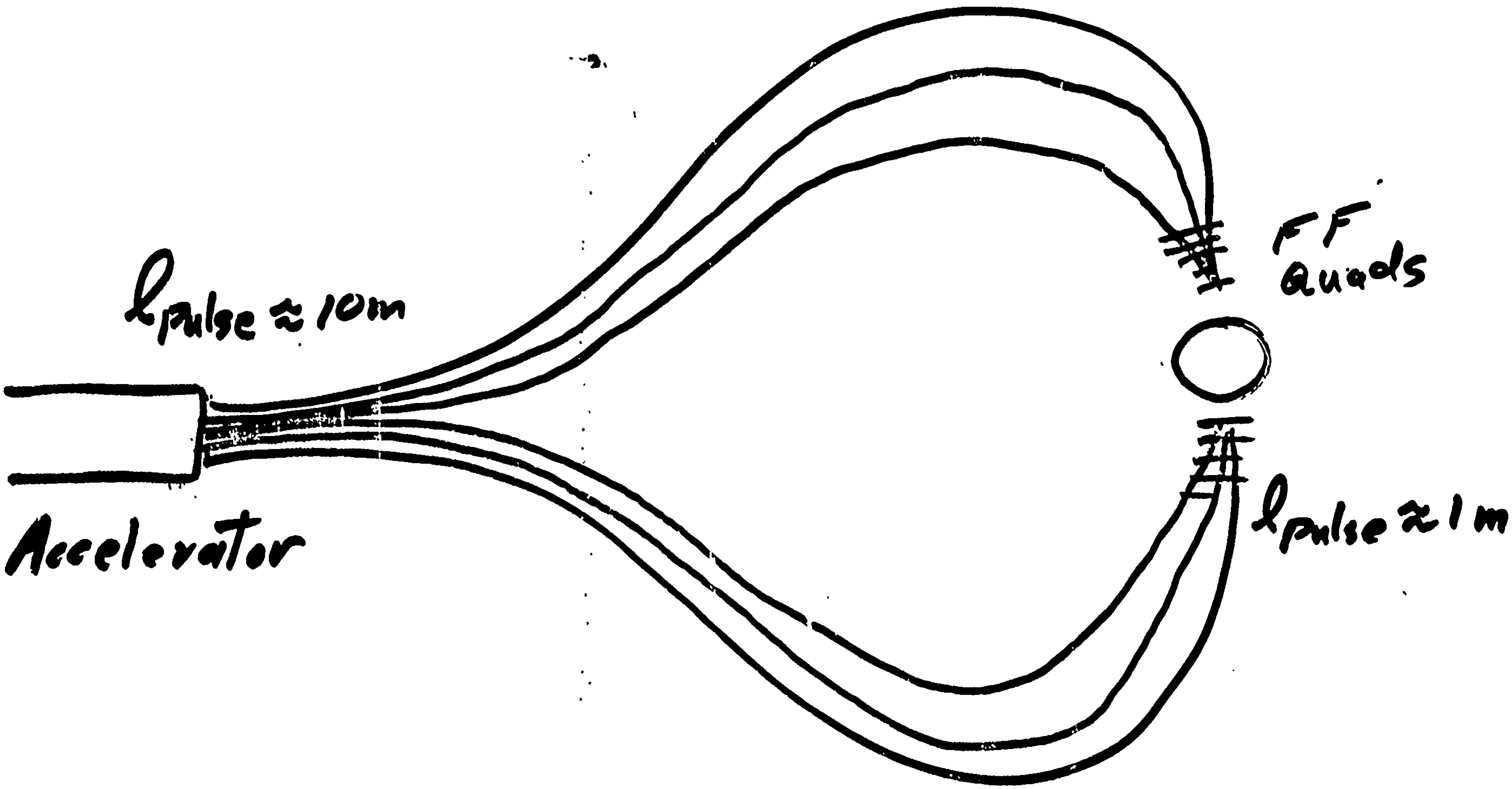

"Velocity Tilt" To Compress $\frac{\Delta v}{v} \approx \frac{10\,m}{400\,m} = 2.5\%$

Can Final Focus Be Moved ~400 m Upstream ??

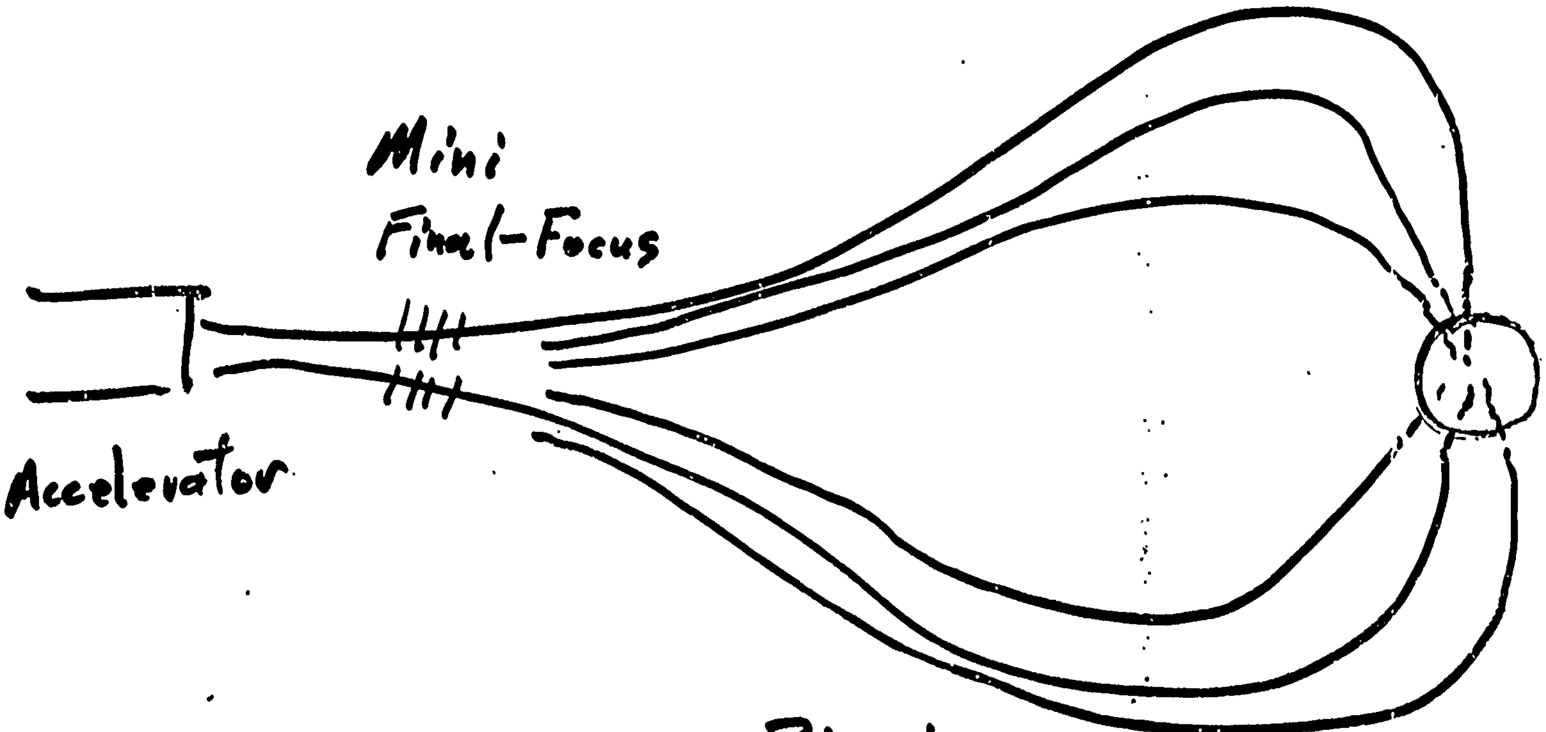

Pinched Transport
in small Pipes
+ Drift Compression

The Mini Final Focus Has Obvious Benefits

Lower current by ×10 → Dont Neutralize

No Neutrons

Low Gas Load

Reduce Focal Length to 1 – 2 m → Much Smaller Magnets

Momentum Spread In Accelerator Increased ×50–100 → stability + Lower Cost

Mini - Final Focus   5.3 GeV Cs^{+}

$B\rho = 122$ T-m

Try Focal Length $F = 1.5$ m
Half Angle $\Theta = 15$ mr

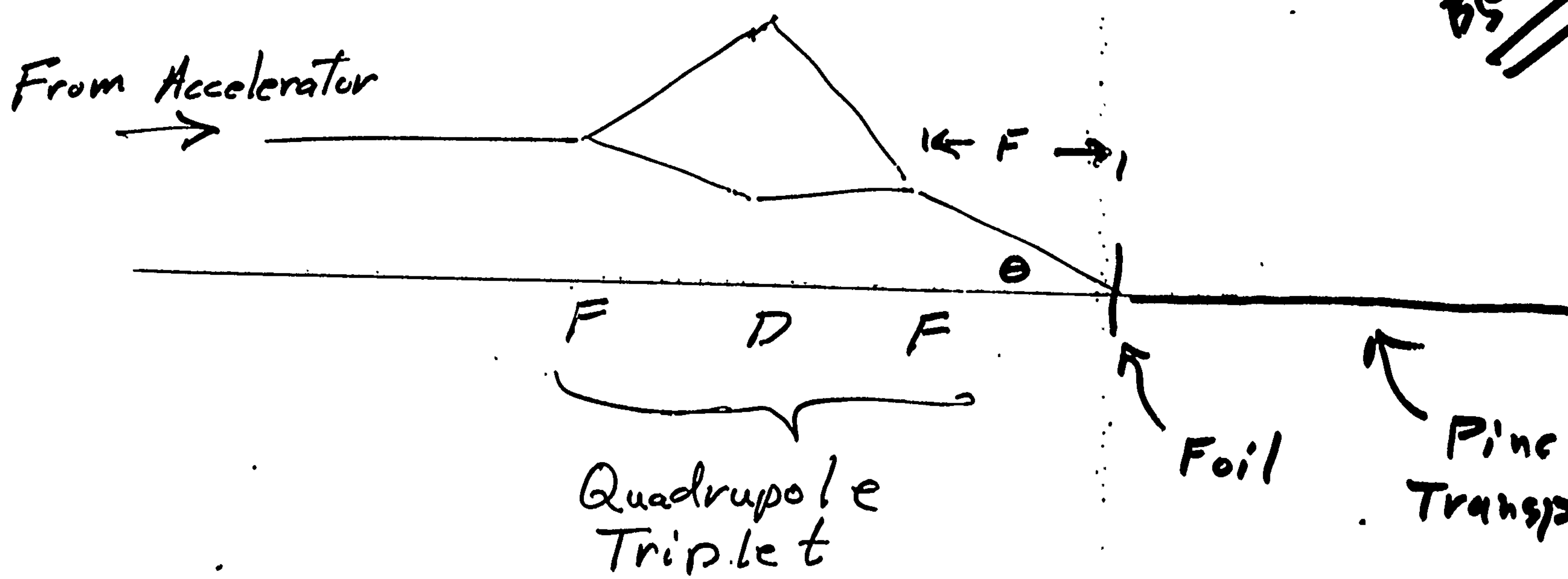

Maximum Radius of beam $= 3F\Theta = 6.75$ cm

Field At Wire ≈ 12 T

(12) Stripped Transport

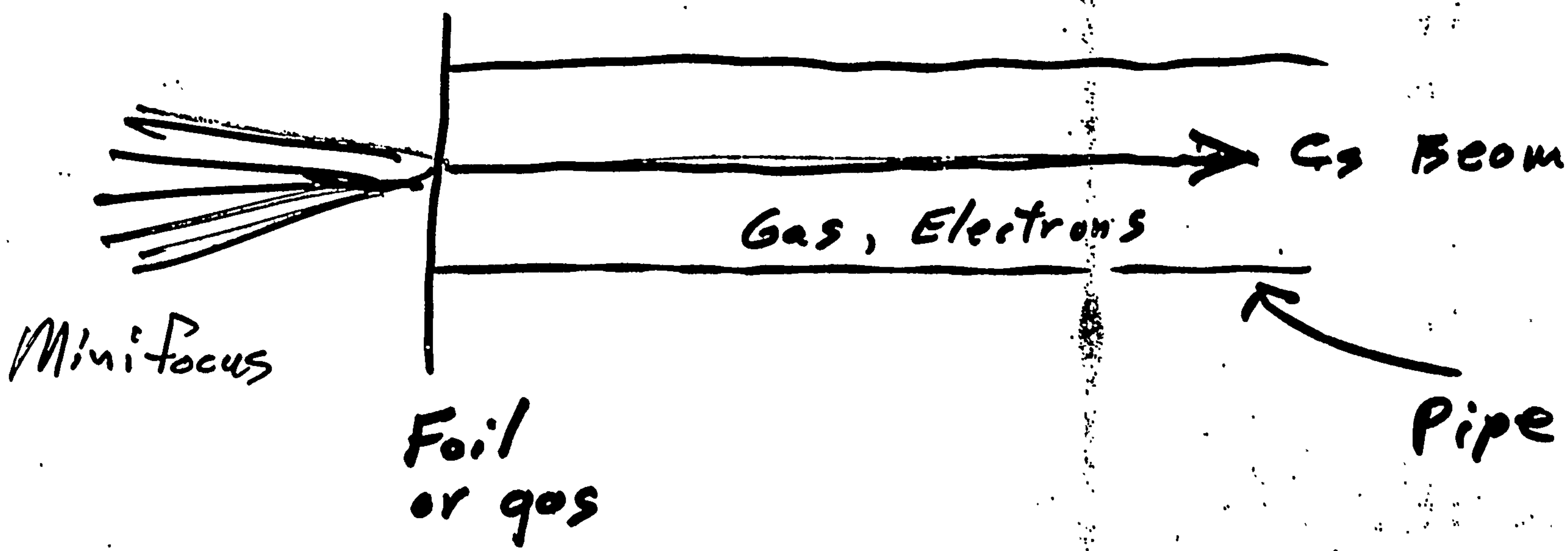

$\gamma = 1$

$I = 750$ Amp

(C_s^{+})

$\gamma = 55$

$I = 750 \times 55 = 41\,kA$

$I \approx 0$

(C_s^{+55})

(14) <u>Stripped Beam</u> Cont.

Bare Beam Electric Field:

$$E_r = \frac{2\lambda}{4\pi\epsilon_0 r}$$

$$\lambda = 55\,\lambda_0 = 483\ \mu C/m$$

$$r = .002\ m$$

$$E_r = \frac{2 \times 483\times10^{-6} \times 9\times10^{9}}{.002} = 4.3\times10^{9}\ \frac{V}{m}$$

Potential to Wall at 10 mm:

$$\phi \approx \frac{2\lambda}{4\pi\epsilon_0} \ln\frac{b}{a}$$

$$= 2\times483\times10^{-6}\times9\times10^{9}\times\ln 5$$

$$= 1.4\times10^{7}\ \text{Volts}$$

The beam will neutralize w.o. gas

Add gas to help

(15) Pinched Transport

eqn of motion
$$\ddot{r} = \frac{ge}{\gamma m}\left(E_r - v B_\theta\right)$$

$$= \frac{ge}{\gamma m}\left[E_{r_0}(1-f_e) - v B_{\theta_0}(1-f_m)\right]$$

Take $f_e = 0$

$$\ddot{r} = -\frac{g e v B_{\theta_0}}{\gamma m}(1-f_m) < 0$$

↑ magnetic neutralization fraction

Encouraged by IPROP Model + Results (D. Welch et al.)

(16) Pinched Transport Cont'

Envelope Eqn

ϵ = edge emittance (un-normalized)

$$a'' = \frac{\epsilon^2}{a^3} - \frac{1}{a}\left[\frac{2\,g^2\, I_{b_0}\,(1-f_m)}{31\times10^6\,\beta\gamma\, A}\right]$$

Equilibrium a : set $a'' = 0$

$$a = \epsilon \sqrt{\frac{31\times10^6\,\beta\gamma A}{g^2\, 2\, I_{b_0}(1-f_m)}}$$

The important thing is to strip when the radius is a minimum ($\simeq$ 2 mm) produced by mini focus.

Pinched Transport (cont.)

The radius (a) depends on emittance and current neutralization factor

Case at Hand: 5.33 GeV Cs^{+55}

$q = 55$

$A = 132.9$

$\beta\gamma = .297$

$I_{b0} = 750$ Amperes $\longrightarrow$ $q I_{b0} = 41300$ Amps

$a = .002$ m (or less)

$\epsilon = 4.4 \times 10^{-6}$ m-r assumed

f_m	$a = 2.43 \times 10^{-4}\,\text{m} / \sqrt{1 - f_m}$
0.0	2.4×10^{-4} m
.9	7.7×10^{-4}
.99	2.4×10^{-3}
.999	7.7×10^{-3}

$2.4 \times 10^{-3} \longleftarrow I_{net} = q I_{b0}(1 - f_m)$

$= 413$ Amps

Pinched Transport - Cont

Beam density $= \dfrac{I_{b0}}{\pi a^2 e v} \simeq 3.7 \times 10^{12}\ cm^{-3} = n_{b0}$

Add H_2 gas to pipe: To supply ample electrons

$n_g \sim 5\% \, n_{b0} \approx 10^{15}\ cm^{-3} \approx 30\ mtorr$

For Compressed beam:

$n_g \sim 10^{16}\ cm^{-3} = 300\ mTorr$

Low Energy Loss:

400 m of 100 mTorr H_2 $= .0004\ gm/cm^2$

Compare Range in Target $\simeq .05\ gm/cm^2$ (H_2 equivalent)

Pinched Transport - Scattering

This may be a problem :

(4 ← for H_2)

$$\sum |\Delta\theta|^2 \cong 4 \cdot \frac{8\pi N_g \ell e^4 q^2}{v^2 p^2} \ln(b_{max}/b_{min})$$

$$\simeq 6.6 \times 10^{-8} \, (rad)^2$$

{ 400 cm, 100 mtorr H_2 }

$$\Delta\varepsilon \sim \sqrt{2}\, r \sqrt{\sum |\Delta\theta|^2} \simeq .7 \times 10^{-6} \text{ m-r}$$

≃ double the assumed value

use less gas ?

get more net current ?

Pinched Transport - Scattering

This may be a problem :

$$\sum |\underset{\sim}{\Delta\theta}|^2 \cong 4 \cdot \frac{8\pi n_g \ell e^4 q^2}{v^2 p^2} \ln(b_{max}/b_{min})$$

(↙ for H_2)

$$\simeq 6.6 \times 10^{-8} \ (\mathrm{rad})^2 \qquad \left\{ \begin{array}{l} 400 \text{ cm} \\ 100 \text{ mtorr} \\ H_2 \end{array} \right.$$

$$\Delta\epsilon \sim \sqrt{2}\, r \sqrt{\sum |\underset{\sim}{\Delta\theta}|^2} \simeq .7 \times 10^{-6} \text{ m-r}$$

≈ double the assumed value

use less gas ?

get more net current ?

Self-Pinched Transport: LIF Concept

C. Olson, D. Welch

Self-pinched transport schemes require a finite net current

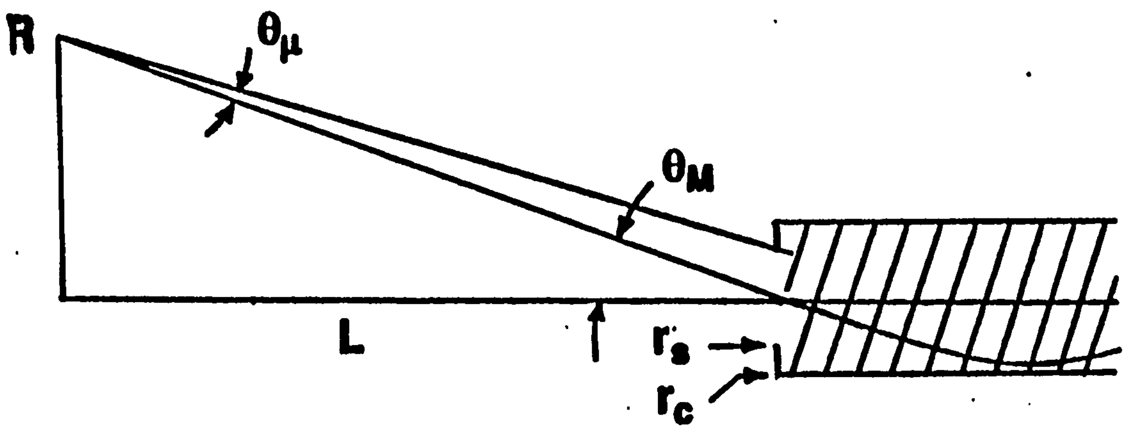

1. $I_c = (1/2)\theta_M^2 I_m^e$
2. $\theta_M = R/L = (R/r_s)\theta_\mu$
3. $r_s = r_c/\sqrt{2}$
4. $I_m^e = \beta\gamma(A/Z)M_p c^3/e$

$$I_c = (1/2)(R/r_s)^2\theta_\mu^2 I_m^e$$

LIF	HIF
I_c = 50 kA for:	I_c = 15.6 kA for:
θ_μ = 6 mrad	θ_μ = 0.3 mrad
R = 12 cm	R = 10 cm
r_c = 0.85 cm	r_c = 0.2 cm
30 MeV Li^{+3}	6 GeV Cs^{+40}
I_p = 1 MA	I_p = 4 kA
I_e = 3 MA	I_e = 160 kA
I_{net}/I_e = 1.7%	I_{net}/I_e = 9.8%

Self-Pinched Transport Should be Ideal for High Yield and Energy

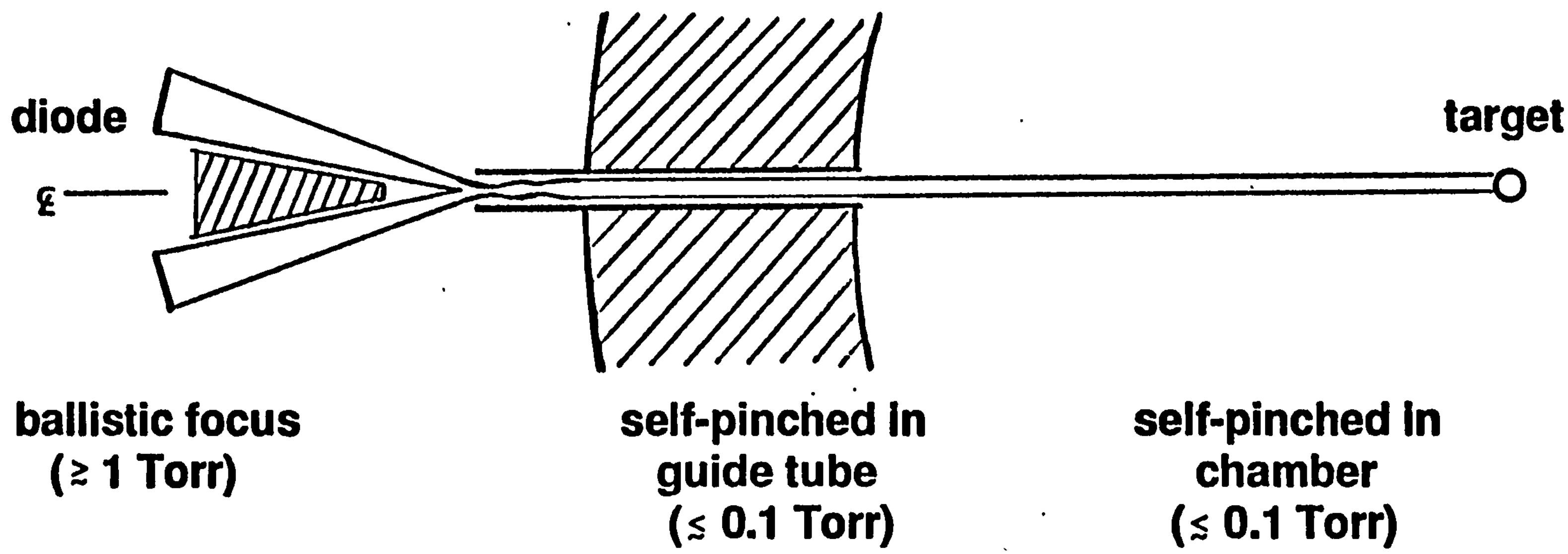

- small holes in chamber wall
- no transport apparatus in chamber
- gas in chamber
- diode shielded

gas breakdown is key issue

Several types of self-pinched transport are being investigated

(1) use gas that is more difficult to ionize (~ helium) and at lower pressure (< 1 Torr)

(2) use laser pre-formed plasma with radius > beam radius

(3) use laser pre-formed annular plasma with inner radius about equal to outer beam radius (annular plasma transport)

Concepts for LIF Transport

D. R. Welch and C. L. Olson
Mission Research Corporation
1720 Randolph Rd, Albuquerque NM 87106

September 20, 1994

Presented at the Workshop on Transport for a Common Ion Driver

LIF Self Pinch Scheme

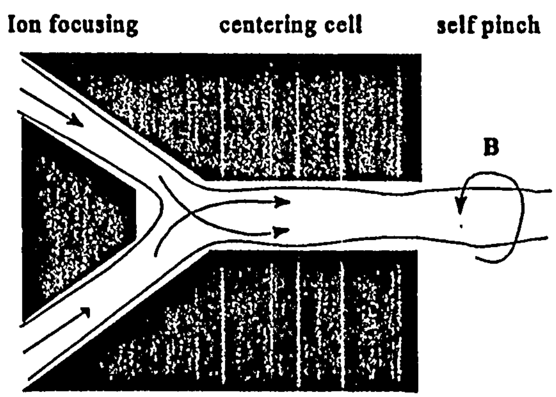

- Hollow beam exits accelerator and is focused to small radius (~1 cm)
- Strong wall forces center beam, directing it to target
- Beam's magnetic field confines beam at small radius to target

Light Ion Fusion Self Pinch Requires 50 kA Net Current

- Required net current increases rapidly with divergence, Θ

$$I_{net} = 17 \gamma \beta \frac{m_i}{z m_e} \Theta^2 \; kA$$

- Co-moving plasma electrons tend to reduce I_{net}
- Rapid ionization by slow moving ions moves optimal pressure for self pinch < 200 mtorr

An Ion Beam Must Pull in Electrons for Neutralization

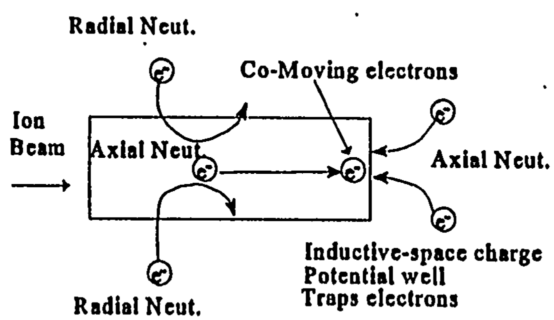

- For self pinch, good charge but poor current neutralization is required
- Radially neutralizing electrons do not remain within the beam unless undergoing a collision
- Axially neutralizing electrons tend more easily to co-movement, particularly at small radii

Self-Pinch in a Sub-Torr Gas Looks Promising

- Breakdown in a l-200 mtorr gas permits significant net current for ion beams
- Self-pinch in a neutral gas has greatest leverage for LIF but may be difficult
- Annular Plasma Transport (APT) and the "Pea Shooter" appear to be more robust in calculations

IPROP Neutral Gas Simulations

- 50 kA, 5 MV protons (cannot move radially)
- 1.5-cm radius, uniform density
- short centering cell
- 5-cm radius, 40-cm length tube
- Nitrogen gas

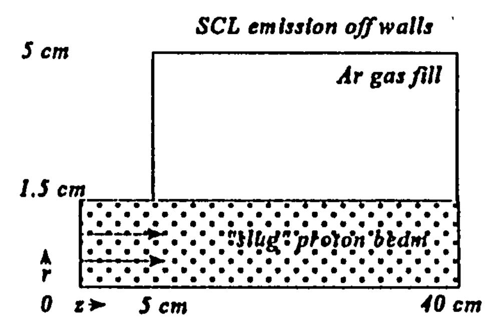

10-20 mtorr Argon Optimizes Pinch Force

- Gas Breakdown is delayed permitting large net currents
- Pinch force does not fall with distance
- magnetic fields at 40 mtorr become repulsive for ions at small radius due to a rapid build up of electrons

Net Current Drops with Distance at Higher Pressures

- 10, 20 and 40 mtorr Ar, 2-ns rise current

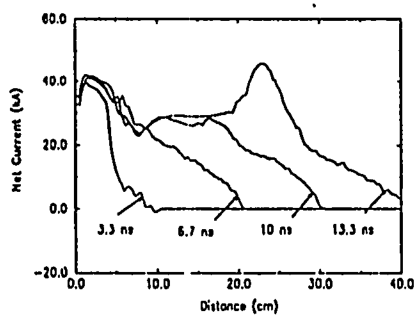

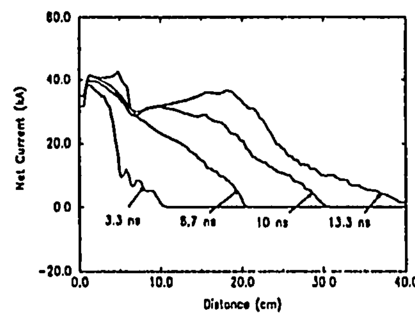

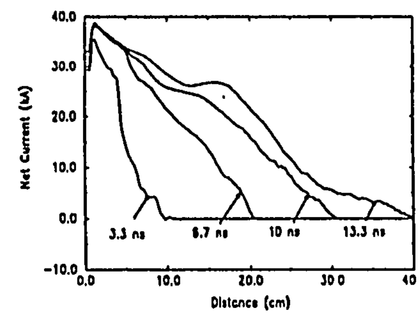

Breakdown More Rapid at Higher Pressures

- Plasma electrons thermalize sooner as shown by their mean velocities (time runs from right to left)

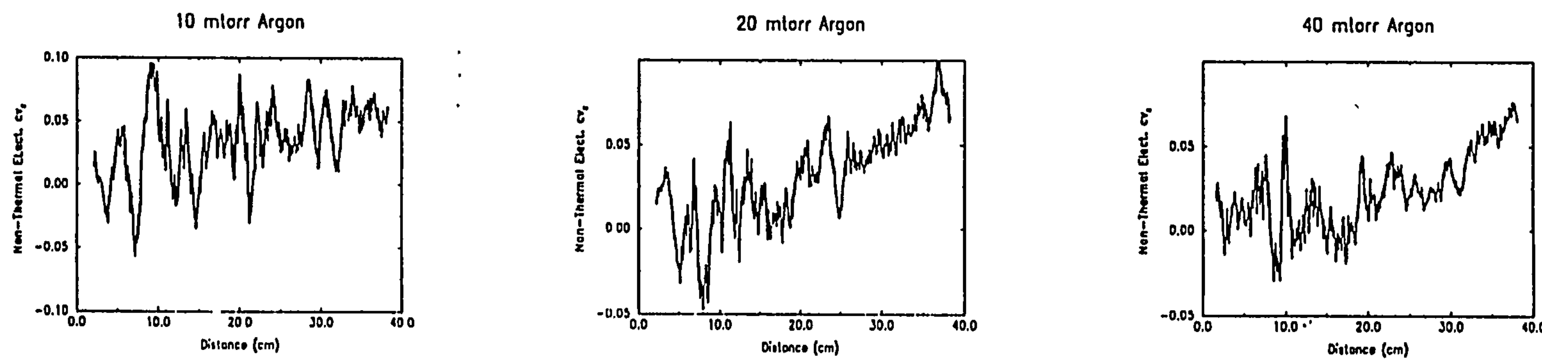

Fast Electrons Build Up Quickly at Higher Pressure

- 10, 20 and 40 mtorr Argon, 2-ns rise current

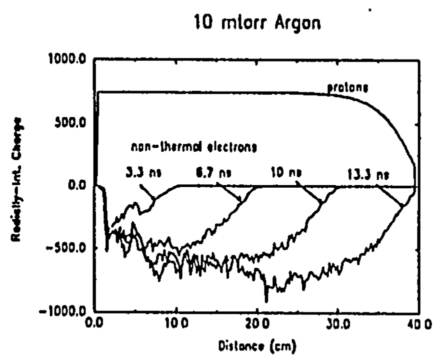

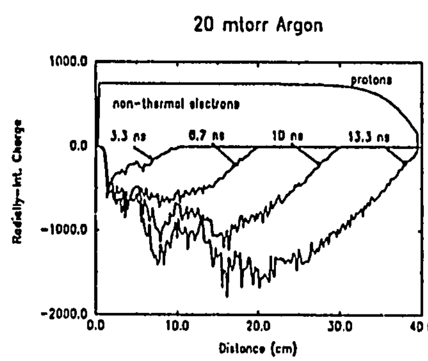

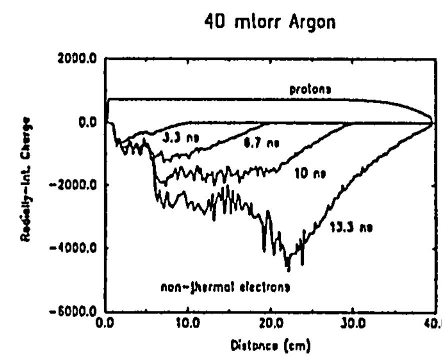

Results of 10-mtorr Simulation

- particles after 13.3 ns

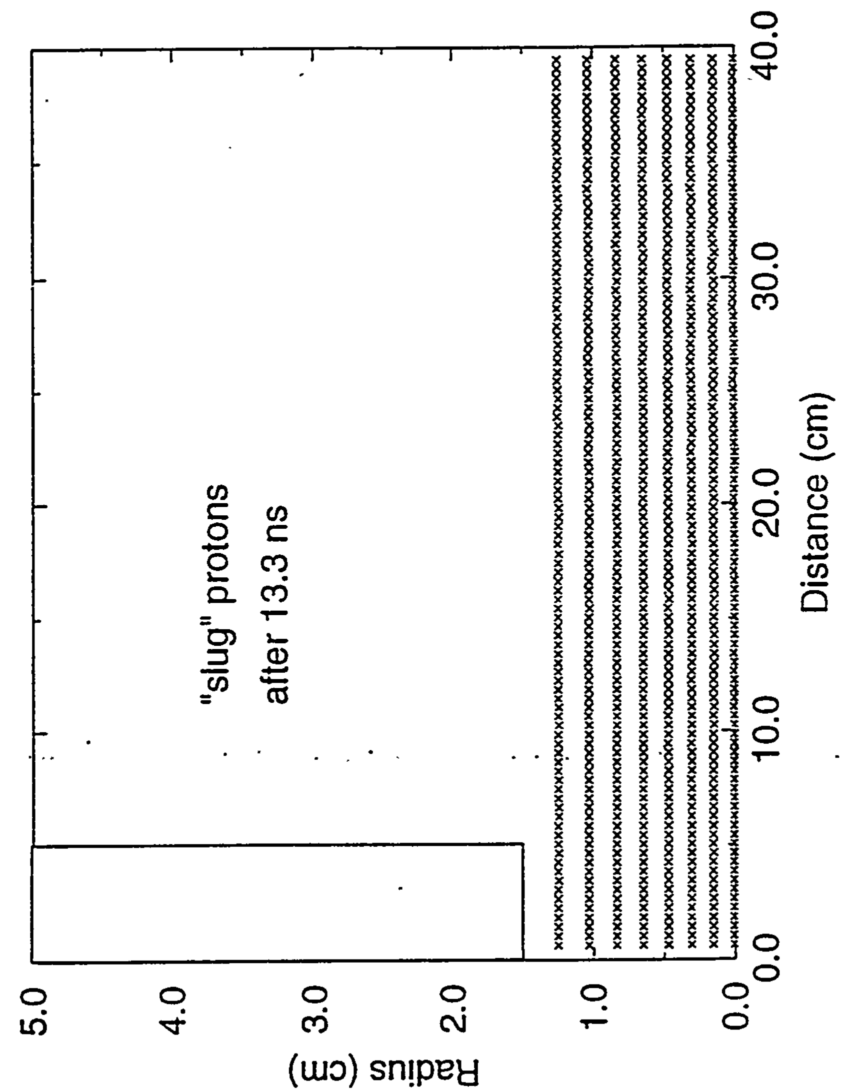
"slug" protons
after 13.3 ns
Radius (cm)
Distance (cm)
0.0
1.0
2.0
3.0
4.0
5.0
0.0
10.0
20.0
30.0
40.0

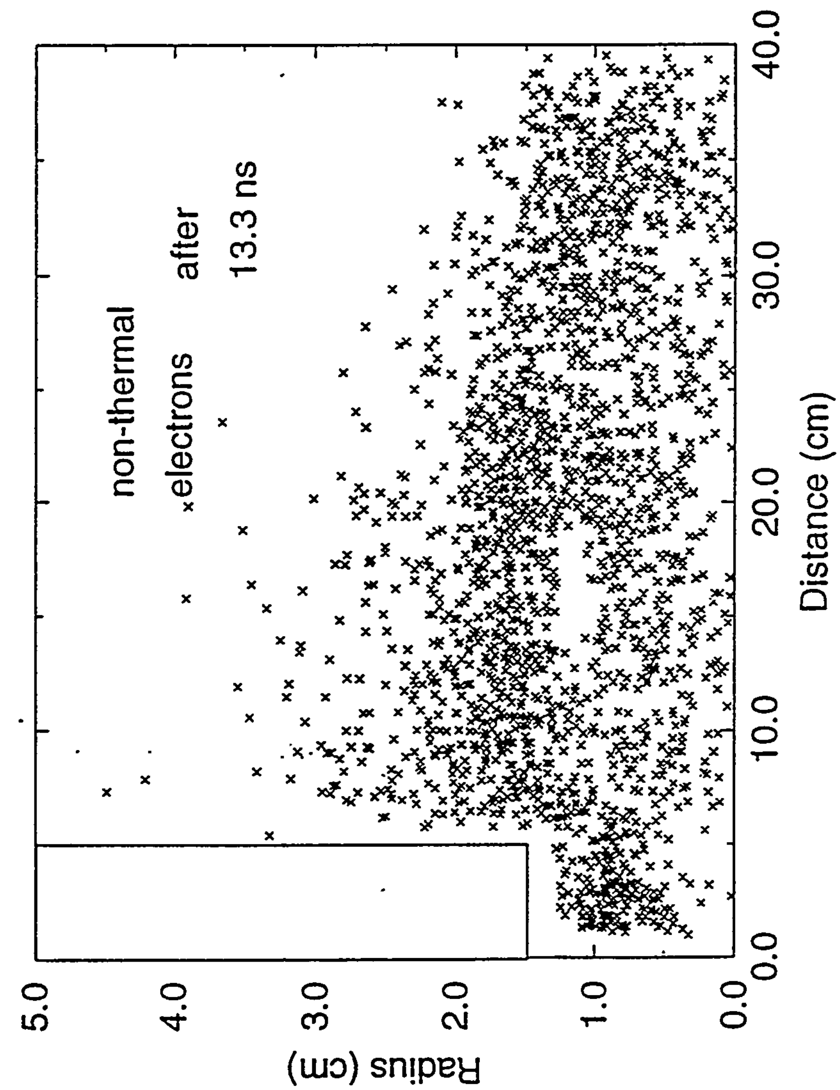
non-thermal electrons after 13.3 ns
Radius (cm)
Distance (cm)
0.0
1.0
2.0
3.0
4.0
5.0
0.0
10.0
20.0
30.0
40.0

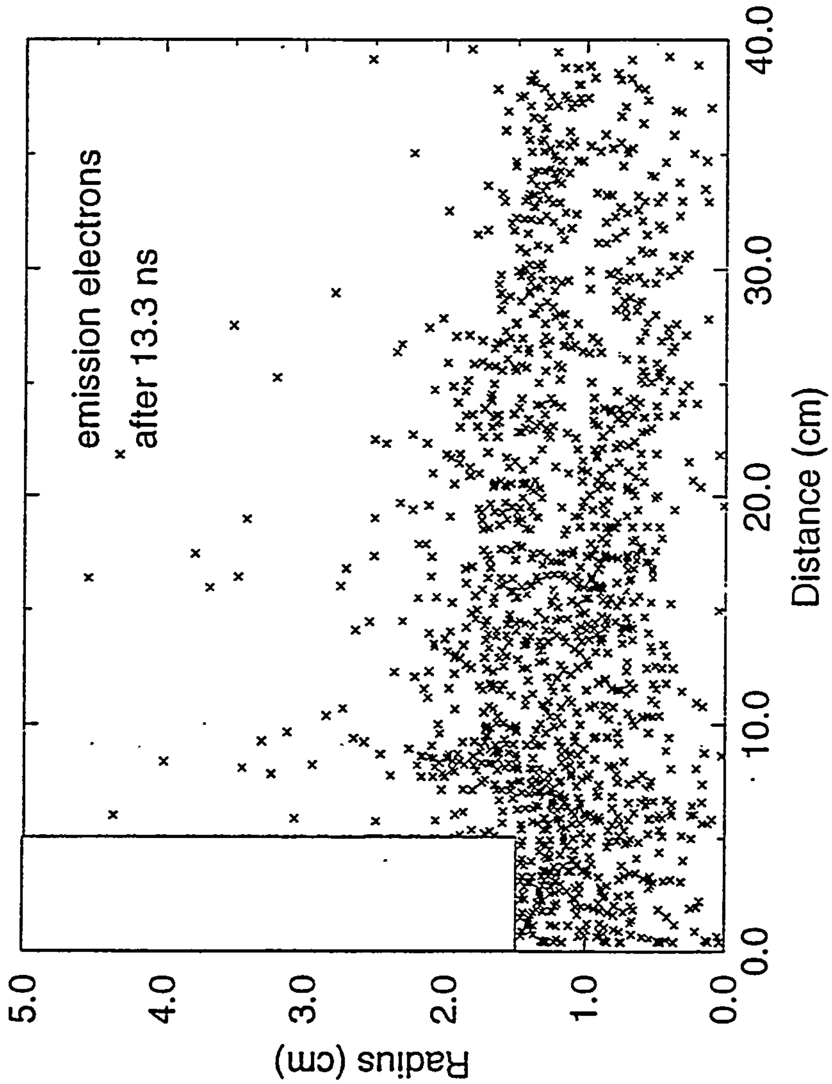
emission electrons
after 13.3 ns
Radius (cm)
Distance (cm)
0.0
1.0
2.0
3.0
4.0
5.0
0.0
10.0
20.0
30.0
40.0

Annular Plasma Transport - APT

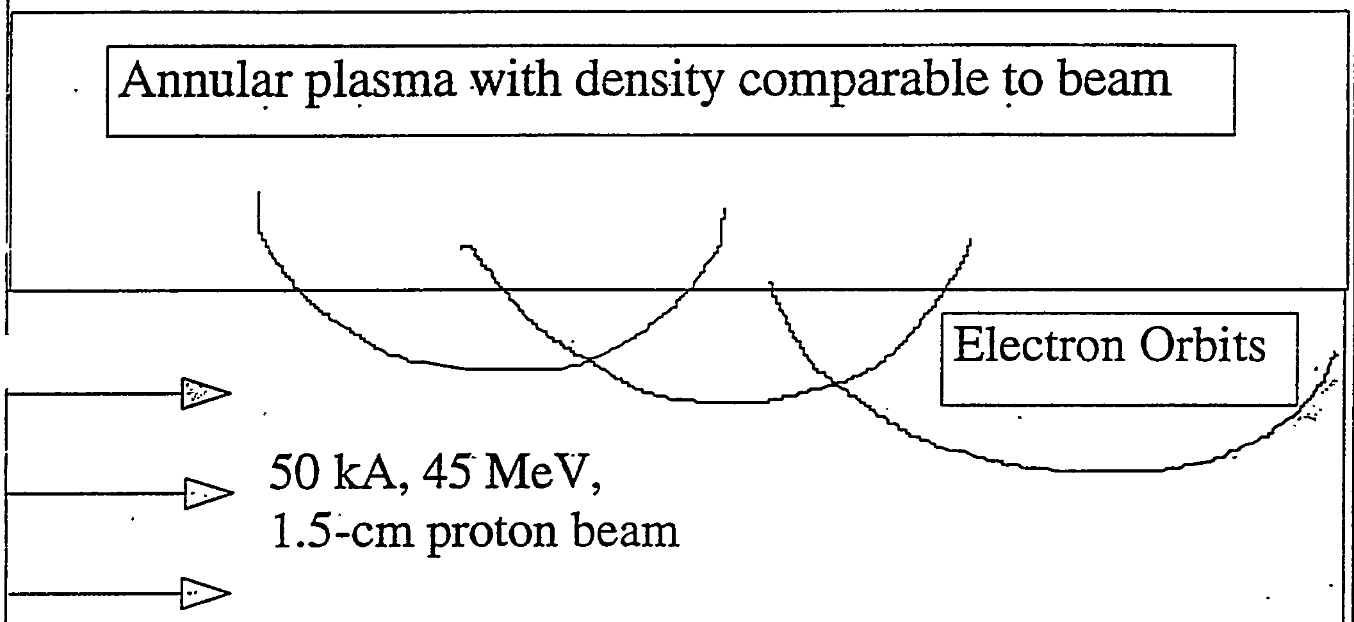

Plasma provides partial charge and current transport with a net pinch force

APT Provides a Significant Net Current

- Laminar flow theory $$I_{net} = \frac{\sqrt{17\beta I_b}}{1+\sqrt{\frac{n_b}{n_p}}}\ kA$$
- Fields initially limited to within skin depth of plasma edge, rapidly diffuse towards axis
- Gas breakdown neutralizes repulsive E_r, leaving full magnetic force to confine and direct beam
- Metal wall behaves as dense plasma

Magnetic fields diffuse inward from plasma

- 50 kA (2-ns rise), 45 MV protons, r=6 skin depths, $n_p = n_b$, no gas

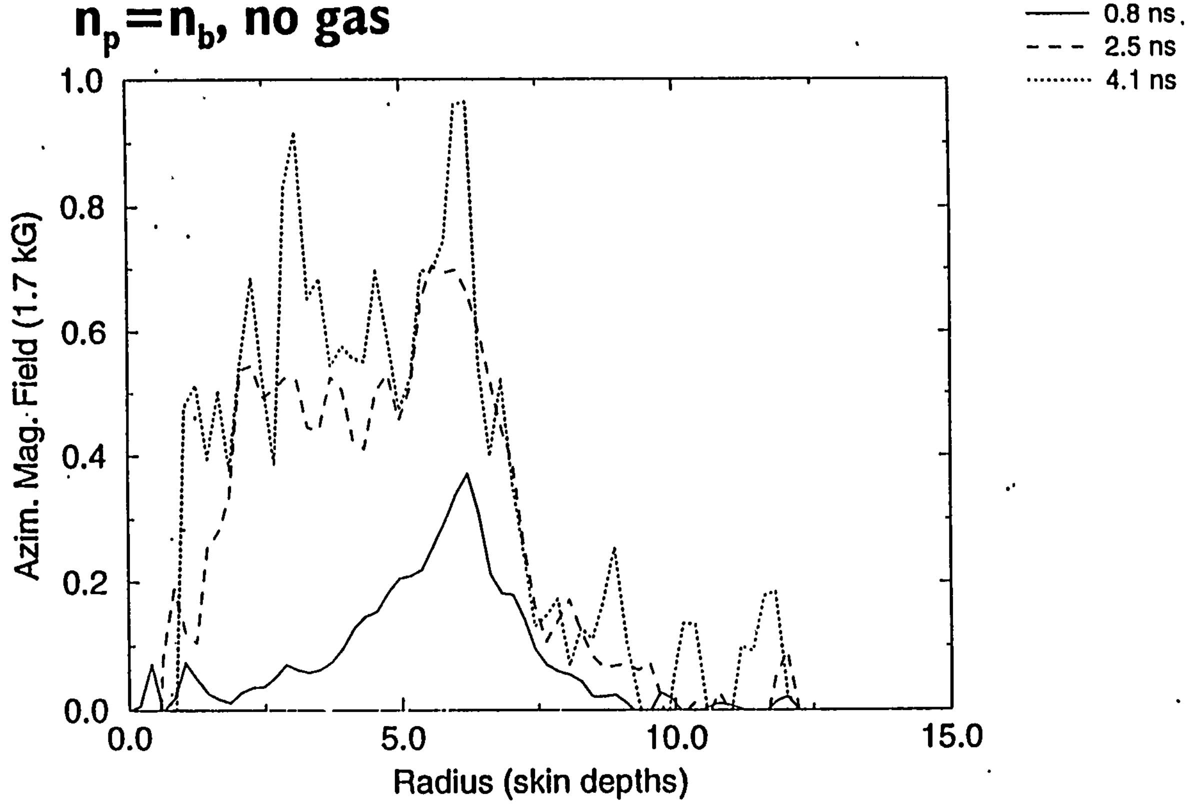

IPROP reproduces theory current scaling

- $r=12$ skin depths, at $t=2.5$ ns

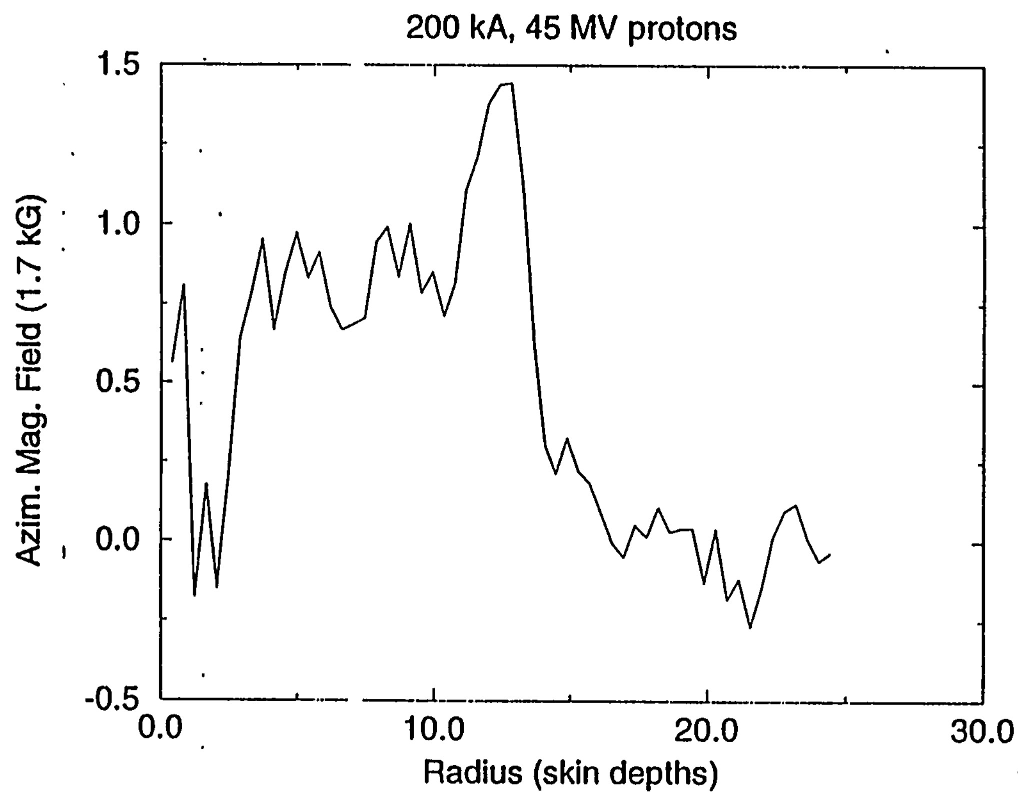

Electric Field also "Diffuses" to entire beam

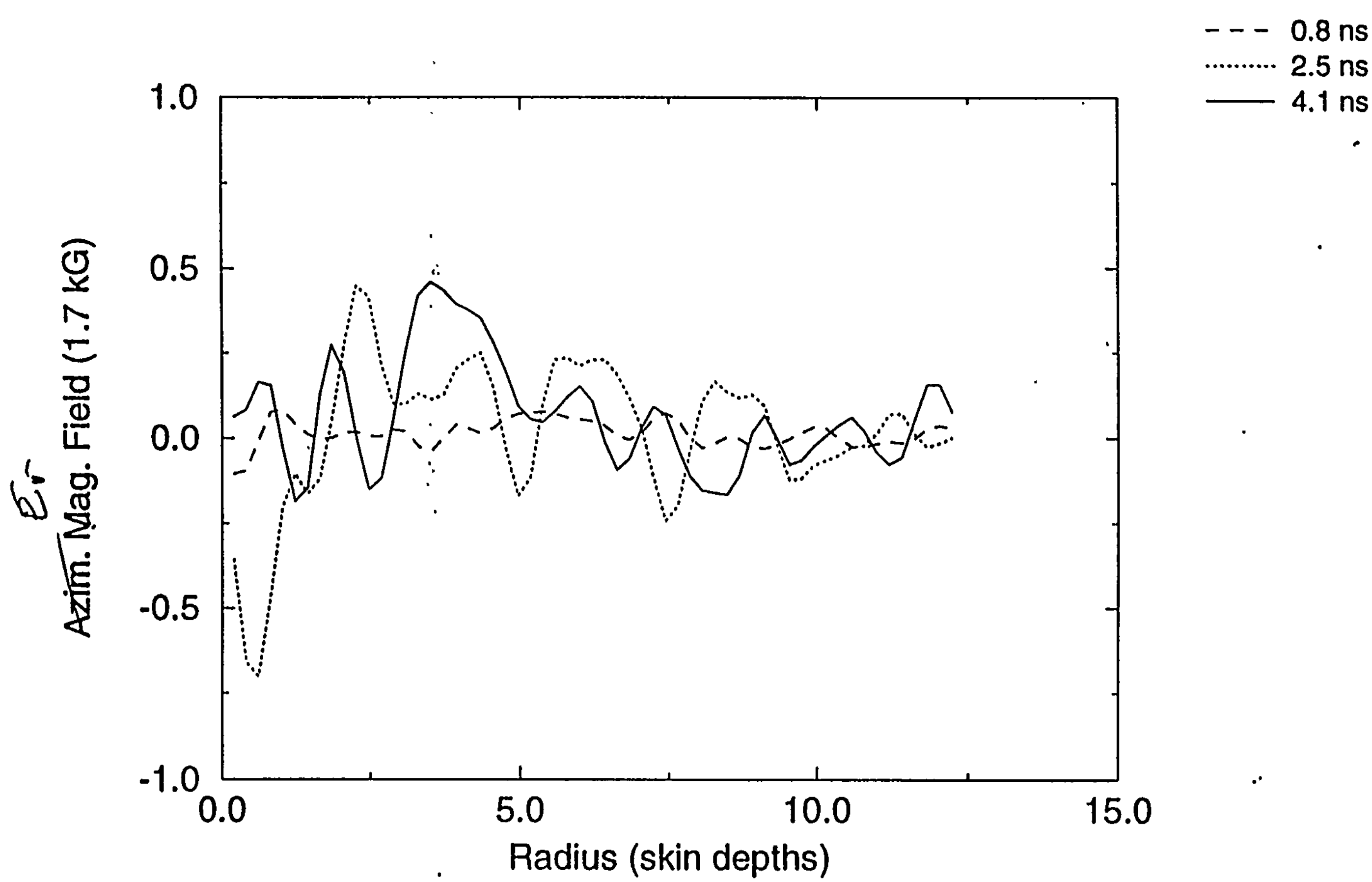

Breakdown Time Depends on Ion Energy and Charge for a Given Gas Pressure (Nitrogen)

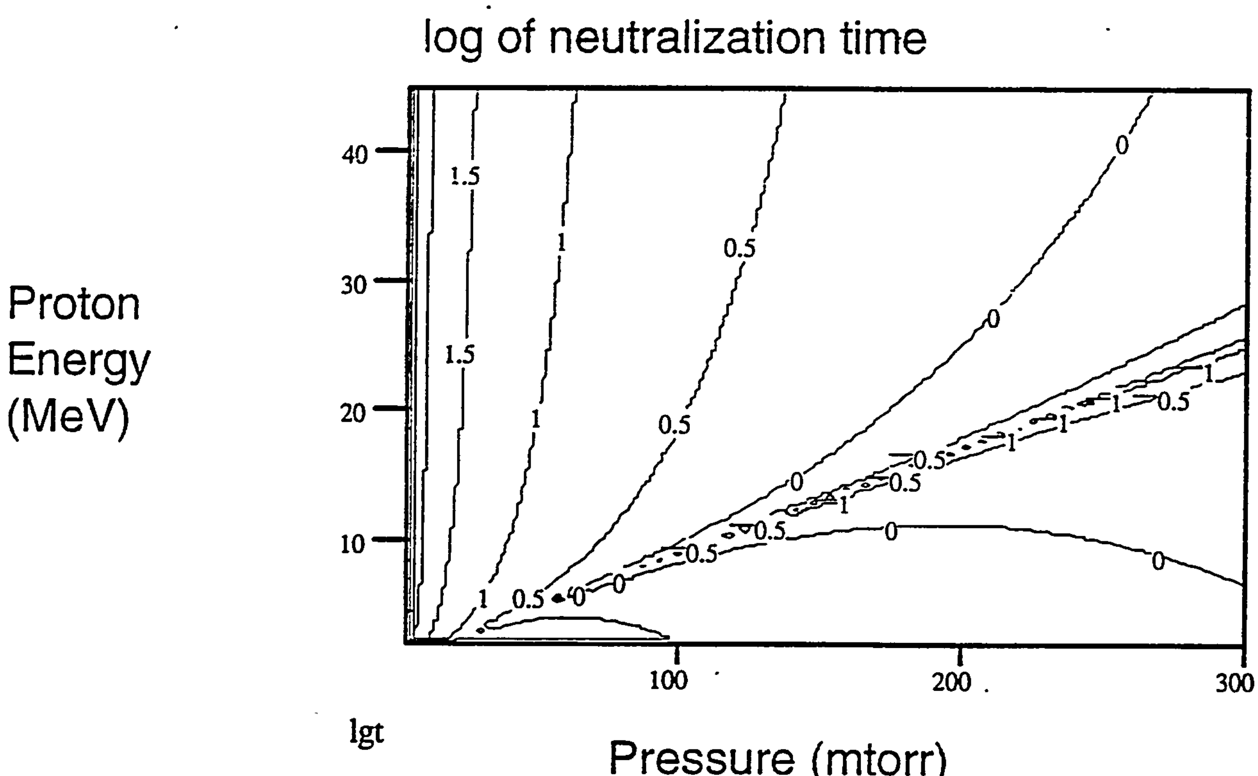

IPROP APT Simulations

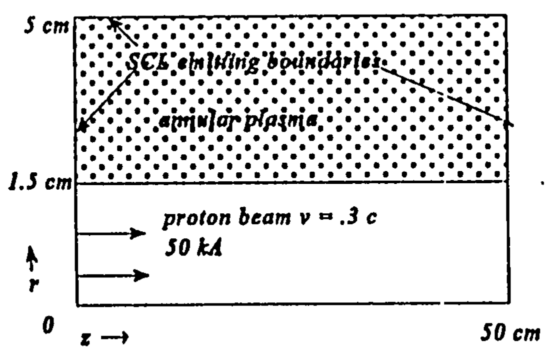

- 50 kA, 45 MV protons
- 1.5-cm radius, uniform density
- 0.033 radian divergence (10 kA matched)
- 5×10^{12} cm^{-3} plasma density

40-100 mtorr Nitrogen Optimizes Pinch With APT

- APT pressure scaling similar to neutral gas - at higher pressures the plasma affects decline
- Pinch force rises quicker with the plasma due to the ready souce of radially neutralizing electrons
- Over the 50 cm length, the simulations with an annular plasma exhibited less sausaging
- A longer current rise time can lead to smaller net current - breakdown occurs before peak current

Net Current Remain Strong at Lower Pressure

- l-ns rise current

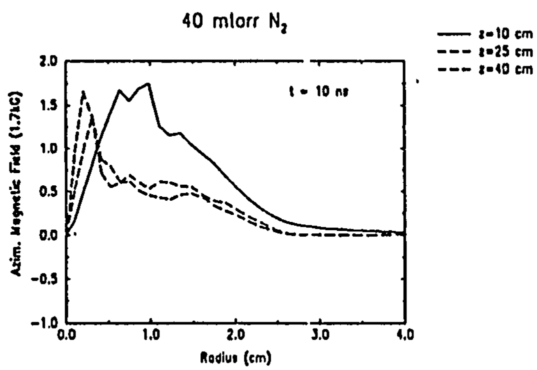

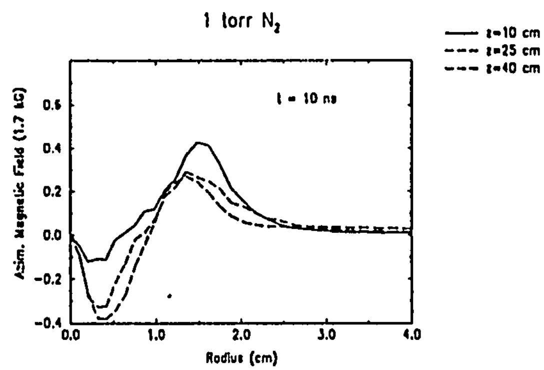

Net Current Rises Sooner, Producing Improved Stability With a Plasma

- I-ns rise current

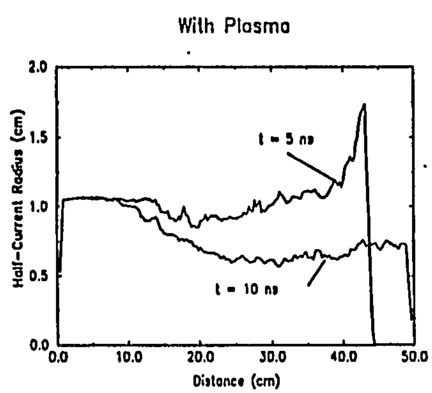

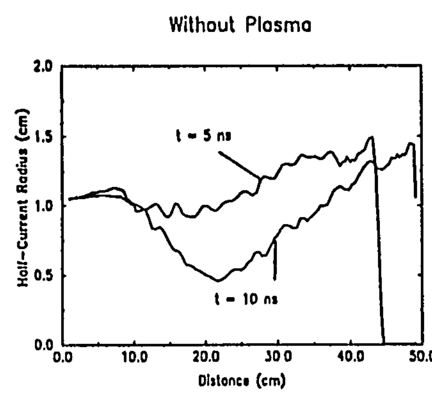

Self Pinch is an Attractive Transport Mode for ICF

- Low-pressure gas yields sufficient net current to confine beam
- Neutral gas transport requires no structures inside target chamber - can be used in repetative mode
- Annular Plasma Improves Transport
- Technical issues to be studied include 3-D stability and long distance propagation

14

STATUS OF PREIONIZED PLASMA CHANNEL PINCH STUDIES

Richard F. Hubbard, Martin Lampe
Richard F. Fernsler, and Steven P, Slinker

Plasma Physics Division
Naval Research Laboratory
Washington, DC 20375

20 September, 1994

Given by: Paul Ottinger

Past Support: **Sandia National Laboratories (LIF)**
Lawrence Berkeley Laboratory (HIF)

RESISTIVE SELF-PINCH FOR LIF AND HIF

- Resistive pinch is known to work for electron beams at 1 torr. Net current I_n is a significant fraction of I_b in this case.

- Investigated by Lee, Yu, and coworkers for HIF using envelope model (1978-80). Recent studies by Fawley, et al. (HIF) and us (HIF and LIF).

- Beam produces conductivity so rapidly that net current is frozen in at a few hundred amps for HIF or a few kA for LIF.

- <u>Pinch is too weak unless emittance is much smaller than expected.</u>

- Fast electrons (knock-ons) are likely to reduce pinch current further or even reverse it. (Hubbard and Goldstein, Yu, et al., Welch)

- Pinch could be enhanced if enough plasma current flows outside the beam or if radiation or atomic physics clamps the conductivity.

BACKGROUND

- Purely resistive self-pinch will probably not generate a strong enough pinch force for ion beam fusion. Simulations show net current I_n or "effective" pinch current I_e much less than beam current I_b.

- In 1990, simulations at NRL using FRIEZR code showed <u>strong</u> pinch ($I_n \sim I_b$) when a collisionless preionized plasma channel was employed. Simulations used "massive" electrons and lower current to limit computer time.

- Key parameter is ratio of plasma skin depth to beam radius ($c/\omega_p a_b$). This ratio was > 1 in early simulations; $\lesssim 1$ in later simulations.

- In 1991-92, further simulation studies revealed potential problems (wakefield effects, tail erosion, etc.). Scaling to the regime of interest for fusion ($c/\omega_p a_b \ll 1$) was uncertain.

- Steady state analytical model developed in 1992-93.

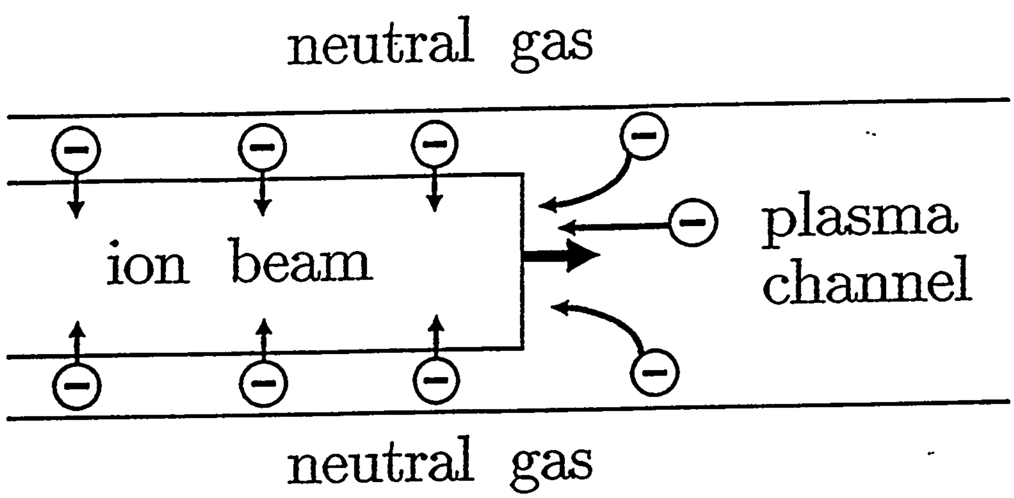
neutral gas
ion beam
plasma
channel
neutral gas

HIGH CURRENT FRIEZR SIMULATION
Overdense channel; no beam ionization

Beam and Net Current

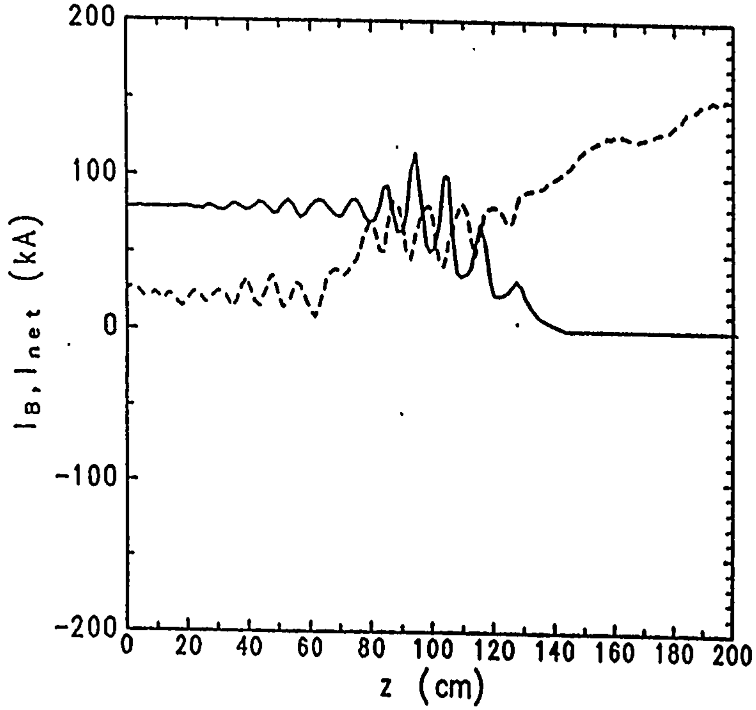

Beam Radius

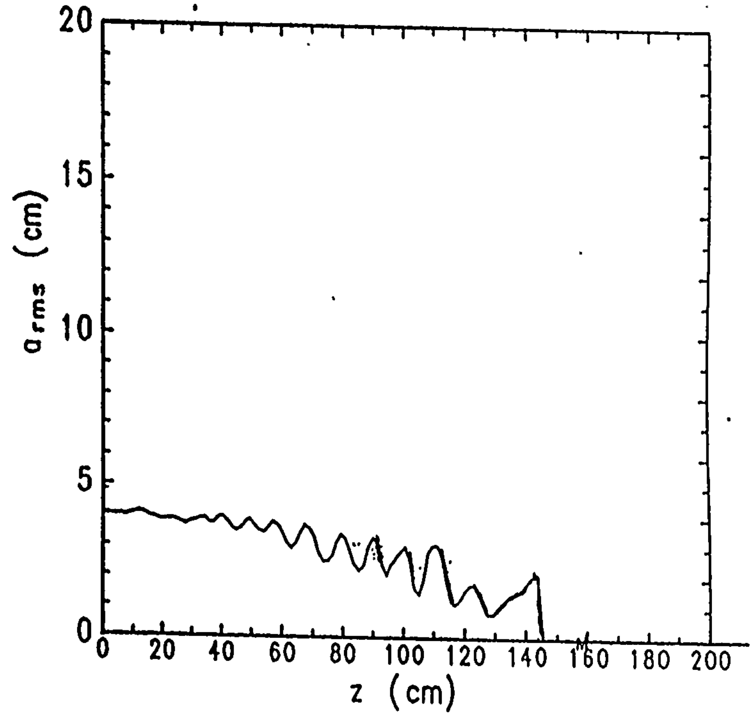

- I_{max} = 80 kA, a_o = 4 cm, a_{ch} = 8 cm, ϵ_n = 0.02 rad-cm
- Strong axial bunching and oscillations but good pinch.

RECENT STUDIES (1993)

- Steady-state anaytical model completed and solved numerically for plasma current J, and net and effective currents I_n and I_b. Analytical solutions obtained for $c/\omega_p a_b << 1$.

- Assumptions: rigid beam slug, collisionless cold fluid channel, steady state achieved in beam frame, plasma velocity much smaller than beam velocity, slow beam rise.

- MAIN RESULT: $I_e \simeq \beta f I_0$, where $\beta = v_b/c$, f is the ratio of the beam charge density to plasma channel density, and $I_0 = 17$ kA. Valid for f << 1, and $c/\omega_p a_b << 1$.

- New simulations with MASK code with $c/\omega_p a_b \sim 0.2$-1 were noisy but showed strong pinch seen in earler FRIEZR simulations. Results generally consistent with numerical solutions to analytical model.

- Wakefield effects NOT expected to be a problem in fusion regime.

PLASMA CURRENT DENSITY J

$$\frac{J(r)}{J_b} = -1 + \frac{a_b\omega_p}{c}\left(K_1^b + I_1^b \frac{K_0^c - LK_1^c}{I_0^c + LI_1^c}\right) I_0\left(\frac{r\omega_p}{c}\right), \quad \text{if } r \le a_b,$$

$$\frac{J(r)}{J_b} = \frac{a_b\omega_p}{c}\left[-I_1^b\, K_0\left(\frac{r\omega_p}{c}\right) + I_1^b \frac{K_0^c - LK_1^c}{I_0^c + LI_1^c}\, I_0\left(\frac{r\omega_p}{c}\right)\right], \quad \text{if } r \ge a_b,$$

where I_0, I_1, K_0, K_1 are modified Bessel functions, and we have used the shorthand superscript-b if the argument is $a_b\omega_p/c$, or superscript-c if the argument is $a_c\omega_p/c$.

- **In the "fusion" regime ($c/\omega_p a_b \ll 1$), this becomes**

$$\frac{J(r)}{J_b} \simeq -1 + \frac{1}{2}\exp\left(-\frac{(a_b - r)\omega_p}{c}\right), \quad \text{if } r \le a_b,$$

$$\frac{J(r)}{J_b} \simeq -\frac{1}{2}\exp\left(\frac{(r - a_b)\omega_p}{c}\right), \quad \text{if } r \ge a_b,$$

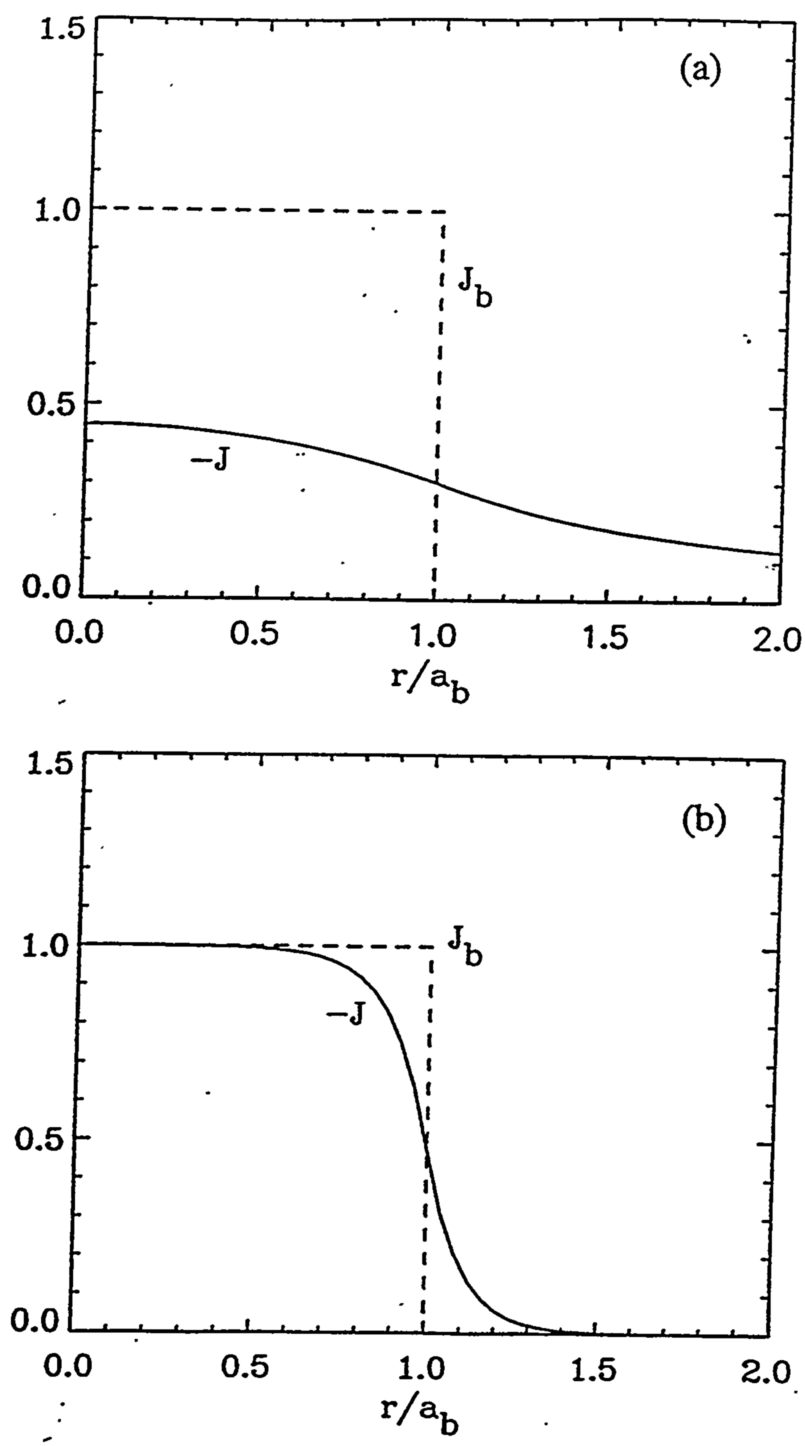

Fig. 1. Plots of the plasma current density profile J(r), from Eqs. (21), for cases with $a_c = 2a_b$. The results are practically independent of the value of the outer radius b. Case (a) has $c/\omega_p a_b = 1$, while Case (b) has $c/\omega_p a_b = 0.1$.

EFFECTIVE OR PINCH CURRENT I_e

- The effective current I_e is a beam-weighted average of the enclosed net current, defined by:

$$\frac{I_e}{I_b} = \int_0^{\infty} \frac{dr 4\pi r J_b(r)}{I_b} \int_0^{r} \frac{dr' 2\pi r' [J_b(r') + J(r')]}{I_b} .$$

- For J given in the earlier viwegraph, this becomes

$$\frac{I_e}{I_b} = \frac{8c}{a_b \omega_p} I_2^b \left(K_1^b + \frac{K_0^c - L K_1^c}{I_0^c + L I_1^c} \right) ,$$

- In the "fusion" regime ($c/\omega_p a_b << 1$), this becomes

$$\frac{I_e}{I_b} \simeq \frac{4c^2}{a_b^2 \omega_p^2} .$$

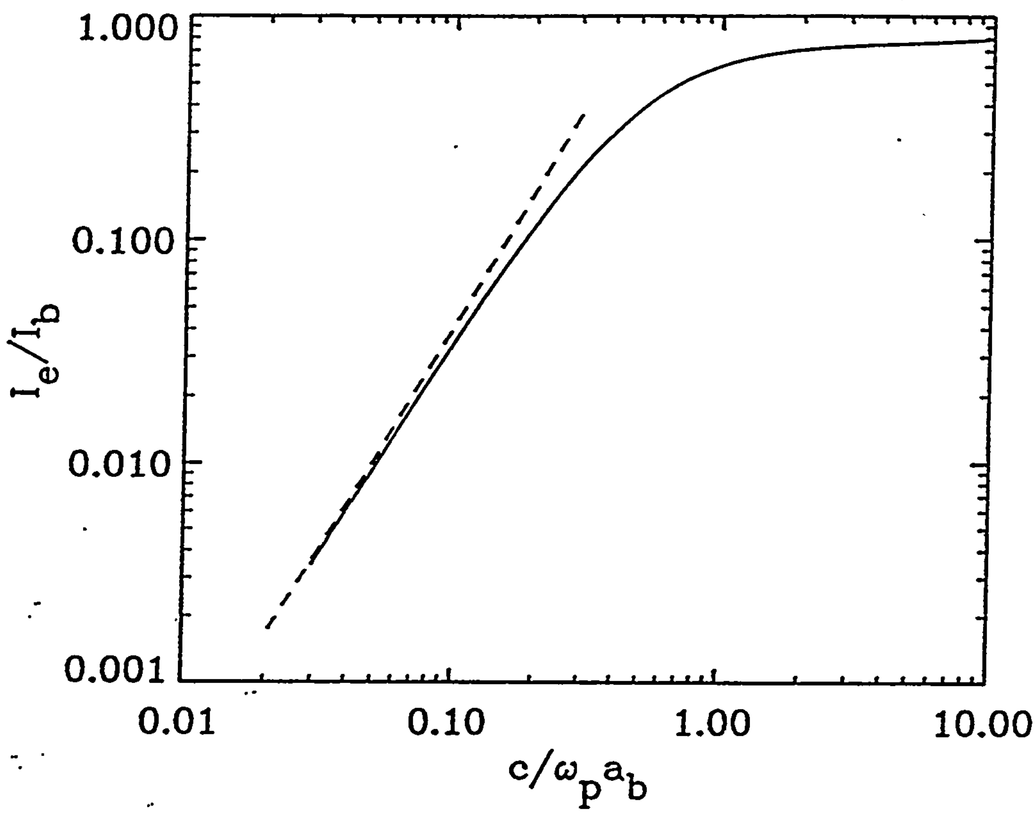

Fig. 2. Plot of the effective pinch current I_e normalized to the beam current I_b, as a function of $c/\omega_p a_b$, from Eq. (25).

SUMMARY AND IMPLICATIONS

- FRIEZR simualtions had shown cases where I_n or I_e was comparable to I_b. For fusion paramters, this would have given a VERY strong pinch.

- In the dense plasma regime for fusion ($c/\omega_p a_b << 1$), the steady state model predicts $I_e = \beta f I_0$, where $I_0 = 17$ kA. Even for f = 1, this is too small for LIF and very marginal for HIF or welterweight ions.

- Analytical model IS consistent with simulation. FRIEZR used massive electrons (100 m_e), so I_0 was 1.7MA in the simulations. Also analytical model predicts $I_e/I_b \gtrsim 0.5$ in regime where simulations were run.

- Stronger pinch may be possible if f is less than 1 inside the beam, and plasma electrons flow in from outside to provide space charge neutralization. This scheme would be prone to wakefield effects and local charge imbalance.

Charged Particle Accelerators for Inertial Fusion Energy

Stanley Humphries, Jr.
Department of Electrical and Computer Engineering
University of New Mexico
Albuquerque, New Mexico 87131

Proc. 1991 PAC
IEEE Vol. 1 of 5

The long history of successful commercial applications of charged-particle accelerators is largely a result of initiatives by private industry. The Department of Energy views accelerators mainly as support equipment for particle physicists rather than components of an energy generation program. In FY 91, the DOE spent over 850 M$ on building and supporting accelerators for physics research versus 5 M$ on induction accelerators for fusion energy[1]. I believe this emphasis is skewed. We must address problems of long-term energy sources to preserve the possibility of basic research by future generations. In this paper, I shall review the rationale for accelerators as inertial fusion drivers, emphasizing that these devices provide a viable path to fusion energy from viewpoints of both physics and engineering.

In the conference talk, I covered the full range of accelerator fusion applications. Because of space limitations, this paper concentrates on induction linacs for ICF, an approach singled out in recent reports by the National Academy of Sciences[2] and the Fusion Policy Advisory Committee[3] as a promising path to long-term fusion power production. Review papers by Cook, Leung, Franzke, Hofmann and Reiser in these proceedings give details on light ion fusion and RF accelerator studies.

Fig. 1*a* illustrates the recently declassified concept of indirect-drive ICF targets. The idea is to convert the energy of a beam into an intense flux of soft X-rays inside a hohlraum, a closed chamber of high-Z material. With proper design of the low-density foam that fills the chamber, the beam can generate a symmetric X-ray flux with optimal time variation to provide strong compression of a high-gain target. In the ion beam target of Fig. 1*a*, two beams pass through the thin chamber shell and heat the foam to about 300 eV. Ideally, the ions should have a normalized range of about 20-30 mg/cm^2 to penetrate the shell and to deposit high energy density in the foam. Longer range ions can be used at the expense of a more complex target with reduced gain (Fig. 1*b*). It is necessary to extend the conversion region and decrease the focal spot size to achieve the required energy density.

Many physics issues of indirect-drive targets have already been resolved. Quoting from Ref. 2, "Experiments (Centurion/Halide) using a tiny fraction of the energy from a fission bomb underground have allowed demonstration of excellent performance, putting to rest fundamental questions about basic feasibility of attaining high

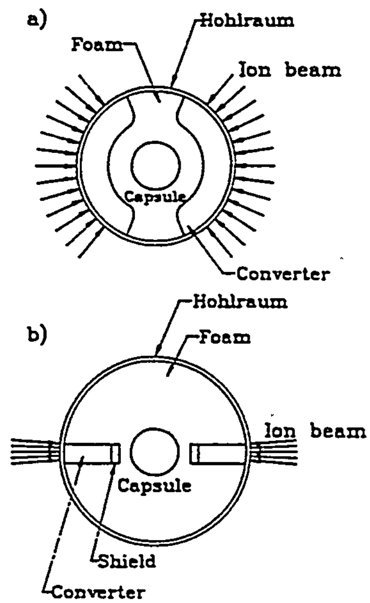

Fig 1. Principle of indirect-drive inertial fusion targets. a) Simple target design with optimum-range ions (20 mg/cm^2). b) Modified target for long-range ions (100 mg/cm^2).

gain." The drawback is that indirect targets require extra drive energy to compensate for the inefficiency of the X-ray conversion process. The estimated energy[4] for ion-driven targets is about 5 MJ for gain in the range 40-100. Although the net energy is modest, the physics challenge is to deliver the energy to small areas in short times (10 ns) at high power levels (5×10^{14} W). The focal spot radius requirement varies from 2 mm for high-energy ions to 1 cm for short-range ions. The beams must propagate a long distance to the focal point. With a target yield in the range 1 GJ, the reactor chamber has a radius of 5-10 m to prevent wall damage.

The power density at the converter must exceed 10^{14} W/cm^2. This precludes the direct application of conventional electromagnetic energy. The Poynting flux in an EM wave with E = 20 MV/m is only 10^8 W/cm^2. Electrodes cannot sustain higher fields in a repetitively-operated system. ICF demands an intermediate stage of power conditioning such as a charged particle accelera- . Accelerators convert electrical energy to stored beam energy that can transform to thermal energy in a material

0-7803-0135-8/91$01.00 ©IEEE

in a small area and short time. For example, focusing a low-emittance beam gives power compression in the transverse direction. High-compression is also possible in the axial direction. In an accelerator, the conversion of electrical to beam energy occurs over an extended distance. Non-relativistic ions can be axially bunched by a velocity tilt during or after acceleration. Finally, charged particles striking a solid material yield their energy in a short range.

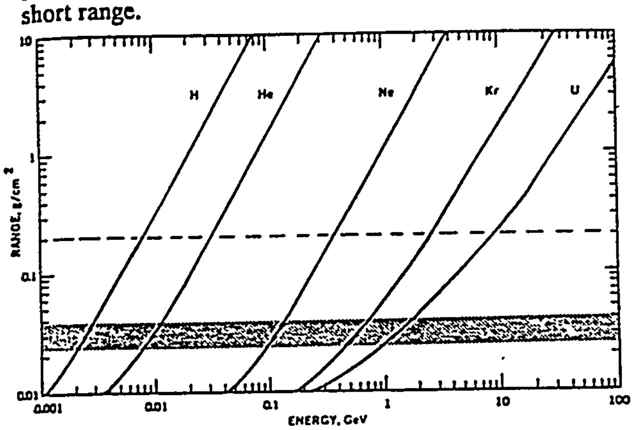

Fig. 2. Normalized ranges for ions in inertial fusion targets. Shaded area: optimum range. Dashed line: range for existing Heavy Ion Fusion studies.

Ions are more attractive than electrons for ICF because of their high stopping power. The variation of range with ion species gives several options for ion accelerator technology. Figure 2 shows that variation of normalized range with kinetic energy and ion species - the range corresponds to 10 MeV He, 100 MeV Ne, or 1500 MeV U. Higher energies are possible with advanced target designs (Fig. 1*b*). The corresponding beam currents to carry 500 TW are 50 MA for 10 MeV He, 5 MA for 100 MeV Ne, and 50 kA for 10 GeV U. Although these currents are beyond present capability, the dramatic advances in beam physics and accelerator technology in the past decade give cause for optimism.

ICF reactors with ion beam drivers have compelling advantages. In contrast to magnetic fusion devices like the Tokomak, the ICF reactor chamber is physically separate from the power source (driver) that creates the thermonuclear plasma. As a result, the engineering of the reactor is simplified. Ion accelerators have several desirable features compared with lasers. Accelerators are reliable, achieve good energy efficiency, and operate at adequate repetition rates (1-10 Hz). Ion beams can be compressed in space and time and focused into the reactor by magnetic lenses with no exposed physical surfaces. Most important, the energy deposition process of ions in matter is predictable. Ref. 3 recognizes these features: "We strongly urge augmenting the [inertial fusion] program for developing a driver of suitable efficiency and reliability to be useful for energy production, with emphasis on heavy ions...."

We can represent the ICF process with an ion beam driver by three stages of power compression (Fig. 3). In the first, electrical energy is stored over an extended period and then converted to beam energy by the accelerator in a time ranging from 20 ns to several ms. Beam manipulations amplify the power. The final stage involves conversion to soft X-rays. We can classify present approaches by their emphasis on electrical versus kinetic energy compression and the power levels for the transfer operations. Fig. 3 shows four current programs. The Kurchatov Institute is the leading laboratory for the study of imploding Z-pinches for fusion[5]. In this process, a large pulsed power generator drives current through an annular foil creating an imploding plasma. The system

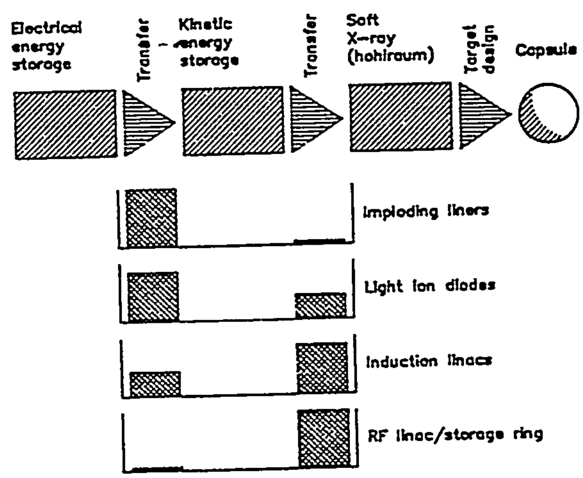

Fig. 3. Schematic view of power compression sequence for ion beam drivers and indirect-drive targets. Four present approaches to ion beam fusion with relative emphasis on electrical versus kinetic energy compression.

produces an intense burst of soft X-rays when the pinch stagnates on axis. In a sense, the plasma is a high-emittance, neutralized ion beam that gives modest power compression in space and time. This method places almost total reliance on electric power amplification. The other three approaches use higher quality beams. The main centers for light-ion fusion are Sandia National Laboratories[6] and the Kernforschungszentrum Karlsruhe[7]. These programs emphasize electrical energy compression, seeking only a factor of about 100 power amplification from beam manipulations. The accelerator electrodes must sustain fields exceeding 200 MV/m to create the necessary high ion current densities. This limits the technology to single shots. Nonetheless, LIF programs can make valuable contributions to energy applications in the areas of beam-target interactions at high intensity, target diagnostics and advanced methods for beam transport.

The other two accelerator options use multi-stage devices to generate lower current beams of heavy ions at higher kinetic energy (heavy ion fusion). High-energy accelerators extend the time and distance for conversion from electrical to kinetic energy; as a result, they can operate reliably at high-repetition-rate. The program at the GSI Darmstadt[8] is based on a conventional RF linac feeding a series of storage rings for beam compression. This approach uses kinetic energy storage and compression exclusively - the electric energy transfer occurs at low power density. The main physical problem of the RF accelerator option is the confinement of intense ion beams in storage rings at a low enough energy to be of interest for ICF. Even with the application of laser induced beam stacking[9] for phase space compression in rings, the ability to meet the focal spot requirement is marginal. Furthermore, there is no latitude to reduce the beam energy below 10 GeV. The main engineering problem is the cost and complexity of kinetic energy storage. Containment of 1 kJ heavy ion beam in a ring costs roughly 10^5 times as much as storing the same electrical energy in a low-inductance capacitor. Clearly, the imperative is to minimize kinetic energy storage in a practical system. Although there is no definitive answer, studies of the storage ring approach to date imply costly and complex systems.

The main center for the induction linac approach is the Lawrence Berkeley Laboratory[10] with assistance from Lawrence Livermore Laboratory. Induction linacs seek a balance between electric and kinetic energy storage for high average power at relatively low cost. The accelerators incorporate acceleration gaps with ferromagnetic isolation cores[11]. Each stage consists of an electrostatic acceleration gap driven directly by a pulsed power generator. The isolation chokes allow series gap stacking to achieve high beam kinetic energy. An advantage of the induction linac is that it can drive pulsed currents in the multi-kA range. The drawback is that the ferromagnetic core cost is high in the low gradient machines.

The induction linac HIF driver is a straight-through device to generate a single beam pulse at moderate repetition rate (<10 Hz). Shaped gap voltage pulses induce a velocity tilt in the non-relativistic ions to compress the beam as it moves through the system. The pulselength varies from several microseconds to about 100 ns. Final bunching to 10 ns occurs in drift transport lines near the reactor. To pass the maximum current, beams propagate near the space-charge limit in a parallel array of quadrupole lens channels. Experiments at LBL have demonstrated the transport of low emittance beams at high flux levels in a quadrupole array with almost a perfect balance between space-charge and focusing forces[12]. The main physics problem is longitudinal control of beam pulses in a heavily loaded accelerator[13] - the papers by Fessenden and Smith in these proceedings discuss this topic. Reference 14 summarizes system studies of power plant drivers carried out by LBL and other groups. Design studies to date use high-vacuum ballistic transport in the reactor as a baseline, limiting the beam kinetic energy to high values. Because induction linacs have low average gradient (<1 MV/m), the cost of cores and other equipment in a 10 GeV exceeds 1 B$.

The main engineering challenge for induction linac drivers is reduction of the driver cost. Two possible solutions are 1) to modify the accelerator technology and 2) to relax the beam requirements. Regarding accelerator technology, papers by Hewett, Yu and Newton in these proceedings report studies of recirculating geometries. A recirculating induction accelerator makes more effective use of isolation cores at expense of a complex acceleration process. In this paper, I will concentrate on second option, lowering requirements on beam quality and kinetic energy through alternative transport techniques in the reactor. Propagation of heavy ion beams through a plasma environment aroused considerable interest a decade ago[15], but lack of funds and a prevailing conservatism in driver design impeded further work. The parameters of conceptual heavy ion drivers to date are set largely by the limitations of ballistic beam propagation in high-vacuum. It is important to note that attractive plasma transport modes exist that can lead to dramatic reductions in the cost of accelerators.

Ballistic transport of a beam to a fusion target in high-vacuum has several drawbacks. The process demands low beam emittance and small energy spread. For example, to focus a 10 GeV U beam over a 10 m span with a compression from 10 cm to 2 mm implies a normalized emittance $\epsilon_n < 6 \times 10^{-6} \pi$-m-r. In vacuum, space-charge expansion limits beams to high kinetic energy and low current. Design studies[14] postulate a large number (20) of parallel beams to circumvent current limitations. Each beam must have its own transport line, final focusing lens array, and reactor entrance port. Transverse space-charge forces and electrostatic target charging preclude reduced beam energy or the acceleration of multiply-charged ions. Finally, it is doubtful that a high-vacuum environment is consistent with a practical reactor design.

One alternative is to improve ballistic focusing with electron neutralization to reduce space charge forces. Although a low emittance is still necessary, there is considerably more latitude to choose beam energy, ion charge state, and the number of reactor entrance ports. In this case, constraints derive mainly from beam transport in the accelerator rather than space-charge forces in the reactor. It may be possible to reduce the beam kinetic energy - although the emittance will be higher, the required focal spot is larger. Also, the use of multiply-charged ions reduces the accelerator length for a given kinetic energy.

An attractive neutralization option is to direct the beam through a preformed plasma cloud at the reactor entrance and then to allow it to propagate through a diffuse reactor plasma generated by the ionization of a low-density background gas. Acceleration of electrons from the plasma cloud by the beam space-charge potential gives effective neutralization. Electron conduction in the diffuse reactor plasma avoids electron heating as the focused ion beam compresses. With this process, it may be possible to transport the full energy beam current from an HIF driver with as few as two beams. Early studies[17] suggested that stable plasma propagation may be limited to a "1 torr window" in analogy with pinched electron beam experiments. Here, the upper limit on background gas pressure is set by beam stripping and the filamentation instability, while the plasma electron-ion two-stream instability sets a lower limit on pressure. The present belief[18] is that the consequences of the two-stream instability are small and that there is no lower limit on background gas pressure. The instability induces negligible beam energy loss through plasma heating and may allow a small fractional imbalance of beam and background electron currents.

An alternative plasma transport mode, self-pinched propagation[19], could dramatically impact the cost of an induction linac ICF driver. The idea is to focus a high-current beam to small spot outside the reactor shield with a short focal length lens. When the beam enters the chamber, a plasma provides complete cancellation of electric fields. In some circumstances, the plasma return current may occupy a larger area than the beam current, leaving enough beam-generated magnetic field to contain the ions in a constant radius pinch. This process does not violate conservation of emittance - it involves only a translation of a preexisting focus. The success of experiments at the Naval Research Laboratory on pinched electron beams in gas[20] and intense ion beam propagation in preformed plasma channels[21] demonstrate the successful control of hose and filamentation instabilities.

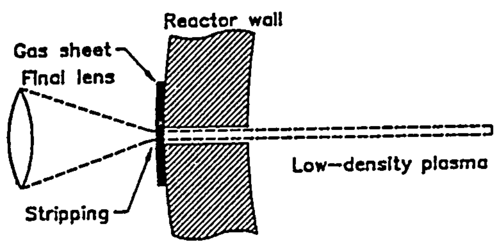

Fig. 4. Injection of a self-pinched beam into a plasma-filled inertial fusion reactor.

Previous work on heavy-ion beam self-pinches concentrated on a homogeneous high-density plasma with beam stripping extended along the propagation path[19]. Because of high predicted plasma conductivity, the residual magnetic field was low. In these studies, self-pinching was marginal. Figure 4 illustrates a better approach. Ion stripping occurs in a dense gas sheet at the external focal point. The highly-charged ions pass into a low-density plasma in the reactor. Simple scaling calculations show that conditions for a pinched beam equilibrium are easy to attain. Ion beams of proper range for ICF optimally have velocities of about 0.2c. This figure corresponds to a beam pulse length of 0.6 m, much shorter than the propagation distance. To avoid charge buildup, the plasma electrons in any cross section of the isolated beam slug must carry a negative current exactly equal to ion current. Suppose the ion current is given by $Z^* I_o$, where I_o is the particle current and Z^* is the ion charge state. A focusing magnetic field exists within the beam volume if the electron current occupies a larger area than the ion current. Inductance in the plasma column is minimized if the areas of the ion beam (A_b) and electron beam (A_e) are equal - the column resistance is lowest when the electrons occupy the maximum area. If A_e is slightly larger than A_b, then the net current inside beam volume is $I_{net} = Z^* I_o f_m$, where $f_m = (A_e - A_b)/A_e$. The paraxial envelope equation implies the following condition for a beam equilibrium,

$$\epsilon_n \cong Z^* r_o \left[\frac{e I_o f_m \beta\gamma}{2\pi\epsilon_o m_i c^3} \right]^{1/2}, \qquad [1]$$

where ϵ_n is the normalized emittance. For a 4 GeV uranium beam ($\beta = 0.2$), vacuum ballistic focusing to a 5 mm radius target requires a value $\epsilon_n = 10^{-5}\pi$-m-r. To see the implications of Eq. 1, consider a value 5 times higher. Two pinched beams with $I_o = 50$ kA irradiate the target - the uranium ions entering the reactor have charge state $Z^* = 40$ entering the reactor. For $r_o = 5$ mm, Eq. 1 implies that $f_m = 0.023$. Because of the high value of Z^*, a pinched equilibrium requires a net current of only 47 kA. Fig. 5 shows the approximate radial variation of field in the beam. The corresponding field energy per meter is

$$U_m = \left[\frac{\mu_o}{16\pi} \right] (I_o Z^* f_m)^2. \qquad [2]$$

For the example discussed, the energy is only 55 J/m. Alternatively, any resistive process that transfers more than 55 J/m from the beam to the plasma electrons will give sufficient magnetic field for a pinched equilibrium. Three resistive process that can account for the energy transfer are ionization of the background gas to create the plasma, heating of drifting electrons by the electron-ion two-stream instability, and acceleration of electrons to achieve approximate current neutralization of the beam. In fact, it is unlikely that a high intensity ion beam could propagate through a plasma without loosing at least 50 J/m. Higher energy loss would create stronger magnetic fields and a more tightly-pinched beam. I feel that a self-pinched equilibrium is a high-probability state for any stripped low-emittance ion beam. Similar optimistic predictions can be made for beams of light ions at reduced energy.

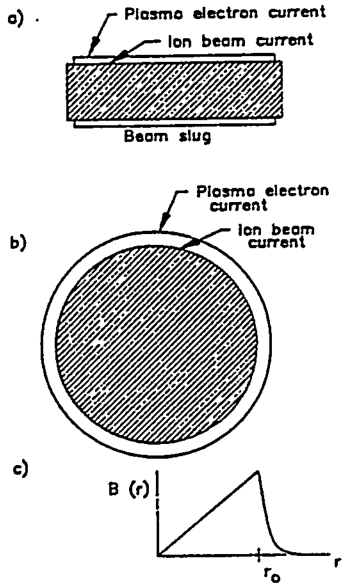

Fig. 5. Physics of the self-pinched heavy ion beam. a) Longitudinal section. b) Radial section. c) Radial variation of azimuthal magnetic field.

The self-pinched mode can alter the baseline parameters of HIF induction linacs for reduced size and cost. Relaxation of reactor transport limits would allow the use of lower beam kinetic energy and multiply charged ions, reducing the accelerator length. The corresponding smaller ion range would allow simple target designs and larger focal spots. The combination of the large focal spot and focusing external to the reactor would relax requirements on beam emittance and energy spread. In turn, a higher beam emittance would permit the use of existing ion sources and shortened quadrupole lenses. Because the limiting current in the accelerator scales inversely as the square of the quadrupole length, the machine can accommodate the higher currents associated with reduced beam energy. The self-pinched transport mode also widens the range of possibilities for reactor design. The problem of beam stripping in the reactor is no longer important and only a few small diameter apertures are necessary for beam injection. In summary, the already attractive option of induction linacs for ICF reactors can be enhanced through application of plasma transport methods.

REFERENCES

1. Physics Today 44, 80 (1991).

2. S.E. Koonin (Chair), Interim Report on Inertial Confinement Fusion (Comm. Phys. Sci., Math. and Resources, National Academy of Sciences, 1990).

3. H. Guyford Stever (Chair), Report of the Technical Panel on Magnetic Fusion of the Energy Research Advisory Board, (U.S. Department of Energy, DOE/S-0081, 1990).

4. To be published, R.O. Bangerter, Proc. Symp. Heavy Ion Fusion, Monterey, December, 1990.

5. V.P. Smirnov, *et.al.*, Proc. 8th Int'l. Conf. High-power Particle Beams, edited by B.N. Breizman and B.A. Knyazev (World Scientific, Singapore, 1991), 61.

6. D.L. Cook, *et. al.*, Proc. 8th Int'l. Conf. High-power Particle Beams, edited by B.N. Breizman and B.A. Knyazev (World Scientific, Singapore, 1991), 3.

7. W. Bauer, *et.al.*, Proc. 8th Int'l. Conf. High-power Particle Beams, edited by B.N. Breizman and B.A. Knyazev (World Scientific, Singapore, 1991), 104.

8. To be published, R. Bock, Proc. Symp. Heavy Ion Fusion, Monterey, December, 1990.

9. To be published, R.W. Muller and I. Hofmann, Proc. Symp. Heavy Ion Fusion, Monterey, December, 1990.

10. Denis Keefe, book on high-brightness beams.

11. See, for instance, S. Humphries, Jr., Principles of Charged Particle Acceleration (Wiley, New York, 1986), Chp. 10.

12. M.G. Tiefenback and D. Keefe, IEEE Trans Nucl. Sci. NS-32, 2483 (1985).

13. S. Humphries, Jr., J. Appl. Phys. 51, 2338 (1980) and E. Lee, Proc. 1981 Linear Acc. Conf. (Los Alamos National Laboratory, LA-9234-C, 1982), 263.

14. D.J. Dudziak (Ed.), "Special Issue on Heavy-Ion Fusion Systems", Fusion Technology 13, 1988.

15. See, for instance, C.L. Olson, J. Fusion Energy 1, 309 (1982).

16. See, for instance, S. Humphries, Jr. and T.R. Lockner, in Applied Charged Particle Optics, Very-high-density Beams, edited by A. Septier (Academic, New York, 1983), 389.

17. To be published, R.F. Hubbard, M. Lampe, G. Joyce, S.P. Slinker, I. Haber and R.F. Fernsler, Proc. Symp. Heavy Ion Fusion, Monterey, December, 1990.

18. Private communication, R. Hubbard (Naval Research Laboratory) and C. Olson (Sandia National Laboratories).

19. S. Yu and E. Lee, Proc. Heavy Ion Fusion Workshop, edited by W.B. Herrmannsfeldt (Lawrence Berkeley Laboratory, LBL-10301, 1980), 504, and R.F. Hubbard, S.A. Goldstein and D.A. Tidman, Ibid., 448.

20. Private communication, R.A. Meger and T. Peyser, Naval Research Laboratory.

21. D. Mosher, *et.al.*, Proc. 8th Int'l. Conf. High-power Particle Beams, edited by B.N. Breizman and B.A. Knyazev (World Scientific, Singapore, 1991), 26.

16

SABRE/Gamble II Possible Experiment to Demonstrate Self-Pinched Propagation

C. Olson

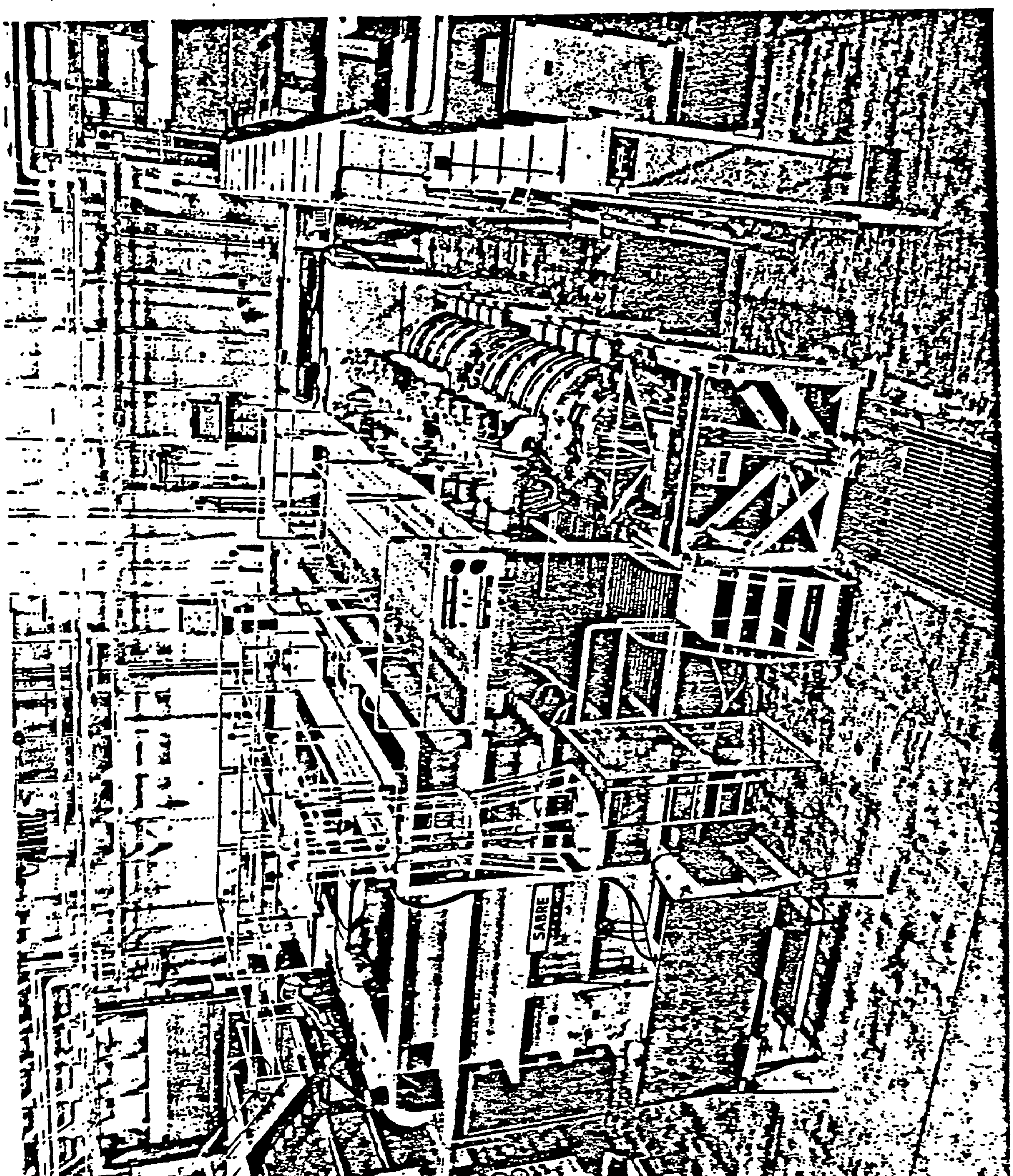
SABRE

The SABRE ion diode has excellent diagnostic access for a wide array of ion beam and plasma diagnostics.

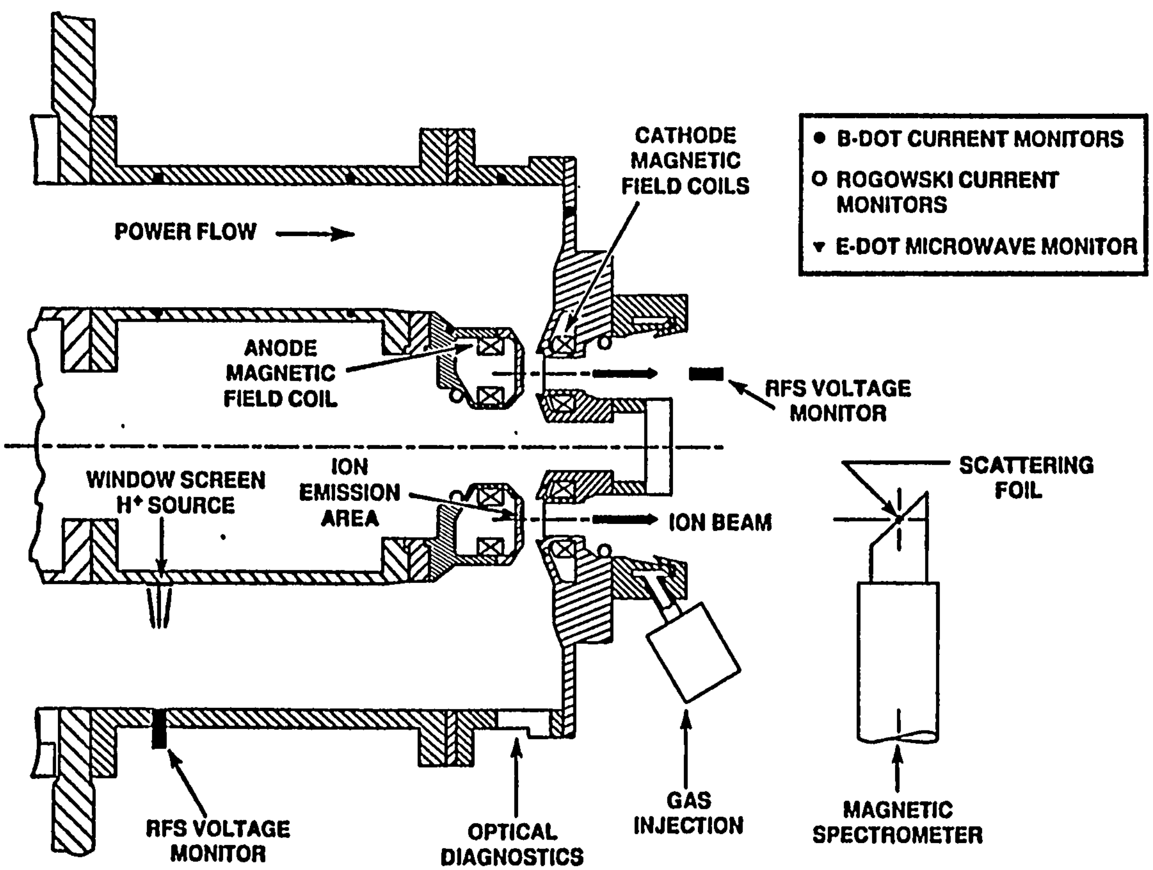

<u>ion beam diagnostics</u>

bare Faraday cups
filtered Faraday cups
shadow boxes
Rutherford pinhole cameras
ion pinhole movie camera
beamlet imaging fiber array
stress gauges
Thomson parabola
magnetic spectrometer
nuclear activation
neutron TOF

<u>plasma diagnostics</u>

visible, VUV spectroscopy
laser deflection
imaging fiber array
anode imaging fiber array

Self-Pinched Transport can be Demonstrated on SABRE

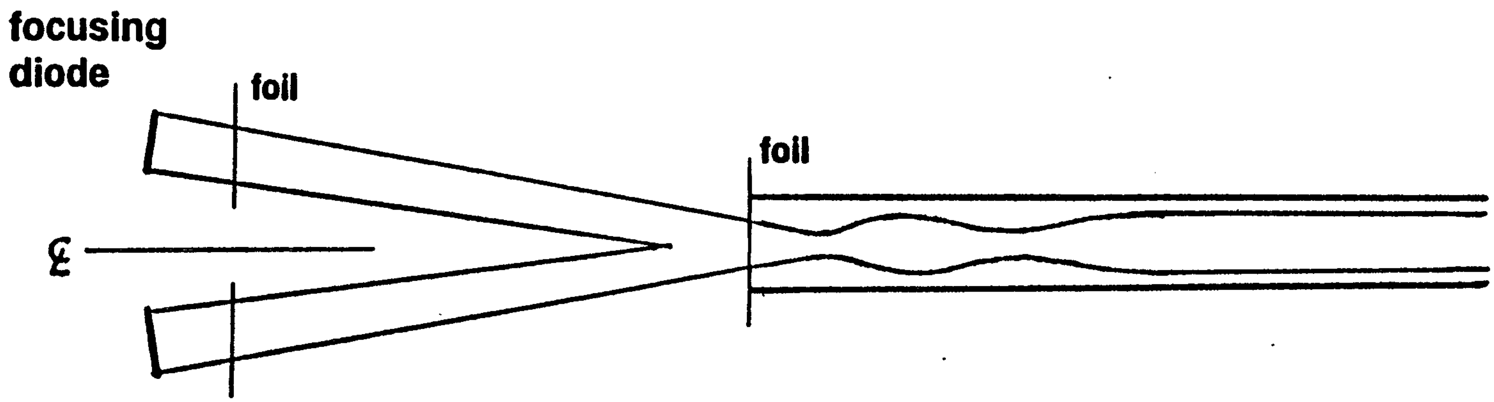

ballistic focus section
(~ few Torr argon)

self-pinched section
(~ 0.02 Torr argon)

INPUT

proton
150 kA
5 MeV ($\beta = 0.1$)
$\theta_\mu = 17$ mrad
$R = 6.5$ cm
$J \approx 2$ kA/cm^2

OUTPUT

$I_{net} \approx 30$ kA
$r_s = 0.8$ cm
$r_c = 1.1$ cm
$J \approx 40$ kA/cm^2

SABRE/Gamble II experiments would demonstrate:

1. ballistic focus to tube entrance.
2. self-pinch transport in tube

   (dependence on gas, pressure, tube radius, current, current risetime, ...)

3. self-pinched transport from tube to free space

   (aiming, tracking, stability issues, ...)

HIF Mainline Transport:
Ballistic / Near Vacuum / Quadrupoles

E. Lee
Lawrence Berkeley Laboratory

Workshop on Transport for a
Common Ion Driver

Sandia National Laboratory
September 20-21, 1994

Ballistic Final Focus

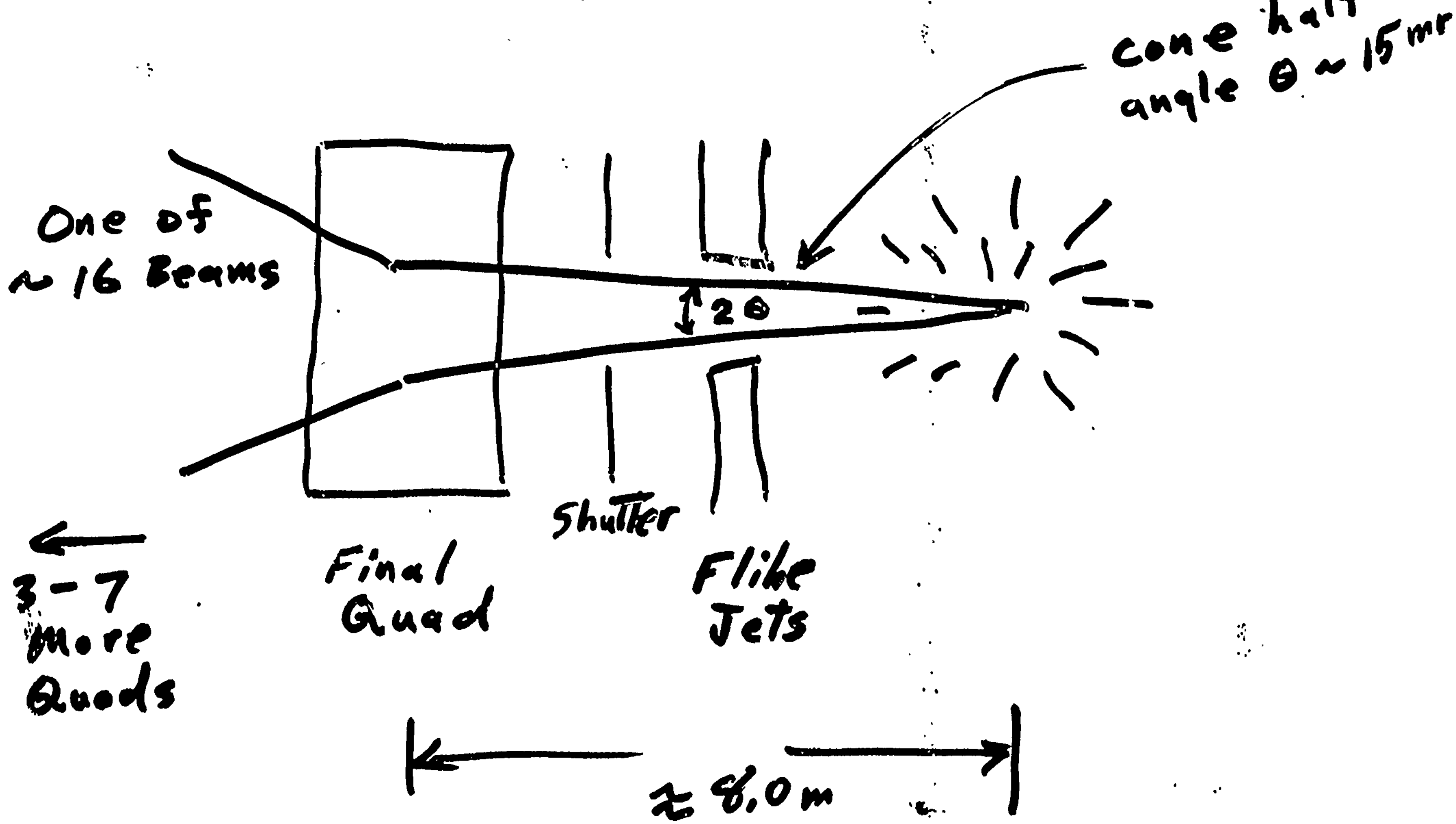

Drift-Compression Lines ~400m Long

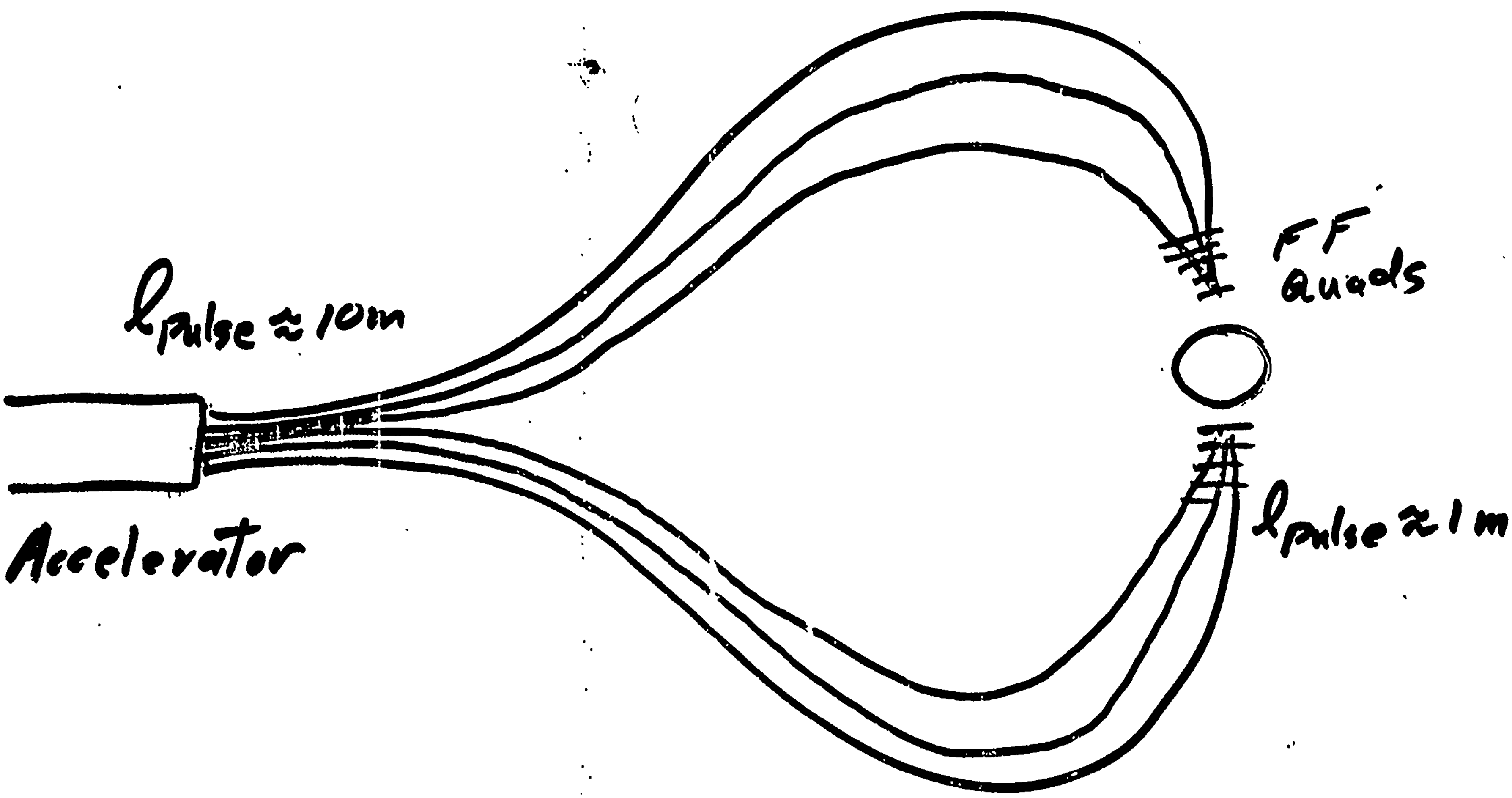

"Velocity Tilt" To Compress $\frac{\Delta v}{v} \approx \frac{10m}{400m} = 2.5\%$

(2)

Typical Final Beam Parameters:

Total Energy	$W =$	5.0 MJ
Ion Type	Cs^+	$A = 132.9$ amu
Ion Range	$R =$	.1 gm/cm²
Ion Energy	$E =$	5.33 GeV
Spot Radius	$r_s =$	2.0 mm
Gain	$G =$	90
Yield	$Y = WG =$	450 MJ
Peak Power	$P =$	480 TW

$\beta = .29$

{Two Sided Indirect Drive}

See R. Bangerter + D. Ho
Proc. 1990 Linac Conf.
also HIFAN-470

3)

Beam Parameters – Cont.

Assume There are $N = 16$ beams & We Use 12 For Peak Power

$$\text{Current Per Beam} = \frac{P}{12\,E} = \frac{480\,TW}{12 \times 5.33\,GV} = \underline{7.5\ kA}$$

This has been compressed by an order of magnitude in final ~400m

Current/beam in Linac $= \underline{750\ \text{Amperes}}$

Spot Radius – Combine Effects "In Quadrature"

$$a^2 = a_\epsilon^2 + a_{sc}^2 + a_{\Delta p}^2 + a_{errors}^2$$

emittance | space charge | chromatic effect | other

$$\downarrow$$

$$(2\,mm)^2 = (1\,mm)^2 + (1\,mm)^2 + (1\,mm)^2 + (1\,mm)^2$$

"Other" includes: higher order aberations
aiming errors
moving spot range

A Typical Beam Cone ½ Angle
$\theta = .015$ Radians

Larger θ: Good For Emittance

Good For Space Charge

Bad For Chromatic Aberation

Bad For Geometric Aberation

Bad For Flux of {Neutrons, Gas, X rays}

Bad For Magnet Size

Maximum Beam Radius in Final Focus $\approx 3F\theta = 3 \times 8 \times .015$

$= .32\ m$

Ballistic Final Focus Has Some Unpleasant Features

Large Magnets → $$ + Space

Gas Load From Chamber → Shutters

Neutrons + Xrays up Beam Line

Momentum Spread $\lesssim$ Few $\times 10^{-4}$ in Accelerator

Neutralization May be Needed

Effects of Stripping Poorly Known

Transverse Emittance Gives A Lower Limit ON Spot Size

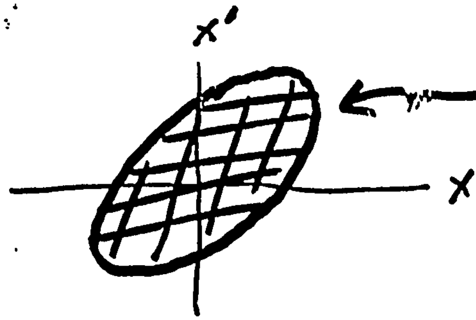

{ related to "microdivergence"

Emittance Dominated Envelope Radius $a(s)$:

$$a'' = \epsilon^2 / a^3$$

$$a_{min} = \epsilon / \theta$$

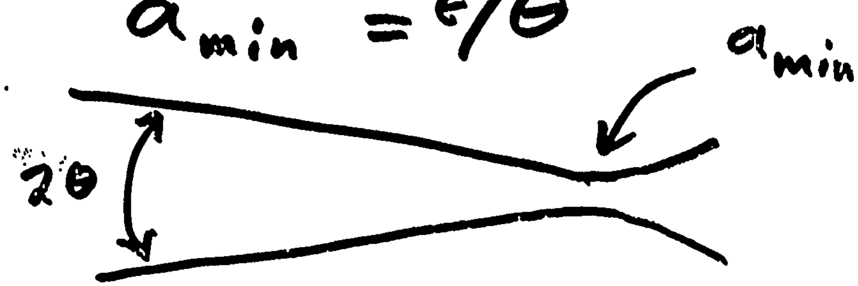

$\epsilon = 1.5 \times 10^{-5}$ m·r
$\theta = .015$ rad

$$\Rightarrow a_{min} = \frac{1.5 \times 10^{-5}}{1.5 \times 10^{-2}} = .001\,m$$

Final Focus Quadrupoles

Layouts are similiar to point-to-point focus

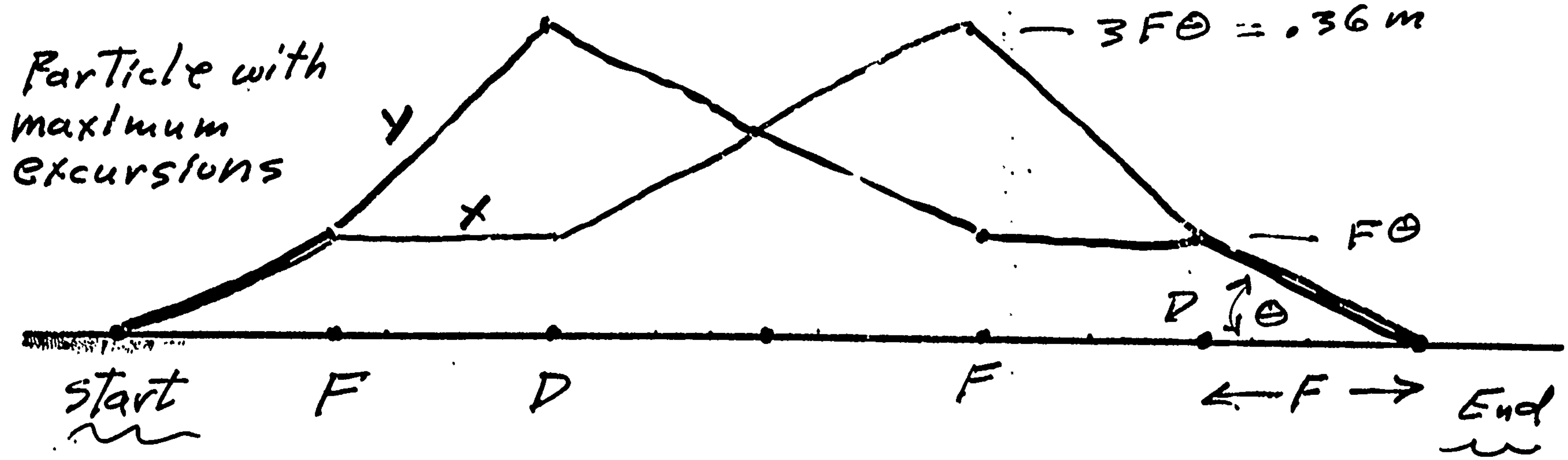

Large Central Magnets:

$[B\rho] = P/e = 122.7$ T-m

Focal length $F = 8.0$ m

effective length $\ell = 4.0$ m

Gradient $B' = [B\rho]/F\ell = 38.3$ T/m

Field at wire $B \approx 2.0$ T

Chromatic Effect

Quad Focal Length ~ Momentum $= P_0 \left(1 + \frac{\Delta P}{P_0}\right)$

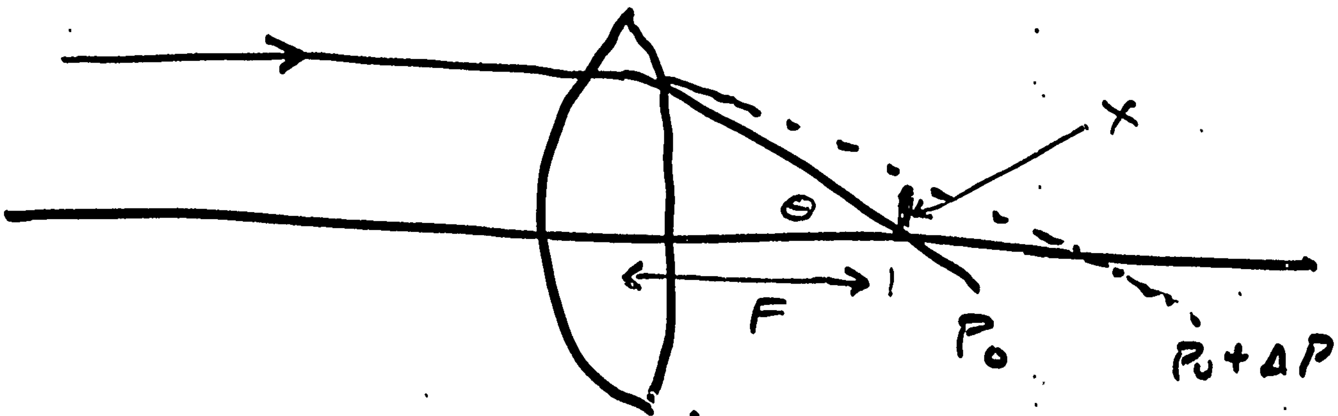

$x = F \theta \, \Delta P / P_0$

(Chromatic Aberation)

For The Four Quad System

$$X_{max} \cong \left[8 F \theta \, \Delta P / P_0 \right] \times \frac{3}{4}$$ ← Space Charge Effect

Require $\left| \frac{\Delta P}{P} \right| \lesssim \frac{a_{\Delta P}}{6 F \theta} = \frac{.001}{6 \times 8 \times .015} = \underline{1.4 \times 10^{-3}}$

Required Degree of Neutralization

Space charge dominated envelope:

$$a'' = K/a$$

$$K = \text{perveance} = \overbrace{\frac{2 q I_b}{31 \times 10^6 (\beta\gamma)^3 A}}^{K_0} (1-f)$$

f = combined neutralization factor

Integrate: $\frac{a'^2}{2} - K \ln(a/a_{min}) = 0$

$$\longrightarrow \quad \frac{\Theta^2}{2} - K_0(1-f) \ln(F\Theta/a_{min}) = 0$$

Require $f \geq 1 - \frac{\Theta^2}{2 K_0 \ln(F\Theta/a_{min})}$ 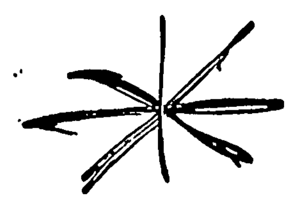

[Note insensitivity to a_{min}]

Neutralization (Cont.)

$I_b = 7500$ Amp $\theta = .015$ rad

$\beta\gamma = .297$ $F = 8.0$ m

$A = 132.9$ $d_{min} = .001$ m

$\gamma = 1$

$K_0 = 1.39 \times 10^{-4}$

Require $f \geq 1 - \frac{(.015)^2}{2 \times 1.39 \times 10^{-4} \ln(120)} = \underline{\underline{.83}}$

[Note 2.0 kA U^+ at 10 GeV

→ Required $f \geq \underline{\underline{.21}}$]

- Most Cases Require Some Neutralization

Stripping By Flibe

$Cs^{+}\ (\beta = .3) \rightarrow \langle\sigma\rangle \approx 2.3 \times 10^{-16}\ cm^{2}$ — Bohr Formula (N. Barboza)

600 °C Flibe: $P \approx .14\ Pa$

$n_g \approx 2.5 \times 10^{13}\ cm^{-3}$

strip length $= \frac{1}{n\sigma} = 174\ cm$

800 °C Flibe: $P \approx 28\ Pa$

$n_g \approx 4 \times 10^{15}\ cm^{-3}$

strip length $= \frac{1}{n\sigma} = 1.1\ cm$

To Strip only 1% of beam in 4.0 m

Require $n_g \lesssim 1.1 \times 10^{11}\ cm^{-3}$

Is This Needed ??

LIF Mainline Transport: ballistic/gas + solenoid focus

C. Olson, P. Ottinger

All LIF transport for high yield and energy requires extraction diodes

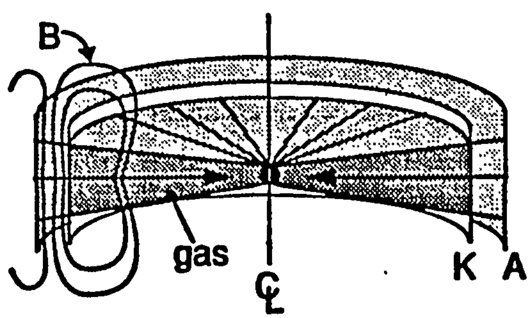

Barrell Diode (Applied B)
PBFA II

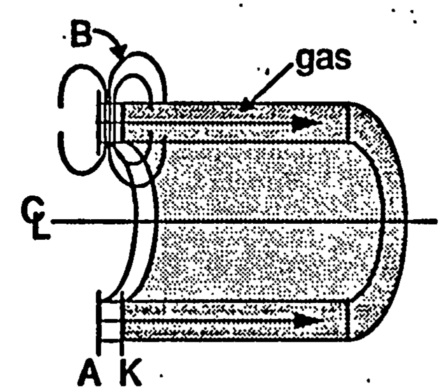

Extraction diode (Applied B)

ALIAS (SNL)
LION (Cornell)
SABRE (SNL)
GAMBLE II (NRL)

KALIF (KfK)
REIDEN IV (ILE, Osaka)

(HERMES III)
(LMF Module)
(ETF Module)
(LIBRA Module)

LMF

LMF has specific transport requirements

extractor diode

microdivergence ~ 6 mrad

voltage-ramped for axial time-of-flight bunching (26 - 35 MV Li^+)

- focusing system must accommodate energy spread

bunching length (400 cm)

lens-to-target length (≥ 100 cm)

diode protection

minimum debris (minimal transport apparatus allowed in chamber)

LMF

The baseline transport scheme for LMF is an achromatic magnetic lens system

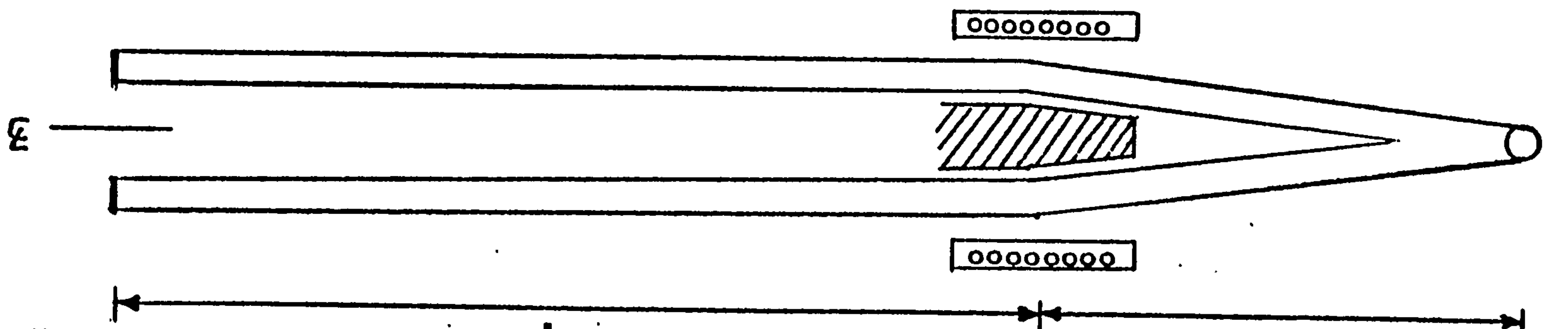

- focuses on target even as diode voltage changes
- spot size determined by $\theta_\mu F$, <u>NOT</u> $\theta_\mu(F+L)$
- no apparatus inside chamber
- diode shielded from debris

- basic elements already in PBFA II: diode lens, gas neutralization, solenoid

gas breakdown is key issue

LMF

Many potential issues have been addressed

applied B near diode
diamagnetic effect in lens
filamentation instability
2-stream instability
scattering (foil & gas)
energy required to ionize & heat gas
optimal gas and gas pressure
diode voltage accuracy
beam instantaneous energy spread
diode/lens alignment tolerances
magnet and chamber survivability
inner beam edge not achromatic
diode lens length
energy/transport efficiency
module packing

Gas breakdown is key remaining issue:

physics understanding
micro charge non-neutrality
current neutralization (want >> 99%)
high σ avoids filamentation
effect of $B_{\perp}$ on σ

LMF has three back-up transport modes

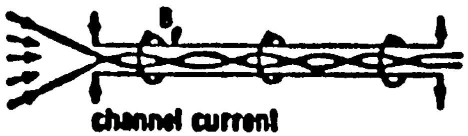

$I_c \sim 50$ kA

Wall-confined channels; demonstrated & "guaranteed to work"

- transport up to 5 meters demonstrated (1 MeV p, 400 kA)
- low mass Kapton tubes demonstrated
- $\eta \sim 75 - 100\%$ (LMF)

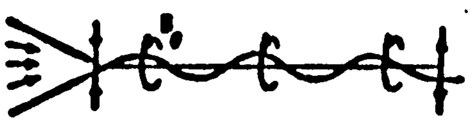

$I_w \sim 50$ kA

Wire-guided transport; demonstrated & "guaranteed to work"

- transport up to 1.5 meters demonstrated (1 MeV p)
- $\eta \sim 50 - 75\%$ (LMF)

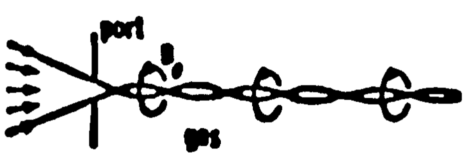

$I_{net} \sim 50$ kA

Self-pinch transport; under study

- several possible scenarios
- need current neutralization ~ 90-98%

Divergence reduction strategy

LMF requires only a moderate decrease in equivalent divergence

Microdivergence (θ_μ): Achieved and Proposed.

Accelerator	Ion	Diode	ε_i(MeV)	θ_μ(mrad)	Status	Equivalent θ_μ(mrad) for LMF (β=0.1; 5 MeV p or 35 MeV Li)
ALIAS	p	1-stage	< 0.6	19	achieved	< 6.6
ALIAS	p	2-stage	> 1	10	achieved	> 4.5
KALIF	p	1-stage	1.7	15	achieved	8.7
PBFA II *	Li	1-stage	9	17	achieved	8.6
SABRE	p	1-stage	5	17	achieved	17
LION	p	1-stage	1	19	achieved	8.5
GAMBLE II	p	1-stage	1	17	achieved	7.6
SABRE	p	1-stage	5	12	proposed	12
Hermes III	Li	2-stage	14	9	proposed	6
LMF	Li	2-stage	35	6	proposed	6

*barrel diode; all other cases are extraction diodes.

LIF Mainline Transport*
Ballistic (gas) Transport with Solenoidal Lens Focusing

Craig Olson
Sandia National Laboratories, Albuquerque, New Mexico
Paul Ottinger
Naval Research Laboratory, Washington, DC

Workshop on Transport for a Common Ion Driver
September 20-21, 1994
Sandia National Laboratories
Albuquerque, New Mexico

*work supported by US DOE

OUTLINE

- Introduction
  - LMF transport
  - BTSF system
- Transport efficiency
- Voltage tuning
- Status for BTSF

THERE ARE MANY PHYSICS ISSUES ASSOCIATED WITH ION BEAM TRANSPORT

self-consistent EM fields

beam charge & current neutralization

beam-induced gas breakdown

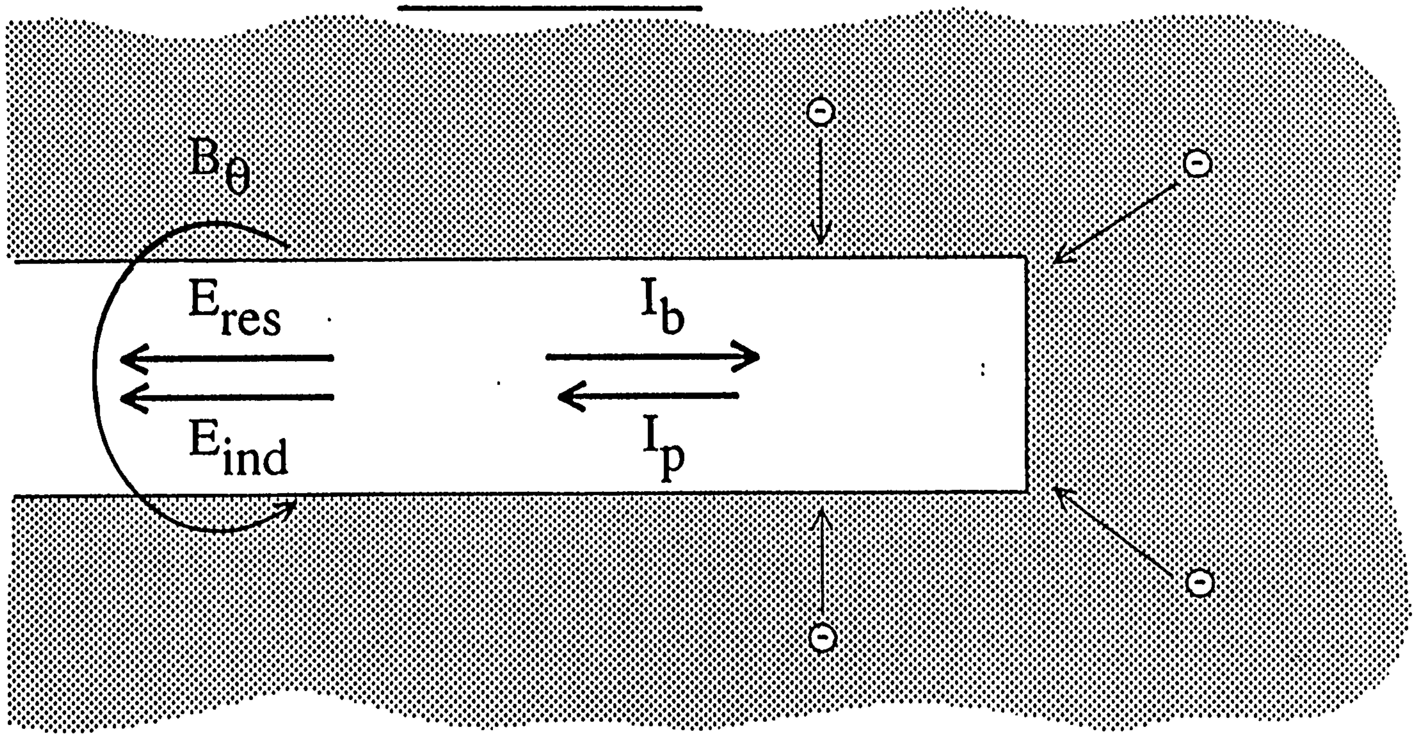

beam ion energy losses

plasma MHD

beam-plasma instabilities

NRL

THE LABORATORY MICROFUSION FACILITY IS PROPOSED TO STUDY HIGH-GAIN ICF TARGETS

Light Ion LMF parameters:

30 MeV Li beam

$r_t = 1$ cm

$E_t \geq 10$ MJ

$\tau_t = 10 - 20$ ns

NRL

CERTAIN ASPECTS OF THE LMF SYSTEM ARE DICTATED BY THE ION SOURCE AND PULSED POWER DRIVER

Driver: Based on Hermes III technology
30 MV, 1 MA, $\tau_p = 40$ ns, $E_p = 1$ MJ (per module)

Ion source: Magnetically insulated extraction diode
$J_i = 2\text{-}10$ kA/cm^2, R = 10-15 cm, $\Theta_\mu = 5\text{-}10$ mrad
(initial point design - $J_i = 2$ kA/cm^2, R = 15 cm, $\Theta_\mu = 5$ mrad)

Consideration	Implication
$\tau_p > \tau_t$	TOF bunching ($\beta = 2\text{-}4$)
$R > r_t$	focusing (F = 1 - 1.5 m)
standoff and TOF bunching	transport (L + F = 4 m)
$E_t > E_p$, symmetry, limits on transportable beam power density	N modules (10 - 30)

NRL

RAMPING THE DIODE VOLTAGE PROVIDES FOR TIME-OF-FLIGHT BEAM BUNCHING

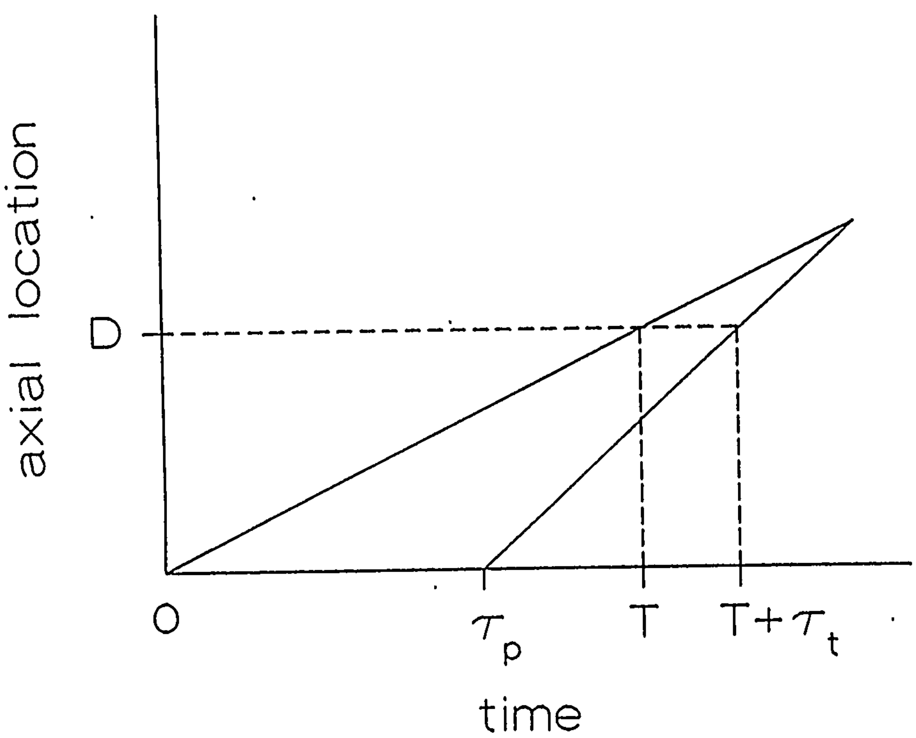

Ideal voltage waveform:

$$V(t) = \frac{V(0)}{\left(1 - \frac{t}{T}\frac{\alpha - 1}{\alpha}\right)^2}$$

where

$\alpha = \tau_p/\tau_t$ = bunching factor

$T = D/\dot{v}(0)$

NRL

THERE ARE A NUMBER OF TRANSPORT SCHEMES BEING CONSIDERED FOR LMF

Ballistic transport with solenoidal lens focusing (BTSF)

Ballistic focusing followed by

- Z-discharge transport (ZDT)
- Wire-guided transport (WGT)
- Self-pinched transport (SPT)

NRL

BALLISTIC TRANSPORT/SOLENOIDAL LENS FOCUSING SYSTEM FOR LMI

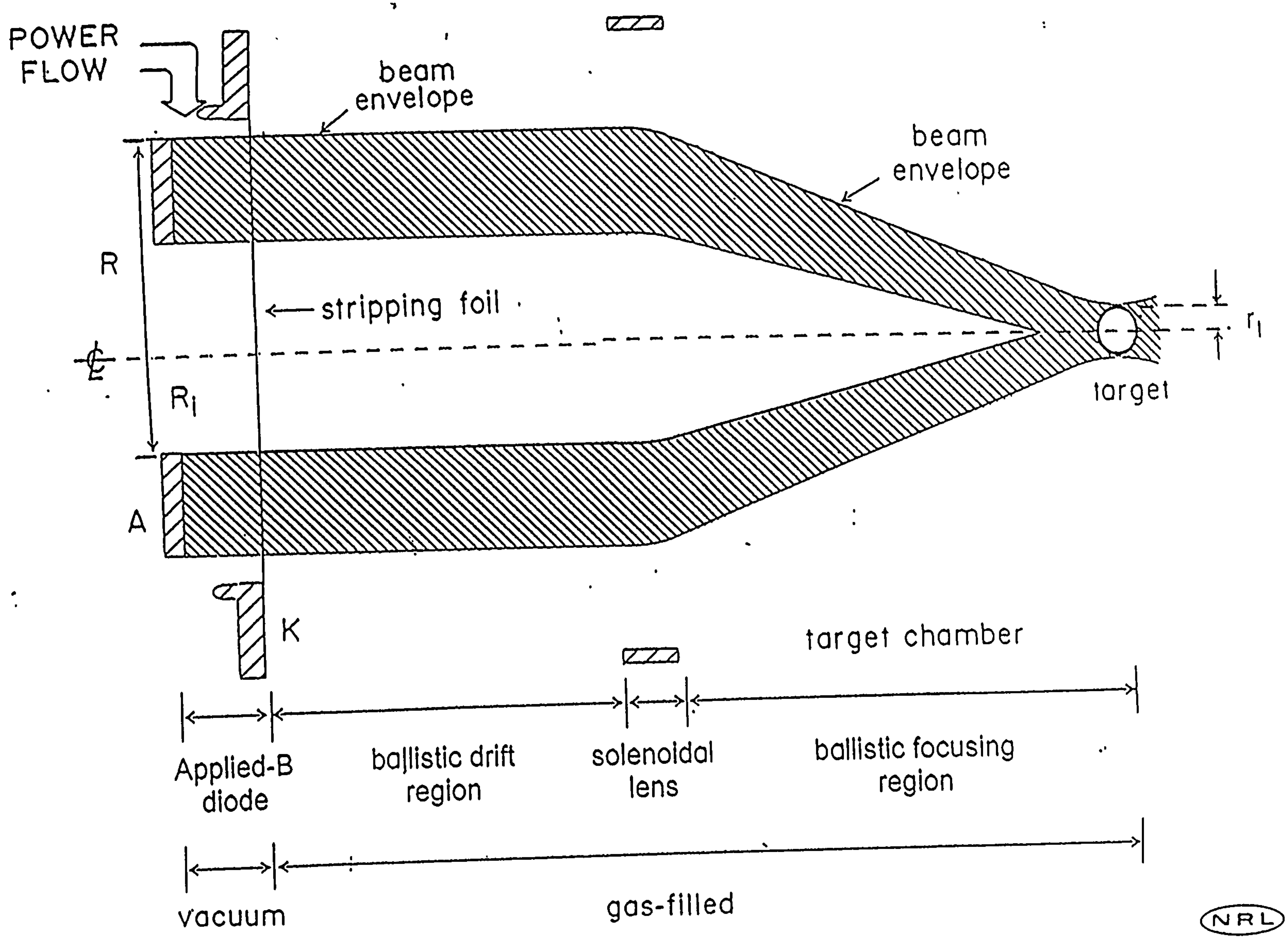

THE DIODE AND SOLENOID FORM A NEARLY ACHROMATIC LENS PAIR FOR BEAM FOCUSING

$$\Theta_d = \underline{\Theta_s(r)} + \underline{\Theta_b(r,t)}$$

$$\underline{\Theta_b} = \omega_c \Delta / v \;\alpha\; V^{3/2}$$

$$\underline{\Theta_F} = r/F \;\alpha\; V^{-1}$$

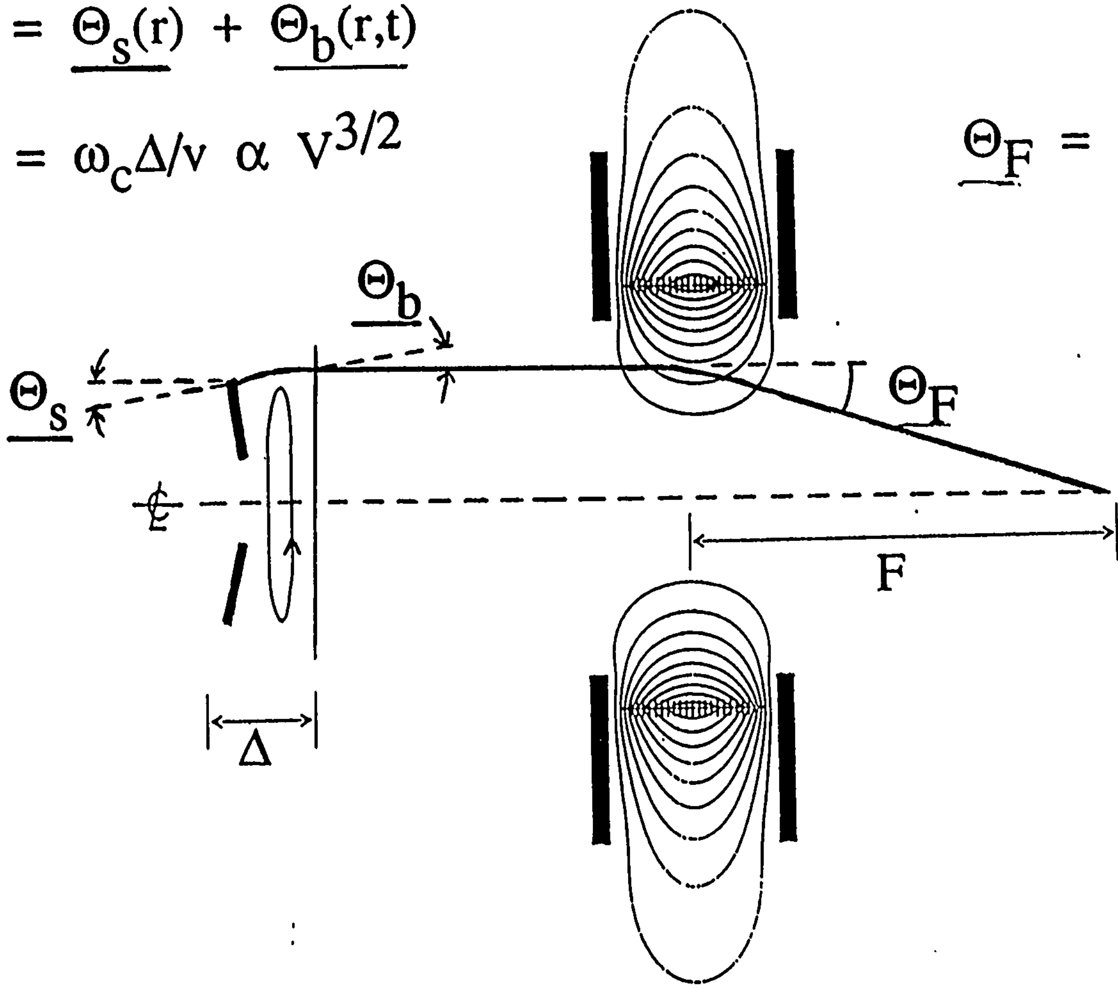

NRL

THE DIODE MODEL AND INJECTION GEOMETRY STRONGLY INFLUENCE TRANSPORT EFFICIENCY

$\Theta_s = \Theta_b(r,t) + \Theta_a(r)$

parallel extraction for BTSF

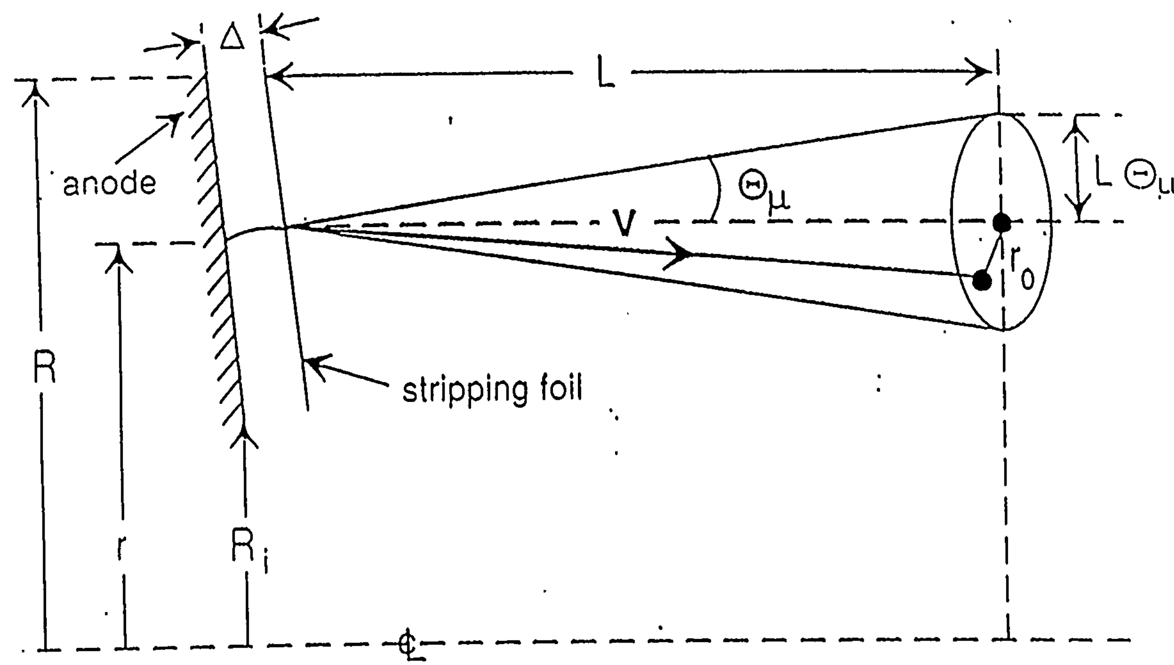

$J_i(r) = const.,$

$R_i = R/2$

$$\Theta_s(r,t) = \Theta_o \left(\frac{V_t}{V_o}\right)^{k-\frac{1}{2}} \left[1 - \left(\frac{V(t)}{V_t}\right)^{k-\frac{1}{2}}\right] \left(\frac{r}{R} - \frac{R}{4r}\right)$$

SWEEPING EFFECT ALSO OCCURS FOR BALLISTIC TRANSPORT

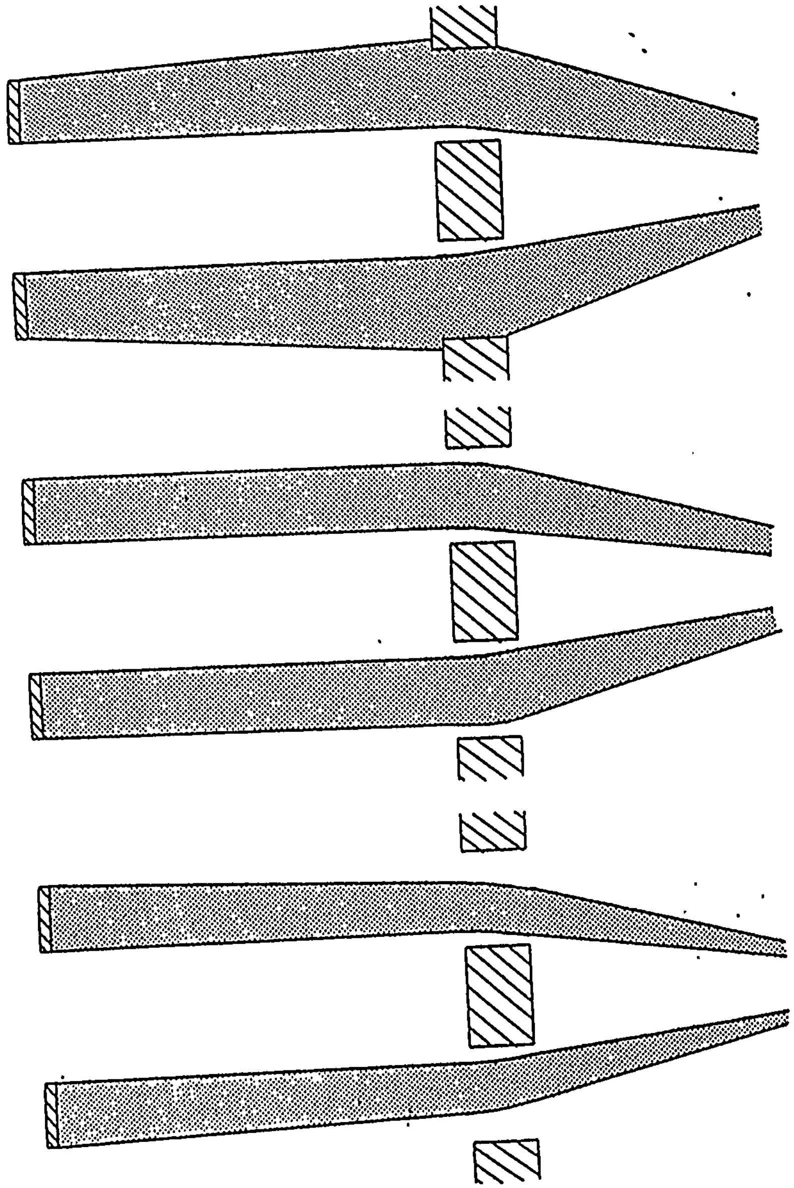

early in pulse;
beam directed outward

mid-pulse;
beam directed forward

late in pulse;
beam directed inward

NRL

FOR BALLISTIC TRANSPORT WITH SOLENOIDAL LENS FOCUSING, rP(r,z) INCREASES RAPIDLY NEAR THE TARGET AS IT FOCUSES AND BUNCHES

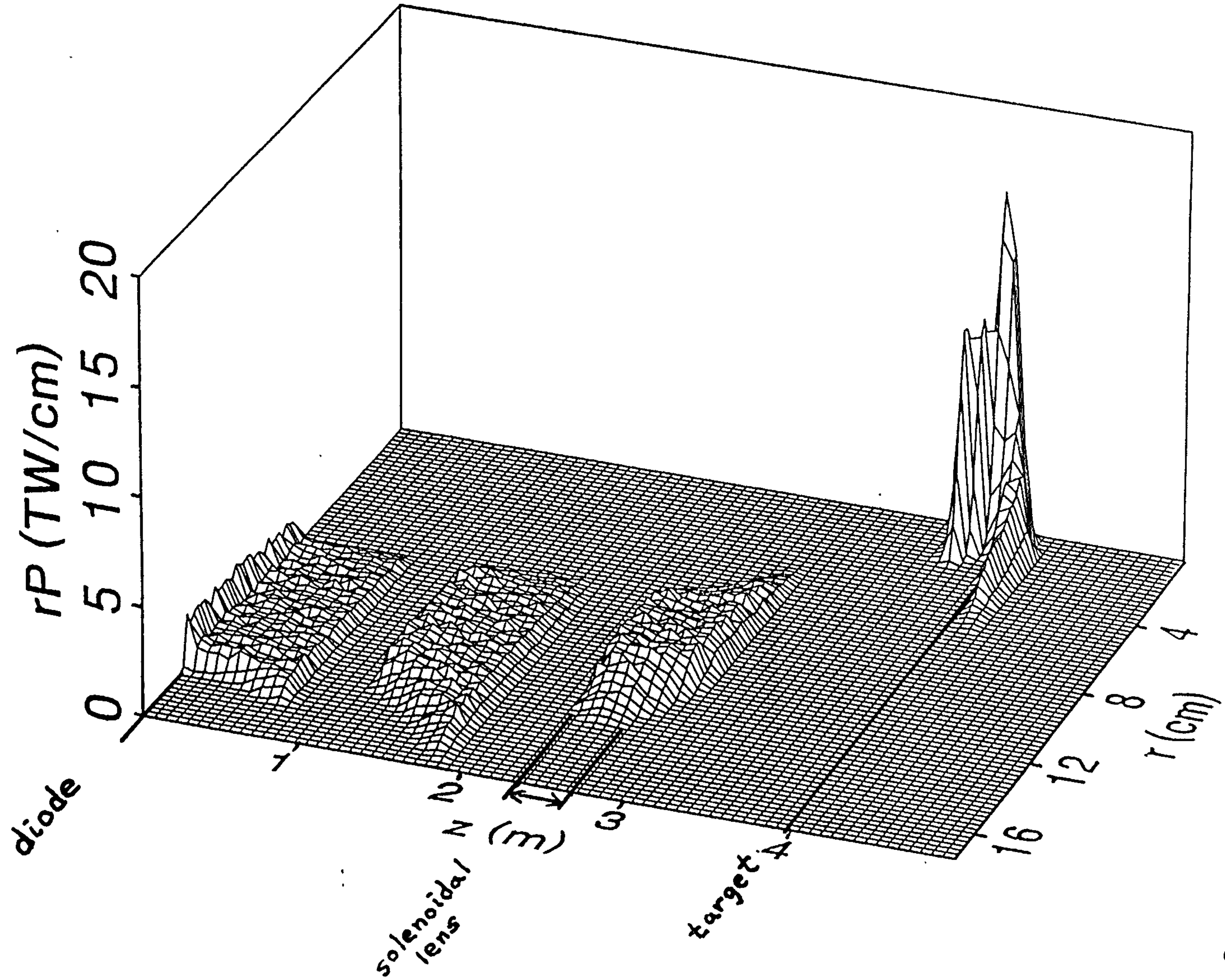

NRL

FOR BALLISTIC TRANSPORT WITH SOLENOIDAL LENS FOCUSING, F IS FIXED BY THE TARGET CHAMBER RADIUS

Analysis assumes:

- complete beam charge- and current-neutrality
- physically reasonable dimensions chosen for solenoid
- center plug for diode protection from blast
- diode/solenoid matched to minimize achromatic effects
- F chosen as smallest acceptable target chamber radius

NRL

FOR BALLISTIC TRANSPORT WITH SOLENOIDAL LENS FOCUSING, TRANSPORT EFFICIENCY IS DETERMINED BY LOSSES TO CENTER PLUG AND THE SPOT SIZE AT THE TARGET

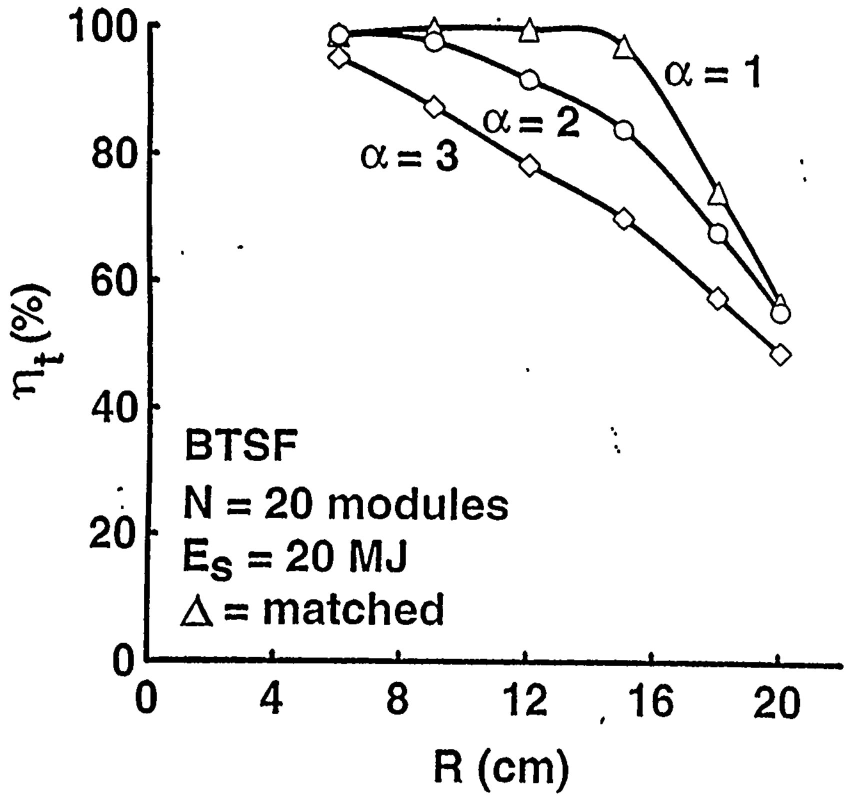

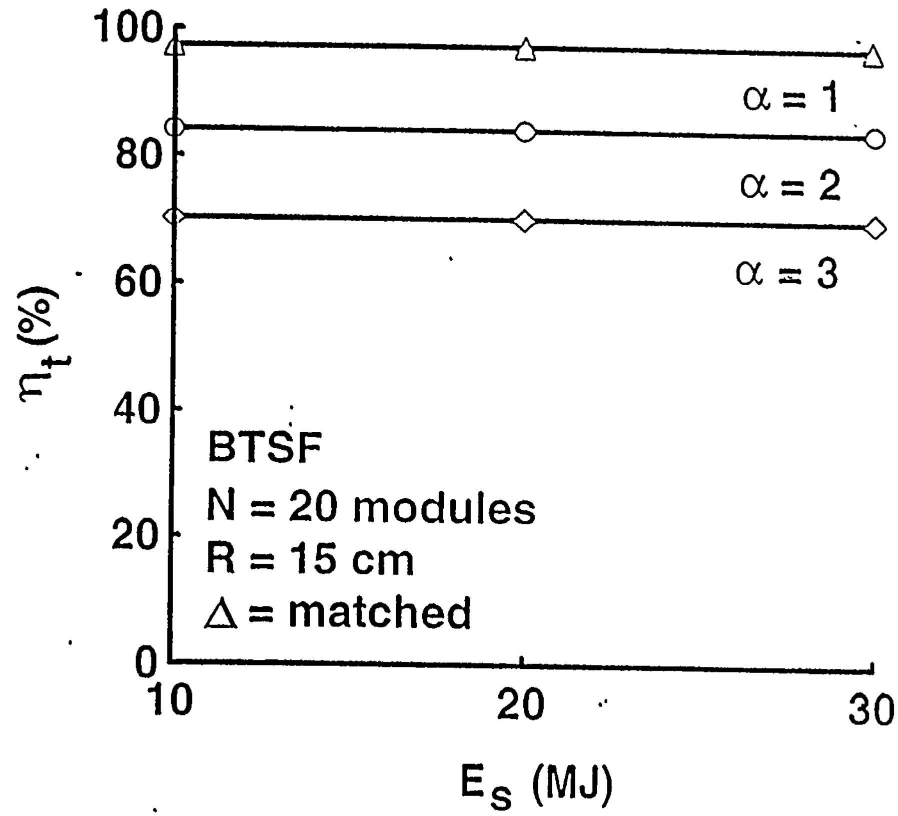

FOR BALLISTIC TRANSPORT WITH SOLENOIDAL LENS FOCUSING, TRANSPORT EFFICIENCY IS DETERMINED BY LOSSES TO CENTER PLUG AND THE SPOT SIZE AT THE TARGET

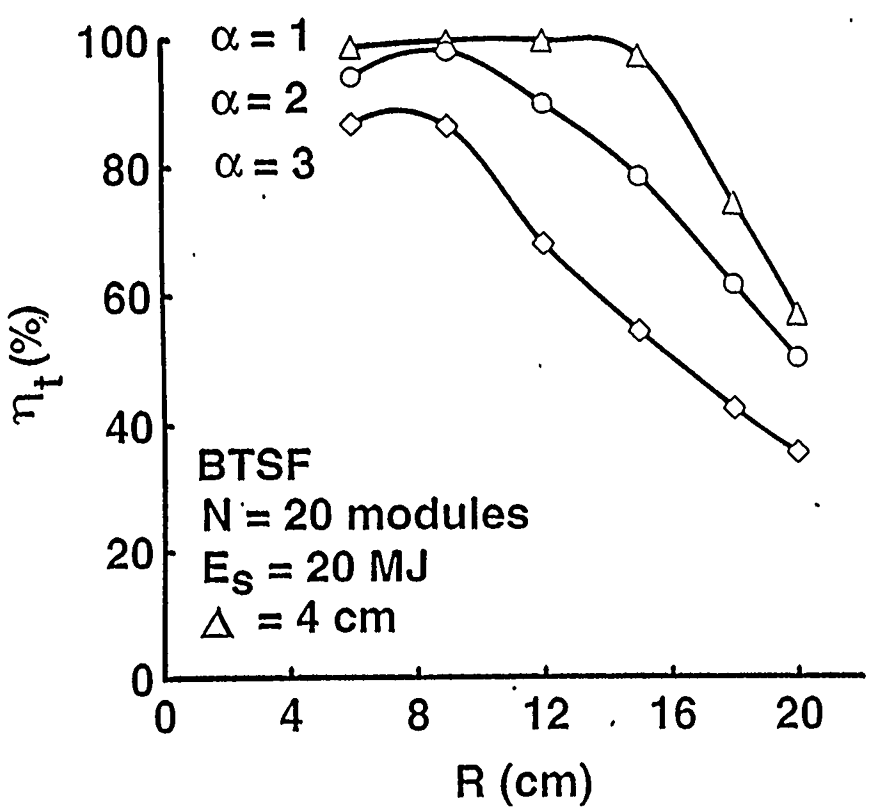

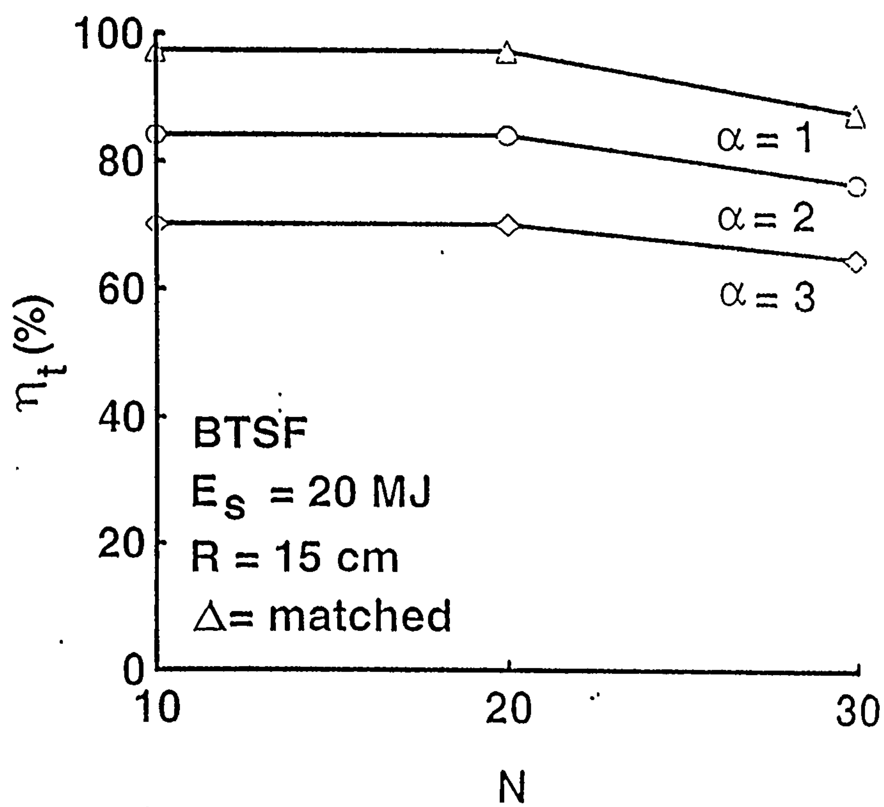

NRL

Tuning the BTSF system so that the beam focuses on target at midpulse provides optimum transport efficiency η_t

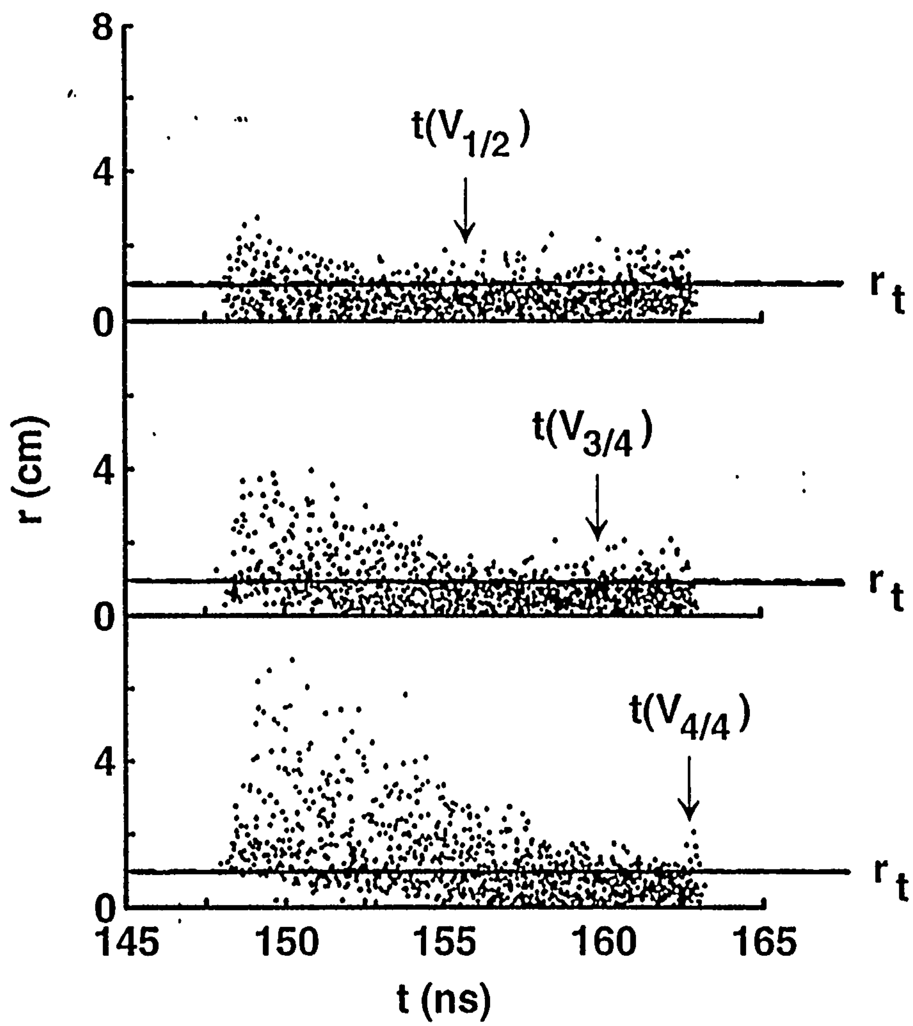

Tuning at 3/4 of the way through the pulse maintains high η_t while providing high intantaneous power efficiency at the end of the pulse

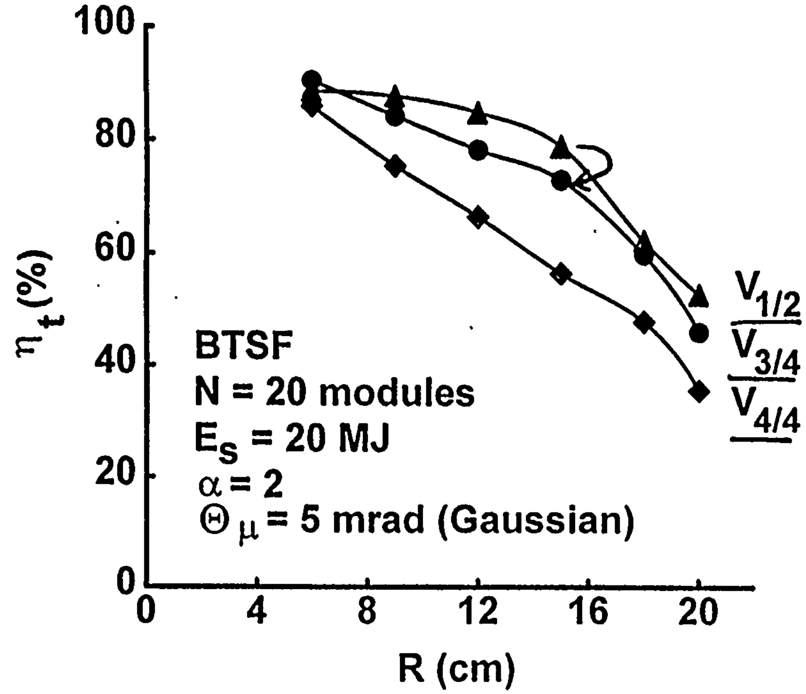

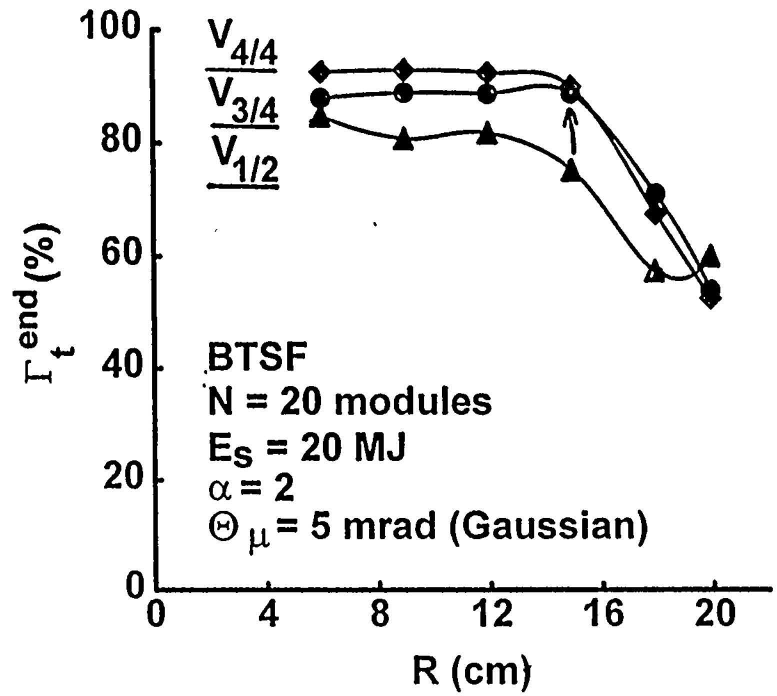

NRL

LMF

The baseline transport scheme for LMF is an achromatic magnetic lens system

NRL

BTSF

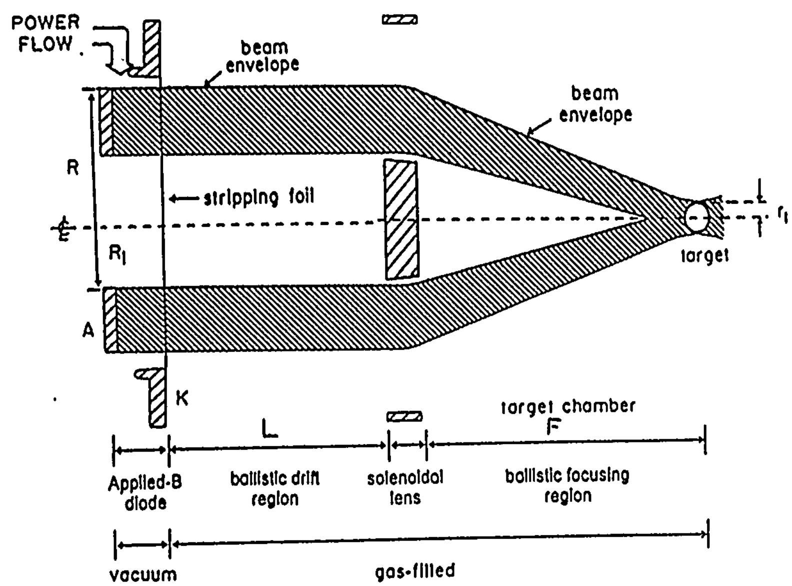

features

- nearly achromatic
- spot size determined by $\theta_\mu F$, not $\theta_\mu(F + L)$
- no apparatus inside chamber
- diode shielded from debris

LMF scaling

$\eta_t \sim 90\%$

status

- high degree of current neutralization is required
- beam-induced gas ionization studies underway

Channel Transport and Wire-Guided Transport

Paul Ottinger
Naval Research Laboratory, Washington, DC

Workshop on Transport for a Common Ion Driver
September 20-21, 1994
Sandia National Laboratories
Albuquerque, New Mexico

*work supported by US DOE

OUTLINE

- ZDT system
- Transport efficiency
- Status for ZDT
- Final focusing
- Transport constraints
- WGT system
- Transport efficiency
- Status for WGT

Z-DISCHARGE TRANSPORT SYSTEM FOR LMF

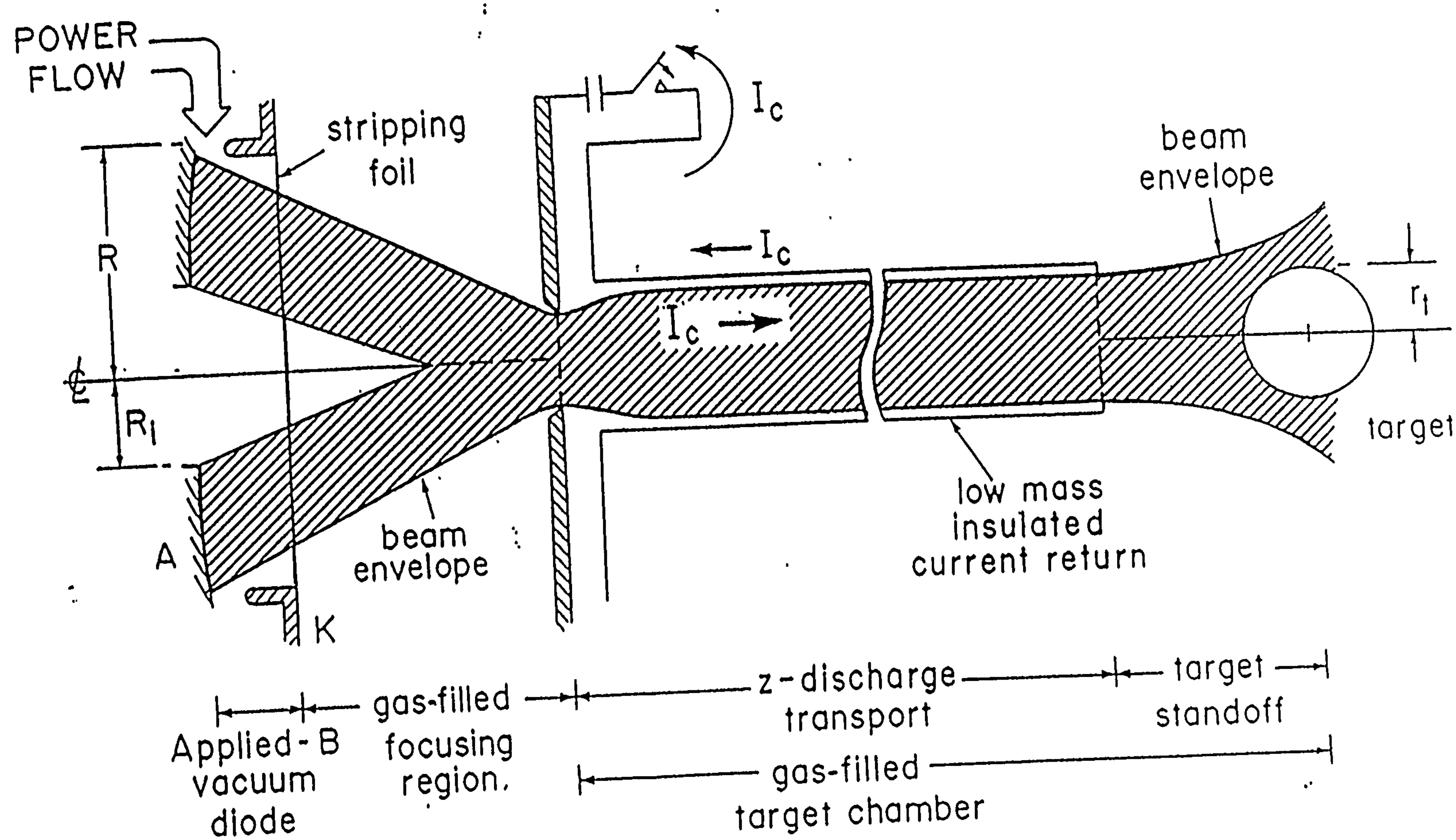

NRL

FOR Z-DISCHARGE TRANSPORT, I_c RADIALLY CONFINES THE BEAM IONS

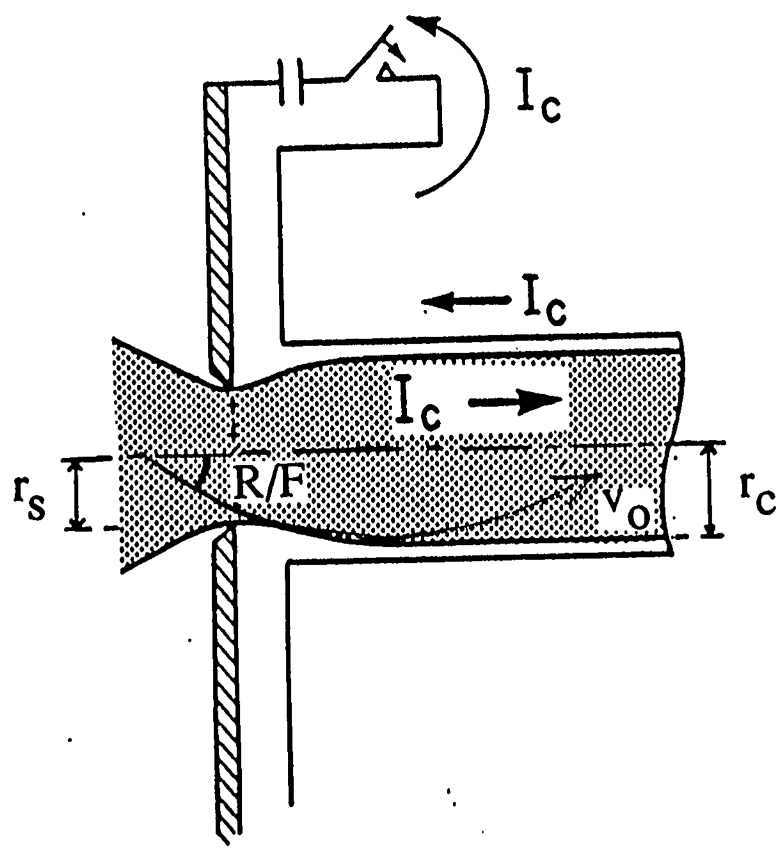

All ions confined to

$r \leq r_c$ when

$$\frac{ZeI_c}{m_i v_o} = \frac{(R/F)^2}{2[1-(r_s/r_c)2]}$$

NRL

ION ORBIT IN Z-DISCHARGE CHANNEL
case with no angular momentum

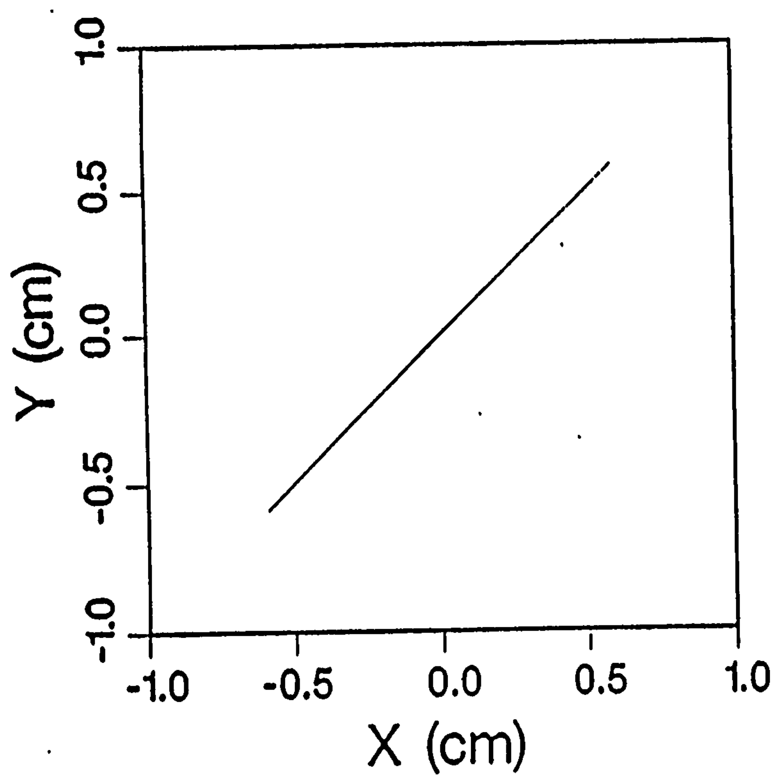

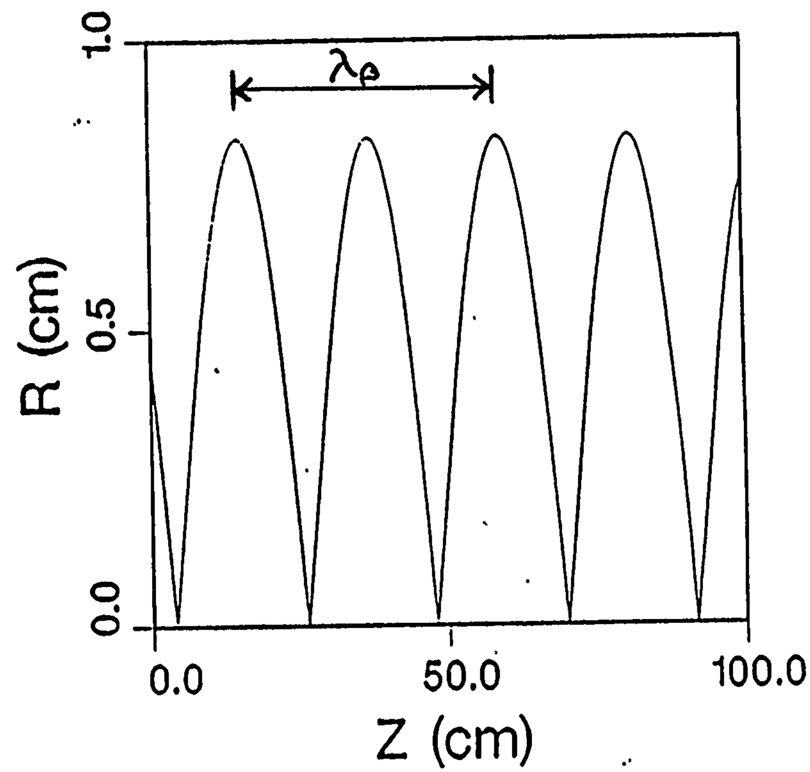

NRL

ION ORBIT IN Z-DISCHARGE CHANNEL

case with angular momentum

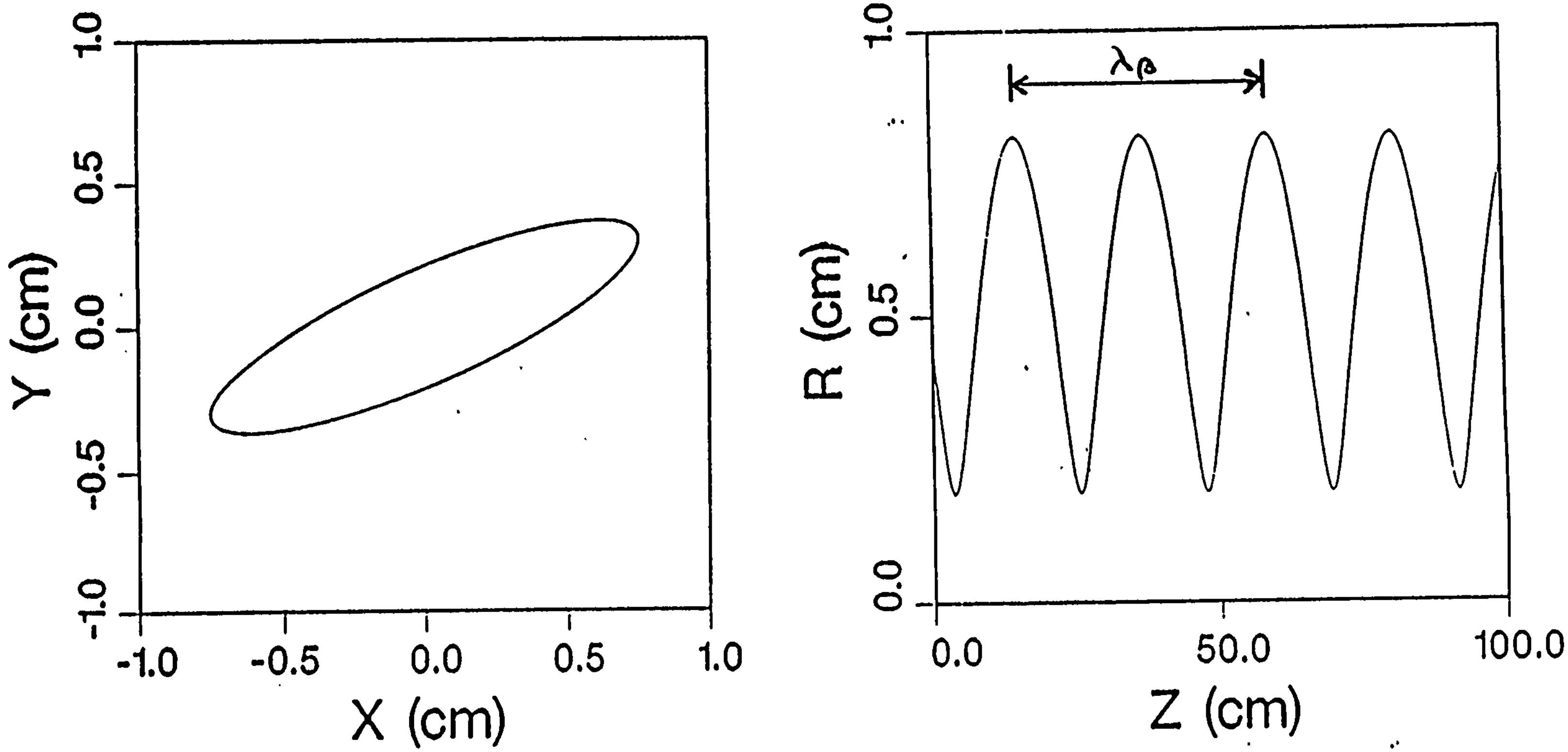

NRL

THE DIODE MODEL AND INJECTION GEOMETRY STRONGLY INFLUENCE TRANSPORT EFFICIENCY

$\Theta_s = \Theta_b(r,t) + \Theta_a(r)$

focused extraction for ZDT or WGT

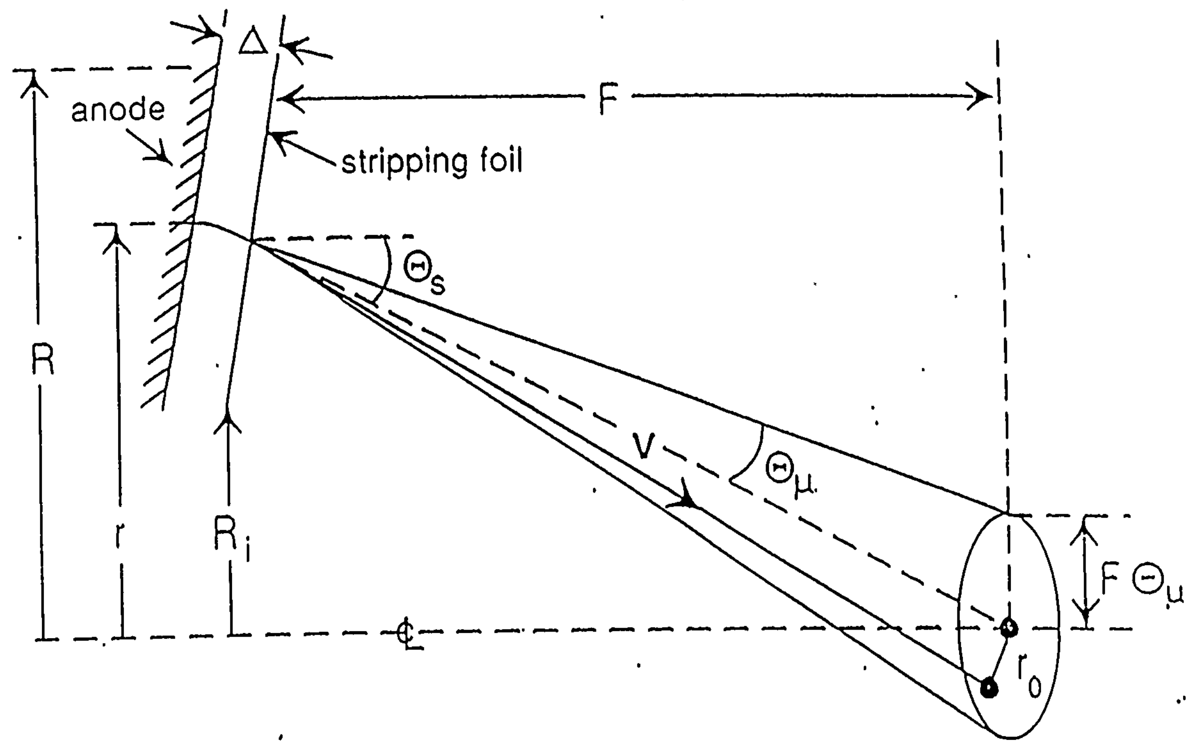

$J_i(r) = const.,$

$R_i = R/2$

$$\Theta_s(r,t) = -\frac{r}{F} + \Theta_o \left(\frac{V_t}{V_o}\right)^{k-\frac{1}{2}} \left[1 - \left(\frac{V(t)}{V_t}\right)^{k-\frac{1}{2}}\right] \left(\frac{r}{R} - \frac{R}{4r}\right)$$

TIME DEPENDENCE OF MAGNETIC BENDING IN DIODE CAUSES FOCUS TO SWEEP INWARD IN TIME

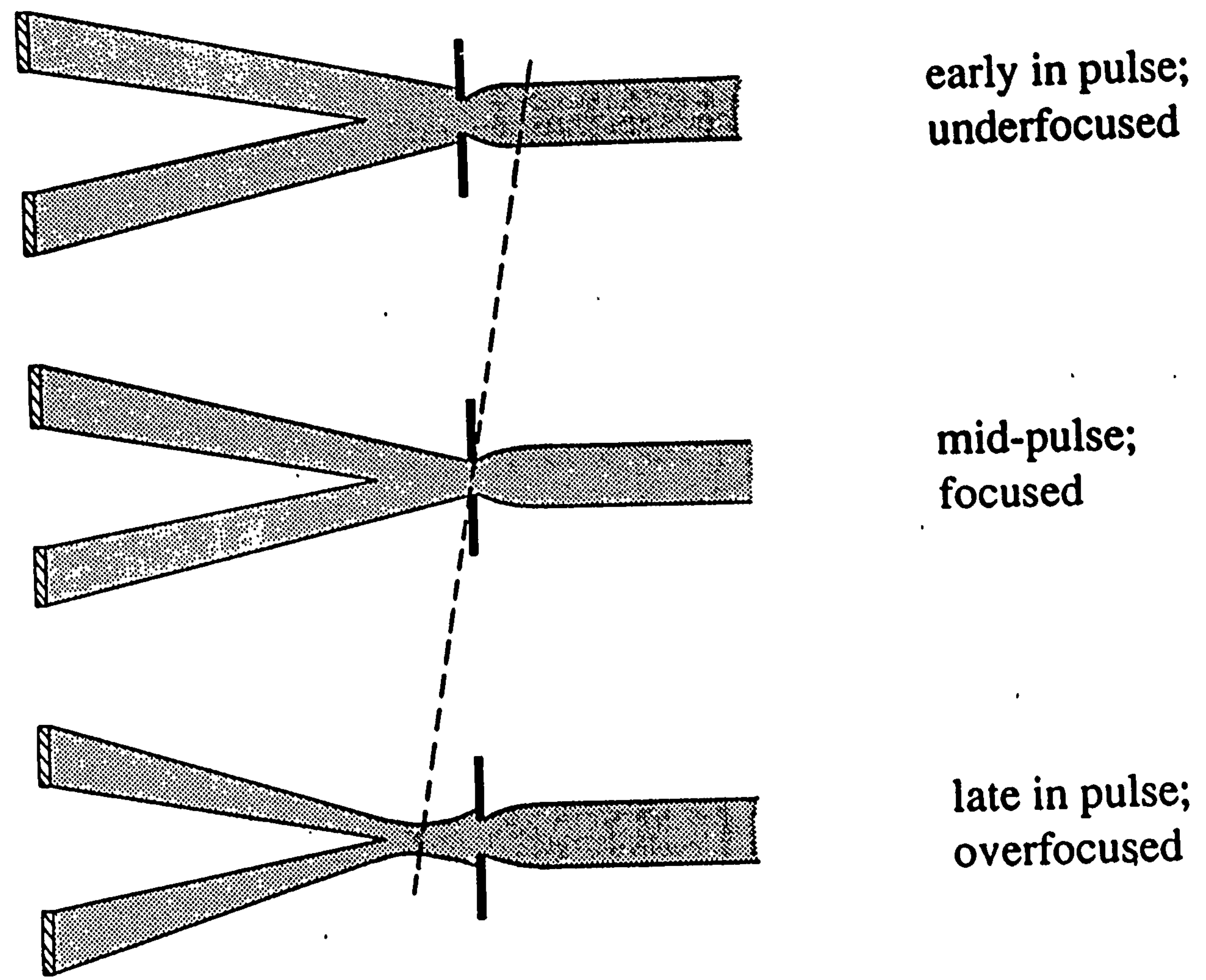

NRL

FOR Z-DISCHARGE TRANSPORT, rP(r,z) INCREASES FIRST AS IT FOCUSES AND THEN AS IT BUNCHES

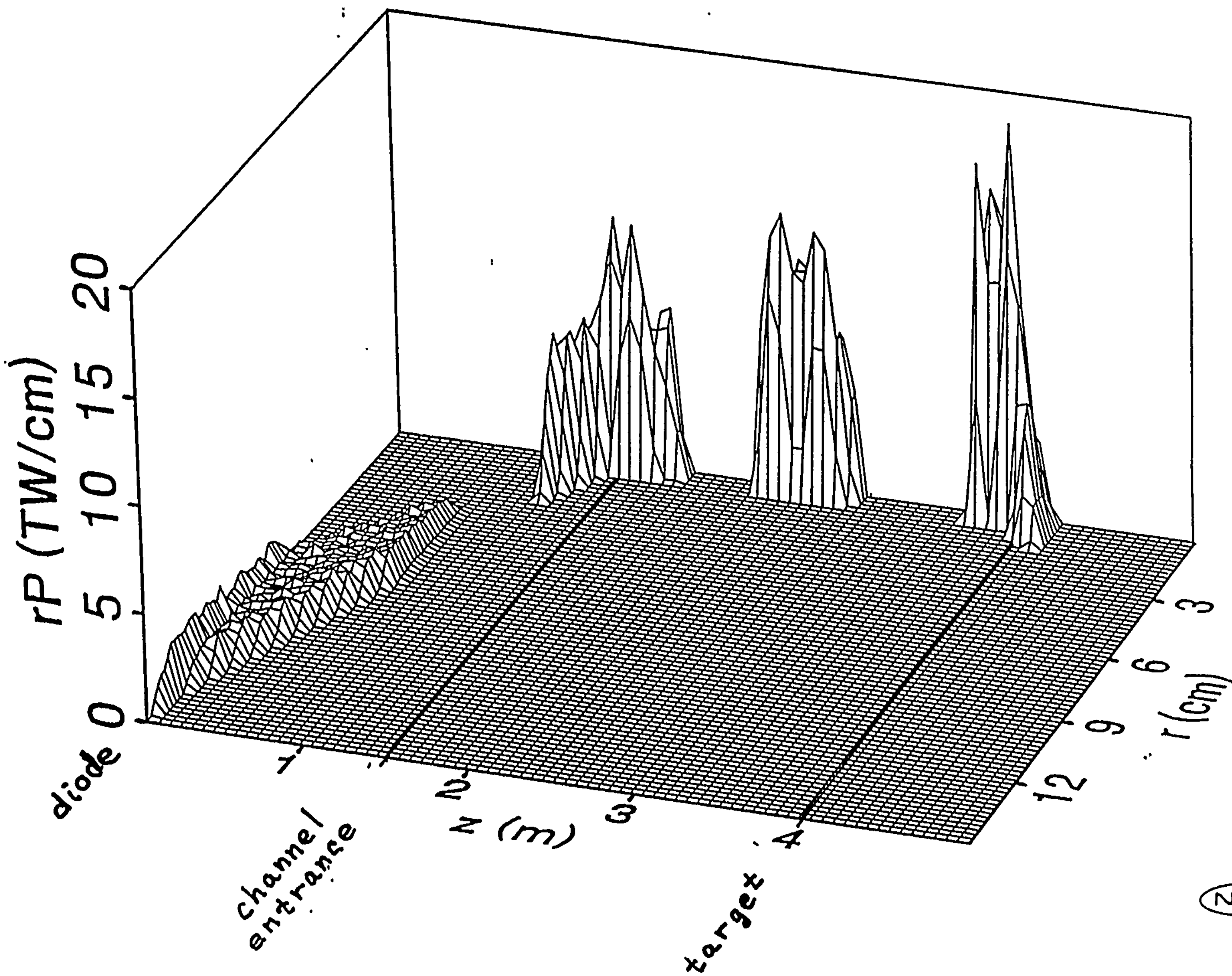

NRL

FOR Z-DISCHARGE TRANSPORT, F and/or I_c CAN BE VARIED TO KEEP r_b COMPARABLE WITH r_t

Analysis assumes:

- complete beam charge- and current-neutrality
- aperture located at $z = F$ with $r_a = \Theta_\mu F$
- $r_c^2 = 2r_a^2$
- $B_\theta \propto r/r_c$
- target standoff from channel exit, $D \propto N^{1/2} r_c$

NRL

FOR Z-DISCHARGE TRANSPORT, TRANSPORT EFFICIENCY IS DETERMINED BY LOSSES TO THE WALL AND THE SPOT SIZE AT THE TARGET

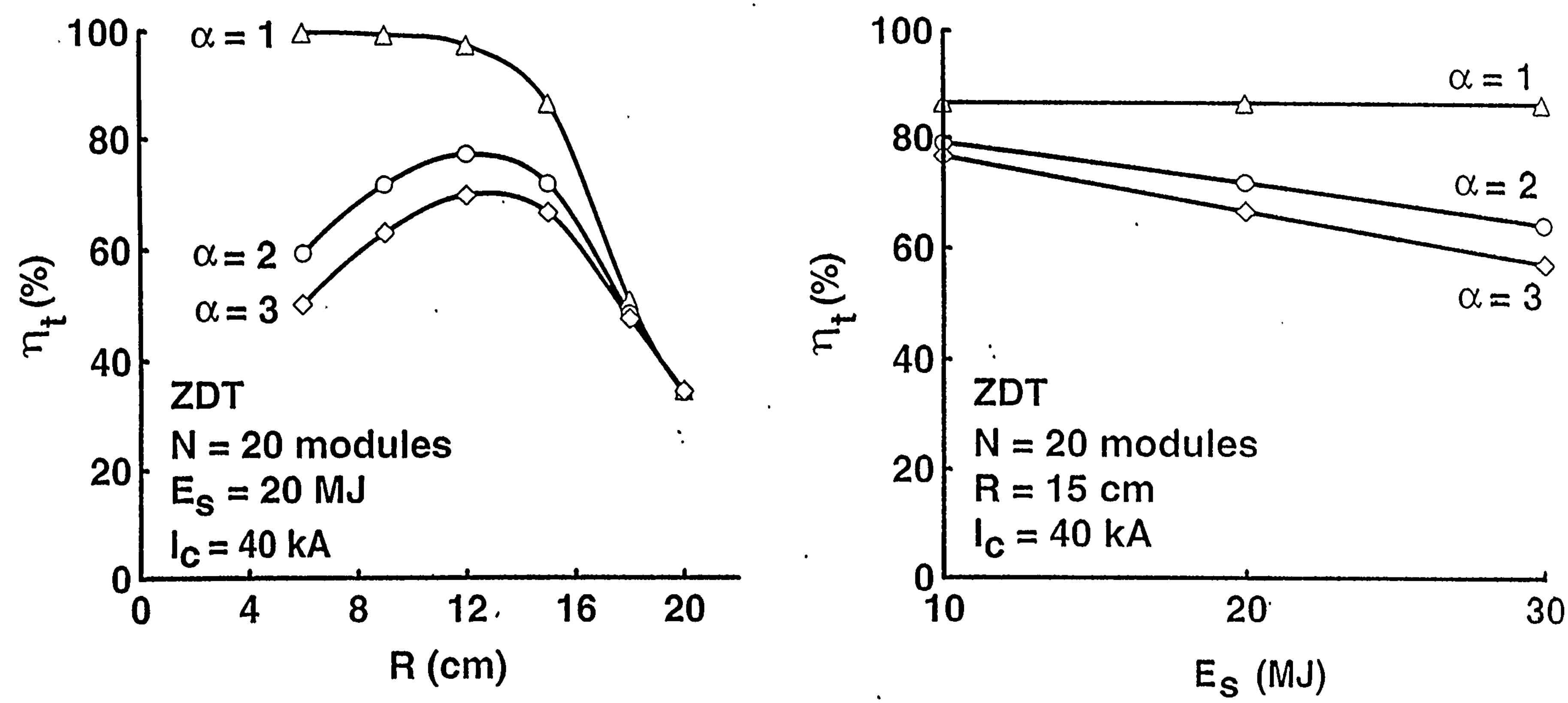

NRL

FOR Z-DISCHARGE TRANSPORT, TRANSPORT EFFICIENCY IS DETERMINED BY LOSSES TO THE WALL AND THE SPOT SIZE AT THE TARGET

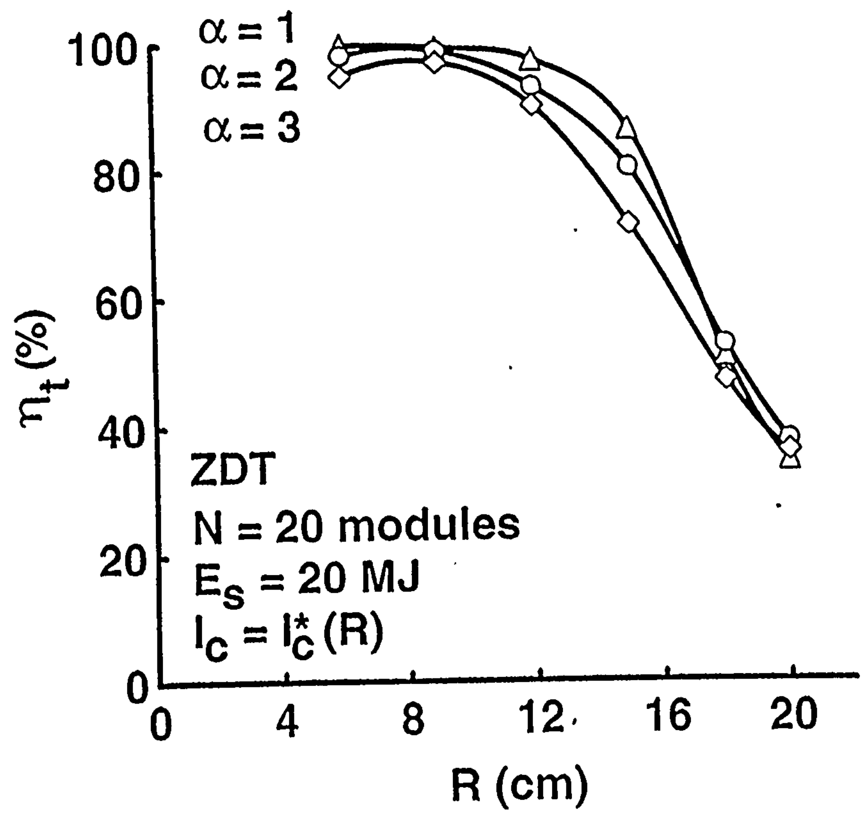

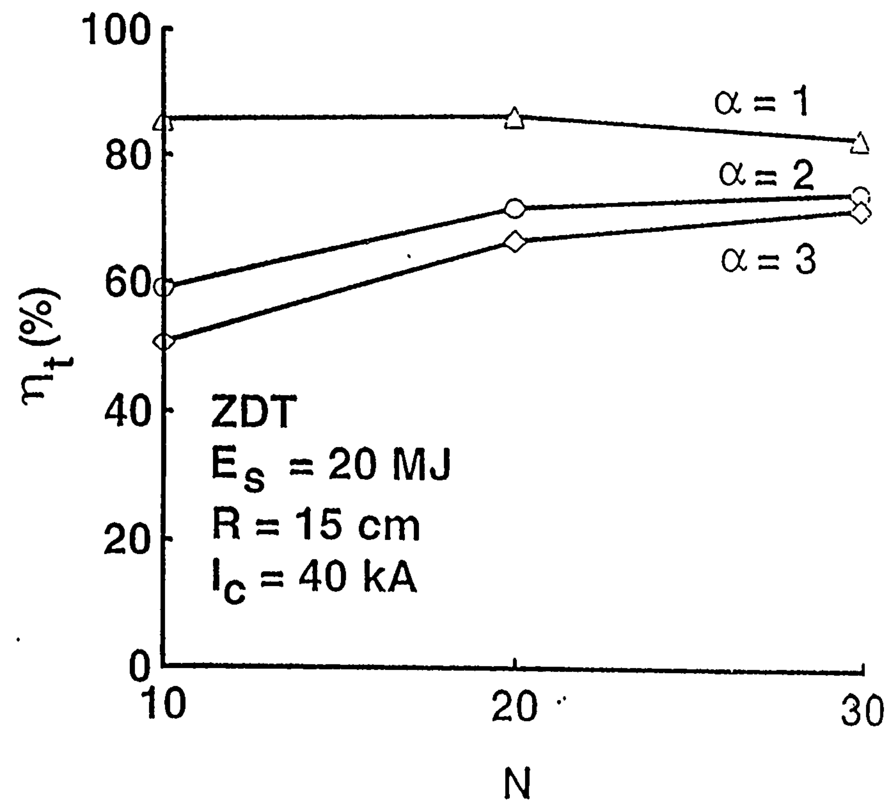

NRL

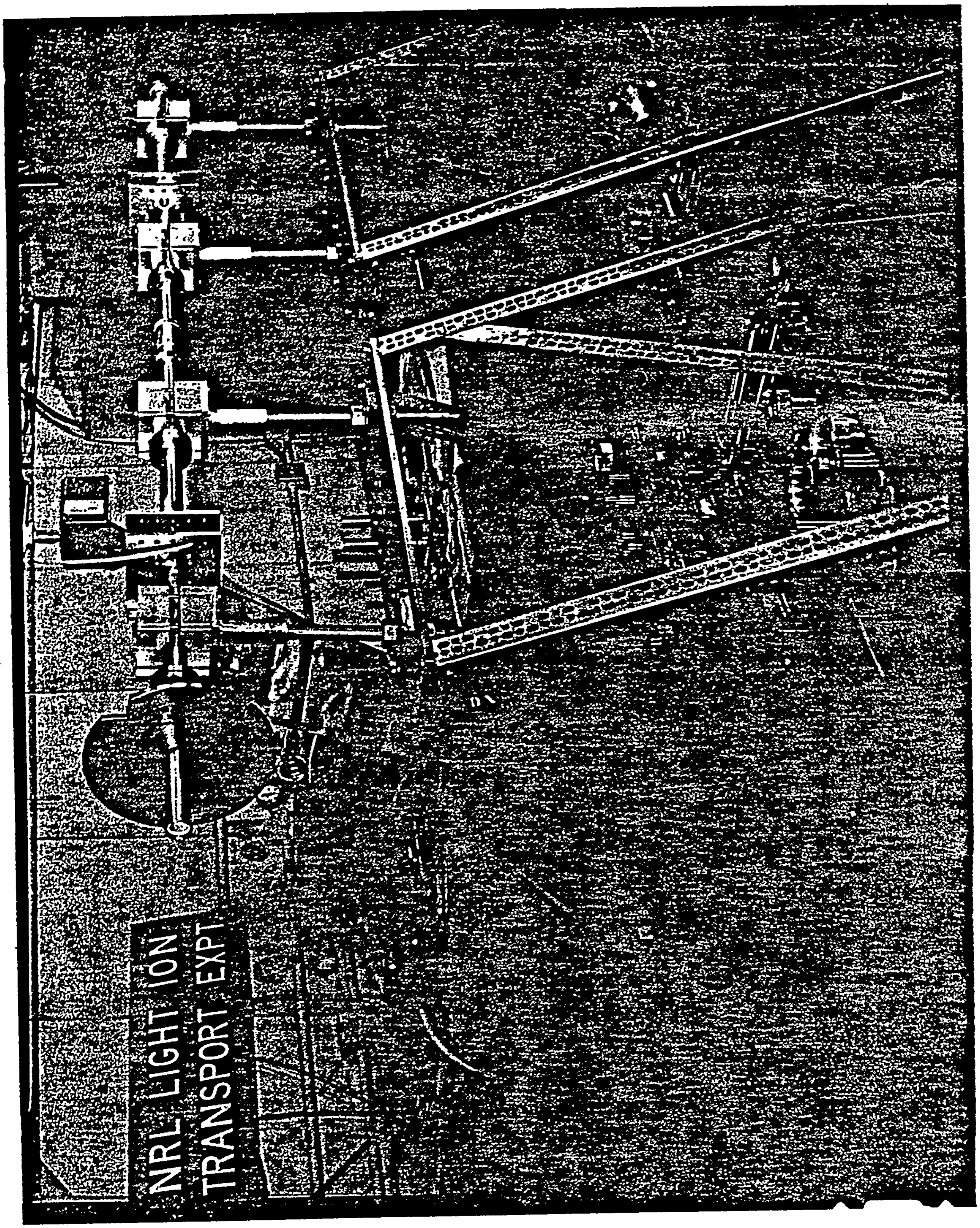
NRL LIGHT ION
TRANSPORT EXPT

Transport Experiment

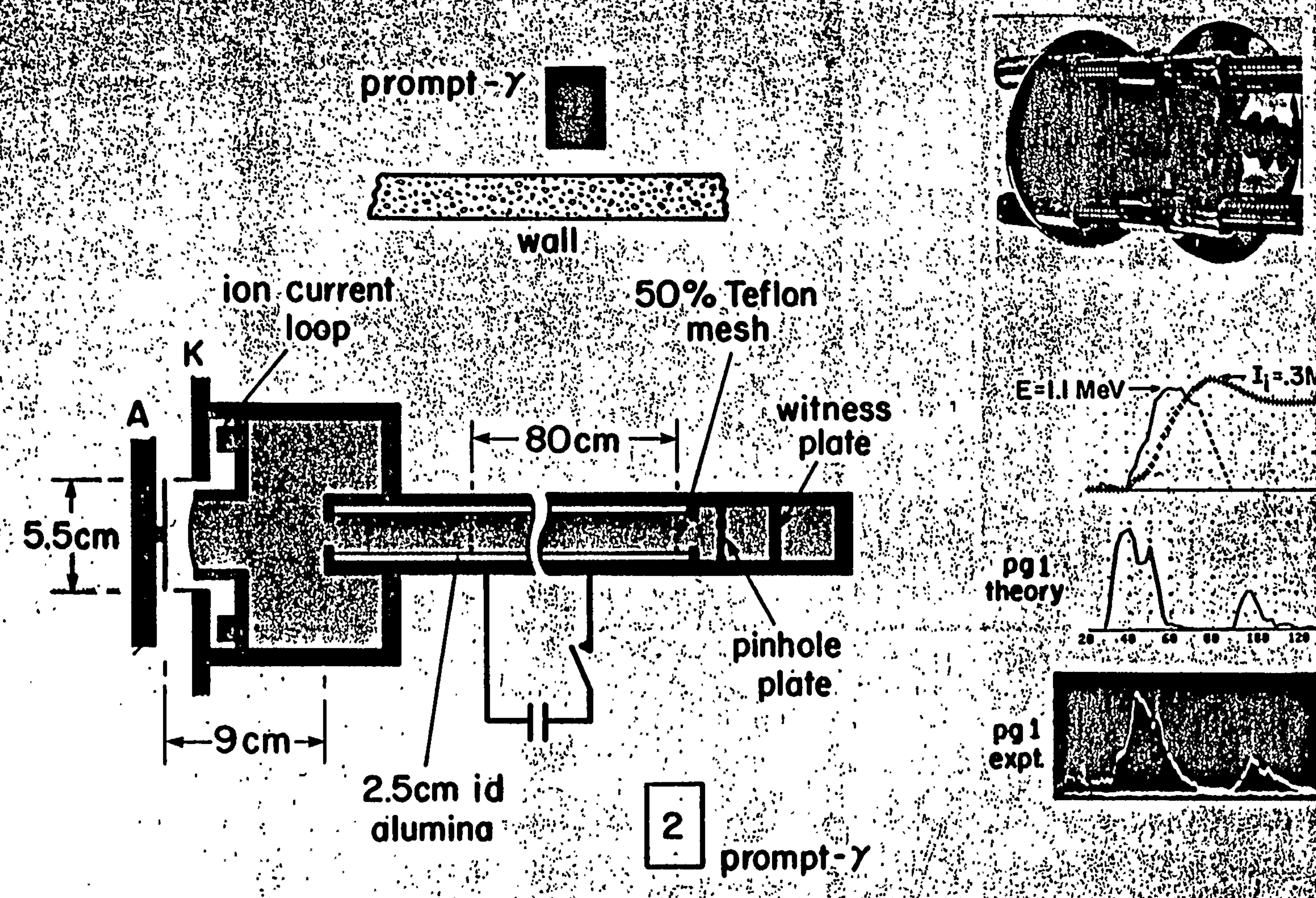

SHADOWBOX IMAGES
FROM Z-DISCHARGE TRANSPORTED BEAMS
IDENTIFY REGION OF PHASE SPACE OCCUPIED BY BEAM

Orbit Analysis

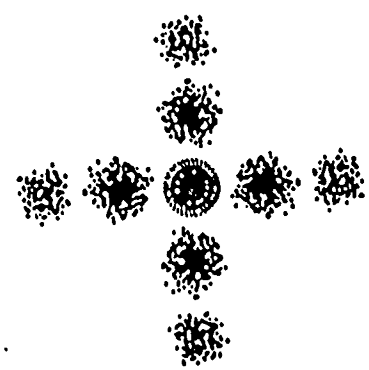

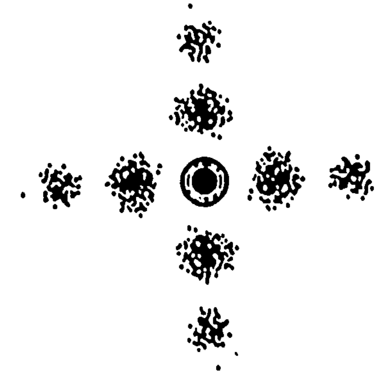

Experiment

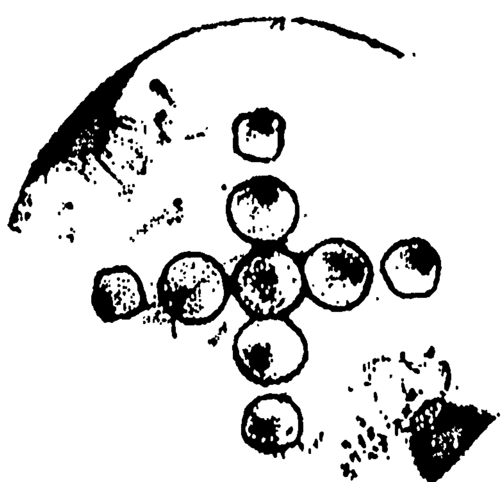

$I_c = 42$ kA
$D = 20$ cm

$I_c = 35$ kA
$D = 30$ cm

NRL

POST-TRANSPORT EXPANSION

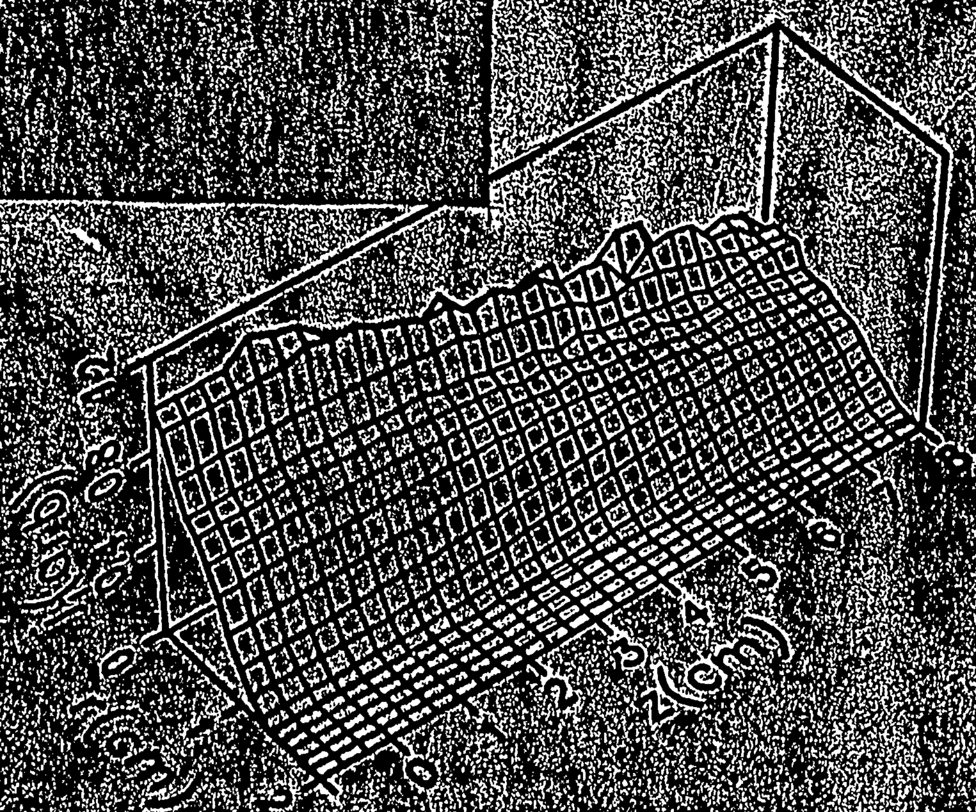

LMF back-up

Wall-confined channels have demonstrated efficient transport over meter distances

NRL

ZDT

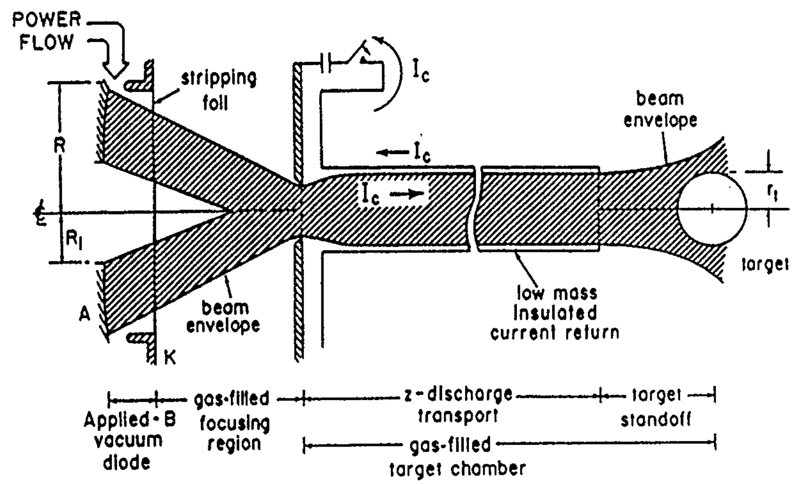

features

- most studied
- large containment vessel possible

experiments

- 1.2 MeV p, up to 400 kA, $r_c \leq 2$ cm
  - $I_c \sim 50$ kA
- transport up to 5 meters demonstrated
- $\eta \sim 100\%$ for channel
- low mass Kapton tubes demonstrated

LMF scaling

- $\eta_t \sim 75\%$

status

- complete, except for high beam-brightness issues

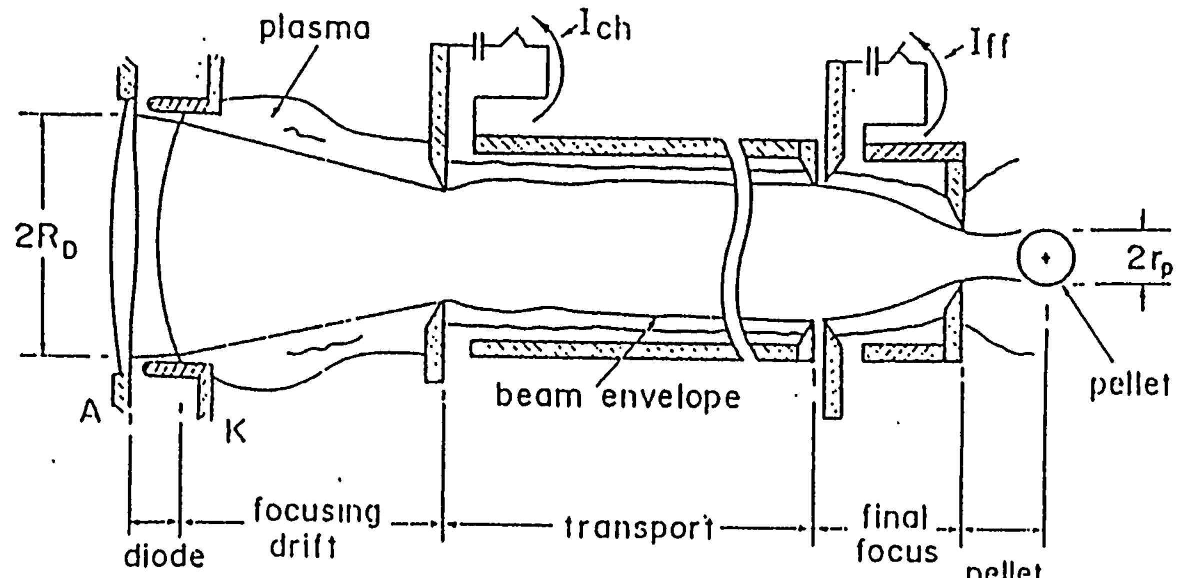

Figure 1: Basic Transport and Final Focus Scheme

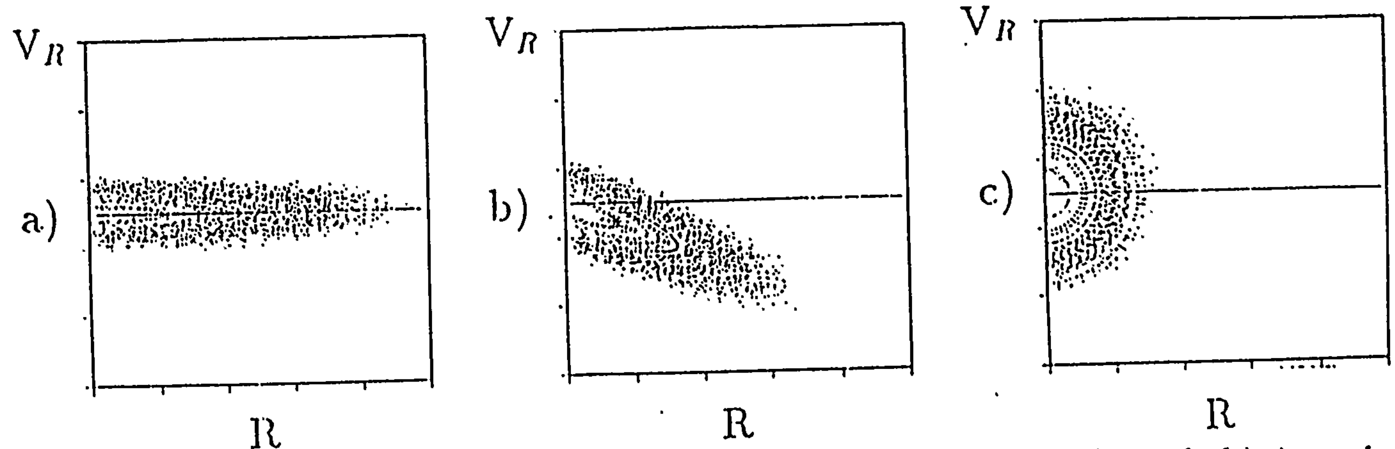

Figure 2: Phase space plots of final focus action. a) At end of transport channel. b) At end of final focus cell. c) At the target. The scale of R is from 0 to 2.5 cm. The scale of V_R is from -1 cm/ns to +1 cm/ns.

CONSTRAINTS DEFINE OPERATIONAL WINDOW FOR BEAM TRANSPORT

Two-stream instability

Filamentation instability

Plasma hydrodynamics

Required energy on target:
- beam transport efficiency
- beam energy losses
- packing constraint

NRL

TWO-STREAM INSTABILITY

Collisional stabilized if:

$$\nu_{ei} \geq 1.52 \frac{\omega_{pb}^2}{\omega_{pe}} \left(\frac{V_b}{\Delta V_{bz}(z)} \right)^2$$

where ν_{ei} is the electron-ion collision frequency, ω_{pb} and ω_{pe} are the beam ion and electron plasma frequencies, V_b is the beam velocity, and ΔV_{bz} is the spread in the beam ion axial velocities.

Tail of the beam (after beam heats plasma) is most vulnerable.

Effect on beam may be minimal:

- required $\Delta V_{bz}/V_b$ for stabilization is small
- k_{max} changes with z in focusing region

NRL

FILAMENTATION INSTABILITY

Significant growth is prevented if:

$$\sigma \geq \frac{\tau_b \omega_{pb}^2}{8\pi\theta^2}$$

where σ is the plasma conductivity, τ_b is the beam pulse duration, and θ is the beam microdivergence before focusing and R/F after focusing.

Tail of beam could be disrupted if plasma conductivity does not grow quickly enough.

NRL

PLASMA HYDRODYNAMICS

Plasma return current in presence of magnetic field from net current or confining channel current can cause significant plasma hydrodynamic expansion if:

$$\frac{J_b B_\theta \tau_b^2}{c\rho_m} \geq \frac{r_b}{10}$$

where J_b is the beam current density and ρ_m is the plasma mass density.

This is only a problem for high-current, small-radius beams (scales as r_b to the fourth power).

NRL

REQUIRED ENERGY ON TARGET

Beam transport efficiency η_t measures the fraction of beam energy from the diode that is directed onto the target.

Beam also loses energy due to:

- collisional stopping in gas
- slowing down in self-consistent axial electric fields

Packing constraint puts upper limit on number of modules N.

Power per beam is given by:

$$P_b = \frac{P_t}{\eta_t \eta_E N}$$

NRL

CONSTRAINTS DERIVED FROM PHYSICS ISSUES COMBINE TO DEFINE AN OPERATIONAL WINDOW FOR TRANSPORT

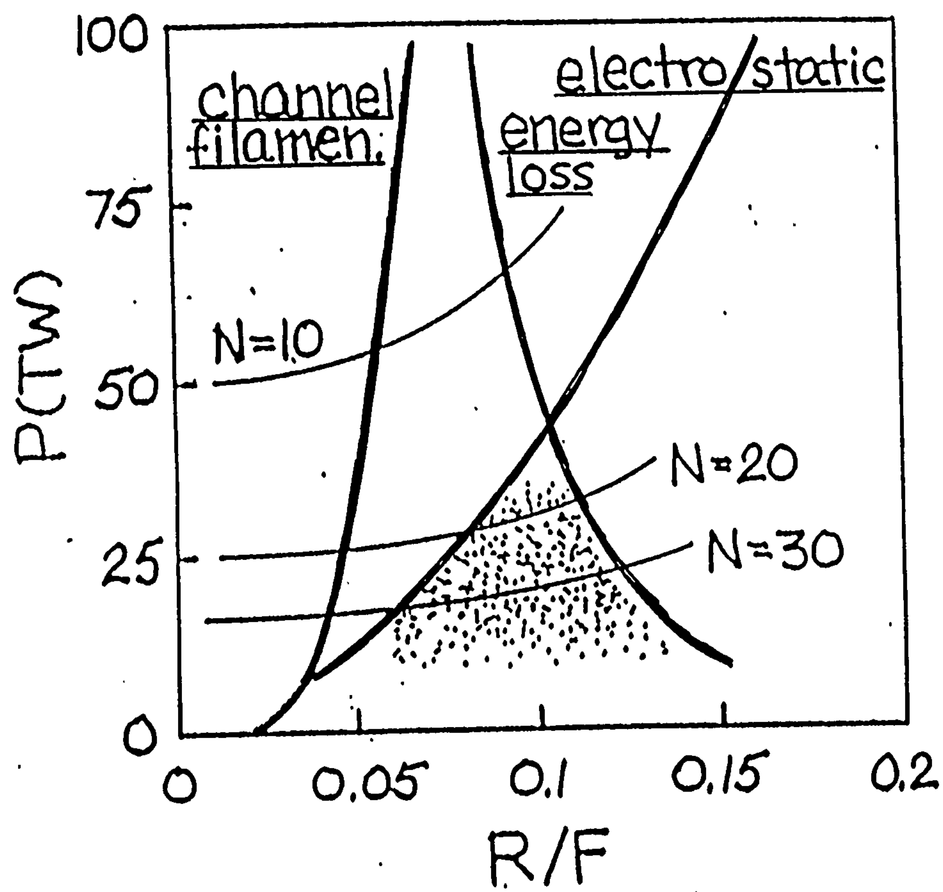

Example: 30 MeV, Li^{+3} beam
$\Theta_{\mu} = 7$ mrad, $\beta = 4$
$r_c = 1$ cm, $L = 330$ cm
$\eta_t = 50\%$, and
1000 TW on target

NRL

WIRE-GUIDED TRANSPORT SYSTEM FOR LMF

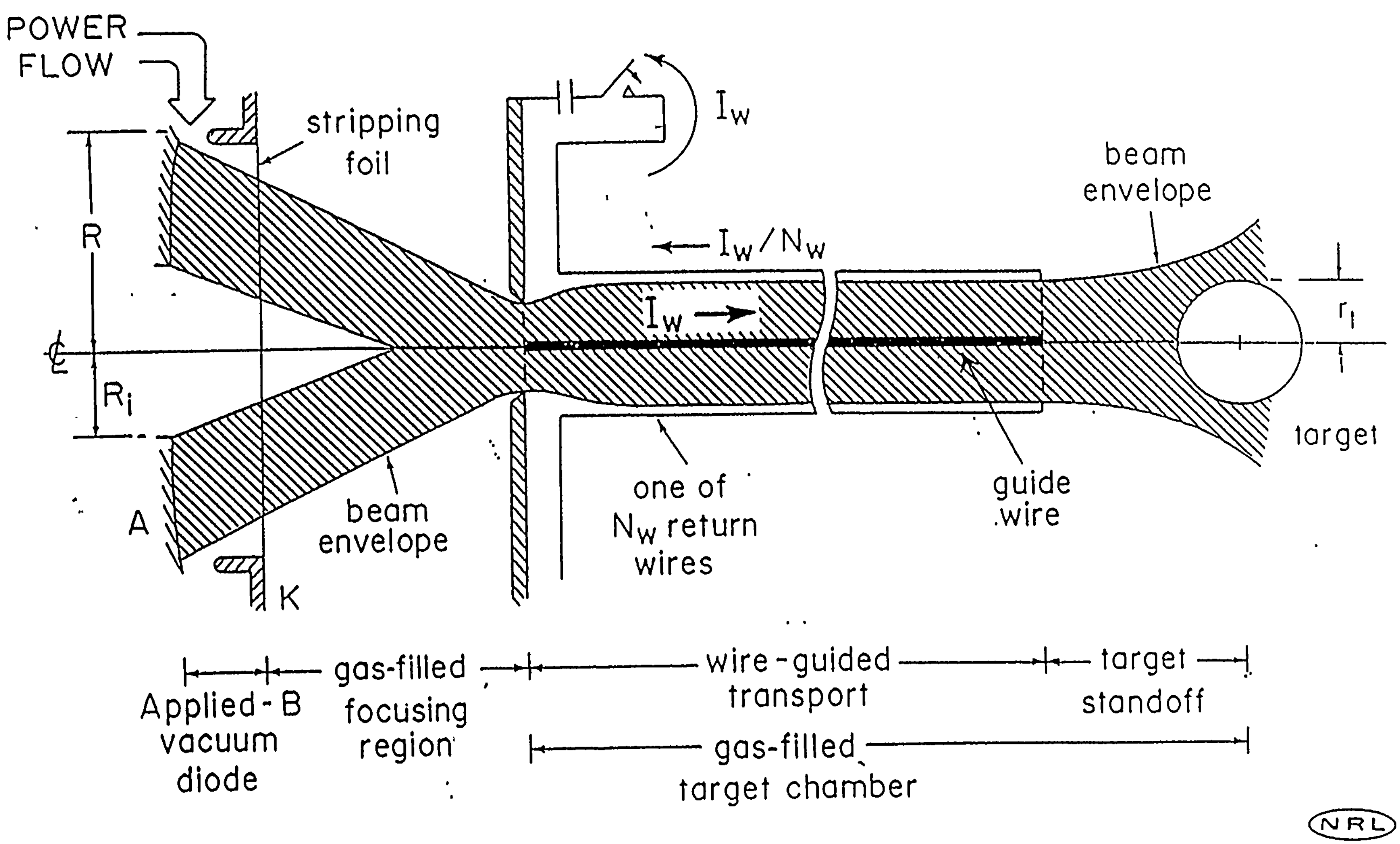

FOR WIRE-GUIDED TRANSPORT, I_w RADIALLY CONFINES THE BEAM IONS

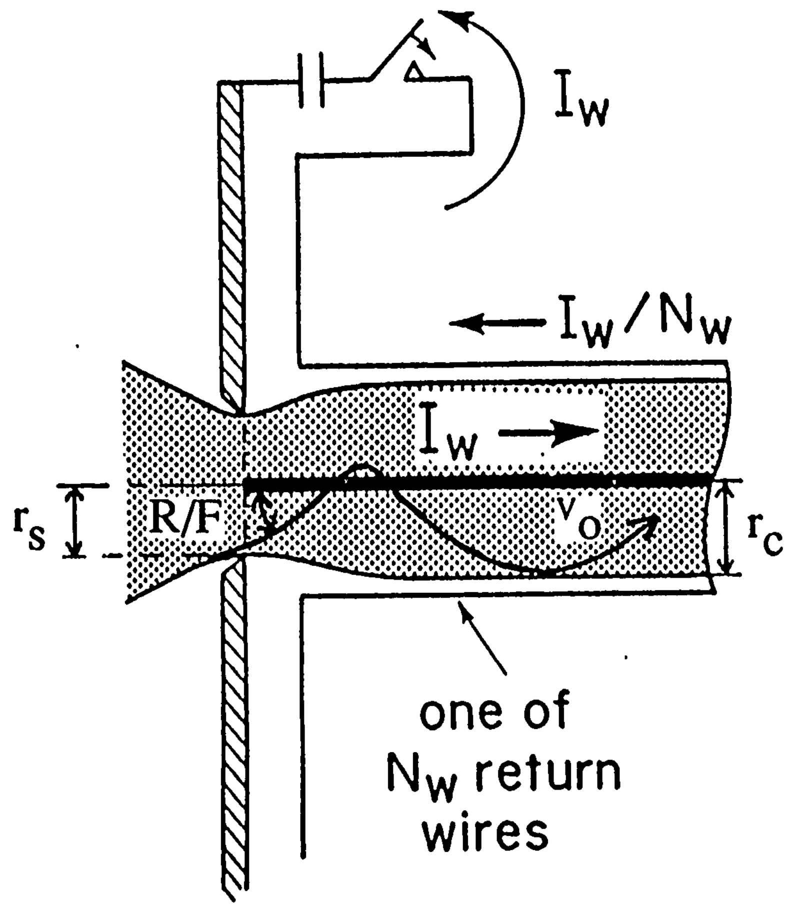

All ions confined to

$r \leq r_c$ when

$$\frac{ZeI_w}{m_i v_o} = \frac{(R/F)^2}{4\ln(r_c/r_s)}$$

NRL

SAMPLE ORBIT IN A WIRE-GUIDED TRANSPORT SYSTEM

$r_0 = r_s$, $\phi = 30°$

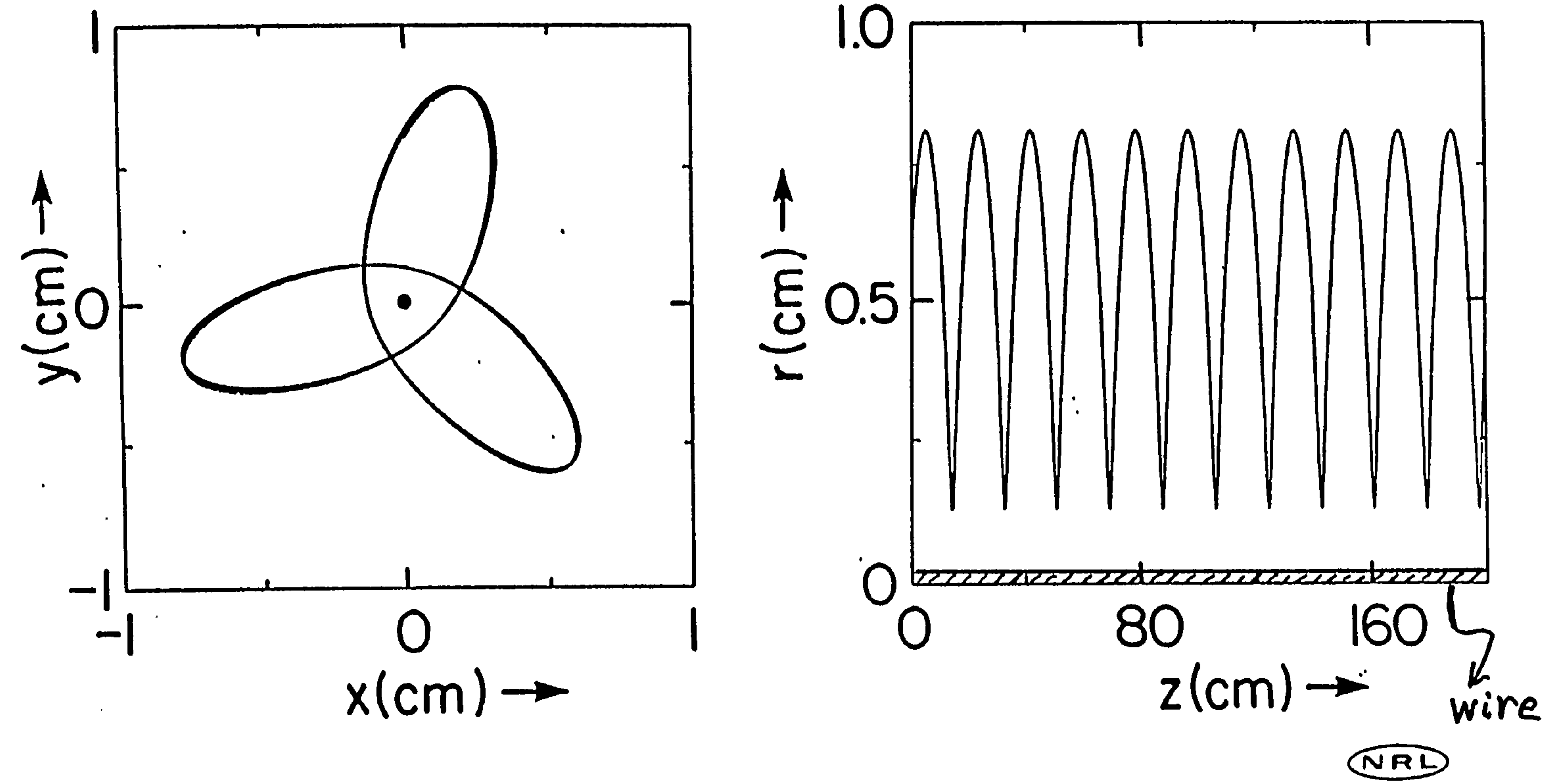

SAMPLE ORBIT IN A WIRE-GUIDED TRANSPORT SYSTEM

$r_0 = r_s \, , \quad \phi = 12^\circ$

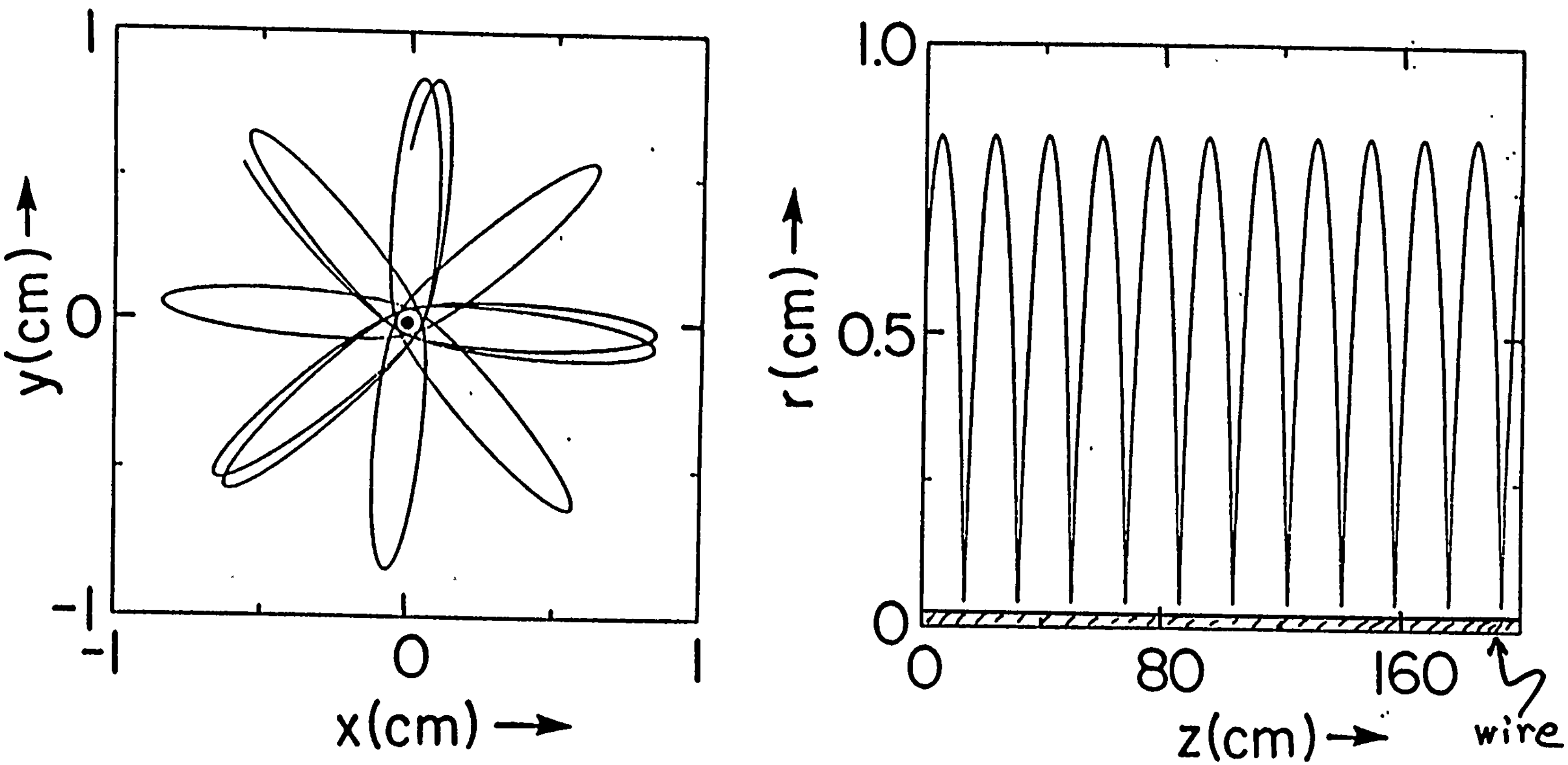

NRL

SAMPLE ORBIT IN A WIRE-GUIDED TRANSPORT SYSTEM

$r_o = r_s$, $\phi = 90°$

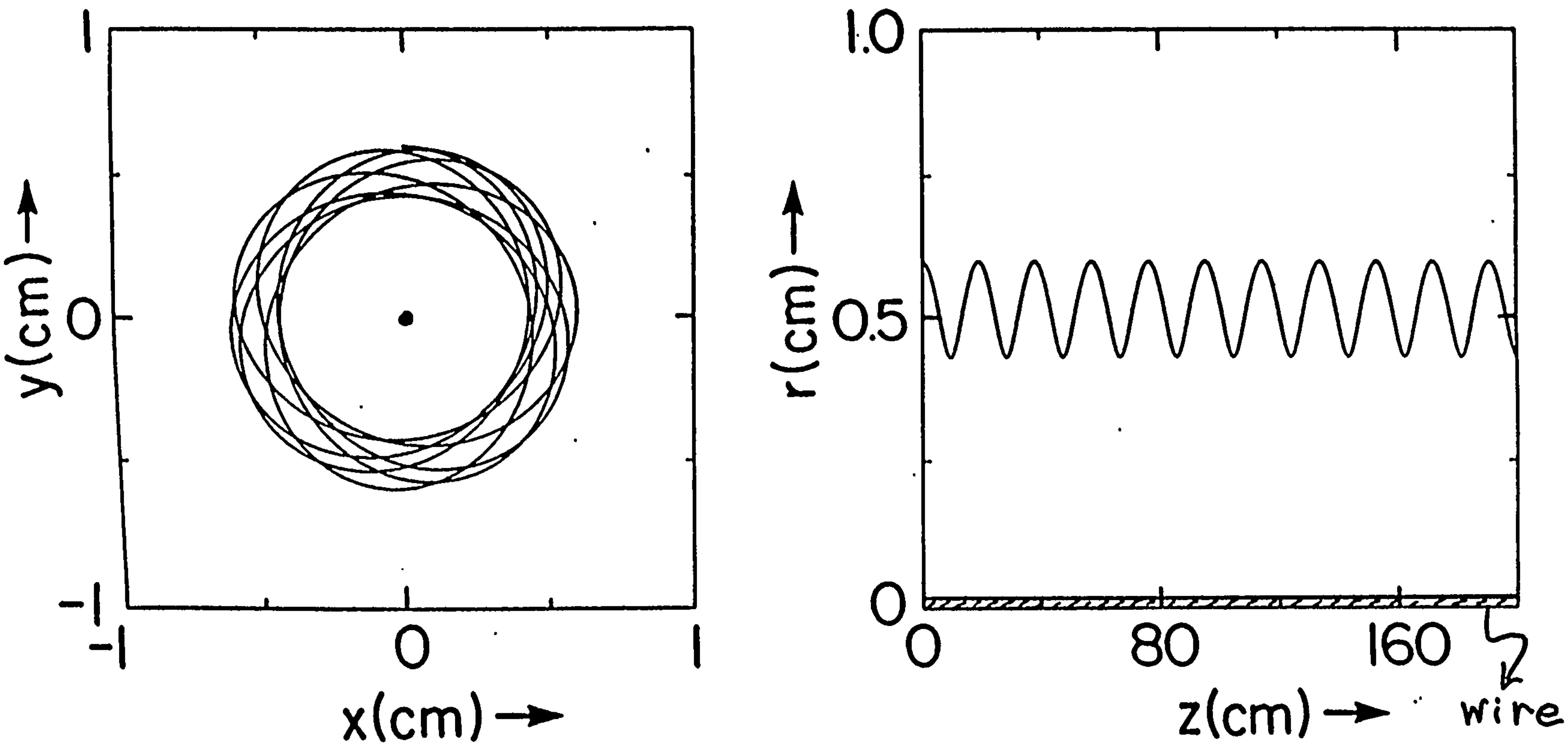

FOR WIRE-GUIDED TRANSPORT, rP(r,z) INCREASES FIRST AS IT FOCUSES AND THEN AS IT BUNCHES

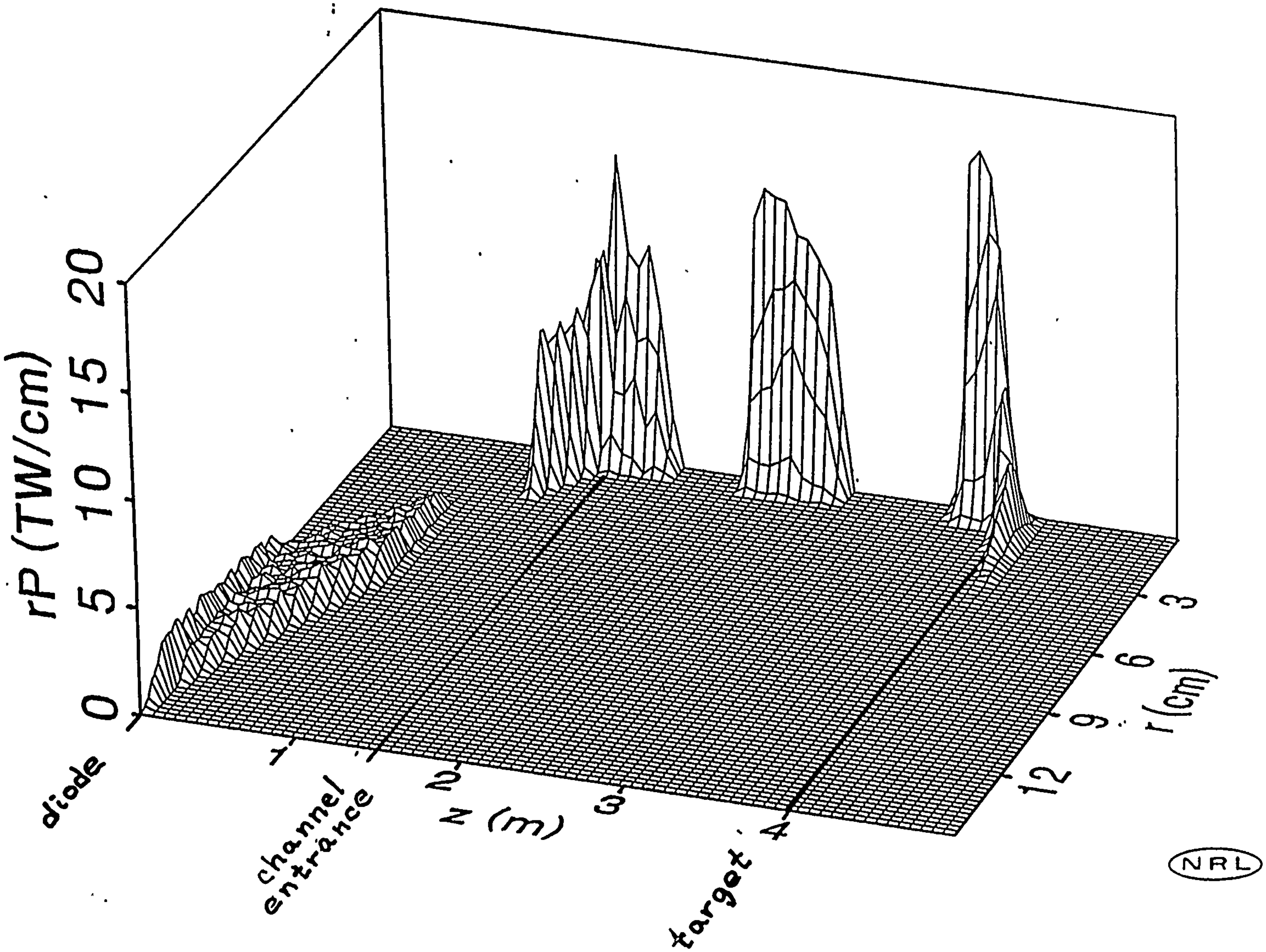

FOR WIRE-GUIDED TRANSPORT, F and/or I_w CAN BE VARIED TO KEEP r_b COMPARABLE WITH r_t

Analysis assumes:

- complete beam charge- and current-neutrality
- aperture located at $z = F$ with $r_a = \Theta_\mu F$
- r_w is minimum radius to avoid melt
- $B_\theta \; \alpha \; r_c/r$
- radial location of return wires, $R_w \; \alpha \; 1.4 r_b$
- target standoff from channel exit, $D \; \alpha \; N^{1/2} R_w$

NRL

FOR WIRE-GUIDED TRANSPORT, TRANSPORT EFFICIENCY IS DETERMINED BY LOSSES TO THE WIRE AND THE SPOT SIZE AT THE TARGET

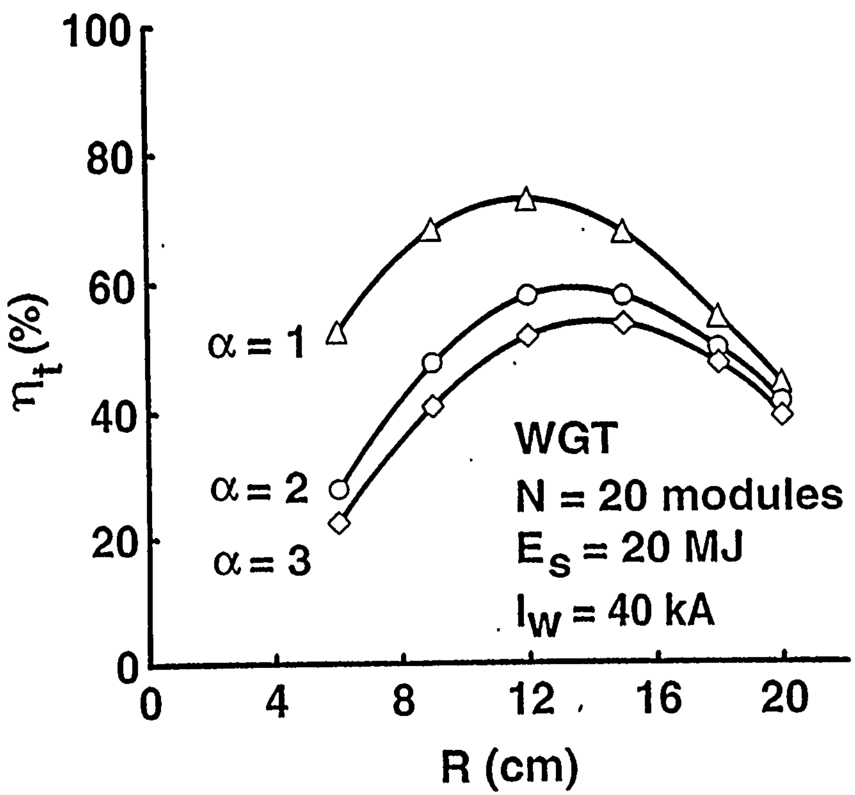

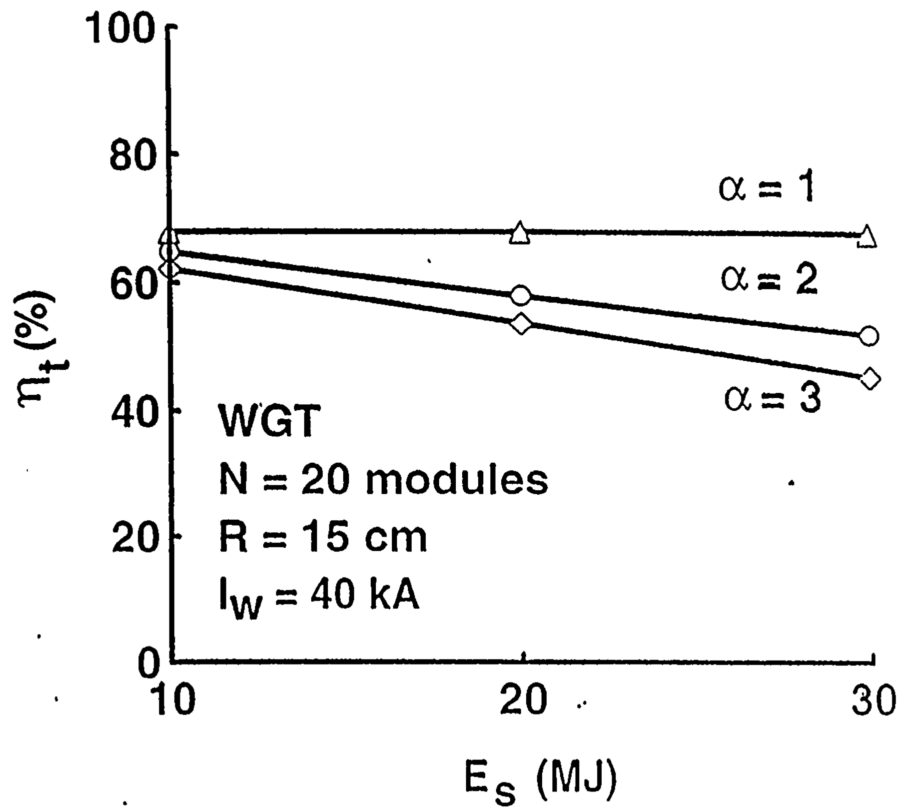

NRL

FOR WIRE-GUIDED TRANSPORT, TRANSPORT EFFICIENCY IS DETERMINED BY LOSSES TO THE WIRE AND THE SPOT SIZE AT THE TARGET

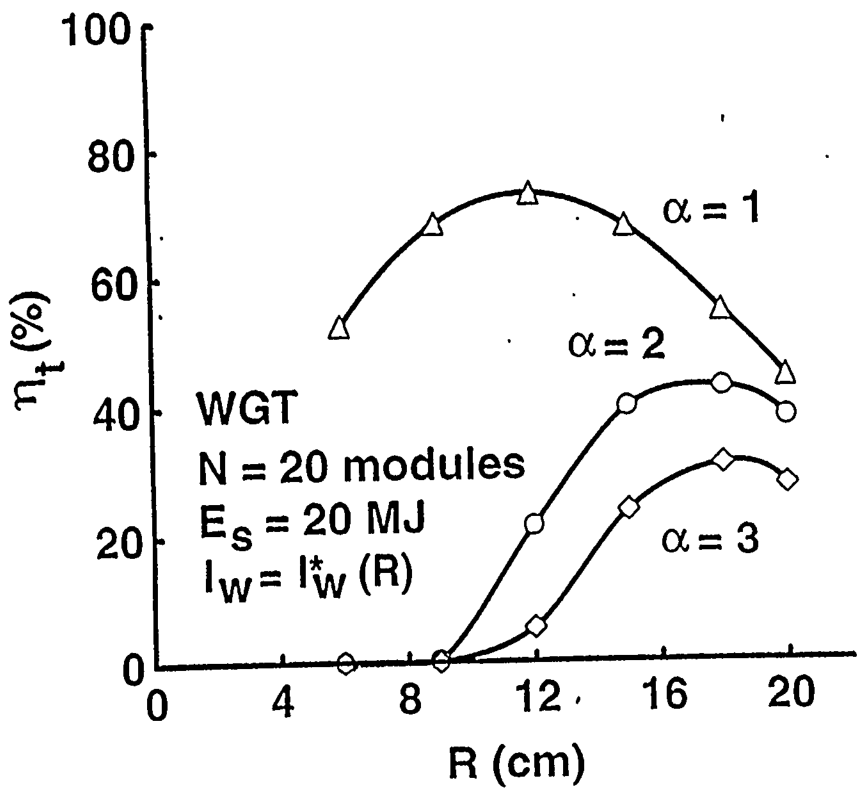

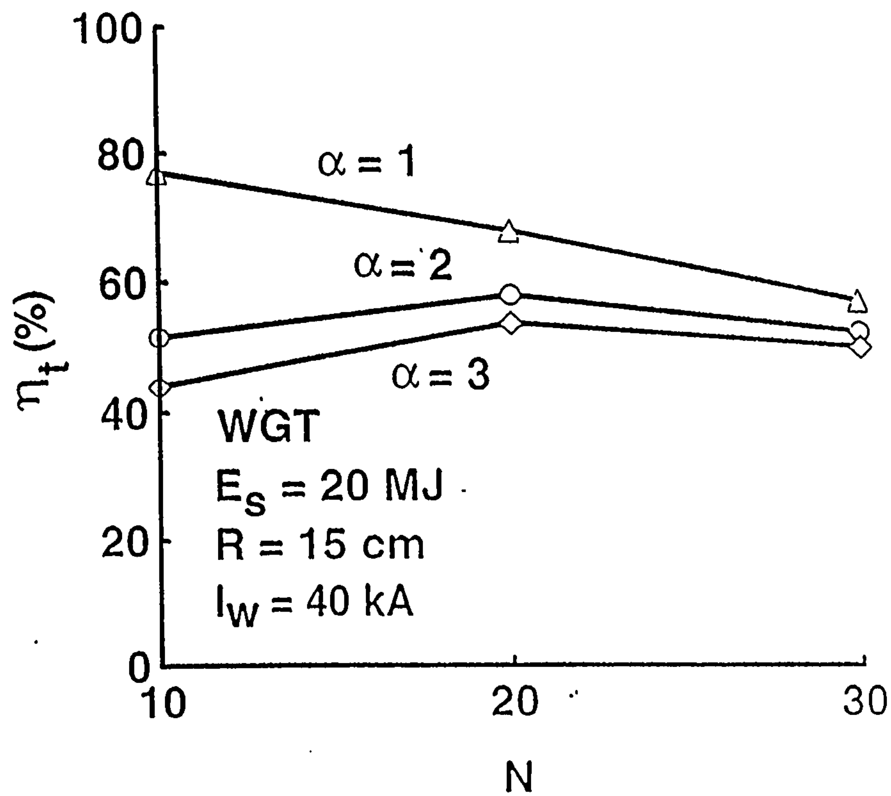

WIRE-GUIDED TRANSPORT SYSTEM ON GAMBLE II AND OPEN SHUTTER PHOTOGRAPH OF ION BEAM

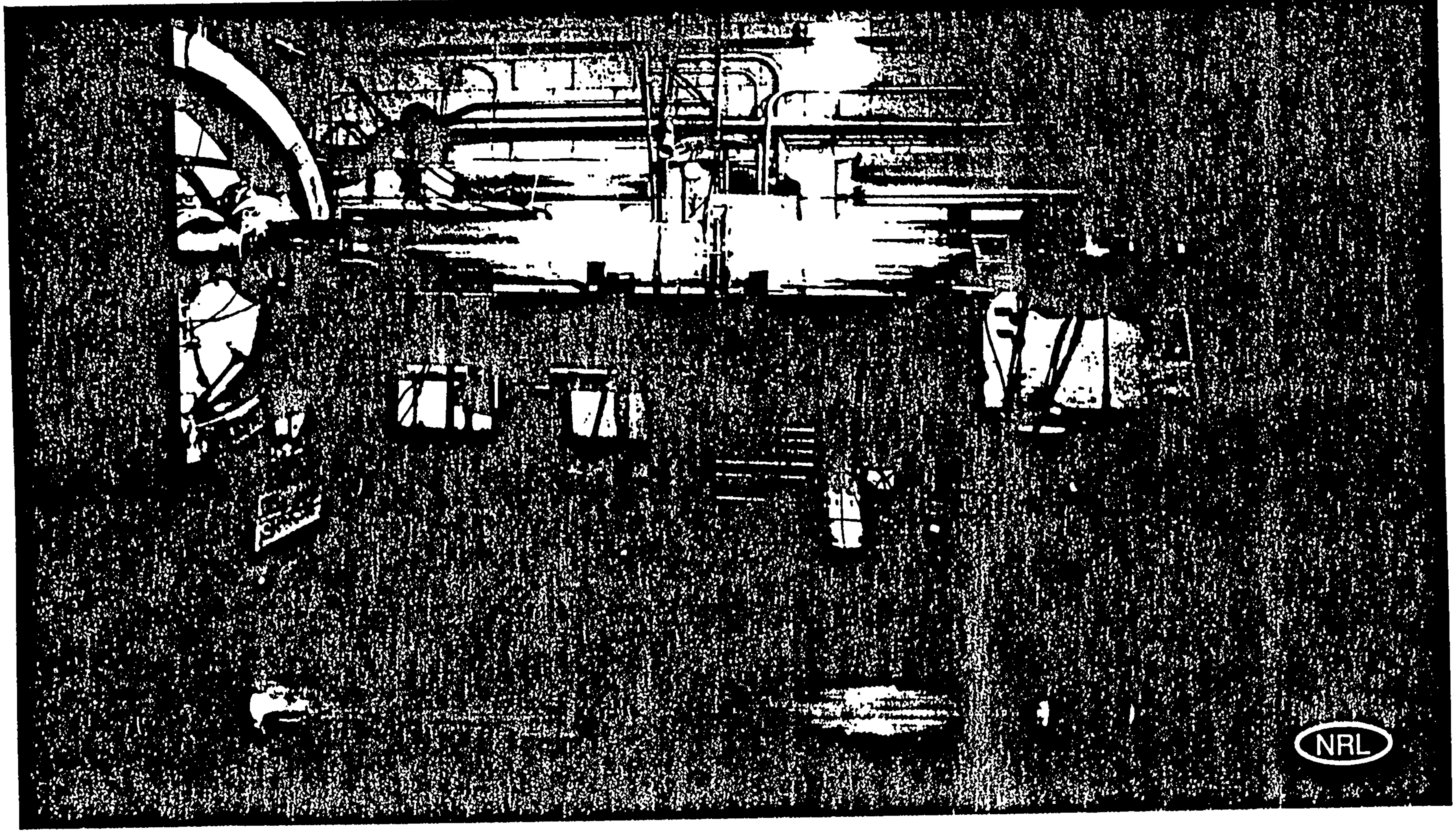

PROMPT-γ RESULTS FROM WIRE-GUIDED BEAM DEMONSTRATE 80% TRANSPORT EFFICIENCY

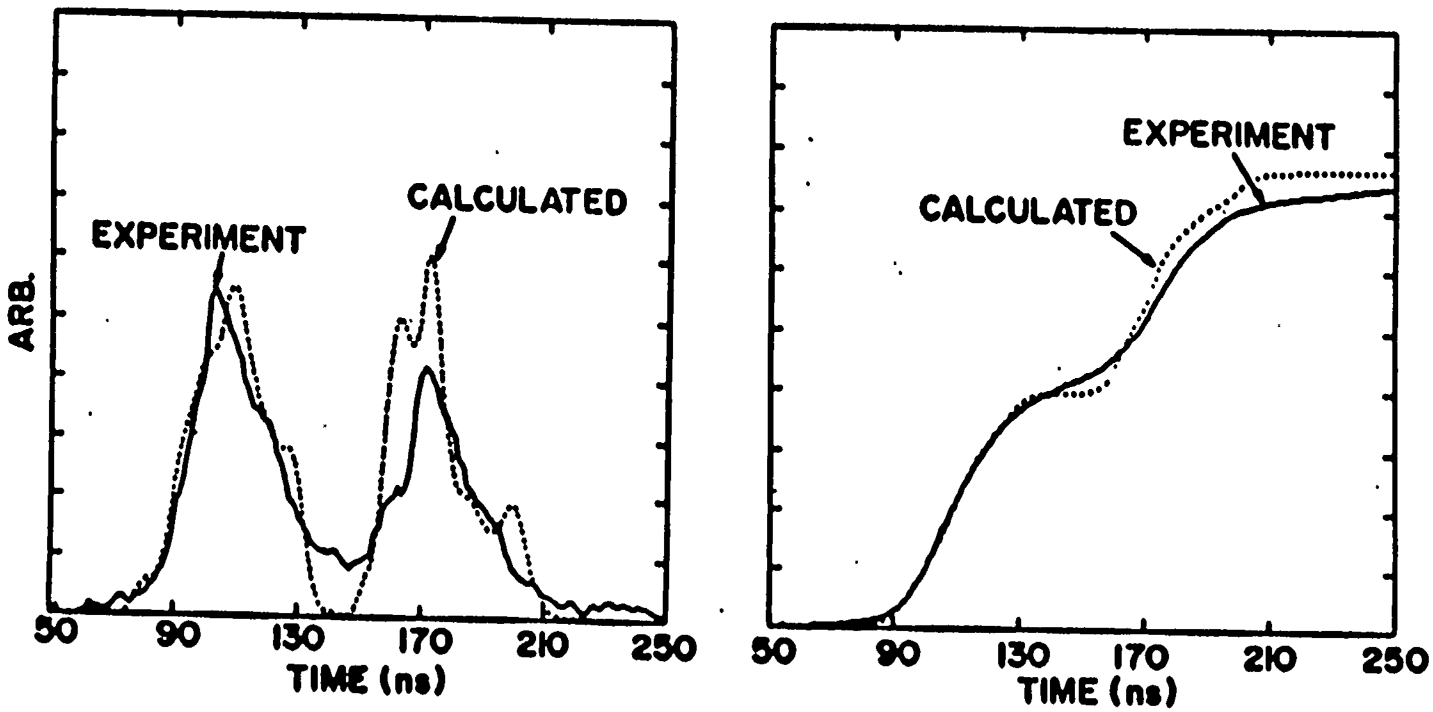

NRL

SHADOWBOX IMAGES FROM WIRE-GUIDED BEAMS REFLECT LOW P_θ LOSSES TO THE GUIDE WIRE

Orbit Analysis

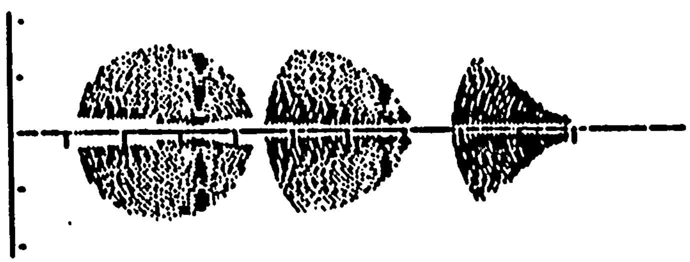

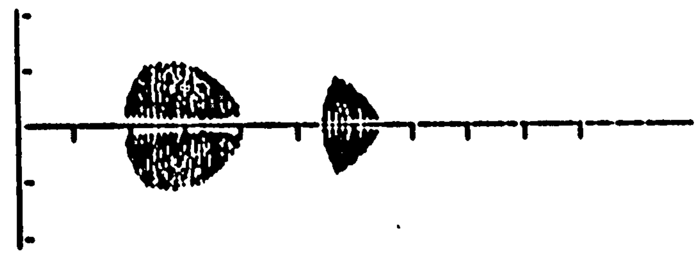

Experiment

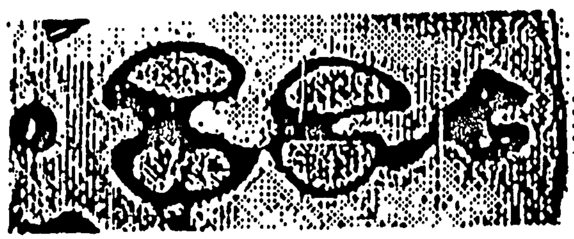

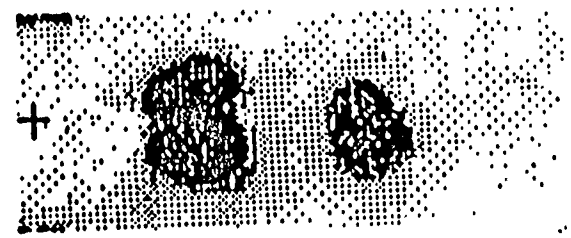

$I_w = 27$ kA
$r_s = 1.27$ cm

$I_w = 15$ kA
$r_s = 0.78$ cm

NRL

LMF back-up

Wire-guided transport has demonstrated efficient transport over meter distances

NRL

WGT

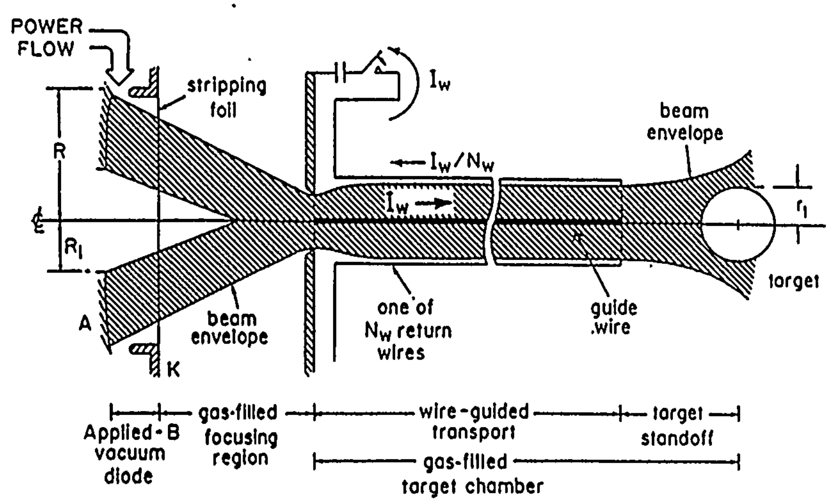

features

large containment vessel possible

experiments

1.2 MeV p, I_c ~ 20-30 kA

transport up to 1.5 meters demonstrated

η ~ 75-80%

LMF scaling

need $N_w \geq 4$ & $r_w \geq 1.4\ r_c$

η_t ~ 60%

status

complete, except for high beam-brightness issues

20

Channel Issues

C. Olson

Free-standing (laser-created) channels (for LIF, HIF, Common Ion) have high voltage breakdown as an unresolved issue

1. free-standing channel is hydro unstable (no nearby walls to stabilize)
2. therefore, must use it for transport before instability grows ($t < \tau_{Alfrien}$) sets Δt
3. channel is very inductive (long, thin)
4. drive voltage α L $\frac{\Delta I_c}{\Delta t}$ ~ MV (very high)
5. high voltage breakdown likely

Channel expansion problems indicate small radius ($\lesssim$ 0.5 cm) channels will not work ; larger radius ($\gtrsim$ 0.5 cm) channels will work

(1) channel hydro expansion (caused by return current)

$r_c = r_0 (1 + \lambda)$

$\lambda = (\pi/c^2) J_p J_c (1/\rho) t^2$

r_0(cm)	λ	$\eta = 1/(1+\lambda)^2$
0.3	0.15	75%
0.2	0.7	34%
0.1	11.7	0.7%

$J_p = 800$ kA/πr^2)
$J_c = 12$ kA/(πr^2)
$\rho = 1.0 \times 10^{-5}$ g/cm^3
(100 Torr H_2)
$t = 20$ ns

(2) channel expansion caused by heating (radiative heat transfer) always end up with same size channel

smallest $r_c \sim 0.5$ cm

Light Ion Fusion Reactors

R.R. Peterson
and the LIBRA
Design Team

University of Wisconsin

Historical Trends in Light Ion Beam Fusion Power Reactor Designs

Driver/Target Related

70's
- Electron Beams
- No Detail on Driver
- High Rep Rate (35 Hz)
- Low Yields (85 MJ)

80's
- Hydrogen Isotope Beams (p,d) @ 6-8 MV
- Lower Rep Rate (3-6 Hz)
- Higher Yields (≈300-800 MJ)
- Channel Transport

90's
- Li & Welterweight Ion Beams
- Helia Technology (30 MV)
- Ballistic & Self-Pinched Transport
- More Realistic LIB Targets

Reactor Chamber Related

70's
- Li "Rain" FW Protection
- "Moving Belt" FW

80's
- Porous Tubes for First Wall Protection
- High Pressure Gas Protection of FW
- Cavity Size 4-5 m Radius

90's
- Final Focusing Magnets Used in Chamber
- Investigate Pb-Li Breeding Alloys
- Smaller Cavity Size (3-3.5 m radius)

Goals of the LIBRA Study

- **Develop a self-consistent conceptual design of a light ion beam fusion commercial power reactor.**

- **Evaluate the potential of light ion fusion as the basis for economically attractive small power plants.**

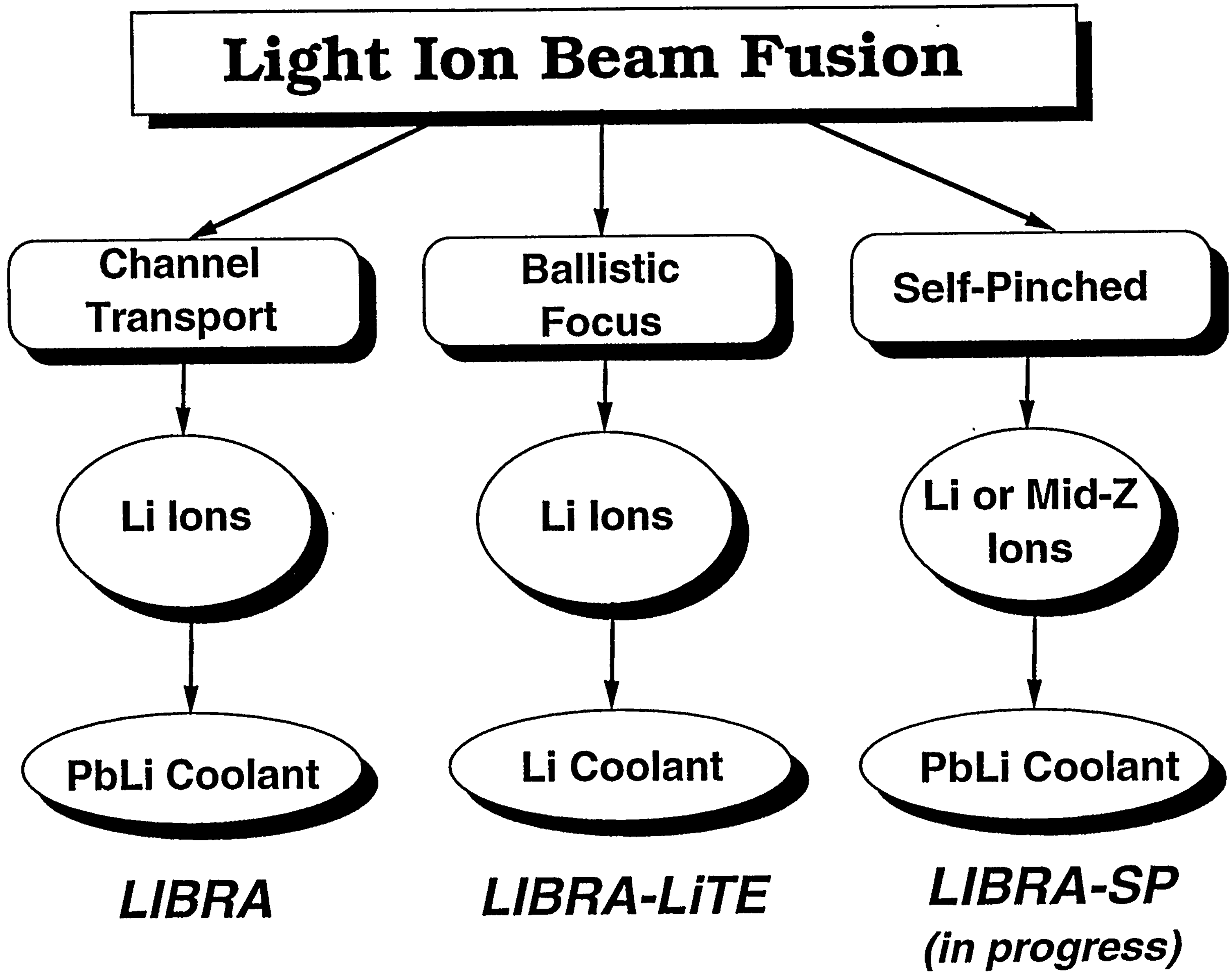
Light Ion Beam Fusion
Channel Transport
Ballistic Focus
Self-Pinched
Li Ions
Li Ions
Li or Mid-Z Ions
PbLi Coolant
Li Coolant
PbLi Coolant
LIBRA
LIBRA-LiTE
LIBRA-SP
(in progress)

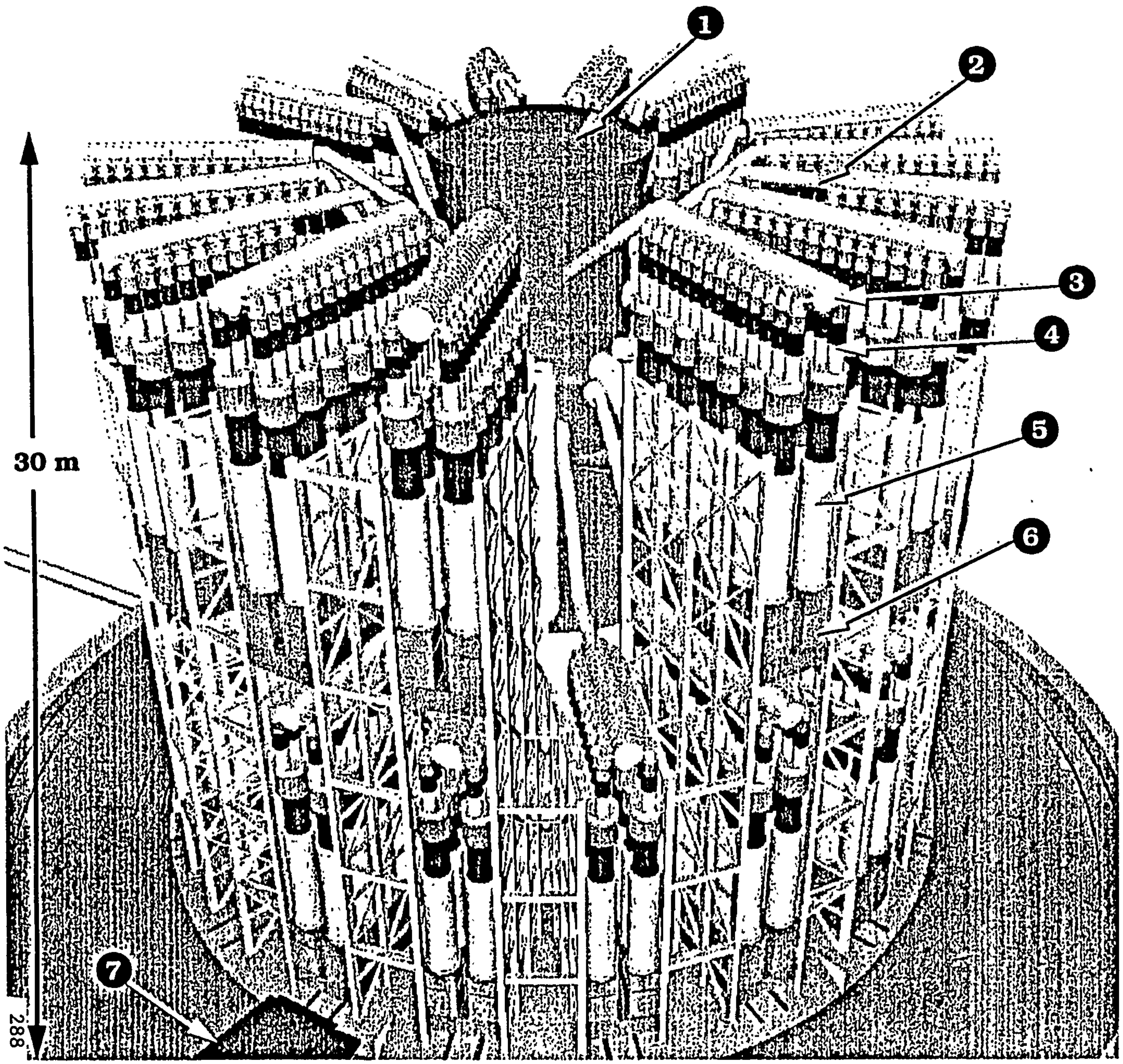

LIBRA-LiTE

View of Reactor from Inside Containment Building

(1) Reactor chamber

(2) Driver

(3) Adder cells

(4) Pulse forming lines

(5) 5 μs stage

(6) Capacitors and switches

(7) Transport carriage

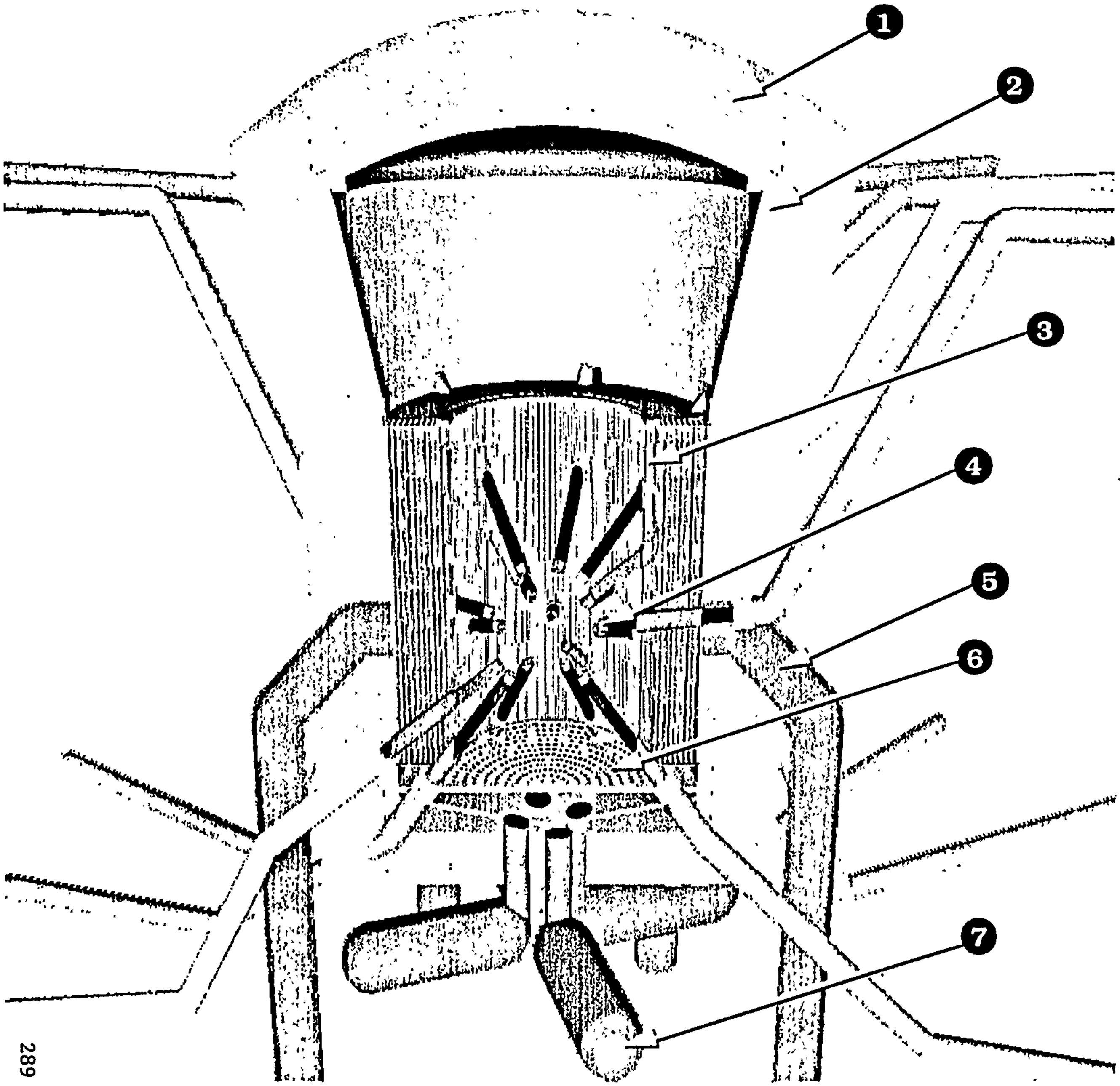

LIBRA-LiTE

Side View Reactor Chamber Cutaway

(1) Shield
(2) Reflector / vacuum chamber
(3) INPORT units
(4) Final focus magnet
(5) Vacuum line
(6) Perforated plate
(7) IHX

The Problem with Channel and Ballistic Transport is that Final Focusing Magnets Must Be Inside the Protective INPORT Units

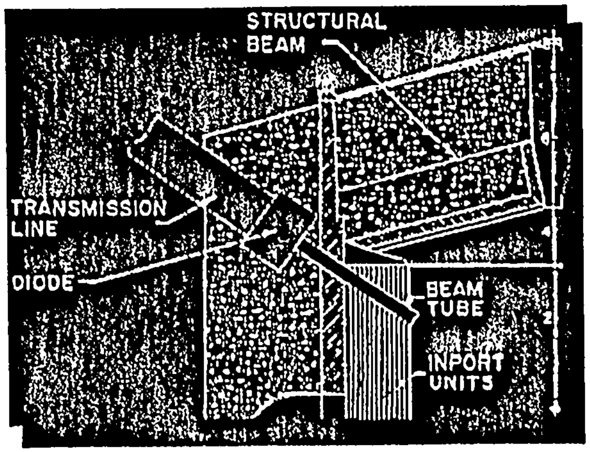

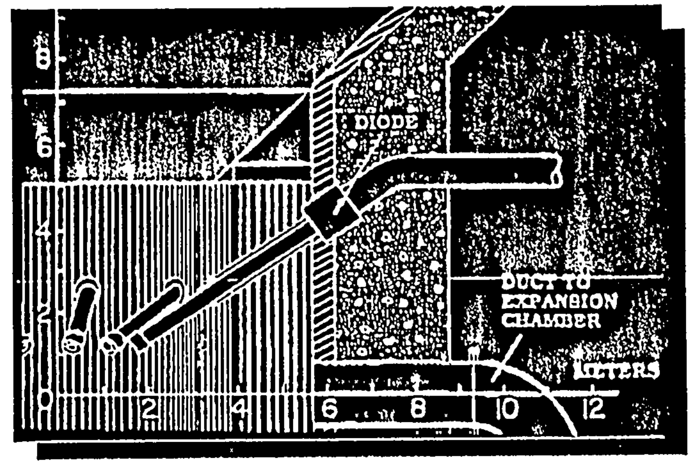

LIBRA		LIBRA-LiTE
18	Number of Beams	30
3 .6	Closest Distance to Magnet (m)	2.0
He/100 torr	Fill Gas	He/1 torr
153	Peak Impulse to the Magnet (Pa-s)	360
4	Neutron Wall Loading (MW/m^2)	29

A Low Ion Source Microdivergence is Required to Place Final Focusing Magnets Farther Away from the Target

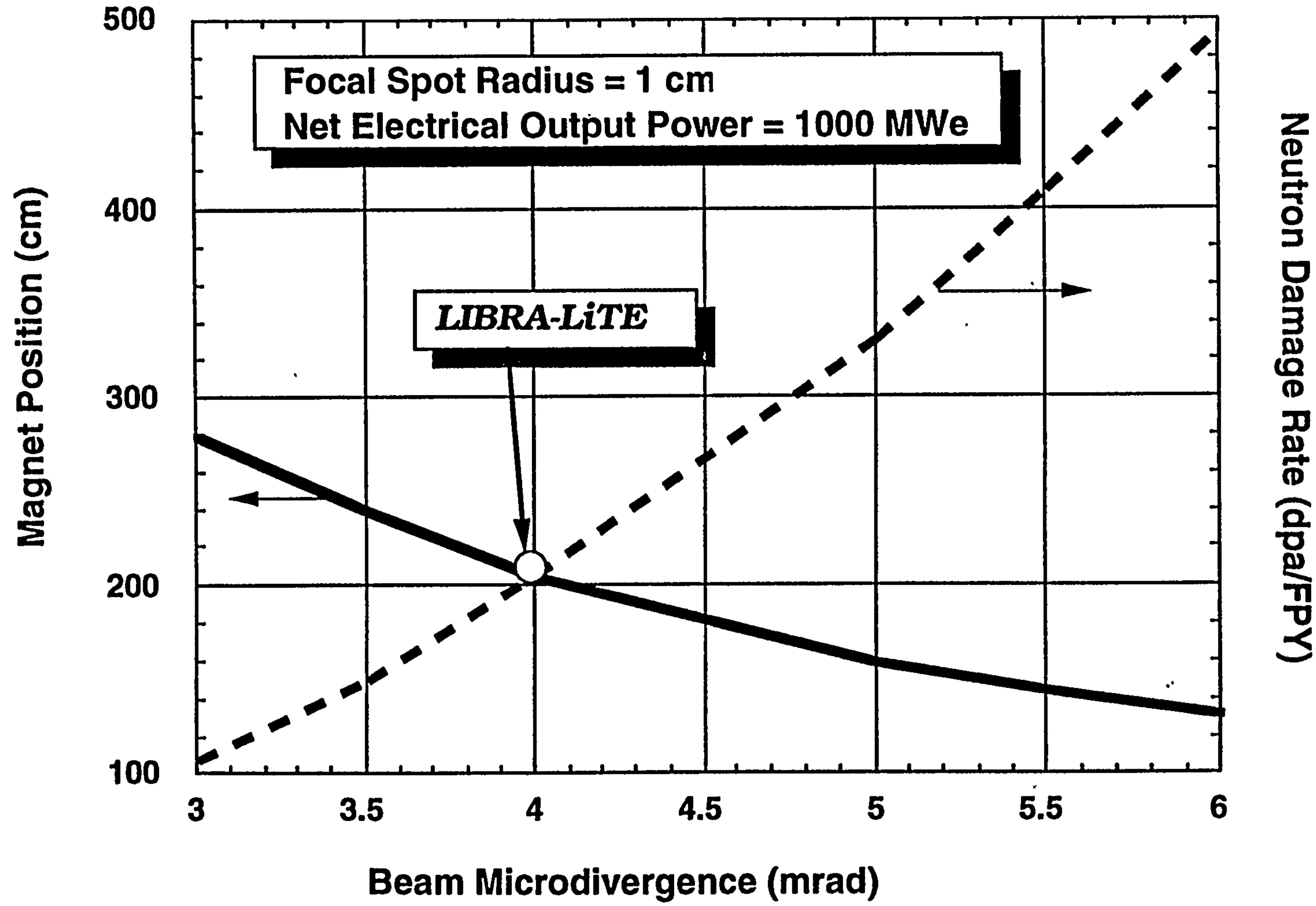

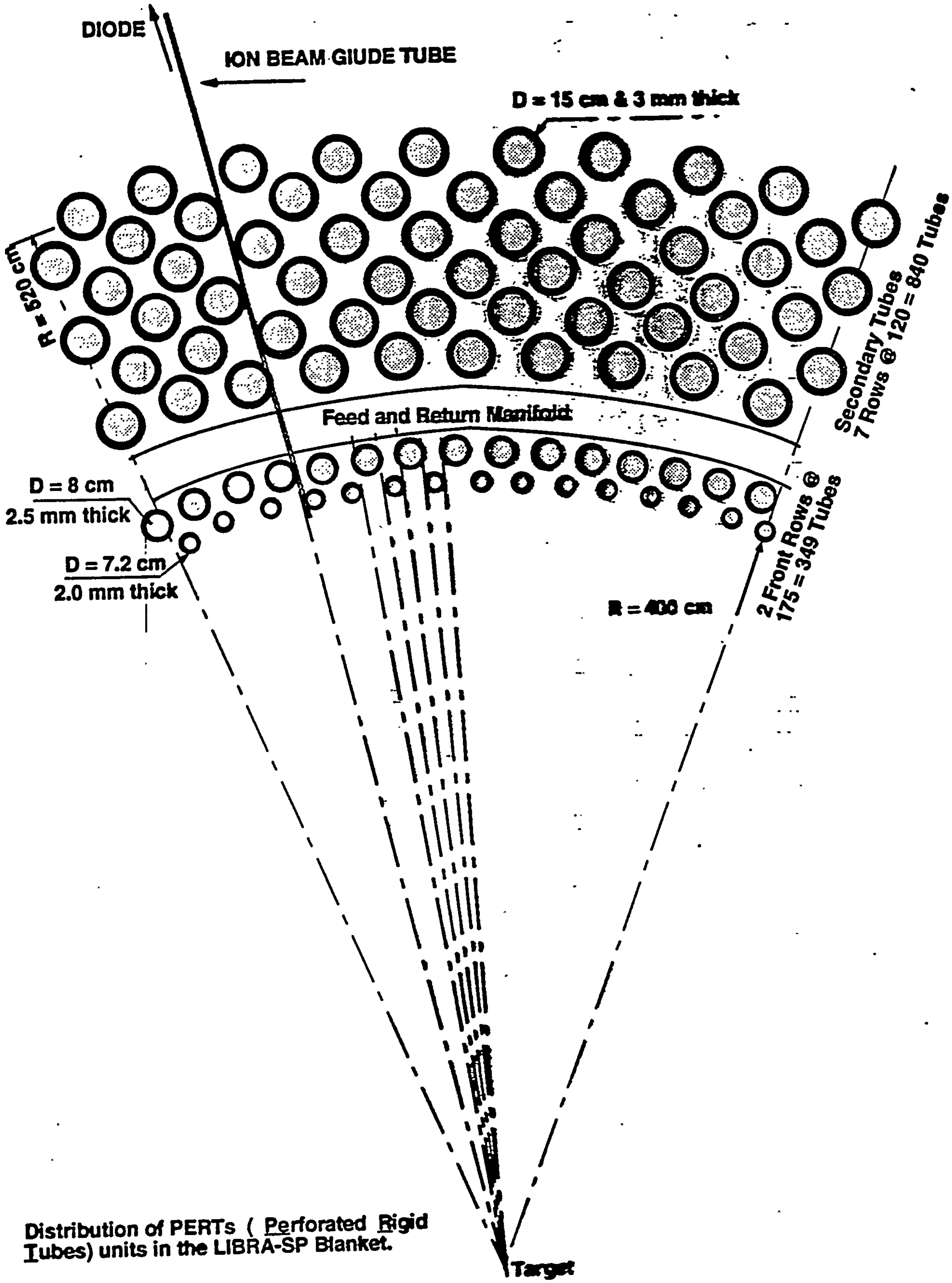

Distribution of PERTs (Perforated Rigid Tubes) units in the LIBRA-SP Blanket.

Reactor Cavity Conditions for Beam Propagation and INPORT/PERIT Units' Performance

Initial Gas Conditions

	LIBRA	*LIBRA-LiTE*	*LIBRA-SP (Preliminary)*
Temperature	500°C	500°C	550°C
Species	He	He	He
# Density	3.55×10^{18} cm^{-3}	3.55×10^{16} cm^{-3}	7.4×10^{16} cm^{-3}

Conditions at INPORTs or PERITs

	LIBRA	*LIBRA-LiTE*	*LIBRA-SP (Preliminary)*
Peak Pressure	100 GPa	4.6 GPa	100 GPa
Pulse Width (FWHM)	1 ns	8 ns	1 ns
Total Impulse	125 Pa-s	100 Pa-s	TBD
Vaporization	7 μm PbLi	66 μm Li	21 μm PbLi

LIBRA Reactors Display Quite Attractive Neutronic Properties

	LIBRA	*LIBRA-LiTE*	*LIBRA-SP* (*Preliminary*)
Neutron Wall Loading (MW/m^2)	6	10.6 (INPORT) 29 (Magnets)	7.2
Breeder	PbLi	Li	PbLi
% ^{6}Li	90	7.4	90
Tritium Breeding Ratio	1.36	1.41	1.48
Overall Energy Multiplication	1.17	1.12	1.18
Damage to INPORT/PERIT Units (dpa/FPY)	60	68	87
Damage to Steel Chamber Walls (dpa/FPY)	6.7	5	3.9

Comparison of LIBRA Power Plants

Parameter	Units	LIBRA	LIBRA-LiTE	LIBSP-1	LIBSP-2	LIBSP-3
Net Electrical Power	MWe	324	957	1001	1002	1000
Ion Beam Transport		Channel	Ballistic	Self-Pinch	Self-Pinch	Self-Pinch
Number of Beams		18	30	24	24	24
Energy on Target	MJ	4	6	7.2	7.2	7.2
Target Gain		80	100	80	80	80
Target Yield	MJ	320	600	576	576	576
Rep Rate	Hz	3	3.9	3.68	3.7	3.76
Fusion Power	MW	960	2340	2120	2131	2166
Fusion Neutron Power	MW	653	1591	1377	1384	1406
Energy Multiplication		1.28	1.211	1.3	1.3	1.3
Total Neutron Power	MW	836	1927	1789	1799	1828
X-ray and Ion Power	MW	286	698	728	732	774
Gamma Power	MW	2.78	6.79	0.13	0.13	0.13
Recirc Power	MW	37.4	88.5	32	32	32
Thermal Power	MW	1142	2671	2534	2548	2589
Thermal Efficiency		0.38	0.44	0.44	0.44	0.44
Gross Elec Power	MWe	434	1175	1115	1121	1139

RRP LIBRA 16 Sep 1994

University of Wisconsin-Madison

Parameters Estimated Based on LIBRA and LIBRA-LiTE

- Costs scaled to LIBRA-LiTE
  - ▷ Driver Direct Cost = $1.04^2 * (271 + (3.41 * RR))(E_{on\ diodes}/8.33)^{0.8}$
  - ▷ Total Direct Cost = Driver Direct Cost + (0.4729 * Thermal Power)
  - ▷ All costs are in millions of 1993 dollars, $E_{on\ diodes}$ is the pulsed power energy into the diodes in MJ, and the thermal power is in MW. RR is the rep rate in Hz.

RRP LIBRA 16 Sep 1994

University of Wisconsin-Madison

Comparison of LIBRA Power Plants (cont.)

Parameter	Units	LIBRA	LIBRA-LiTE	LIBSP-1	LIBSP-2	LIBSP-3
Driver Efficiency		0.49	0.376	0.376	0.376	0.376
Prime Energy Storage	MJ	17.01	33.24	22.40	23.64	28.37
Diode Type		1 stage	1 stage	2 stage	2 stage	2 stage
Diode Efficiency		0.8	0.8	0.9	0.9	0.9
Energy into Diode	MJ	8.33	12.50	8.42	8.89	10.67
Transport Efficiency		0.6	0.6	0.95	0.9	0.75
Energy into Beam	MJ	6.67	10.00	7.58	8.00	9.60
Net Driver Efficiency		0.235	0.180	0.321	0.305	0.254
Gain*Net driver Eff.		18.8	18.0	25.7	24.4	20.3
Net Efficiency		0.0894	0.0794	0.1415	0.1340	0.1117
Gain*Efficiency		7.15	7.94	11.32	10.72	8.93
Driver Power	MWe	51.0	129.7	82.4	87.5	106.7
Magnet Power	MWe	27	75	0	0	0
Aux. Power	MWe	32	13.5	32	32	32
Recirc. Power Fract		0.254	0.186	0.103	0.107	0.122
Direct Driver Cost	M$ (1993)	304	426	309	323	374
Total Direct Cost	M$ (1993)	845	1689	1508	1528	1598
Unite Direct Cost	$/W (1993)	2.61	1.76	1.51	1.53	1.60

RRP LIBRA 16 Sep 1994

University of Wisconsin-Madison

The Direct Unit Cost of the LIBRA Reactors Compares Favorably with Other ICF and MCF DT Power Plants at the 1000 MWe Level

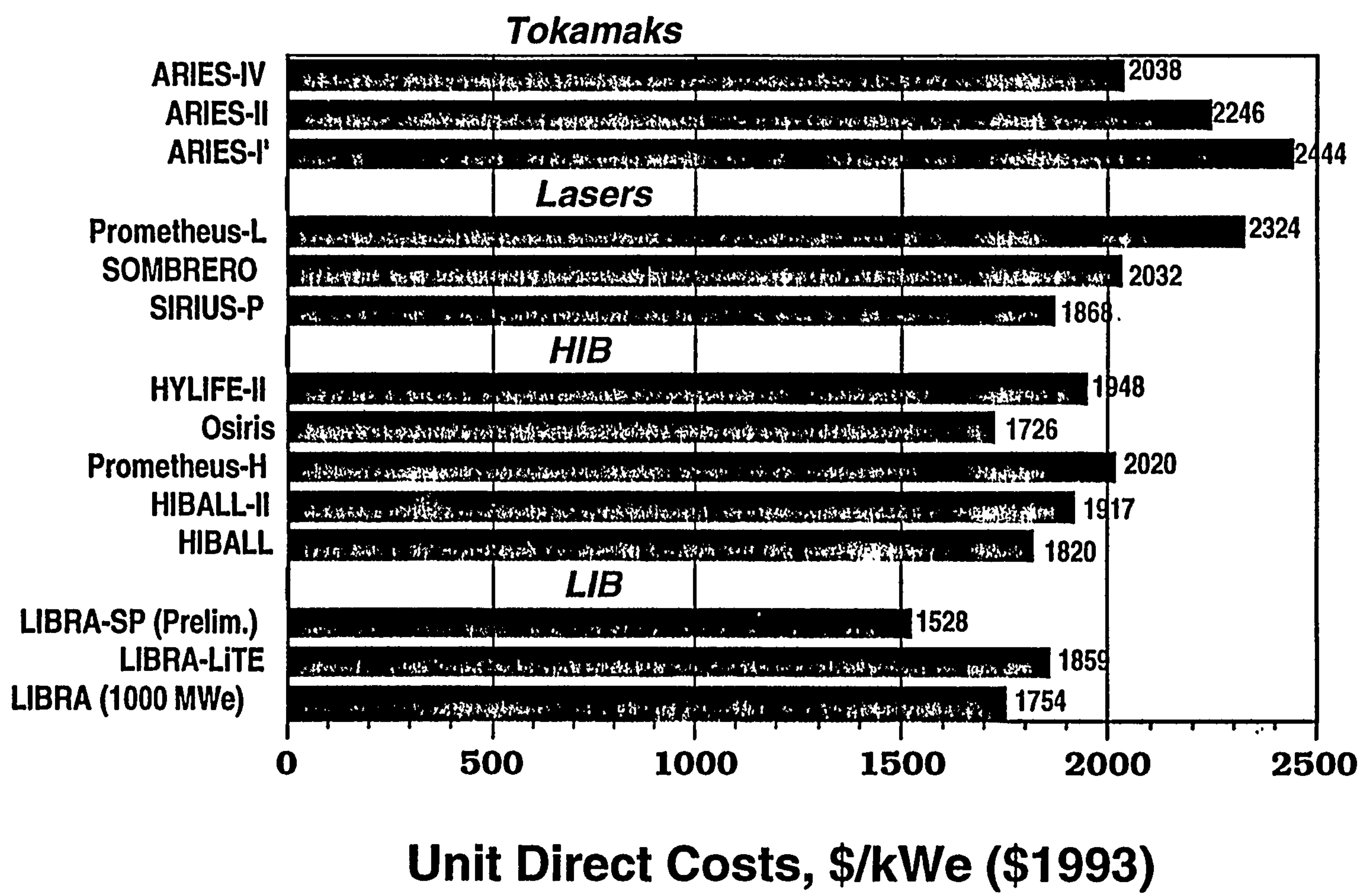

The LIBRA-SP Target Uses Internal Pulse Shaping

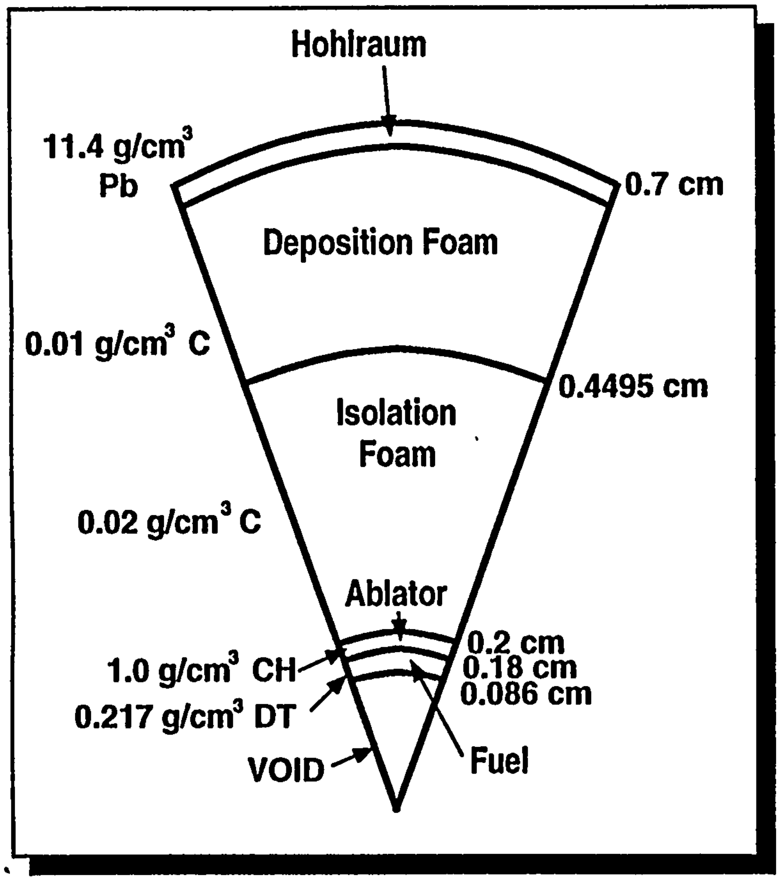

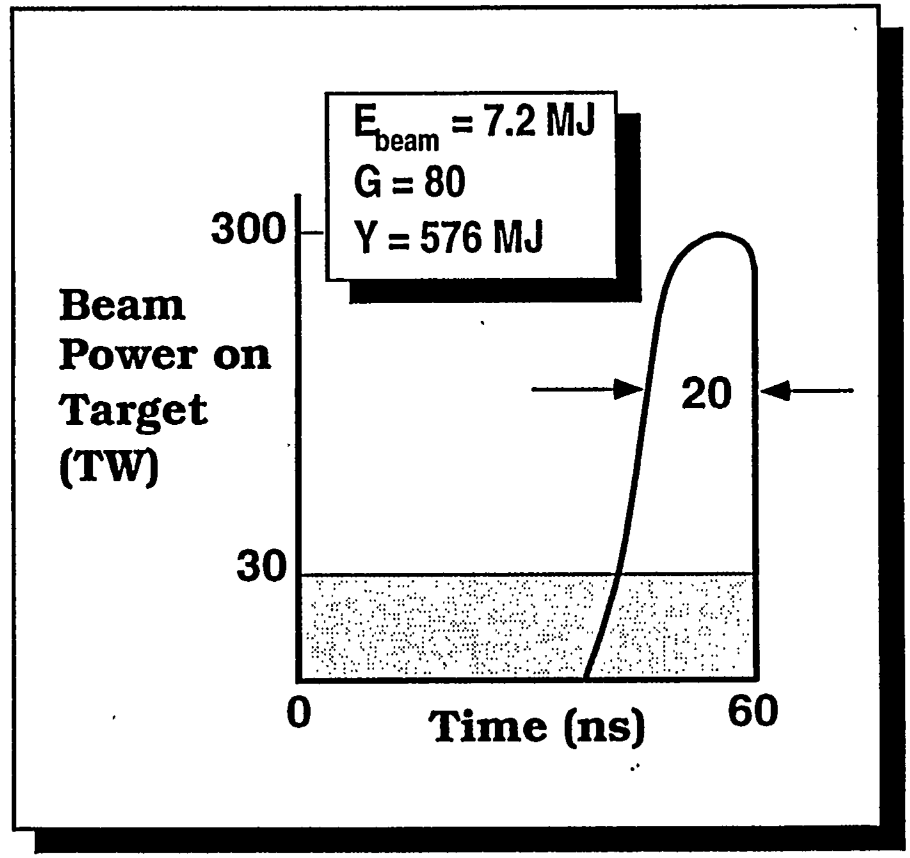

Indirect Drive Ion Beam Gain Curves are Lower than for Lasers

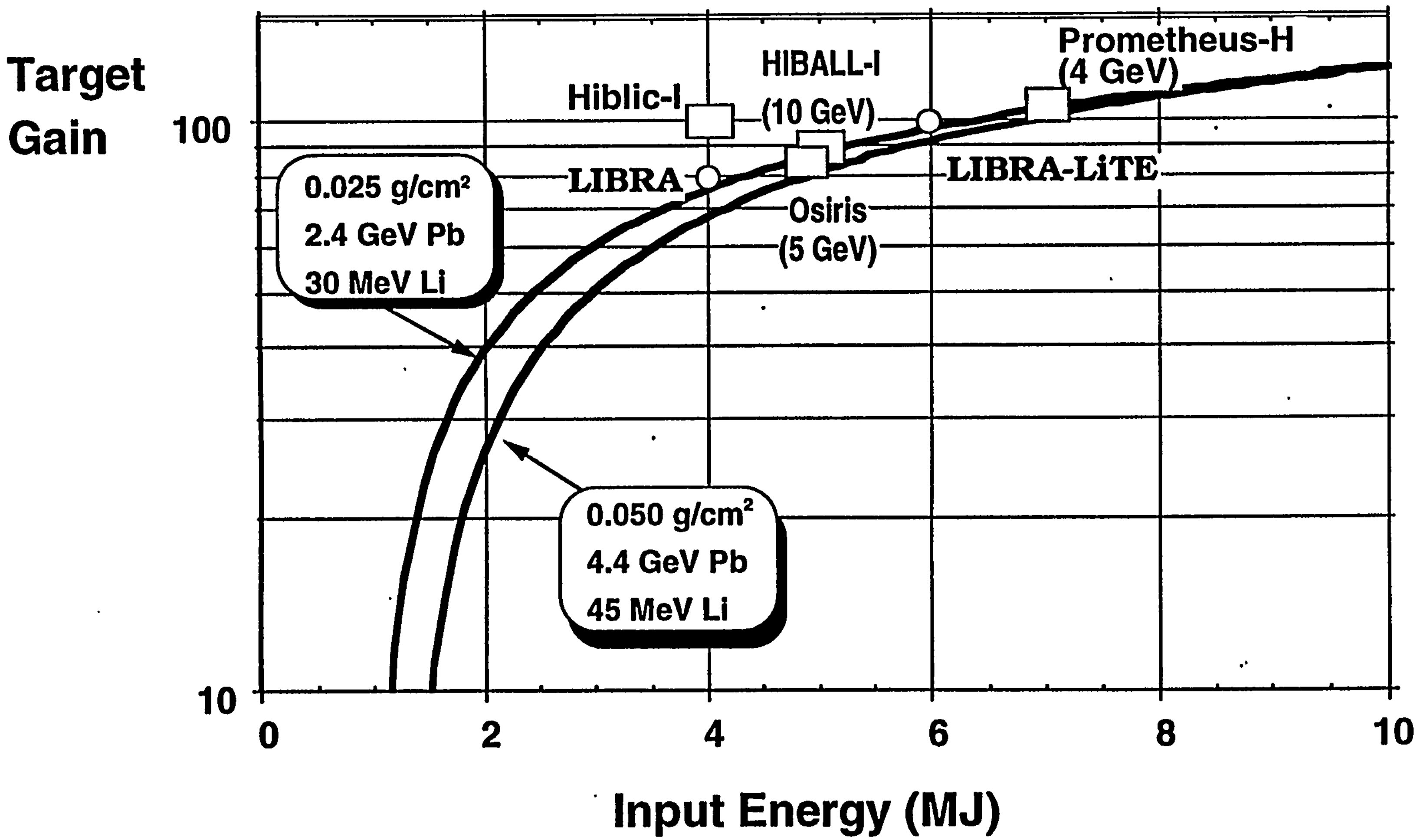

The Use of Helia Driver Technology and Li Ion Applied B Diodes Allow Efficient Energy Transport to the Target

	Prime Energy Storage (MJ)	η_D	Energy to Diode (MJ)	η_{DD}	Energy to Beam (MJ)	η_T	Energy on Target (MJ)	Net Driver Efficiency
LIBRA (18 beams)	17	49%	8.3	80%	6.7	60%	4	23.5%
					channel transport			
LIBRA-LiTE (30 beams)	33	38%	12.5	80%	10	60%	6	18.0%
					ballistic transport			
LIBRA-SP (24 beams)	24	38%	8.9	90%	8.0	90%	7.2	30.5%
					self-pinch			

Ion Transport Parameters for LIBRA-SP Base Case

General

Parameter	Units	Total	Main	Prepulse
Energy Leaving Diodes	MJ	8.0	6.67	1.33
Energy Transport Efficiency	%		90	90
Energy Delivered to Target	MJ	7.2	6.0	1.2
Number of Beams		24	12	12
Transport Length	m		7	7
Pulse Widths				
at Diode	ns		40	40
at Target	ns		20	40
Ion Energy	MeV		30	30
Ion Species			Li	Li

RRP LIBRA 16 Sep 1994

University of Wisconsin-Madison

Ion Transport Parameters for LIBRA-SP Base Case

Total For All Beams

Parameter	Units	Total	Main	Prepulse
Power at Diodes	TW	200	167	33
Power at Target	TW	330	300	30
Anode Area	cm^2		1111	222
Current at Diodes	MA	6.67	5.56	1.11
Current at Target	MA	11	10	1
Target Radius	cm	0.7		
Current Density at Diodes	MA/cm^2		0.005	0.005
Current Density at Target	MA/cm^2	1.79	1.62	0.16
Power Density at Diodes	TW/cm^2		0.15	0.15
Power Density at Target	TW/cm^2	53.6	48.7	4.9

RRP LIBRA 16 Sep 1994

University of Wisconsin-Madison

Ion Transport Parameters for LIBRA-SP Base Case

For Each Beam

Parameter	Units	Main	Prepulse
Energy Leaving Diode	MJ	0.556	0.111
Energy on Target	MJ	0.5	0.1
Power at Diode	TW	13.9	2.78
Power at Target	TW	25	2.5
Anode Area	cm^2	92.6	18.5
Current at Diode	MA	0.463	0.093
Current at Target	MA	0.833	0.0833
Focal Spot Radius	cm	0.7	0.7
Current Density at Diode	MA/cm^2	0.005	0.005
Current Density at Target	MA/cm^2	0.541	0.0541
Power Density at Diode	TW/cm^2	0.15	0.15
Power Density at Target	TW/cm^2	16.2	1.62

RRP LIBRA 16 Sep 1994

University of Wisconsin-Madison

Ion Transport Critical Issues for Reactors

- Background Gas Conditions
  density, species, impurities, temperature
- Beam Requirements
  Divergence, Microdivergence, current
- Pointing
- Transport Efficiency

Ion Transport Parameters for 170 MeV Na Ions
For Each Beam and LIBRA-SP Base Case

Parameter	Units	Main			Prepulse			
Energy Leaving Diode	MJ	0.556			0.111			
Energy on Target	MJ	0.5			0.1			
Power at Diode	TW	13.9			2.78			
Power at Target	TW	25			2.5			
Anode Area	cm^2	16.3	36.4	13.2	3.27	7.28	2.6	
Current at Diode	MA	0.0817	0.182	.066	0.0164	0.0364		0.013
Current at Target	MA	0.147	.327	.12	0.0147	0.0327		0.012
Focal Spot Radius	cm	0.7			0.7			
Current Density at Diode	MA/cm^2	0.005	0.08		0.005			
Current Density at Target	MA/cm^2	0.0955	0.213		0.00955	0.0213	0.008	
Power Density at Diode	TW/cm^2	0.85	0.38	1.05	0.85	0.38	1.05	
Power Density at Target	TW/cm^2	16.2			1.62			

76 Mev Na.
211 Mev

RRP LIBRA 17 Sep 1994

University of Wisconsin-Madison

Extension to Welterweight Ions

- higher power density in diodes (assuming 5 kA/cm²). Will it damage diodes?
- Lower current per accelerator module. Will Induction voltage adders still work?
- Transport in chamber? Lower current density, higher particle energy and mass.

HIF power plant designs: issues affecting beam transport

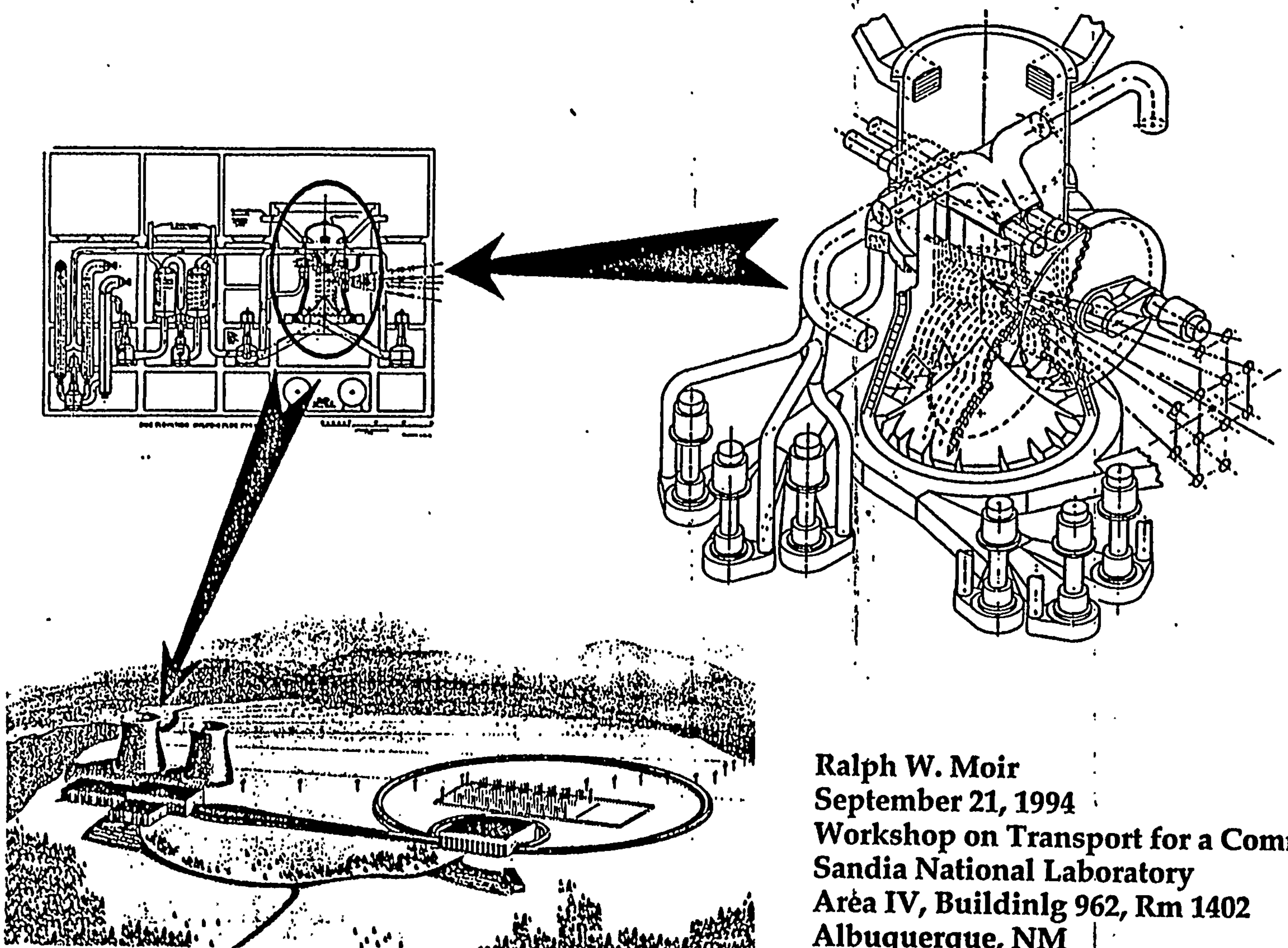

Ralph W. Moir
September 21, 1994
Workshop on Transport for a Common Ion Driver
Sandia National Laboratory
Arěa IV, Buildinlg 962, Rm 1402
Albuquerque, NM

22

Recirculator-driven, Heavy-Ion Fusion Power Plant

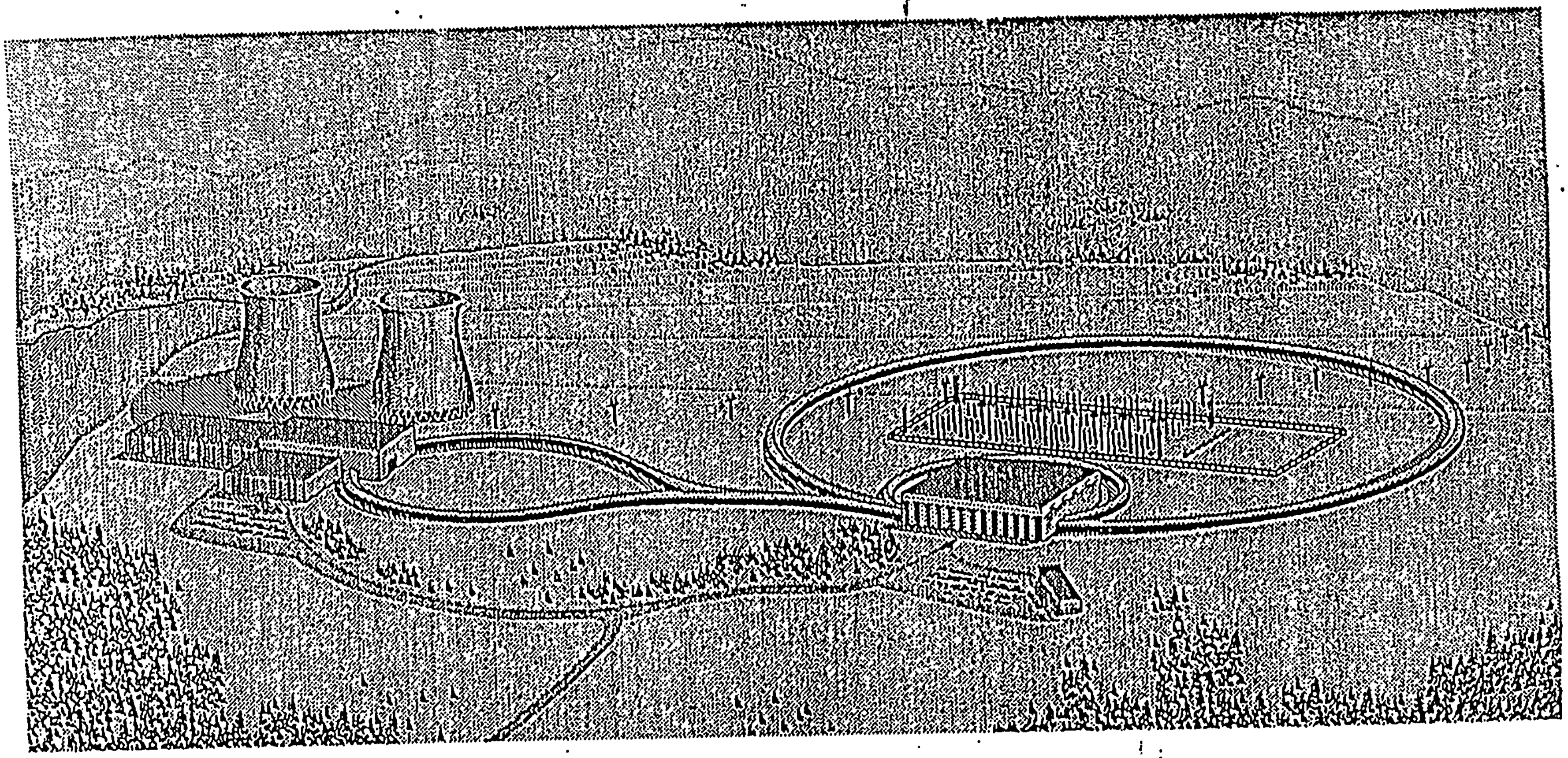

A plausible 400 m final transport section for single sided illumination has been scoped

Correct length for
drift compression

Minimum angle beam
array for higher gain

Longer path length for
8 beams for pulse shaping

3D neutronics calculation
needed

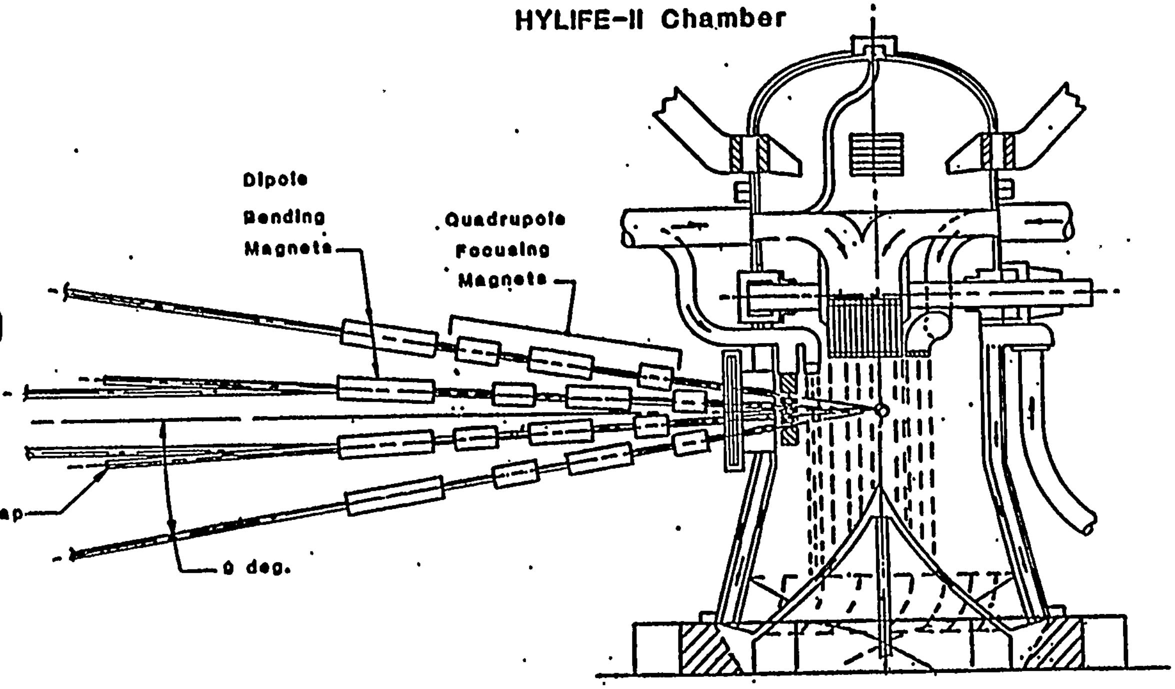

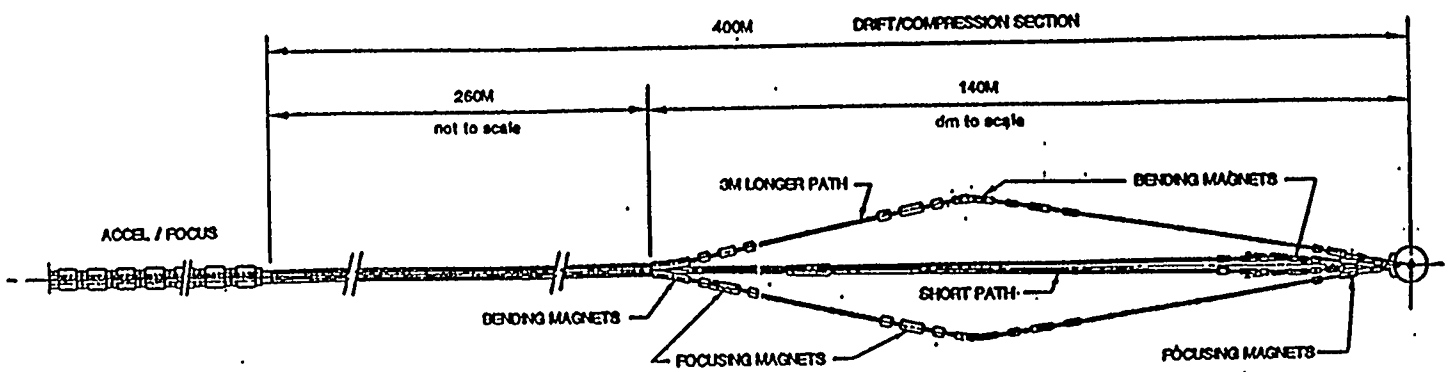

Rotating shutters will close 0.14 m dia holes in 0.001 s stopping liquid splash slower that 1000 m/s

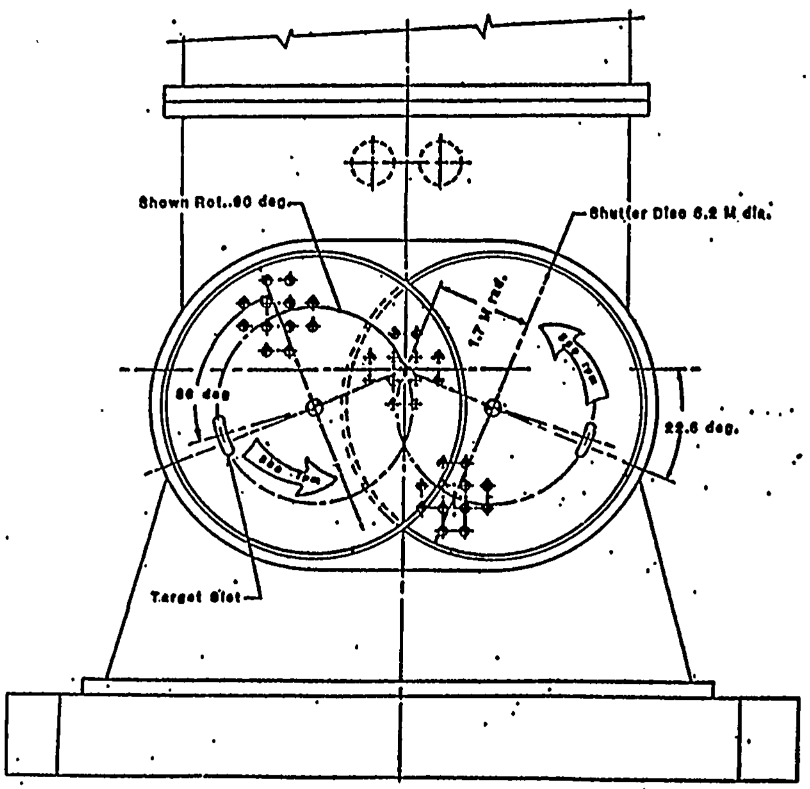

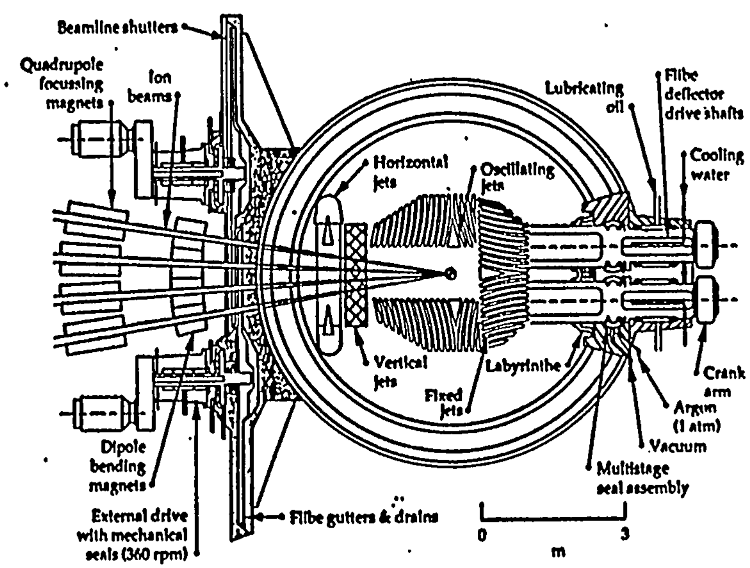

Single-sided illumination will result in cost savings of final transport components

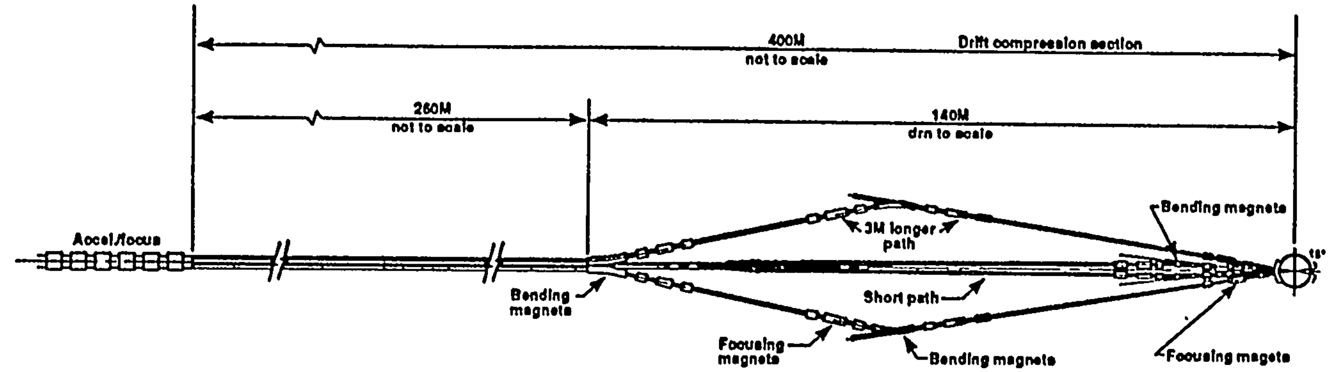

FIGURE 1 The last 400 m of the heavy-ion beam system is used to accomplish drift compression of the beams and the last 50 m is used for final focus from one side onto the target in the example shown. The desired pulse shape can be obtained by compressing, delaying, and stacking the 12 beams.

148 *W.R. Meier / Fusion Engineering and Design 25 (1994) 145–157*

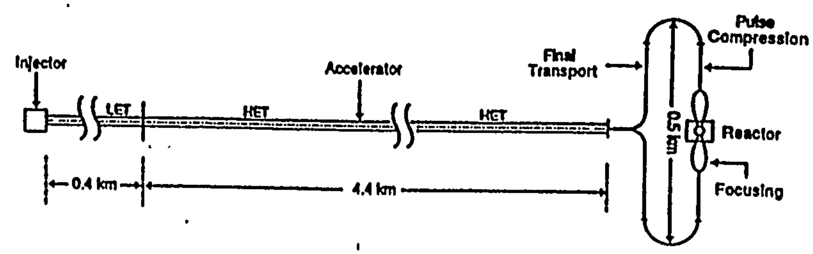

	Into LET	Into HET	Out of HET
Distance from Injector (km)	0	0.4	4.8
Acceleration Gradient (MV/m)	0.013	0.85	0.85
Ion Voltage (MV)	3	78	3830
Beam Current (A)	3.5	170	1090
Pulse Duration (ms)	34.1	0.70	0.10
Pulse Length (m)	71.4	7.5	7.5

Fig. 2. The Osiris driver is a 12-beam linac using Xe^{+} ions. Design parameters at various locations along the accelerator are shown.

Heavy-ion target can be designed for single-sided illumination while minimizing asymmetry

Radiation-Driven Targets for Heavy-Ion Fusion

IAEA-CN-60/B-P-13

D. D.-M. Ho, J. A. Harte, and M. Tabak
Lawrence Livermore National Laboratory
Livermore, CA 94550

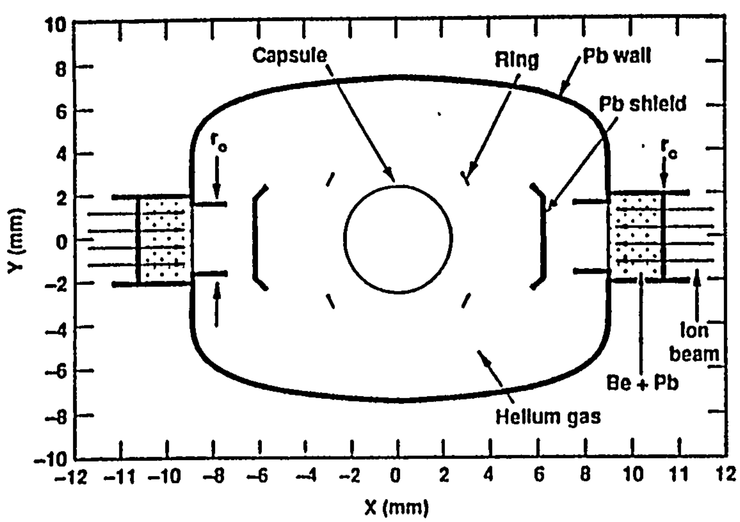

50-01-0894-3177pb02
18DMH/Awh

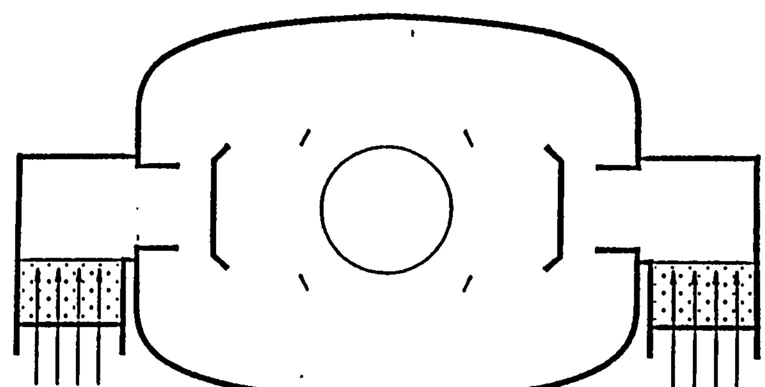

50-01-0894-3177pb01
18DMH/Awh

Target injection will be more challenging

Beam propagation may be possible in two density regions: low density or channel transport

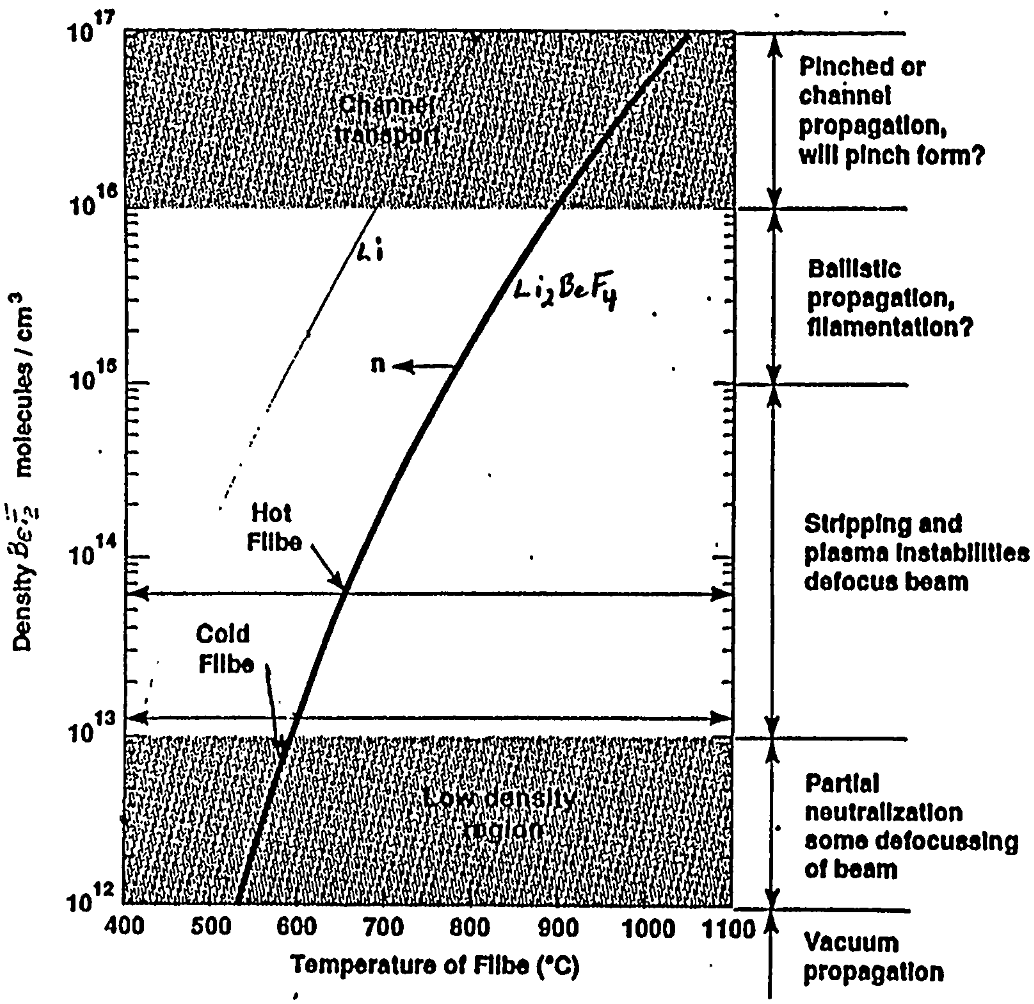

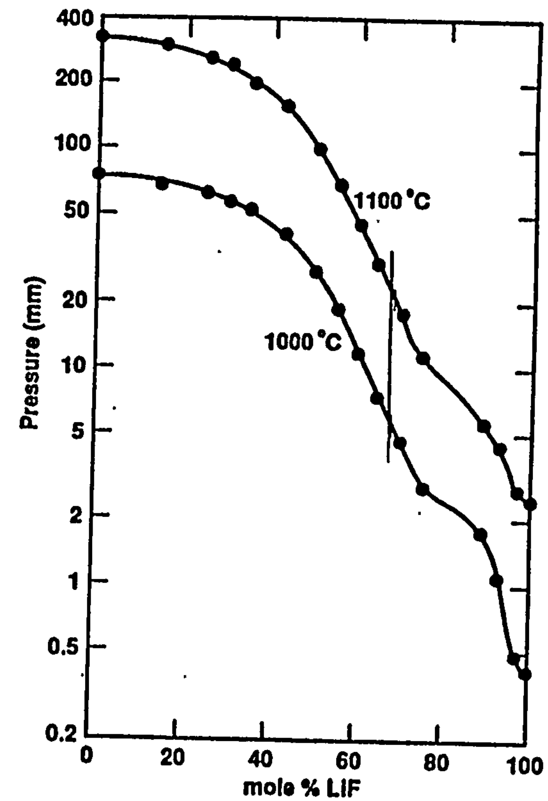

Fig. 6-1. Vapor pressures in the LiF·BeF_2 system.

OSIRIS is an example of an HIF Reaction chamber

W.R. Meier / Fusion Engineering and Design 25 (1994) 145–157 147

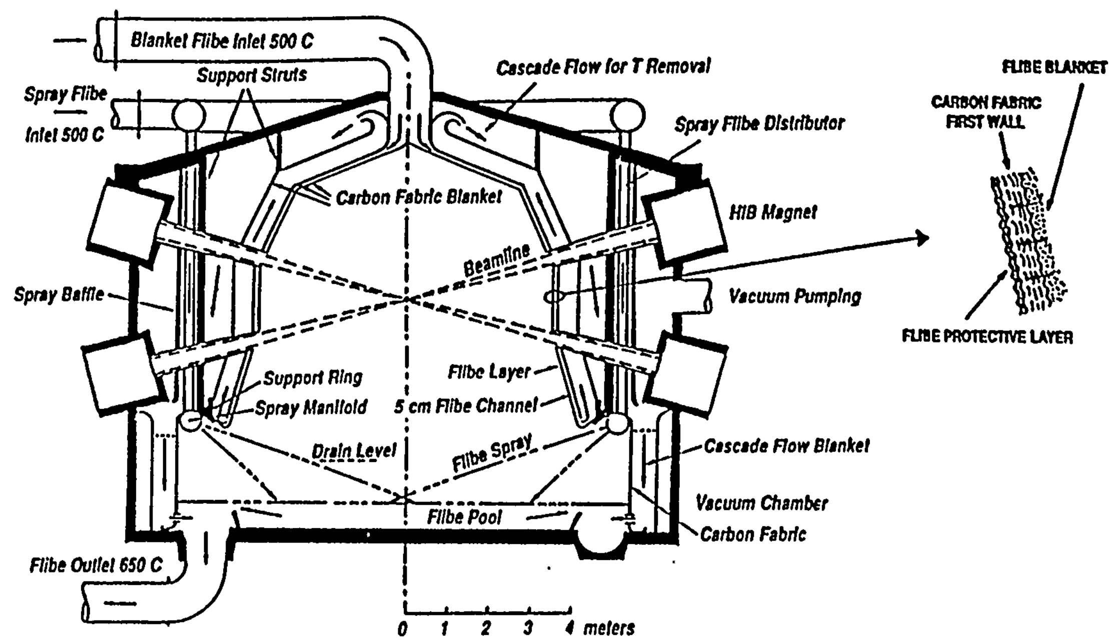

Fig. 1. The Osiris chamber features a porous carbon-fabric blanket filled with molten salt Flibe.

Flibe
Condensation on Flibe spray
Carbon fiber walls

Prometheus-H is an example of an HIF Reaction chamber

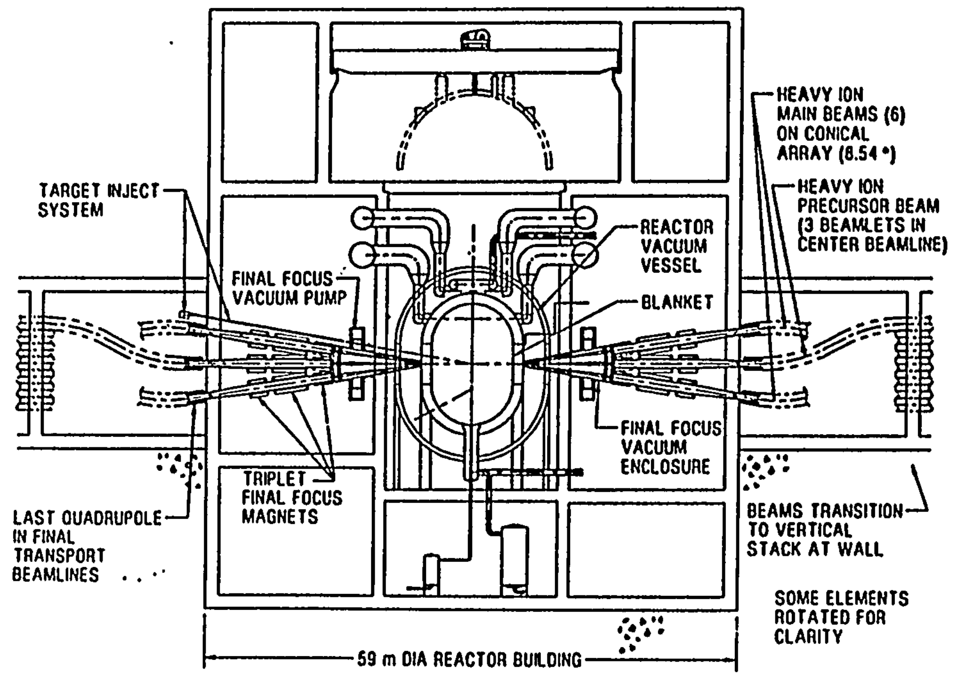

Fig. 14. Prometheus-H reactor cavity arrangement.

$Li_{17}Pb_{83}$

Condensation on $Li_{17}Pb_{83}$ coated walls

SiC walls

Cascade is an example of an HIF Reaction chamber

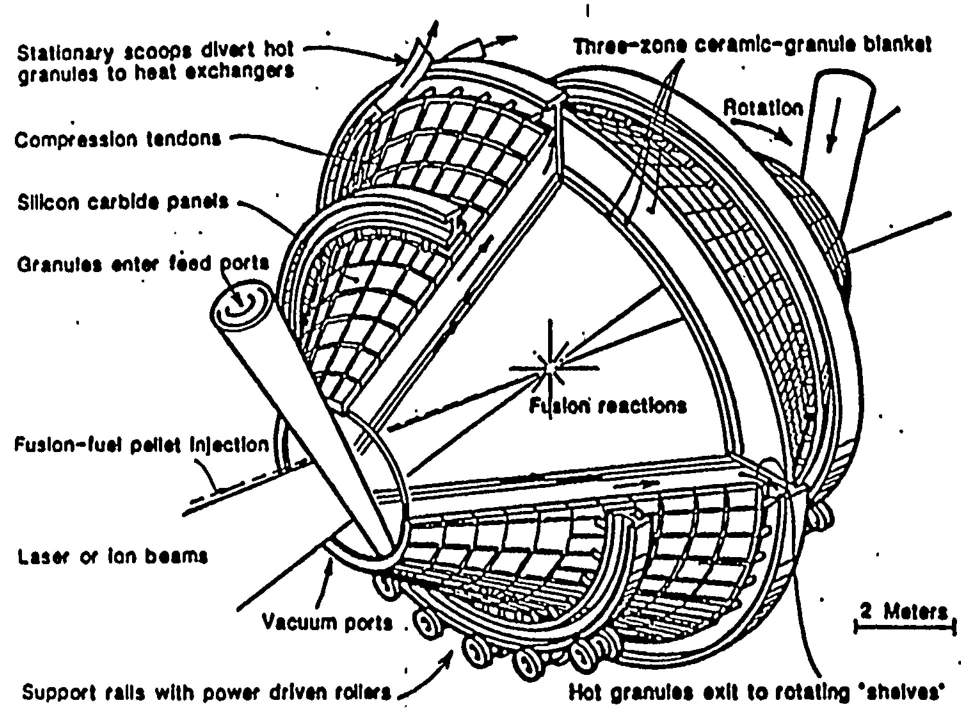

Pb condensation on walls exterior to chamber carbon granules

HIBALL-II is an example of an HIF Reaction chamber

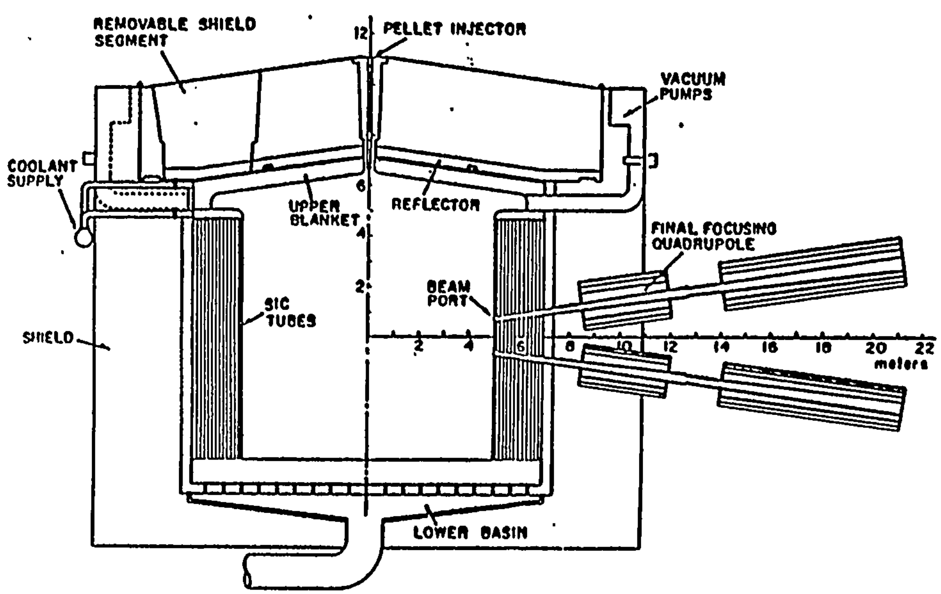

Cross section of HIBALL chamber.

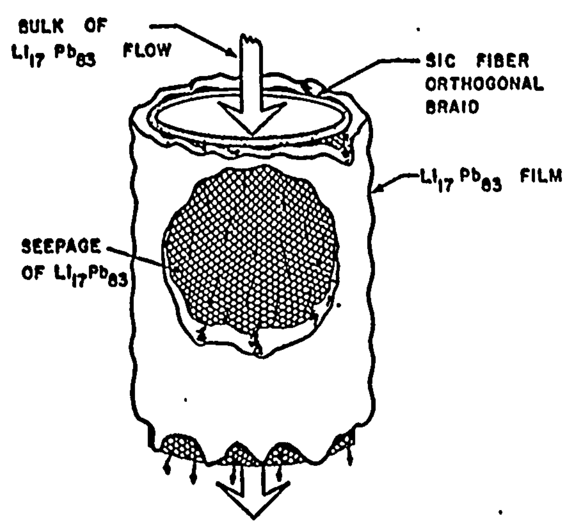

Schematic of INPORT unit concept.

$Li_{17}Pb_{83}$
Condensation on $Li_{17}Pb_{83}$ coated walls
SiC walls

HYLIFE-II is based on liquid wall protected chambers

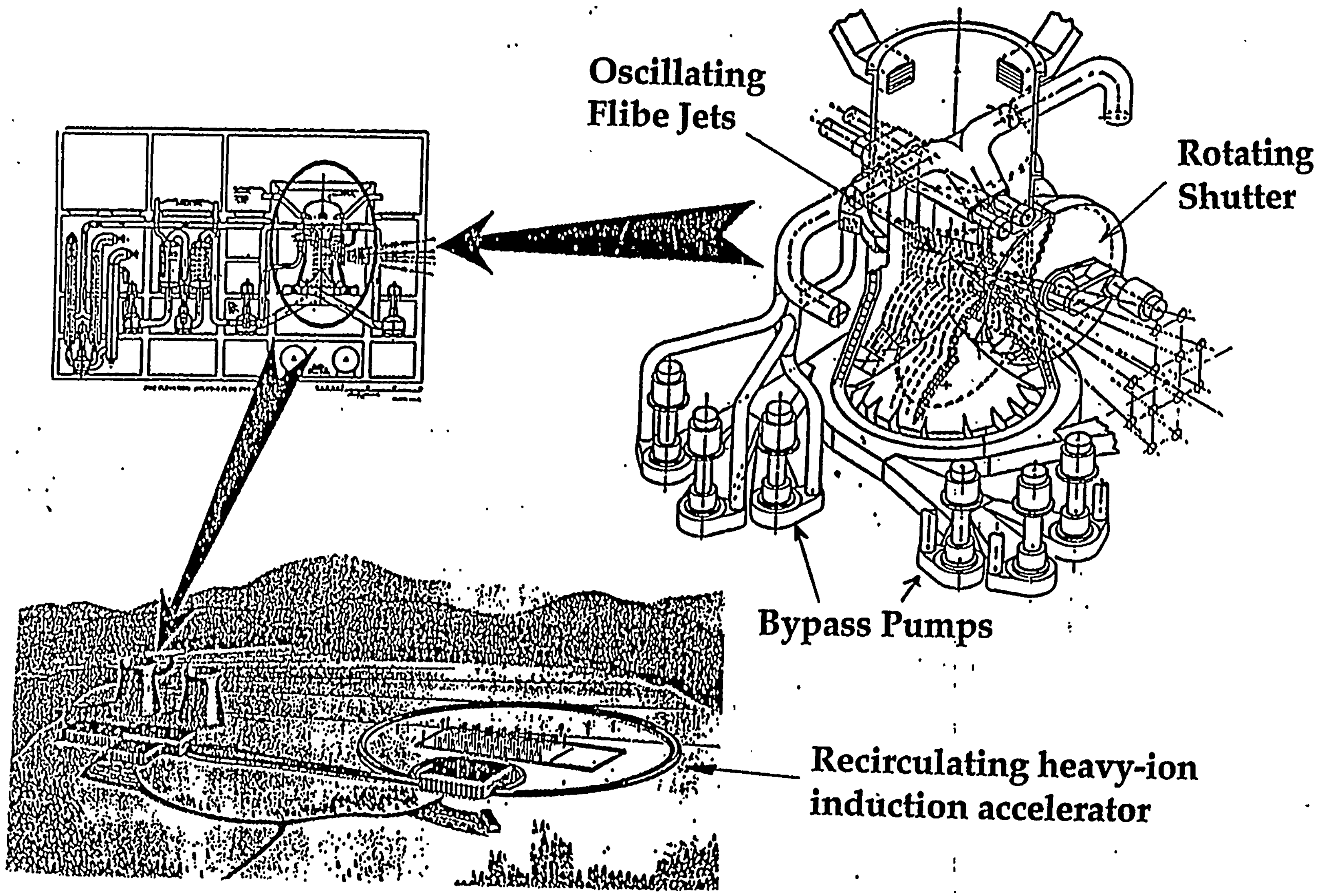

Heavy ions illuminate single-sided targets

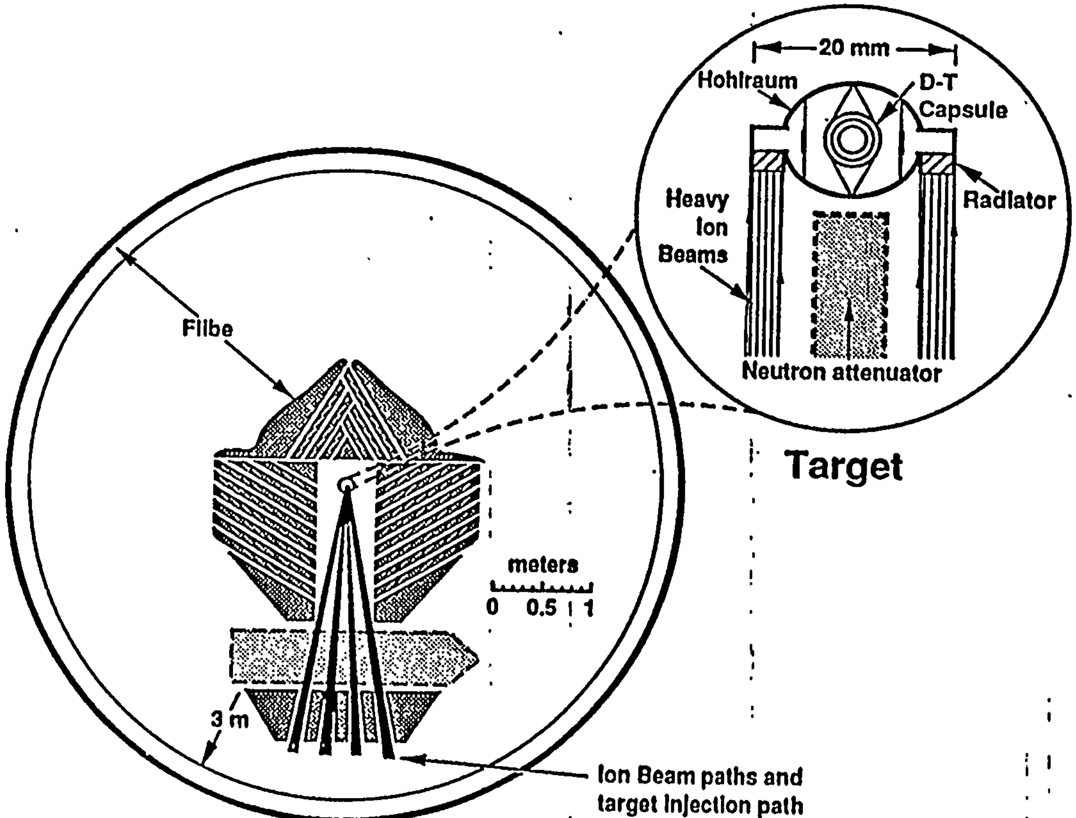

Cross Section through liquid
Top View

Chamber

Flibe
Condensation on Flibe spray
304 stainless steel walls behind 0.5 m Flibe

A liquid "pocket" surrounds the microexplosion and protects the walls from neutron damage

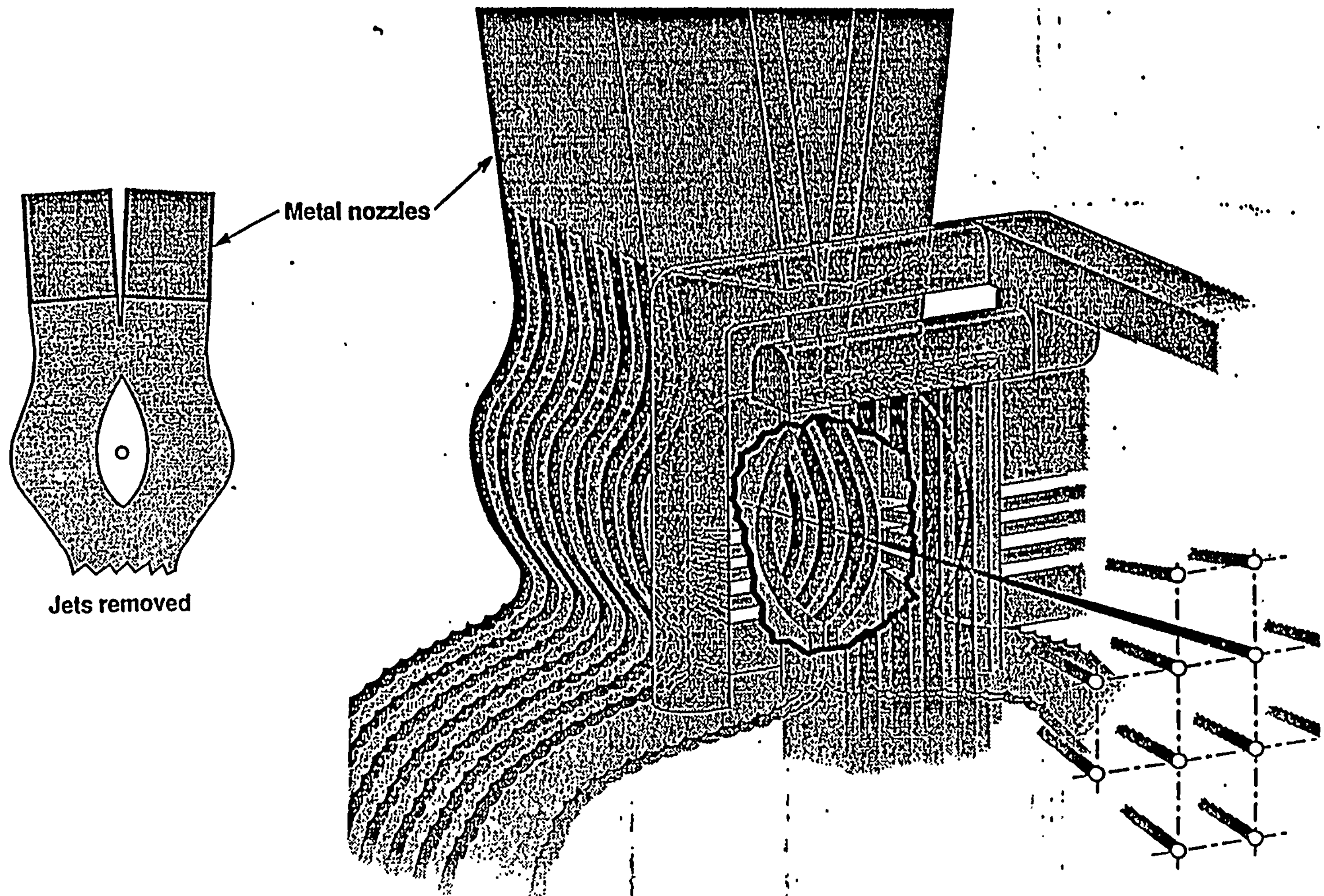

With thick liquid walls, the 304 SS structures will last 30 yrs and qualify for shallow burial

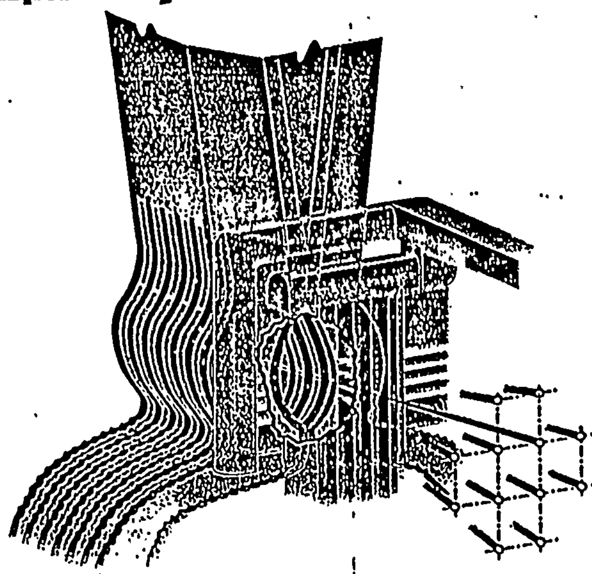

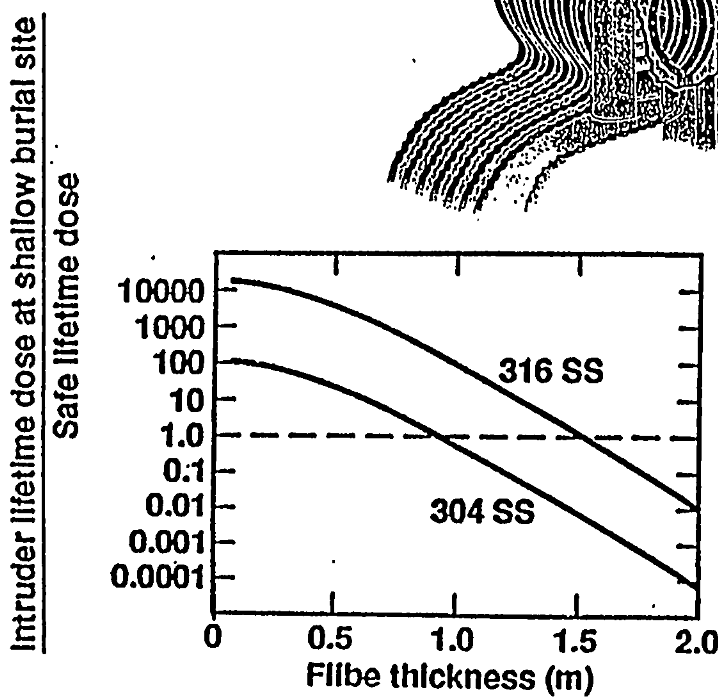

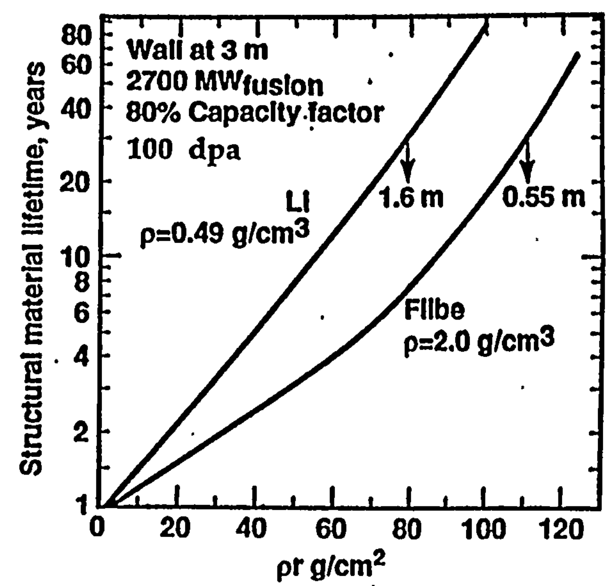

HYLIFE-II

Design function	Advantage
Flibe coolant	nonflammable
liquid wall protection	structures last 30 years shallow burial using 304 SS 30% reduction in Cost of electricity due to: 1-less down time for first wall replacement 2-avoiding first wall replacement reduces cost 3-less remote equipment needed 4.4 ¢/kWh
oscillating jets	active chamber clearing (6 Hz)

Requires demonstration of:
1-high gain (>50) targets
2-reliable and low cost (<600M$ direct) driver
3-reliable and low cost target factory (est. cost~60M$ direct)

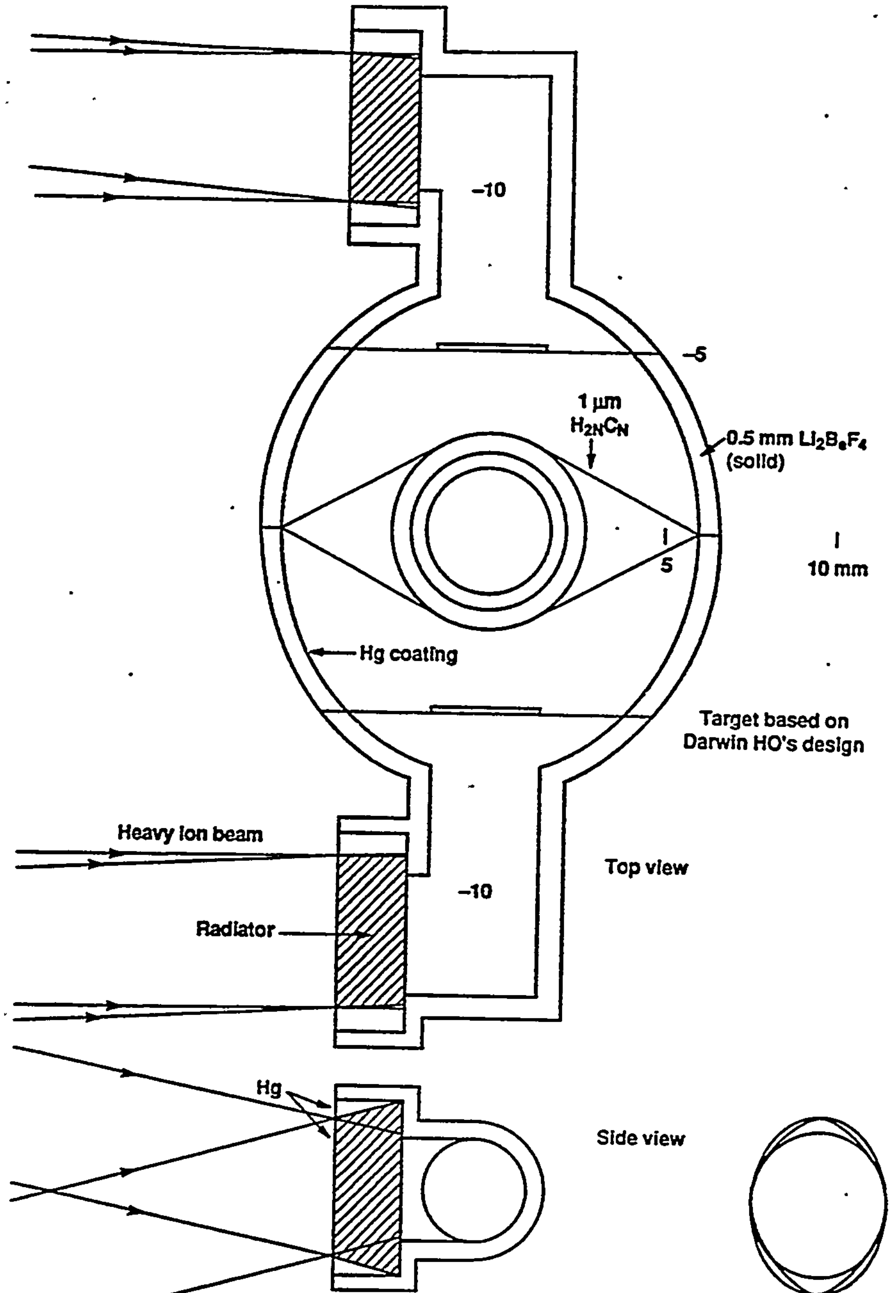

Fig. 1. Heavy-ion target for HYLIFE-II

40-00-0394-0626pub

The beam ports are protected from neutron damage

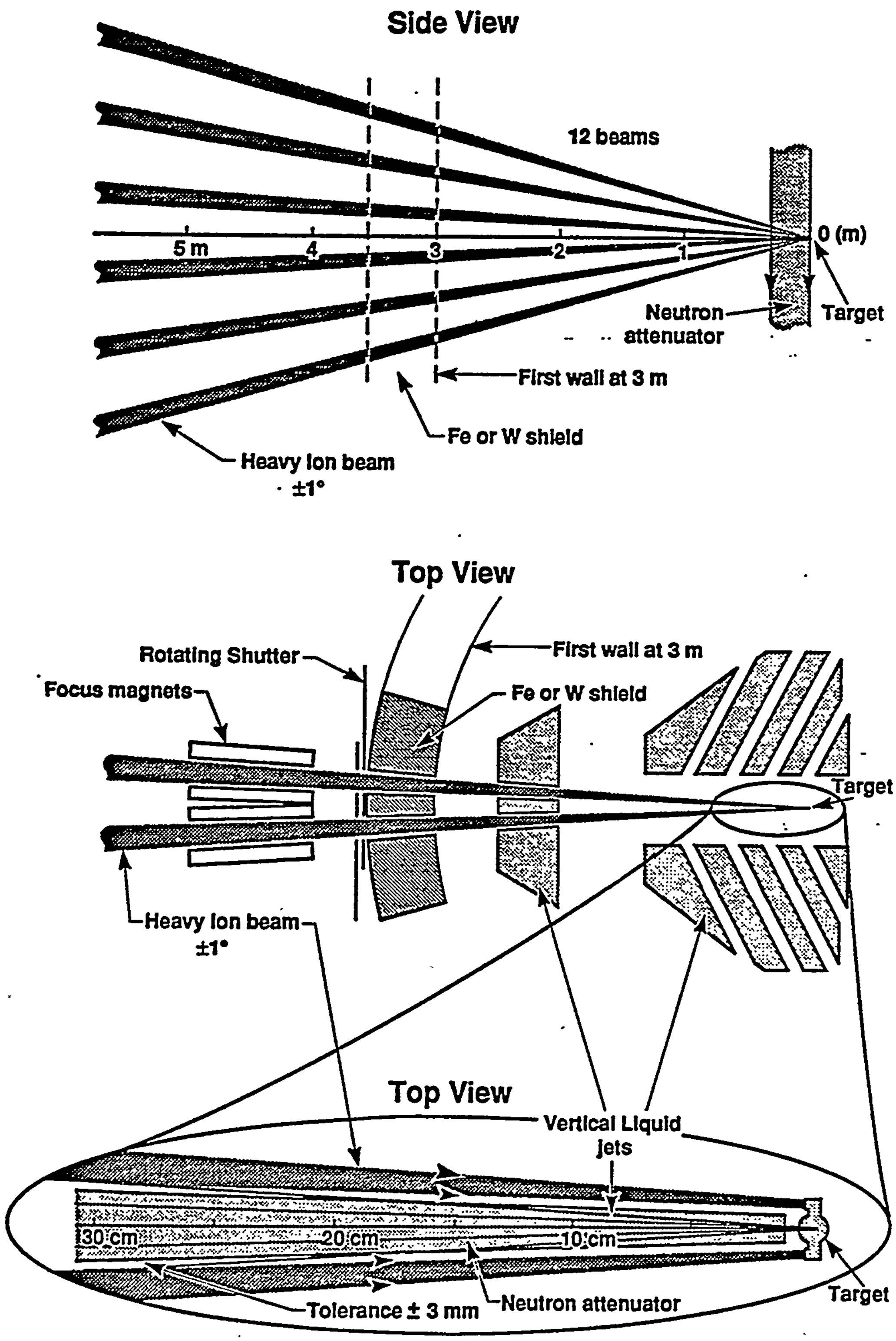

MFE-IFE-rm-0684-6

The six beams overlap when they near the target

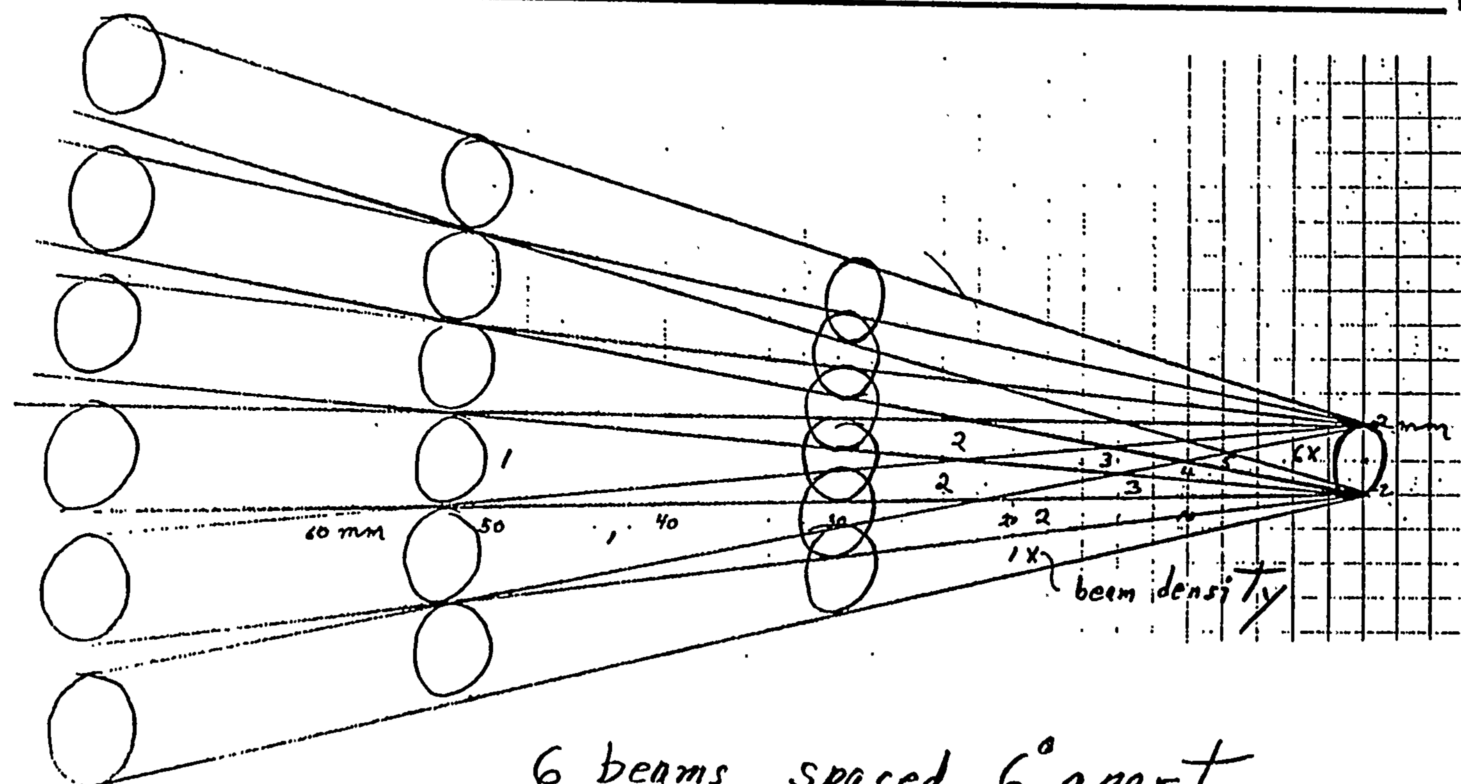

6 beams spaced 6° apart
± 1° spread
$r = 2$ mm spot size
$\theta = \pm 0.017$ rad.
$r\theta = 0.035$ mm rad.

Future work

Experiments on liquid jets to show configuration is possible and clearing will likely work. Applicable to LMF/ETF.

Experiments on condensation to show vapor density can be reduced to the desired value in ~0.2 s. Verify Tsunami and other codes. Applicable to LMF/ETF.

Experiments to show single-side, illuminated targets can be injected accurately enough. Targets illuminated from each end can use spin stabilization and can be symmetric.

23

Recent Work in Atomic Modeling at the University of Wisconsin

J.J. MacFarlane and P. Wang

Fusion Technology Institute
University of Wisconsin–Madison

Presented at:

Workshop on Transport for a Common Ion Driver
Sandia National Laboratories
20–21 September 1994

Overview of ICF Plasma Physics Work at UW

- Over the past 4–5 years, we have developed computational tools to study the radiative and atomic properties of non-LTE plasmas (LTE = local thermodynamic equilibrium).

- These tools have been applied to studies of:

  - spectroscopic analyses of K_α line emission measured in intense light ion beam-target interaction experiments (SNL and KfK);

  - emission spectra obtained from the PBFA-II gas cell region (SNL);

  - anode plasma investigations (KfK and SNL);

  - ICF (post-explosion) target chamber plasmas for high-gain ICF facilities;

  - plasmas created during tokamak disruptions;

  - astrophysical plasmas (stellar winds).

- This work complements previous and ongoing efforts at UW-FTI to simulate the radiation-hydrodynamic properties of ICF-related plasmas.

Goals of This Presentation

- Summarize atomic modeling capabilities at UW.

  $\Longrightarrow$ How can such models effectively be used to better understand ion beam transport.

- Show as example: PBFA-II K_α Spectral Analysis

  $\Longrightarrow$ Utilizes beam-impact ionization cross sections, as well as "usual" collisional-radiative processes.

Schematic Illustration of the Transitions in a 3-Level Atom

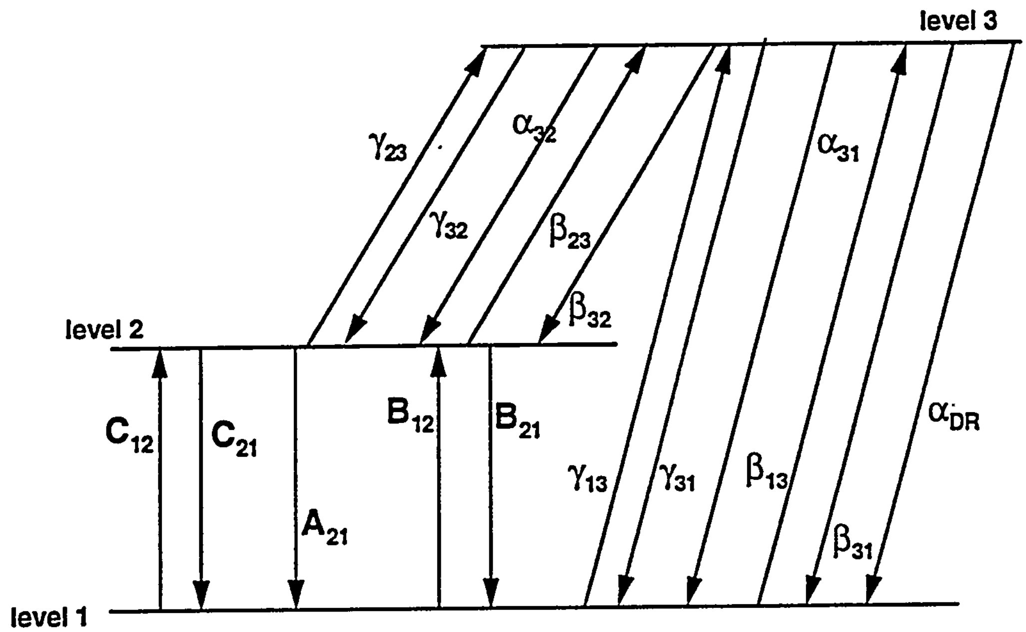

C_{ij} --> collisional excitation (i<j) or deexcitation (i>j)
A_{ij} --> spontaneous emission
B_{ij} --> photoexcitation (i<j) or stimulated emission (i>j)
γ_{ij} --> collisional ionization (i<j) or recombination (i>j)
α_{ij} --> radiative recombination
α_{DR} --> dielectronic recombination
β_{ij} --> photoionization (i<j) or stimulated recombination (i>j)

Also: inner-shell processes
ion beam-impact ionization and excitation
autoionization

Fundamentals

Rate Equations: (L ≡ number of atomic levels)

$$\frac{dn_1}{dt} = n_1 P_{11} + n_2 P_{12} + \dots + n_L P_{1L}$$
$$\frac{dn_2}{dt} = n_1 P_{21} + n_2 P_{22} + \dots + n_L P_{2L}$$
$$\vdots \qquad\qquad \vdots$$
$$\frac{dn_L}{dt} = n_1 P_{L1} + n_2 P_{L2} + \dots + n_L P_{LL}$$

The $\{P_{ij}\}$ consist of collisional and radiative terms:

Radiative rate coefficient:

$$\overline{J}_{ij} = \frac{1}{4\pi} \int_0^\infty d\nu \, \phi_\nu \oint d\Omega \, I_{\mu\nu}$$

Transport equation:

$$\mu \left(\frac{\partial I_{\mu\nu}}{\partial \tau_\nu} \right) = I_\nu - S_\nu$$

Major Features of Atomic Data Base Calculations

- A configuration interaction (CI) model with multi-configuration Hartree-Fock wavefunctions is used to compute E levels, oscillator strengths, and photoionization cross sections.

- Collisional data (e^--impact) are computed using a combination of distorted wave, Coulomb-Born, and semiclassical impact parameter models.

- Ion-impact ionization (inner-shell and outer-shell) and excitation cross sections are computed using a plane-wave Born approximation model with Hartree-Fock wavefunctions; includes corrections for binding energy, Coulomb deflection, and relativistic effects (MPWBA).

- Multiple ionization cross sections are computed using an independent event model with MPWBA cross sections.

- Auger rates and fluorescence yields are computed for each autoionization level.

Major Features of Collisional-Radiative Equilibrium Code

- Atomic level populations are determined by solving multilevel atomic rate equations self-consistently with the radiation field and ion beam properties.

- Any state in the atomic model can be coupled to any other state; thus, transitions between excited states of differing ions can be considered, as can transitions between non-adjacent ions.

- Ion beam-induced multiple ionization effects are included as direct transitions in the statistical equilibrium matrix equations.

- Emission and absorption spectra include contributions from bound-bound (lines), bound-free (recombinations), and free-free transitions (Bremsstrahlung).

- Line shapes include effects of natural, Doppler, Auger, and Stark broadening.

- Radiation transport is modeled using either:

  (i) an angle- and frequency-averaged escape probability method, or

  (ii) a multiangle, multifrequency model based on the second-order form of the transfer equation.

- For Al calculations, we consider a total of 1250 atomic levels distributed over all 14 ionization stages. Roughly 60% are autoionizing levels.

Detailed Atomic Models Are Used to Analyze the Complex Structure in Measured Spectra

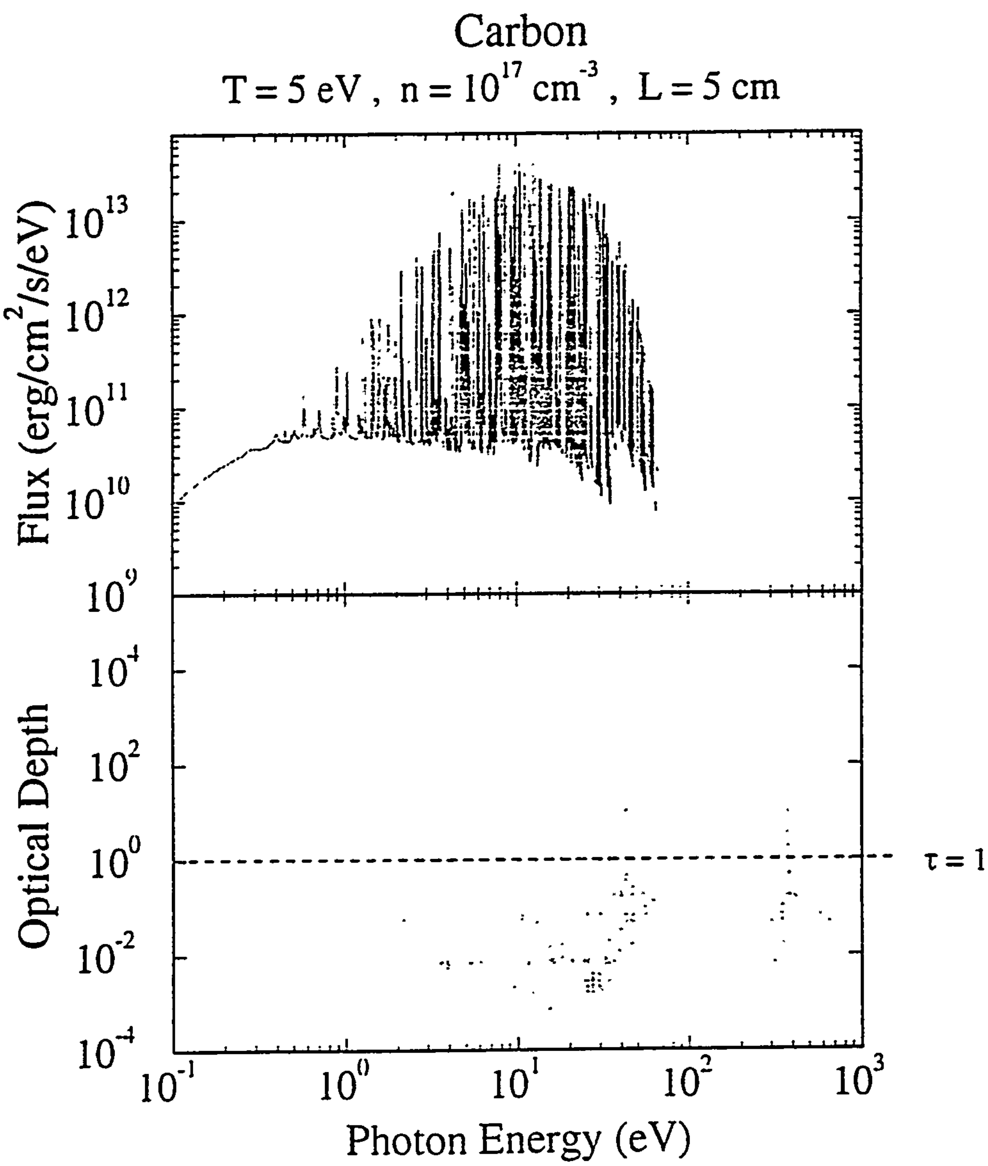

- Spectra are dominated by line emission.
- Even at moderate densities ($n \approx 10^{17}$ cm^{-3}), plasmas with cm-size dimensions are optically thick to the strongest lines.

Schematic of Light Ion Beam Experiment

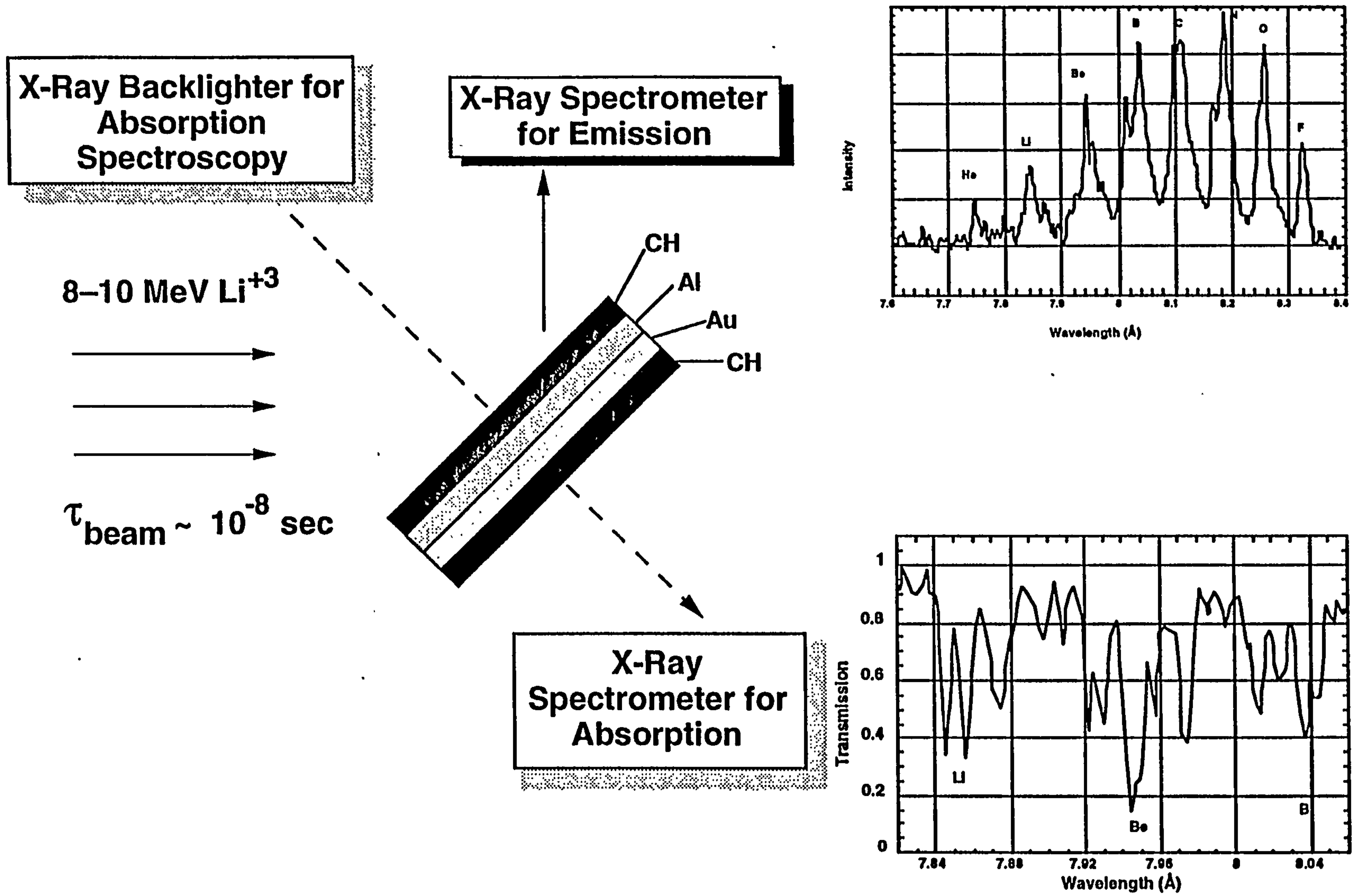

Production of K_α and K_β Fluorescence Lines

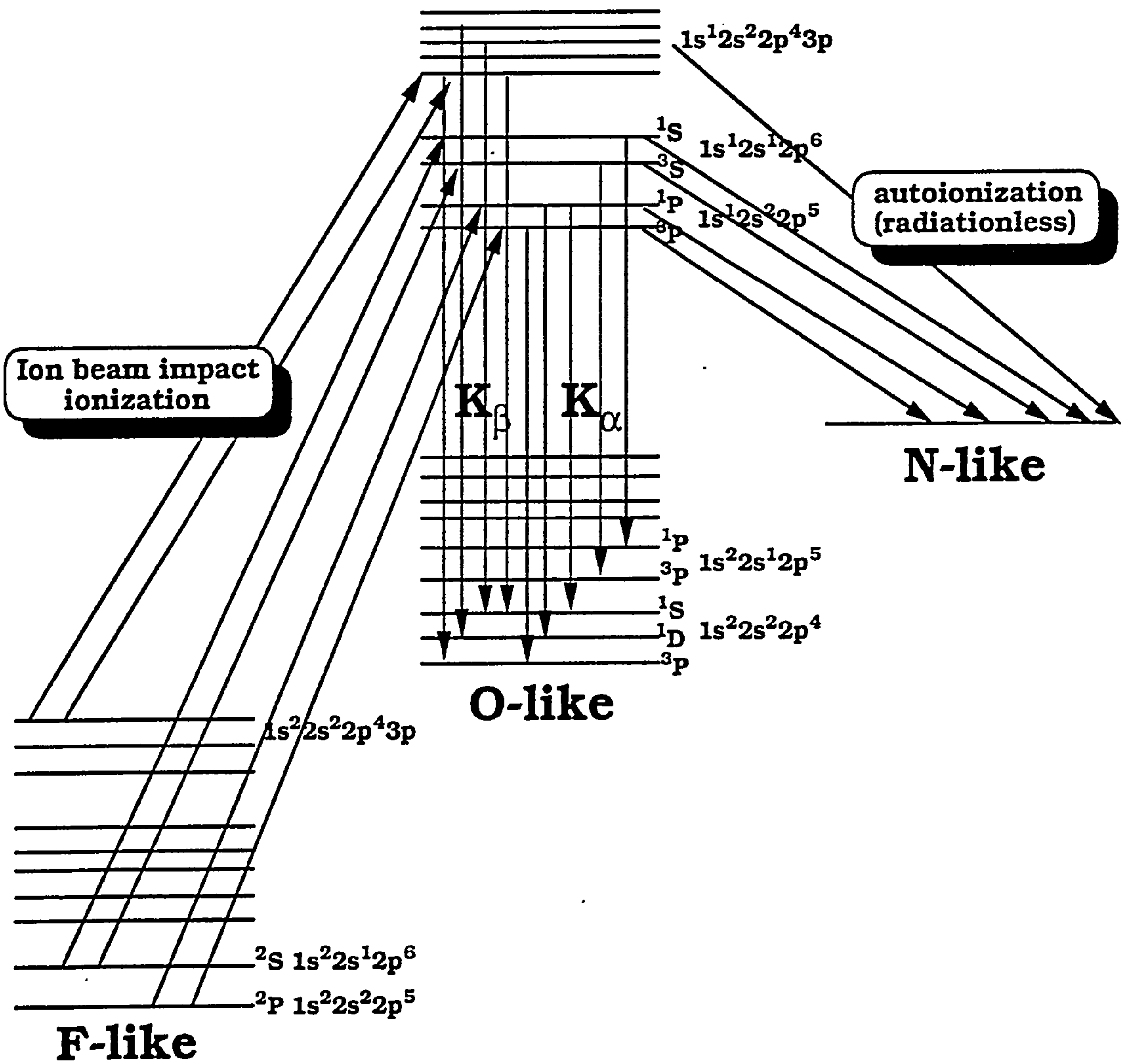

K_α and K_β satellites provide constraints on plasma T,ρ.

Comparison of Calculated Ion Beam-Impact Ionization Cross Sections with Experiment

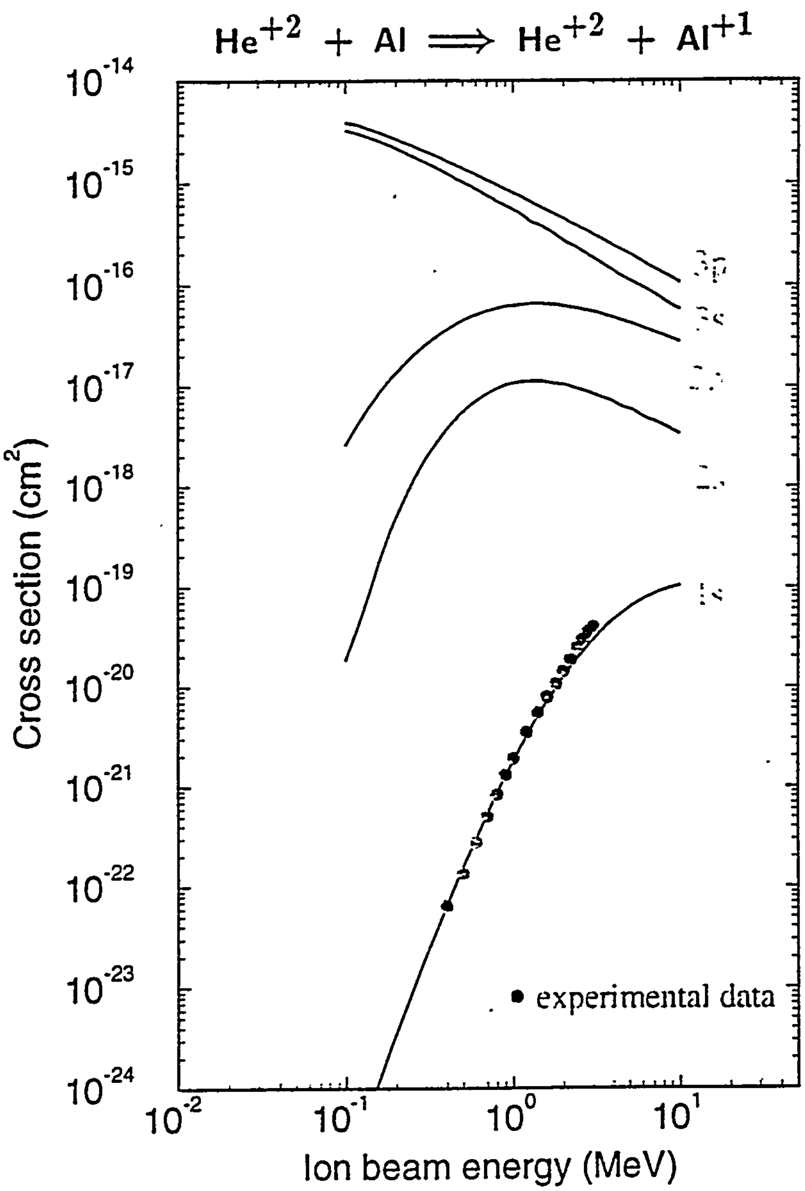

- Outer-shell cross sections are much larger
  ⟹ affect ionization, heating

- Inner-shell cross sections are important for spectral diagnostics analyses.

Multiple Ionization Processes in Lithium Beam Experiments

- In ion-atom collisions K-shell ionization is often accompanied by multiple L-shell ionization.

- It is important to consider this process when determining the plasma temperature and ionization state from K_α emission spectra.

$$\text{F-like:}\begin{cases} 1s^2 2s^2 2p^5 \xrightarrow{1e^-} 1s^1 2s^2 2p^5 \xrightarrow{K_\alpha} 1s^2 2s^2 2p^4 \\ 1s^2 2s^2 2p^5 \xrightarrow{2e^-} 1s^1 2s^2 2p^4 \longrightarrow 1s^2 2s^2 2p^3 \\ 1s^2 2s^2 2p^5 \xrightarrow{4e^-} 1s^1 2s^1 2p^3 \longrightarrow 1s^2 2s^1 2p^2 \end{cases}$$

O-like: $1s^2 2s^2 2p^4$

N-like: $1s^2 2s^2 2p^3$

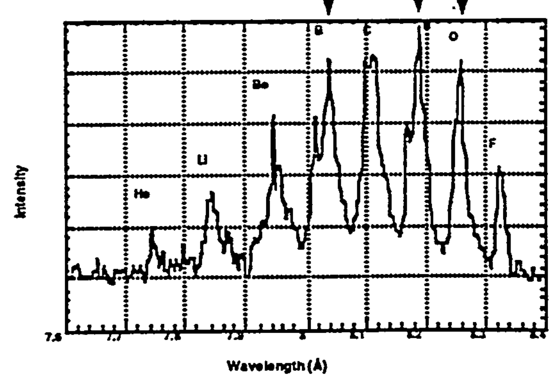

- We have developed a model for computing single ionization, multiple ionization, and electron capture cross sections for ion-atom collisions.

Calculated Emission Spectrum for 2000 Å-Thick Al Target Heated by 9 MeV Li Beam

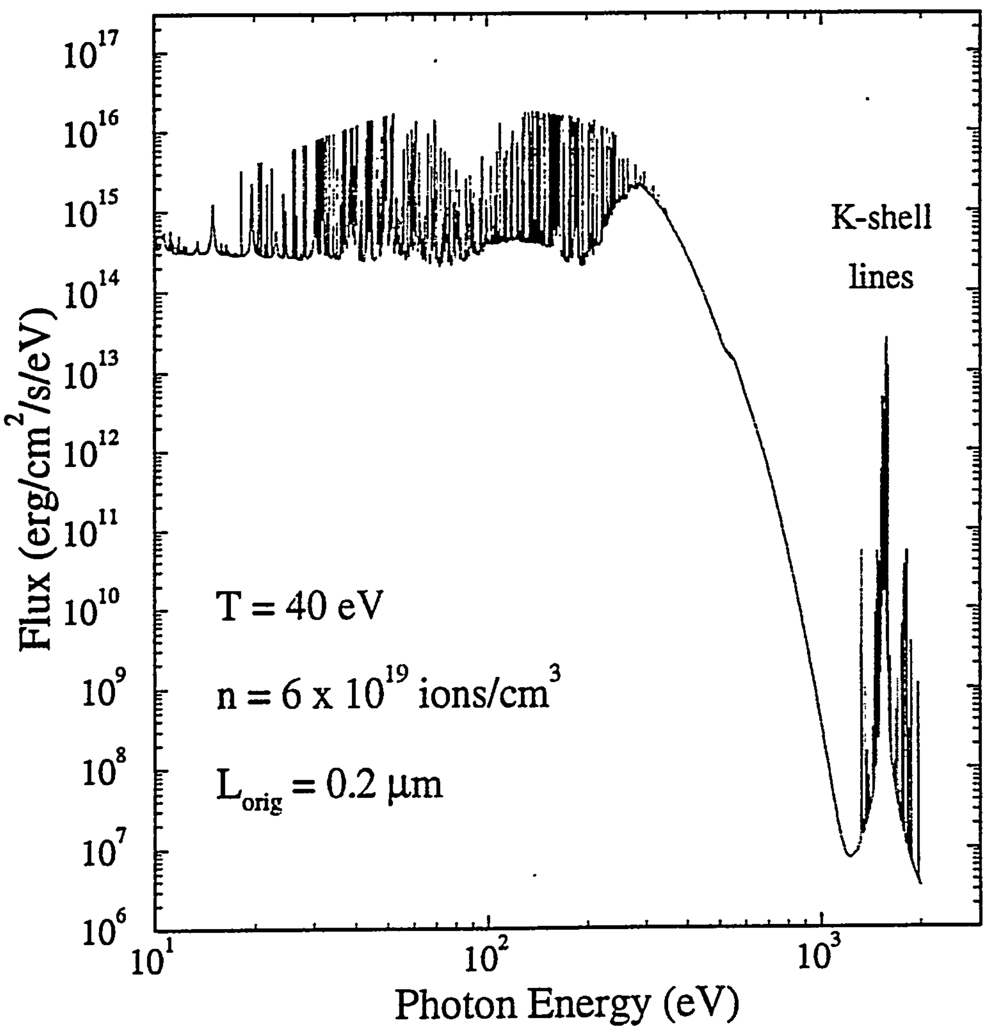

- K_α satellites are emitted at 1.5 keV (opacity effects from tampers are reduced).
- "Thermal" portion of spectrum is line-dominated.

Comparison of Theory and Al K_α Absorption Spectrum

LLNL Laser-Produced Plasma (Perry et al. 1991)

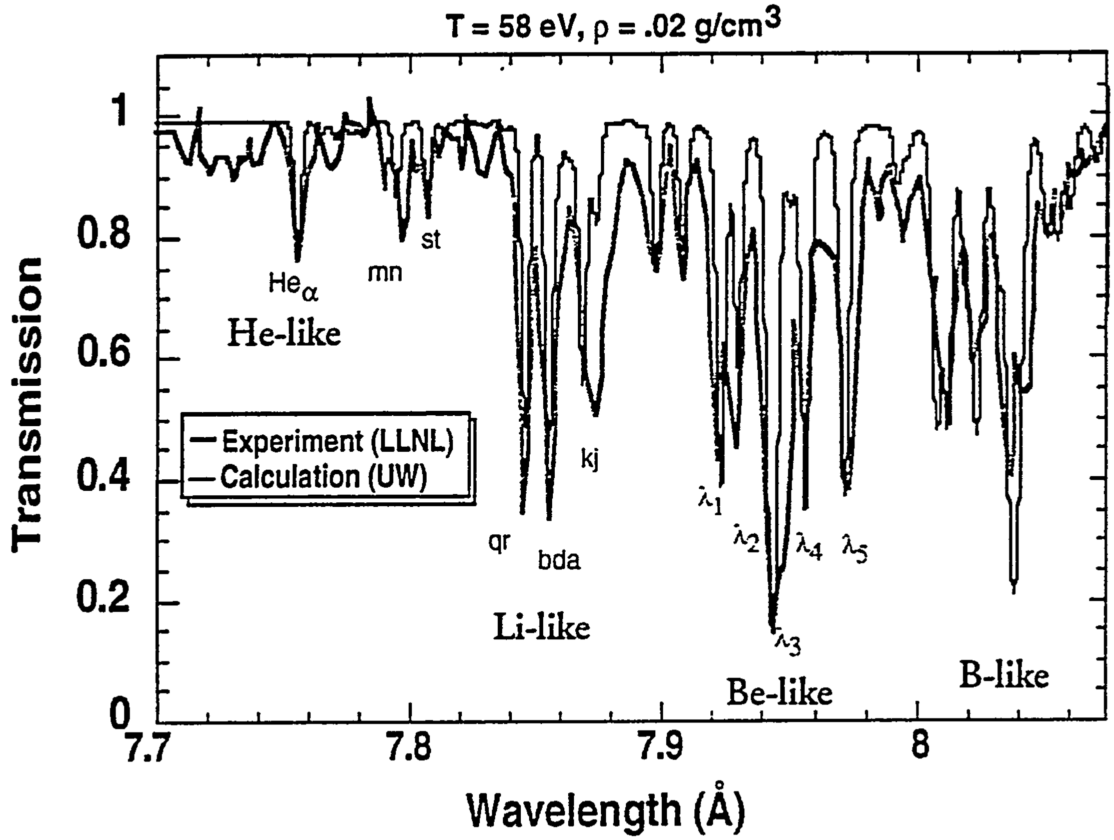

- Good agreement is obtained with "high-resolution" absorption spectrum.

- This allows us to confidently ID lines in PBFA-II emission spectra.

Al K_α Satellite Spectrum Observed in PBFA-II Li Beam Experiments

Shot 5881 (Time-Integrated)

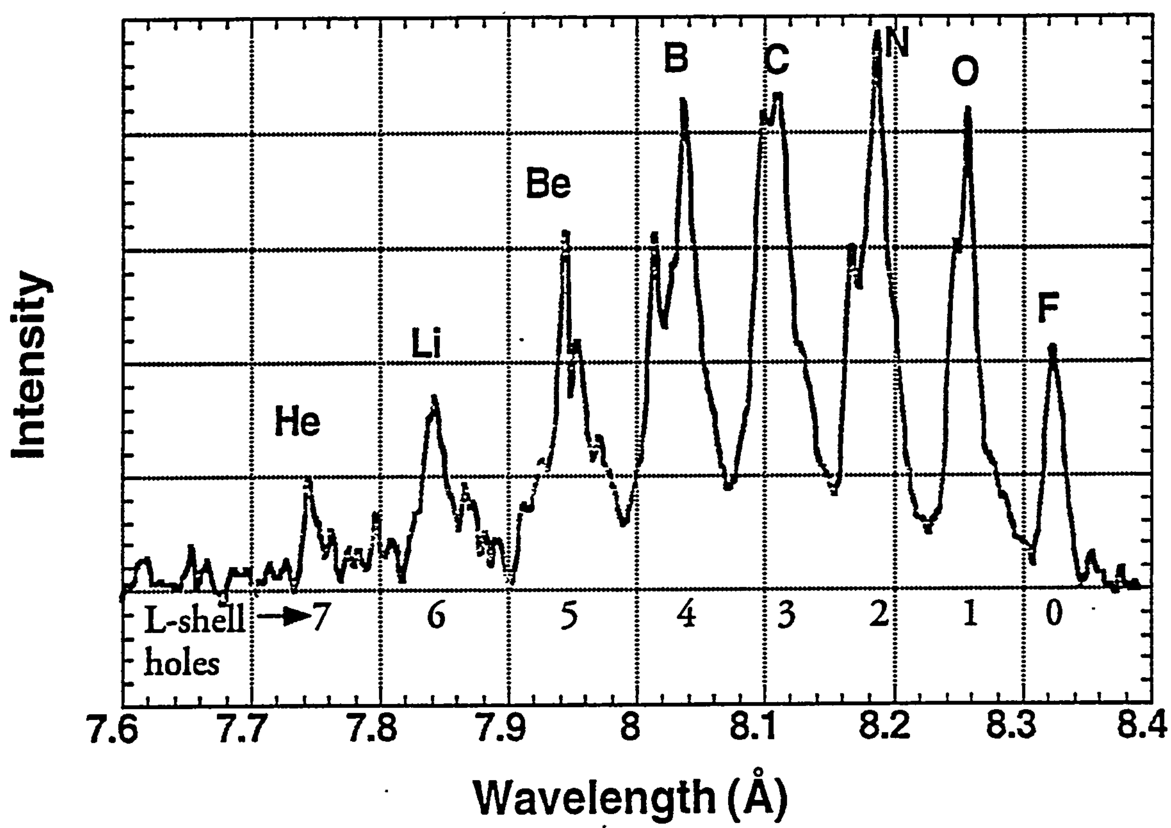

- Satellites are observed from F-like (cold) Al through He-like Al.

- Considerable structure is seen within each of the major satellite features.

Temperature Dependence of Al K_α Satellite Spectrum

$n = 10^{20}$ ions/cm^3; $L_o = 2000$ Å

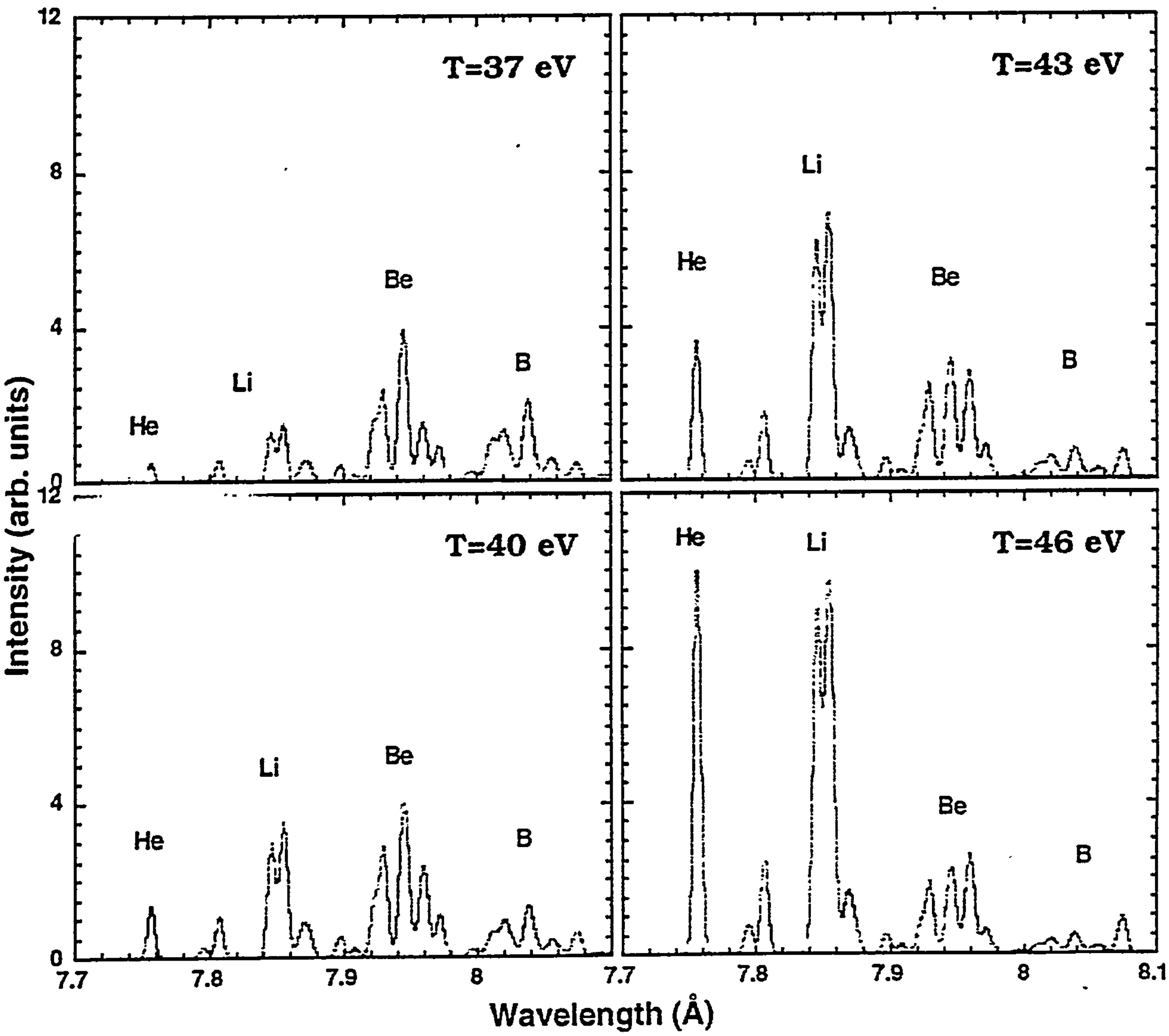

- K_α satellite spectrum shows good temperature sensitivity.

- Intensity ratios of Li-like satellites to He_α can be used to determine plasma conditions.

Dielectronic Recombination Cross Sections Are Computed to Assess Influence on PBFA-II K_α Spectra

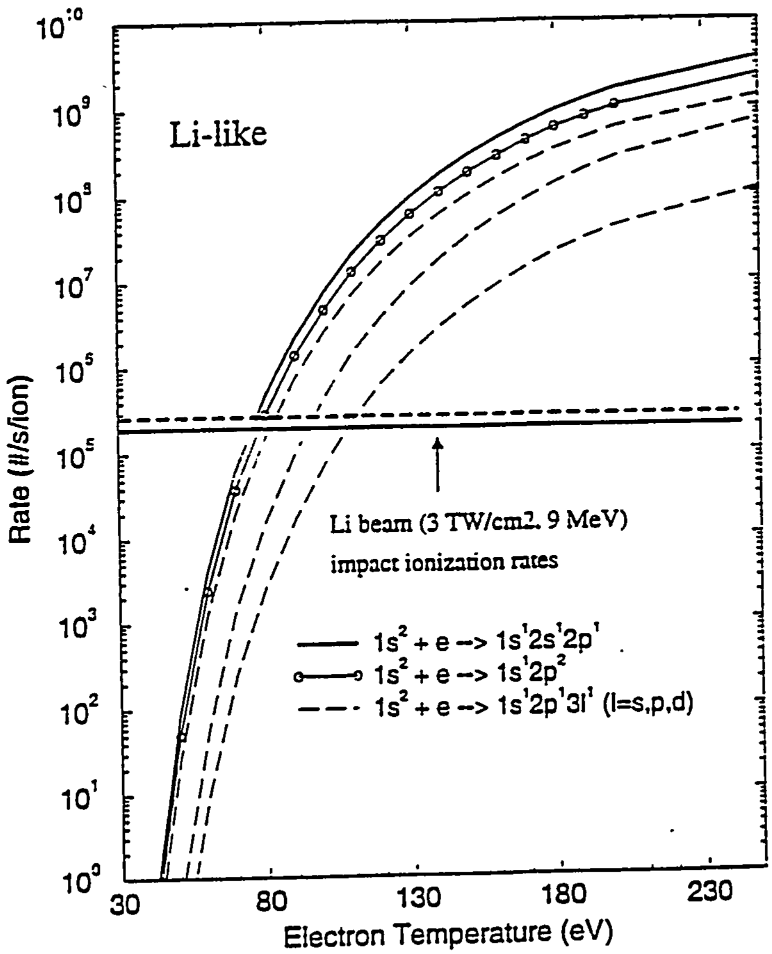

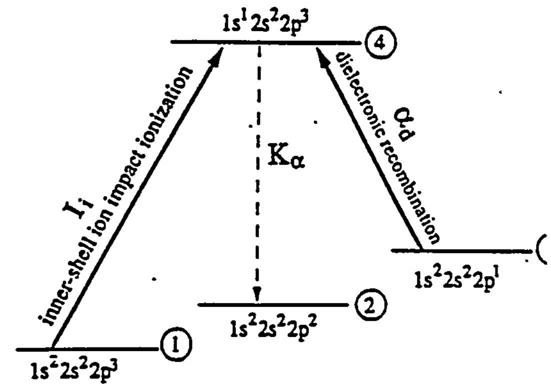

- DR exceeds beam-impact ionization as dominant populating mechanism for autoionization states at $T \gtrsim$ 60–80 eV.

A Comparison of EOSOPA and STA for High-*Z* Plasma
(Au: T = 20 eV, ρ = 0.1 g/cm^3)

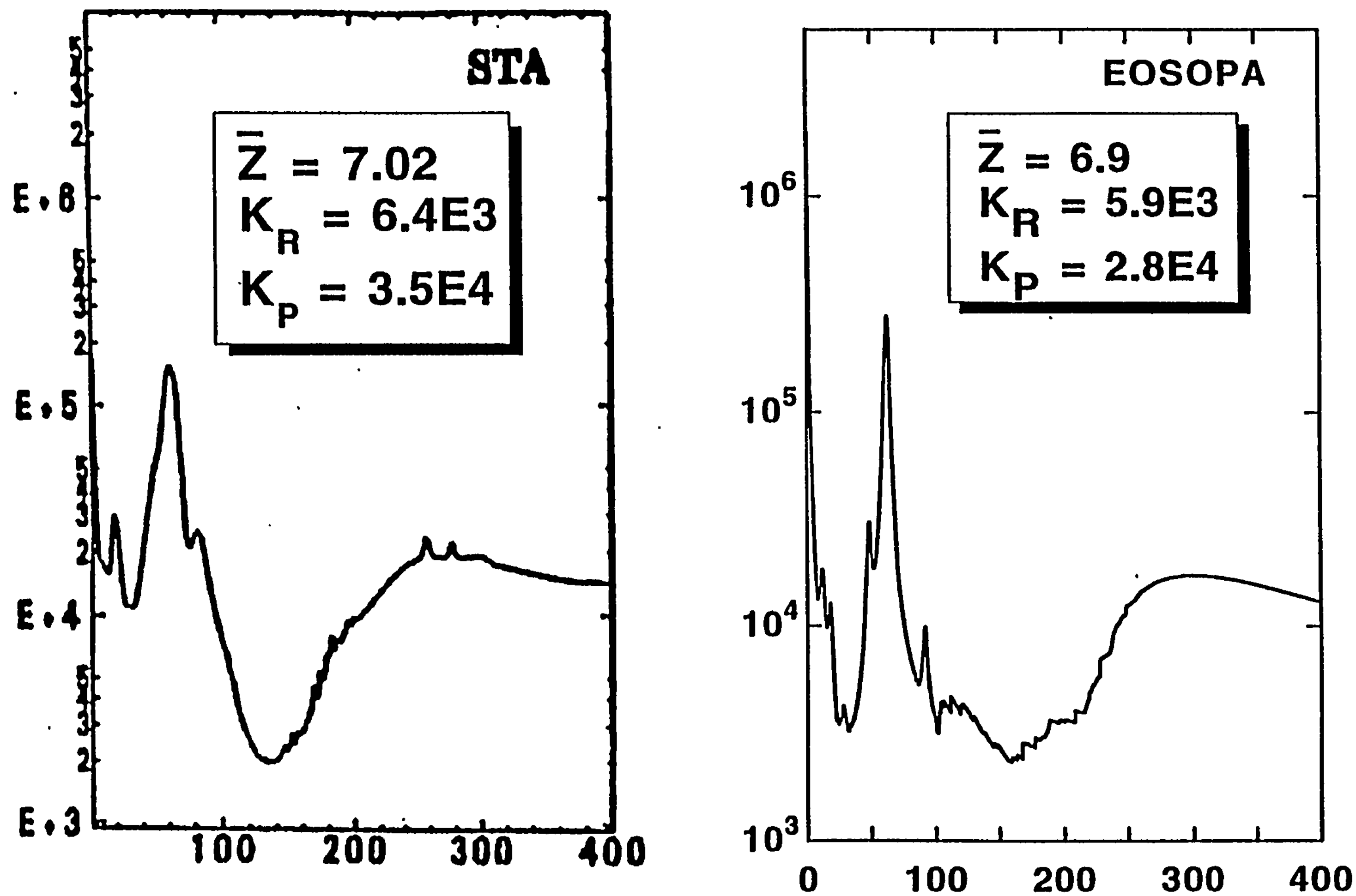

Ongoing and Future ICF Work at UW

- Time-dependent collisional-radiative modeling of SNL gas cell and anode plasmas ($n_e \sim 10^{17}$ cm^{-3}, $\tau \sim 10^{-9}$ s).

- Spectral analysis of PBFA-II and KALIF beam-plasma interaction experiments.

- Continued expansion of atomic data bases, including high-Z opacities and high-ρ EOS.

- Rad-hydro: 1-D with C-R modeling
  2-D with MHD

- Parallel and distributed computing.

The IPROP and IVORY Gas Breakdown Codes

D. R. Welch
Mission Research Corporation
1720 Randolph Rd, Albuquerque NM 87106

September 21, 1994

Presented at the Workshop on Transport for a Common Ion Driver

24

IPROP has been used for a variety of problems

- IPROP was originally developed to study atmospheric propagation of intense relativistic electron beams
- Recently, the IPROP modeling has been extended to near vacuum problems.
- IPROP has been benchmarked against ion and electron beam experiments (GAMBLE II and HERMES III) at pressures from 200 mtorr to an atmosphere.

IPROP in good agreement with HERMES III experiment

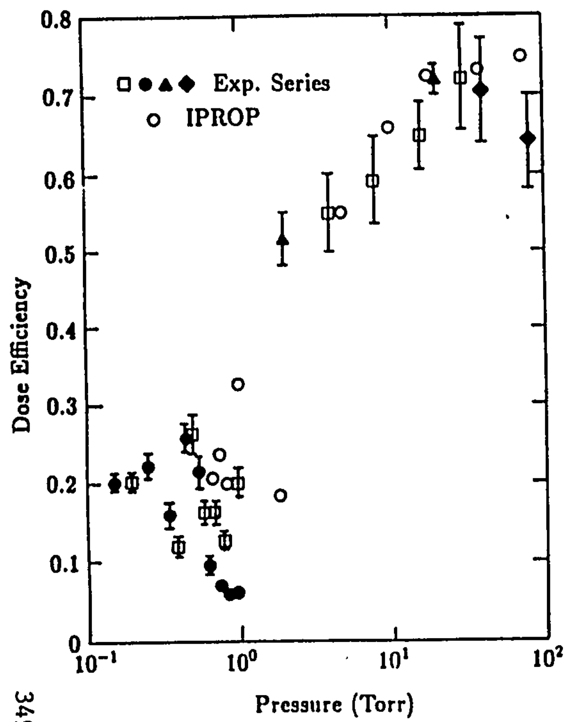

FIG. 4. The efficiency of radiation transport (dose efficiency) to 435 cm of the HERMES III beam plotted from experimental data and IPROP simulations.

- Net currents and radiation calculations at the outer, far walls compare well in detail

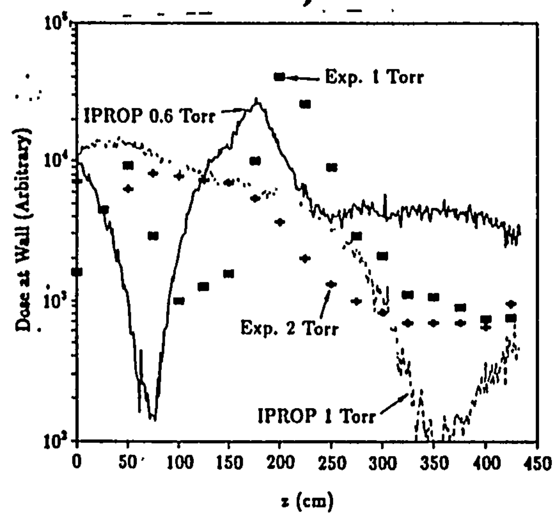

FIG. 7. The measured and calculated radiation dose at the outer wall as a function of z is plotted for 1 and 2 Torr in the experiment and 0.6 and 1 Torr in the IPROP simulations.

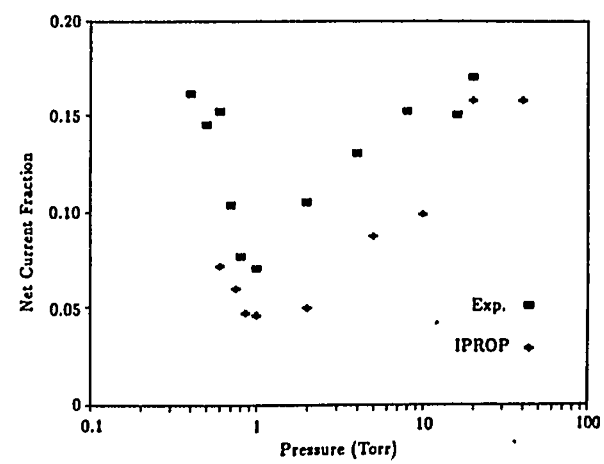

FIG. 6. The net-current fraction (net current/beam current) at peak beam power as a function of pressure is plotted for the HERMES III experiment (z=230 cm) and IPROP simulations (z=150 cm).

IPROP is quasi-3d with electromagnetic fields

- Arbitrary orthogonal coordinates with the third dimension Fourier analyzed into an arbitrary number of modes
- EM flds solved implicitly, large time steps possible
- EM flds can be solved in a moving frame 0-c
- Lab frame EM solver includes internal conductors, particle emission, charge-conserving particle push and wave launcher.

IPROP has macro-particle and thermal-fluid components for electrons

- Typically, electrons with energies < 100 eV constitute a tensor conductivity. Electrons at higher energies are followed as particles.

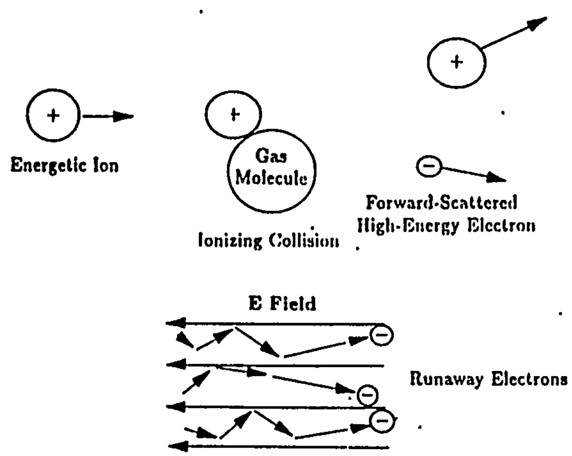

- Particles are created due to runaway or in energetic collisions.

- Fluid electrons produced due to ionization, from particles decellerating <100 eV and avalanche.

Fluid treated with simple PIC MHD

- EOM includes pressure and JxB terms calculated on double grid to minimize numerical self forces
- energy equation includes Ohmic, high-energy collision and PdV terms
- EM flds and plasma currents interpolated from mesh to fluid particles. Electron densities and collision frequencies interpolated from particles to mesh.

IPROP has simple atomic physics models

- Ionization rates, derived from the Bethe equation, are only valid for the first ionization
- Elastic scattering of particles assumes Rutherford cross section, Moliere multiple scattering used at higher pressures
- Noble gas recombination rates need work

IVORY is pure PIC with gas collision physics

- Used to study low-pressure e-beam transport for HERMES III and gas breakdown in the PBFA II ion diode
- Handles basic nitrogen and hydrogen chemistries: ionization, stripping, charge exchange and elastic scattering included
- Quasi-3d, fast EM solve with time-biasing, graphical interface

WARP Code Capabilities and Needed Development*

Alex Friedman, Debra A. Callahan, David P. Grote, A. Bruce Langdon, and Steven M. Lund, *LLNL*

Irving Haber, *NRL*

Presented at:

Workshop on Transport for a Common Ion Driver
Sandia National Laboratories, September 20-21, 1994

*Work performed under the auspices of the U.S. D.O.E. by Lawrence Livermore National Laboratory under contract W-7405-ENG-48, and by the Naval Research Laboratory under contracts DE-AI05-92ER54177 and DE-AI05-83ER40112.

We are using particle simulations to understand HIF beam transport.

- The quality of these "space-charge-dominated" beams—which are non-neutral plasmas—is crucial, since they must be focused onto small (few mm) fusion target spots.
- If all forces were linear functions of the transverse coordinates, the beam's emittance would be preserved.
- However, nonlinear beam self-fields (and applied fields) can lead to emittance growth, especially when the beam undergoes many manipulations: nonuniform acceleration, bends, transport through misalignments, ...
- A self-consistent-field description is necessary.
- Because of the beam's low plasma frequency and short residence time, particle-in-cell techniques are particularly well suited to HIF applications.
- Codes must be fast, to follow beam over hundreds of accelerator lattice periods.
- Codes must be flexible, with user-selectable levels of detail.

WARP combines features of PIC & accelerator codes

- Main elements are:
  - 3d ("warped Cartesian") PIC & fieldsolver: WARP3d
  - Axisymmetric PIC with module-impedance model: WARPrz
  - Envelope equation solver (for loading "matched" beams)
- Uses Basis development system / interactive interpreter for full control over computations, diagnostics
- *Time* (not "*s*") is independent coordinate for particle motion
- The self-field is assumed electrostatic, and is solved for by FFT or SOR in 3d, FFT/tridiagonal in *r,z*.

  The field mesh is a window which moves with the beam.
- WARP3d accelerator lattice models a fully general set of finite-length focusing, bending, and accelerating elements:
  - Idealized sharp-edged elements
  - Electrostatic elements from "first principles" by specifying potentials on internal conductors
  - E and B fields as sums of multipole components at each axial grid point

Some interesting aspects of WARP3d

Techniques

- Subgrid-scale placement of conductor surfaces in Poisson solution, via modified finite difference stencil; eliminates "Lego-land" restriction. (To date only for convex rods).
- Quasi-time dependent simulation for efficient determination of equilibrium solutions: $\Delta t_{\text{fields}} > \Delta t_{\text{particles}}$
- No grids for E; obtain for each particle from ϕ in neighborhood.
- "Warped" coordinate system to model bent beam lines
- "Residence corrections" in finite-length, hard-edged external fields to ensure that particles receive the correct impulse
- One-plane and two-plane symmetries

Capabilities

- Beam injection at constant current
- Time-dependent accelerating-gap and dipole fields

Why subgrid-scale placement of conductor boundaries

Conductor non-aligned with the computational mesh.

Conductor has curved boundary.

The finite difference form of Poisson's equation for the points near the surface is changed to explicitly include the surface.

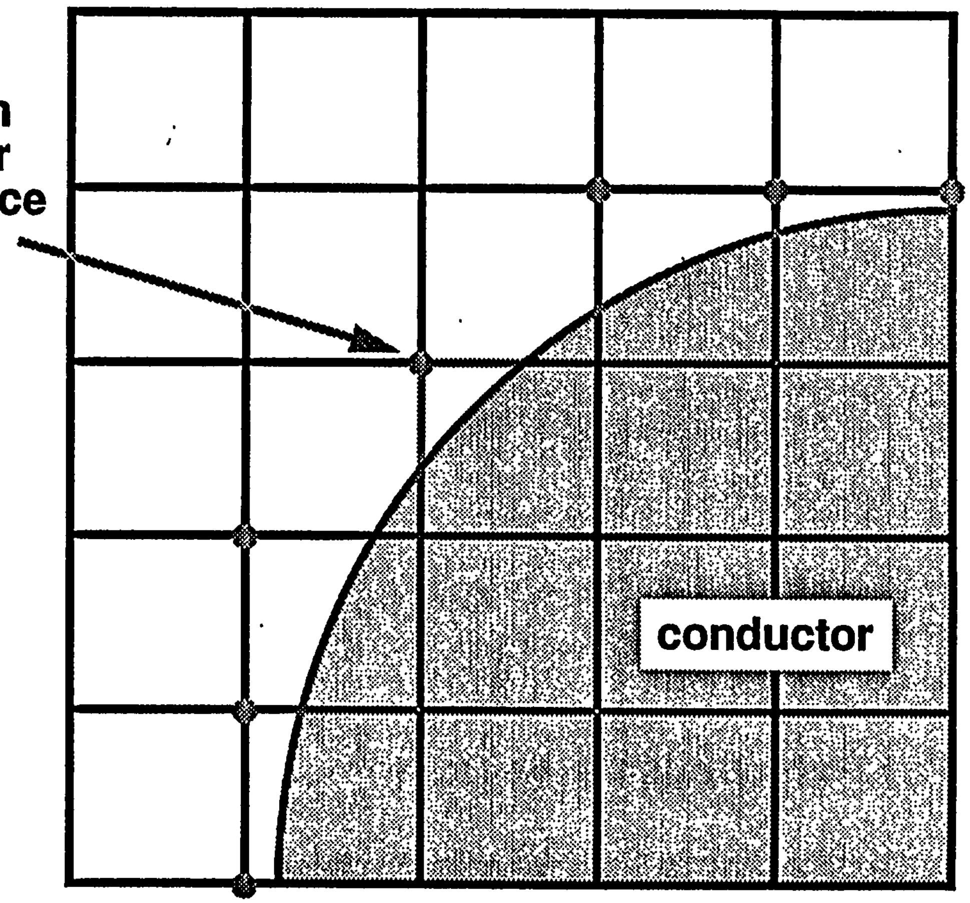

9/16/94 DPG

Subgrid-scale placement of conductor boundaries*

Needed to accurately include focusing (and other) conductors self-consistently while using a minimal number of grid cells.

In one dimension:

- Given ϕ on conductor and at the grid point a distance δ outside the conductor, ϕ just inside the conductor is given by extrapolation.

$$\phi_{inside} = \frac{\phi_{boundary} - (1-\delta)\,\phi_{outside}}{\delta}$$

- That expression is used in the finite difference form of Poisson's equation for ϕ outside the conductor.

$$\frac{(\phi_{boundary} - (1-\delta)\,\phi_{outside})/\delta - 2\phi_{outside} + \phi_{bulk}}{\Delta^2} = -\frac{\rho_{outside}}{\varepsilon_0}$$

- This is rearranged to be explicit and is used in place of the usual expression in the field solver at the conductor boundary.

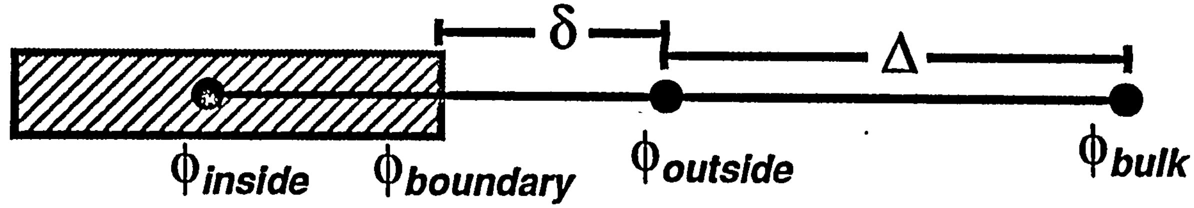

*The technique is based on a technique EGUN uses.

9/16/94 DPG

Mesh motion in WARP3d

- Mesh is like a window that moves to overlay beam.
- When internal accelerator structures are to be modeled from "first principles," it is usually best that the mesh remain in a fixed relationship to them. In this case the mesh cannot move smoothly to track the beam.

  Instead, the mesh moves in "fits and starts," waiting until the beam has moved far enough, and then moving by Δz. This is like a "treadmill." Zones are removed from well behind the beam's tail, and inserted well ahead of its head.
- When particles are being injected (initially or upon restart), the mesh remains fixed until all are in, then begins moving.

  Future enhancement may allow "short" mesh which "grows" while beam is being injected.
- Thus, in many cases the beam drifts through the mesh.

  Must avoid finite-grid (aliasing) instability—axial beam temperature, and spatial filtering in z, are of help here.

Some applications of WARP

- Propagation and axial compression of beam in presence of non-linear fields: 3-D simulations of drift-compression experiments on LBL's MBE-4 facility
- R,Z simulation studies of "longitudinal instability" (a resistive wall mode driven by module impedance)
- Long-time behavior of beams, approach to equilibrium
- Temperature equilibration between transverse and longitudinal degrees of freedom
- (ILSE and Small Recirculator applications, described separately)

WARP3d models effects of nonlinear self- and applied fields in ILSE

- ESQ injector was simulated from "first principles."
- Straight matching section for 1-beam "Elise" injector designed
- "Bent" matching section for 4-beam injector begun
- Misalignments in ILSE-scale drift compression studied
- Understanding of emittance evolution in planned ILSE achromatic bend (earlier version) obtained
- Combiner modeling just beginning

The electrostatic quadrupole units simultaneously focus and accelerate the ion beam to 2 MV

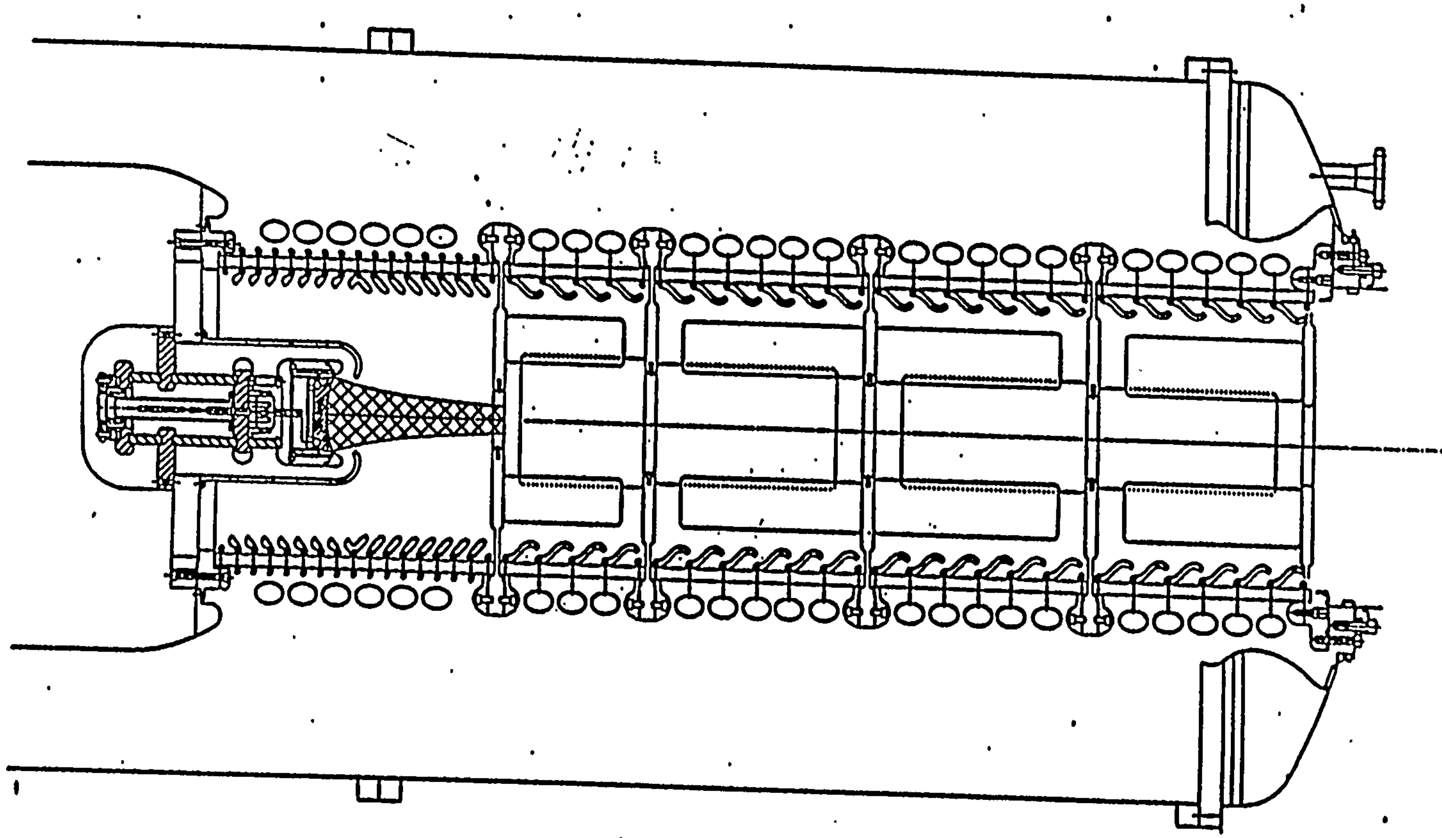

5SSY93

WARP was a principal design tool for Electrostatic Quadrupole injector design

- Aberrations arise because:
  - $V_{foc} \lesssim E_{beam}$, motion not paraxial.
  - Applied fields not perfectly quadrupolar.
- Major aberrations: terms in $\varphi \propto r^4$. Can be reduced by:
  - moving rods in / out
  - other changes to ESQ geometry
  - higher V_{diode}.
- Good agreement with scaled experiment. Also with actual ESQ injector, within uncertainty of initial conditions.

Injector geometry

Cross Section

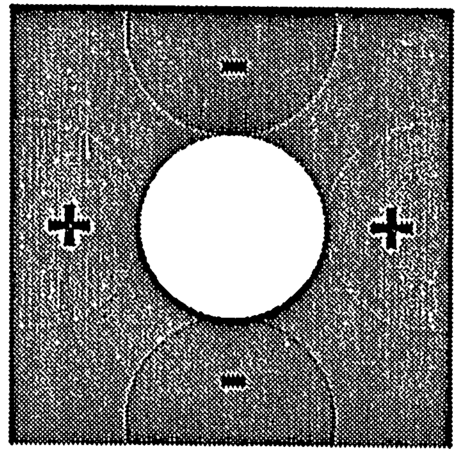

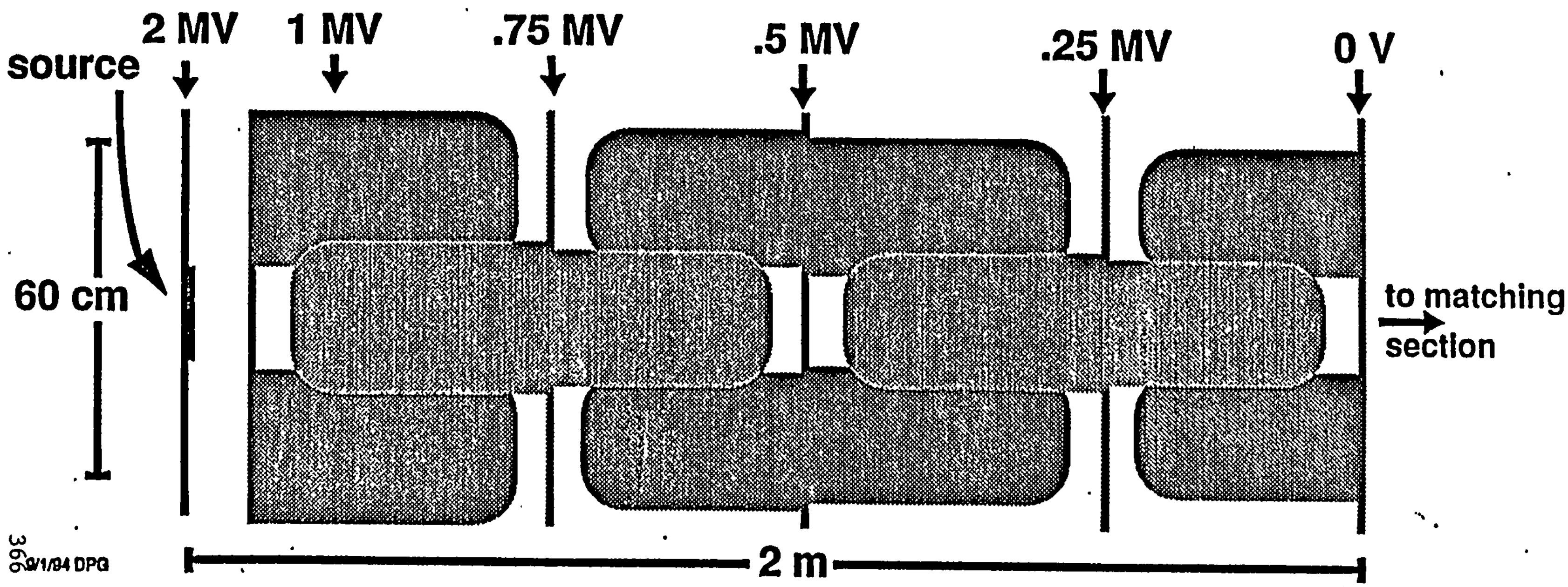

9/1/84 DPG

WARP3d features used in ESQ simulation

- beam formulation by constant current injection
- four-fold transverse symmetry - model one quadrant
- subgrid-scale placement of electrode surfaces
- limited time dependence, Δt fields ~ 100 Δt particles

Typical: mesh 50x50x200-600, 70K-300K particles

Runtime: ~3-30 minutes on Cray C90, single processor

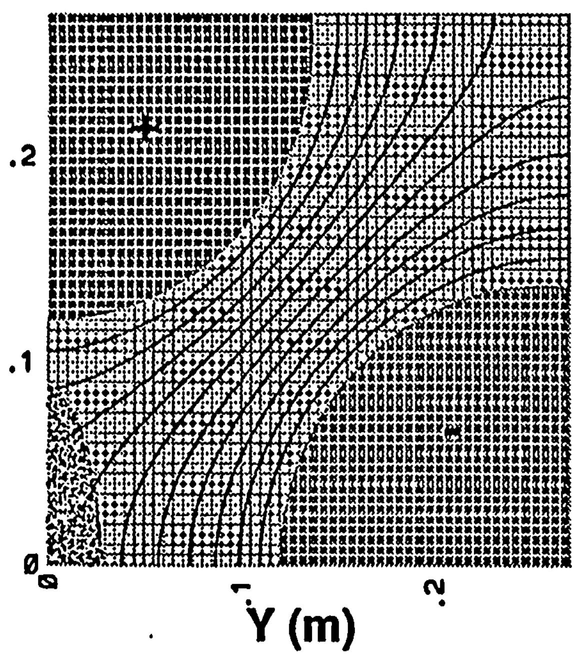

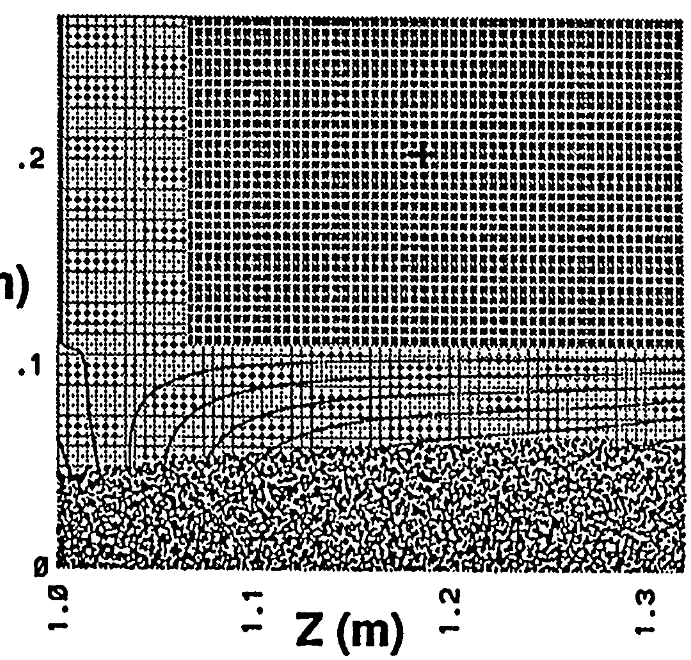

9/1/94 DPG

Initial Results

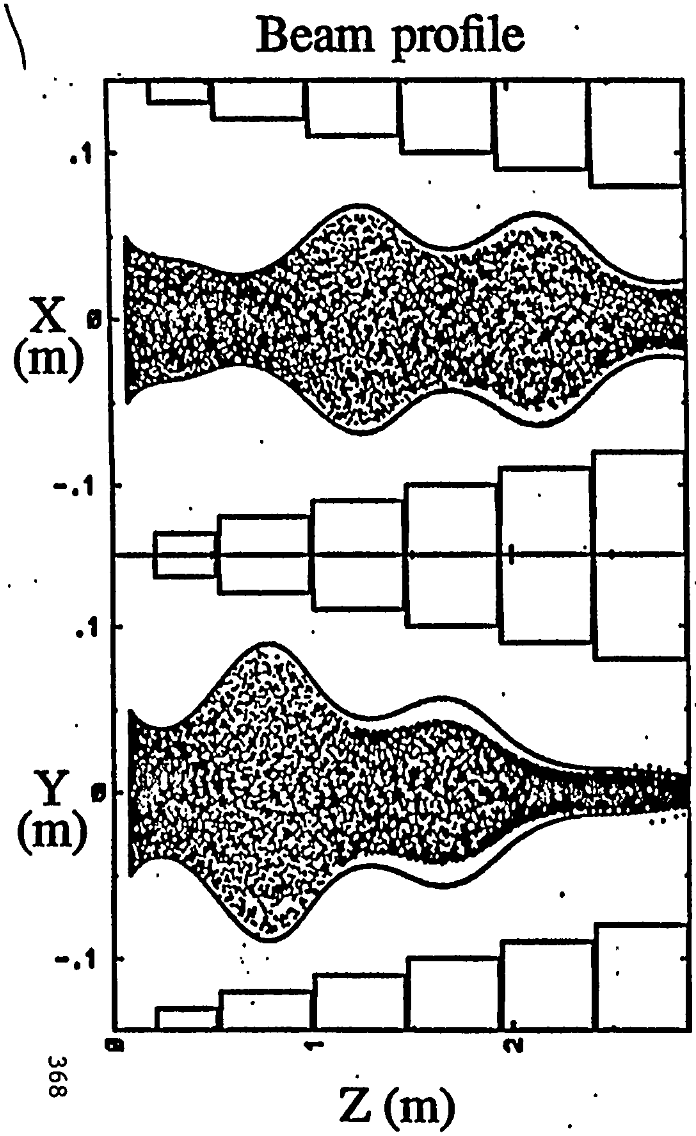

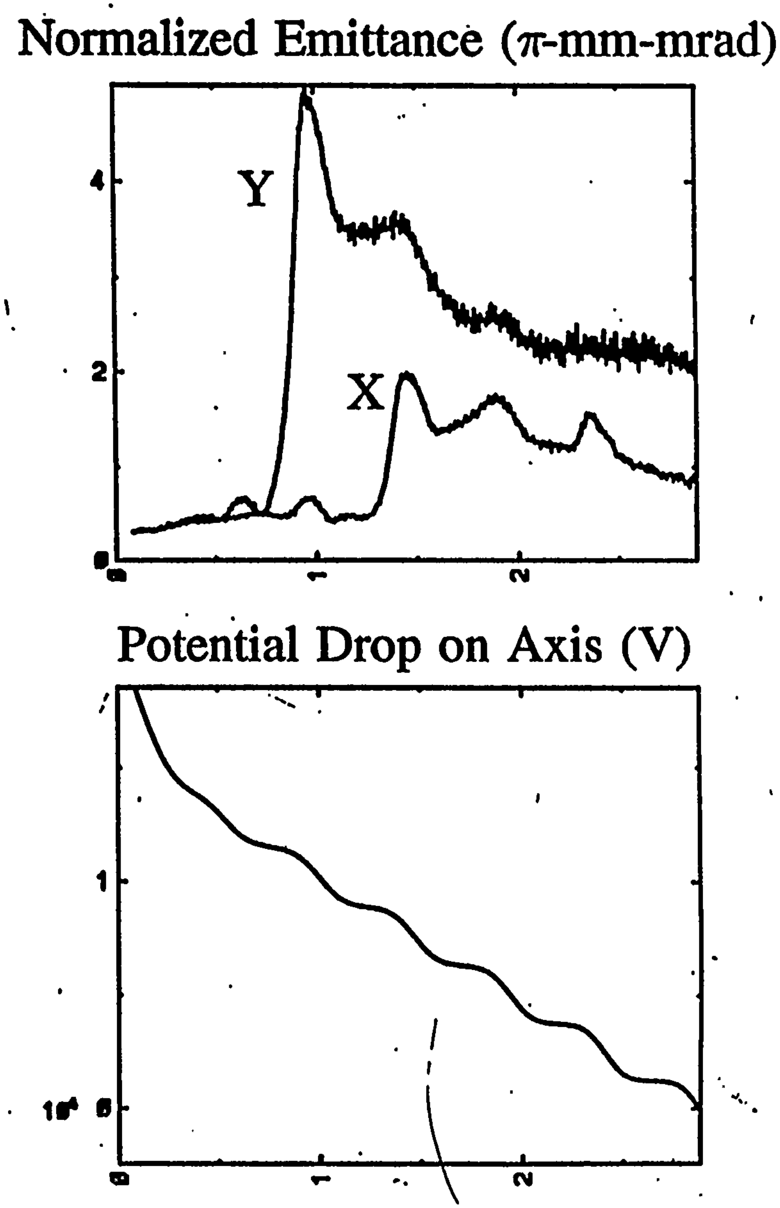

Scaled Injector With Corrections

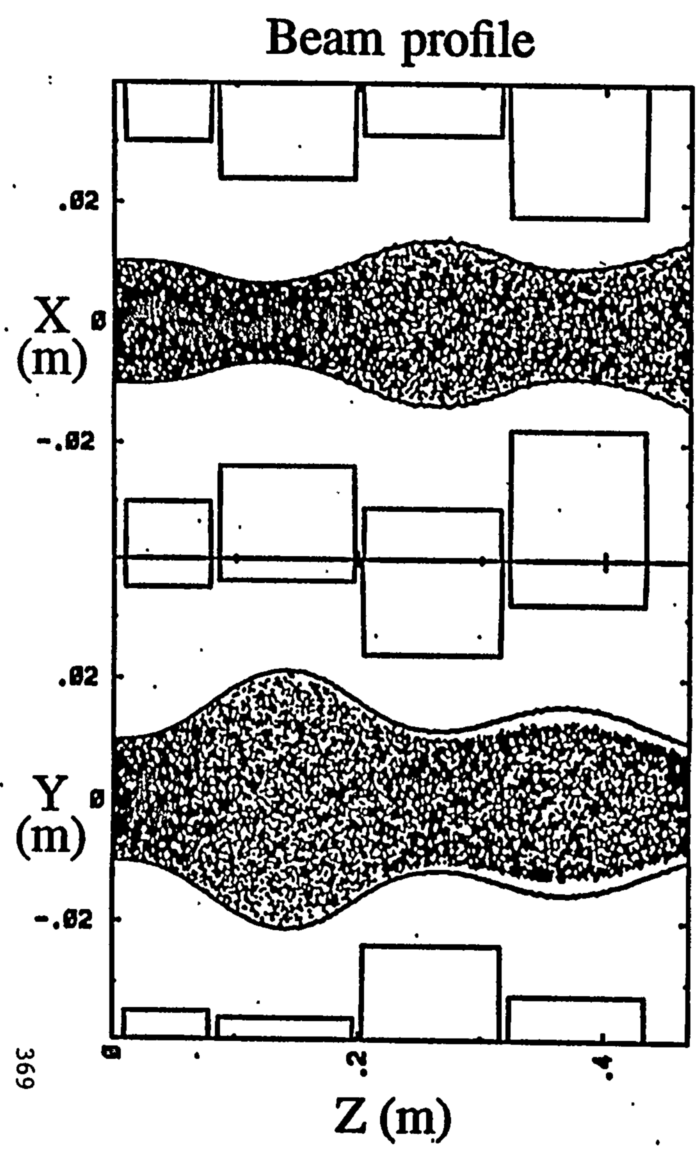

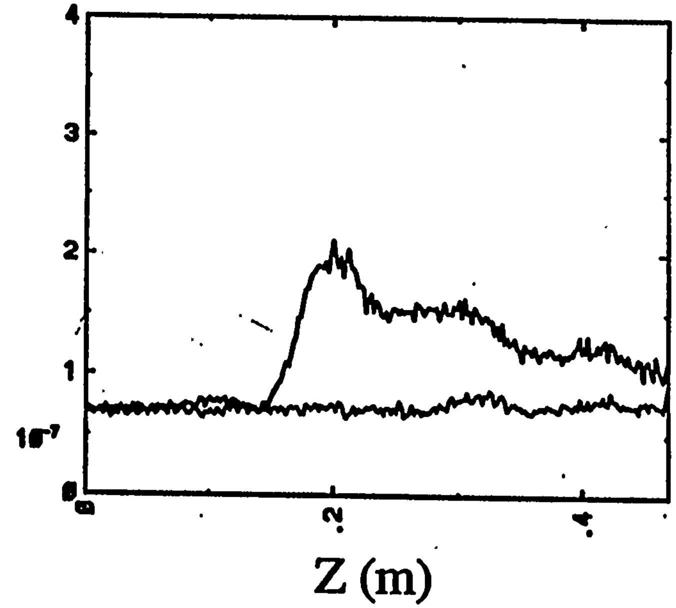

Comparison between scaled experiment and WARP3d

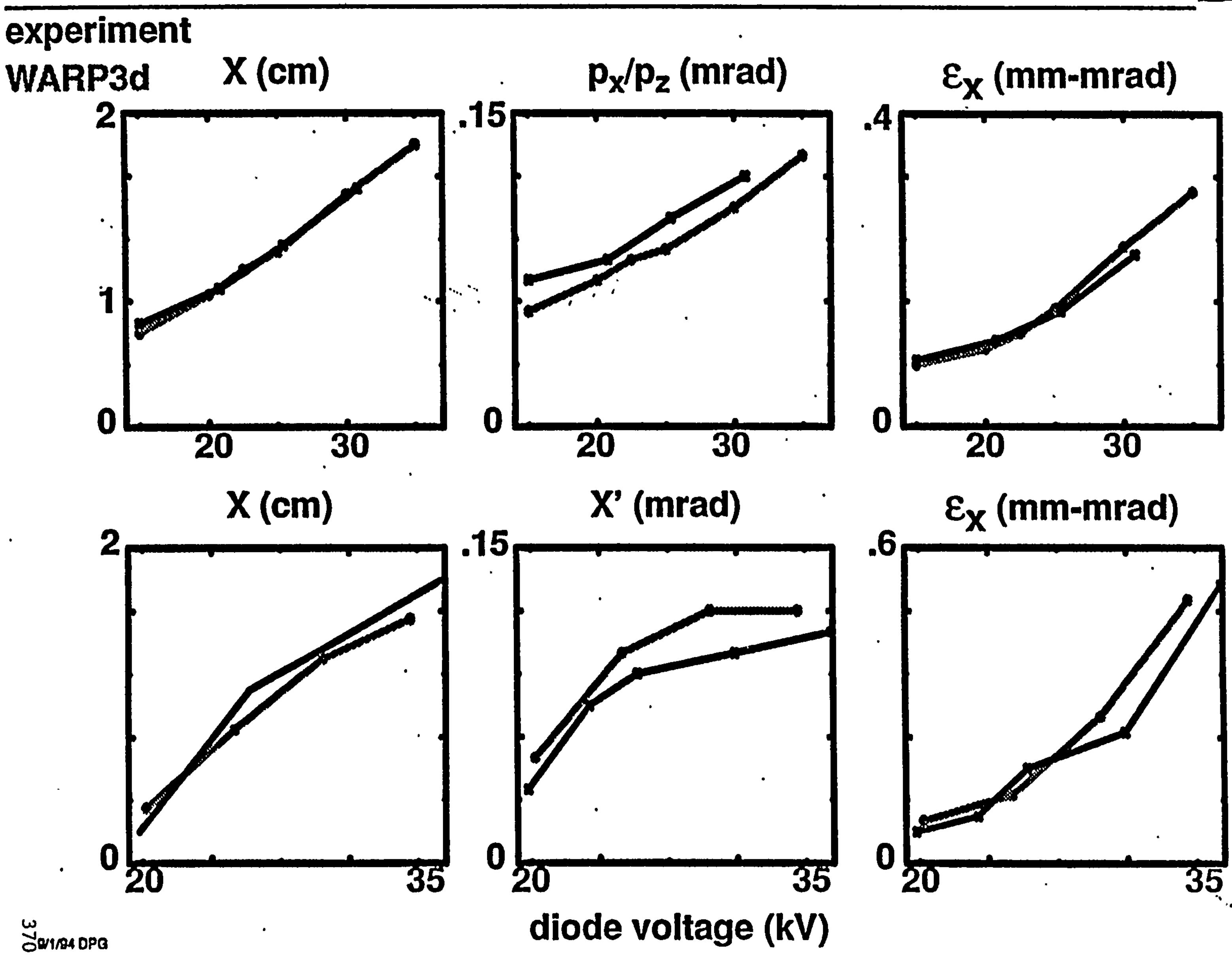

370 9/1/94 DPG

WARP3d models effects of nonlinear self- and applied fields in small recirculator

- Focusing, energy effects in electric dipoles as affected by dipole geometry, location; need "first principles" model:
  - Potential variation along trajectory gives linear focusing in accelerator plane *(x)*.
  - Fringe fields give nonlinear focusing in *x*.
  - Finite transverse plate size gives focusing in *y*.
- Higher-order multipole moments of permanent magnet quads
- Emittance growth due to bends
- Thermalization of space-charge waves from mismatches
- Post-injector matching section
- Insertion/extraction sections (not yet ready—may be hard)
- 15-lap "nearly-first-principles" simulations with 50 k steps, 160 k particles, 32x16x256 mesh:
  - 15 hours on single Cray C-90 processor
  - 70 hours on HP 735 workstation

Small recirculator experiment

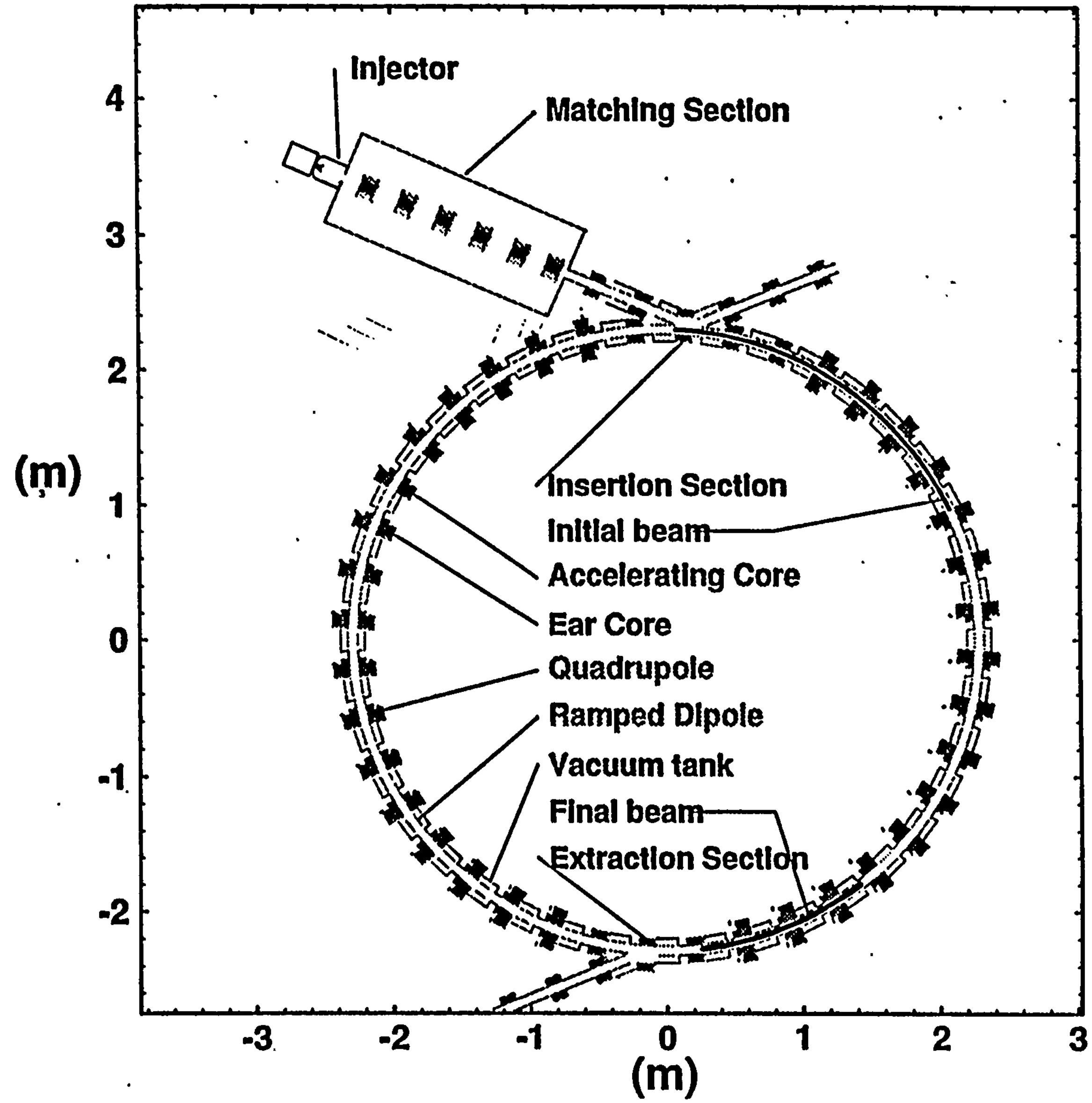

9/1/94 DPG

A small recirculator is being developed at LLNL

Scale of planned device is roughly 1:100

no of laps	15	
circumference	14.4 m	
total path length	216 m	
beam-pipe radius	3.5 cm	
ion mass	39 amu	K^+
beam radius	1.1 cm → 1.3 cm	
beam energy	80 keV → 320 keV	
beam current	2 mA → 8 mA	
beam duration	4 μs → 1 μs	
beam length	2.5 m → 1.25 m	

Lattice will be novel electric-magnetic hybrid

- permanent-magnet quadrupoles for alternating-gradient focusing
- time-varying electric dipoles for bending and steering
- FET-based modulators to generate acceleration waveforms

8/30/94 3

What will the small recirculator look like?

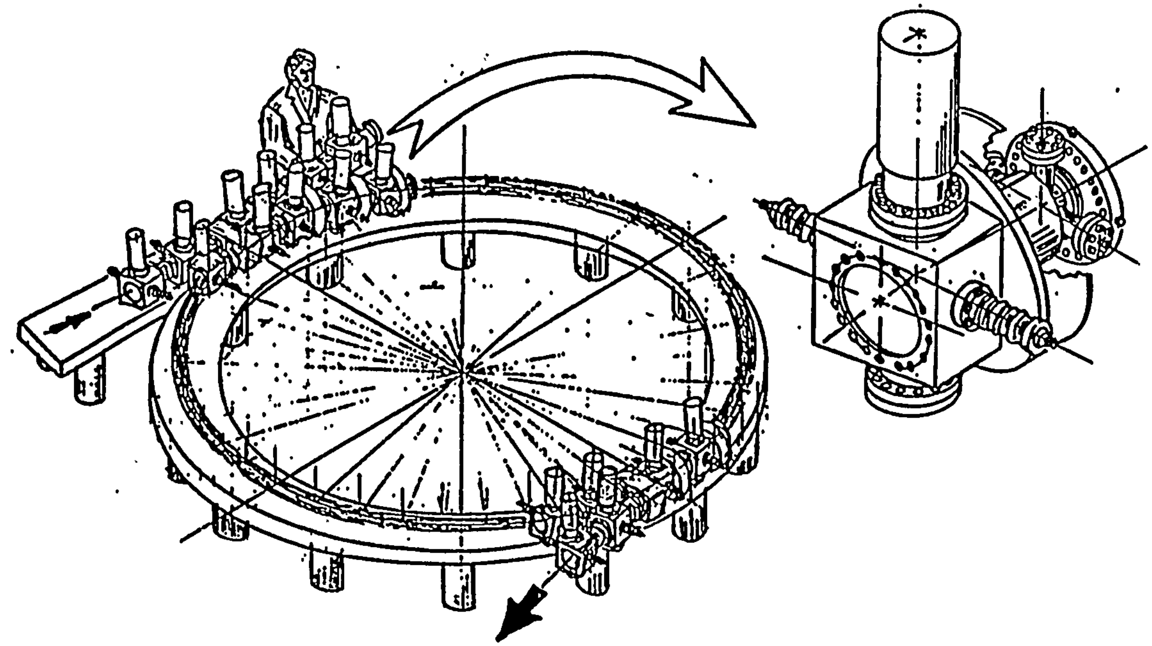

Recirculator lattice geometry: flat plates

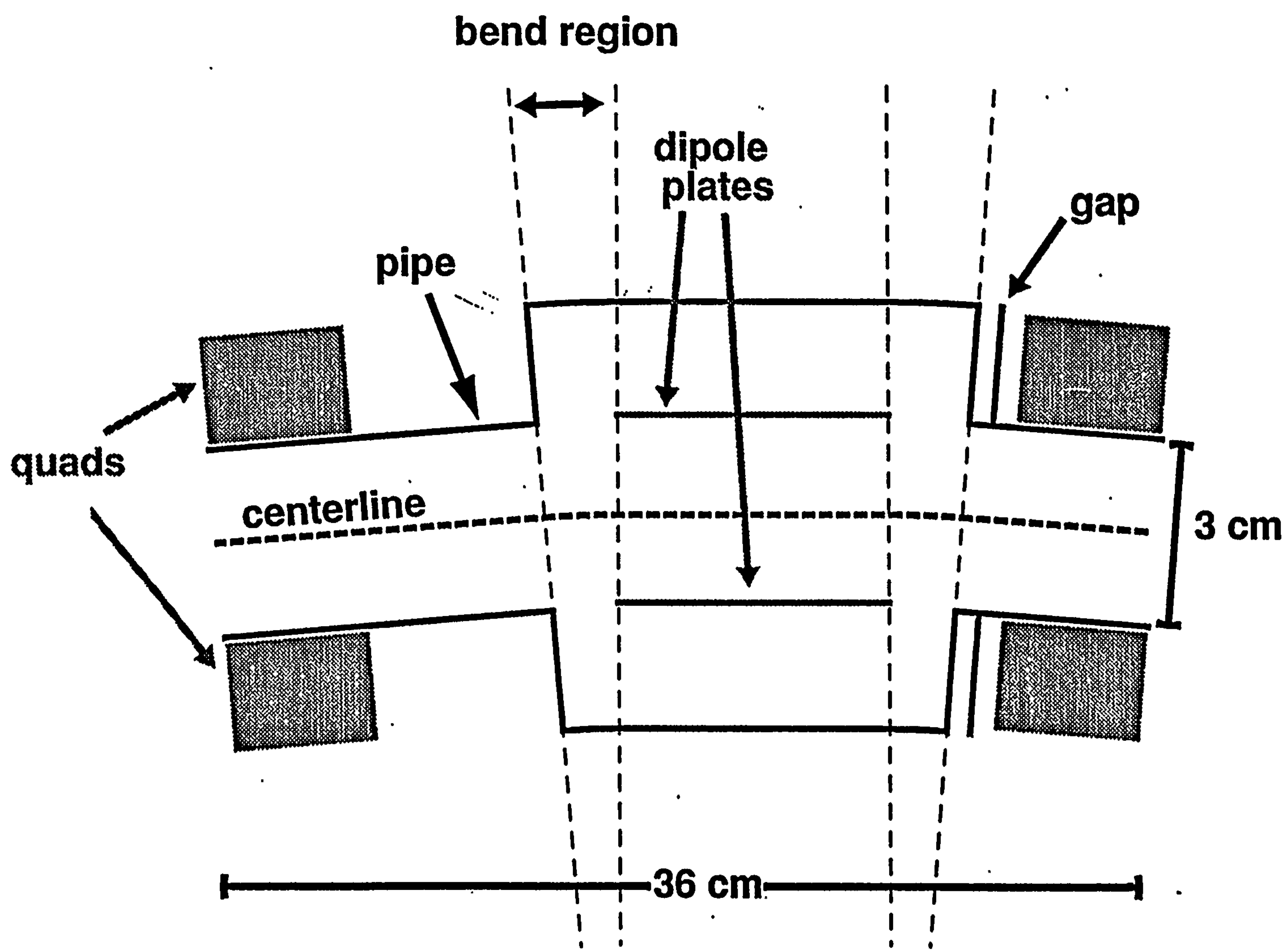

9/1/94 DPG

Recirculator lattice geometry: sector plates

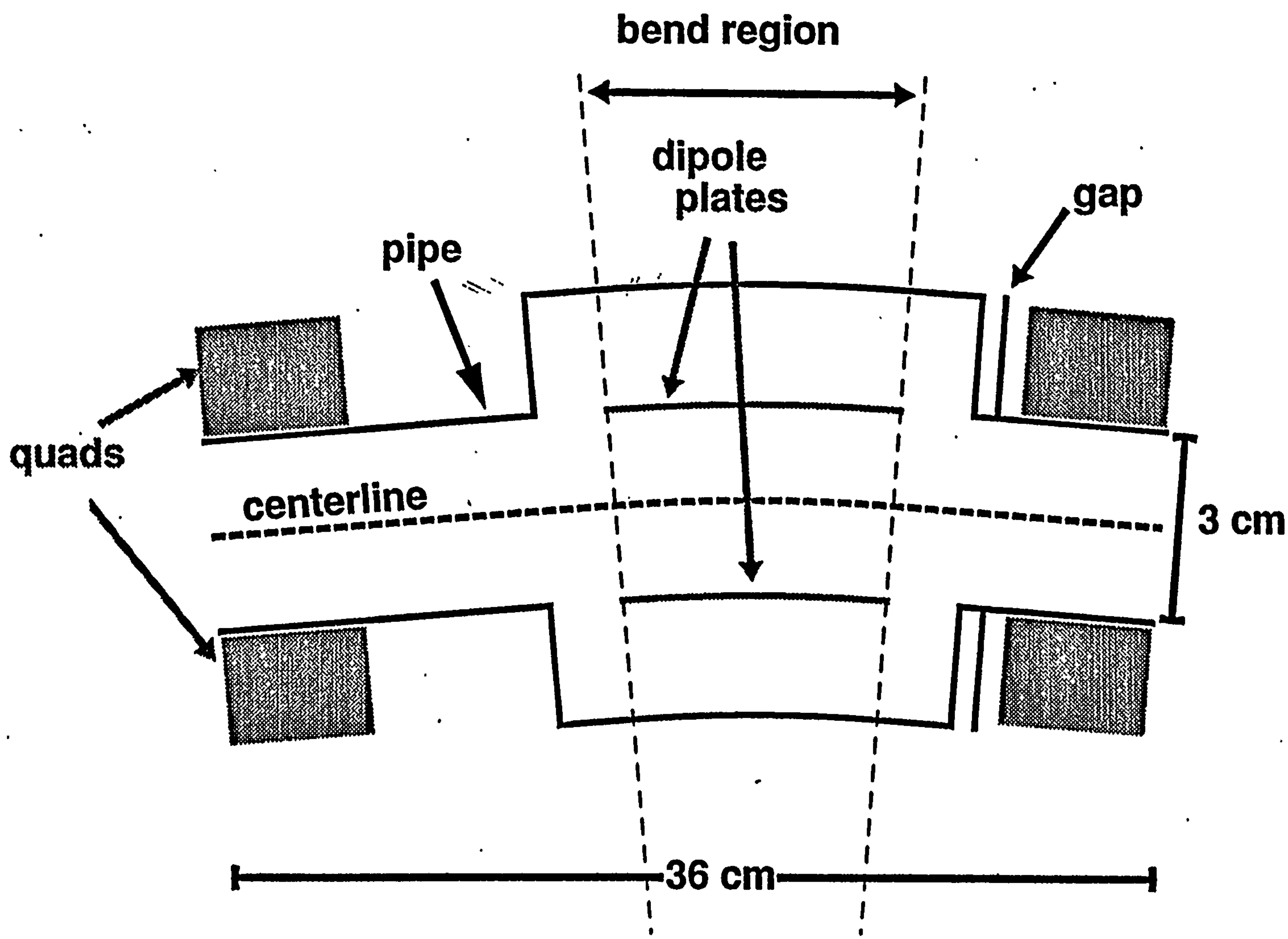

9/1/94 DPG

Drifting beam in recirculator

- For efficiency, the dipole field is calculated once.
  - The dipole field is calculated in WARP3d from Laplace's equation using SOR solver and saved.
  - The potential is then overlaid onto the FFT solution of the beam self-fields in a conducting pipe.
- Two models of magnetic quadrupoles were used.
  - ideal, hard edged, using residence corrections
  - multipole components, including non-linear fields
- Axially confining ear field is applied either continuously (not fixed to the gaps) or as a time varying field in finite-lengthed accelerating gaps.
- The beam is loaded into a straight section and enters the ring through an ideal insertion section.
- One plane symmetry is used: only the top of the beam is modeled.

Typical: 32x16x64 mesh, 75K particles

Runtimes: for 50K time steps, ~6 hours C90 single processor

9/1/94 DPG

Drifting beam profiles at start of run

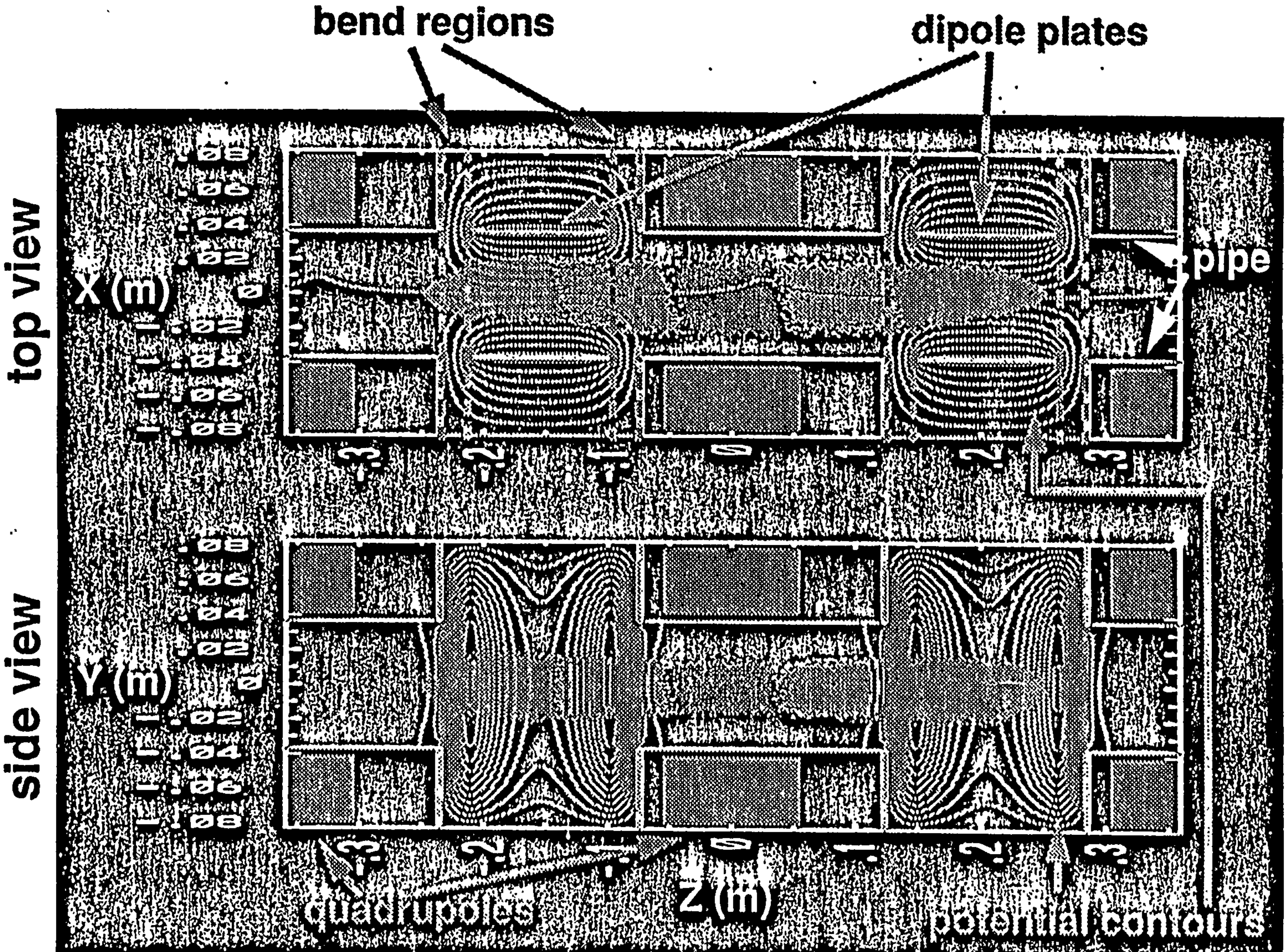

9/1/94 DPG

Axial velocity profile

In the dipoles, the axial variation of the potential spreads the velocity profile. This is the energy effect.

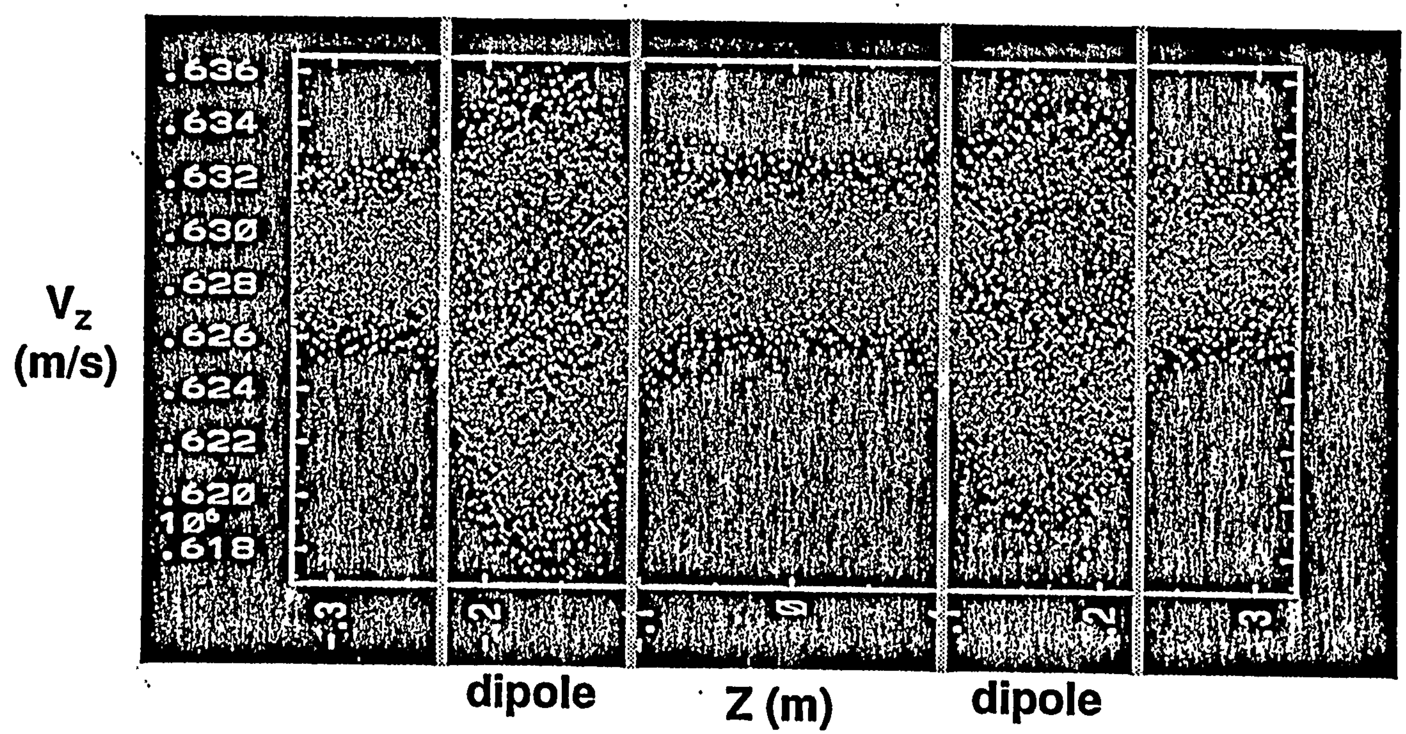

The particle color is determined by *x*, the location in plane of the bend.

Green is smaller *x*, pink is larger *x*.

9/1/94 DPG

Constant physical length results

After the initial jump in emittance from matching to the bends, there is no emittance growth in the plane of the bends (*x*) after 15 laps.

We believe ε_y can be reduced by shaping the plates.

Normalized ε_x at mid-pulse

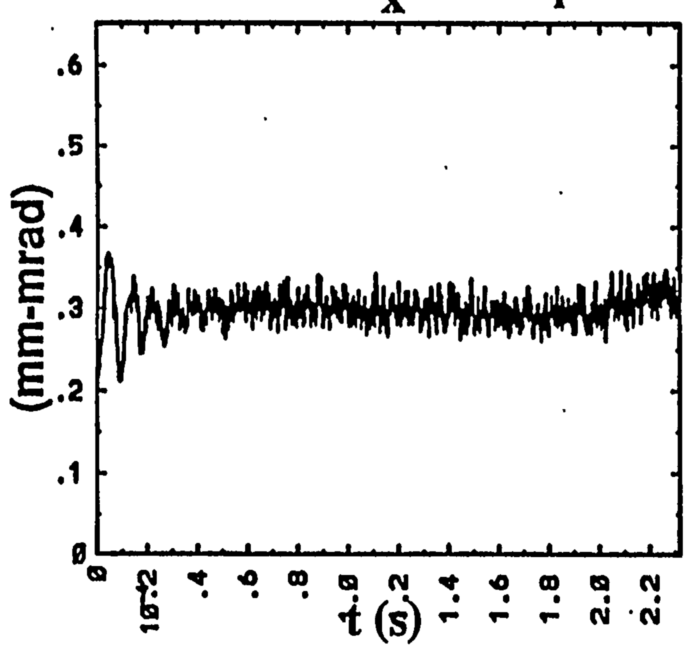

Normalized ε_y at mid-pulse

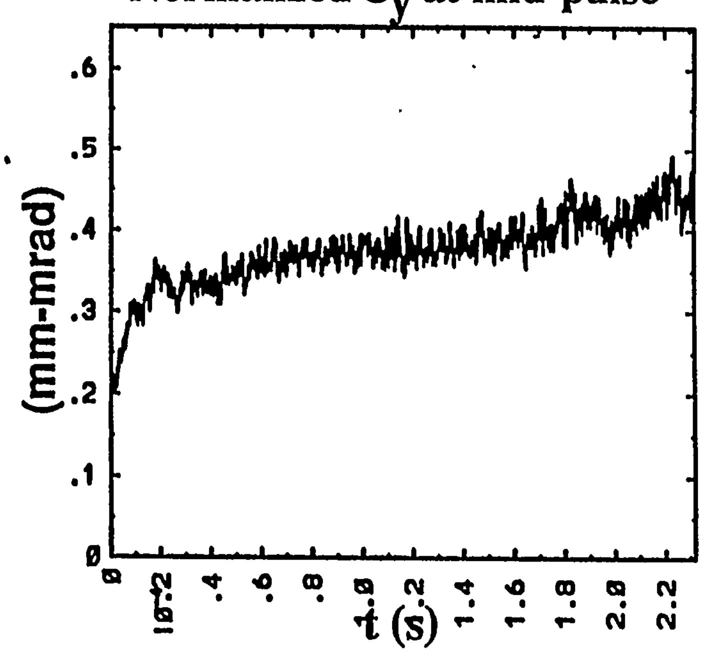

9/1/94 DPG

Plans for WARP3d model of 4-into-1 combiners

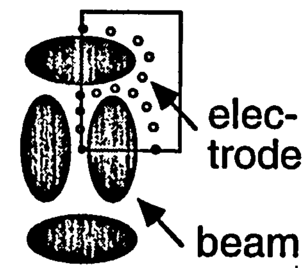

- Small experiment on MBE-4, now getting underway at LBL, will use “Stonehenge” geometry to minimize entrained empty space.
- Need simulate only one quadrant, as shown. Upstream of where beams see each other, need simulate only half of a single beam, using warped coordinates to follow inward motion.
- Focusing and bending are provided by electrostatic electrodes. Final set of electrodes is a multi-wire “squirrel cage” with many wires at different potentials (those in one quadrant are shown in above cartoon). We plan to simulate it using electrodes in WARP, with a very fine grid.
- An important application of run linking.
- Geometry for ILSE combiner not yet finalized.

These goals set direction for code development.

- End-to-end 3-D simulation of LBL's planned ILSE accelerator and experiments, and of LLNL's small recirculator experiments
  - Analysis and design of some individual stages has been done
- Simulation of driver-scale beam physics in *r,z* and 3-D
  - Already well underway
- End-to-end simulation of linear driver beams
  - Present-day computers "adequate" for simplified lattices
  - Better computers will allow detailed models, "routine" use
- End-to-end PIC modeling of recirculator drivers, with their 30x greater path length, is a genuine "grand challenge."

Planned improvements to & applications of WARP

- Improvements:
  - Time-dependent space-charge limited injection, planar/curved
  - More general internal conductor shapes; link to CAD system
  - Linkage of runs using data saved as beam passes thru a plane
  - Final-focus model (requires dynamic mesh?)
  - Higher-order "residence corrections" for fringe fields
  - WARPrz enhancements: Discrete-modules / feedforward
  - Relativistic field calculation (mover already relativistic)
  - Parallelization (first C-90; massively parallel?)
- Applications
  - Combiner experiment
  - Integrated modeling of ILSE
  - Integrated modeling of small recirculator, including insertion/extraction, steering
  - Driver modeling, including pulse shaping using WARPrz, and linkage into chamber code BIC

Code features chosen for propagation model

SEE PAPER (7) FOR MORE INFORMATION ON BICrz

- Electromagnetic fields, particle-in-cell ions
  - Need at least a time-dependent r, z model with self-consistent electrostatic, inductive electric, and magnetic fields (Darwin model also provides this).

- Orthogonal curvilinear quadrilateral mesh
  - concentrates expensive resolution where it is needed: near the target.

- Particle-in-cell electrons created by photoionization and collisions
  - Unless neutralization is quite complete, electrons will be energetic enough to warrant kinetic modeling.

QUICKSILVER, A 3D, Time-Domain, Finite-Difference PIC Code for the Simulation of Complex Structures

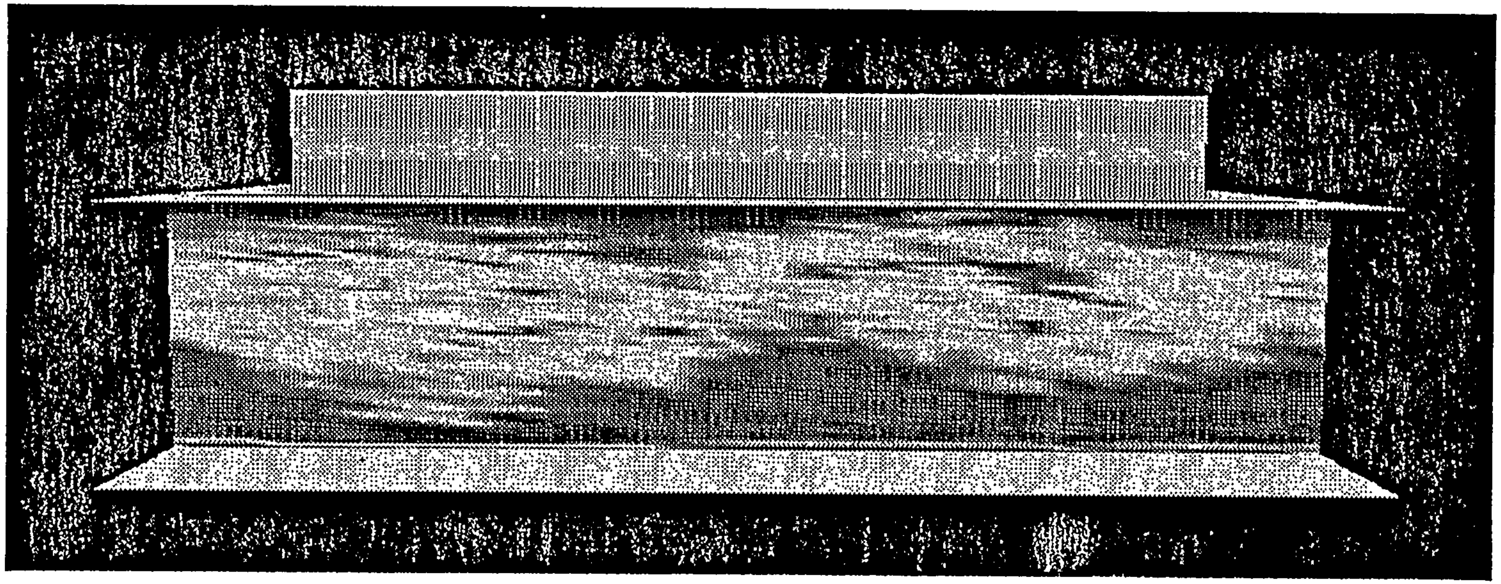

David B. Seidel, Mark L. Kiefer, Rebecca S. Coats, Timothy D. Pointon, and Jeffrey P. Quintenz

Pulsed Power Sciences Center

Sandia National Laboratories

Albuquerque, NM 87185-1186

Presented to:

Workshop on Transport for a Common Ion Driver

Sandia National Laboratories

September 20-21, 19942

QUICKSILVER implements basic physical laws and consequently is applicable to many problems

QUICKSILVER simulates electromagnetics in the time-domain and also, with the inclusion of charged particles, high-current, high voltage plasma physics

- 3D full-wave Finite-Difference Time-Domain (FDTD) Maxwell equation solver with multi-block capabilities
- Charged Particle-In-Cell (PIC) capability
- Models geometrically complex systems of conductors and dielectrics
- A wide range of boundary conditions available.

QUICKSILVER has been ported to many types of computers

- Cray Supercomputers (utilizes multiple CPUs)
- RISC Workstations (HP 700)
- Port to Sandia's Intel Paragon (1800+ CPUs) is in progress for performing very ambitious simulations and/or fast-turnaround

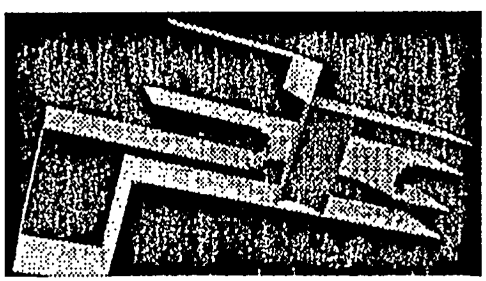

Example of a complex plasma physics device (post-hole convolute) simulated with QUICKSILVER

The QUICKSILVER suite consists of several individual elements

Geometry, Grid, Diagnostics

↓

Crunch Numbers

↓

Commercial Software for Data Analysis, Movie Generation

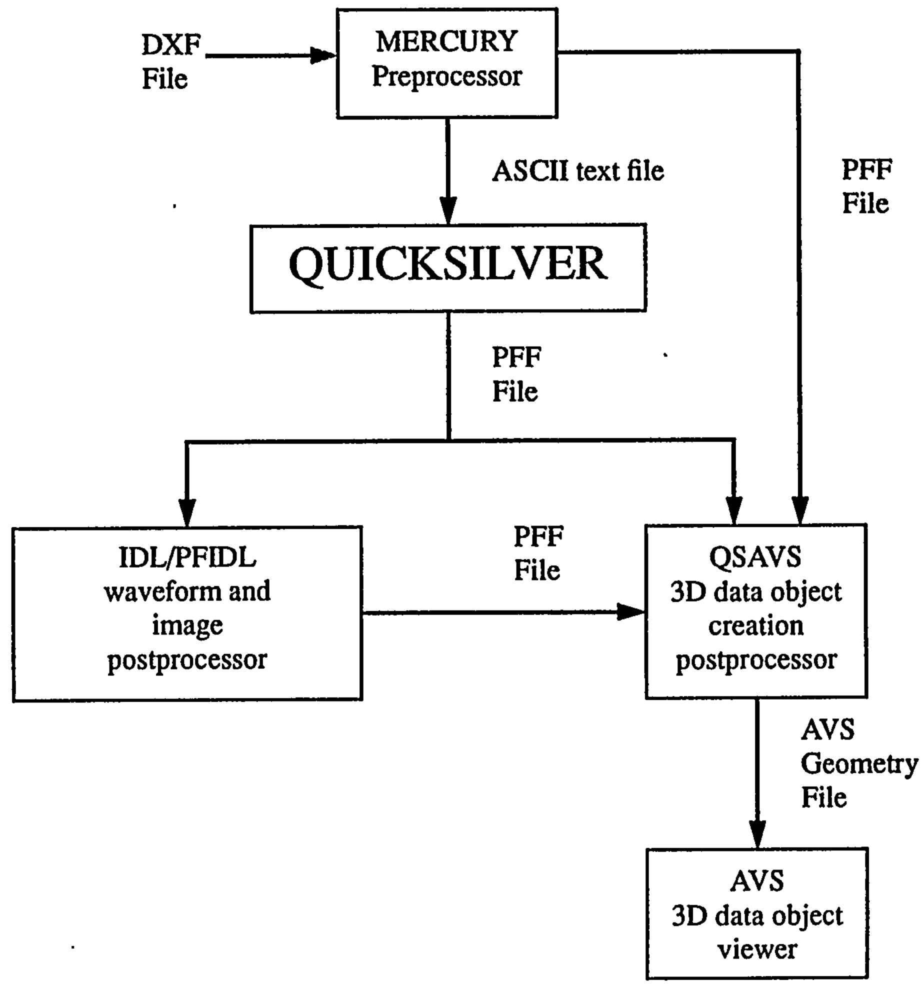

QUICKSILVER's presently provides an excellent base of set-up and post-analysis tools

Easy setup using MERCURY:

- Menu-driven
- On-line help
- Extensive error-detection
- Straightforward specification of complex 3D objects
- Perfect conductors and (lossy) dielectrics

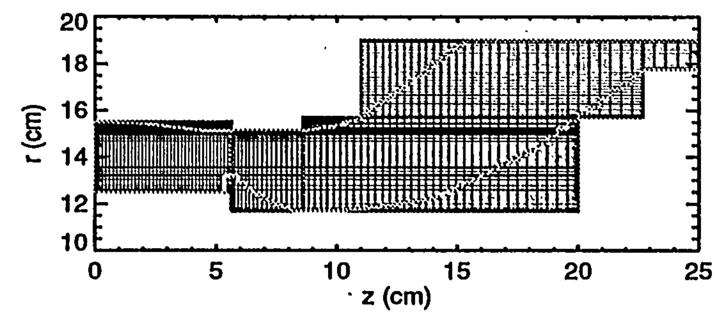

- (New) Graphical editor for using DXF-formatted geometry definitions

Commercial postprocessing capabilities for data visualization and analysis --

- PFIDL analysis tool is based upon commercial IDL software
- QSAVS 3D animation tool is based upon commercial AVS software.

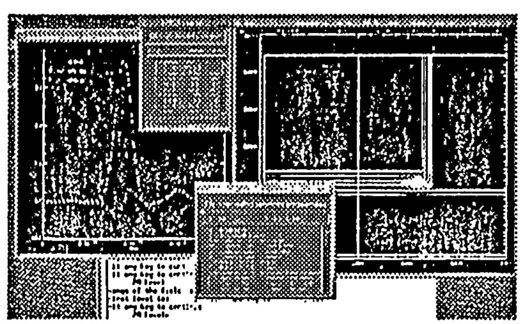

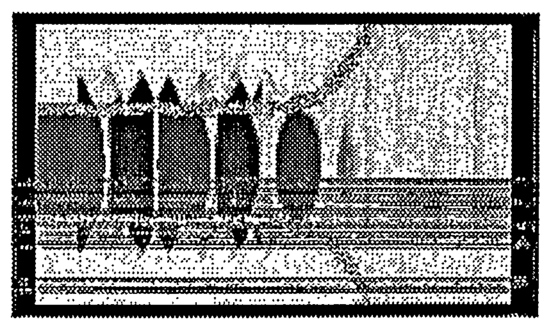

Sandia National Laboratories
MLK:HP/Santa Rosa:8/94

TWOQUICK is a 2D version of QUICKSILVER and Uses the same postprocessors

TWOQUICK is an ***extensively*** reworked derivative of MAGIC

Its input/output model has been completely replaced and is now similar to that of QUICKSILVER

- Its input processor supports command files, aliasing, variable substitution, and FOR loops.
- Its output (PFF data files) are totally compatible with QUICKSILVER's postprocessors

New physics and algorithms have been added:

- Slanted surface emission
- Completely vectorized charge and current density allocation
- Charge conservation diagnostics

Shaded cones can be used to display snapshots of vector data

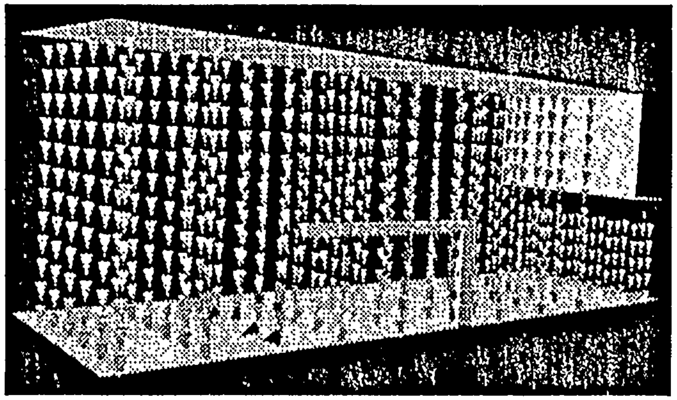

Electron Launcher Voltage Probe Simulation -- Electric Field

Shaded spheres can be used to display snapshots of particle position

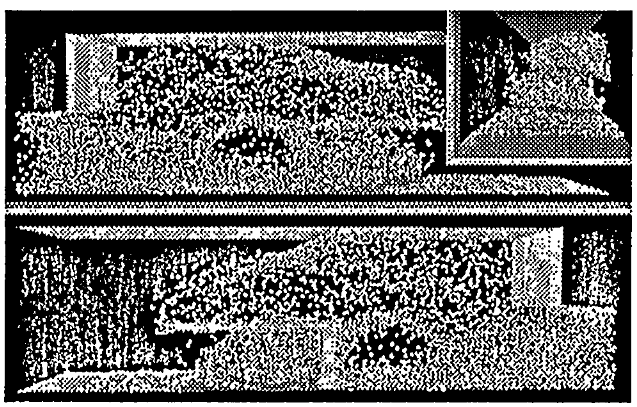

Three Views of Electrons in Electron Launcher Voltage Probe Simulation

Shaded surfaces can be used to display slices of scalar snapshot data

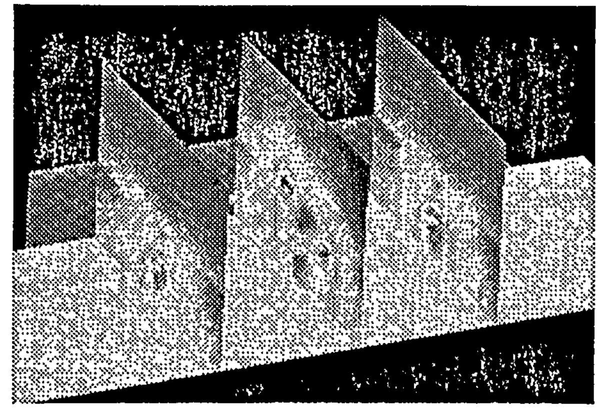

Surfaces of electric field magnitude for a simple interconnect structure

QUICKSILVER simulations illuminate a complex evolution of diode instabilities

early time diocotron

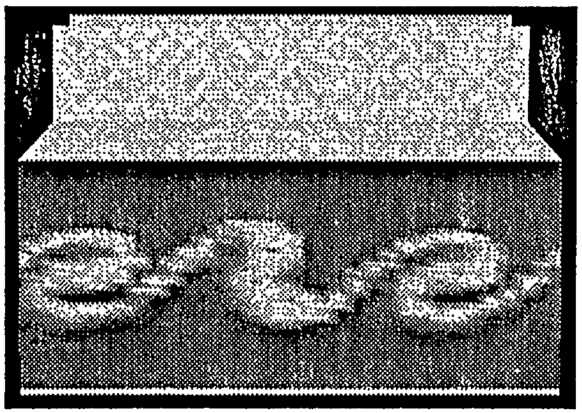

late time ion mode

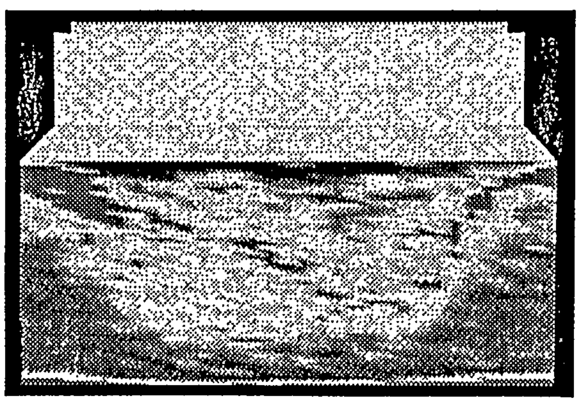

Linear growth rate of diocotron mode and saturation by electron trapping

↓

Growth of other modes followed by mode coupling

↓

Evolution towards frequency spectrum peaked at lowest ion mode resonance or lower

We are using 2- and 3-dimensional simulations to understand the SABRE extraction ion diode

2-D TWOQUICK simulations address geometry and power flow

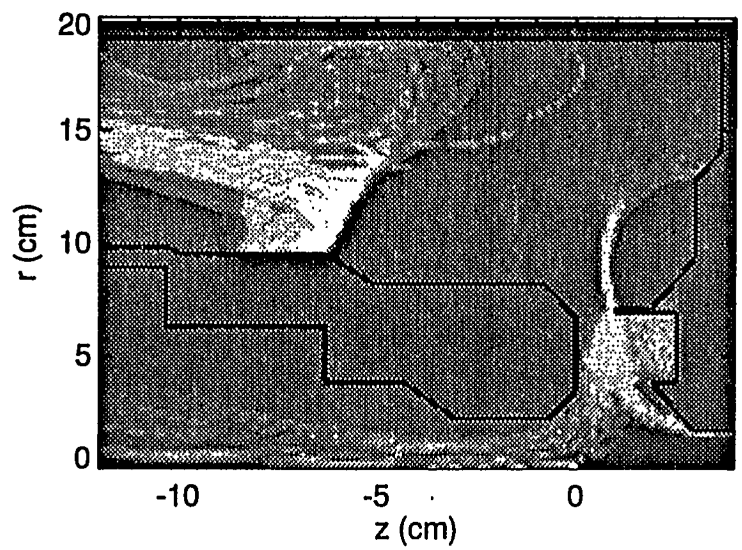

Resolving the electron space-charge into feed electron and cathode-tip electron populations helps clarify their roles.

3-D QUICKSILVER simulations study instabilities in the diode

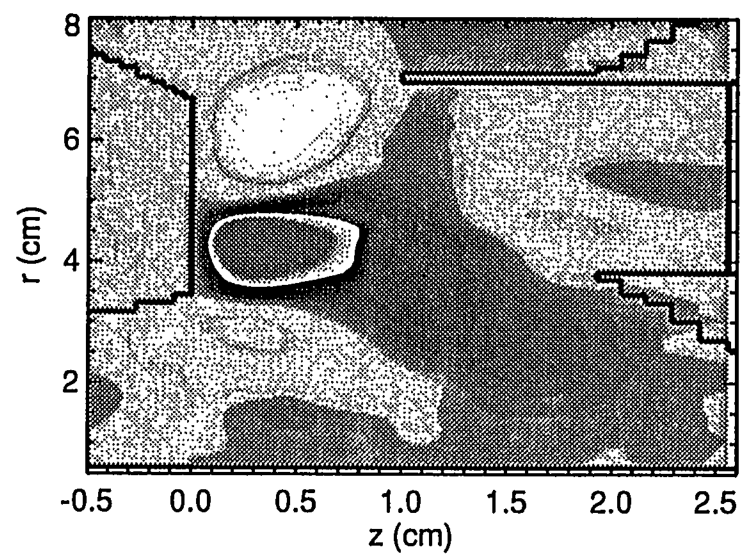

The real part of the l = 8 mode of E_ϕ for the ion mode shows radial structure, unlike the dioctron mode

To Increase the Ion Diode Voltage We Must Improve the PBFA Adder to Provide Increased Z_f .

From TWOQUICK Model of Half PBFA Vacuum Voltage Adder:

Raised Cone, No POS: t = 60.10 ns

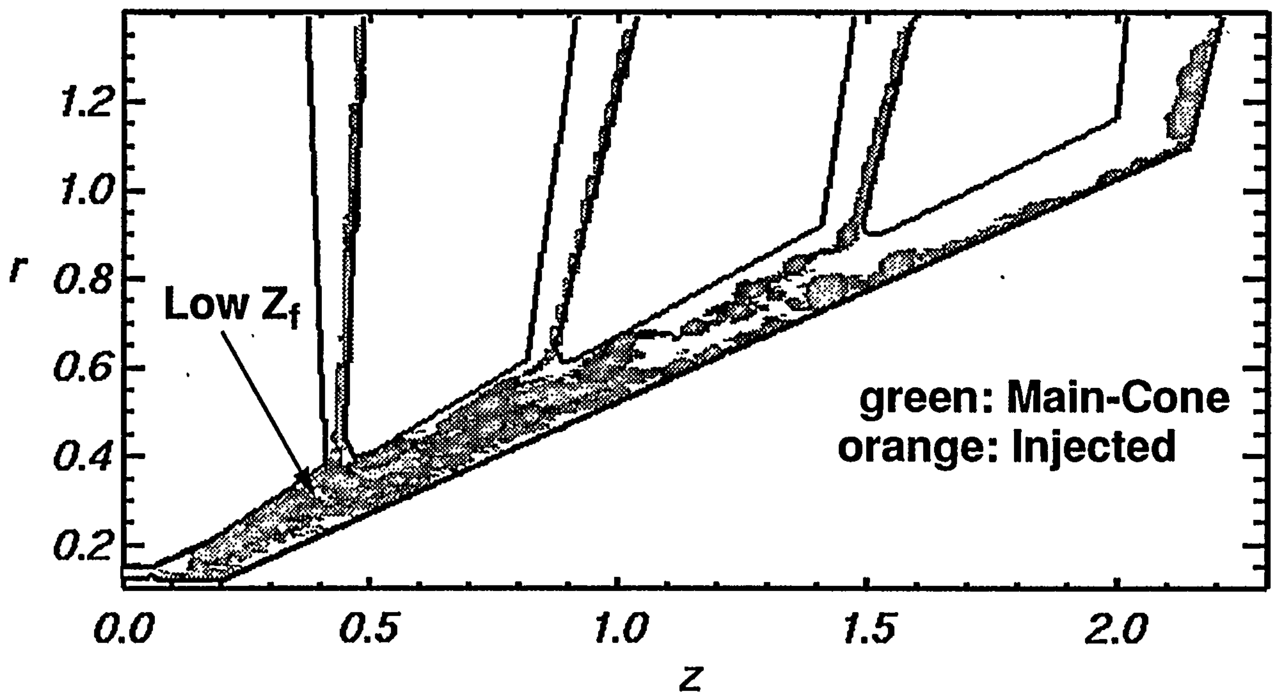

- Which flow components contribute most to producing an electron charge density centroid near the anode, giving low Z_f?
- Can we influence these components by feasible modifications of the system, or with POS?

Pulsed Power Sciences, Sandia National Laboratories
S. E. Rosenthal: 11/15/93

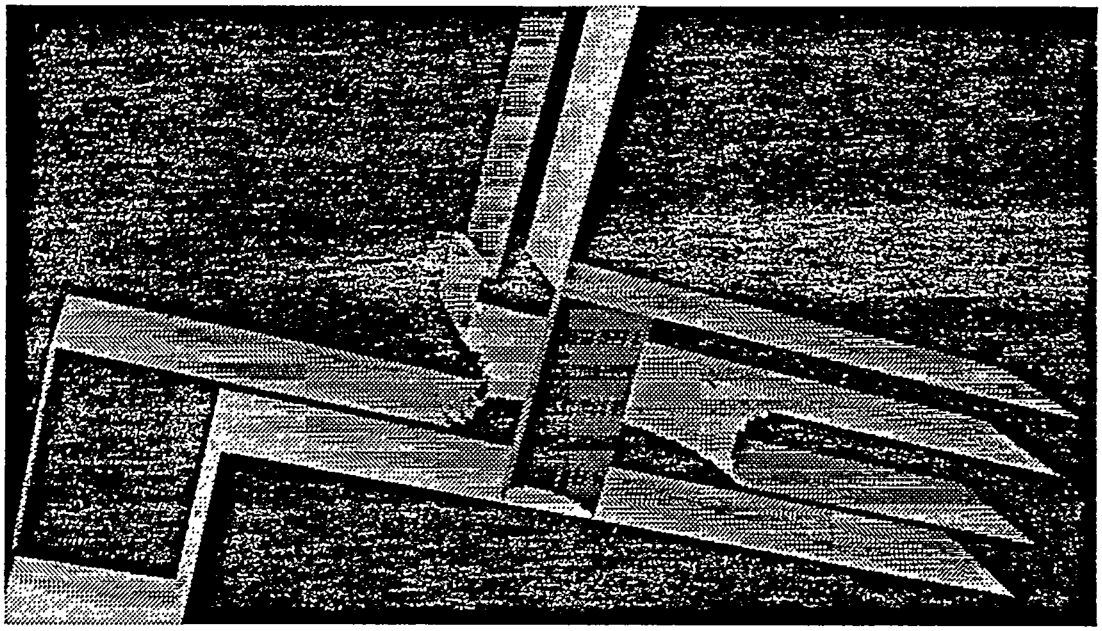

Perspective view of simulation geometry. Two MITL power feeds are at far right. The inductive load is at far left. The MITL feed from top models the effect of the upper half of the Double Post-Hole Convolute.

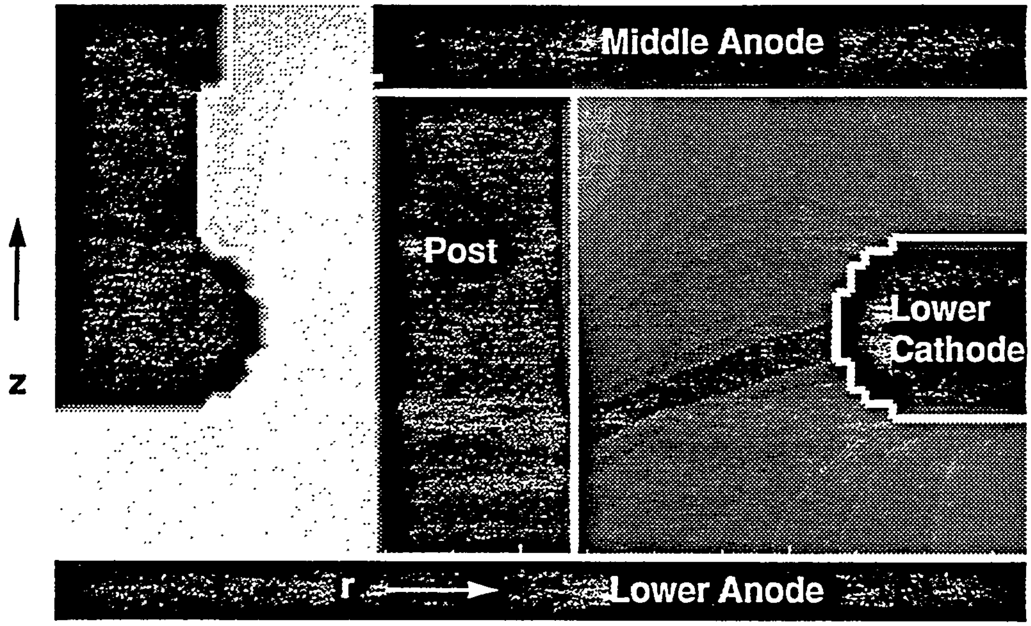

The magnetic null between the upstream edge of hole and the upstream side of post from simulation. |B| is shown in rz-plane through post axis.

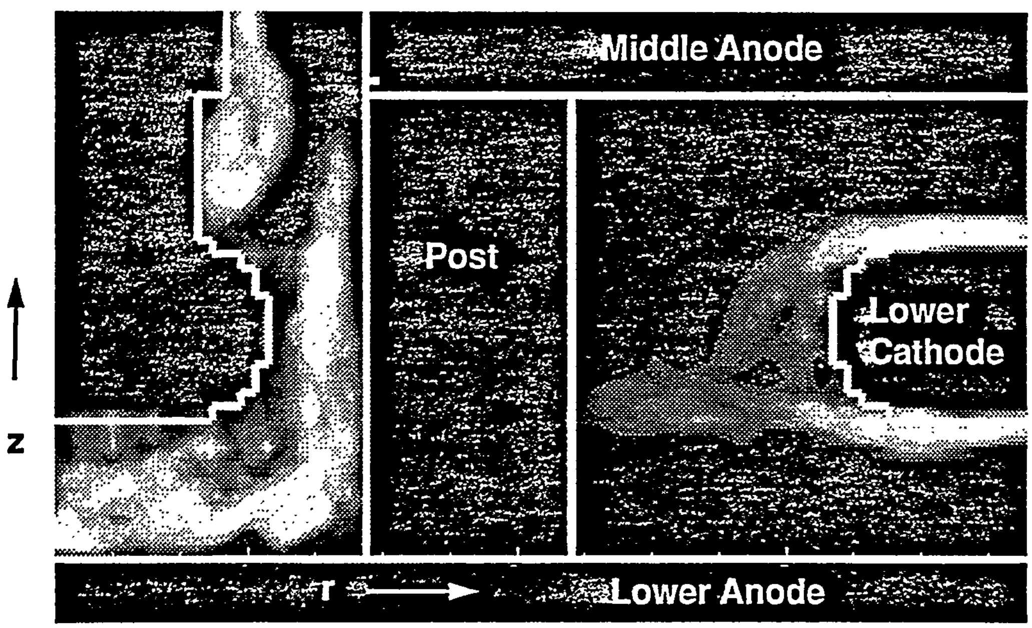

The electron flow follows the magnetic null between the upstream edge of hole and the upstream side of post from simulation.

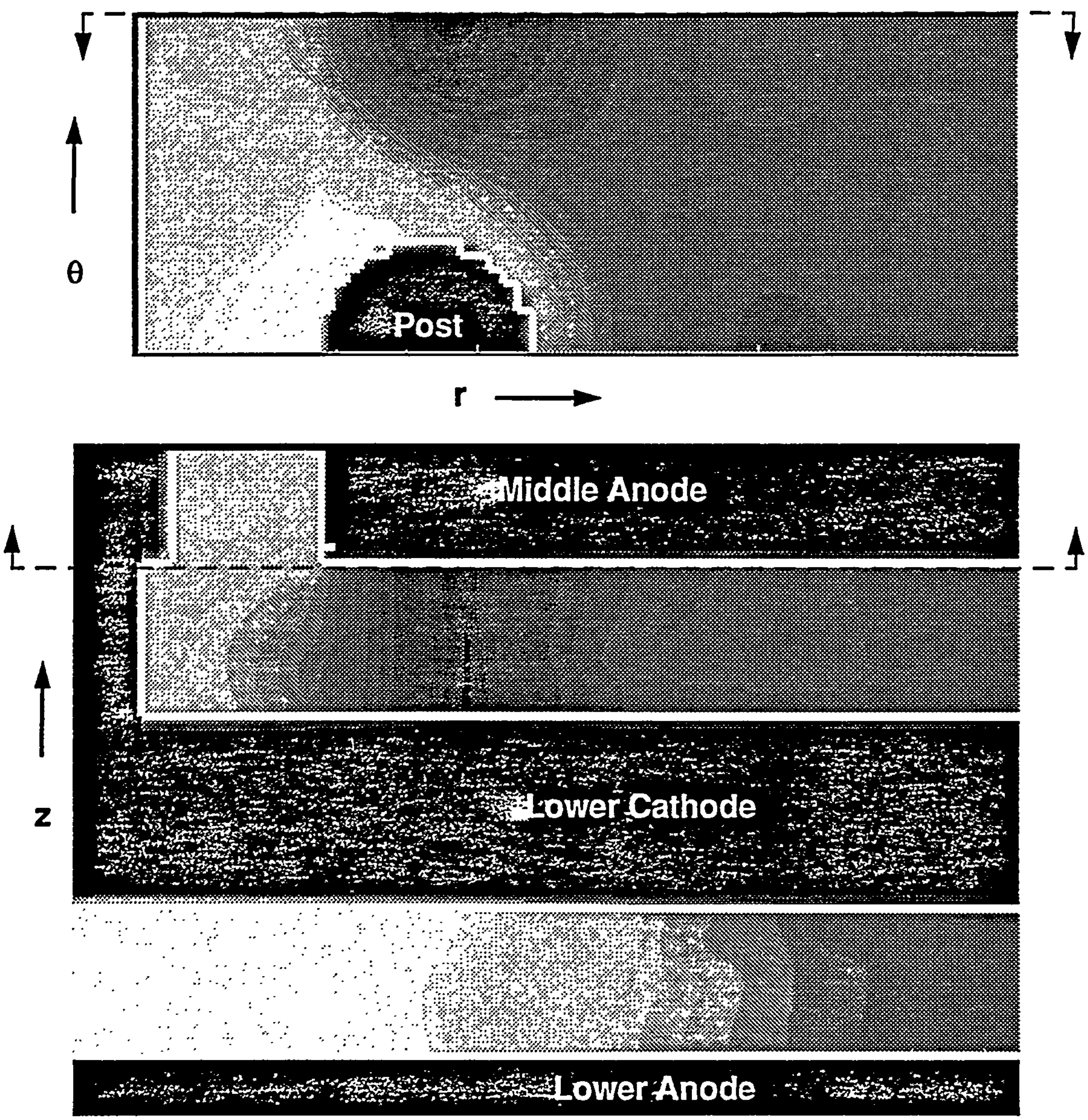

The magnetic null between lower cathode and underside of middle anode from simulation. Top view shows |B| in plane of underside of middle anode (rθ). Bottom view shows |B| in rz-plane midway between posts.

Comparison of simulation predictions to measured data is a critical element of our program

Microstrip Lowpass Filter

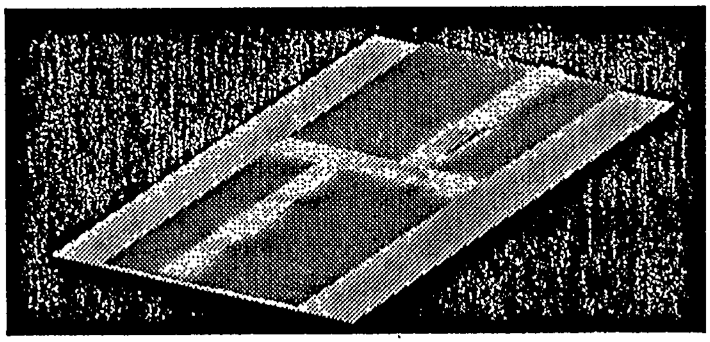

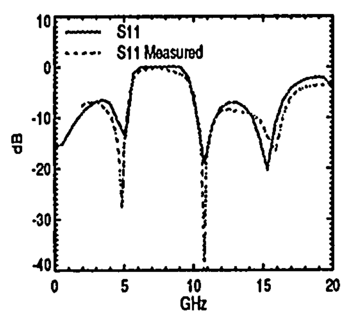

S_{11}

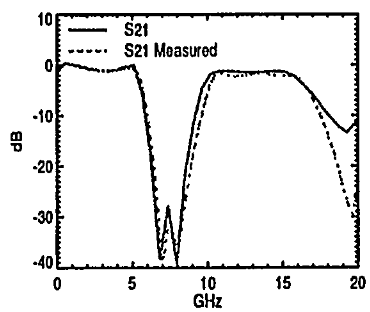

S_{21}

Matching Structure X1-45-D1

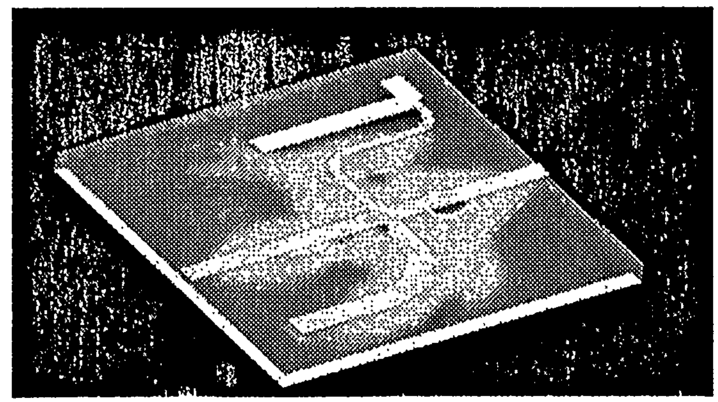

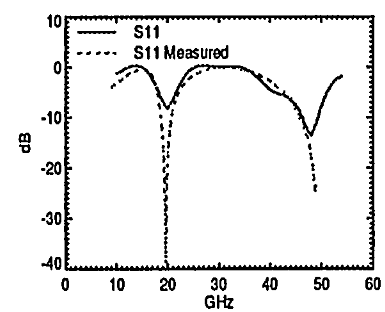

S_{11}

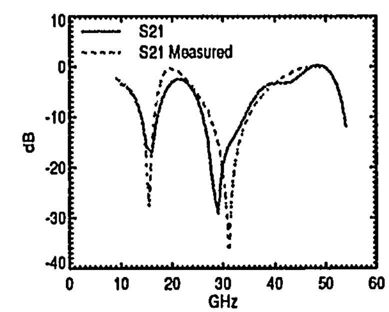

S_{21}

Sandia National Laboratories
MLK:HP/Santa Rosa:8/94

BUCKSHOT

A 3-D 'Gridless' Particle Code For End-To-End Accelerator Research

John S. Wagner, SNL-NM

Transport for a Common Ion Driver Workshop
Albuquerque, New Mexico
September 21-21, 1994

Developed at Sandia (circa 1986), Buckshot has special features for high current, end-to-end, beam transport simulations.

- *Very easy to use*
- *Fast (10-1000x faster than 3-D EM PIC)*
- *Fully 3-D*
- *Gridless field solvers for space charge/current effects relaxes courant condition and allows large timesteps*
- *Particle pusher is fully relativistic*
- *Multi-species particles with realistic charge/mass allows study of background plasmas, channels, and charge neutralization*
- *Gaps, bends, boundaries, laser or beam driven ionization*
- *Applied time dependent fields from formulas or meshes*
- *Many other field solvers available (gridded EM, multipole, nlogn, unstructured lists)*
- *Portable and parallelized versions*

Typically a magnetostatic force law approximation is used by BUCKSHOT to compute particle self-forces.

- *Particles are spheres or cylindrical filaments that interact magnetostatically. Particles feel their neighbors charge and currents, but no self-radiation**
- *Particles are sorted axially to distinguish near from far neighbors. 'Near-same-slice' neighbors are accounted for exactly, distant neighbors are ignored or approximated*
- *Particles move self-consistently with self and applied forces*
- *Self-consistent forces may be computed by direct summation*
- *Particles are finite-size to eliminate numerical heating..... finite Δt permits anomalous very near collisions of particles interacting with $1/r$ or $1/r^2$ forces.*
- *Equation of motion integrated with standard leapfrog*

* *in the 'classic' BUCKSHOT*

JSW:1241:ssc:9/21/94

Typical Applications

- Theoretical and laboratory research of IFR-beam physics
- Laser guided high current REB's in ionosphere
- Recirculating and spiral line accelerator end-to-end design
- Spacecraft charging
- SSC H^- injector, LEBT and RFQ
- Electron & ion beam lithography
- Collisional/Collisionless Neutral Gas Dynamics
- HPM

- Bridges the gap between beam-optics / envelope models and fully 3-D EM-PIC (with the kitchen sink)

MEASURED ION HOSE GROWTH RATE IS LOWER THAN SIMPLE MODEL PREDICTIONS BUT AGREES WITH ADVANCED CODE.

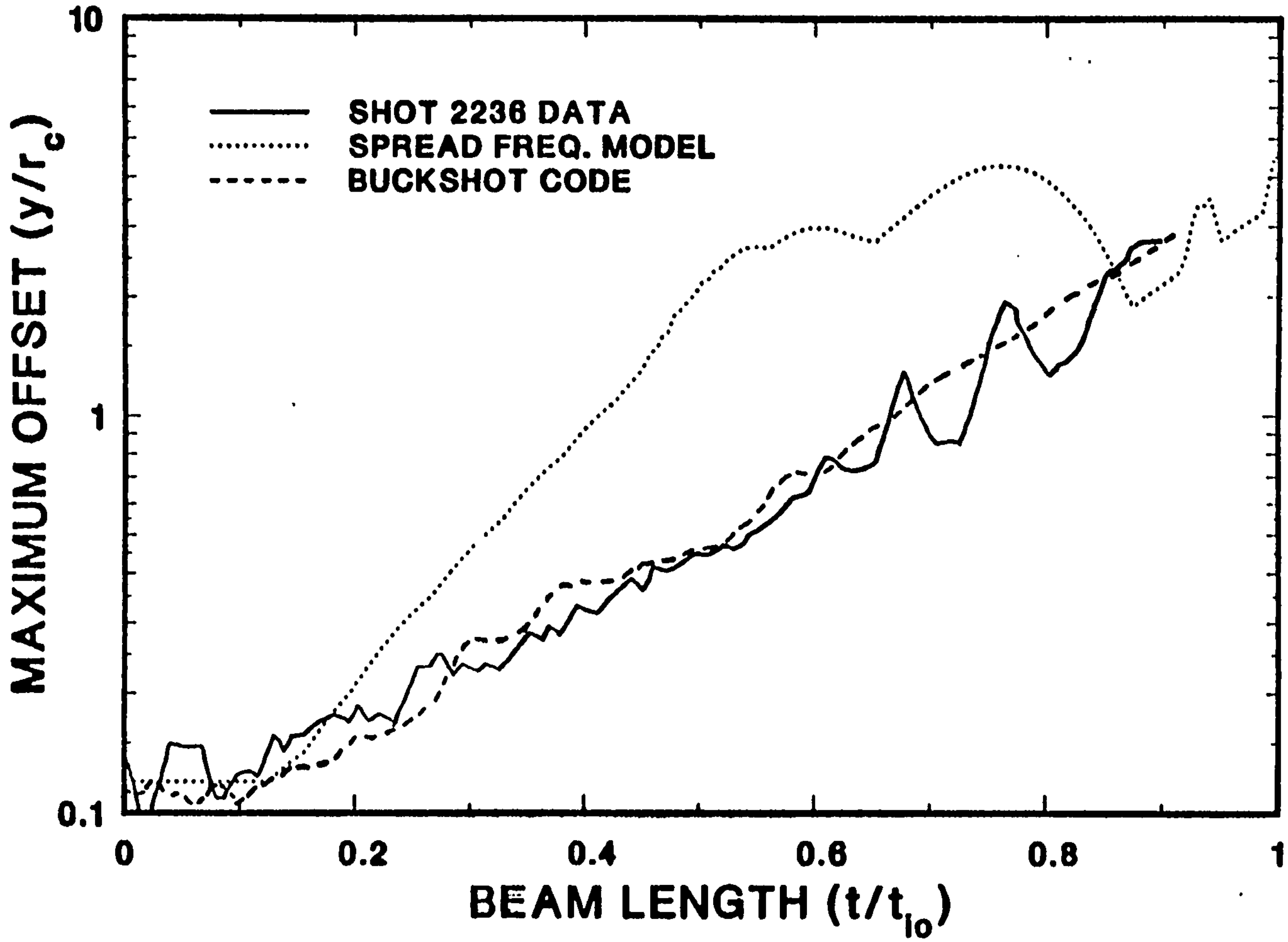

Example: Buckshot-Magic Comparison

- *RADLAC IFR conditioning cell*
- *40 KA*
- *Annular beam*
- γ*=40*
- *30 cm tank*

BUCKSHOT shows excellent agreement with electromagnetic MAGIC code

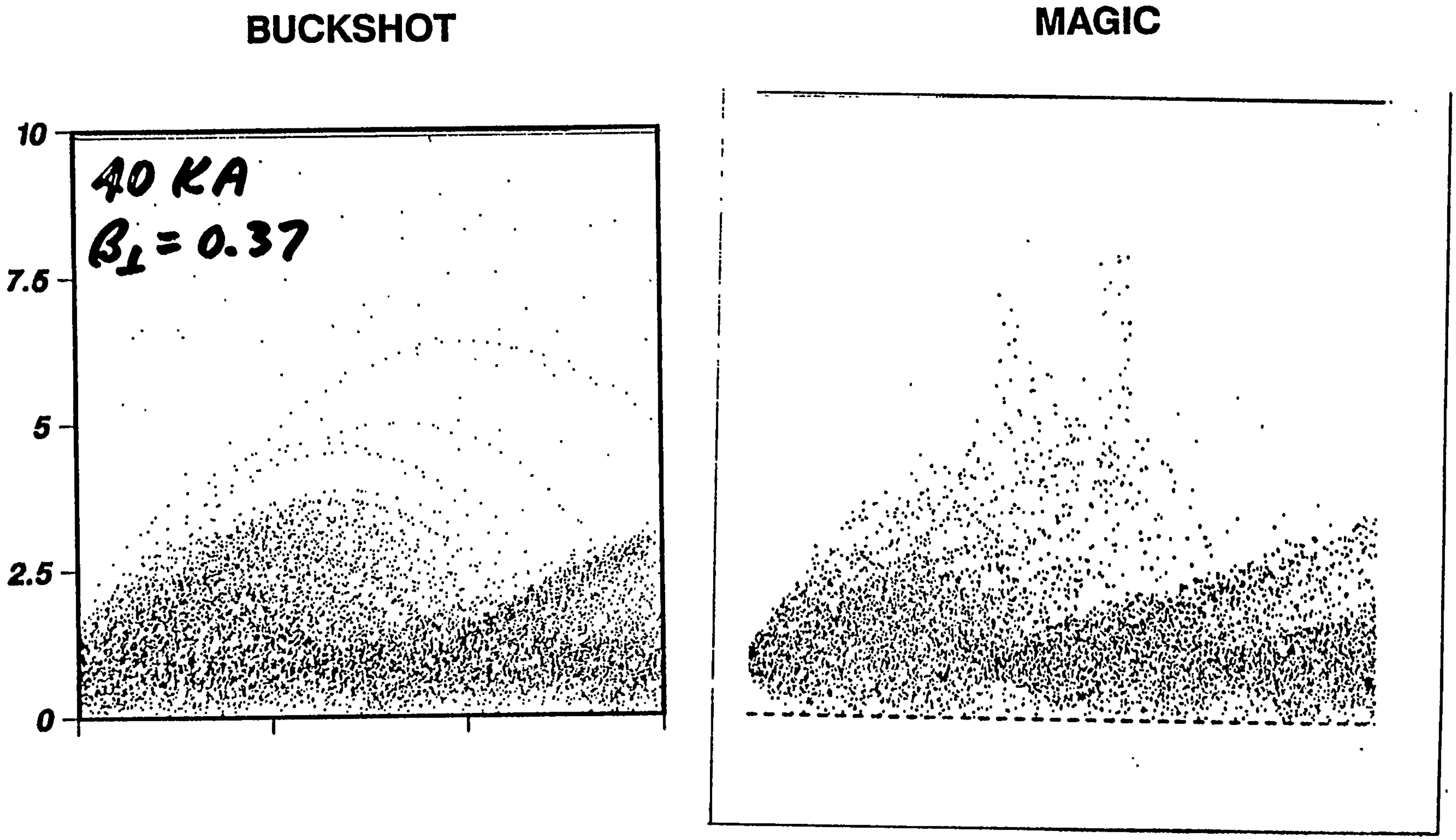

Spiral line application accelerator has been simulated with BUCKSHOT

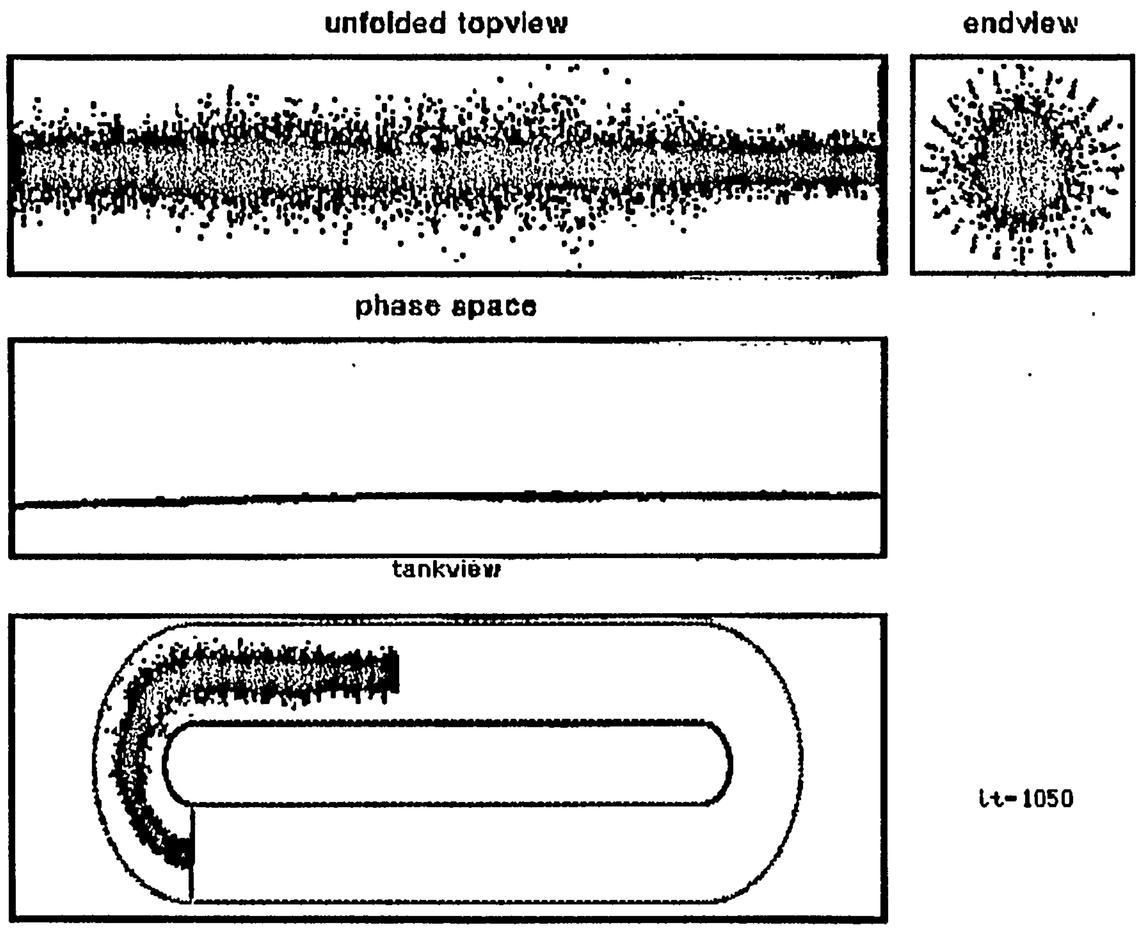

I = 25 kA
r_b = 1.1 cm
r_c = 0.5 cm
f = 0.3
38 gaps
4 passes

After the first pass, the emittance is well below the criteria

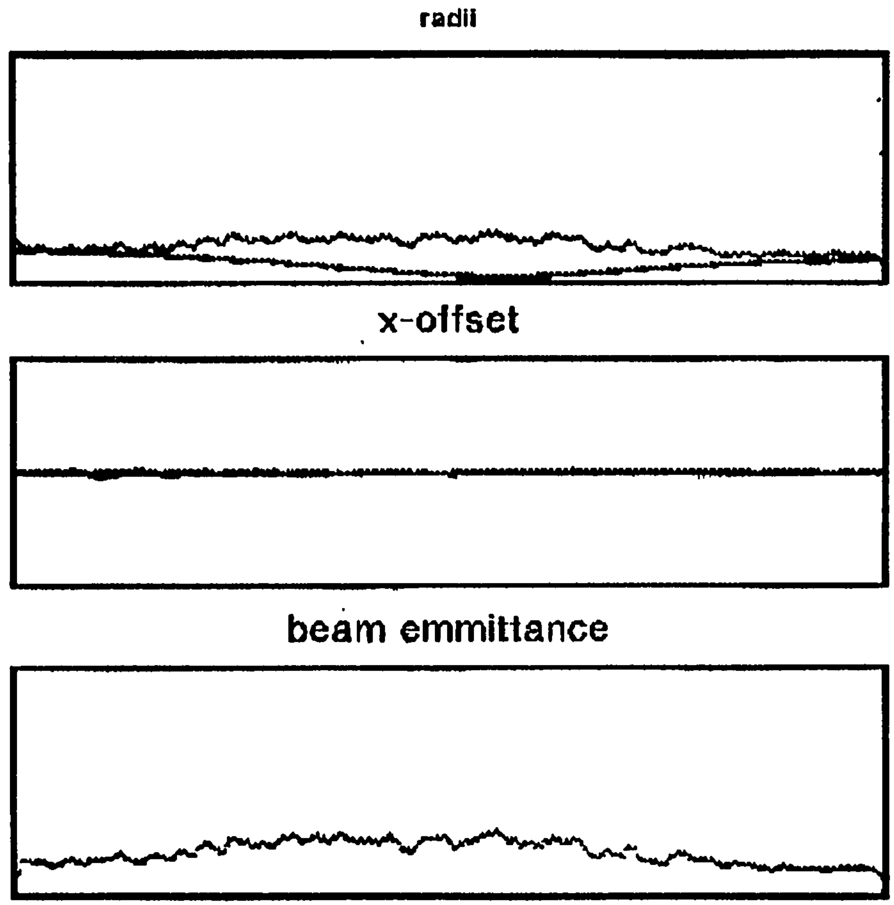

Lt-1050

After four passes, the beam has 100% current transport

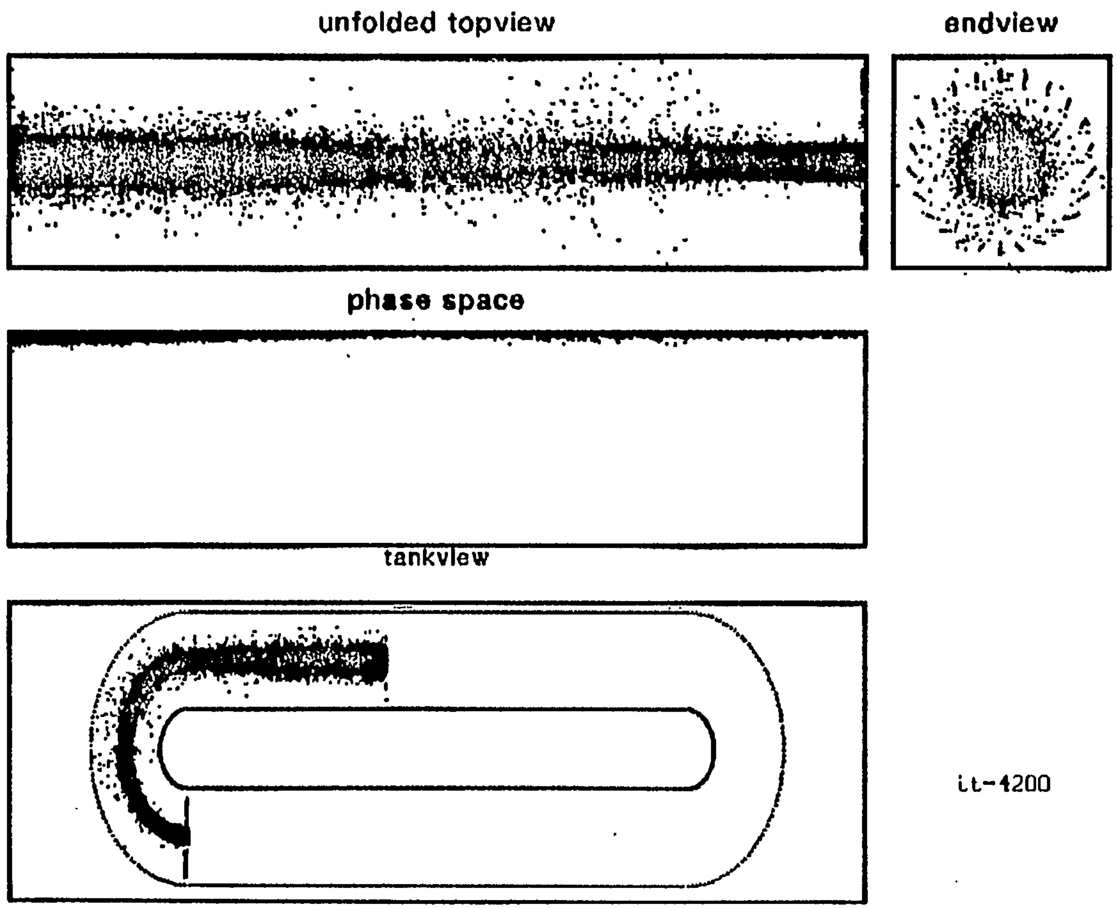

After four passes, the full energy beam meets the emittance criteria

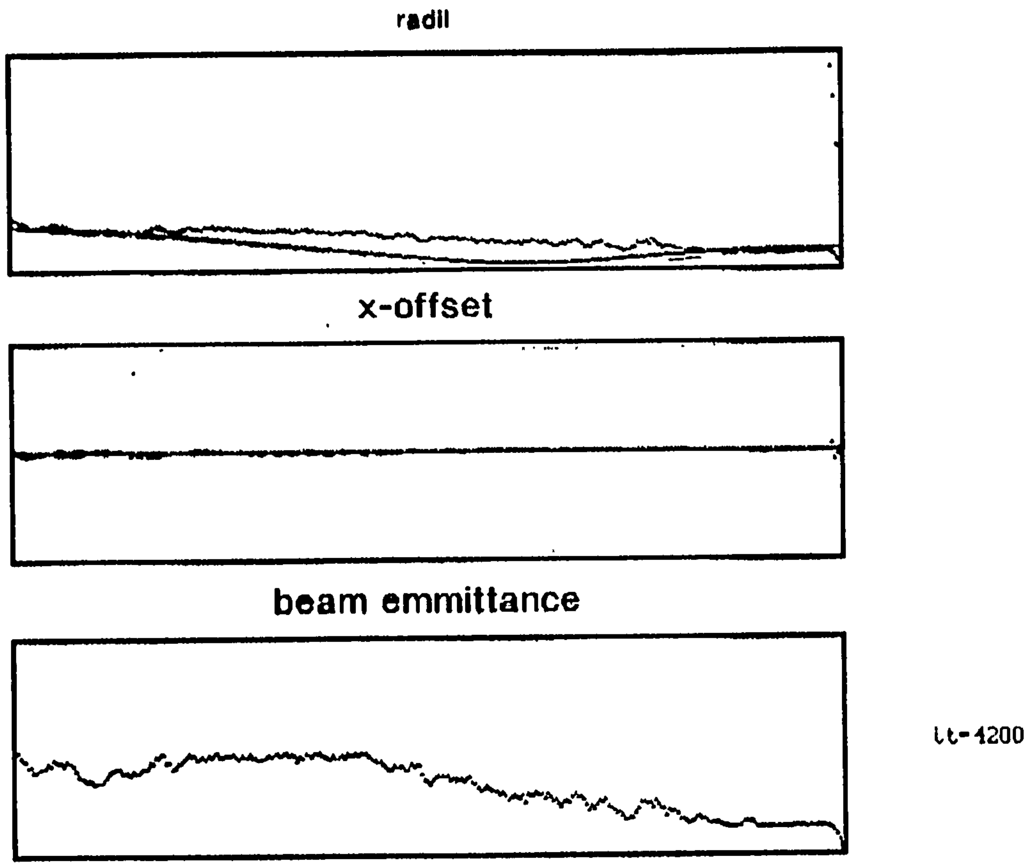

Example: benchmarking the code on a typical SSC-HESQ example

- Canonical Parameters are:
- L=22.5 cm
- λ= 15 cm
- V=7000 volts
- R=1.5 cm
- Fields from analytical approximation for a HESQ

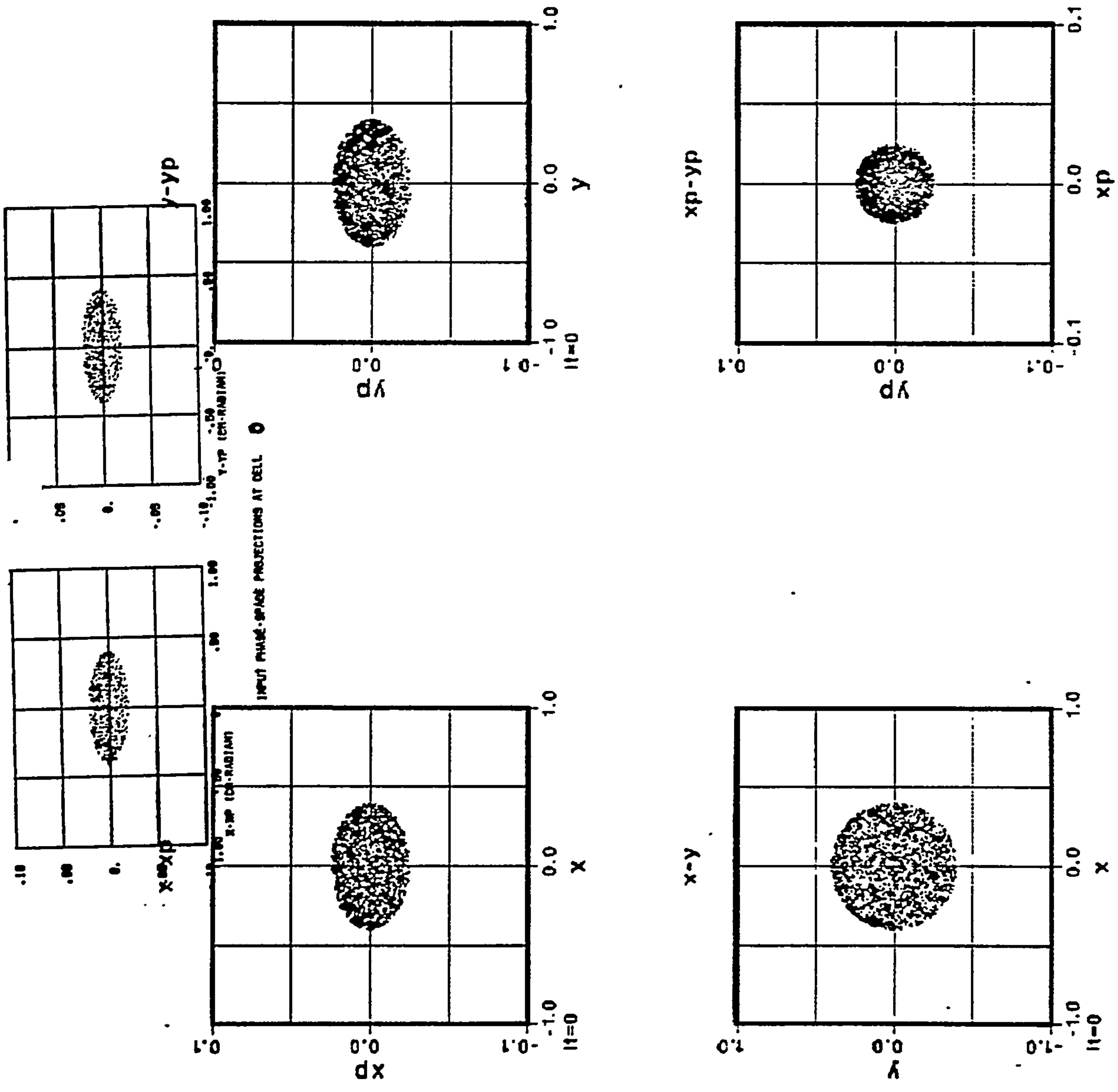
INPUT PHASE-SPACE PROJECTIONS AT CELL 0
x-xp
y-yp
x-y
xp-yp

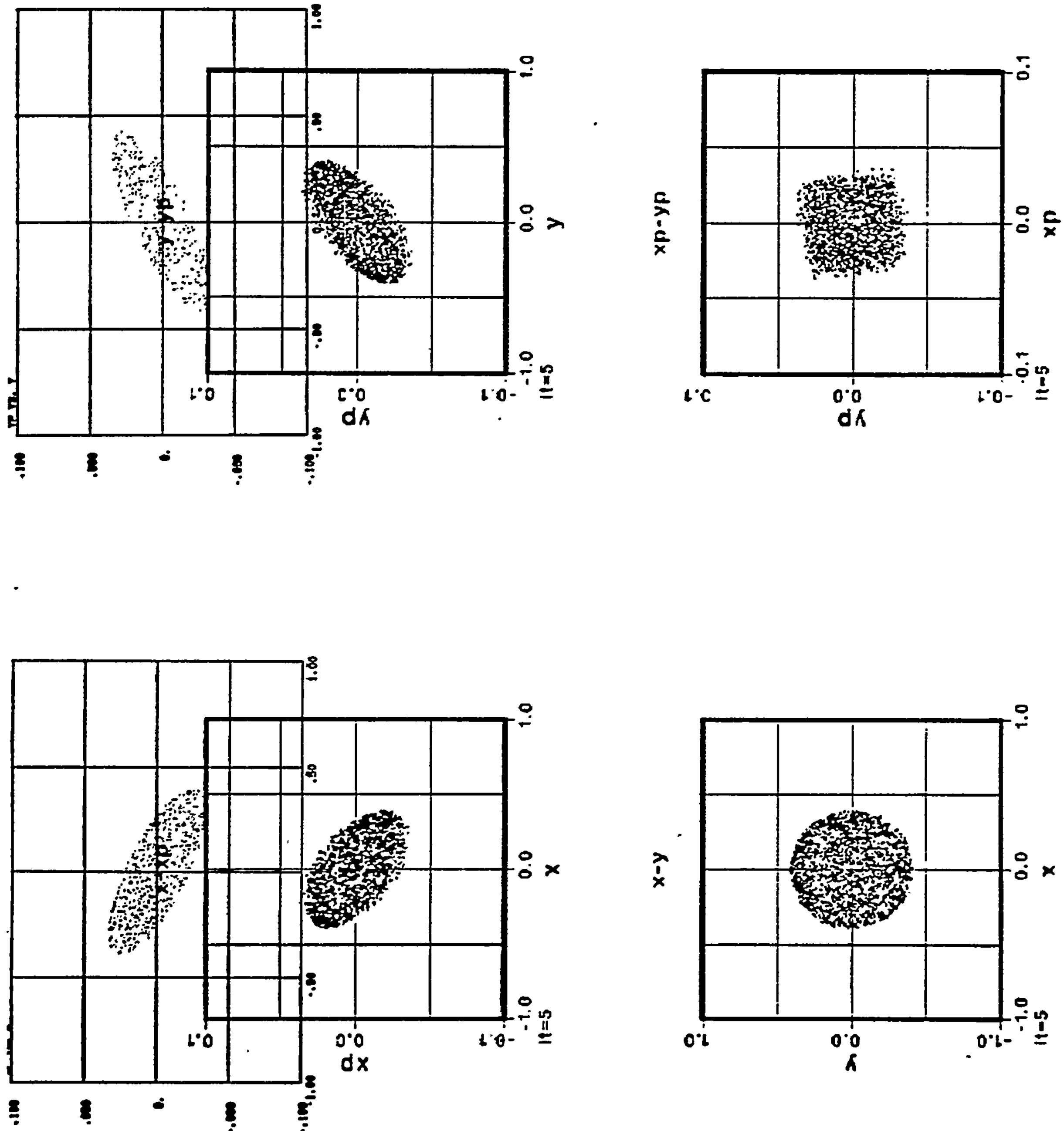
y-yp
x-xp
xp-yp
x-y
xp
yp
x
y
t=5

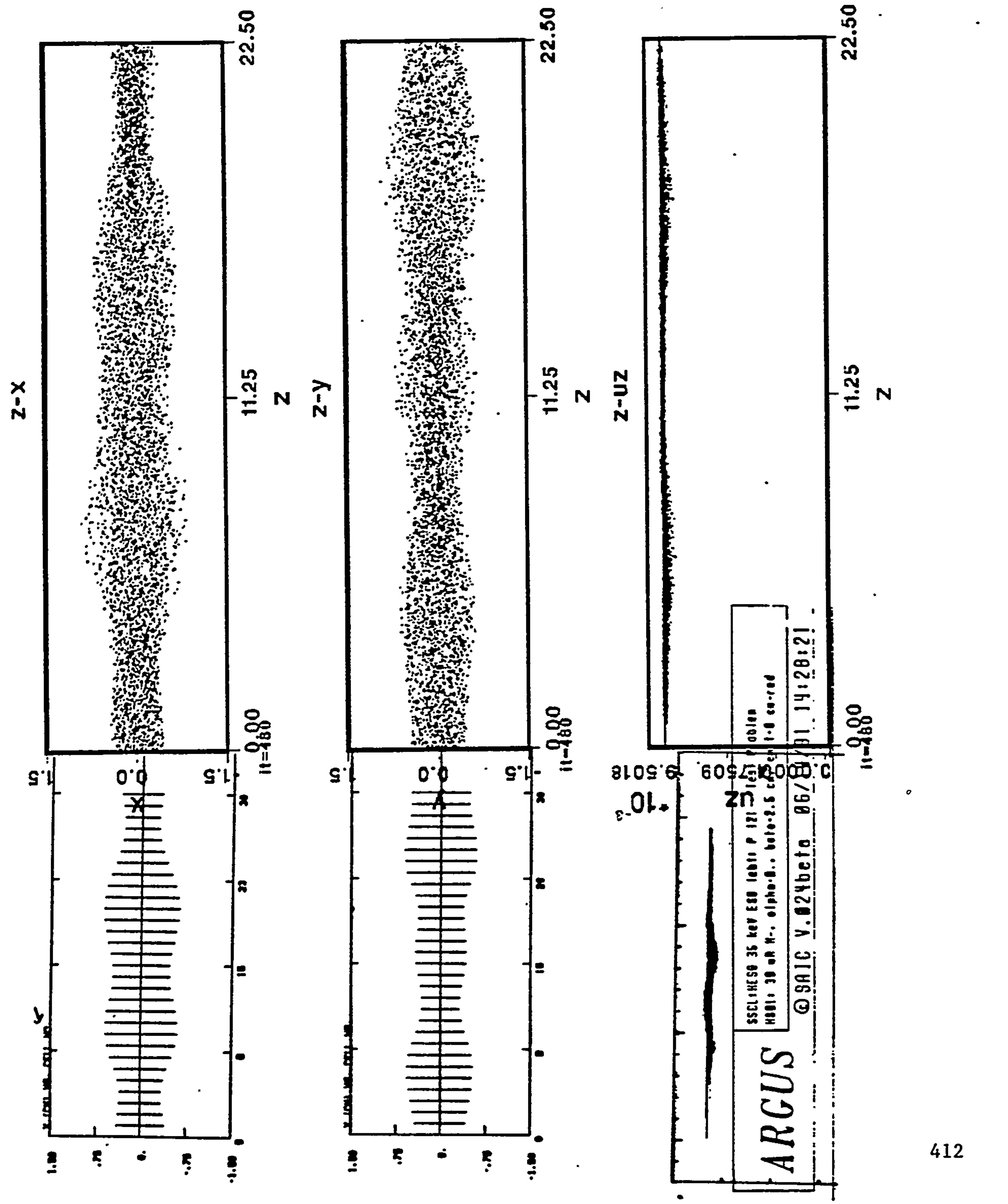

Z-X
Z-y
Z-UZ
Z
0.00
11.25
22.50
1.5
0.0
-1.5
ARGUS

POLAROID
D025 7194 C

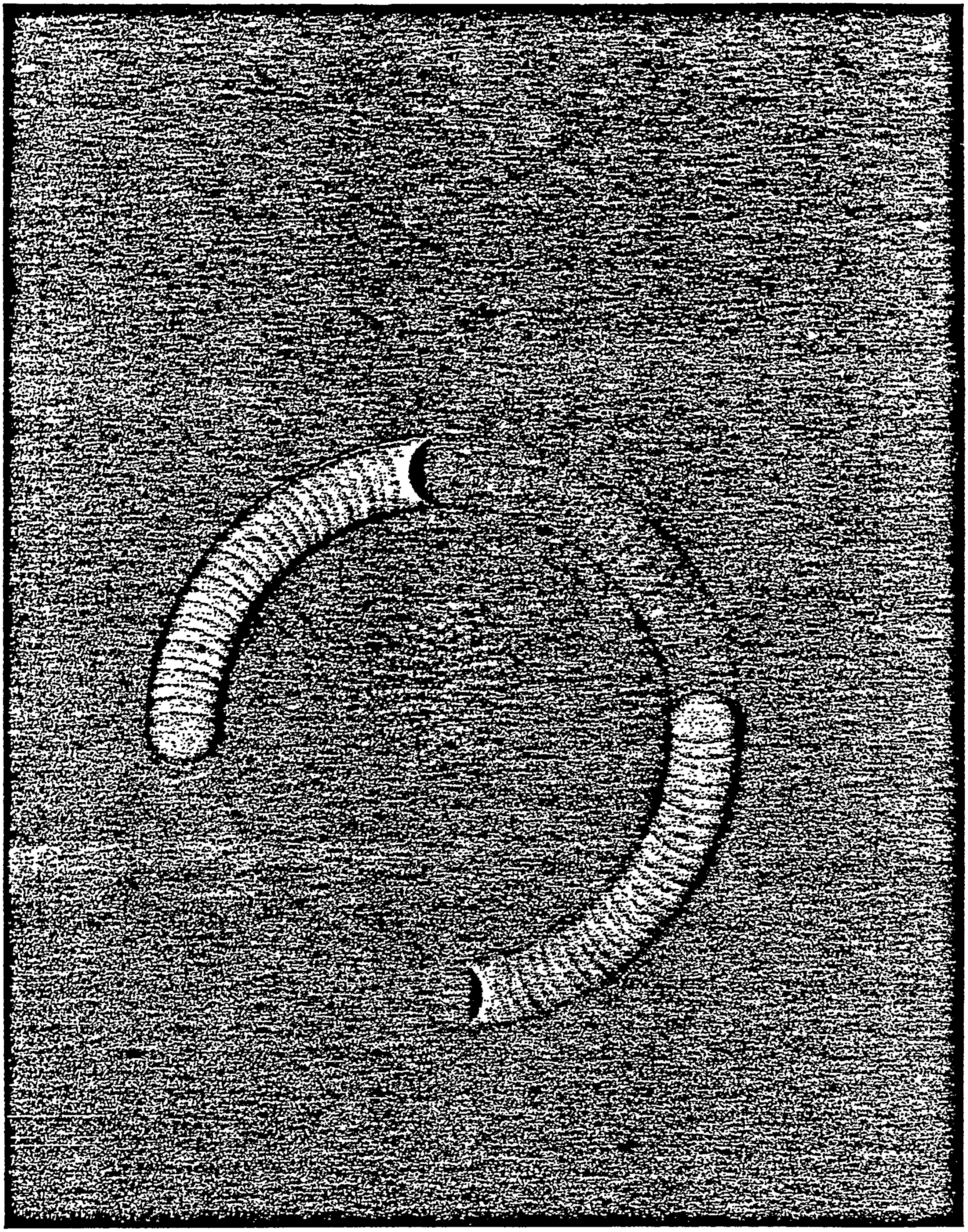

Olson

COPIED FROM BOARD
- RESULTS AT END OF
WORKSHOP 9-21-94

(1)

Common set of parameters

$R \sim 10$ cm $\quad < r_t$

$L \sim 2$-7 m in gas part in reactor

$r_t \sim 0.2$-1 cm

~~$A \sim$??~~

~~$Z \sim$~~

~~$\gamma \sim$~~

~~N~~

ϵ

θ_μ

multi-gap, neutralized between gaps

1-2 GAP $\quad A < 6$?

multi-gap $\quad A > 50$?

(5)

Stability theory – first look for trouble

Atomic physics – ion impact σ

stripping σ

diagnostic signatures

relevant gas chemistry

(4)

recommendations:

experiment: self-pinched on SABRE
ILSE neut. experiment
light ion machine — neut. exp.?
pre-formed channels —
stripping, etc., for $A>1$

code development: IPROP: self pinch for high Z ions (HIF, LIF, Conversion)
WARP 3D: multi-gap with neut.?
BICFE: with plasma LIF Ballistic
QUICKSILVER: beam overlap problem (HIF, LIF): very 3D
BUCKSHOT: { Delta ray (HIP) for pinched & final focus; stripping }
Z-discharge codes

(3)

system sensitivity study,
systematic evaluation of a common ion
for transport

interface – accel./~~tran~~transport

diagnostics – e.g. I_{max}, σ
probe beam interior

"Cooperative approaches to ion driven fusion"

" Commonality of inertial fusion materials, issues, technology

Chromatic effects abberations

(2)

TRANSPORT AREAS & ISSUES

self-pinched : small r equilibria
& accessibility
adequate f_m & f_i
efficiency of trapping beam
stability (hose, sausage, 2-stream
filamentation)
charge to target?
multi-beam overlap
aiming & tracking

charge neutralization - ballistic
neut. between gaps

Channel issues - small r limit
free-standing channel HV breakdown

HIF lens aberrations, realistic lenses

LIF current neut. in B, demo.